

# Insights in microorganisms in vertebrate digestive systems 2022

**Edited by**  
Weiqi He

**Published in**  
Frontiers in Microbiology



## FRONTIERS EBOOK COPYRIGHT STATEMENT

The copyright in the text of individual articles in this ebook is the property of their respective authors or their respective institutions or funders. The copyright in graphics and images within each article may be subject to copyright of other parties. In both cases this is subject to a license granted to Frontiers.

The compilation of articles constituting this ebook is the property of Frontiers.

Each article within this ebook, and the ebook itself, are published under the most recent version of the Creative Commons CC-BY licence. The version current at the date of publication of this ebook is CC-BY 4.0. If the CC-BY licence is updated, the licence granted by Frontiers is automatically updated to the new version.

When exercising any right under the CC-BY licence, Frontiers must be attributed as the original publisher of the article or ebook, as applicable.

Authors have the responsibility of ensuring that any graphics or other materials which are the property of others may be included in the CC-BY licence, but this should be checked before relying on the CC-BY licence to reproduce those materials. Any copyright notices relating to those materials must be complied with.

Copyright and source acknowledgement notices may not be removed and must be displayed in any copy, derivative work or partial copy which includes the elements in question.

All copyright, and all rights therein, are protected by national and international copyright laws. The above represents a summary only. For further information please read Frontiers' Conditions for Website Use and Copyright Statement, and the applicable CC-BY licence.

ISSN 1664-8714  
ISBN 978-2-8325-4300-9  
DOI 10.3389/978-2-8325-4300-9

## About Frontiers

Frontiers is more than just an open access publisher of scholarly articles: it is a pioneering approach to the world of academia, radically improving the way scholarly research is managed. The grand vision of Frontiers is a world where all people have an equal opportunity to seek, share and generate knowledge. Frontiers provides immediate and permanent online open access to all its publications, but this alone is not enough to realize our grand goals.

## Frontiers journal series

The Frontiers journal series is a multi-tier and interdisciplinary set of open-access, online journals, promising a paradigm shift from the current review, selection and dissemination processes in academic publishing. All Frontiers journals are driven by researchers for researchers; therefore, they constitute a service to the scholarly community. At the same time, the *Frontiers journal series* operates on a revolutionary invention, the tiered publishing system, initially addressing specific communities of scholars, and gradually climbing up to broader public understanding, thus serving the interests of the lay society, too.

## Dedication to quality

Each Frontiers article is a landmark of the highest quality, thanks to genuinely collaborative interactions between authors and review editors, who include some of the world's best academicians. Research must be certified by peers before entering a stream of knowledge that may eventually reach the public - and shape society; therefore, Frontiers only applies the most rigorous and unbiased reviews. Frontiers revolutionizes research publishing by freely delivering the most outstanding research, evaluated with no bias from both the academic and social point of view. By applying the most advanced information technologies, Frontiers is catapulting scholarly publishing into a new generation.

## What are Frontiers Research Topics?

Frontiers Research Topics are very popular trademarks of the *Frontiers journals series*: they are collections of at least ten articles, all centered on a particular subject. With their unique mix of varied contributions from Original Research to Review Articles, Frontiers Research Topics unify the most influential researchers, the latest key findings and historical advances in a hot research area.

Find out more on how to host your own Frontiers Research Topic or contribute to one as an author by contacting the Frontiers editorial office: [frontiersin.org/about/contact](https://frontiersin.org/about/contact)



# Insights in microorganisms in vertebrate digestive systems: 2022

## Topic editor

Weiqi He — Soochow University, China

## Citation

He, W., ed. (2024). *Insights in microorganisms in vertebrate digestive systems: 2022*. Lausanne: Frontiers Media SA. doi: 10.3389/978-2-8325-4300-9

# Table of contents

- 05 **Editorial: Insights in microorganisms in vertebrate digestive systems: 2022**  
Yu-Ting Tang and Wei-Qi He
- 07 **New insights into bacterial mechanisms and potential intestinal epithelial cell therapeutic targets of inflammatory bowel disease**  
Bing Liang, Changhao Wu, Chao Wang, Wenshe Sun, Wujun Chen, Xiaokun Hu, Ning Liu and Dongming Xing
- 22 **Traditional Chinese medicine improves myasthenia gravis by regulating the symbiotic homeostasis of the intestinal microbiota and host**  
Mingli Zhao, Li Liu, Fanzhao Liu, Lei Liu, Zhijuan Liu, Yanli Gao and Jianxi Cao
- 33 **Communication of gut microbiota and brain *via* immune and neuroendocrine signaling**  
Kaja Kasarello, Agnieszka Cudnoch-Jedrzejewska and Katarzyna Czarzasta
- 46 **Dynamic changes in fecal microbiota in donkey foals during weaning: From pre-weaning to post-weaning**  
Zhenwei Zhang, Bingjian Huang, Xu Gao, Xiaoyuan Shi, Xinrui Wang, Tianqi Wang, Yonghui Wang, Guiqin Liu and Changfa Wang
- 62 **Effects of several flavonoids on human gut microbiota and its metabolism by *in vitro* simulated fermentation**  
Lixia Pan, Hangyu Ye, Xionge Pi, Wei Liu, Zhao Wang, Yinjun Zhang and Jianyong Zheng
- 77 **Glucose oxidase as an alternative to antibiotic growth promoters improves the immunity function, antioxidative status, and cecal microbiota environment in white-feathered broilers**  
Wenyu Zhao, Yuan Huang, Na Cui, Ruiguo Wang, Zhiming Xiao and Xiaou Su
- 94 **Development of a reproducible small intestinal microbiota model and its integration into the SHIME<sup>®</sup>-system, a dynamic *in vitro* gut model**  
Stef Deyaert, Frédéric Moens, Walter Pirovano, Bartholomeus van den Bogert, Eline Suzanne Klaassens, Massimo Marzorati, Tom Van de Wiele, Michiel Kleerebezem and Pieter Van den Abbeele
- 112 **Landscape in the gallbladder mycobiome and bacteriome of patients undergoing cholelithiasis with chronic cholecystitis**  
Junqing Hu, Jichao Tang, Xinpeng Zhang, Kaijin Yang, Ayan Zhong, Qin Yang, Yanjun Liu, Yi Li and Tongtong Zhang
- 126 **Association between salivary microbiota and renal function in renal transplant patients during the perioperative period**  
Xuyu Xiang, Bo Peng, Kai Liu, Tianyin Wang, Peng Ding, Hao Li, Yi Zhu and Yingzi Ming

- 138 **Hybridization alters the gut microbial and metabolic profile concurrent with modifying intestinal functions in Tunchang pigs**  
Jiayi He, Yunchao Zhang, Hui Li, Yanshe Xie, Guiqing Huang, Chen Peng, Pengju Zhao and Zhengguang Wang
- 155 **Virulence-related factors and antimicrobial resistance in *Proteus mirabilis* isolated from domestic and stray dogs**  
Lijuan Liu, Zhiyou Dong, Shengquan Ai, Shanyu Chen, Mengyao Dong, Qianlan Li, Ziyao Zhou, Haifeng Liu, Zhijun Zhong, Xiaoping Ma, Yanchun Hu, Zhihua Ren, Hualin Fu, Gang Shu, Xianmeng Qiu and Guangneng Peng
- 165 **House ammonia exposure causes alterations in microbiota, transcriptome, and metabolome of rabbits**  
Keyao Li, Shuo Pang, Zhechen Li, Xiaoning Ding, Yating Gan, Qianfu Gan and Shaoming Fang
- 182 **Effects of different manganese sources on nutrient digestibility, fecal bacterial community, and mineral excretion of weaning dairy calves**  
Huimin Ji, Dejin Tan, Yuhua Chen, Zhiqiang Cheng, Jingwen Zhao and Miao Lin
- 195 **Salidroside ameliorates memory impairment following long-term ethanol intake in rats by modulating the altered intestinal microbiota content and hippocampal gene expression**  
Yu Jiao, Zhenglin Zhao, Xin Li, Lulu Li, Dan Xiao, Siyuan Wan, Tong Wu, Tong Li, Ping Li and Rongjie Zhao
- 209 **Microbiota as key factors in inflammatory bowel disease**  
Zachary White, Ivan Cabrera, Isabel Kapustka and Teruyuki Sano



## OPEN ACCESS

EDITED AND REVIEWED BY  
Knut Rudi,  
Norwegian University of Life Sciences, Norway

\*CORRESPONDENCE  
Wei-Qi He  
✉ whe@suda.edu.cn

RECEIVED 27 November 2023  
ACCEPTED 18 December 2023  
PUBLISHED 05 January 2024

CITATION  
Tang Y-T and He W-Q (2024) Editorial: Insights  
in microorganisms in vertebrate digestive  
systems: 2022. *Front. Microbiol.* 14:1344969.  
doi: 10.3389/fmicb.2023.1344969

COPYRIGHT  
© 2024 Tang and He. This is an open-access  
article distributed under the terms of the  
[Creative Commons Attribution License \(CC  
BY\)](#). The use, distribution or reproduction in  
other forums is permitted, provided the  
original author(s) and the copyright owner(s)  
are credited and that the original publication  
in this journal is cited, in accordance with  
accepted academic practice. No use,  
distribution or reproduction is permitted  
which does not comply with these terms.

# Editorial: Insights in microorganisms in vertebrate digestive systems: 2022

Yu-Ting Tang and Wei-Qi He\*

Jiangsu Key Laboratory of Neuropsychiatric Diseases and Cambridge-Suda (CAM-SU) Genomic Resource Center, Medical College of Soochow University, Suzhou, Jiangsu, China

## KEYWORDS

gut microbiota, human diseases, animal husbandry, microbial imbalances, physiological impact

## Editorial on the Research Topic

### Insights in microorganisms in vertebrate digestive systems: 2022

The entire microbiota of the digestive tract, spanning from the oral cavity to the rectum, is established through interactions with the external environment, a process initiated during the fetal stage (Martino et al., 2022). Microorganisms intricately influence host physiological activities (Westermann and Vogel, 2021), engaging with the nervous system, immune system, and various organs (Morais et al., 2021; Tilg et al., 2022). Imbalances in the microecology impact diverse aspects of the host's cognition, emotions, diet, and metabolism (Fan and Pedersen, 2021). Deyaert et al. established an *in vitro* dynamic ileal microbiota model to investigate bacterial activity. Additionally, Pan et al. highlighted the regulatory role of flavonoids in shaping the human gut microbiota structure. We underscore that an understanding of microbial ecology can unveil the host's health status. This Research Topic aims to provide a comprehensive overview of cutting-edge studies on the symbiotic relationship between microorganisms and digestive system. This aligns with the summaries provided by Liang et al., Kasarello et al., and White et al. contributing insights and addressing current challenges in the exploration of microorganism interactions across multiple systems.

The gut microbiota actively participates in the human physiological and pathological activities (Shalon et al., 2023). Its potential as prognosis indicators or treatment targets has been deeply explored. Hu et al. illustrated the microbial landscape of the gallbladder in patients with gallstones, revealing significant alterations in bacterial taxonomic composition and strengthened correlation between bacterial and fungal communities in bile, potentially linked to gallstone formation. Xiang et al. connected the saliva microbiota changes with the renal function recovery in renal transplant patients during the perioperative period, suggesting them as biomarkers for postoperative recovery. Jiao et al. reported that a rising abundance of *Actinobacteria* and *Bifidobacterium* in the intestine following salidroside treatment, correlated with downregulation of *Tomm7* (translocase of outer mitochondrial membrane 7) in the hippocampus, ameliorating memory impairment after long-term ethanol intake in rats. Zhao M. et al. proposed that an increase in *Shigella* and a decrease in *Prevotella* and *Bacteroides* may contribute to the occurrence and development of myasthenia gravis. The imbalance of the microbial community can



be adjusted by Modified Buzhong Yiqi Decoction treatment, further enhancing host immune function.

Beyond its implications for human diseases, the gut microbiota holds the potential for developments in animal husbandry. Ji et al. proposed that organic Mn supplementation in the diet had more advantages than the sulfate forms in weaning calves, maintaining a more stable microbial community. Zhao W. et al. demonstrated that a diet supplemented with glucose oxidase may strengthen the immunologic barrier and maintain a healthy intestinal microecology. A deeper understanding of the microbiota community aids in optimizing gut function and improving feeding efficiency. Zhang et al. documented dynamic changes in fecal microbiota in donkey foals during weaning, while He et al. manipulated gut microbial and metabolic profiles through hybridization in Tunchang pigs. Regarding microbial structure, composition, and functional capacity as crucial assessment, Li et al. disclosed that house ammonia exposure in rabbits may impact on local immune responses and inflammatory processes. Liu et al. disclosed a higher prevalence of multidrug-resistant *Proteus mirabilis* in domestic dogs, along with corresponding antibiotic resistance genes. This finding emphasizes the importance of prudent antibiotic management by veterinarians. The study of vertebrate microbiota offers an opportunity to comprehensively monitor the health status of livestock, ensuring the high-quality of husbandry products (Wen et al., 2021).

It is inspiring that our Research Topic has garnered attention from researchers worldwide, including those from the USA, Poland, Belgium, the Netherlands, and China. We extend our gratitude to all authors who contributed their original work to this Research Topic and the reviewers for their invaluable comments. We also express our sincere thanks to the editorial office of Frontiers in Microbiology for their excellent support and for providing us with the opportunity to successfully host this hot topic issue.

## References

- Fan, Y., and Pedersen, O. (2021). Gut microbiota in human metabolic health and disease. *Nat. Rev. Microbiol.* 19, 55–71. doi: 10.1038/s41579-020-0433-9
- Martino, C., Dillmore, A. H., Burcham, Z. M., Metcalf, J. L., Jeste, D., and Knight, R. (2022). Microbiota succession throughout life from the cradle to the grave. *Nat. Rev. Microbiol.* 20, 707–720. doi: 10.1038/s41579-022-00768-z
- Morais, L. H., Schreiber, H. L., and Mazmanian, S. K. (2021). The gut microbiota-brain axis in behaviour and brain disorders. *Nat. Rev. Microbiol.* 19, 241–255. doi: 10.1038/s41579-020-00460-0
- Shalon, D., Culver, R. N., Grembi, J. A., Folz, J., Treit, P. V., Shi, H., et al. (2023). Profiling the human intestinal environment under physiological conditions. *Nature*. 617, 581–591. doi: 10.1038/s41586-023-05989-7
- Tilg, H., Adolph, T. E., and Trauner, M. (2022). Gut-liver axis: Pathophysiological concepts and clinical implications. *Cell Metab.* 34, 1700–1718. doi: 10.1016/j.cmet.2022.09.017
- Wen, C., Yan, W., Mai, C., Duan, Z., Zheng, J., Sun, C., et al. (2021). Joint contributions of the gut microbiota and host genetics to feed efficiency in chickens. *Microbiome*. 9, 126. doi: 10.1186/s40168-021-01040-x
- Westermann, A. J., and Vogel, J. (2021). Cross-species RNA-seq for deciphering host-microbe interactions. *Nat. Rev. Genet.* 22, 361–378. doi: 10.1038/s41576-021-00326-y

## Author contributions

Y-TT: Writing—original draft, Writing—review & editing. W-QH: Funding acquisition, Writing—original draft, Writing—review & editing.

## Funding

The author(s) declare financial support was received for the research, authorship, and/or publication of this article. This work was supported by the National Natural Science Foundation of China (31971062), the Open Fund of National Facility for Translational Medicine (Shanghai) (TMSK-2021-301), and the Natural Science Foundation of the Jiangsu Higher Education Institutions of China (20KJA180003).

## Conflict of interest

The authors declare that the research was conducted in the absence of any commercial or financial relationships that could be construed as a potential conflict of interest.

The author(s) declared that they were an editorial board member of Frontiers, at the time of submission. This had no impact on the peer review process and the final decision.

## Publisher's note

All claims expressed in this article are solely those of the authors and do not necessarily represent those of their affiliated organizations, or those of the publisher, the editors and the reviewers. Any product that may be evaluated in this article, or claim that may be made by its manufacturer, is not guaranteed or endorsed by the publisher.



## OPEN ACCESS

## EDITED BY

Weiqi He,  
Soochow University,  
China

## REVIEWED BY

Yukiko Miyamoto,  
University of California, San Diego,  
United States  
Graham J. Britton,  
Icahn School of Medicine at Mount Sinai,  
United States

## \*CORRESPONDENCE

Ning Liu  
leirum\_ln@qdu.edu.cn  
Dongming Xing  
xdm\_tsinghua@163.com

## SPECIALTY SECTION

This article was submitted to  
Microorganisms in Vertebrate  
Digestive Systems, a section of the journal  
Frontiers in Microbiology

RECEIVED 10 October 2022

ACCEPTED 30 November 2022

PUBLISHED 16 December 2022

## CITATION

Liang B, Wu C, Wang C, Sun W, Chen W,  
Hu X, Liu N and Xing D (2022) New insights  
into bacterial mechanisms and potential  
intestinal epithelial cell therapeutic targets  
of inflammatory bowel disease.  
*Front. Microbiol.* 13:1065608.  
doi: 10.3389/fmicb.2022.1065608

## COPYRIGHT

© 2022 Liang, Wu, Wang, Sun, Chen, Hu,  
Liu and Xing. This is an open-access article  
distributed under the terms of the [Creative  
Commons Attribution License \(CC BY\)](#). The  
use, distribution or reproduction in other  
forums is permitted, provided the original  
author(s) and the copyright owner(s) are  
credited and that the original publication in  
this journal is cited, in accordance with  
accepted academic practice. No use,  
distribution or reproduction is permitted  
which does not comply with these terms.

# New insights into bacterial mechanisms and potential intestinal epithelial cell therapeutic targets of inflammatory bowel disease

Bing Liang<sup>1</sup>, Changhao Wu<sup>2</sup>, Chao Wang<sup>1</sup>, Wenshe Sun<sup>1</sup>,  
Wujun Chen<sup>1</sup>, Xiaokun Hu<sup>3</sup>, Ning Liu<sup>1\*</sup> and Dongming Xing<sup>1,4\*</sup>

<sup>1</sup>Cancer Institute, The Affiliated Hospital of Qingdao University, Qingdao, China, <sup>2</sup>Department of Biochemistry and Physiology, Faculty of Health and Medical Sciences, University of Surrey, Guildford, United Kingdom, <sup>3</sup>Intervention Neurosurgery, The Affiliated Hospital of Qingdao University, Qingdao, China, <sup>4</sup>School of Life Sciences, Tsinghua University, Beijing, China

The global incidence of inflammatory bowel disease (IBD) has increased rapidly in recent years, but its exact etiology remains unclear. In the past decade, IBD has been reported to be associated with dysbiosis of gut microbiota. Although not yet proven to be a cause or consequence of IBD, the common hypothesis is that at least some alterations in the microbiome are protective or pathogenic. Furthermore, intestinal epithelial cells (IECs) serve as a protective physical barrier for gut microbiota, essential for maintaining intestinal homeostasis and actively contributes to the mucosal immune system. Thus, dysregulation within the intestinal epithelium increases intestinal permeability, promotes the entry of bacteria, toxins, and macromolecules, and disrupts intestinal immune homeostasis, all of which are associated with the clinical course of IBD. This article presents a selective overview of recent studies on bacterial mechanisms that may be protective or promotive of IBD in biological models. Moreover, we summarize and discuss the recent discovery of key modulators and signaling pathways in the IECs that could serve as potential IBD therapeutic targets. Understanding the role of the IECs in the pathogenesis of IBD may help improve the understanding of the inflammatory process and the identification of potential therapeutic targets to help ameliorate this increasingly common disease.

## KEYWORDS

inflammatory bowel disease, gut microbiota, bacterial mechanisms, intestinal epithelial cells (IECs), therapeutic targets

## Introduction

Inflammatory bowel disease (IBD) is a multifactorial chronic inflammatory disease, which primarily includes Crohn's disease (CD) and Ulcerative colitis (UC). IBD causes severe gastrointestinal (GI) tract symptoms, including diarrhea, abdominal pain, bleeding, anemia, and weight loss, and poses a severe but incurable threat to human life and health.

The etiology and pathogenesis of IBD remain unknown. However, they may be linked to genetic susceptibility, intestinal microbial homeostasis imbalance, impaired intestinal mucosal barrier function, disorders of innate and adaptive immune regulation in the intestine, and stimulation by external environmental factors. IBD primarily affects genetically predisposed individuals in a specific environment where the intestinal mucosal immune system produces an abnormally amplified immune response to intestinal microbial antigens, resulting in inflammatory damage to the intestinal mucosa.

There are ~400 species of bacteria in the human intestine, including resident and some transient bacteria. The sites of IBD are the colon, rectum, and ileum, where the intestine is most exposed to bacteria. Some clinical features of IBD are similar to those of some infectious diseases of the GI. Several studies have shown that a large quantity of bacteria in the human intestine affects the function of the intestinal mucosal immune system and that a large number of intestinal antigens, such as enteric bacteria and bacterial products, induce abnormal immune responses in the intestine of individuals with genetic susceptibility to IBD, leading to the development of IBD. Although the current research data do not support that infection with a specific pathogenic microorganism causes the development of IBD, clinical observations suggest that intestinal infections caused by these microorganisms can induce the recurrence of IBD in remission. In addition, many experiments have confirmed the involvement of intestinal bacteria in the development of experimental colitis. About 99.9% of human GI microbiota are bacteria, and the other 0.1% are fungi, archaea, and viruses (Qin et al., 2010; Sommer and Backhed, 2013). Bacteria have been extensively reported to have an important role in the pathogenesis of IBD. Intestinal epithelial cells (IECs) line the surface of the intestinal epithelium and perform a variety of functions, including the physical isolation of commensal bacteria and the integration of microbial signals (Peterson and Artis, 2014). IECs also react to immune cell-produced factors that regulate epithelial barrier function, proliferation, and differentiation (Soderholm and Pedicord, 2019). Dysregulation of the IECs can lead to increased intestinal permeability, abnormal IEC interactions with immune cells, and disruption of intestinal immune homeostasis, all of which are associated with the clinical course of IBD (Coskun, 2014).

Many medications, including aminosalicylates, corticosteroids, immunomodulatory drugs, biologics, and antibiotics, can help reduce inflammation and alleviate IBD symptoms. Among them, the introduction of tumor necrosis factor (TNF) inhibitors is an outstanding achievement, allowing for long-term remission and modification of the IBD course in many patients (Nielsen and Ainsworth, 2013). The clinical treatment of IBD has advanced dramatically due to the development and application of these medications and the updating of therapeutic targets. However, these conventional treatments still focus on inducing and maintaining clinical remission, which is not yet wholly curable. A substantial proportion of patients still have long-term chronic active

inflammatory reactions and the need for surgical procedures, which significantly impacts patients' quality of life and imposes a major social and medical burden. Therefore, it is critical to investigate the pathogenesis of IBD, identify new targets for IBD treatment and implement precision medicine to develop the best treatment for patients.

## Bacteria species and functional pathways involved in the protection and pathogenicity of inflammatory bowel disease

The gut microbiota is considered to be a nonnegligible factor in the pathogenesis of IBD and an important target for the research of therapeutic drugs for IBD, which can regulate the host's vital activities, modulate the immune response and counteract the dysbiosis of gut microbiota, and play a vital role in protecting the host's health. Many studies have found that IBD patients have a disturbed intestinal microecological balance, characterized by reduced diversity, increased bacterial instability, increased *Actinobacteria*, and *Proteobacteria*, and decreased *Bacteroidetes* and *Firmicutes*, especially a significant decrease in bacteria producing short-chain fatty acids (SCFAs; Caruso et al., 2020). The pathophysiological mechanisms by which gut microbiota antigens induce abnormal responses in the innate and adaptive immune systems of the intestinal mucosa remain unknown. In addition to SCFAs, tryptophan metabolism, bile acid metabolism, Polysaccharide A (PSA) production, and virulence factor genes are balanced in the normal intestine, whereas tryptophan derivatives are reduced, secondary bile acids are reduced, PSA gene expression is reduced, and microbial virulence gene expression is increased in IBD patients' intestines.

## Bacteria species and functional pathways that are potentially protective of inflammatory bowel disease

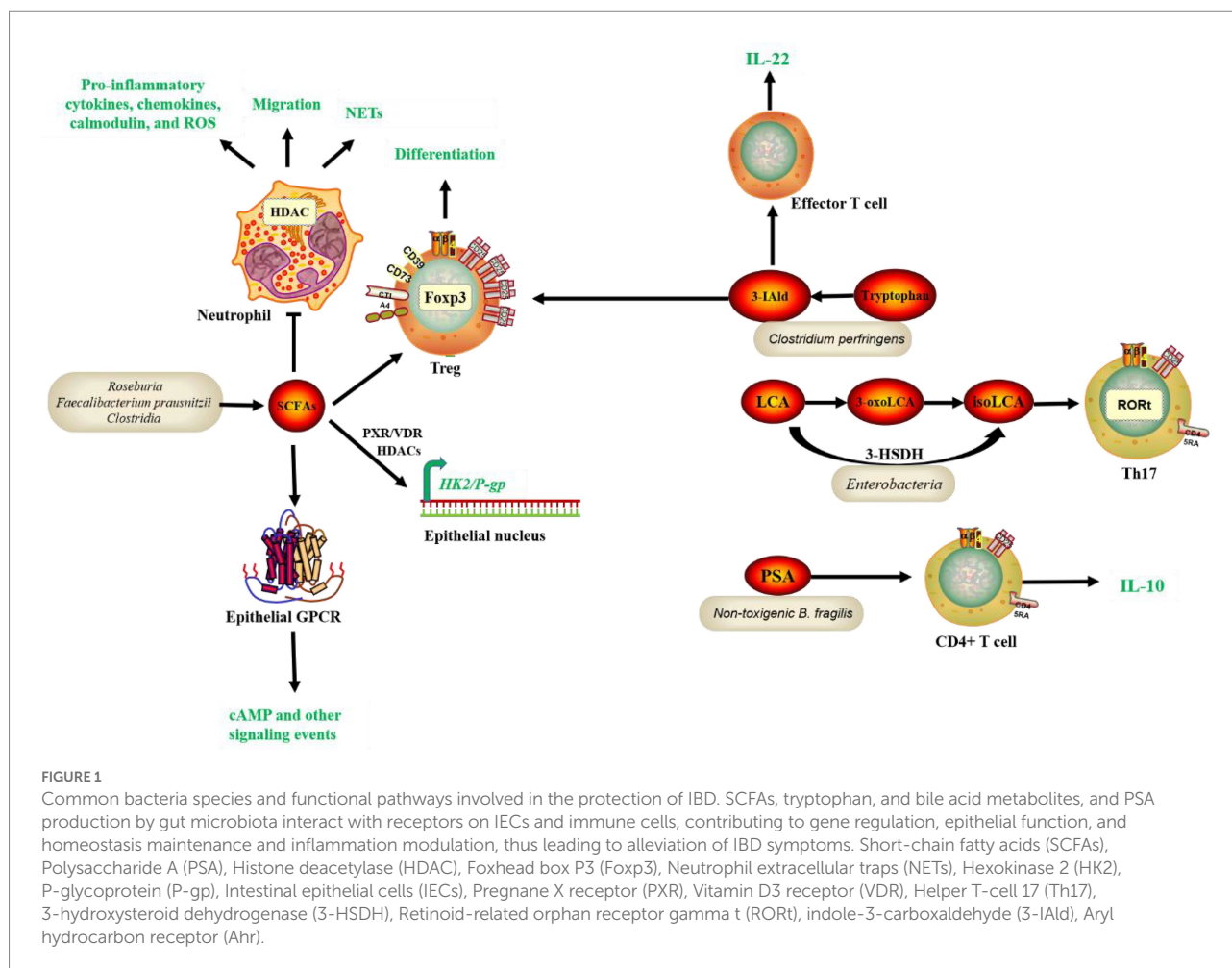
The first bacterial metabolite to play a potentially protective role for IBD is SCFA. The major SCFAs, including acetate, propionate, and butyrate, account for over 95% of the total SCFA content in feces (Kim et al., 2019). SCFAs can be produced by bacteria such as *Roseburia* and *Faecalibacterium prausnitzii*. Intestinal microorganisms convert dietary fiber fatty acids into SCFAs, which then enter the intestinal lumen. SCFAs can bind to G protein-coupled receptors (GPCRs), like GPR41 (Brown et al., 2003), GPR43 (Maslowski et al., 2009), and GPR109A (Thangaraju et al., 2009), to activate signaling cascades that control immune functions and improving intestinal barrier integrity (Vieira et al., 2015). SCFAs can also modulate immune cells, reduce pro-inflammatory factors, and mitigate the development of IBD (Luis et al., 2021); (Renga et al., 2022); (Rösch et al., 2017); (Nicolas and Chang, 2019). Back in 2013, butyrate, a by-product

from *Clostridia* fermentation of indigestive dietary fiber, was discovered to increase histone H3 acetylation at the *Foxhead box P3 (Foxp3)* promoter and conserved noncoding regions, promoting Treg differentiation and alleviate the development of colitis in mice (Furusawa et al., 2013). Similarly, Li et al. reported that butyrate inhibited neutrophil migration, formation of neutrophil extracellular traps (NETs), and production of pro-inflammatory cytokines, chemokines, and calmodulin in IBD patients by inhibiting histone deacetylase (HDAC). RNA sequencing analysis revealed that butyrate's immunomodulatory effects on neutrophils included leukocyte activation, innate immune response regulation, and oxidative stress (Li et al., 2021). Recent studies demonstrated previously unknown intracellular signaling network mediated by butyrate. For instance, butyrate could exert a protective effect against colitis by downregulating Hexokinase 2 (HK2) in the intestinal epithelium via HDAC8 (Hinrichsen et al., 2021). Moreover, a subsequent study revealed that butyrate increased *P-glycoprotein (P-gp)* transcription by inhibiting HDACs and activating nuclear receptors, pregnane X receptor (PXR) and vitamin D3 receptor (VDR). P-gp is a component of Intestinal epithelial cells (IECs) that plays an essential role in the excretion of endogenous cannabinoid toxins, the prevention of excessive inflammation, and the maintenance of endocytosis (Foley et al., 2022; Figure 1). The second pathway that protects against IBD is the metabolism of bile acids. Bile acids are synthesized in the liver, then processed and modified before being secreted into the duodenum, where intestinal microorganisms convert them to secondary bile acids (Ahmad and Haeusler, 2019). There are two secondary bile acids: lithocholic acid (LCA) and chenodeoxycholic acid (CDCA). They modulate immune cells, reduce pro-inflammatory factors, decrease systemic inflammation and alleviate the development of IBD (Postler and Ghosh, 2017); (Sinha et al., 2020). Bile acids can affect host metabolism, cancer progression, and innate immunity, but their effects on adaptive immune cells such as Helper T-cell 17 (Th17) cells and Regulatory T (Treg) cells have not been clarified. Previous research has shown that 3-oxoLCA and isoalloLCA, 2 lithocholic acid (LCA) derivatives, can inhibit the differentiation of Th17 cells and promote the differentiation of Treg, respectively. 3-oxoLCA inhibits the differentiation of Th17 cells by directly binding to the key transcription factor RAR-related orphan receptor gamma t (*RORyt*) and isoalloLCA promotes Treg differentiation by enhancing *Foxp3* expression and inducing the production of mitochondrial reactive oxygen species (mROS; Hang et al., 2019); however, the relationship between 3-oxoLCA and IBD remains unknown. A recent study discovered *Enterobacteria* and bacterial enzyme 3-hydroxysteroid dehydrogenase (3-HSDH) that convert LCA to 3-oxoLCA and then to isoLCA through *in vitro* culture screening. IsoLCA, like 3-oxoLCA, inhibits the transcriptional activity of *RORyt* and thus reduces Th17 cell differentiation (Paik et al., 2022). This study adds to our understanding of *Enterobacteria*-metabolite-host immune interactions and highlight the critical role of microbe-derived bile acid metabolites in regulating host immunity,

shedding new light on the treatment of immune diseases such as IBD (Figure 1). Treg cells have an important role in maintaining intestinal homeostasis, and their differentiation is influenced by the products of gut microbiota. A recently published study identified two new secondary bile acids,  $\omega$ -muricholic acid ( $\omega$ -MCA) and 3 $\beta$ -hydroxydeoxycholic acid (isoDCA) that effectively induce Treg differentiation *in vitro*, with isoDCA being more abundant in the intestine (Campbell et al., 2020). Further studies showed that isoDCA enhances its Treg induction by interacting with the farnesol X receptor (FXR) in dendritic cells (DCs), and by constructing engineered bacteria and colony colonization experiments, it was confirmed in mice that isoDCA-producing colonies promote peripheral Treg. The third pathway is tryptophan metabolism. Tryptophan is a necessary amino acid. Dietary tryptophan can undergo the kynurenine ammonia pathway in response to microbial and other inflammatory stimuli, producing a variety of compounds (Ma et al., 2020). Microbial action breaks down tryptophan to an indole derivative, which can modulate immune cells by stimulating IL-22, secreting antimicrobial peptides, and inhibiting the expression of inflammatory factors (Zelante et al., 2013). *Clostridium perfringens* can participate in the metabolism of tryptophan, which is also protective of IBD. According to a recent study, a tryptophan metabolite, indole-3-carboxaldehyde (3-IAld) reduces immune checkpoint inhibitor (ICI)-induced colitis in mice by influencing the structure and function of the mouse gut microbiota, resulting in an increase in sugar-fermenting bacteria and SCFA-producing bacteria and regulating Aryl hydrocarbon receptor (Ahr)/IL-22, and IL-10+ Treg cells (Renga et al., 2022; Figure 1). PSA production, the fourth potentially protective pathway for IBD, is primarily produced by *Bacteroides fragilis*. *B. fragilis* can deliver the immunomodulatory molecule PSA to immune cells by releasing outer membrane vesicles (OMVs), activate TLR 2 on the surface of DCs, resulting in the release of cytokines that promote IL-10 production by T cells (Wang et al., 2006; Shen et al., 2012; Dasgupta et al., 2014). This process is enhanced by direct binding of PSA to TLR2 expressed on Foxp3+ Tregs, which increases IL-10 production even further (Round and Mazmanian, 2010; Figure 1). PSA-induced IL-10 production inhibits the activity of mucosal effector T cells, particularly TH17 cells, and thus protects mice in colitis models (Mazmanian et al., 2008; Dasgupta et al., 2014). Here, *B. fragilis* refers mainly to non-toxicogenic *B. fragilis*, or NTBF. On the other hand, Enterotoxigenic *B. fragilis* (ETBF) is toxin-producing, which is likely to promote the development of IBD (Chung et al., 2018).

In addition to the four metabolite pathways associated with gut microbiota mentioned previously, other microbial species and functional molecules/pathways have been studied extensively recently (Figure 2). *Akkermansia muciniphila* (Akk) binds to a receptor on the membrane of IECs, affecting downstream immune regulatory responses, lowering lipopolysaccharide (LPS), reducing inflammation, regulating lipids, and lowering blood glucose in mouse models (Plovier et al., 2017). The literature has reported that Akk and its outer membrane protein, Amuc\_1100, can



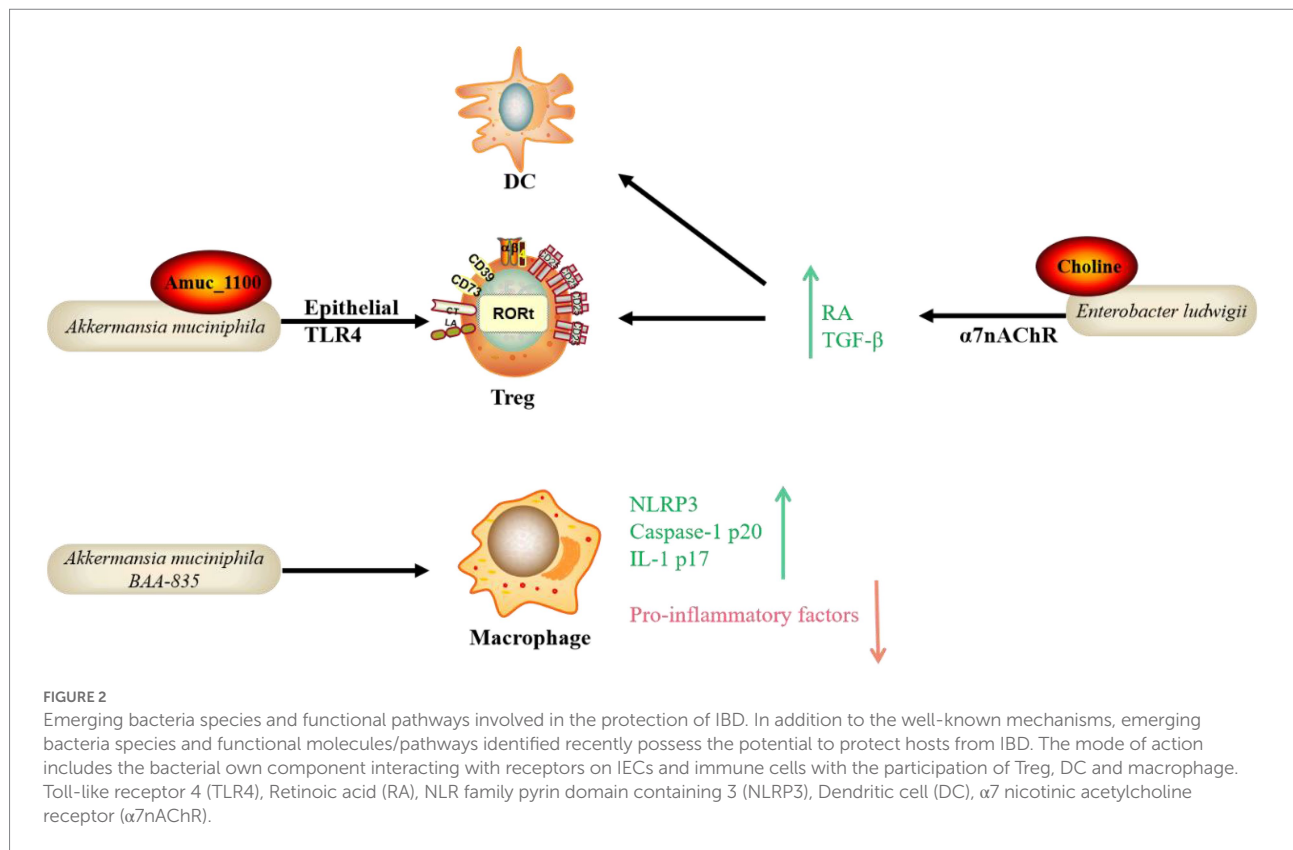


alleviate enteritis in mice (Zhai et al., 2019). Toll-like receptor 4 (TLR4) is a critical mediator in the interactions between gut microbiota and host immunity. Yang et al. recently discovered that TLR4 protects mice from colitis by promoting Akk colonization in the intestine, which upregulates RORt+ Treg cell-mediated immune responses (Liu et al., 2022). Furthermore, in a previous study, oral administration of Akk bacteria strain BAA-835 significantly improved the phenotype of Dextran sulfate sodium (DSS)-induced acute colitis in mice. Mechanistically, Akk increased the expression of *NLR family pyrin domain containing 3* (*NLRP3*), *caspase-1 p20*, and *IL-1 p17* improved intestinal barrier function, and inhibited the expression of pro-inflammatory factors such as *TNF-α* and *IL-6* (Qu et al., 2021). However, an earlier study found that Akk can cause colitis in sterile IL-10 gene-deficient mice (Seregin et al., 2017). Therefore, whether Akk can be used to treat IBD is still debatable. Furthermore, according to a recent study by Wang et al., *Enterobacter ludwigii* isolated from metronidazole-treated mouse feces could enhance DCs and promote Tregs differentiation through its metabolite choline and its receptor  $\alpha 7$  nicotinic acetylcholine receptor ( $\alpha 7$ nAChR)-mediated upregulation of retinoic acid (RA) and TGF- $\beta$ , thereby increasing the CD103+ DC/Treg-dependent tolerance response

and ultimately reducing the susceptibility of mice to DSS-induced colitis. Thus, this study provides a potential therapeutic approach for IBD (Li et al., 2022).

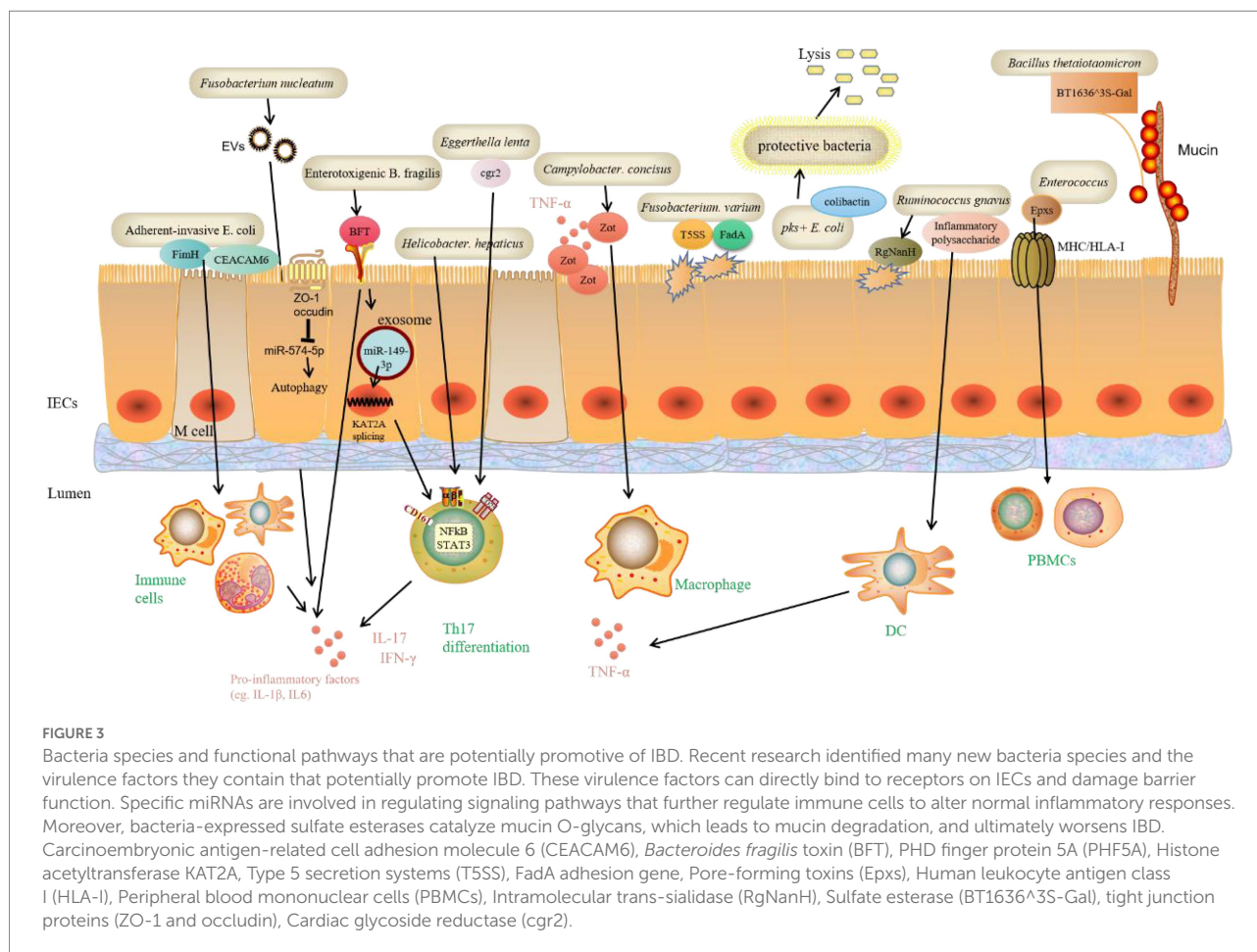
## Bacteria species and functional pathways that are potentially promotive of inflammatory bowel disease

Previous research has found that some pathobionts play a pro-IBD role in genetically susceptible individuals, such as *Mycobacterium paratuberculosis* and *Helicobacter pylori*. In addition, the efficacy of antibiotics and probiotics targeting gut microbiota further suggests a role for microorganisms in IBD. New research has recently emerged identifying many new bacteria species and the virulence factors they contain that potentially promote IBD (Figure 3). Adherent-invasive *E. coli* (AIEC) is distinct from typical *E. coli*, which AIEC is enriched in the intestinal microbiota of CD patients and promotes intestinal inflammation, development of IBD and even colorectal cancer (CRC). However, it is unclear how the nutrient metabolism of AIEC affects intestinal homeostasis. AIEC can adhere to the IECs



layer *via* the FimH and carcinoembryonic antigen-related cell adhesion molecule 6 (CEACAM6), enter the lamina propria and Peyer's patch *via* Microfold (M) cells, and interact with immune cells in the intestinal lumen to increase the production of inflammatory factors (Barnich et al., 2007; Palmela et al., 2018; Viladomiu et al., 2021). A recent article reported that in CD, propionate metabolism by AIEC is critical in promoting intestinal T cell inflammation. Meanwhile, CX3CR1<sup>+</sup> mononuclear phagocytes produce IL-1 $\beta$  upon sensing the AIEC metabolite propionate, which induces Th17 cells and drives intestinal inflammation (Viladomiu et al., 2021). Moreover, ETBF is strongly associated with the development of IBD, colitis associated cancer (CAC), and CRC. However, the mechanisms by which ETBF induces intestinal inflammation and tumorigenesis are unclear. *B. fragilis* contains the virulence gene *B. fragilis toxin* (BFT), which encodes the virulence protein BFT, interacting with the membrane receptors of IECs and immune cells *via* the STAT3 and NF- $\kappa$ B pathways, causing the expression of IL-17 downstream, promoting the expression of inflammatory factors and thus influencing the development of CRC (Chung et al., 2018). Recent study has discovered that ETBF-stimulated cells deliver miR-149-3p *via* exosomes and promote Th17 cell differentiation. ETBF induced CRC by suppressing miR-149-3p and promoting PHD finger protein 5A (PHF5A)-mediated histone acetyltransferase KAT2A mRNA alternative splicing (Cao et al., 2021). *Campylobacter concisus* is involved in a wide range of inflammatory diseases, including IBD. The *zonula occludens*

*toxin* (*Zot*) gene, discovered in *Asiatic cholera* and had a pathogenic effect, is found in 30% of *C. concisus* (Zhang et al., 2014). In a large study of Danish subjects, 962 people were infected with *C. concisus* and 1725 with *C. jejuni*. The risk of colitis was significantly higher in *C. concisus*-infected subjects than in controls, with a risk ratio of 32.4 (Nielsen et al., 2020). This also implies that *C. Concisus* likely hasten the onset of IBD. Further research has revealed that the enteropathogenic *Zot* virulence protein of *C. concisus* disrupts the intestinal epithelial barrier and induces the production of pro-inflammatory cytokines, particularly TNF- $\alpha$ , by intestinal epithelial and macrophage cells (Mahendran et al., 2016). *Fusobacterium varium* was found in up to 54.6% of 163 inflamed mucosal samples from 152 UC patients in Japan using real-time quantitative PCR (Tahara et al., 2015). A genome-wide analysis of an *F. varium* Fv113-g1 isolate from a UC patient's intestine revealed numerous virulence factors, including 44 *Type 5 secretion systems* (T5SS) and 13 *FadA adhesion gene* homologs in mucosal inflammation (Sekizuka et al., 2017). Some gut microbiota (for example, pks + *E. coli*) produce colibactin, a chemically unstable small molecule genotoxin whose genotoxicity to host cells can increase the host's risk of CRC. The effects of colibactin on other microorganisms in the gut have received little attention. A recent study discovered that colibactin could target surrounding bacteria containing prophages and activate prophages within the bacteria, causing phage replication and bacterial lysis. The induction of prophages by colibactin-producing bacteria has been observed in



various human and gut-associated phage-bacterial systems and in mouse fecal flora. These findings shed light on the potential mechanisms by which colibactin influences gut microbiota and the relationship between bacterial products and phagosomal behavior. As a result, it is possible that bacteria evolved this genotoxin to inhibit other bacteria rather than poison the host and that the cancer-promoting effects of colibactin are a “misuse” of the host (Silpe et al., 2022). *Enterococci* are a group of bacteria widely found in the intestines of humans and other animals that cause multi-drug resistant infections. However, a family of potent protein-like toxins specifically targeting human and animal cells has not been previously identified in *Enterococcus* spp. Min’s group have recently identified and resolved a novel family of *Pore-forming toxins* (Epxs) expressed in *Enterococcus* spp. They discovered that Epx is a subclass of small  $\beta$ -barrel pore-forming toxins, with the  $\beta$ -barrel serving as the top structural domain and forming homo-octameric pores. The whole-genome CRISPR-Cas9 screen revealed that Epx2/3 binds to human leukocyte antigen class I (HLA-I). Through Epx2 virulence, Epx2+ *E. faecalis* strains harm peripheral blood mononuclear cells (PBMCs) and intestinal-like organs (Xiong et al., 2022). *Ruminococcus gnavus* is a type of commensal bacteria found in the human intestine. Several studies have found that they are

significantly more abundant in IBD patients than in healthy subjects. *R. gnavus*. Can reduce intestinal mucin, which is mediated by intramolecular trans-sialidase (RgNanH; Tailford et al., 2015). Moreover, *R. gnavus*. Can stimulate DCs via the production of inflammatory polysaccharides, increasing the inflammatory cytokine TNF- $\alpha$ , promoting IBD’s development (Henke et al., 2019). Other bacteria that potentially contribute to IBD are *Helicobacter hepaticus* and *H. bilis*, both of which are from the genus *Helicobacter*. Bacteria from the genus *Helicobacter* that are not *H. pylori* often positively associated with IBD. In contrast, *H. pylori* and IBD show a negative correlation, meaning that people infected with *H. pylori* are less likely to develop IBD, possibly due to the ability of *H. pylori* to inhibit the growth of other bacteria. According to one study, in a mouse model of *IL-10* gene-deficient colitis, *H. hepaticus* induced inflammatory Th17, increased IL-17A and IFN- $\gamma$  expression, and aided in the development of colitis (Xu et al., 2018). Some gut microbiota can colonize the intestinal mucus layer and feed on mucin, a major component of the mucus layer. Mucin is a heavily glycosylated protein with numerous O-glycan chains. Mucin O-glycan ends are frequently sulfated in the distal colon. Bacterial degradation of colonic mucin requires specific sulfatases to remove sulfate groups on O-glycans. However, little is known about the bacterial

sulfate esterases that act on colonic mucin and how they work. A recently published study discovered a sulfate esterase expressed by *Bacillus thetaiotaomicon*, a common human intestinal commensal that uses sulfated colonic mucin O-glycans as its sole carbon source. The knockout of sulfate esterases from *B. thetaiotaomicon* revealed that one of the enzymes (BT1636<sup>Δ</sup>3S-Gal) is required to utilize sulfated mucin O-glycan and plays an important role in the intestinal colonization of the bacterium (Luis et al., 2021). These findings shed light on how gut microbiota degrade colonic mucins and the mechanisms associated with bacterial colonization and IBD. Blocking this enzymatic pathway could be a potential intervention strategy to prevent pro-IBD bacteria from disrupting the intestinal mucus layer barrier. *Fusobacterium nucleatum* infection may contribute to the worsening of UC, but its mechanism is not yet clear. Dong's team recently published findings that EVs of *F. nucleatum* could promote the expression of pro-inflammatory factors (IL-1 $\beta$ , IL-6, TNF- $\alpha$ ) and down-regulate the expression of anti-inflammatory factors (IL-10) and tight junction proteins (ZO-1 and occludin) in IECs by down-regulating the expression of *miR-574-5p* to promote the activation of autophagy, leading to barrier dysfunction and worsen DSS-induced colitis in mice (Wei et al., 2022). Furthermore, another recent study discovered that *Eggerthella lenta* could promote colitis in mice by activating Th17 cells and promoting IL-17a production through its expression of a drug-metabolizing enzyme, Cardiac glycoside reductase (*cgr2*). *E. lenta* was found to be enriched in patients with IBD, while the expression of the *cgr2* gene was increased in patients with rheumatoid arthritis. *Cgr2* metabolizes steroidal saponins, which inhibit Th17 cell activity and are negatively associated with IBD severity. Furthermore, dietary arginine supplementation inhibited *cgr2*-induced Th17 cell activation and colitis in mice (Alexander et al., 2022).

## Targeting potential modulators and signaling pathways in intestinal epithelial cells to treat inflammatory bowel disease

Recent advances in various treatments have directly changed the clinical management model for IBD patients. The introduction of immunosuppressants and biologics significantly reduces the use of corticosteroids. In addition, the alpha 4 $\beta$ 7 integrin blocker vedolizumab has also been included in the clinical IBD treatment. While these strategies expand the arsenal of IBD physicians, a significant percentage of patients do not respond to these treatments (Singh et al., 2018). Several new cytokine inhibitors, modulators of cytokine signaling pathways, inhibitors of transcription factors, and new anti-adhesion and anti-T cell activation and migration strategies are undergoing clinical trial evaluation. More therapeutic targets and signaling pathways need to be found to provide patients with more choices and personalized services in treatment decisions (Table 1).

An essential function of the intestinal epithelium is to act as a barrier limiting the interaction between the luminal contents, such as intestinal microorganisms, and the immune system, absorbing nutrients while limiting microbial translocation (Allaire et al., 2018). Impaired intestinal barrier function leads to increased membrane permeability of IECs, which promotes the entry of intraperitoneal bacteria, toxins, and macromolecules into the body, thus inducing an inflammatory immune response. Intestinal epithelial barrier injury is of great interest in the study of the cellular and molecular pathogenesis of IBD, and reconstruction and regeneration of the intestinal epithelium is essential to restore intestinal homeostasis after injury (Sommer et al., 2021). Patients with IBD exhibit defects in multiple components of the mucosal barrier. Future research should focus on the modulation of the intestinal epithelial barrier as a possible therapeutic target for IBD.

By analyzing the function of the creatine transporter protein SLC6A8 (also known as CRT) in IECs, a recent study found that CRT is localized around tight junction proteins and can maintain intestinal epithelial barrier function by regulating the energy balance of IECs to promote the expression and localization of tight junction proteins. The deficiency of CRT inhibited creatine uptake, barrier formation, and healing function in IECs (Hall et al., 2020). Mechanistically, CRT deletion increased *Claudin-2* expression and decreased *Claudin-1* expression to promote the "leaky gut" phenotype, altered the localization of tight junction proteins, and inhibited actin polymerization. The study also found that the expression of *CRT* was significantly reduced in the colon tissue of IBD patients, suggesting that CRT may be a potential target for treating IBD (Hall et al., 2020). Recently, the protective role of IECs Golgi membrane protein 1 (GOLM1) in IBD has been demonstrated. IECs-specific deletion of GOLM1 leads to greater susceptibility to DSS-induced colitis and Azoxymethane (AOM)/DSS-induced colonic carcinogenesis in mice. GOLM1 interacts with the Notch2 intracellular structural domain to maintain intestinal epithelial barrier homeostasis by regulating the balance of the Notch signaling pathway in IECs, thereby inhibiting the development of colitis and colorectal carcinogenesis (Pu et al., 2021). Moreover, myosin light chain kinase (MLCK) is also a key regulator of intestinal barrier function. A unique structural domain within the MLCK splice variant MLCK1 mediates its recruitment to the tightly linked peri-junctional actomyosin ring (PAMR). A small molecule divertin was identified previously through screening that blocked acute TNF-induced MLCK1 recruitment, downstream myosin light chain (MLC) phosphorylation, barrier dysfunction, and diarrhea *in vitro* and *in vivo*, and inhibited the progression of experimental IBD (Graham et al., 2019). Another recent study has found that MLCK1 can interact with the tacrolimus-binding protein FKBP8 peptidyl-prolyl cis/trans isomerase (PPIase) structural domain and that these interactions are critical for MLCK1 recruitment, MLC phosphorylation, and TNF-induced barrier loss. Tissue biopsies from CD patients revealed an increased number of intercellularly linked MLCK1-FKBP8 interactions compared to controls. Blocking MLCK1-FKBP8 binding reversed MLCK1-FKBP8



TABLE 1 Targeting IEC modulators or signaling pathways to treat IBD.

Modulators/pathways	Mode of action	Biological process	References
Creatine transporter protein SLC6A8	Promote expression and localization of tight junction proteins Claudin1/2 and actin polymerization	Regulate energy balance and maintain barrier formation and healing function	<a href="#">Hall et al. (2020)</a>
Golgi membrane protein 1 (GOLM1)	Regulate the balance of the Notch signaling pathway	Maintain barrier homeostasis	<a href="#">Pu et al. (2021)</a>
Myosin light chain kinase splice variant (MLCK1)	TNF-induced MLCK1 recruitment to peri-junctional actomyosin ring (PAMR) mediates MLC phosphorylation. Interact with FKBP8 PPIase for MLCK1 recruitment and MLC phosphorylation	Maintain barrier function	<a href="#">Graham et al. (2019)</a>
miR-181 family members	Regulate Wnt and immune processes	Promote intestinal recovery after injury	<a href="#">Jimenez et al. (2022)</a>
Histone H3K9 methyltransferase SETDB1	Silence endogenous retroviruses to inhibit DNA damage	Maintain IECs survival, barrier function, and homeostasis	<a href="#">Juznic et al. (2021)</a>
m6A methyltransferase METTL14	Regulate <i>NF-kB</i> mRNA stability, affecting the activity of the NF-kB pathway and inhibiting TNF-mediated apoptosis	Regulate the development and apoptosis of colonic epithelial cells and colonic stem cells	<a href="#">Zhang et al. (2022)</a>
DNA methyltransferase 3A (DNMT3A)	DNMT3A deficiency leads to hypomethylation	Maintain intestinal epithelial barrier function and regeneration	<a href="#">Fazio et al. (2022)</a>
Special AT-rich sequence-binding protein 2 (SATB2)	Increase the expression of the Cl-/HCO <sub>3</sub> -transport protein SLC26A3	Maintain diversity and composition of the gut microbiota	<a href="#">Ni et al. (2021)</a>
5-Hydroxytryptamine (5-HT)	Reduce TGF- $\beta$ secretion and inhibit the TGF- $\beta$ /SMAD pathway Enhance AKT activity through 5-HT <sub>2B</sub> and activate the IL-6/STAT3 pathway	Tumor-suppressive effects at the initiation stage of CAC Promote tumor progression in the later stages of CAC	<a href="#">Mao et al. (2022)</a>
Spermidine oxidase (SMOX)	Promote spermidine production and inhibit alpha-defensin expression	Maintain diversity and composition of the gut microbiota	<a href="#">Gobert et al. (2022)</a>
Stromal interaction molecule 1 (STIM1)	STIM1 deficiency controls the stimulation of the intestinal epithelium by reducing endoplasmic reticulum stress caused by an imbalance in Ca <sup>2+</sup> homeostasis	Maintain intestinal barrier	<a href="#">Liang et al. (2022)</a>
RhoB	Reduced or absent RhoB inhibits the Wnt pathway and activates the p38 MAPK pathway	Promote goblet cell differentiation and IECs proliferation, increase SCFA-producing bacteria abundance and elevate the levels of SCFAs and receptors	<a href="#">Yang et al. (2022)</a>
Leukemia inhibitory factor (LIF)	Inhibit Th17 cells differentiation by phosphorylating and activating STAT4 and suppressing STAT3-induced IL17 gene expression	Alleviate colonic inflammation	<a href="#">Zhang et al. (2019)</a>
Alpha B-crystallin (CRYAB)	Reduce cellular inflammatory factor (TNF- $\alpha$ , IL-6, IL-1 $\beta$ , IL-8) production by inhibiting IKK $\beta$ activity	Protect barrier integrity	<a href="#">Xu et al. (2019)</a>
deSUMOylase SENP7	Ubiquitin ligase SIAH2 downregulates SENP7 through ubiquitination, which reduces pro-inflammatory mechanisms through $\gamma\delta$ T cells.	Control intestinal inflammation	<a href="#">Suhail et al. (2019)</a>
Epithelial NF- $\kappa$ B2 signaling	Amplify RelA activity and increase RelA-driven inflammatory gene expression	Induce abnormal intestinal inflammation	<a href="#">Chawla et al. (2021)</a>
Guanylate cyclase C (GC-C)	Regulate intestinal ion and fluid secretion through cGMP production and activation of cGMP-dependent protein kinase II	Loss of overall internal environmental homeostasis, fluid ion imbalance, and dysregulation of the intestinal microbiota	<a href="#">Mishra et al. (2021)</a>
Epithelial autonomous NAIP/NLRC4 inflammasomes	Drive IEC pyroptosis or apoptosis and promote IEC expulsion	Mitigate TNF-induced disruption of the intestinal epithelial barrier	<a href="#">Fattinger et al. (2021)</a>
NLRP3 Inflammasomes	miR223 mediates NLRP3 regulation and NLRP3 pathway blockage reduces IL-1 $\beta$ production	Inhibition of inflammasomes suppresses excessive inflammatory responses in the intestine	<a href="#">Kanneganti (2017)</a>

(Continued)

TABLE 1 (Continued)

Modulators/pathways	Mode of action	Biological process	References
ADP/P2Y1	ADP activates NLRP3 inflammasomes <i>via</i> P2Y1 receptors and promotes NLRP3 inflammasomes component ASC phosphorylation to increase IL-1 $\beta$ production		Zhang et al. (2020)
NLRP6 inflammasomes	Deubiquitinating enzyme Cyld binds to NLRP6, removes its ubiquitination modifications, inhibits NLRP6-ASC inflammasome formation, and regulates the maturation process of IL-18.		Mukherjee et al. (2020)
Nicotinamide adenine dinucleotide phosphate (NADPH) oxidase 1 (NOX1)	The absence of intestinal epithelial NOX1 combined with TNF $\alpha$ stimulation alters the stem cell microenvironment and stem cell differentiation	Promote lymphoplasmacytosis	Hsu et al. (2022)
Superoxide dismutase 1 (SOD1)	Restoring SOD activity inhibits p38-MAPK/NF- $\kappa$ B signal-mediated inflammation and apoptosis.	SOD1 deletion enhances oxidative stress and disrupts the intestinal epithelial barrier, reduces antioxidant enzyme activity, and increases colonic infiltration of pro-inflammatory immune cells	Hwang et al. (2020)
Multidrug resistance 1 (MDR1)	Reduce mROS	Protect mitochondria against xenotoxins through its efflux function	Ho et al. (2018)
3-mercaptopyruvate sulfurtransferase (MPST)	Regulate the AKT/apoptotic axis in IECs, inhibit pro-inflammatory cytokines expression, ROS production	Protect the intestine from inflammation and apoptosis incidence	Zhang et al. (2022)
Reductively modified albumin (r-Alb)	Inhibit cellular ROS and superoxide production through sulfhydryl (-SH)	Reduce the cellular damage caused by oxidative stress	Yang et al. (2021)

interactions, MLCK1 recruitment, and barrier loss *in vitro* and *in vivo* (Zuo et al., 2022). These studies provide a new potential therapeutic target for diseases related to intestinal barrier dysfunction, such as IBD.

There are fewer studies on post-transcriptional regulation in the maintenance of intestinal homeostasis and the development of colitis. A recently published study showed that the conserved miR-181 family members in the intestinal epithelium are down-regulated in IBD and mouse colitis samples, and their expression promotes intestinal recovery after injury by regulating Wnt and immune processes, which could be a potential new target for the treatment of intestinal inflammation (Jimenez et al., 2022). Furthermore, SETDB1 is a histone H3K9 methyltransferase that plays a regulatory role in intestinal epithelial homeostasis and IBD. Recent studies reveal that SETDB1 can maintain intestinal epithelial homeostasis by silencing endogenous retroviruses to inhibit DNA damage. Mice specifically deficient in SETDB1 in the intestinal epithelium exhibited impaired intestinal epithelial differentiation, impaired intestinal barrier, enhanced intestinal inflammation, and reduced survival. Meanwhile, some missense mutations associated with SETDB1 loss of function were significantly enriched in IBD patients (Juznic et al., 2021). Taken together, the results of this study suggest that SETDB1 may be a potential target for the treatment of IBD. In recent years, many studies have found that the methylation modification of RNA N6-methyladenosine (m6A) is involved in the maintenance of many types of stem cells, but whether RNA m6A also plays a vital

role in intestinal stem cells is unclear. Recently, Li's group found that m6A methyltransferase METTL14 plays an essential role in colonic stem cell self-renewal, and it may regulate the development and apoptosis of colonic epithelial cells and colonic stem cells by regulating the stability of *NF- $\kappa$ B* mRNA, affecting the activity of *NF- $\kappa$ B* pathway, and inhibiting TNF-mediated apoptosis (Zhang et al., 2022). Therefore, m6A is closely related to the development of colitis and can be used as a potential clinical target for the treatment of colitis. DNA methyltransferase 3A (DNMT3A) is involved in DNA methylation modifications and its genetic variants are associated with IBD. A recent study observed downregulation of *DNMT3A* expression in IECs in CD patients. Mechanistically, DNMT3A deficiency leads to hypomethylation, which impairs the function and regeneration of the intestinal epithelial barrier, making mice more susceptible to DSS-induced colitis, implying a role for impaired epithelial DNMT3A function in the etiology of IBD (Fazio et al., 2022).

Recently, the role of some regulatory factors known to be associated with colorectal carcinogenesis and development in IBD has also been revealed. Special AT-rich sequence-binding protein 2 (SATB2) is a potential diagnostic and prognostic marker for CRC, but its role in colitis and CAC is unclear. A recent study found that intestinal epithelial cell-specific SATB2 deficiency worsened colitis and CAC in mice by altering the diversity and composition of the gut microbiota and decreasing the expression of the Cl-/HCO<sub>3</sub>-transport protein SLC26A3 (Ni et al., 2021). Moreover, 5-hydroxytryptamine (5-HT) is commonly associated

with CAC, and the conclusions on how 5-HT affects CAC are not yet uniform. 5-HT<sub>2B</sub> is one of the receptors for 5-HT, which is expressed in IECs. A recent study revealed that 5-HT/5-HT<sub>2B</sub>/TGF- $\beta$  signaling exerts tumor-suppressive effects at the initiation stage of CAC while promoting tumor progression in the later stages. 5-HT<sub>2B</sub>-deficient IECs, on the one hand, reduce TGF- $\beta$  secretion and inhibit the TGF- $\beta$ /SMAD pathway; on the other hand, it enhances AKT activity through 5-HT<sub>2B</sub> and thus activate the IL-6/STAT3 pathway, enhance the intestinal inflammatory response, and exacerbates IEC destruction, thus promoting CAC tumorigenesis. Antibody blockade of IL-6 reverses the promoting effect of 5-HT<sub>2B</sub> deficiency on CAC development. TCGA data show a positive correlation between 5-HT<sub>2B</sub> expression and prognosis in CRC patients (Mao et al., 2022). Previous studies have shown that spermidine oxidase (SMOX) promotes spermidine production and regulates colitis. In a recent study, SMOX deficiency in mice worsened DSS-induced colitis and AOM/DSS-induced colonic tumorigenesis, increased alpha-defensin expression, and induced dysbiosis of gut microbiota, leading to reduced abundance of *Prevotella* and increased *Proteobacteria* and *Deferribacteres*. In contrast, spermidine supplementation reversed the above phenotype. In addition, down-regulation of SMOX expression was observed in inflamed colonic tissues from patients with UC and patients with colitis-associated heterotypic hyperplasia (Gobert et al., 2022). Furthermore, stromal interaction molecule 1 (STIM1) is an integral component of the store-operated calcium entry (SOCE) process that promotes CRC and T-cell-mediated inflammatory diseases. However, it is unclear whether STIM1 in IECs is involved in the pathological process of IBD. Recent studies have found that STIM1 deficiency in the intestinal epithelium in colitis controls the stimulation of the intestinal epithelium by commensal bacteria by reducing endoplasmic reticulum stress caused by an imbalance in Ca<sup>2+</sup> homeostasis, reducing loss of goblet cells, and maintaining the integrity of the mucus layer (Liang et al., 2022). STIM1 is a vital regulator of maintaining the intestinal barrier and a potential target for IBD treatment. RhoB, a member of the small Rho GTPase family, exhibits rapid upregulation when the organism is induced by genotoxic stress, LPS, inflammatory cytokines, growth factors and toxins, and is involved in a variety of cellular processes; however, the role of RhoB in colitis remains unclear. Recently, Wang Quan's team found that RhoB is significantly upregulated in UC, and that reduced or absent RhoB promotes goblet cell differentiation and proliferation of IECs by inhibiting the Wnt pathway and activating the p38 MAPK pathway. In addition, decreased RhoB increased the abundance of SCFA-producing bacteria and elevated the levels of SCFAs and their receptors. These findings suggest that RhoB is a potential molecular marker for the diagnosis of IBD, as well as a potential therapeutic target (Yang et al., 2022).

The intestine is the fastest self-renewing tissue in the adult mammalian organism, and its primary stem cells are located in the crypt of the intestinal villi. Stem cells in this location have a high capacity for self-renewal and differentiation and can differentiate

into intestinal epithelial absorptive cells and intestinal epithelial endocrine cells after 4–5 mitotic divisions. Among them, Paneth cells and Tuff cells are involved in the maintenance of intestinal stem cells. Different subtypes of cells differentiated from intestinal stem cells are essential in maintaining intestinal homeostasis by producing a mucus layer covering the surface of the intestinal epithelial cells, recognizing pathogens, and producing antimicrobial peptides to ensure an effective immune response (Peterson and Artis, 2014). Moreover, a recent study found that leukemia inhibitory factor (LIF), a cytokine in the IL-6 family secreted by IECs, alleviates colonic inflammation by inhibiting the differentiation of Th17 cells in a mouse model of colitis. Mechanistically, LIF inhibits the differentiation of Th17 cells by phosphorylating and activating STAT4 and suppressing STAT3-induced *IL17* gene expression (Zhang et al., 2019). The results of this study provide new potential therapeutic targets for the treatment of IBD. Alpha B-crystallin (CRYAB) is a small heat shock protein that plays a protective role in intestinal inflammation. A recent study found that *CRYAB* expression was significantly reduced in both IBD patients and DSS-induced colitis mouse models and negatively correlated with TNF- $\alpha$  and IL-6 levels; *CRYAB* could reduce cellular inflammatory factors (TNF- $\alpha$ , IL-6, IL-1 $\beta$ , IL-8) production *in vitro* by inhibiting IKK $\beta$  activity, and in colitis mice *in vivo* (Xu et al., 2019). This suggests that *CRYAB* may be a potential therapeutic target for IBD, as it protects the integrity of the intestinal barrier and alleviates colitis symptoms. Previous studies have found that epithelial deSUMOylation is associated with IBD. The deSUMOylase SENP7 and its interacting group regulate epithelial-immune cross-reactivity. In healthy cells, the ubiquitin ligase SIAH2 negatively regulates SENP7 through ubiquitination. Upregulation of epithelial SENP7 induces pro-inflammatory mechanisms through  $\gamma\delta$  T cells. Knockdown of SENP7 or clearance of  $\gamma\delta$  T cells suppressed DSS-induced intestinal inflammation; upregulation of *SENP7* expression was strongly statistically correlated with higher clinical disease indices in IBD patients (Suhail et al., 2019). This study shows that epithelial SENP7 is necessary to control intestinal inflammation and highlights its importance as a potential drug target.

In addition, excessive activation of RelA/NF- $\kappa$ B causes abnormal inflammation associated with IBD. The canonical NF- $\kappa$ B module regulates intranuclear activation of RelA dimers and induces a pro-inflammatory gene expression, and uncontrolled RelA activity induces abnormal intestinal inflammation. A recently published study found that atypical NF- $\kappa$ B2 signaling amplifies RelA activity in colonic epithelial cells, increases RelA-driven inflammatory gene expression, and exacerbates intestinal pathogenesis in IBD patients and mice with colitis, suggesting that the atypical NF- $\kappa$ B2 pathway may be a potential therapeutic target for inflammatory diseases (Chawla et al., 2021). Activating mutations in guanylate cyclase C (GC-C), a target receptor for the gastrointestinal peptide hormone guanylate and urinary guanylate, and bacterial heat-stable enterotoxins can both cause early-onset diarrhea and chronic

IBD. GC-C regulates intestinal ion and fluid secretion through cGMP production and activation of cGMP-dependent protein kinase II. A recent study constructing activating mutant mice with the *guanylate cyclase C* (*Gucy2c*) gene found that mutant mice have increased intestinal cGMP, leading to loss of overall internal environmental homeostasis, fluid ion imbalance, dysregulation of the intestinal microbiota, and susceptibility to colitis, suggesting that gut-associated cGMP signaling pathway may mediate colitis and flora dysbiosis (Mishra et al., 2021).

Inflammasomes are an important natural immune component expressed in both immune cells and non-immune cells (Lamkanfi and Dixit, 2014). By regulating the degree of inflammation and cell death in response to pathogen-associated molecular patterns (PAMPs) or danger-associated molecular patterns (DAMPs), they can either protect or harm the host (Man, 2018). Inflammasomes play an important role in inflammation and pathogen clearance. However, the mechanisms by which endogenous danger signals activate inflammasomes and the association of inflammasomes with inflammatory diseases have not been clarified. Earlier studies have shown that *Salmonella typhimurium* expresses a specific PAMP, a ligand for NLR family of apoptosis inhibitory proteins (NAIPs), during infection of IECs and high expression of NAIP/NLRC4 inflammasomes in IECs specifically inhibits the dissemination of *S. typhimurium* from the intestine to the whole body (Rauch et al., 2017; Hausmann et al., 2020). A recent study demonstrated that epithelial autonomous NAIP/NLRC4 inflammasomes mitigate TNF-induced disruption of the intestinal epithelial barrier by driving IEC pyroptosis or apoptosis and promoting IEC expulsion (Fattinger et al., 2021). *miR-223* expression is increased in inflammatory tissues in IBD (Zhang et al., 2021). NLRP3 is a component of inflammasomes, and *NLRP3* expression is elevated in colon and myeloid cells in *miR-223*-deficient environments. Drugs block the *NLRP3* pathway, reduce IL-1 $\beta$  production, and attenuate colitis (Kanneganti, 2017). Recently, Zhang et al. revealed the mechanism by which endogenous danger signals activate inflammasomes to promote IBD. ADP, a danger signal released during colonic injury from IECs, activates NLRP3 inflammasomes via P2Y1 receptors and promotes phosphorylation of NLRP3 inflammasomes component ASC to increase IL-1 $\beta$  production, thereby worsening DSS-induced colitis in mice. Extracellular ADP activates NLRP3 inflammasomes via P2Y1 receptor-mediated calcium signaling, and deletion of P2Y1 receptors or treatment with P2Y1 receptor inhibitors inhibits NLRP3 inflammasomes activation to alleviate colitis (Zhang et al., 2020). The results of this study suggest that ADP/P2Y1 may serve as a potential therapeutic target for IBD. NLRP6 inflammasomes regulate the intestinal inflammatory response and the organism's resistance to microbial responses, but the molecular mechanism of how to inhibit NLRP6 function to avoid tissue damage caused by excessive inflammatory response is not clear. A recent study showed that the deubiquitinating enzyme Cyld binds to NLRP6, removes its ubiquitination modifications, inhibits NLRP6-ASC inflammasomes formation, regulates the maturation process of IL-18, and suppresses excessive

inflammatory responses in the intestine (Mukherjee et al., 2020). This finding may provide new ideas for the treatment of intestinal inflammation.

The intestinal epithelium is constantly exposed to inducers of ROS, such as commensal microorganisms (Kajino-Sakamoto et al., 2010). In addition to an excessive inflammatory response, oxidative stress is considered a major feature of IBD (Tian et al., 2017). In the gastrointestinal tract, ROS production by nicotinamide adenine dinucleotide phosphate (NADPH) oxidase (NOX/DUOX) is a key biological mechanism regulating pathogen killing, host-microbe interactions and tissue repair after injury (Aviello et al., 2019). ROS production via enterocyte NOX1 has been shown to transduce microbial signals that promote epithelial wound healing (Alam et al., 2014) and mutations in genes that induce ROS production, such as Nox1, are highly associated with IBD (Aviello et al., 2019; Hsu et al., 2022). Mechanistically, the absence of intestinal epithelial NOX1 combined with TNF $\alpha$  stimulation can alter the stem cell microenvironment and stem cell differentiation, promote the number of lymphoplasmacytes and thus accelerate the progression of colitis, which may provide new insights into the prevention and treatment of IBD (Hsu et al., 2022). Superoxide dismutase 1 (SOD1) is one of the three superoxide dismutases responsible for the destruction of free superoxide radicals in the body. However, the role of SOD1 in oxidative stress in colitis is unclear. Hwang et al. found that SOD1 deletion enhances oxidative stress in mice and disrupts the intestinal epithelial barrier, reduces antioxidant enzyme activity, and increases colonic infiltration of pro-inflammatory immune cells to worsen DSS-induced colitis in mice. Restoring SOD activity can inhibit p38-MAPK/NF- $\kappa$ B signal-mediated inflammation and apoptosis, thereby alleviating colitis (Hwang et al., 2020). In mice, loss of multidrug resistance 1 (MDR1) function leads to colitis similar to human IBD. Ho et al. showed that MDR1 has a protective effect on mitochondria, where MDR1 deficiency leads to mitochondrial dysfunction, while increased mROS drive the development of colitis. Since MDR1 protects against xenotoxins primarily through its efflux function, the results of this study suggest a unique mitochondrial toxin genetic susceptibility interaction leading to mitochondrial dysfunction, a novel pathogenic mechanism that could provide many new therapeutic opportunities for IBD (Ho et al., 2018). Moreover, endogenous hydrogen sulfide (H<sub>2</sub>S) has anti-inflammatory activity in IBD, and the role of 3-mercaptopyruvate sulfurtransferase (MPST), a key enzyme regulating endogenous H<sub>2</sub>S biosynthesis, in IBD is not yet clear. A recent study found that MPST likely protects the intestine from inflammation by regulating the AKT/apoptotic axis in IECs, inhibiting the expression of pro-inflammatory cytokines, ROS production, and the incidence of apoptosis, providing a new therapeutic strategy for colitis (Zhang et al., 2022). Albumin is the most abundant matrix protein in the body and performs a variety of biological functions, including the ability to resist oxidative stress through free sulfhydryl groups (-SH). Oxidative stress is an important feature of colitis, and studies have shown that colitis can



significantly reduce albumin and increase oxidized albumin (Krzystek-Korpacz et al., 2008; Khan et al., 2017). However, no studies have yet explored the potential efficacy of albumin in the treatment of colitis. A recent work showed that DSS-induced administration of reductively modified albumin (r-Alb) to mice with colitis effectively improved the colitis phenotype by the mechanism that r-Alb inhibits cellular ROS and superoxide production through sulfhydryl (-SH) and reduces the cellular damage caused by oxidative stress. The results of this study provide a new intervention technique for the clinical treatment of colitis, while r-Alb has a promising application as an effective antioxidant (Yang et al., 2021).

## Conclusion

Multiple factors are involved in the pathogenesis of IBD, such as genetic, environmental, infectious, and immunological factors, among which intestinal inflammation and immune dysfunction play an important role. In IBD patients, molecules such as SCFAs, bile acids and microbial tryptophan metabolites are altered (Sun et al., 2017; Heinken et al., 2019; Scott et al., 2020). These microbe-derived compounds function as signaling molecules, mediating host-microbiota communication and regulating immune homeostasis. Recent research suggests that SCFAs, particularly butyrate, have immunomodulatory properties. Furthermore, SCFAs can activate the signaling cascade that controls immune function *via* GPCRs. With the advancement of molecular biology techniques, the value of epigenetics as one of the pathways regulating gene expression in IBD has been gradually explored and established to be particularly relevant to IBD. Butyrate has recently been discovered to regulate epithelial gene expression or immune cells *via* epigenetic pathways. Besides, the latest evidence suggests that specific bile acid metabolites, tryptophan metabolites, and PSA interact with adaptive immune cells to improve the inflammatory environment of IBD. In addition to traditional bacterial metabolites, certain new bacteria species and their effector molecules have been identified to regulate immune factors release and improve IBD by binding to IECs or immune cell surface receptors. On the contrary, many new bacteria species and the virulence factors they contain potentially promote IBD by disrupting epithelial barrier, promoting pro-inflammatory factors secretion, and interfering normal gut microbiota. Recent research has confirmed the importance of miRNAs in targeting specific molecules in signaling pathways that regulate intestinal barrier homeostasis, inflammation, and autophagy. Several studies have found specific miRNAs linked to IBD and attempted to use them as diagnostic biomarkers (Soroosh et al., 2018).

The long-term persistence of chronic inflammation in IBD is a major contributor to tumor transformation and the development of CAC. In the past decades, significant progress has been made in the immunological mechanisms of IBD,

providing new strategies and ideas for treating IBD. The subsequent introduction of biologics, such as TNF- $\alpha$  blocker, replaced nonselective anti-inflammatory corticosteroids in IBD management. However, these therapies still have the potential for primary unresponsiveness, secondary loss of response, opportunistic infections, and cancer development. Therefore, there is an urgent need to develop novel and effective therapies that target specific signaling pathways in the pathogenesis of IBD. Disruption of the intestinal barrier, abnormal death of epithelial cells, and subsequent inflammation are at the heart of chronic inflammatory and infectious gastrointestinal diseases (Patankar and Becker, 2020). Recent studies have shown that the Notch, Wnt, and Nf $\kappa$ B signaling pathways are involved in the pathogenesis of IBD and different upstream signaling molecules can activate these pathways, thus serving as potential targets for the treatment of IBD. Moreover, RNA methylation is a new class of RNA epigenetic modifications discovered in recent years and can regulate mRNA expression. One of the most common modifications is m6A. There is a growing body of research involving RNA methylation and disease, covering tumors (Su et al., 2019), neurological disorders (Jiang et al., 2022), obesity (Li et al., 2020), and immune response (Wang et al., 2020), but the relationship with IBD needs further investigation. Elevated levels of NLRP3 inflammasome and pro-inflammatory cytokines are the main pathological mechanisms of IBD (Zhen and Zhang, 2019). Therefore, targeting NLRP3 inflammasome offers a promising strategy for the treatment of IBD. Chronic intestinal inflammation is related with the overproduction of ROS, which leads to oxidative stress. Recent studies have identified several key molecules that play varying degrees of regulatory functions in the production of ROS and could be explored as possible targets for IBD therapy. In the future, altering specific genetic loci may be a promising therapeutic approach for IBD. In addition, novel antibodies or inhibitors, combination therapy regimens, and multifactor blockers are also expected to break the bottleneck of IBD treatment and improve disease for patients with IBD. Furthermore, in the past three decades, there has been a rapid development in the clinical diagnosis and treatment of IBD. However, numerous issues still need to be explored in depth, such as genetic testing, serological markers in the disease population, imaging of the disease, endoscopic assessment, monitoring, drug specificity, and FMT. It is the future trend to further develop relatively specific novel drugs, develop IBD assessment models through extensive sample population studies, and provide personalized treatment to patients.

## Author contributions

BL and CnW wrote the paper. CoW, WS, and XH made figures. WC made the table. NL and DX conceived of the presented idea. All authors contributed to the article and approved the submitted version.

## Funding

This work is financially supported by the Qingdao Postdoctoral Applied Research Project (grant no. RZ2200001423).

## Conflict of interest

The authors declare that the research was conducted in the absence of any commercial or financial relationships

## References

- Ahmad, T. R., and Haeusler, R. A. (2019). Bile acids in glucose metabolism and insulin signalling – mechanisms and research needs. *Nat. Rev. Endocrinol.* 15, 701–712. doi: 10.1038/s41574-019-0266-7
- Alam, A., Leoni, G., Wentworth, C. C., Kwal, J. M., Wu, H., Ardita, C. S., et al. (2014). Redox signaling regulates commensal-mediated mucosal homeostasis and restitution and requires formyl peptide receptor 1. *Mucosal Immunol.* 7, 645–655. doi: 10.1038/mi.2013.84
- Alexander, M., Ang, Q. Y., Nayak, R. R., Bustion, A. E., Sandy, M., Zhang, B., et al. (2022). Human gut bacterial metabolism drives Th17 activation and colitis. *Cell Host Microbe* 30, 17–30.e9. doi: 10.1016/j.chom.2021.11.001
- Allaire, J. M., Crowley, S. M., Law, H. T., Chang, S. Y., Ko, H. J., and Vallance, B. A. (2018). The intestinal epithelium: central coordinator of mucosal immunity. *Trends Immunol.* 39, 677–696. doi: 10.1016/j.it.2018.04.002
- Aviello, G., Singh, A. K., O'Neill, S., Conroy, E., Gallagher, W., D'Agostino, G., et al. (2019). Colitis susceptibility in mice with reactive oxygen species deficiency is mediated by mucus barrier and immune defense defects. *Mucosal Immunol.* 12, 1316–1326. doi: 10.1038/s41385-019-0205-x
- Barnich, N., Carvalho, F. A., Glasser, A. L., Darcha, C., Jantschke, P., Allez, M., et al. (2007). CEACAM6 acts as a receptor for adherent-invasive *E. coli*, supporting ileal mucosa colonization in Crohn disease. *J. Clin. Invest.* 117, 1566–1574. doi: 10.1172/JCI30504
- Brown, A. J., Goldsworthy, S. M., Barnes, A. A., Eilert, M. M., Tcheang, L., Daniels, D., et al. (2003). The orphan G protein-coupled receptors GPR41 and GPR43 are activated by propionate and other short chain carboxylic acids. *J. Biol. Chem.* 278, 11312–11319. doi: 10.1074/jbc.M211609200
- Campbell, C., McKenney, P. T., Konstantinovskiy, D., Isaeva, O. I., Schizas, M., Verter, J., et al. (2020). Bacterial metabolism of bile acids promotes generation of peripheral regulatory T cells. *Nature* 581, 475–479. doi: 10.1038/s41586-020-2193-0
- Cao, Y., Wang, Z., Yan, Y., Ji, L., He, J., Xuan, B., et al. (2021). Enterotoxigenic *Bacteroides fragilis* promotes intestinal inflammation and malignancy by inhibiting exosome-packaged miR-149-3p. *Gastroenterology* 161, 1552–1566.e12. doi: 10.1053/j.gastro.2021.08.003
- Caruso, R., Lo, B. C., and Nunez, G. (2020). Host-microbiota interactions in inflammatory bowel disease. *Nat. Rev. Immunol.* 20, 411–426. doi: 10.1038/s41577-019-0268-7
- Chawla, M., Mukherjee, T., Deka, A., Chatterjee, B., Sarkar, U. A., Singh, A. K., et al. (2021). An epithelial Nfkb2 pathway exacerbates intestinal inflammation by supplementing latent RelA dimers to the canonical NF-kappaB module. *Proc. Natl. Acad. Sci. U. S. A.* 118:e2024828118. doi: 10.1073/pnas.2024828118
- Chung, L., Thiele Orberg, E., Geis, A. L., Chan, J. L., Fu, K., DeStefano Shields, C. E., et al. (2018). *Bacteroides fragilis* toxin coordinates a pro-carcinogenic inflammatory cascade via targeting of colonic epithelial cells. *Cell Host Microbe* 23, 203–214.e5. doi: 10.1016/j.chom.2018.01.007
- Coskun, M. (2014). Intestinal epithelium in inflammatory bowel disease. *Front. Med. (Lausanne)*. 1:24. doi: 10.3389/fmed.2014.00024
- Dasgupta, S., Erturk-Hasdemir, D., Ochoa-Reparaz, J., Reinecker, H. C., and Kasper, D. L. (2014). Plasmacytoid dendritic cells mediate anti-inflammatory responses to a gut commensal molecule via both innate and adaptive mechanisms. *Cell Host Microbe* 15, 413–423. doi: 10.1016/j.chom.2014.03.006
- Fattinger, S. A., Geiser, P., Samperio Ventayol, P., Di Martino, M. L., Furter, M., Felmy, B., et al. (2021). Epithelium-autonomous NAIP/NLRC4 prevents TNF-driven inflammatory destruction of the gut epithelial barrier in salmonella-infected mice. *Mucosal Immunol.* 14, 615–629. doi: 10.1038/s41385-021-00381-y
- Fazio, A., Bordoni, D., Kuiper, J. W. P., Weber-Stiehl, S., Stengel, S. T., Arnold, P., et al. (2022). DNA methyltransferase 3A controls intestinal epithelial barrier function and regeneration in the colon. *Nat. Commun.* 13:6266. doi: 10.1038/s41467-022-33844-2
- Foley, S. E., Dente, M. J., Lei, X., Sallis, B. F., Loew, E. B., Meza-Segura, M., et al. (2022). Microbial metabolites orchestrate a distinct multi-tiered regulatory network in the intestinal epithelium that directs P-glycoprotein expression. *mBio* 13:e0199322. doi: 10.1128/mbio.01993-22
- Furusawa, Y., Obata, Y., Fukuda, S., Endo, T. A., Nakato, G., Takahashi, D., et al. (2013). Commensal microbe-derived butyrate induces the differentiation of colonic regulatory T cells. *Nature* 504, 446–450. doi: 10.1038/nature12721
- Gobert, A. P., Latour, Y. L., Asim, M., Barry, D. P., Allaman, M. M., Finley, J. L., et al. (2022). Protective role of Spermidine in colitis and colon carcinogenesis. *Gastroenterology* 162, 813–827.e8. doi: 10.1053/j.gastro.2021.11.005
- Graham, W. V., He, W., Marchiando, A. M., Zha, J., Singh, G., Li, H. S., et al. (2019). Intracellular MLCK1 diversion reverses barrier loss to restore mucosal homeostasis. *Nat. Med.* 25, 690–700. doi: 10.1038/s41591-019-0393-7
- Hall, C. H. T., Lee, J. S., Murphy, E. M., Gerich, M. E., Dran, R., Glover, L. E., et al. (2020). Creatine transporter, reduced in colon tissues from patients with inflammatory bowel diseases, regulates energy balance in intestinal epithelial cells, epithelial integrity, and barrier function. *Gastroenterology* 159, 984–998.e1. doi: 10.1053/j.gastro.2020.05.033
- Hang, S., Paik, D., Yao, L., Kim, E., Trinath, J., Lu, J., et al. (2019). Bile acid metabolites control T(H)17 and T(reg) cell differentiation. *Nature* 576, 143–148. doi: 10.1038/s41586-019-1785-z
- Hausmann, A., Böck, D., Geiser, P., Berthold, D. L., Fattinger, S. A., Furter, M., et al. (2020). Intestinal epithelial NAIP/NLRC4 restricts systemic dissemination of the adapted pathogen salmonella Typhimurium due to site-specific bacterial PAMP expression. *Mucosal Immunol.* 13, 530–544. doi: 10.1038/s41385-019-0247-0
- Heinken, A., Ravcheev, D. A., Baldini, F., Heirendt, L., Fleming, R. M., and Thiele, I. (2019). Systematic assessment of secondary bile acid metabolism in gut microbes reveals distinct metabolic capabilities in inflammatory bowel disease. *Microbiome*. 7, 1–18.
- Henke, M. T., Kenny, D. J., Cassilly, C. D., Vlamakis, H., Xavier, R. J., and Clardy, J. (2019). *Ruminococcus gnavus*, a member of the human gut microbiome associated with Crohn's disease, produces an inflammatory polysaccharide. *Proc. Natl. Acad. Sci. U. S. A.* 116, 12672–12677. doi: 10.1073/pnas.1904099116
- Hinrichsen, F., Hamm, J., Westermann, M., Schroder, L., Shima, K., Mishra, N., et al. (2021). Microbial regulation of hexokinase 2 links mitochondrial metabolism and cell death in colitis. *Cell Metab.* 33, 2355–2366.e8. doi: 10.1016/j.cmet.2021.11.004
- Ho, G. T., Aird, R. E., Liu, B., Boyapati, R. K., Kennedy, N. A., Dorward, D. A., et al. (2018). MDR1 deficiency impairs mitochondrial homeostasis and promotes intestinal inflammation. *Mucosal Immunol.* 11, 120–130. doi: 10.1038/mi.2017.31
- Hsu, N.-Y., Nayar, S., Gettler, K., Talware, S., Giri, M., Alter, I., et al. (2022). NOX1 is essential for TNF $\alpha$ -induced intestinal epithelial ROS secretion and inhibits M cell signatures. *Gut:gutjnl-2021-326305*. doi: 10.1136/gutjnl-2021-326305
- Hwang, J., Jin, J., Jeon, S., Moon, S. H., Park, M. Y., Yum, D.-Y., et al. (2020). SOD1 suppresses pro-inflammatory immune responses by protecting against oxidative stress in colitis. *Redox Biol.* 37:101760. doi: 10.1016/j.redox.2020.101760

that could be construed as a potential conflict of interest.

## Publisher's note

All claims expressed in this article are solely those of the authors and do not necessarily represent those of their affiliated organizations, or those of the publisher, the editors and the reviewers. Any product that may be evaluated in this article, or claim that may be made by its manufacturer, is not guaranteed or endorsed by the publisher.

- Jiang, L., Li, X., Wang, S., Yuan, Z., and Cheng, J. (2022). The role and regulatory mechanism of m(6)a methylation in the nervous system. *Front. Genet.* 13:962774. doi: 10.3389/fgene.2022.962774
- Jimenez, M. T., Clark, M. L., Wright, J. M., Michieletto, M. F., Liu, S., Erickson, I., et al. (2022). The miR-181 family regulates colonic inflammation through its activity in the intestinal epithelium. *J. Exp. Med.* 219:e20212278. doi: 10.1084/jem.20212278
- Juznic, L., Peuker, K., Striglic, A., Brosch, M., Herrmann, A., Hasler, R., et al. (2021). SETDB1 is required for intestinal epithelial differentiation and the prevention of intestinal inflammation. *Gut* 70, 485–498. doi: 10.1136/gutjnl-2020-321339
- Kajino-Sakamoto, R., Omori, E., Nighot, P. K., Blikslager, A. T., Matsumoto, K., and Ninomiya-Tsuji, J. (2010). TGF- $\beta$ -activated kinase 1 signaling maintains intestinal integrity by preventing accumulation of reactive oxygen species in the intestinal epithelium. *J. Immunol.* 185, 4729–4737. doi: 10.4049/jimmunol.0903587
- Kanneganti, T.-D. (2017). Inflammatory bowel disease and the NLRP3 Inflammasome. *N. Engl. J. Med.* 377, 694–696. doi: 10.1056/NEJMcibr1706536
- Khan, N., Patel, D., Shah, Y., Trivedi, C., and Yang, Y. X. (2017). Albumin as a prognostic marker for ulcerative colitis. *World J. Gastroenterol.* 23, 8008–8016. doi: 10.3748/wjg.v23.i45.8008
- Kim, K. N., Yao, Y., and Ju, S. Y. (2019). Short chain fatty acids and fecal microbiota abundance in humans with obesity: a systematic review and meta-analysis. *Nutrients* 11:2512. doi: 10.3390/nul1102512
- Krzystek-Korpacz, M., Neubauer, K., Berdowska, I., Boehm, D., Zielinski, B., Petryszyn, P., et al. (2008). Enhanced formation of advanced oxidation protein products in IBD. *Inflamm. Bowel Dis.* 14, 794–802. doi: 10.1002/ibd.20383
- Lamkanfi, M., and Dixit, V. M. (2014). Mechanisms and functions of inflammasomes. *Cells* 157, 1013–1022. doi: 10.1016/j.cell.2014.04.007
- Li, G., Lin, J., Zhang, C., Gao, H., Lu, H., Gao, X., et al. (2021). Microbiota metabolite butyrate constrains neutrophil functions and ameliorates mucosal inflammation in inflammatory bowel disease. *Gut Microbes* 13:1968257. doi: 10.1080/19490976.2021.1968257
- Li, Q., Sun, X., Yu, K., Lv, J., Miao, C., Yang, J., et al. (2022). Enterobacter ludwigii protects DSS-induced colitis through choline-mediated immune tolerance. *Cell Rep.* 40:111308. doi: 10.1016/j.celrep.2022.111308
- Li, Y., Wang, J., Huang, C., Shen, M., Zhan, H., and Xu, K. (2020). RNA N6-methyladenosine: a promising molecular target in metabolic diseases. *Cell Biosci.* 10:19. doi: 10.1186/s13578-020-00385-4
- Liang, X., Xie, J., Liu, H., Zhao, R., Zhang, W., Wang, H., et al. (2022). STIM1 deficiency in intestinal epithelium attenuates colonic inflammation and tumorigenesis by reducing ER stress of goblet cells. *Cell. Mol. Gastroenterol. Hepatol.* 14, 193–217. doi: 10.1016/j.jcmgh.2022.03.007
- Liu, Y., Yang, M., Tang, L., Wang, F., Huang, S., Liu, S., et al. (2022). TLR4 regulates RORgammat(+) regulatory T-cell responses and susceptibility to colon inflammation through interaction with *Akkermansia muciniphila*. *Microbiome*. 10:98. doi: 10.1186/s40168-022-01296-x
- Luis, A. S., Jin, C., Pereira, G. V., Glowacki, R. W. P., Gugel, S. R., Singh, S., et al. (2021). A single sulfatase is required to access colonic mucin by a gut bacterium. *Nature* 598, 332–337. doi: 10.1038/s41586-021-03967-5
- Ma, N., He, T., Johnston, L. J., and Ma, X. (2020). Host-microbiome interactions: the aryl hydrocarbon receptor as a critical node in tryptophan metabolites to brain signaling. *Gut Microbes* 11, 1203–1219. doi: 10.1080/19490976.2020.1758008
- Mahendran, V., Liu, F., Riordan, S. M., Grimm, M. C., Tanaka, M. M., and Zhang, L. (2016). Examination of the effects of campylobacter concisus zonula occludens toxin on intestinal epithelial cells and macrophages. *Gut Pathog.* 8:18. doi: 10.1186/s13099-016-0101-9
- Man, S. M. (2018). Inflammasomes in the gastrointestinal tract: infection, cancer and gut microbiota homeostasis. *Nat. Rev. Gastro Hepat.* 15, 721–737. doi: 10.1038/s41575-018-0054-1
- Mao, L., Xin, F., Ren, J., Xu, S., Huang, H., Zha, X., et al. (2022). 5-HT2B-mediated serotonin activation in enterocytes suppresses colitis-associated cancer initiation and promotes cancer progression. *Theranostics*. 12, 3928–3945. doi: 10.7150/thno.70762
- Maslowski, K. M., Vieira, A. T., Ng, A., Kranich, J., Sierro, F., Yu, D., et al. (2009). Regulation of inflammatory responses by gut microbiota and chemoattractant receptor GPR43. *Nature* 461, 1282–1286. doi: 10.1038/nature08530
- Mazmanian, S. K., Round, J. L., and Kasper, D. L. (2008). A microbial symbiosis factor prevents intestinal inflammatory disease. *Nature* 453, 620–625. doi: 10.1038/nature07008
- Mishra, V., Bose, A., Kiran, S., Banerjee, S., Shah, I. A., Chaukimath, P., et al. (2021). Gut-associated cGMP mediates colitis and dysbiosis in a mouse model of an activating mutation in GUCY2C. *J. Exp. Med.* 218:e20210479. doi: 10.1084/jem.20210479
- Mukherjee, S., Kumar, R., Tsakem Lenou, E., Basrur, V., Kontoyiannis, D. L., Ioakeimidis, F., et al. (2020). Deubiquitination of NLRP6 inflammasome by Cyld critically regulates intestinal inflammation. *Nat. Immunol.* 21, 626–635. doi: 10.1038/s41590-020-0681-x
- Ni, H., Chen, Y., Xia, W., Wang, C., Hu, C., Sun, L., et al. (2021). SATB2 defect promotes colitis and colitis-associated colorectal cancer by impairing cl-/HCO3-exchange and homeostasis of gut microbiota. *J. Crohns Colitis* 15, 2088–2102. doi: 10.1093/ecco-jcc/jjab094
- Nicolas, G. R., and Chang, P. V. (2019). Deciphering the chemical lexicon of host-gut microbiota interactions. *Trends Pharmacol. Sci.* 40, 430–445. doi: 10.1016/j.tips.2019.04.006
- Nielsen, O. H., and Ainsworth, M. A. (2013). Tumor necrosis factor inhibitors for inflammatory bowel disease. *N. Engl. J. Med.* 369, 754–762. doi: 10.1056/NEJMc1209614
- Nielsen, H. L., Dalager-Pedersen, M., and Nielsen, H. (2020). High risk of microscopic colitis after campylobacter concisus infection: population-based cohort study. *Gut* 69, 1952–1958. doi: 10.1136/gutjnl-2019-319771
- Paik, D., Yao, L., Zhang, Y., Bae, S., D'Agostino, G. D., Zhang, M., et al. (2022). Human gut bacteria produce TauEta17-modulating bile acid metabolites. *Nature* 603, 907–912. doi: 10.1038/s41586-022-04480-z
- Palmela, C., Chevarin, C., Xu, Z., Torres, J., Sevrin, G., Hirten, R., et al. (2018). Adherent-invasive Escherichia coli in inflammatory bowel disease. *Gut* 67, 574–587. doi: 10.1136/gutjnl-2017-314903
- Patankar, J. V., and Becker, C. (2020). Cell death in the gut epithelium and implications for chronic inflammation. *Nat. Rev. Gastro Hepat.* 17, 543–556. doi: 10.1038/s41575-020-0326-4
- Peterson, L. W., and Artis, D. (2014). Intestinal epithelial cells: regulators of barrier function and immune homeostasis. *Nat. Rev. Immunol.* 14, 141–153. doi: 10.1038/nri3608
- Plovier, H., Everard, A., Druart, C., Depommier, C., Van Hul, M., Geurts, L., et al. (2017). A purified membrane protein from *Akkermansia muciniphila* or the pasteurized bacterium improves metabolism in obese and diabetic mice. *Nat. Med.* 23, 107–113. doi: 10.1038/nm.4236
- Postler, T. S., and Ghosh, S. (2017). Understanding the Holobiont: how microbial metabolites affect human health and shape the immune system. *Cell Metab.* 26, 110–130. doi: 10.1016/j.cmet.2017.05.008
- Pu, Y., Song, Y., Zhang, M., Long, C., Li, J., Wang, Y., et al. (2021). GOLM1 restricts colitis and colon tumorigenesis by ensuring notch signaling equilibrium in intestinal homeostasis. *Signal Transduct. Target. Ther.* 6:148. doi: 10.1038/s41392-021-00535-1
- Qin, J., Li, R., Raes, J., Arumugam, M., Burgdorf, K. S., Manichanh, C., et al. (2010). A human gut microbial gene catalogue established by metagenomic sequencing. *Nature* 464, 59–65. doi: 10.1038/nature08821
- Qu, S., Fan, L., Qi, Y., Xu, C., Hu, Y., Chen, S., et al. (2021). *Akkermansia muciniphila* alleviates dextran sulfate sodium (DSS)-induced acute colitis by NLRP3 activation. *Microbiol. Spectr.* 9:e0073021. doi: 10.1128/Spectrum.00730-21
- Rauch, I., Deets, K. A., Ji, D. X., von Moltke, J., Tenthorey, J. L., Lee, A. Y., et al. (2017). NAIP-NLRC4 Inflammasomes coordinate intestinal epithelial cell expulsion with eicosanoid and IL-18 release via activation of Caspase-1 and -8. *Immunity* 46, 649–659. doi: 10.1016/j.immuni.2017.03.016
- Renga, G., Nunzi, E., Pariano, M., Puccetti, M., Bellet, M. M., Pieraccini, G., et al. (2022). Optimizing therapeutic outcomes of immune checkpoint blockade by a microbial tryptophan metabolite. *J. Immunother. Cancer* 10:e003725. doi: 10.1136/jitc-2021-003725
- Rösch, C., Taverne, N., Venema, K., Gruppen, H., Wells, J. M., and Schols, H. A. (2017). Effects of in vitro fermentation of barley  $\beta$ -glucan and sugar beet pectin using human fecal inocula on cytokine expression by dendritic cells. *Mol. Nutr. Food Res.* 61:1600243. doi: 10.1002/mnfr.201600243
- Round, J. L., and Mazmanian, S. K. (2010). Inducible Foxp3<sup>+</sup> regulatory T-cell development by a commensal bacterium of the intestinal microbiota. *Proc. Natl. Acad. Sci. U. S. A.* 107, 12204–12209. doi: 10.1073/pnas.0909122107
- Scott, S. A., Fu, J., and Chang, P. V. (2020). Microbial tryptophan metabolites regulate gut barrier function via the aryl hydrocarbon receptor. *Proc. Natl. Acad. Sci. U. S. A.* 117, 19376–19387. doi: 10.1073/pnas.2000047117
- Sekizuka, T., Ogasawara, Y., Ohkusa, T., and Kuroda, M. (2017). Characterization of *Fusobacterium varium* Fv113-g1 isolated from a patient with ulcerative colitis based on complete genome sequence and transcriptome analysis. *PLoS One* 12:e0189319. doi: 10.1371/journal.pone.0189319
- Seregin, S. S., Golovchenko, N., Schaf, B., Chen, J., Pudlo, N. A., Mitchell, J., et al. (2017). NLRP6 protects Il10<sup>-/-</sup> mice from colitis by limiting colonization of *Akkermansia muciniphila*. *Cell Rep.* 19, 733–745. doi: 10.1016/j.celrep.2017.03.080
- Shen, Y., Giardino Torchia, M. L., Lawson, G. W., Karp, C. L., Ashwell, J. D., and Mazmanian, S. K. (2012). Outer membrane vesicles of a human commensal mediate immune regulation and disease protection. *Cell Host Microbe* 12, 509–520. doi: 10.1016/j.chom.2012.08.004

- Silpe, J. E., Wong, J. W. H., Owen, S. V., Baym, M., and Balskus, E. P. (2022). The bacterial toxin colibactin triggers prophage induction. *Nature* 603, 315–320. doi: 10.1038/s41586-022-04444-3
- Singh, S., George, J., Boland, B. S., Vande Castele, N., and Sandborn, W. J. (2018). Primary non-response to tumor necrosis factor antagonists is associated with inferior response to second-line biologics in patients with inflammatory bowel diseases: a systematic review and meta-analysis. *J. Crohns Colitis* 12, 635–643. doi: 10.1093/ecco-jcc/jjy004
- Sinha, S. R., Haileselassie, Y., Nguyen, L. P., Tropini, C., Wang, M., Becker, L. S., et al. (2020). Dysbiosis-induced secondary bile acid deficiency promotes intestinal inflammation. *Cell Host Microbe* 27, 659–670.e5. doi: 10.1016/j.chom.2020.01.021
- Soderholm, A. T., and Pedicord, V. A. (2019). Intestinal epithelial cells: at the interface of the microbiota and mucosal immunity. *Immunology* 158, 267–280. doi: 10.1111/imm.13117
- Sommer, F., and Backhed, F. (2013). The gut microbiota—masters of host development and physiology. *Nat. Rev. Microbiol.* 11, 227–238. doi: 10.1038/nrmicro2974
- Sommer, K., Wiendl, M., Müller, T. M., Heidbreder, K., Voskens, C., Neurath, M. F., et al. (2021). Intestinal mucosal wound healing and barrier integrity in IBD—crosstalk and trafficking of cellular players. *Front. Med. (Lausanne)* 8:643973. doi: 10.3389/fmed.2021.643973
- Soroosh, A., Koutsoumpa, M., Pothoulakis, C., and Iliopoulos, D. (2018). Functional role and therapeutic targeting of microRNAs in inflammatory bowel disease. *Am. J. Physiol. Gastrointest. Liver Physiol.* 314, G256–G262. doi: 10.1152/ajpgi.00268.2017
- Su, Y., Huang, J., and Hu, J. (2019). m6A RNA methylation regulators contribute to malignant progression and have clinical prognostic impact in gastric cancer. *Front. Oncol.* 9:1038. doi: 10.3389/fonc.2019.01038
- Suhail, A., Rizvi, Z. A., Mujagond, P., Ali, S. A., Gaur, P., Singh, M., et al. (2019). DeSUMOylase SENP7-mediated epithelial signaling triggers intestinal inflammation via expansion of Gamma-Delta T cells. *Cell Rep.* 29, 3522–3538.e7. doi: 10.1016/j.celrep.2019.11.028
- Sun, M., Wu, W., Liu, Z., and Cong, Y. (2017). Microbiota metabolite short chain fatty acids, GPCR, and inflammatory bowel diseases. *J. Gastroenterol.* 52, 1–8. doi: 10.1007/s00535-016-1242-9
- Tahara, T., Shibata, T., Kawamura, T., Okubo, M., Ichikawa, Y., Sumi, K., et al. (2015). Fusobacterium detected in colonic biopsy and clinicopathological features of ulcerative colitis in Japan. *Dig. Dis. Sci.* 60, 205–210. doi: 10.1007/s10620-014-3316-y
- Tailford, L. E., Owen, C. D., Walshaw, J., Crost, E. H., Hardy-Goddard, J., Le Gall, G., et al. (2015). Discovery of intramolecular trans-sialidases in human gut microbiota suggests novel mechanisms of mucosal adaptation. *Nat. Commun.* 6:7624. doi: 10.1038/ncomms8624
- Thangaraju, M., Cresci, G. A., Liu, K., Ananth, S., Gnanaprakasam, J. P., Browning, D. D., et al. (2009). GPR109A is a G-protein-coupled receptor for the bacterial fermentation product butyrate and functions as a tumor suppressor in colon. *Cancer Res.* 69, 2826–2832. doi: 10.1158/0008-5472.CAN-08-4466
- Tian, T., Wang, Z., and Zhang, J. (2017). Pathomechanisms of oxidative stress in inflammatory bowel disease and potential antioxidant therapies. *Oxidative Med. Cell. Longev.* 2017:4535194. doi: 10.1155/2017/4535194
- Vieira, A. T., Macia, L., Galvão, I., Martins, F. S., Canesso, M. C., Amaral, F. A., et al. (2015). A role for gut microbiota and the metabolite-sensing receptor GPR43 in a murine model of gout. *Arthritis Rheumatol.* 67, 1646–1656. doi: 10.1002/art.39107
- Viladomiu, M., Metz, M. L., Lima, S. F., Jin, W. B., Chou, L., Guo, C. J., et al. (2021). Adherent-invasive *E. coli* metabolism of propanediol in Crohn's disease regulates phagocytes to drive intestinal inflammation. *Cell Host Microbe* 29, 607–19.e8. doi: 10.1016/j.chom.2021.01.002
- Wang, Q., McLoughlin, R. M., Cobb, B. A., Charrel-Dennis, M., Zaleski, K. J., Golenbock, D., et al. (2006). A bacterial carbohydrate links innate and adaptive responses through toll-like receptor 2. *J. Exp. Med.* 203, 2853–2863. doi: 10.1084/jem.20062008
- Wang, Y. N., Yu, C. Y., and Jin, H. Z. (2020). RNA N(6)-Methyladenosine modifications and the immune response. *J. Immunol. Res.* 2020:6327614. doi: 10.1155/2020/6327614
- Wei, S., Zhang, J., Wu, X., Chen, M., Huang, H., Zeng, S., et al. (2022). Fusobacterium nucleatum extracellular vesicles promote experimental colitis by modulating autophagy via the miR-574-5p/CARD3 Axis. *Inflamm. Bowel Dis.* 23:izac177. doi: 10.1093/ibd/izac177
- Xiong, X., Tian, S., Yang, P., Lebreton, F., Bao, H., Sheng, K., et al. (2022). Emerging enterococcus pore-forming toxins with MHC/HLA-I as receptors. *Cells* 185, 1157–1171.e22. doi: 10.1016/j.cell.2022.02.002
- Xu, W., Guo, Y., Huang, Z., Zhao, H., Zhou, M., Huang, Y., et al. (2019). Small heat shock protein CRYAB inhibits intestinal mucosal inflammatory responses and protects barrier integrity through suppressing IKKbeta activity. *Mucosal. Immunol.* 12, 1291–1303. doi: 10.1038/s41385-019-0198-5
- Xu, M., Pokrovskii, M., Ding, Y., Yi, R., Au, C., Harrison, O. J., et al. (2018). C-MAF-dependent regulatory T cells mediate immunological tolerance to a gut pathobiont. *Nature* 554, 373–377. doi: 10.1038/nature25500
- Yang, X., Mao, Z., Huang, Y., Yan, H., Yan, Q., Hong, J., et al. (2021). Reductively modified albumin attenuates DSS-induced mouse colitis through rebalancing systemic redox state. *Redox Biol.* 41:101881. doi: 10.1016/j.redox.2021.101881
- Yang, J., Pei, G., Sun, X., Xiao, Y., Miao, C., Zhou, L., et al. (2022). RhoB affects colitis through modulating cell signaling and intestinal microbiome. *Microbiome* 10:149. doi: 10.1186/s40168-022-01347-3
- Zelante, T., Iannitti, R. G., Cunha, C., De Luca, A., Giovannini, G., Pieraccini, G., et al. (2013). Tryptophan catabolites from microbiota engage aryl hydrocarbon receptor and balance mucosal reactivity via interleukin-22. *Immunity* 39, 372–385. doi: 10.1016/j.immuni.2013.08.003
- Zhai, R., Xue, X., Zhang, L., Yang, X., Zhao, L., and Zhang, C. (2019). Strain-specific anti-inflammatory properties of two Akkermansia muciniphila strains on chronic colitis in mice. *Front. Cell. Infect. Microbiol.* 9:239. doi: 10.3389/fcimb.2019.00239
- Zhang, J., Cen, L., Zhang, X., Tang, C., Chen, Y., Zhang, Y., et al. (2022). MPST deficiency promotes intestinal epithelial cell apoptosis and aggravates inflammatory bowel disease via AKT. *Redox Biol.* 56:102469. doi: 10.1016/j.redox.2022.102469
- Zhang, T., Ding, C., Chen, H., Zhao, J., Chen, Z., Chen, B., et al. (2022). M(6)a mRNA modification maintains colonic epithelial cell homeostasis via NF-kappaB-mediated antiapoptotic pathway. *Sci. Adv.* 8:eabl5723. doi: 10.1126/sciadv.abl5723
- Zhang, L., Lee, H., Grimm, M. C., Riordan, S. M., Day, A. S., and Lemberg, D. A. (2014). Campylobacter concisus and inflammatory bowel disease. *World J. Gastroenterol.* 20, 1259–1267. doi: 10.3748/wjg.v20.i5.1259
- Zhang, C., Qin, J., Zhang, S., Zhang, N., Tan, B., Siwko, S., et al. (2020). ADP/P2Y1 aggravates inflammatory bowel disease through ERK5-mediated NLRP3 inflammasome activation. *Mucosal Immunol.* 13, 931–945. doi: 10.1038/s41385-020-0307-5
- Zhang, J., Wang, C., Guo, Z., Da, B., Zhu, W., and Li, Q. (2021). miR-223 improves intestinal inflammation through inhibiting the IL-6/STAT3 signaling pathway in dextran sodium sulfate-induced experimental colitis. *Immun. Inflamm. Dis.* 9, 319–327. doi: 10.1002/iid3.395
- Zhang, Y. S., Xin, D. E., Wang, Z., Song, X., Sun, Y., Zou, Q. C., et al. (2019). STAT4 activation by leukemia inhibitory factor confers a therapeutic effect on intestinal inflammation. *EMBO J.* 38, 1–20. doi: 10.15252/embj.201899595
- Zhen, Y., and Zhang, H. (2019). NLRP3 Inflammasome and inflammatory bowel disease. *Front. Immunol.* 10:276. doi: 10.3389/fimmu.2019.00276
- Zuo, L., Kuo, W. T., Cao, F., Chanez-Paredes, S. D., Zeve, D., Mannam, P., et al. (2022). Tacrolimus-binding protein FKBP8 directs myosin light chain kinase-dependent barrier regulation and is a potential therapeutic target in Crohn's disease. *Gut:gutjnl-2021-326534*. doi: 10.1136/gutjnl-2021-326534





## OPEN ACCESS

## EDITED BY

Weiqi He,  
Soochow University,  
China

## REVIEWED BY

Fang Xiang,  
South China Agricultural University, China  
Manoj Baranwal,  
Thapar Institute of Engineering and  
Technology, India

## \*CORRESPONDENCE

Jianxi Cao  
✉ wkyxb2013@126.com

<sup>†</sup>These authors have contributed equally to  
this work

## SPECIALTY SECTION

This article was submitted to  
Microorganisms in Vertebrate Digestive  
Systems,  
a section of the journal  
Frontiers in Microbiology

RECEIVED 28 October 2022

ACCEPTED 12 December 2022

PUBLISHED 06 January 2023

## CITATION

Zhao M, Liu L, Liu F, Liu L, Liu Z, Gao Y and  
Cao J (2023) Traditional Chinese medicine  
improves myasthenia gravis by regulating  
the symbiotic homeostasis of the intestinal  
microbiota and host.  
*Front. Microbiol.* 13:1082565.  
doi: 10.3389/fmicb.2022.1082565

## COPYRIGHT

© 2023 Zhao, Liu, Liu, Liu, Liu, Gao and  
Cao. This is an open-access article  
distributed under the terms of the [Creative  
Commons Attribution License \(CC BY\)](#). The  
use, distribution or reproduction in other  
forums is permitted, provided the original  
author(s) and the copyright owner(s) are  
credited and that the original publication in  
this journal is cited, in accordance with  
accepted academic practice. No use,  
distribution or reproduction is permitted  
which does not comply with these terms.

# Traditional Chinese medicine improves myasthenia gravis by regulating the symbiotic homeostasis of the intestinal microbiota and host

Mingli Zhao<sup>1†</sup>, Li Liu<sup>2†</sup>, Fanzhao Liu<sup>1</sup>, Lei Liu<sup>1</sup>, Zhijuan Liu<sup>1</sup>,  
Yanli Gao<sup>1</sup> and Jianxi Cao<sup>1\*</sup>

<sup>1</sup>Department of Cardio-Thoracic Surgery, The First Affiliated Hospital of Henan University of  
Traditional Chinese Medicine, Zhengzhou, China, <sup>2</sup>Department of Thoracic Surgery, Henan  
Province Hospital of Traditional Chinese Medicine, Zhengzhou, China

Myasthenia gravis (MG) is an autoimmune disease caused by autoantibodies that is dependent on T-cell immunity and complement participation and mainly involves neuromuscular junctions. In this study, 30 patients with myasthenia gravis were selected and divided into pretreatment (Case group) and posttreatment (Treatment group) and 30 healthy volunteers (CON group) were included. Among them, the treatment group was treated with Modified Buzhong Yiqi Decoction (MBZYQD), and the levels of antibodies such as AChR, Musk and Titin in blood and intestinal microbiota were compared before treatment (Case group), after treatment (Treatment group) and in healthy volunteers (CON group). The results showed that after treatment with MBZYQD, the antibody levels of AChR, MuSK, and Titin and the inflammatory factor level of IL-6, IL-1 $\beta$ , and IL-22 in MG patients decreased significantly and nearly returned to a healthy level. In addition, after treatment with MBZYQD, the diversity, structure and function of intestinal microorganisms in MG patients also recovered to a healthy level. At the phylum level, the relative abundance of Proteobacteria in the Case group increased significantly, accompanied by a significant decrease in the relative abundance of Bacteroides compared with that in the CON group, the relative abundance of Proteobacteria and Bacteroides in the Treatment group was similar to that in the CON group. At the genus level, the relative abundance of *Shigella* in the Case group was significantly increased, accompanied by a significant decrease in the relative abundance of *Prevotella*, and the relative abundance of *Shigella* and *Prevotella* in Treatment group was similar to that in the CON group. Moreover, the fluorobenzoate degradation pathway (KO00364) was significantly increased in the Case group, while this pathway was significantly decreased in the Treatment group. In conclusion, MBZYQD can improve the immune function of the host by regulating the diversity, structure and function of the intestinal microbiota to treat myasthenia gravis.

## KEYWORDS

myasthenia gravis, traditional Chinese medicine, intestinal microbiota,  
immunological function, SCFAs



## Introduction

Myasthenia gravis (MG) is an autoimmune mediated disease (Gilhus and Verschuuren, 2015). Its etiology includes environmental factors and genetic factors. At present, antibodies to acetylcholine receptor (AChR), muscle specific receptor tyrosine kinase (MuSK), and Rankine receptor (RyR) are known (Zhao et al., 2008; Sieb, 2014; Müllges and Stoll, 2019). These antibodies can interfere with the aggregation of AChR and affect the function of AChR and the signal transmission of nerve-muscle junctions, resulting in the failure of nerve-to-muscle action potential transmission (Gomez et al., 2010). Its main clinical manifestations are skeletal muscle weakness, fatigue, aggravation after activity, ptosis, diplopia, dysphagia, unclear articulation, and weak mastication (Zhao et al., 2011).

There are a large number of microorganisms in the human intestine, and they gradually form a complex relationship of mutualism with humans (Hugon et al., 2015). The intestinal microbiota play a variety of role; they are not only responsible for digesting and absorbing nutrients, but also play an important role in regulating the proliferation and differentiation of epithelial cells and resisting the invasion of pathogens (Soderholm and Pedicord, 2019; Rohr et al., 2020; Stacy et al., 2021). Moreover, the intestinal microbiota play an important role in promoting the occurrence and development of host innate immunity and its acquired immune system (Thaiss et al., 2016; Pascal et al., 2018). Studies have shown that there are obvious defects in the development and maturation of the spleen, mesenteric lymph nodes and intestinal-associated lymphoid tissues of sterile mice, and the administration of microbiota or some metabolites of microbiota can induce the above tissues to become normal, which indicates that intestinal microbiota are indispensable in the maturation of the host immune system (Kamada et al., 2013). Moreover, the immunosuppressive effect of intestinal microbiota on T lymphocytes is mainly reflected in the two cell helper T lymphocytes - helper T cells and regulatory T cells (Yang et al., 2020). Regulatory T cells in the intestine have the anti-inflammation functions, maintaining the immune tolerance of the body to its own harmful substances, and preventing the occurrence of autoimmune disorders in the host (Lan et al., 2007; Gao et al., 2016; Elmadfa and Meyer, 2019).

Previous research found that compared with a normal group, the diversity of microorganisms in the feces of patients in an MG group decreased as a whole, and the structure of the microbial community also changed, especially the SCFA level in the feces of patients in the MG group, which decreased significantly (Qiu et al., 2018; Liu et al., 2021). The same study also found that the

Firmicutes/Bacteroides ratio (F/B ratio) in the intestinal microbiota of MG patients was significantly lower than that of the healthy control group, and the F/B ratio can be regarded as a pro-inflammatory environment. The inflammatory microbiota may cause damage to intestinal epithelial cells and trigger an immune response, eventually leading to the occurrence of various autoimmune diseases and an imbalance in the immune system (Qiu et al., 2018; Rinaldi et al., 2018). Other research explored the fecal microbiota of MG experimental mice (experimental autoimmune myasthenia gravis, EAMG) and healthy mice: At the phylum level, the ratio of Tenericutes/Verrucomicrobiota in the experimental autoimmune myasthenia gravis (EAMG) model group significantly decreased compared with that in the healthy control group, and Tenericutes/Verrucomicrobiota ratio partially recovered after probiotic treatment. At the family level, Lachnospiraceae decreased significantly in the EAMG group, and the ratio of Ruminococcaceae/Lachnospiraceae increased significantly. After treatment with probiotics, the ratio of Ruminobacteriaceae to Lachnospiraceae decreased significantly (Rinaldi et al., 2019). Additionally, Zheng et al. colonized germ-free mice with MG microbiota and healthy microbiota. The MG microbiota mice exhibited markedly impaired motor performance compared with healthy microbiota mice, and this insufficiency could be reversed by cocolonization of germ-free mice with MG microbiota and healthy microbiota mice. The above experimental results further support the correlation between gut microbiota and MG (Zheng et al., 2019).

In recent years, the role of intestinal microbiota in the immune system and their correlation with autoimmune diseases have been gradually explored. Intestinal microbiota may play a role in the occurrence and development of MG by affecting key factors in the anti-inflammatory process (Rinaldi et al., 2019). Traditional Chinese medicine (TCM) treatment is now considered a new immunomodulatory tool and a potential treatment that may be used to improve the symptoms of MG. Traditional Chinese medicine believes that MG belongs to the category of “flaccidity syndrome.” Most studies also show that the method of invigorating the spleen and replenishing qi is the key to the treatment of MG, and most of them use Buzhong Yiqi Decoction as the base prescription, which is treated according to syndrome differentiation, and has achieved remarkable effects (Jiang et al., 2018; Li et al., 2021; Zong et al., 2021). In our clinical work, we found that MBZYQD has a significant effect in the treatment of myasthenia gravis. Its main ingredients are nine medicines, including *Astragalus*, *Codonopsis*, *Atractylodes macrocephala*, *Cohosh*, and *Bupleurum chinense*, et al., among which the main active ingredients are flavonoids, including quercetin, luteolin, kaempferol, and naringenin. These active ingredients have anti-inflammatory and antioxidant effects (Imran et al., 2019; Kracht et al., 2020). However, the effect of MBZYQD on the intestinal microbiota of myasthenia gravis is unknown. By using the hypervariable marker sequence of the V3-V4 region of the 16S rRNA gene, this study established the systematic pattern spectrum of the intestinal microbial population, compared the differences in fecal microbiota between MG patients and a healthy control

Abbreviations: MG, Myasthenia gravis; MBZYQD, Modified Buzhong Yiqi Decoction; SCFAs, Short chain fatty acids; AChR, Acetylcholine receptor; MuSK, Muscle specific receptor tyrosine kinase; RyR, Rankine receptor; F/B, Firmicutes/Bacteroides; TCM, Traditional Chinese Medicine; KEGG, Kyoto Encyclopedia of Genes and Genomes; NMDS, Non-metric multidimensional scaling; PCoA, Principal Co-ordinates analysis; FMT, Fecal microbiota transplantation.

group, as well as MG patients treated with MBZYQD before and after treatment, and discussed the possible mechanism of traditional Chinese medicine in the treatment of MG to lay a solid foundation for the discovery of new diagnosis and treatment methods.

## Materials and methods

### Case source

MG patients who met the inclusion criteria in the cardiothoracic surgery clinic of the First Affiliated Hospital of Henan University of Traditional Chinese Medicine were selected, and a sample size of  $n=90$  was obtained according to the case-control study design. That is, 30 MG patients (before (Case group,  $n=30$ ) and after treatment (Treatment group,  $n=30$ )) and 30 healthy volunteers (CON group,  $n=30$ ) were selected in this study (Volunteers with one of the following conditions were excluded: liver and/or kidney disease, mental disease, tumor, gastrointestinal disease, metabolic disease or any other disease that might affect the results of the study. Antibiotics, glucocorticoids, anti-obesity agents, monoclonal drugs, hypoglycemic agents or probiotics within 3 months were excluded).

### Ethical review

The clinical research plan met the ethical standards of and was approved by the clinical ethics committee of the scientific research project of The First Affiliated Hospital of Henan University of Traditional Chinese Medicine: HECABX-20210185.

### Diagnostic criteria

#### Inclusion criteria

According to the diagnostic criteria of myasthenia gravis in Western medicine, the condition of patients with myasthenia gravis is in a stable stage. In line with the diagnostic criteria of TCM syndrome differentiation, the disease belongs to deficiency of spleen and stomach qi. The age of the patients with myasthenia gravis in Henan was between 18 and 70 years old. No patients had thymoma. The test design was explained to the patients to help them understand the test contents, and the consent form was signed. Patients with myasthenia gravis who could cooperate with this treatment scheme and persist in treatment for 4 months were permitted to complete the detection of the main observation indices. Those who met the above conditions could be selected.

TCM syndrome was referenced from the National Standard of the People's Republic of China Terms for Clinical Diagnosis and Treatment of Traditional Chinese Medicine-Symptoms, issued by the State Administration of Technical Supervision and from the Guidelines for Diagnosis and Treatment of Common Diseases in

Internal Medicine of Traditional Chinese Medicine - Western Medicine Diseases issued by the Chinese Society of Traditional Chinese Medicine in 2008. Spleen and stomach qi deficiency syndrome was characterized by main symptoms, including drooping eyelids, light twilight, limb weakness, and dysphagia, chewing difficulty or chewing weakness; secondary symptoms, including a lack of qi and laziness, stuffiness and shortness of breath in the chest, choking after drinking water, inability to lift the neck, loss of appetite, abdominal distension, fatigue, body fatigue, sallow complexion, and loose stool. Tongue pulse was characterized by the tongue being light and fat, with tooth marks on the edge, with thin and white fur, and a weak pulse. TCM syndrome differentiation required that the main symptoms be and at least one secondary symptom was present, along with the tongue pulse meeting the described criteria.

#### Exclusion criteria

Exclusion criteria included the following: MG symptoms did not conform to TCM syndrome types (spleen stomach qi deficiency syndrome); myasthenic crisis and cholinergic crisis had occurred in the last 6 months; for women, being pregnant or lactating; having experienced the surgical removal of thymoma; being diagnosed with a serious mental illness or being unable to cooperate with the clinical investigation; having complications of serious heart, kidney, blood, or other important organ diseases; being allergic to drugs that might be used in this study; and having recently participated in other clinical studies.

### Treatment plan

Thirty patients with myasthenia gravis of spleen stomach deficiency of vital energy type were treated with MBZYQD (drug composition: *Astragalus membranaceus* (reuse), *Atractylodes macrocephala*, *Radix Pseudostellariae*, *Poria cocos*, *Angelica sinensis*, *Tangerine peel*, *Bupleurum*, *Cohosh*, *Roasted licorice*, etc.), which was uniformly decocted by the decoction machine in the preparation room of the First Affiliated Hospital of Henan University of Traditional Chinese Medicine, 1 dose/day, 2 times/day).

### Research period and sample collection

The study period was 3 months (The overall framework of this study is shown in Figure 1A). The index collection time point at which feces and blood samples were collected occurred once the MG patients were enrolled (i.e., before the intervention of MBZYQD). Within 3 months of treatment, it was indicated that it was effective or cured according to the efficacy evaluation criteria. Combined with the absolute and relative score table of myasthenia gravis, feces and blood samples were taken again for patients with a relative score of more than 50%. The absolute and relative clinical scoring criteria for myasthenia gravis were determined in

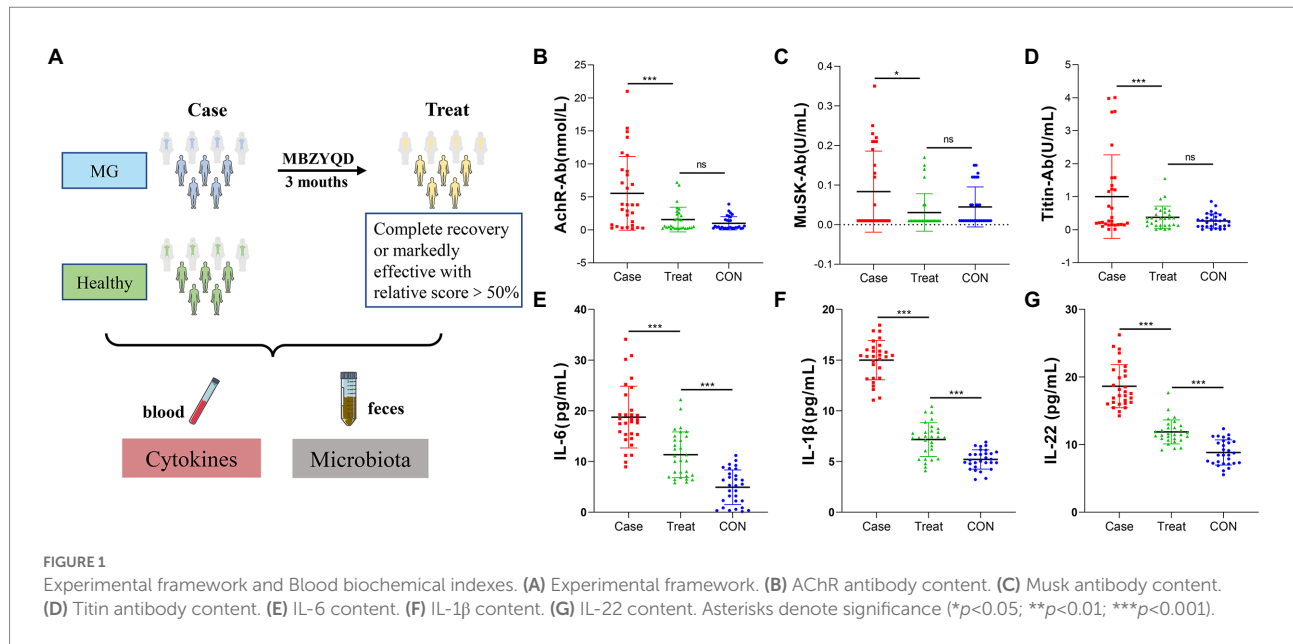


**TABLE 1** The clinical symptoms of myasthenia gravis patients before and after treatment.

Variables	Case group	Treatment group	<i>p</i> value
Gender (Female)	15 (50%)	15 (50%)	NA
Age-years	59.47 $\pm$ 13.33	59.47 $\pm$ 13.33	NA
ASMG	13.56 $\pm$ 9.36	3.52 $\pm$ 3.06	0.001
RSMG (Total efficiency)	NA	93.86 $\pm$ 5.62	NA
MGFA	9.56 $\pm$ 4.23	2.36 $\pm$ 1.56	0.025
ADLMG	6.52 $\pm$ 3.17	1.65 $\pm$ 1.03	0.032

Note: ASMG, Absolute score of myasthenia gravis; RSMG, Relative score of myasthenia gravis; MGFA, Myasthenia gravis foundation of America; ADLMG, Activities of daily living of myasthenia gravis.

**Supplementary material S1.** Fecal samples were collected once the healthy control group was enrolled. Blood test items mainly included AChR antibody, MuSK antibody, Titin antibody levels and inflammatory factor levels (IL-6, IL-1 $\beta$ , and IL-22). The clinical symptoms of myasthenia gravis patients before and after treatment are shown in [Table 1](#).

## Extraction and database construction of fecal genomic DNA

From the CON, Case and Treatment groups of fecal samples, 10, 17, and 13 samples were randomly selected for 16S rRNA gene sequencing. Total genomic DNA samples of bacteria in feces were extracted using the fecal DNA Extraction Kit (MP biomedical, Santa Ana, CA, United States) according to the manufacturer's instructions and stored at  $-20^{\circ}\text{C}$  before

further analysis. The concentration and quality of extracted DNA were measured by the NanoDrop ND-1000 spectrophotometer and agarose gel electrophoresis, respectively. The V3-V4 region of the bacterial 16S rRNA gene was amplified by PCR using forward primer (5'-ACTCCTACGGGAGGGCAGCA-3') and reverse primer (5'-GGACTACHVGGTWTCTAAT-3'). Illumina's TruSeq Nano DNA LT Library Prep Kit was used to prepare the sequencing library.

## Bioinformatics analysis

### Alpha and beta diversity analysis

In this study, the alpha diversity index and beta diversity index were used to characterize the diversity of species within and between habitats respectively, to comprehensively evaluate their overall diversity. Alpha diversity was calculated as follows: Using QIIME2 (2019.4) and the ggplot2 package in R language, calculate the alpha diversity index (mainly including Chao1, observed species, Shannon, Simpson, Faith's, PD Pielou's evenness and Good's coverage) was calculated according to the ASV/OTU table that was not flattened to detect biological diversity. Then, the R language was used to draw the specaccum species accumulation curve for the total number of ASVs/OTUs corresponding to each sample in the ASV/OTU abundance matrix to test whether the sample size of this study was sufficient. Beta diversity was calculated as follows: The vegan package in the R script was used for NMDS analysis. Through the dimensionality reduction decomposition of the sample distance matrix, the data structure was simplified, and the distribution characteristics of samples were described at a specific distance scale to show the composition differences of microbial communities.

## Species composition analysis

Called the “QIIME taxa barplot” command in QIIME2, statistical calculations were performed on the feature table after removing singletons; the composition distribution of each sample at the phylum and genus levels was visualized; and the analysis results were presented in a histogram. In addition to showing the formation of taxonomic composition in the form of a tree diagram, in this study, ggtree was used as an evolutionary tree to show the position of ASV/OTU in the evolutionary tree and the evolutionary distance between them and to reflect their composition, abundance, taxonomy and other information through a heatmap and histogram (Wang et al., 2020).

## Species difference and standard species analysis

After exploring the differences in microbial community composition, we also need to know which species are mainly caused by these differences. LEfSe analysis is a difference analysis method that which can directly analyze the differences of all classification levels at the same time. At the same time, LEfSe puts more emphasis on finding robust differential species between groups, namely marker species (biomarkers). One of its characteristics is that it is not only limited to analyzing the differences in community composition in different sample groups but can also go deep into different subgroups and identify the marker microbial groups that are consistent in different subgroups. At present, it has been widely used in the fields of microbial amplification analysis and is especially suitable for finding biomarkers in medical research. To further compare the species composition differences between samples, the pheatmap package in R language was used to calculate the clustering results of each sample and each taxon, which is presented in the form of an interactive graph to display the distribution trend of species abundance of each sample. By default, the abundance data of the top 20 genera of average abundance were used to draw the heatmap.

## Functional potential prediction

The above analysis focuses on the diversity and species composition of the microbiota. With the development of data analysis technology, we can refer to known microbial genome data to predict the composition of microbiota genes or functional units for samples with only microbiota marker gene sequencing data. The obtained functional units were used to obtain the abundance value of metabolic pathways according to the metabolic pathway database and R language analysis. Then, using the normalized functional unit abundance table, the R script was used to calculate the distance matrix in R and conduct PCoA. The PCoA coordinates of the sample points were output and drawn into a two-dimensional scatter diagram. Finally, after obtaining the abundance data of metabolic pathways, we attempted to identify the metabolic pathways with significant differences between groups.

## Statistical analysis

A completely randomized test design was used in the study. The significance of the difference between the means of the groups was determined by one-way ANOVA. Differences with  $p < 0.05$  (\*),  $p < 0.01$  (\*\*), and  $p < 0.01$  (\*\*\*) were considered to be statistically significant. The statistical calculations used in this study were performed with IBM SPSS 25.0.

## Results

### Blood biochemical indices

The results showed that the levels of AChR, MuSK, Titin and inflammatory factors (IL-6, IL-1 $\beta$ , and IL-22) in the Treatment group were significantly lower than those in the Case group, and there were no significant differences in the antibody levels of AChR, MuSK and Titin between the Treatment group and the CON group of healthy volunteers (Figures 1B–G).

### Species composition

To further compare the species composition differences between samples and display the distribution trend of species abundance of each sample, a heatmap can be used for species composition analysis. At the phylum level, the relative abundance of Bacteroidetes in the Case group was significantly lower than that in the CON group, and the relative abundance of Proteus was significantly higher than that in the CON group. After treatment, the relative abundance of Bacteroidetes and Proteobacteria returned to the level of the CON group (Figures 2A,C). At the genus level, *Prevotella* and *Megamonas* were hardly detected in the Case group, but the relative abundance of *Shigella* was significantly higher than that in the CON group, and all bacteria returned to the level of the CON group after treatment (Figures 2B,D). Phylotree results show that *Bacteroides* and *Prevotella* are closely related, and both belong to Bacteroidia. They had high relative abundance in the Case group but low relative abundance in Treatment group and CON group. In addition, *Roseburia* and *Bifidobacterium* were closely related, and *Bifidobacterium* had a high relative abundance in the Treatment group (Figure 2E). The correlation analysis results of intestinal microbiota and cytokines showed that antibodies (AChR, MuSK, and Titin) and inflammatory factors (IL-6, IL-1 $\beta$ , and IL-22) were mainly positively correlated with *Shigella* and *Enterococcus*, but negatively correlated with *Prevotella*, *Bacteroides*, and *Bifidobacterium* (Figure 2F).

### Alpha and beta diversity

Alpha diversity refers to the indicators of richness, diversity and evenness of species in locally uniform habitats. It is also



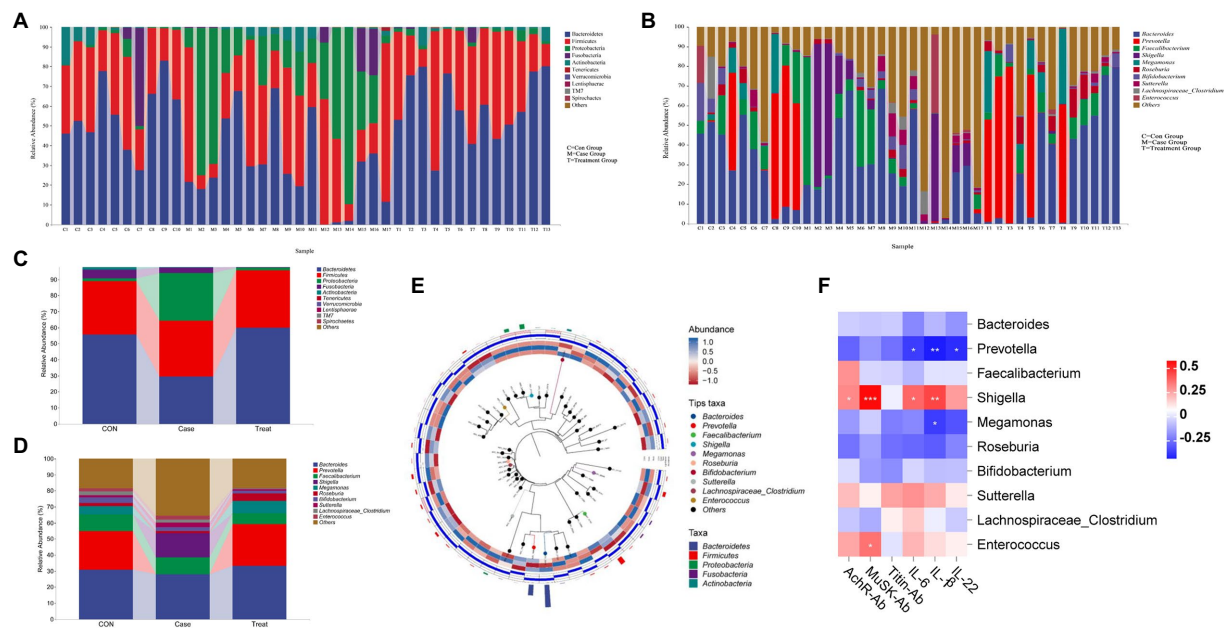


FIGURE 2

Species composition and association analysis. (A,C) Composition and distribution of intestinal microbiota at phylum level in Case group, Treatment group and CON group. (B,D) Composition and distribution of intestinal microbiota at genus level in Case group, Treatment group and CON group. (E) Phylotree evolutionary tree. (F) Correlation analysis of intestinal microbiota (Genus Level) and Cytokines. Asterisks denote significance (\* $p < 0.05$ ; \*\* $p < 0.01$ ; \*\*\* $p < 0.001$ ).

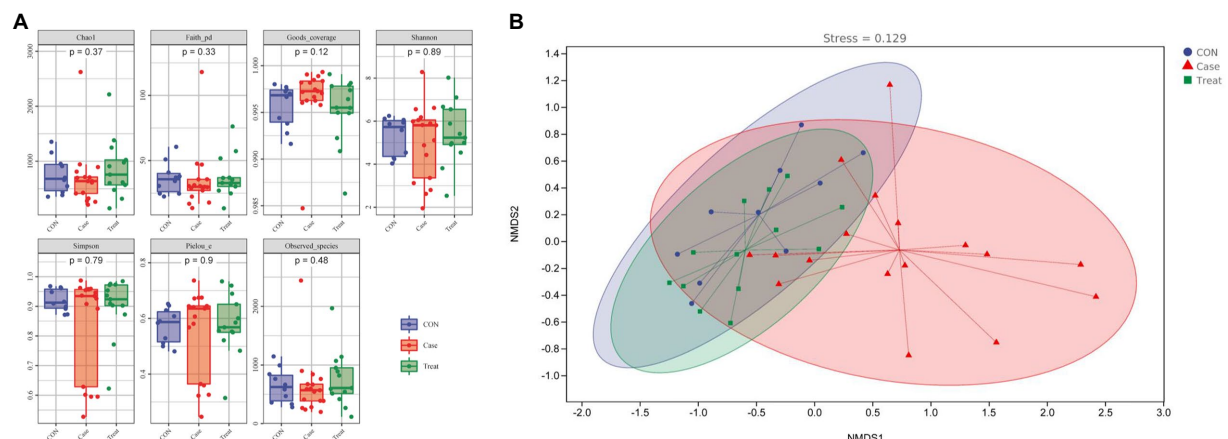


FIGURE 3

Alpha and beta diversity. (A) Alpha diversity indexes. (B) Nonmetric Multidimensional scaling (NMDS).

known as within-habitat diversity. In this study, the alpha diversity results showed that the Chao1 index, Faith PD index, Shannon index, Simpson and observed species index of the case group were lower than those of the CON group, while the coverage index was higher than that of the CON group. In the Treatment group, these alpha diversity indices were restored (Figure 3A). NMDS results showed that the dispersion degree among samples in the Case group was large. After MBZYQD treatment, the dispersion distance among samples in the Treatment group decreased, and

there was a great difference between the Case group and the Treatment group, while the distribution degree of samples in the Treatment group was closer to that of the CON group (Figure 3B).

## Species differences and marker species

LEfSe analysis showed that *Proteobacteria*, *Coprobacillus*, *Bacteroidia*, *Bacteroidales*, and *Bacteroidetes* were the most



significantly different bacteria in Case group, CON group and Treatment group, respectively (Figure 4A). To further compare the species composition differences between samples and display the distribution trend of species abundance of each sample, the species composition of the top 20 relative abundances was analyzed by a heatmap. The results showed that the microbiota of the Case group was significantly different from that of the CON group and Treatment group, such as *Sutterella*, *Oscillospira*, *Fusobacterium*, *Dorea*, *[Ruminococcus]*, *Phascolarctobacterium*, *Shigella*, and *[Eubacterium]*, while the relative abundance of *Prevotella*, *Bacteroides*, and *Megamonas* were significantly lower than those of the CON group. After treatment, the relative abundances of these bacteria returned to the normal level, reaching the level of the CON group (Figure 4B).

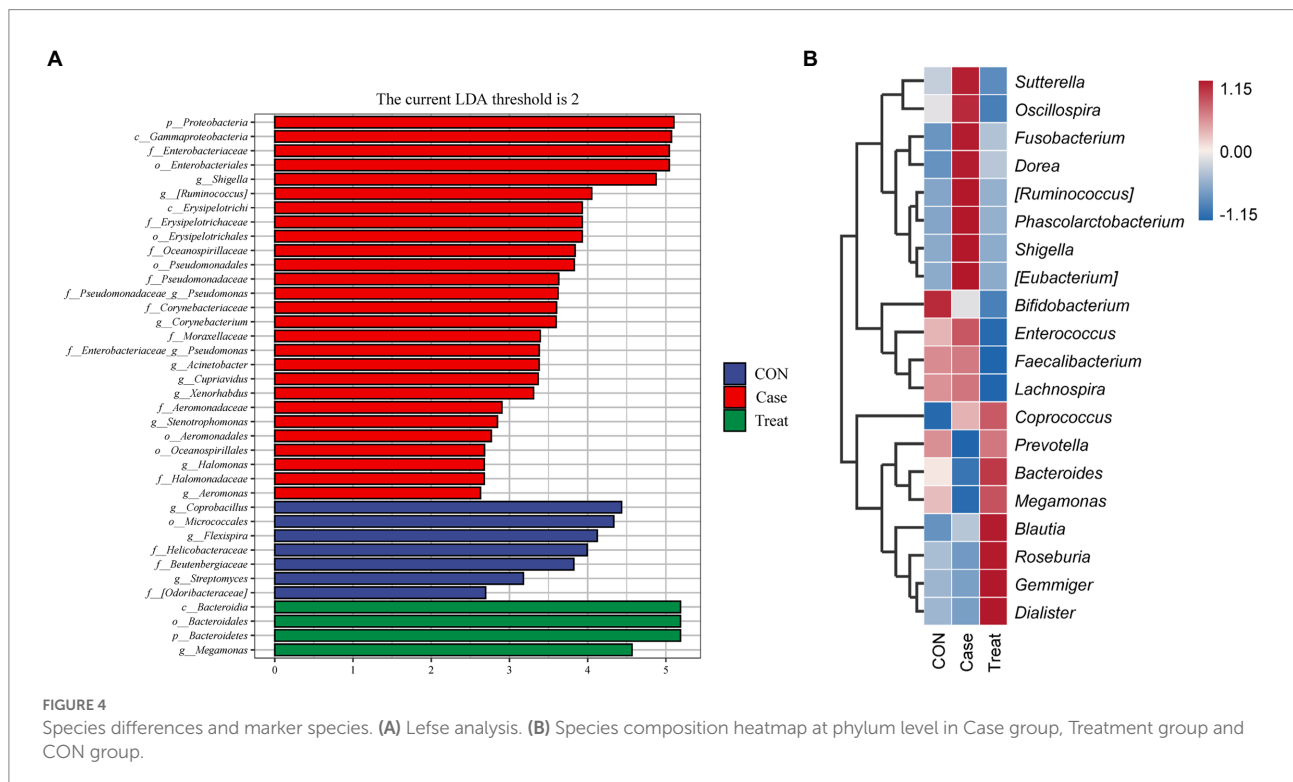
## KEGG metabolic pathway

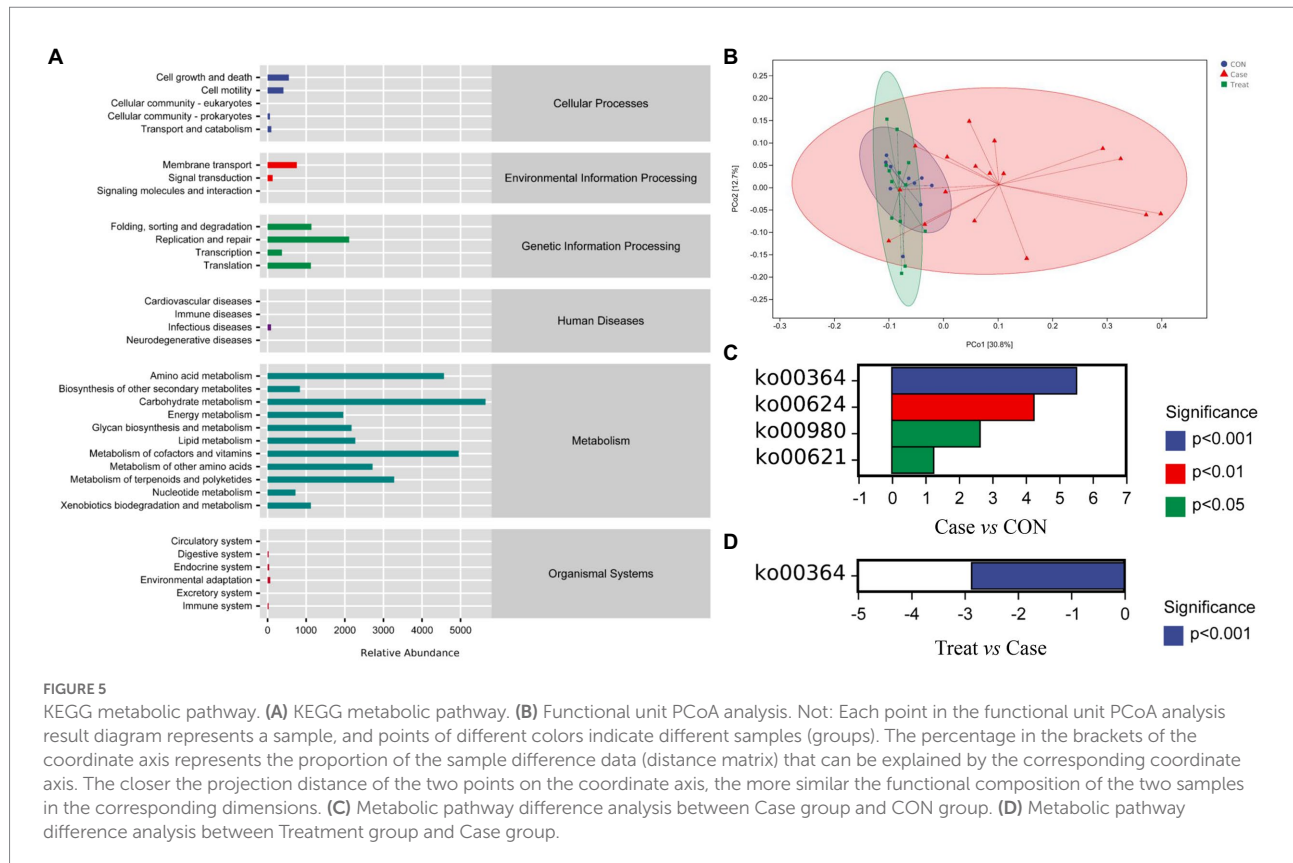
In this study, the microbiota was mainly involved in metabolic pathways, including amino acid metabolism, carbohydrate metabolism, coenzyme factor and vitamin metabolism (Figure 5A). The results of functional unit PCoA analysis were consistent with the NMDS results in the beta diversity analysis results; that is, the dispersion degree between samples in the Case group was large. After MBZYQD treatment, the dispersion ranges between samples in the Treatment group decreased, and there were great differences between the Case group and the Treatment group, while the distribution degree

of samples in the Treatment group was closer to that in the CON group (Figure 5B). Further analysis of the differences in KEGG metabolic pathways among the three groups showed that the Case group significantly upregulated KO00364, KO00624, KO00980, and KO00621 compared with the CON group. The KO00364 pathway was significantly downregulated in the Treatment group compared with the Case group (Figures 5C,D).

## Discussion

Myasthenia gravis (MG) refers to an autoimmune disease in which the lesion occurs at the junction of the nerve and muscle, and the acquired neuromuscular junction transmission disorder is mediated by autoantibodies (Narayanawami et al., 2021). The etiology of myasthenia gravis blepharoptosis is related to many factors (Mantegazza et al., 2018). At present, the commonly used treatment methods include cholinesterase inhibitors, immunosuppressants, thymectomy and so on (Farmakidis et al., 2018). However, because the disease is a chronic disease and has a long course, long-term use of the above drugs will produce a variety of adverse reactions, and surgical treatment is painful (Gajdos et al., 2012). Modern studies have found that there is a new cholinesterase inhibitor in MBZYQD (Liu et al., 2010; Cui et al., 2015). MBZYQD may affect the key factors in the anti-inflammatory process by regulating





intestinal microbiota (Wang et al., 2022) and may play a role in the occurrence and development of MG (Li et al., 2021; Zong et al., 2021). However, it is unclear whether MBZYQD can improve myasthenia gravis by regulating intestinal microbiota. Therefore, this study analyzed the difference in intestinal microbiota in myasthenia gravis patients before and after MBZYQD treatment by high-throughput sequencing technology.

The results of this study showed that compared with the CON group, the diversity of microorganisms in the feces of patients in the MG group decreased as a whole, and the structure of the microbial community also changed. The study also found that the Firmicutes/Bacteroides ratio (F/B ratio) in the intestinal microbiota of MG patients was significantly lower than that of the healthy control group, and the F/B ratio can be regarded as a pro-inflammatory environment (Liu et al., 2021). The intestinal microbiota may cause damage to intestinal epithelial cells and trigger an immune response, eventually leading to the occurrence of various autoimmune diseases and an imbalance in the immune system (De Luca and Shoenfeld, 2019; Nakamoto et al., 2019; Di Tommaso et al., 2021). The view that the change in the F/B ratio is related to a series of autoimmune mediated diseases has also been supported by the research of Bibbò et al. (2017) and Shen et al. (2022). After MBZYQD treatment, the diversity and structure of the intestinal microbiota of MG

patients recovered, and the ratio of Firmicutes/Bacteroides (F/B ratio) in the intestinal microbiota of MG patients also returned to normal.

Further analysis showed that the relative abundance of *Shigella* was significantly increased in Case group, the relative abundance of *Shigella* was restored in Treatment group, and the relative abundance of *Shigella* was closely related to that found in Alzheimer's disease (AD), colitis and pancreatitis (Cattaneo et al., 2017; Li et al., 2020; Fan et al., 2021; Pivari et al., 2022). In addition, the relative abundance of *Prevotella* and *Bacteroides* was significantly reduced in the Case group and the relative abundance of *Prevotella* and *Bacteroides* was restored in the Treatment group, while *Prevotella* can use carbohydrates in the intestine to produce SCFAs, and the quantities and relative abundance of SCFAs can be considered biomarkers of health (Wu et al., 2011; Martínez et al., 2015; Yao et al., 2022). Atarashi et al. and Furusawai et al. found that SCFAs can directly regulate T cells to differentiate into CD4+FoxP3+ T cells, change the phenotype of dendritic cells, induce the expression of Raldh1 in dendritic cells, promote the production of retinoic acid (RA), and induce the differentiation of CD4+FoxP3+ T cells (Atarashi et al., 2013; Furusawa et al., 2015). Based on previous studies and the comparison between MG patients and healthy controls, it is speculated that the change in intestinal microbiota composition may lead to the lack or dysfunction of CD4+FoxP3+ T cells induced by intestinal bacteria,

which has a profound impact on immunity (Kwon et al., 2010; Chae et al., 2012). When the number of *Prevotella* and *Bacteroides* colonizing in the host decreases, the content of SCFAs in the intestine will be affected, and the number of CD4+FoxP3+ T cells in the corresponding mucosal lamina propria will also be reduced, leading to an imbalance in the immune response (Mangalam et al., 2017; Shahi et al., 2019, 2020).

These results indicate that the increase in *Shigella* abundance and the decrease in *Prevotella* and *Bacteroides* abundance may be important reasons for the occurrence and development of myasthenia gravis. Moreover, the researchers fed EAMG rats mixed probiotic preparations of two lactobacilli and two *Bifidobacteria*. It was found that the mixed probiotic preparations could significantly reduce the clinical symptoms of EAMG rats by influencing the level of regulatory dendritic cells and inducing CD4+ T cells to transform into CD4+Foxp3+ T cells. In addition, such preparations can reduce the level of AChR antibody and IFN- $\gamma$ , TNF- $\alpha$ , IL-6, IL-17, and other immune factors levels, which is similar to the results of this study, indicating that intestinal microbiota can participate in the pathogenesis and development of MG (Chae et al., 2012). It can be inferred from the pathogenesis of myasthenia gravis and the immune regulation mechanism of intestinal microbiota that the immune response to stimulate T lymphocytes may be the key link of intestinal microbiota leading to MG (Chen and Tang, 2021).

Furthermore, in the analysis of KEGG metabolic pathways, it was found that the Case group significantly upregulated the pathways of fluorobenzoate degradation (KO00364), polycyclic aromatic hydrocarbon degradation (KO00624), metabolism of xenobiotics by cytochrome P450 (KO00980) and dioxin degradation (KO00621) compared with the CON group. The KO00364 pathway significantly downregulated in the Treatment group compared with the Case group. This result suggests that KO00364 may be the key metabolic pathway involved in myasthenia gravis. Previous reports have shown that this pathway is related to the severity of intestinal inflammation, such as Crohn's disease (Montassier et al., 2015). In addition, the KO pathway related to the fluorobenzoic acid degradation pathway is often observed in the intestinal microbiota of patients with *Clostridium difficile* infection, and Proteobacteria bacteria involved in this pathway are significantly enriched (mainly including *Klebsiella*, *Escherichia coli*, unclassified *Enterobacteriaceae*, and *Salmonella*; Fujimoto et al., 2021). Subsequently, Fujimoto et al. significantly reduced the relative abundance of the KO pathway related to the fluorobenzoic acid degradation pathway and Proteobacteria (mainly including *Klebsiella*, *Escherichia coli*, unclassified *Enterobacteriaceae*, and *Salmonella*) in the intestinal microbiota of patients infected with *Clostridium difficile* through fecal microbiota transplantation (FMT; Fujimoto et al., 2021). This is consistent with the results of this study, indicating that MBZYQD can improve the intestinal environment, regulate the host immune level, and achieve intestinal microbiota host symbiosis and stability by reducing the relative abundance of Proteobacteria

and the degradation pathway of fluorobenzoic acid in the intestine.

## Conclusion

Intestinal microbiota plays an essential role in the pathogenesis of myasthenia gravis. The results of this study show that the imbalance of the microbial community may be one of the causes of myasthenia gravis. Treatment with MBZYQD can adjust the diversity and structure of the intestinal microbiota and the function of the microbial community in MG patients. Reconstruction of the microbiota can further improve the immune function of the host, indicating that MBZYQD may play a role in the treatment of myasthenia gravis by regulating the intestinal microbiota and achieving intestinal microbiota host symbiosis and stability.

## Data availability statement

The datasets presented in this study can be found in online repositories. The names of the repository/repositories and accession number(s) can be found at: <https://www.ncbi.nlm.nih.gov/genbank/>, PRJNA895190.

## Ethics statement

The studies involving human participants were reviewed and approved by the clinical ethics committee of the scientific research project of The First Affiliated Hospital of Henan University of Traditional Chinese Medicine. Written informed consent to participate in this study was provided by the participants' legal guardian/next of kin.

## Author contributions

MZ and LiL: data curation and writing — original draft. FL, LeL, and ZL: methodology. YG: visualization. JC: writing — reviewing and editing. JC: supervision, resources, and funding acquisition. All authors contributed to the article and approved the submitted version.

## Funding

This work was supported by the Special project for scientific research of traditional Chinese medicine in Henan Province (2019ZY1003). The funders had no role in the study design, data collection and interpretation or the decision to submit the work for publication.

## Conflict of interest

The authors declare that the research was conducted in the absence of any commercial or financial relationships that could be construed as a potential conflict of interest.

## Publisher's note

All claims expressed in this article are solely those of the authors and do not necessarily represent those of their affiliated

organizations, or those of the publisher, the editors and the reviewers. Any product that may be evaluated in this article, or claim that may be made by its manufacturer, is not guaranteed or endorsed by the publisher.

## Supplementary material

The Supplementary material for this article can be found online at: <https://www.frontiersin.org/articles/10.3389/fmicb.2022.1082565/full#supplementary-material>

## References

- Atarashi, K., Tanoue, T., Oshima, K., Suda, W., Nagano, Y., Nishikawa, H., et al. (2013). Treg induction by a rationally selected mixture of clostridia strains from the human microbiota. *Nature* 500, 232–236. doi: 10.1038/nature12331
- Bibbò, S., Dore, M. P., Pes, G. M., Delitala, G., and Delitala, A. P. (2017). Is there a role for gut microbiota in type 1 diabetes pathogenesis? *Ann. Med.* 49, 11–22. doi: 10.1080/07853890.2016.1222449
- Cattaneo, A., Cattane, N., Galluzzi, S., Provati, S., Lopizzo, N., Festari, C., et al. (2017). Association of brain amyloidosis with pro-inflammatory gut bacterial taxa and peripheral inflammation markers in cognitively impaired elderly. *Neurobiol. Aging* 49, 60–68. doi: 10.1016/j.neurobiolaging.2016.08.019
- Chae, C. S., Kwon, H. K., Hwang, J. S., Kim, J. E., and Im, S. H. (2012). Prophylactic effect of probiotics on the development of experimental autoimmune myasthenia gravis. *PLoS One* 7:e52119. doi: 10.1371/journal.pone.0052119
- Chen, P., and Tang, X. (2021). Gut microbiota as regulators of Th17/Treg balance in patients with myasthenia gravis. *Front. Immunol.* 12:803101. doi: 10.3389/fimmu.2021.803101
- Cui, L., Wang, Y., Liu, Z., Chen, H., Wang, H., Zhou, X., et al. (2015). Discovering new acetylcholinesterase inhibitors by mining the Buzhongyiqi decoction recipe data. *J. Chem. Inf. Model.* 55, 2455–2463. doi: 10.1021/acs.jcim.5b00449
- De Luca, F., and Shoenfeld, Y. (2019). The microbiome in autoimmune diseases. *Clin. Exp. Immunol.* 195, 74–85. doi: 10.1111/cei.13158
- Di Tommaso, N., Gasbarrini, A., and Ponziani, F. R. (2021). Intestinal barrier in human health and disease. *Int. J. Environ. Res. Public Health* 18:12836. doi: 10.3390/ijerph182312836
- Elmadfa, I., and Meyer, A. L. (2019). The role of the status of selected micronutrients in shaping the immune function. *Endocr Metab Immune Disord Drug Targets* 19, 1100–1115. doi: 10.2174/1871530319666190529101816
- Fan, L., Qi, Y., Qu, S., Chen, X., Li, A., Hendi, M., et al. (2021). *B. adolescentis* ameliorates chronic colitis by regulating Treg/Th2 response and gut microbiota remodeling. *Gut Microbes* 13, 1–17. doi: 10.1080/19490976.2020.1826746
- Farmakidis, C., Pasnoor, M., Dimachkie, M. M., and Barohn, R. J. (2018). Treatment of myasthenia gravis. *Neurol. Clin.* 36, 311–337. doi: 10.1016/j.ncl.2018.01.011
- Fujimoto, K., Kimura, Y., Allegretti, J. R., Yamamoto, M., Zhang, Y. Z., Katayama, K., et al. (2021). Functional restoration of bacteriomes and viromes by fecal microbiota transplantation. *Gastroenterology* 160, 2089–2102.e12. doi: 10.1053/j.gastro.2021.02.013
- Furusawa, Y., Obata, Y., and Hase, K. (2015). Commensal microbiota regulates T cell fate decision in the gut. *Semin. Immunopathol.* 37, 17–25. doi: 10.1007/s00281-014-0455-3
- Gajdos, P., Chevret, S., and Toyka, K. V. (2012). Intravenous immunoglobulin for myasthenia gravis. *Cochrane Database Syst. Rev.* 12:CD002277. doi: 10.1002/14651858.CD002277.pub4
- Gao, W., Guo, Y., Wang, C., Lin, Y., Yu, L., Sheng, T., et al. (2016). Indirubin ameliorates dextran sulfate sodium-induced ulcerative colitis in mice through the inhibition of inflammation and the induction of Foxp3-expressing regulatory T cells. *Acta Histochem.* 118, 606–614. doi: 10.1016/j.acthis.2016.06.004
- Gilhus, N. E., and Verschuuren, J. J. (2015). Myasthenia gravis: subgroup classification and therapeutic strategies. *Lancet Neurol.* 14, 1023–1036. doi: 10.1016/S1474-4422(15)00145-3
- Gomez, A. M., Van Den Broeck, J., Vrolix, K., Janssen, S. P., Lemmens, M. A., Van Der Esch, E., et al. (2010). Antibody effector mechanisms in myasthenia gravis-pathogenesis at the neuromuscular junction. *Autoimmunity* 43, 353–370. doi: 10.1010/08916930903555943
- Hugon, P., Dufour, J. C., Colson, P., Fournier, P. E., Sallah, K., and Raoult, D. (2015). A comprehensive repertoire of prokaryotic species identified in human beings. *Lancet Infect. Dis.* 15, 1211–1219. doi: 10.1016/S1473-3099(15)00293-5
- Imran, M., Rauf, A., Shah, Z. A., Saeed, F., Imran, A., Arshad, M. U., et al. (2019). Chemo-preventive and therapeutic effect of the dietary flavonoid kaempferol: a comprehensive review. *Phytother. Res.* 33, 263–275. doi: 10.1002/ptr.6227
- Jiang, X., Chen, G., Huang, J., Xie, L., Shen, D., Jiang, K., et al. (2018). Modified Buzhong Yiqi decoction for myasthenia gravis: a systematic review protocol. *Medicine (Baltimore)* 97:e13677. doi: 10.1097/md.00000000000013677
- Kamada, N., Seo, S. U., Chen, G. Y., and Núñez, G. (2013). Role of the gut microbiota in immunity and inflammatory disease. *Nat. Rev. Immunol.* 13, 321–335. doi: 10.1038/nri3430
- Kracht, M., Müller-Ladner, U., and Schmitz, M. L. (2020). Mutual regulation of metabolic processes and proinflammatory NF-κB signaling. *J. Allergy Clin. Immunol.* 146, 694–705. doi: 10.1016/j.jaci.2020.07.027
- Kwon, H. K., Lee, C. G., So, J. S., Chae, C. S., Hwang, J. S., Sahoo, A., et al. (2010). Generation of regulatory dendritic cells and CD4+Foxp3+ T cells by probiotics administration suppresses immune disorders. *Proc. Natl. Acad. Sci. U. S. A.* 107, 2159–2164. doi: 10.1073/pnas.0904055107
- Lan, R. Y., Mackay, I. R., and Gershwin, M. E. (2007). Regulatory T cells in the prevention of mucosal inflammatory diseases: patrolling the border. *J. Autoimmun.* 29, 272–280. doi: 10.1016/j.jaut.2007.07.021
- Li, X., He, C., Li, N., Ding, L., Chen, H., Wan, J., et al. (2020). The interplay between the gut microbiota and NLRP3 activation affects the severity of acute pancreatitis in mice. *Gut Microbes* 11, 1774–1789. doi: 10.1080/19490976.2020.1770042
- Li, J., Qi, G., and Liu, Y. (2021). Effect of Buzhong Yiqi decoction on anti-acetylcholine receptor antibody and clinical status in juvenile ocular myasthenia gravis. *Medicine (Baltimore)* 100:e27688. doi: 10.1097/md.00000000000027688
- Liu, X. Y., Chen, S. L., and Zhang, W. X. (2010). Clinical study of strengthening pi and nourishing shen therapy combined with Western medicine on patients with glucocorticoid resistant myasthenia gravis. *Zhongguo Zhong Xi Yi Jie He Za Zhi* 30, 271–274. PMID: 20535925.
- Liu, P., Jiang, Y., Gu, S., Xue, Y., Yang, H., Li, Y., et al. (2021). Metagenome-wide association study of gut microbiome revealed potential microbial marker set for diagnosis of pediatric myasthenia gravis. *BMC Med.* 19:159. doi: 10.1186/s12916-021-02034-0
- Mangalam, A., Shahi, S. K., Luckey, D., Karau, M., Marietta, E., Luo, N., et al. (2017). Human gut-derived commensal bacteria suppress CNS inflammatory and demyelinating disease. *Cell Rep.* 20, 1269–1277. doi: 10.1016/j.celrep.2017.07.031
- Mantegazza, R., Bernasconi, P., and Cavalcante, P. (2018). Myasthenia gravis: from autoantibodies to therapy. *Curr. Opin. Neurol.* 31, 517–525. doi: 10.1097/wco.0000000000000596
- Martínez, I., Stegen, J. C., Maldonado-Gómez, M. X., Eren, A. M., Siba, P. M., Greenhill, A. R., et al. (2015). The gut microbiota of rural Papua new guineans: composition, diversity patterns, and ecological processes. *Cell Rep.* 11, 527–538. doi: 10.1016/j.celrep.2015.03.049
- Montassier, E., Gastinne, T., Vangay, P., Al-Ghalith, G. A., Bruley Des Varannes, S., Massart, S., et al. (2015). Chemotherapy-driven dysbiosis in the intestinal microbiome. *Aliment. Pharmacol. Ther.* 42, 515–528. doi: 10.1111/apt.13302



- Müllges, W., and Stoll, G. (2019). Myasthenia gravis. *Nervenarzt* 90, 1055–1066. doi: 10.1007/s00115-019-00798-8
- Nakamoto, N., Sasaki, N., Aoki, R., Miyamoto, K., Suda, W., Teratani, T., et al. (2019). Gut pathobionts underlie intestinal barrier dysfunction and liver T helper 17 cell immune response in primary sclerosing cholangitis. *Nat. Microbiol.* 4, 492–503. doi: 10.1038/s41564-018-0333-1
- Narayanaswami, P., Sanders, D. B., Wolfe, G., Benatar, M., Cea, G., Evoli, A., et al. (2021). International consensus guidance for Management of Myasthenia Gravis: 2020 update. *Neurology* 96, 114–122. doi: 10.1212/wnl.00000000000011124
- Pascal, M., Perez-Gordo, M., Caballero, T., Escribese, M. M., Lopez Longo, M. N., Luengo, O., et al. (2018). Microbiome and allergic diseases. *Front. Immunol.* 9:1584. doi: 10.3389/fimmu.2018.01584
- Pivari, F., Mingione, A., Piazzini, G., Ceccarani, C., Ottaviano, E., Brasacchio, C., et al. (2022). Curcumin supplementation (Meriva®) modulates inflammation, lipid peroxidation and gut microbiota composition in chronic kidney disease. *Nutrients* 14:231. doi: 10.3390/nu14010231
- Qiu, D., Xia, Z., Jiao, X., Deng, J., Zhang, L., and Li, J. (2018). Altered gut microbiota in myasthenia gravis. *Front. Microbiol.* 9:2627. doi: 10.3389/fmicb.2018.02627
- Rinaldi, E., Consonni, A., Cordiglieri, C., Sacco, G., Crasà, C., Fontana, A., et al. (2019). Therapeutic effect of Bifidobacterium administration on experimental autoimmune myasthenia gravis in Lewis rats. *Front. Immunol.* 10:2949. doi: 10.3389/fimmu.2019.02949
- Rinaldi, E., Consonni, A., Guidesi, E., Elli, M., Mantegazza, R., and Baggi, F. (2018). Therapeutic effect of Bifidobacterium administration on experimental myasthenia gravis? *Ann. N. Y. Acad. Sci.* 1413, 49–58. doi: 10.1111/nyas.13567
- Rohr, M. W., Narasimhulu, C. A., Rudeski-Rohr, T. A., and Parthasarathy, S. (2020). Negative effects of a high-fat diet on intestinal permeability: a review. *Adv. Nutr.* 11, 77–91. doi: 10.1093/advances/nmz061
- Shahi, S. K., Freedman, S. N., Murra, A. C., Zarei, K., Sompallae, R., Gibson-Corley, K. N., et al. (2019). Prevotella histicola, a human gut commensal, is as potent as COPAXONE® in an animal model of multiple sclerosis. *Front. Immunol.* 10:462. doi: 10.3389/fimmu.2019.00462
- Shahi, S. K., Jensen, S. N., Murra, A. C., Tang, N., Guo, H., Gibson-Corley, K. N., et al. (2020). Human commensal Prevotella histicola ameliorates disease as effectively as interferon-Beta in the experimental autoimmune encephalomyelitis. *Front. Immunol.* 11:578648. doi: 10.3389/fimmu.2020.578648
- Shen, J., Yang, L., You, K., Chen, T., Su, Z., Cui, Z., et al. (2022). Indole-3-acetic acid alters intestinal microbiota and alleviates ankylosing spondylitis in mice. *Front. Immunol.* 13:762580. doi: 10.3389/fimmu.2022.762580
- Sieb, J. P. (2014). Myasthenia gravis: an update for the clinician. *Clin. Exp. Immunol.* 175, 408–418. doi: 10.1111/cei.12217
- Soderholm, A. T., and Pedicord, V. A. (2019). Intestinal epithelial cells: at the interface of the microbiota and mucosal immunity. *Immunology* 158, 267–280. doi: 10.1111/imm.13117
- Stacy, A., Andrade-Oliveira, V., McCulloch, J. A., Hild, B., Oh, J. H., Perez-Chaparro, P. J., et al. (2021). Infection trains the host for microbiota-enhanced resistance to pathogens. *Cells* 184, 615–627. doi: 10.1016/j.cell.2020.12.011
- Thaiss, C. A., Zmora, N., Levy, M., and Elinav, E. (2016). The microbiome and innate immunity. *Nature* 535, 65–74. doi: 10.1038/nature18847
- Wang, L. G., Lam, T. T., Xu, S., Dai, Z., Zhou, L., Feng, T., et al. (2020). Treeio: an R package for phylogenetic tree input and output with richly annotated and associated data. *Mol. Biol. Evol.* 37, 599–603. doi: 10.1093/molbev/msz240
- Wang, Y., Shi, C., Yu, W., Jiao, W., and Shi, G. (2022). Efficacy of Yougui pill combined with Buzhong Yiqi decoction in alleviating the sexual dysfunction in female rats through modulation of the gut microbiota. *Pharm. Biol.* 60, 46–55. doi: 10.1080/13880209.2021.2010774
- Wu, G. D., Chen, J., Hoffmann, C., Bittinger, K., Chen, Y. Y., Keilbaugh, S. A., et al. (2011). Linking long-term dietary patterns with gut microbial enterotypes. *Science* 334, 105–108. doi: 10.1126/science.1208344
- Yang, W., Yu, T., Huang, X., Bilotta, A. J., Xu, L., Lu, Y., et al. (2020). Intestinal microbiota-derived short-chain fatty acids regulation of immune cell IL-22 production and gut immunity. *Nat. Commun.* 11:4457. doi: 10.1038/s41467-020-18262-6
- Yao, Y., Kim, G., Shafer, S., Chen, Z., Kubo, S., Ji, Y., et al. (2022). Mucus sialylation determines intestinal host-commensal homeostasis. *Cells* 185, 1172–1188. doi: 10.1016/j.cell.2022.02.013
- Zhao, L., Zhang, S. L., Tao, J. Y., Jin, F., Pang, R., Guo, Y. J., et al. (2008). Anti-inflammatory mechanism of a folk herbal medicine, Duchesnea indica (Andr) Focke at RAW264.7 cell line. *Immunol. Investig.* 37, 339–357. doi: 10.1080/08820130802111589
- Zhao, C. B., Zhang, X., Zhang, H., Hu, X. Q., Lu, J. H., Lu, C. Z., et al. (2011). Clinical efficacy and immunological impact of tacrolimus in Chinese patients with generalized myasthenia gravis. *Int. Immunopharmacol.* 11, 519–524. doi: 10.1016/j.intimp.2010.12.012
- Zheng, P., Li, Y., Wu, J., Zhang, H., Huang, Y., Tan, X., et al. (2019). Perturbed microbial ecology in myasthenia gravis: evidence from the gut microbiome and fecal metabolome. *Adv. Sci.* 6:1901441. doi: 10.1002/adv.201901441
- Zong, G., Liu, S., Chen, Z., and Hu, Y. (2021). Efficacy and safety of Buzhong Yiqi decoction combined with western medicine in the treatment of myasthenia gravis: a protocol for systematic review and meta-analysis. *Medicine (Baltimore)* 100:e24807. doi: 10.1097/md.00000000000024807





## OPEN ACCESS

## EDITED BY

Weiqi He,  
Soochow University, China

## REVIEWED BY

Arunachalam Muthaiyan,  
University of New Mexico Gallup, United States  
Richard Agans,  
Air Force Research Laboratory, United States

## \*CORRESPONDENCE

Katarzyna Czarzasta  
✉ katarzyna.czarzasta@wum.edu.pl

## SPECIALTY SECTION

This article was submitted to  
Microorganisms in Vertebrate Digestive  
Systems,  
a section of the journal  
Frontiers in Microbiology

RECEIVED 07 December 2022

ACCEPTED 12 January 2023

PUBLISHED 25 January 2023

## CITATION

Kasarello K, Cudnoch-Jedrzejewska A and  
Czarzasta K (2023) Communication of gut  
microbiota and brain *via* immune  
and neuroendocrine signaling.  
*Front. Microbiol.* 14:1118529.  
doi: 10.3389/fmicb.2023.1118529

## COPYRIGHT

© 2023 Kasarello, Cudnoch-Jedrzejewska and  
Czarzasta. This is an open-access article  
distributed under the terms of the [Creative  
Commons Attribution License \(CC BY\)](#). The use,  
distribution or reproduction in other forums is  
permitted, provided the original author(s) and  
the copyright owner(s) are credited and that the  
original publication in this journal is cited, in  
accordance with accepted academic practice.  
No use, distribution or reproduction is  
permitted which does not comply with  
these terms.

# Communication of gut microbiota and brain *via* immune and neuroendocrine signaling

Kaja Kasarello, Agnieszka Cudnoch-Jedrzejewska and  
Katarzyna Czarzasta\*

Chair and Department of Experimental and Clinical Physiology, Laboratory of Centre for Preclinical  
Research, Medical University of Warsaw, Warsaw, Poland

The gastrointestinal tract of the human is inhabited by about  $5 \times 10^{13}$  bacteria (of about 1,000 species) as well as archaea, fungi, and viruses. Gut microbiota is known to influence the host organism, but the host may also affect the functioning of the microbiota. This bidirectional cooperation occurs in three main inter-organ signaling: immune, neural, and endocrine. Immune communication relies mostly on the cytokines released by the immune cells into circulation. Also, pathogen-associated or damage-associated molecular patterns (PAMPs or DAMPs) may enter circulation and affect the functioning of the internal organs and gut microbiota. Neural communication relies mostly on the direct anatomical connections made by the vagus nerve, or indirect connections *via* the enteric nervous system. The third pathway, endocrine communication, is the broadest one and includes the hypothalamic-pituitary-adrenal axis. This review focuses on presenting the latest data on the role of the gut microbiota in inter-organ communication with particular emphasis on the role of neurotransmitters (catecholamines, serotonin, gamma-aminobutyric acid), intestinal peptides (cholecystokinin, peptide YY, and glucagon-like peptide 1), and bacterial metabolites (short-chain fatty acids).

## KEYWORDS

gut-brain axis, gut microbiota, HPA axis, immune system, vagus nerve

## 1. Gastrointestinal tract as a living environment of the gut microbiota

The gastrointestinal tract (GI) is the external environment for our body. Therefore, the GI epithelium has to act as the protective barrier for the organism. Tight junctions connecting the epithelial cells and mucus produced by goblet cells are the physical barriers ([Vancamelbeke and Vermeire, 2017](#)). Moreover, enterocytes produce antimicrobial peptides (AMPs) which act directly on the bacterial cell membrane, causing its disruption and cell lysis ([Chung and Raffatellu, 2018](#)). Furthermore, the gut-associated lymphoid tissue (GALT) defends the organism against pathogens and, more importantly, maintains homeostasis in the GI tract ([Mörbe et al., 2021](#)). The molecules which allow our immune system to recognize potentially harmful microorganisms are the microorganism-associated molecular patterns (MAMPs), or in general for pathogens—the pathogen-associated molecular patterns (PAMPs). Such patterns are recognized by pattern recognition receptors (PRRs) present on the host cells of the innate immune system ([Takeuchi and Akira, 2010](#); [Wang and Wang, 2016](#)). All these factors contribute

to limiting the direct contact of the gastrointestinal epithelium with the microbiota. Therefore, the symbiotic gut microbiota which colonizes our intestines influences the GI epithelium, and interacts with the immune system, but in a limited scope (Hooper et al., 2012).

## 2. Gut microbiota—Characteristics

The term gut microbiota describes the microorganisms that exist in the GI, consisting mainly of bacteria, but also of archaea, fungi, and viruses (Quigley, 2017; Zhao and Elson, 2018; Zhao et al., 2021). The term microbiome, which is a broader concept that refers to microorganisms, their genomes, and the habitat they reside in, is often used instead of the term gut microbiota.

The colonization of the GI tract mostly takes place during birth, but there is evidence of trans-placental gut colonization (Quigley, 2017). It was shown that the gut microbiota profile in humans changes with the age of the host and is most stable in adulthood (Nicholson et al., 2012; Carabotti et al., 2015). In the healthy adult human, there are about  $5 \times 10^{13}$  bacteria (of about 1000 species) in the gut, mostly represented by the two phyla, *Firmicutes* and *Bacteroidetes* (Quigley, 2017; Zhao and Elson, 2018; Zhao et al., 2021), as well as less numerous *Actinobacteria*, *Proteobacteria*, *Fusobacteria*, *Verrucomicrobia*, and *Archaea* (Dubinski et al., 2021). The available data suggest that gender may have a significant influence on the composition and activity of gut microbiota (Makris et al., 2021). Clinical studies have shown that men when compared with women have an increased number of *Bacteroides* and *Prevotella*, as well as *Clostridia*, *Bacteroidetes*, and *Proteobacteria* phylum (Kovacs et al., 2011). However, the mechanisms explaining the above observation remain unclear (Bolnick et al., 2014).

The condition in which the balance between the commensal microflora and pathogenic microorganisms is maintained is called eubiosis (Iebba et al., 2016). Each deviation from the normal composition of gut microbiota (instability or a decrease in the number of *Firmicutes* and *Bacteroidetes*) and the accompanying violation of the intestinal epithelial barrier is referred to as dysbiosis, i.e., a deviation leading to an inflammatory state (Ahlawat et al., 2021; Dubinski et al., 2021).

The host organism creates favorable conditions for the development of gut microbiota, which in turn exert many positive effects on the host. Bacteria, through fermentation processes, produce metabolites such as lactates and short-chain fatty acids (SCFAs), which include acetate (C2), propionate (C3), and butyrate (C4) (Silva et al., 2020). These substances, synthesized in the gastrointestinal tract, can enter the circulation through the portal vein, and then *via* the blood to the peripheral tissues and organs, and also to the brain (Lerner et al., 2017). For example, butyrate is the most abundant of the SCFAs. It is synthesized in the large intestine by the following types of bacteria: *Clostridium*, *Eubacterium*, and *Butyrivibrio* (Bourassa et al., 2016; Czerwińska et al., 2021; Amiri et al., 2022; Table 1). It has been shown that butyrate has anti-inflammatory properties and has a positive effect on the intestinal epithelium, which may have a positive effect on the gut microbiota, increasing the number of the ENS cholinergic neurons, as well as modulating appetite through vagal and hypothalamic stimulation (Liu et al., 2018). Additionally, gut microbiota plays an important role in the synthesis of vitamins (K, riboflavin, biotin, nicotinic acid, pantothenic acid, pyridoxine, thiamine, and

folic acid), and the metabolism of bile acids (Thursby and Juge, 2017). However, gut microbiota can also have adverse effects on the host organism, including the synthesis and release into the blood of lipopolysaccharide (LPS), also called endotoxin, which is a component of the cell wall of gram-negative bacteria and plays a key role in the initiation and progression of inflammation (Cani et al., 2012; Dubinski et al., 2021).

The gut microbiota has been shown to influence the host organism in three major pathways: (a) *via* immune systems, (b) *via* neurotransmitters, and (c) *via* microbial metabolites (Wang and Wang, 2016).

### 2.1. Gut microbiota and immune system interaction

As previously mentioned, the mucus layer reduces to a large extent the direct contact of the gut microbiota with the GI epithelium. Bacteria that reach deeper into the mucosal surface are sampled by the protrusions of the dendritic cells (DCs), which are the specialized antigen-presenting cells (APCs). Next, the DCs go to the mesenteric lymph node, where the sampled antigens are presented to T and B lymphocytes (Hooper et al., 2012).

In the state of eubiosis, physical barriers are intact and molecules such as IgA and AMPs, present in the gut lumen, provide the control mechanisms inhibiting the pathogen spreading. Moreover, symbiotic bacteria itself produces the AMPs against pathogenic strains (Iebba et al., 2016). Immune cells composing GALT present the tolerogenic phenotype as the result of the influence of transforming growth factor  $\beta$  (TGF $\beta$ ) produced by the epithelial cells. TGF $\beta$  causes the differentiation of immune cells toward the anti-inflammatory tolerogenic phenotype. In addition, CD103 + DCs residing in the lamina propria produce anti-inflammatory interleukin 10 (IL-10), which further influences T and B cell differentiation (Siddiqui and Powrie, 2008; Moro-Sibilot et al., 2016; Pathak et al., 2020). B cells in the mesenteric lymph nodes produce the IgA antibodies against the bacterial antigens, and next go to the lamina propria and secrete the IgA into the intestinal lumen. Here, the IgA binds to the bacterial antigens and prevents bacterial translocation through the gut epithelium. In case of bacterial penetration under the epithelium, the resident macrophages and DCs in the lamina propria phagocyte the microorganisms (Hooper et al., 2012). In turn, naive T cells under the influence of the commensal bacteria antigens are differentiated into regulatory T cells (Tregs) (Lathrop et al., 2011). Such a mechanism underlies the mechanism of oral tolerance, which prevents the evoking of an immune response against dietary antigens and against symbiotic microflora. Furthermore, induced Tregs secrete the anti-inflammatory cytokines, IL-10, and TGF- $\beta$ . When the pathogenic bacteria encounter GALT, naive T cells differentiate into Th1/Th17 subtypes, producing proinflammatory cytokines (Zhao and Elson, 2018). Moreover, CD103<sup>+</sup> DCs also contribute to the production of retinoic acid (RA) from vitamin A, which is induced by the SCFAs obtained from dietary fibers. RA is also the factor inducing Tregs differentiation (Luu et al., 2017). In such a homeostatic state, tolerance to dietary antigens and antigens from commensal microflora is maintained.

On the other hand, during dysbiosis, pathogens and their harmful metabolites are recognized by the PRRs on the surface of the

TABLE 1 The butyrate-producing bacteria.

Domain	Phylum	Class	Order	Family	Genus	Species
Bacteria	Firmicutes	Clostridia	Eubacteriales	Clostridiaceae	<i>Butyricoccus</i>	<i>Butyricoccus pullicaecorum</i>
					<i>Clostridium</i>	<i>Clostridium acetobutylicum</i>
						<i>Clostridium butyricum</i>
						<i>Clostridium saccharobutylicum</i>
						<i>Clostridium tyrobutyricum</i>
						<i>Clostridium orbiscidens</i>
						<i>Clostridium hathewayi</i>
						<i>Clostridium indolis</i>
						<i>Clostridium nexile</i>
					<i>Subdoligranulum</i>	<i>Subdoligranulum variabile</i>
				Lachnospiraceae	<i>Anaerostipes</i>	<i>Anaerostipes butyraticus</i>
						<i>Anaerostipes caccae</i>
						<i>Anaerostipes hadrus</i>
						<i>Anaerostipes rhamnosivorans</i>
					<i>Butyrivibrio</i>	<i>Butyrivibrio crossotus</i>
						<i>Butyrivibrio fibrisolvens</i>
						<i>Butyrivibrio proteoclasticus</i>
					<i>Coprococcus</i>	<i>Coprococcus catus</i>
						<i>Coprococcus comes</i>
						<i>Coprococcus eutactus</i>
					<i>Roseburia</i>	<i>Roseburia cecicola</i>
						<i>Roseburia faecis</i>
						<i>Roseburia hominis</i>
						<i>Roseburia intestinalis</i>
						<i>Roseburia inulinivorans</i>
					<i>Shuttleworthia</i>	<i>Shuttleworthia satelles</i>
				Oscillospiraceae	<i>Anaerotruncus</i>	<i>Anaerotruncus colihominis</i>
					<i>Faecalibacterium</i>	<i>Faecalibacterium prausnitzii</i>
					<i>Papillibacter</i>	<i>Papillibacter cinnamivorans</i>
					<i>Ruminococcus</i>	<i>Ruminococcus gnavus</i>
						<i>Ruminococcus obeum</i>
				Eubacteriaceae	<i>Eubacterium</i>	<i>Eubacterium cylindroides</i>
						<i>Eubacterium hallii</i>
						<i>Eubacterium limosum</i>
						<i>Eubacterium ramulus</i>
						<i>Eubacterium rectale</i>
						<i>Eubacterium ruminantium</i>
			Thermoanaerobacterales	Thermosediminibacteraceae	<i>Caldicellulosiruptor</i>	<i>Caldicellulosiruptor saccharolyticus</i>
	Negativicutes		Veillonellales	Veillonellaceae	<i>Megasphaera</i>	<i>Megasphaera elsdenii</i>

immune cells of the host, and an innate immune response is evoked. Enterotoxins released by pathogens, such as LPS, cause damage to the intestinal epithelium, which results in gut permeability and the entrance of pathogens into the circulation. The damage to the gut epithelium may also contribute to intestinal inflammation. Environmental factors, such as a western diet, antibiotics, stress, or injury may cause damage to the gut epithelium, allowing bacterial gut

penetration, which induces an immune reaction (Cresci and Bawden, 2015; Lobionda et al., 2019). Mediators released by the immune cells during an inflammatory reaction enter the circulation to attract more immune cells. PAMPs released from damaged pathogens may also enter the circulation.

Two examples of PRRs are toll-like receptors (TLRs) and nucleotide-binding oligomerization domain (NOD)-like receptors

(McCusker and Kelley, 2013). The interaction of PRRs and PAMPs results in the activation of intracellular signaling pathways, leading to nuclear factor kappa-light-chain-enhancer of activated B cells (NF- $\kappa$ B) translocation to the nucleus, and results in the activation of gene transcription for proinflammatory cytokines (e.g., interleukin-1, IL-1; tumor necrosis factor  $\alpha$ , TNF $\alpha$ ; interferon gamma, IFN $\gamma$ ) (McCusker and Kelley, 2013). Interestingly, the TLRs of the innate immune systems can distinguish between the MAMPs of the symbiotic bacteria from those present on the surface of the pathogens (Korecka and Arulampalam, 2012).

The above-mentioned cells and molecules, such as immune cells differentiated under the influence of symbiotic or pathogenic microflora, cytokines, inflammatory mediators, pathogen toxins, and PAMPs after translocation into the systemic circulation, may further infiltrate the central nervous system (CNS) and influence its functioning (Zhang et al., 2021).

## 2.2. Gut microbiota and neurotransmitters interaction

The main neurotransmitters that may play a role in the gut-brain axis communication are serotonin, dopamine, noradrenaline, and gamma-aminobutyric acid (GABA) (Cox and Weiner, 2018; Makris et al., 2021). These substances are synthesized not only in the CNS but also in enteroendocrine (EEC) cells that have the ability to synthesize neurotransmitters under the influence of intestinal peptides, as well as the gut microbiota itself (Makris et al., 2021).

It is worth emphasizing that one percent of the intestinal epithelial cells are EEC cells, the role of which is to synthesize and release substances into the intestinal lumen in the presence of ingested carbohydrates, triglycerides, and proteins, and to regulate intestinal motility, secretion, and food intake (Näslund and Hellström, 2007; Gunawardene et al., 2011; Wu et al., 2013).

It has been shown that EEC cells synthesize approximately 90 percent of the total serotonin produced in the human body (Bellono et al., 2017). Moreover, an important role in the synthesis of serotonin is played by the liver expressing the enzyme tryptophan-2,3-dioxygenase (TDO, tryptophan pyrolase), degrading tryptophan to N-formylkynurenine, which is then deformed by formidases to kynurenine. This reduces the concentration of tryptophan which may be converted to the serotonin in the brain (Wirleitner et al., 2003; Müller and Daya, 2008). In the digestive system, serotonin is involved in the activation of innate intestinal reflexes, mediating intestinal-brain communication, regulating the immune system, and has a protective/regenerative effect on neuronal cells and the interstitial cells of Cajal, but on the other hand it may cause enteritis (Mawe and Hoffman, 2013). Studies indicate that the level and activity of serotonin, synthesized both in the CNS and peripherally, is strongly influenced by the gut microbiota. In particular, a few representatives of the gut microbiota such as *Candida*, *Streptococcus*, *Escherichia*, and *Enterococcus* are capable of producing serotonin directly (Holzer and Farzi, 2014; Jameson and Hsiao, 2018). Nevertheless, it was noticed that serotonin has a significant effect on the composition and activity of the gut microbiota. Fung et al. (2019) observed that elevated intestinal serotonin levels increased the relative abundance of spore-forming bacteria.

Serotonin as well as other neurotransmitters, including dopamine and norepinephrine, are involved in gut-brain communication

(Makris et al., 2021). It has been found that both dopamine and norepinephrine can be synthesized directly by the gut microbiota. Dopamine can be synthesized by the following microorganisms: *Bacillus cereus*, *Bacillus mycoides*, *Bacillus subtilis*, *Escherichia coli*, *Hafnia alvei*, *Klebsiella pneumoniae*, *Morganella morganii*, *Proteus vulgaris*, and *Staphylococcus aureus*. In turn, norepinephrine can be synthesized by: *Bacillus mycoides*, *Bacillus subtilis*, *Escherichia coli*, and *Proteus vulgaris* (Strandwitz, 2018). Moreover, gut microbiota is capable of synthesizing oxidases such as laccase, which has oxidizing properties, and catabolize catecholamines to reactive oxygen species (ROS) and dopamine quinone (DAQ), which is associated with mitochondrial dysfunction and dementia in patients with Parkinson's disease (Sharma et al., 2018). Gut microbiota may also play a role in the transport of catecholamines (Singh et al., 2007). In addition, gut microbiota may affect the availability of tryptophan, a precursor to catecholamines (Rackers et al., 2018). These data appear to have important implications because the nucleus tractus solitarius (NTS), the main site for catecholamine synthesis, receives signals from the phrenic and vagus nerves (Paton et al., 2000). In turn, the NTS, via noradrenergic neurons and catecholamines, can activate the hypothalamic-pituitary-adrenal (HPA) axis, which has a significant impact on the composition and activity of the gut microbiota (Herman et al., 2016).

It has also been shown that GABA is directly synthesized by some types of intestinal bacteria, mainly: *Bifidobacterium* spp. and *Lactobacillus* spp. (Strandwitz, 2018). In addition, it was found that lactate, a substrate for the SCFAs produced by gut microbiota, through the pathway dependent on the brain G protein-coupled receptor 81 (GPR81), induces anti-GABA-transmitting effects (Caspani et al., 2019). On the other hand, the administration of *Lactobacillus rhamnosus* contributed to an increase in the expression of GABA receptors in the cingulate cortex and a decrease in the expression of GABA receptors in the hippocampus, amygdala, and the locus coeruleus, leading to a reduction in anxiety and depressive-like behavior in adult male BALB/c mice (Tanida et al., 2005; Bravo et al., 2011).

## 2.3. Gut microbiota metabolites and brain interaction

It appears that SCFAs can influence the brain indirectly by activating the immune system and the autonomic nervous system (Stilling et al., 2016). First, SCFAs are able to stimulate the activity of microglia and change the selectivity of the blood-brain barrier (BBB) permeability (Strandwitz, 2018). It is likely that the abundant exposure of H<sup>+</sup> dependent monocarboxylate transporters (MCTs) in endothelial cells may facilitate the penetration of SCFAs by BBB. Clinical studies have shown the presence of SCFAs in human cerebrospinal fluid (CSF) in the following range: acetate 0–171  $\mu$ M, propionate 0–6  $\mu$ M, and butyrate 0–2.8  $\mu$ M. In addition, the mean level of SCFAs in the human brain is 17.0 pmol/mg of tissue for butyrate, and 18.8 pmol/mg of tissue for propionate (Silva et al., 2020). The SCFAs also appear to play a significant role in maintaining the integrity of the BBB. Studies on germ-free mice showed decreased expression of tight junction proteins such as claudin and occludin in the endothelium, leading to increased BBB permeability. In turn, colonization of adult germ-free mice with complex microflora or monocolonization with SCFA-producing bacterial strains restored BBB integrity (Braniste et al., 2014).



It has also been shown that SCFAs can act indirectly on the CNS by binding SCFAs to their receptors on EEC cells, stimulating the secretion of GLP-1 and PYY, which can act on the CNS *via* the vagus nerve (Bliss and Whiteside, 2018). Another mechanism by which SCFAs respond to systemic functions is the inhibition of histone deacetylase (HDAC) activity, thereby promoting the acetylation of a lysine residue present in histones and nucleosomes in various cell populations, including the intestine, the autonomic nervous system (ANS), and the CNS (Stilling et al., 2016).

It was also found that SCFAs can affect the synthesis of neurotransmitters in the CNS, butyrate and propionate are able to stimulate the synthesis of dopamine and norepinephrine, and propionic acid can modulate serotonergic neurotransmission and affect the levels of GABA, dopamine, and serotonin (Nankova et al., 2014; El-Ansary et al., 2015; Stilling et al., 2016). The available data suggest that the SCFAs synthesized by the gut microbiota after entering the host cells (passive diffusion and/or active transport) inhibit the histone deacetylase inhibitor (HDAC) or, by interacting with membrane receptors, activate various intracellular signaling pathways that modify the expression of a given gene (Nankova et al., 2014; Stilling et al., 2016). It has been shown that butyric and propionic acids can regulate tyrosine hydroxylase (TH) mRNA levels through various transcription factors, including the activation of the cAMP-response element binding protein (CREB) and, consequently, may lead to increased production of catecholamines (Nankova et al., 2014).

Short-chain fatty acids may also modulate the expression of signaling molecules important for learning and memory, such as brain-derived neurotrophic factor (BDNF), *N*-methyl-D-aspartate receptor subtype 2B (NR2B) subunit, the serotonin transporter, and the neuropeptide Y system. It has been shown that sodium butyrate is able to stimulate BDNF expression, neurogenesis, and neuronal proliferation in rodents, and facilitate long-term consolidation (Silva et al., 2020). Moreover, SCFAs influence several nervous functions, such as the regulation of the circadian rhythm and the control of appetite (Silva et al., 2020; Williams et al., 2020; Makris et al., 2021). It appears that SCFAs may affect neuronal function through a pathway dependent on GPR41 and GPR43 receptors or HDAC inhibitory activity (Nankova et al., 2014; Patnala et al., 2017).

### 3. Gut-brain axis (GBA)

The observed concordance of the phylogenetic trees of the gut microbiota and primates indicates co-evolution of the host organism, including humans, with the resident microorganisms. Through co-evolution, the gut microbiota influenced the formation of the host's immune system, which developed complex mechanisms for identifying and destroying microbes (Dominguez-Bello et al., 2019). Moreover, available data suggest that gut microbiota may influence host brain activities such as behavior, appetite regulation, and serotonin metabolism (Schroeder and Bäckhed, 2016). Changes in gut microbiota composition have been linked to many neurological diseases such as neurodegenerative disorders (Vogt et al., 2017). The above effects on the host brain are likely to be exerted by gut microbiota *via* the gut-brain axis (GBA). Moreover, the same pathway enables the CNS to influence the composition and activity of the gut microbiota (Ahlawat et al., 2021; Makris et al., 2021). The gut-brain axis is a bidirectional signaling pathway between the gut and the CNS

(Bauer et al., 2016), and this action is possible through three GBA communication pathways: (1) immunological; (2) neuroanatomical; and (3) neuroendocrine (Wang and Wang, 2016).

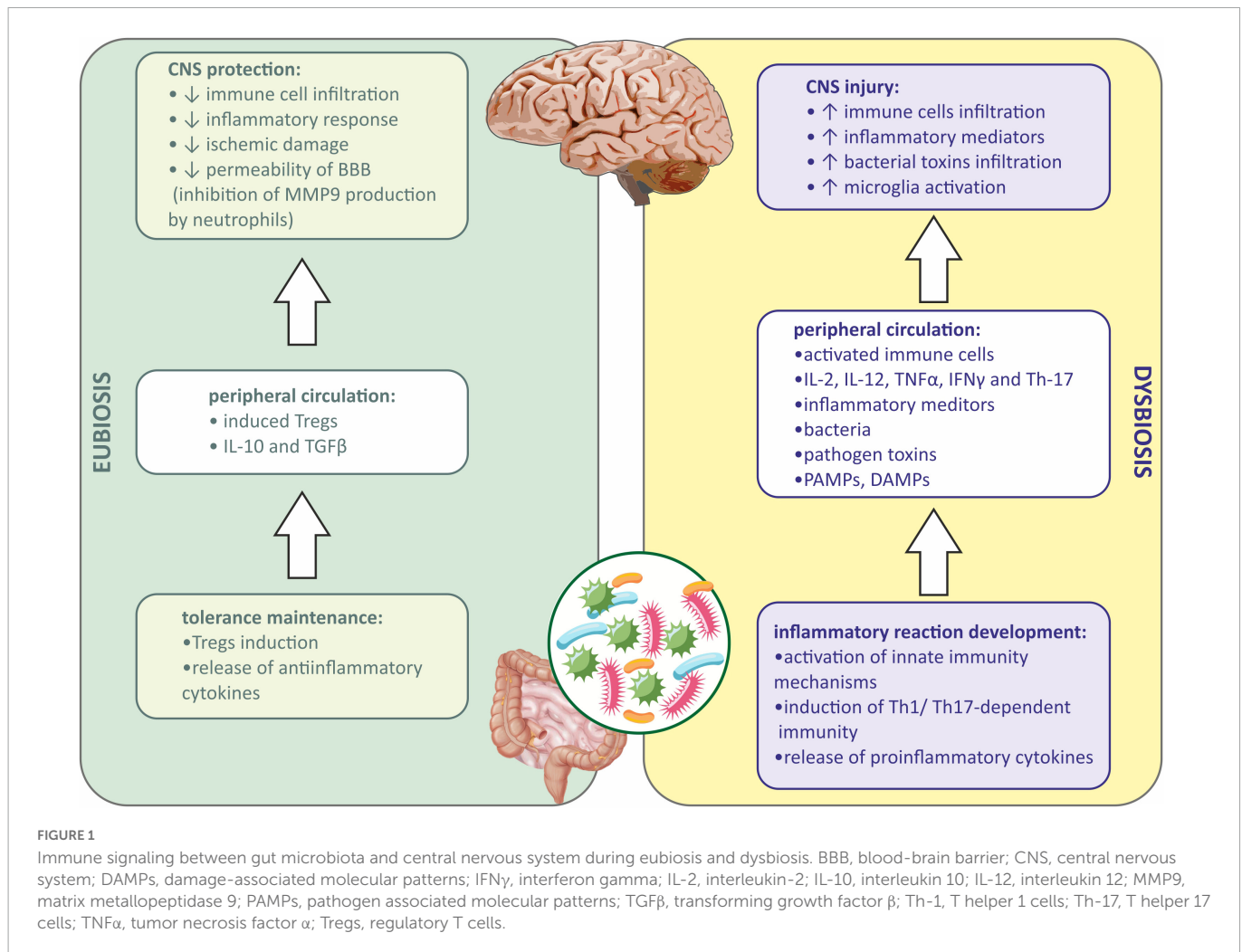
#### 3.1. Immunological signalization in the GBA

As described above, the immune mechanisms are shifted to anti-inflammatory responses in the state of eubiosis in the gut (Lee and Kim, 2017). Tregs are generated when antigens are presented by DCs to lymphocytes in the GALT during the eubiotic state (Lathrop et al., 2011). Tregs produce anti-inflammatory cytokines, such as IL-10 and TGF $\beta$ , which are responsible for the inhibition of proinflammatory cytokine production, switching the immune response from Th1/Th17-dependent to Th2-dependent (Li et al., 2021), and therefore quenching the immune reaction and promoting the repair process in the damaged tissue (Mingomataj and Bakiri, 2016). Induced Tregs may also translocate into circulation and inhibit the inflammatory responses in the organism (Weiner and Wu, 2011). The depletion of Tregs was shown to increase CNS damage in mice after stroke (Liesz et al., 2009). It was also presented that Tregs may influence the CNS from the periphery. In rodents with ischemic stroke evoked, injection of Tregs diminished immune cell infiltration, inflammatory response, and ischemic damage of the brain. This was due to the inhibition of matrix metalloproteinase-9 (MMP-9) production by neutrophils, which suppressed the remodeling of the BBB and decreased its permeability (Li et al., 2013; Figure 1).

When dysbiosis occurs, a local inflammatory response in the gut is observed first, and then peripheral inflammation develops when inflammatory mediators, bacteria, metabolites, PAMPs, etc., enter the systemic circulation (Lobionda et al., 2019). Both innate and adaptive immune mechanisms are involved. PAMPs *via* PRR receptors on the host cells activate innate immunity mechanisms (Bergstrom et al., 2012). In addition, the immune cells in GALT are involved during dysbiosis, and lymphocytes under the influence of inflammatory mediators and PAMPs differentiate into proinflammatory subtype (Th1 and Th17), and further produce proinflammatory cytokines, such as interleukin-2 (IL-2), interleukin-12 (IL-12), TNF $\alpha$ , IFN $\gamma$ , and Th-17. Peripheral inflammation affects the BBB integrity, allowing the infiltration of immune cells and inflammatory mediators into the CNS (Amoo et al., 2021). Besides, bacterial toxins present in the circulation may also infiltrate into the CNS (Abdel-Haq et al., 2019; Zhang et al., 2021). Microglia, resident immune cells in the CNS may be further activated by infiltrating proinflammatory cytokines from the periphery, and sterile immune reaction may be evoked, eventually causing CNS injury (Cryan et al., 2019; Gwak and Chang, 2021; Figure 1).

The gut-brain immune communication acts in both ways. After injury of the CNS caused by mechanical injury, stroke, infection, etc., the damaged tissue releases damage-associated molecular patterns (DAMPs) activating resident microglia. Activated microglia of the proinflammatory (M1) phenotype release inflammatory mediators acting as chemoattractants and are responsible for recruiting peripheral immune cells to the inflammation site. Those cells, neutrophils, monocytes, and CD4<sup>+</sup> T cells, also produce proinflammatory cytokines, which together with DAMPs may enter the peripheral circulation and affect the peripheral tissues (Shichita et al., 2009). If the intestinal barrier is reached, gut inflammation





may be evoked, causing gut permeability, epithelial injury, and the entrance of pathogenic bacteria into circulation. This may eventually lead to systemic inflammation (Arya and Hu, 2018). Moreover, intestinal inflammation causes the reduction in Tregs differentiation and IL-10 and TGF $\beta$  secretion and the promotion of a Th1/Th17-dependent immune reaction. Such a lack of anti-inflammatory signaling and promotion of proinflammatory mechanisms further activates the immune cells and exacerbates the inflammation of the CNS (Rahman and Dandekar, 2021; Schächtle and Rosshart, 2021; Figure 2).

### 3.2. Neuroanatomicsignaling in gut microbiota-brain communication

Based on the available data, it can be concluded that the gut microbiota-induced vagal signaling affects the critical immune components of the microbiota-gut-brain axis and allows the vagus nerve to be seen as an integral part of the bidirectional neuroimmunoendocrine pathway (Liu et al., 2021; Figure 3). Therefore, two pathways can be distinguished at the neuroanatomical level. The first direct way between the GI and the brain consists of the vagus nerve and the ANS. While the second indirect way is made by the connection between the ANS and the enteric nervous system (ENS) (Wang and Wang, 2016).

It has been proven that the vagus nerve plays a key role in the communication between the gut microbiota and the brain *via* anatomical signaling (Czerwińska et al., 2021; Makris et al., 2021). Some researchers believe that the vagus nerve innervates the entire digestive tract, while others argue that it only innervates to the left colon flexion (Bonaz et al., 2018). Vagal afferent fibers are distributed in all layers of the gastrointestinal wall but do not penetrate the epithelial layer into the lumen of the intestine (Wang and Powley, 2007). The afferent endings of the vagus nerve have been divided into three subtypes: (1) afferent endings located at the apices of the intestinal villi directly under the epithelial wall; (2) afferent endings around the intestinal glands or crypts located below the crypt-villus junction; (3) afferent endings along the antral glands of the stomach (afferent endings of the antral gland) forms the end concentrations directly below the luminal epithelial wall (Powley et al., 2011). All of the above vagus nerve endings are both chemosensitive and mechanosensitive (Bonaz et al., 2018). Vagus nerve chemoreceptors are presumed to be involved in communication between the gut microbiota and the brain by detecting SCFAs and/or intestinal peptides (Raybould, 2010; Figure 3). Oleate (one of the SCFAs) acts on the vagal afferent fibers *via* cholecystokinin (CCK), while butyrate can directly activate the vagus nerve (Lal et al., 2001). Similarly, the LPS synthesized by the gut microbiota can interact with the TLRs located on the vagus nerve fibers at the nodose ganglion level (Hosoi et al., 2005; Figure 3).

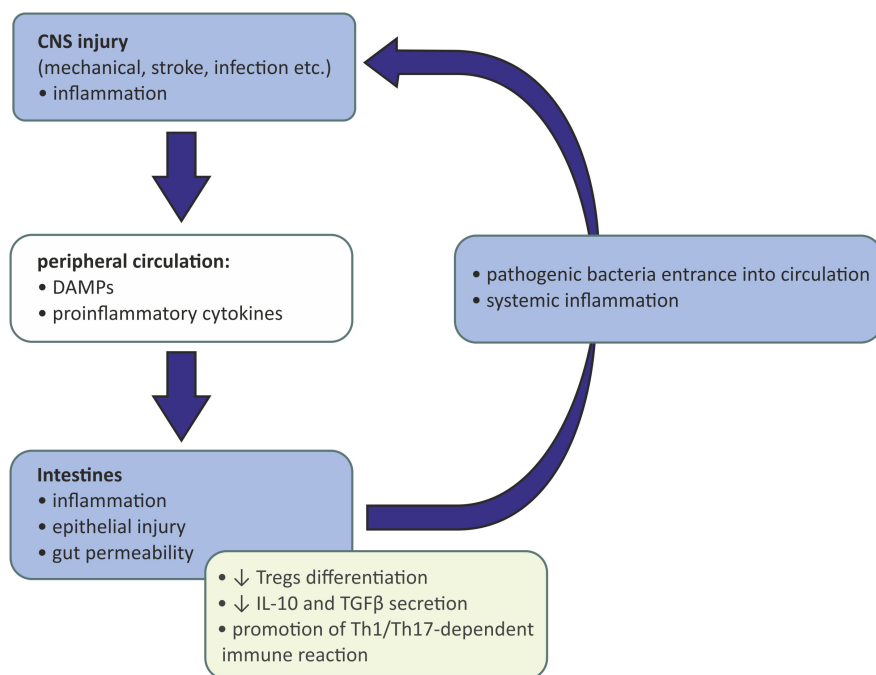


FIGURE 2

Influence of injured and inflamed central neurons system on gut microbiota. CNS, central nervous system; DAMPs, damage-associated molecular patterns; IL-10, interleukin 10; TGFβ, transforming growth factor β; Th-1, T helper 1 cells; Th-17, T helper 17 cells; Tregs, regulatory T cells.

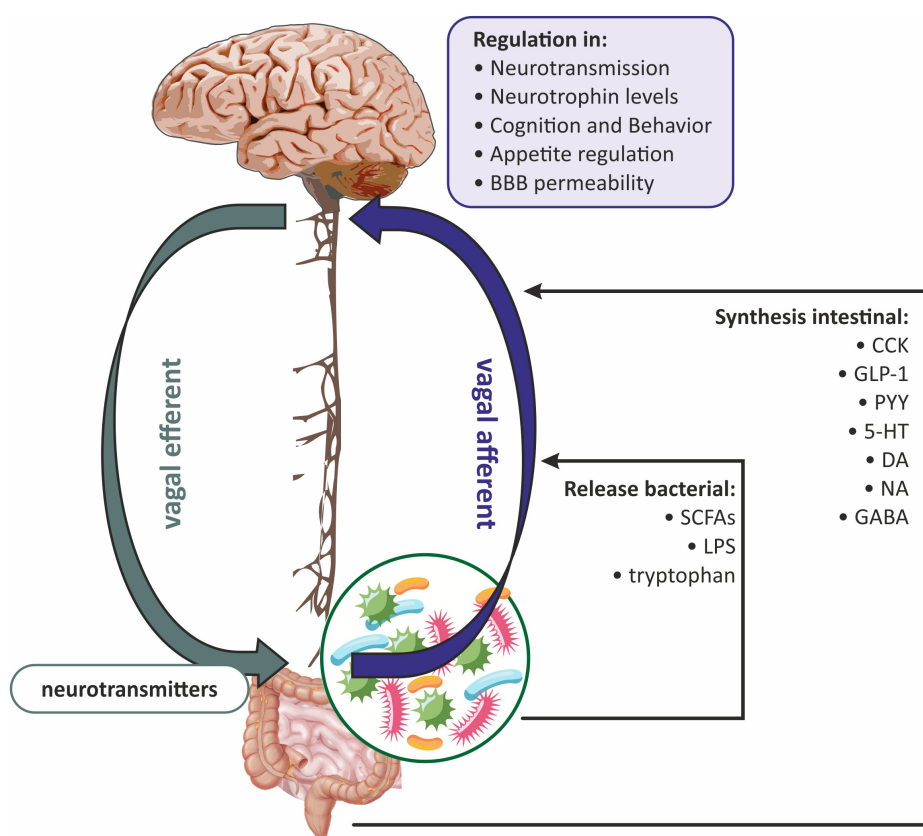


FIGURE 3

The role of the vagus nerve in gut microbiota-brain communications. BBB, blood-brain barrier; CCK, cholecystokinin; DA, dopamine; GABA, gamma-aminobutyric acid; GLP-1, glucagon-like peptide-1; 5-HT, serotonin; LPS, lipopolysaccharide; NA, noradrenaline; PYY, peptide YY (PYY); SCFAs, short-chain fatty acids.

The vagus nerve can also receive signals from the gastrointestinal tract indirectly, involving the ENS, which is part of the autonomic nervous system. The ENS consists mainly of enteric glial cells (EGCs), which resemble astrocytes in the CNS (Ahlawat et al., 2021). The ENS is distributed throughout the intestinal wall, including the lamina propria of the mucosa (Obata and Pachnis, 2016; Kho and Lal, 2018). From the ganglia of the ENS, the neuron fibers go to the prevertebral ganglia and then to the spinal cord at the level of the T5-L2 and S2-S4 segments, and to the vagal nuclei. Afferent fibers of the vagus nerve and spinal cord concentrate hormonal and mechanical stimuli in the NTS and in the dorsal motor nucleus, where the signal is integrated, and next sent to the hypothalamus, as well as to the basal ganglia and brain stem nuclei (Sobrinho Crespo et al., 2014; Bauer et al., 2016; Zhao et al., 2018). NTS signaling is mediated by proopiomelanocortin (POMC), catecholaminergic neurons, and N-methyl-D-aspartate (NMDA) glutamate receptors (Bauer et al., 2016; Bliss and Whiteside, 2018). The vagus nerve can also receive information from the intestinal lumen *via* enteroendocrine (EEC) cells, which make up one percent of all intestinal epithelial cells (Bonaz et al., 2018). It has been shown that EEC can release serotonin (5-HT), which then activates 5-HT<sub>3</sub> receptors on the vagal afferent fibers (Li et al., 2000). EEC effects on the vagus nerve may also be indirect through intestinal peptides such as CCK, glucagon-like peptide-1 (GLP-1), and peptide YY (PYY) (Strader and Woods, 2005). In general, gut hormones fall into two broad categories: orexigenic, for example, ghrelin, which together with neuropeptide Y (NPY) and agouti-related peptide (AGRP) neurons, increases hunger; and anorexigenic, i.e., appetite-suppressing peptides such as GLP-1, PYY, and CCK (Weltens et al., 2018). The vagus nerve has receptors for both anorexigenic and orexigenic intestinal peptides (Strader and Woods, 2005). Subsequently, the signal is sent to the CNS, ultimately leading to the modulation of reward regions (amygdala and nucleus accumbens) and appetite regulation (Weltens et al., 2018; Czerwińska et al., 2021; Figure 3).

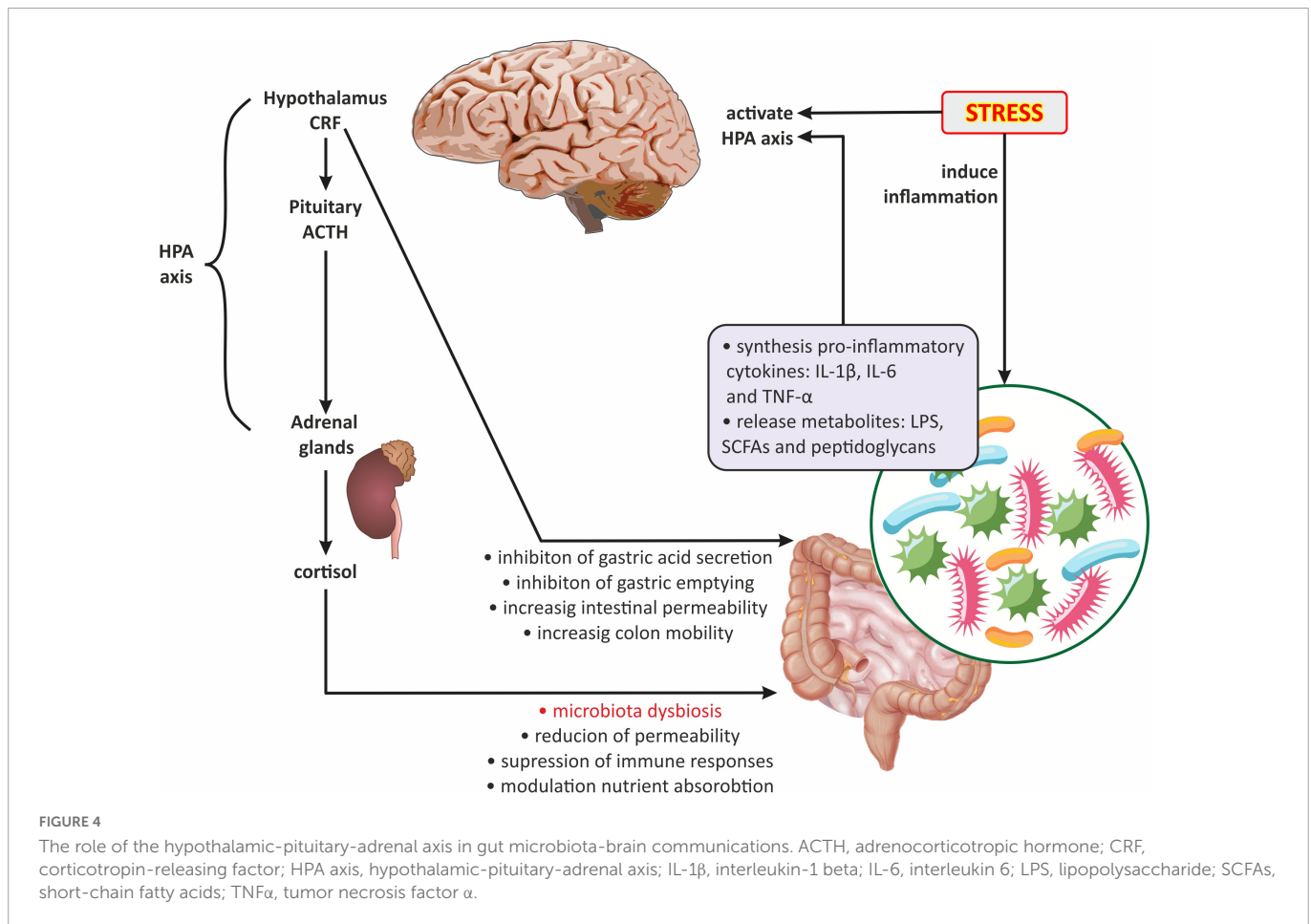
Evidence for the direct influence of the gut microbiota on the activation of the vagus nerve is provided by a few experimental studies. *Ex vivo* studies have shown that the application of *Lactobacillus johnsonii* to the isolated fragment of the jejunum contributed to an increase in the firing rate of the vagus nerve fibers, which was prevented by the previous subdiaphragmatic vagotomy (Perez-Burgos et al., 2013). It was reported that duodenal injection of *Lactobacillus johnsonii* in male Wistar rats caused an increase in gastric activity of the vagus nerve (Tanida et al., 2005). It was also shown that signals sent by the gut microbiota *via* the vagus nerve can go directly to the CNS. Male mice receiving *Lactobacillus rhamnosus* for 14 days showed a reduction in anxiety-like behavior and a decrease in the HPA axis activity. Whereas vagotomy in these mice abolished the anxiolytic effects induced by *Lactobacillus rhamnosus* (Liu et al., 2021). Bravo et al. (2011) observed that chronic oral administration of *Lactobacillus rhamnosus* (JB-1) in healthy adult male BALB/c mice increased gamma-aminobutyric acid (GABA) expression in the cingulate cortex and decreased GABA in the hippocampus, amygdala, and locus coeruleus. Interestingly, the above effects were abolished by vagotomy. In addition, studies in healthy Sprague Dawley rats have shown that one of the bacterial metabolites, indole, can stimulate the ECC of the colon to secrete GLP-1, which in turn stimulated colonic vagal afferent activity (Buckley et al., 2020). Recently, Tashtush et al. (2022) showed that administration of fecal supernatant from patients with active inflammatory bowel disease (IBD) on the C57/Bl6 mouse vagal afferent neurons (nodose

ganglion; NG) increased their excitability, possibly due to mediators such as cysteine protease, activating protease-activated receptor 2 (PAR2) dependent signaling pathways, which leads to the inhibition of voltage-gated K<sup>+</sup> currents.

Moreover, available data have shown that gut microbiota can affect the nervous system of the host by altering the metabolism of neurotransmitters. Studies (Engevik et al., 2021) on adult germ-free Swiss Webster mice treated with live *Bifidobacterium dentium* *via* oral gavage showed that bacterial-produced acetate contributed not only to increased 5-HT release from the EEC, but also increased 5-HT<sub>2a</sub> receptor expression in the hippocampus and lowered the anxiety-like behaviors in the tested mice. In turn, a study (Peng et al., 2022) revealed that another bacterial metabolite, succinate, has a protective effect on dopaminergic neurons in the substantia nigra. In addition, it was shown that oral supplementation of the three major SCFAs (acetate, propionate, and butyrate) in C57BL/6J mice undergoing psychosocial stress reduced disturbance in food-seeking behavior as well as reducing anti-depressant and anti-anxiety effects (van de Wouw et al., 2018). SCFAs are presumed to affect the host nervous system in a hormone-like fashion *via* specific G-protein coupled receptors (GPCRs) (Barki et al., 2022), which also include many metabotropic neurotransmitter receptors. On the other hand, emotional disorders such as chronic stress not only affect the metabolism of neurotransmitters but also have strong implications on the composition of the gut microbiota (Yang et al., 2021). Moreover, norepinephrine, a stress-related hormone has been shown to increase the abundance of *Desulfovibrio vulgaris*. A significant population increase of this bacterium is observed in patients with inflammatory bowel disease and irritable bowel syndrome (Coffman et al., 2022).

### 3.3. Neuroendocrine signaling in the gut microbiota-brain communication

The neuroendocrine level primarily includes the HPA axis, which plays a key role in the stress response and is also one of the main components of the gut-brain axis. The HPA axis begins in the paraventricular nucleus of the hypothalamus, where the corticotropin releasing factor (CRF) is synthesized. In turn, CRF stimulates the pituitary gland to produce the adrenocorticotrophic hormone (ACTH), which leads to the release of glucocorticoids (cortisol and corticosterone) from the adrenal cortex (Misiak et al., 2020). In addition, CRF stimulates the locus coeruleus to synthesize catecholamines, thus leading to an increase in the noradrenergic activity of the brain (Jedema and Grace, 2004). There is evidence that the gut microbiota develops in parallel with the HPA axis, moreover, they are in constant communication (de Weerth, 2017; Frankiensztajn et al., 2020; Misiak et al., 2020; Williams et al., 2020). Interestingly, the two-way communication between the gut microbiota and the HPA axis is increasingly emphasized (Dinan and Cryan, 2017; Foster et al., 2017; Morris and Ridlon, 2017; Figure 4). It has been reported that the abnormal formation of the HPA axis during brain development may affect microbial colonization and visceral sensitivity (Pellissier and Bonaz, 2017). Irritable bowel syndrome studies have shown that cortisol can directly activate resident immune cells and external primary afferent fibers in the gastrointestinal tract (Moloney et al., 2016). Moreover, both experimental and clinical researchers have demonstrated that the stress-related HPA axis response can increase intestinal permeability



leading to dysbiosis (Vicario et al., 2012; Vanuytsel et al., 2014; Figure 4).

Significant information on the existence of interactions between the gut microbiota and the HPA axis was provided by Sudo et al. (2004). These researchers demonstrated that germ-free mice (GF; mice raised in the absence of microbes) were more sensitive to restraint stress than mice with normally functioning microbiota but in the absence of specific pathogens (SPF; specific pathogen-free mice). GF mice also showed decreased levels of cortical glucocorticoid receptor mRNA expression and increased levels of CRF mRNA and protein in the hypothalamus compared with SPF mice. Moreover, the same researchers observed that the increase in plasma ACTH and corticosterone levels in response to restrictive stress was significantly greater in GF mice compared with SPF mice. Probably the observed differences in stress response between GF and SPF mice could also be caused by decreased expression of POMC and encoding CRF receptor type 1 (Crhr1) genes (Vagnerová et al., 2019).

Experimental studies have also shown that numerous stressors causing an increase in the activity of the HPA axis may affect the development of dysbiosis (Dubinski et al., 2021). It has been shown that chronic s.c. injection of ACTH hormone fragment in female Wistar rats not only caused their depressive-like behavior, but also caused changes in the community of gut microbiota, namely a marked increase in *Ruminococcus* and *Klebsiella* and a reduction in the population of *Akkermansia* and *Lactobacillus* (Song et al., 2019). Wu et al. (2020) in research carried out on rats with stress-induced hypertension (SIH) noted a reduction in HPA axis hyperactivity and blood pressure due to the administration of an

antibiotic cocktail containing ampicillin, vancomycin, neomycin, and metronidazole. Catecholamines released in response to stress probably play an important role in this process. It was proven that catecholamines can stimulate the growth of gram-negative bacteria (Lyte and Ernst, 1992). The above data seem to confirm studies conducted in patients suffering from irritable bowel syndrome (IBS) in combination with emotional distress including anxiety and depressive symptoms. In these patients, already slightly lower concentrations of serotonin and norepinephrine corresponded to significant changes in the composition of gut microbiota. Namely, serotonin levels were positively correlated with the abundance of *Proteobacteria*, and norepinephrine was positively correlated with *Bacteroidetes* and negatively correlated with *Firmicutes* (Barandouzi et al., 2022). Similarly, clinical data confirmed that stress and the accompanying increased cortisol blood level have a significant impact on the development of gut dysbiosis (Misiak et al., 2020).

In contrast, both experimental and clinical studies revealed that probiotics based on *Bacillus licheniformis*, *Saccharomyces boulardii*, *Lactobacillus rhamnosus*, and *Bifidobacterium* spp. contributed to the inhibition of stress-induced HPA axis hyperactivity, as well as alleviated depressive-like behavior and anxiety-related behavior (Eutamene et al., 2007; Gareau et al., 2007; Desbonnet et al., 2010).

It appears that the gut microbiota can act on the HPA axis through several mechanisms (Figure 4): (1) gut dysbiosis contributes to the increased release of pro-inflammatory cytokines, including IL-1, IL-6, and TNF- $\alpha$  which can cross the BBB and activate the HPA axis (Turnbull and Rivier, 1995; Banks, 2005); (2) the HPA axis can be activated by bacterial metabolites such as LPS, SCFAs, and



peptidoglycans (components of bacterial cell walls) (Arentsen et al., 2017; van de Wouw et al., 2018); (3) by the influence of gut microbiota on the HPA axis *via* the vagus nerve, affecting the NTS activity of noradrenergic neurons (Paton et al., 2000; Herman et al., 2016); and (4) by changes in HPA axis activity caused by the modulation of central gene expression in the hippocampus and hypothalamus by gut microbiota (Frankensztajn et al., 2020).

## 4. The role of the gut-brain axis in the treatment of CNS diseases

Currently, many researchers emphasize the possibility of using the gut-brain axis in the treatment of many neurological diseases such as autism spectrum disorder (ASD), Alzheimer's disease (AD), and Parkinson's disease (PD) (Metta et al., 2022; Taniya et al., 2022; Varesi et al., 2022).

Clinical studies increasingly point to a link between ASD and intestinal dysfunction. It is estimated that up to 70% of children with ASD have impaired function of the digestive tract (Sajdel-Sulkowska et al., 2019). In the case of gut microbiota, these abnormalities concern the development of an excessive number of pathogenic bacteria such as *Clostridium tetani* (Shaw, 2010). In turn, treating children with ASD with anti-clostridium antibiotics resulted in a decrease in typical behaviors for them (Kang et al., 2017). Moreover, high hopes are attached to Microbiota Transfer Therapy (MTT) in the treatment of patients with ASD (Taniya et al., 2022).

Currently, the role of disorders in the functioning of the gut brain-axis in the pathogenesis of neurodegenerative diseases such as AD and PD is increasingly emphasized. Damage to the intestinal barrier is hypothesized to lead to a systemic inflammatory response, which in turn impairs BBB function and promotes neuroinflammation leading to neurodegeneration and neuron damage. Consequently, damaged GBA potentiates  $\beta$ -amyloid deposition in AD and misfolding and aggregation of  $\alpha$ -synuclein in PD (Quigley, 2017). Similar to patients with ASD, also in the case of therapy of patients with neurodegenerative diseases, much attention is paid to the need to restore the proper composition of the gut microbiota with fecal microbiota transplantation (FMT) or probiotics (Metta et al., 2022; Varesi et al., 2022). It is likely that FMT has a beneficial effect on reducing symptoms in patients with PD through neuroprotective effects against toxicity induced by the TLR4/TNF- $\alpha$  signaling pathway and 1-methyl-4-phenyl-1,2,3,6-tetrahydropyridine (MPTP) (Metta et al., 2022). So far, few clinical trials have shown the beneficial effect of FMT on improving cognition, memory, and mood, as well as gut microbiota biodiversity and SCFA production in patients with AD (Hazan, 2020; Park et al., 2021). However, the results of studies on the effect of probiotics on symptom improvement in patients with AD are inconclusive. Akbari et al. (2016) showed that after 12 weeks of daily administration of a mixture of *Lactobacillus acidophilus*, *Lactobacillus casei*, *Bifidobacterium bifidum*, and *Lactobacillus fermentum*, AD patients showed a significant improvement in mini-mental state exam results. On the other hand, the administration of two different probiotic mixtures: one containing *Lactobacillus fermentum*, *Lactobacillus plantarum*, and *Bifidobacterium lactis* and the other containing *Lactobacillus acidophilus*, *Bifidobacterium bifidum*, and *Bifidobacterium longum*, did not contribute to the improvement of cognitive functions in patients with severe Alzheimer's disease

(Agahi et al., 2018). Moreover, numerous studies indicate a well-chosen diet as a quick way to modify the composition and metabolism of the gut microbiota, reduce inflammation, and help maintain eubiosis and proper dependencies in the gut-brain axis (Metta et al., 2022; Varesi et al., 2022).

## 5. Conclusion

Gut microbiota, which is an integral part of the human body, is able to summon and control many of its physiological processes. The host organism also has great influence on the composition and activity of the gut microbiota. Recent studies show that the gut-brain axis is a well-established concept, indicating the bidirectional cooperation between two organs of the human body, the brain, and the gut, and in particular the microbiota residing in the intestines. Many studies have shown the engagement of different routes of communication able to transmit information between the two separate organs, such as immune, nervous, and endocrine. It was also proved that disturbances in one of the organs may affect the proper functioning of the other, also in a bidirectional manner. Unfortunately, the routes for signal transduction involved in the gut-brain communication are still not fully known as well as what roles are played by inflammation, neurotransmitters, intestinal peptides, and bacterial metabolites. In addition, a significant amount of information on the gut-brain axis activity comes from studies on animal models, which, while providing relevant information, should not be directly extrapolated to the human population. Therefore, more research is needed to elucidate the importance of gut microbiota not only for adult organisms, but also for developing ones, with the target of preventing or treating CNS diseases.

## Author contributions

KK and KC: methodology, resources, and writing—original draft preparation. KC and AC-J: supervision. KC: project administration. All authors conceptualization, writing—review and editing, read, and agreed to the published version of the manuscript.

## Conflict of interest

The authors declare that the research was conducted in the absence of any commercial or financial relationships that could be construed as a potential conflict of interest.

## Publisher's note

All claims expressed in this article are solely those of the authors and do not necessarily represent those of their affiliated organizations, or those of the publisher, the editors and the reviewers. Any product that may be evaluated in this article, or claim that may be made by its manufacturer, is not guaranteed or endorsed by the publisher.

## References

- Abdel-Haq, R., Schlachetzki, J. C. M., Glass, C. K., and Mazmanian, S. K. (2019). Microbiome-microglia connections via the gut-brain axis. *J. Exp. Med.* 216, 41–59. doi: 10.1084/jem.20180794
- Agahi, A., Hamidi, G. A., Daneshvar, R., Hamdieh, M., Soheili, M., Alinaghypour, A., et al. (2018). Does severity of Alzheimer's disease contribute to its responsiveness to modifying gut microbiota? A double blind clinical trial. *Front. Neurol.* 9:662. doi: 10.3389/fneur.2018.00662
- Ahlatwat, S., Asha, and Sharma, K. K. (2021). Gut-organ axis: A microbial outreach and networking. *Lett. Appl. Microbiol.* 72, 636–668. doi: 10.1111/lam.13333
- Akbari, E., Asemi, Z., Daneshvar Kakhaki, R., Bahmani, F., Kouchaki, E., Tamtaji, O. R., et al. (2016). Effect of probiotic supplementation on cognitive function and metabolic status in Alzheimer's disease: A randomized, double-blind and controlled trial. *Front. Aging Neurosci.* 8:256. doi: 10.3389/fnagi.2016.00256
- Amiri, P., Hosseini, S., Ghaffari, S., Tutunchi, H., Ghaffari, S., Mosharkesh, E., et al. (2022). Role of Butyrate, a gut microbiota derived metabolite, in cardiovascular diseases: A comprehensive narrative review. *Front. Pharmacol.* 12:837509. doi: 10.3389/fphar.2021.837509
- Amoo, M., O'Halloran, P. J., Henry, J., Husien, M., Ben Brennan, P., Campbell, M., et al. (2021). Permeability of the blood-brain barrier after traumatic brain injury: radiological considerations. *J. Neurotrauma* 39, 20–34. doi: 10.1089/neu.2020.7545
- Arentsen, T., Qian, Y., Gkotsis, S., Femenia, T., Wang, T., Udekwu, K., et al. (2017). The bacterial peptidoglycan-sensing molecule Pglyrp2 modulates brain development and behavior. *Mol. Psychiatry* 22, 257–266. doi: 10.1038/mp.2016.182
- Arya, A. K., and Hu, B. (2018). Brain-gut axis after stroke. *Brain Circ.* 4, 165–173. doi: 10.4103/bc.bc\_32\_18
- Banks, W. A. (2005). Blood-brain barrier transport of cytokines: A mechanism for neuropathology. *Curr. Pharm. Des.* 11, 973–984. doi: 10.2174/1381612053381684
- Barandouzi, Z. A., Lee, J., del Carmen Rosas, M., Chen, J., Henderson, W. A., Starkweather, A. R., et al. (2022). Associations of neurotransmitters and the gut microbiome with emotional distress in mixed type of irritable bowel syndrome. *Sci. Rep.* 12, 1–11. doi: 10.1038/s41598-022-05756-0
- Barki, N., Bolognini, D., Börjesson, U., Jenkins, L., Riddell, J., Hughes, D. I., et al. (2022). Chemogenetics defines a short-chain fatty acid receptor gut-brain axis. *Elife* 11:e73777. doi: 10.7554/eLife.73777
- Bauer, P. V., Hamr, S. C., and Duca, F. A. (2016). Regulation of energy balance by a gut-brain axis and involvement of the gut microbiota. *Cell. Mol. Life Sci.* 73, 737–755. doi: 10.1007/s00018-015-2083-z
- Bellono, N. W., Bayrer, J. R., Leitch, D. B., Castro, J., Zhang, C., O'Donnell, T. A., et al. (2017). Enterochromaffin cells are gut chemosensors that couple to sensory neural pathways. *Cell* 170, 185–198.e16. doi: 10.1016/j.cell.2017.05.034
- Bergstrom, K. S., Sham, H. P., Zarepour, M., and Vallance, B. A. (2012). Innate host responses to enteric bacterial pathogens: A balancing act between resistance and tolerance. *Cell. Microbiol.* 14, 475–484. doi: 10.1111/j.1462-5822.2012.01750.x
- Bliss, E. S., and Whiteside, E. (2018). The gut-brain axis, the human gut microbiota and their integration in the development of obesity. *Front. Physiol.* 9:900. doi: 10.3389/fphys.2018.00900
- Bolnick, D. I., Snowberg, L. K., Hirsch, P. E., Lauber, C. L., Org, E., Parks, B., et al. (2014). Individual diet has sex-dependent effects on vertebrate gut microbiota. *Nat. Commun.* 5:4500. doi: 10.1038/ncomms5500
- Bonaz, B., Bazin, T., and Pellissier, S. (2018). The vagus nerve at the interface of the microbiota-gut-brain axis. *Front. Neurosci.* 12:49. doi: 10.3389/fnins.2018.00049
- Bourassa, M. W., Alim, I., Bultman, S. J., and Ratan, R. R. (2016). Butyrate, neuroepigenetics and the gut microbiome: Can a high fiber diet improve brain health? *Neurosci. Lett.* 625, 56–63. doi: 10.1016/j.neulet.2016.02.009
- Braniste, V., Al-Asmakh, M., Kowal, C., Anuar, F., Abbaspour, A., Tóth, M., et al. (2014). The gut microbiota influences blood-brain barrier permeability in mice. *Sci. Transl. Med.* 6:263ra158. doi: 10.1126/scitranslmed.3009759
- Bravo, J. A., Forsythe, P., Chew, M. V., Escaravage, E., Savignac, H. M., Dinan, T. G., et al. (2011). Ingestion of *Lactobacillus* strain regulates emotional behavior and central GABA receptor expression in a mouse via the vagus nerve. *Proc. Natl. Acad. Sci. U.S.A.* 108, 16050–16055. doi: 10.1073/pnas.1102999108
- Buckley, M. M., O'Brien, R., Brosnan, E., Ross, R. P., Stanton, C., Buckley, J. M., et al. (2020). Glucagon-like peptide-1 secreting l-cells coupled to sensory nerves translate microbial signals to the host rat nervous system. *Front. Cell. Neurosci.* 14:95. doi: 10.3389/fncel.2020.00095
- Can, P. D., Osto, M., Geurts, L., and Everard, A. (2012). Involvement of gut microbiota in the development of low-grade inflammation and type 2 diabetes associated with obesity. *Gut Microbes* 3, 279–288. doi: 10.4161/gmic.19625
- Carabotti, M., Scirocco, A., Maselli, M. A., and Severi, C. (2015). The gut-brain axis: Interactions between enteric microbiota, central and enteric nervous systems. *Ann. Gastroenterol.* 28, 203–209.
- Caspani, G., Kennedy, S., Foster, J. A., and Swann, J. (2019). Gut microbial metabolites in depression: Understanding the biochemical mechanisms. *Microb. Cell* 6, 454–481. doi: 10.15698/mic2019.10.693
- Chung, L. K., and Raffatellu, M. (2018). G.I. pros: Antimicrobial defense in the gastrointestinal tract. *Semin. Cell Dev. Biol.* 88, 129–137. doi: 10.1016/j.semcdb.2018.02.001
- Coffman, C. N., Varga, M. G., Alcock, J., Carrol-Portillo, A., Singh, S. B., Xue, X., et al. (2022). Norepinephrine induces growth of *Desulfovibrio vulgaris* in an iron dependent manner. *Anaerobe* 75:102582. doi: 10.1016/j.anaerobe.2022.102582
- Cox, L. M., and Weiner, H. L. (2018). Microbiota signaling pathways that influence neurologic disease. *Neurother. J. Am. Soc. Exp. Neurother.* 15, 135–145. doi: 10.1007/s13311-017-0598-8
- Cresci, G. A., and Bawden, E. (2015). Gut microbiome: What we do and don't know. *Nutr. Clin. Pract.* 30, 734–746. doi: 10.1177/0884533615609899
- Cryan, J. F., O'Riordan, K. J., Cowan, C. S. M., Sandhu, K. V., Bastiaansen, T. F. S., Boehme, M., et al. (2019). The microbiota-gut-brain axis. *Physiol. Rev.* 99, 1877–2013. doi: 10.1152/physrev.00018.2018
- Czerwińska, M., Czarzasta, K., and Cudnoch-Jędrzejewska, A. (2021). New peptides as potential players in the crosstalk between the brain and obesity, metabolic and cardiovascular diseases. *Front. Physiol.* 12:692642. doi: 10.3389/fphys.2021.692642
- de Weerth, C. (2017). Do bacteria shape our development? Crosstalk between intestinal microbiota and HPA axis. *Neurosci. Biobehav. Rev.* 83, 458–471. doi: 10.1016/j.neubiorev.2017.09.016
- Desbonnet, L., Garrett, L., Clarke, G., Kiely, B., Cryan, J. F., and Dinan, T. G. (2010). Effects of the probiotic *Bifidobacterium infantis* in the maternal separation model of depression. *Neuroscience* 170, 1179–1188. doi: 10.1016/j.neuroscience.2010.08.005
- Dinan, T. G., and Cryan, J. F. (2017). Microbes immunity and behavior: Psychoneuroimmunology Meets the microbiome. *Neuropsychopharmacology* 42, 178–192. doi: 10.1038/npp.2016.103
- Dominguez-Bello, M., Godoy-Vitorino, F., Knight, R., and Blaser, M. (2019). Role of the microbiome in human development. *Gut* 68, 1108–1114. doi: 10.1136/gutjnl-2018-317503
- Dubinski, P., Czarzasta, K., and Cudnoch-Jędrzejewska, A. (2021). The influence of gut microbiota on the cardiovascular system under conditions of obesity and chronic stress. *Curr. Hypertens. Rep.* 23:31. doi: 10.1007/s11906-021-01144-7
- El-Ansary, A., Bhat, R. S., Al-Daihan, S., and Al Dbass, A. M. (2015). The neurotoxic effects of ampicillin-associated gut bacterial imbalances compared to those of orally administered propionic acid in the etiology of persistent autistic features in rat pups: Effects of various dietary regimens. *Gut Pathog.* 7:7. doi: 10.1186/s13099-015-0054-4
- Engvik, M. A., Luck, B., Visuthranukul, C., Ihekweazu, F. D., Engvik, A. C., Shi, Z., et al. (2021). Human-derived *Bifidobacterium dentium* modulates the mammalian serotonergic system and gut-brain axis. *Cell. Mol. Gastroenterol. Hepatol.* 11, 221–248. doi: 10.1016/j.jcmgh.2020.08.002
- Eutamene, H., Lamine, F., Chabo, C., Theodorou, V., Rochat, F., Bergonzelli, G. E., et al. (2007). Synergy between *Lactobacillus paracasei* and its bacterial products to counteract stress-induced gut permeability and sensitivity increase in rats. *J. Nutr.* 137, 1901–1907. doi: 10.1093/jn/137.8.1901
- Foster, J. A., Rinaman, L., and Cryan, J. F. (2017). Stress & the gut-brain axis: Regulation by the microbiome. *Neurobiol. Stress* 7, 124–136. doi: 10.1016/j.yynstr.2017.03.001
- Frankiyszajn, L. M., Elliott, E., and Koren, O. (2020). The microbiota and the hypothalamus-pituitary-adrenocortical (HPA) axis, implications for anxiety and stress disorders. *Curr. Opin. Neurobiol.* 62, 76–82. doi: 10.1016/j.conb.2019.12.003
- Fung, T. C., Vuong, H. E., Luna, C. D. G., Pronovost, G. N., Aleksandrova, A. A., Riley, N. G., et al. (2019). Intestinal serotonin and fluoxetine exposure modulate bacterial colonization in the gut. *Nat. Microbiol.* 4, 2064–2073. doi: 10.1038/s41564-019-0540-4
- Gareau, M. G., Jury, J., MacQueen, G., Sherman, P. M., and Perdue, M. H. (2007). Probiotic treatment of rat pups normalises corticosterone release and ameliorates colonic dysfunction induced by maternal separation. *Gut* 56, 1522–1528. doi: 10.1136/gut.2006.117176
- Gunawardene, A. R., Corfe, B. M., and Staton, C. A. (2011). Classification and functions of enteroendocrine cells of the lower gastrointestinal tract. *Int. J. Exp. Pathol.* 92, 219–231. doi: 10.1111/j.1365-2613.2011.00767.x
- Gwak, M. G., and Chang, S. Y. (2021). Gut-brain connection: Microbiome, gut barrier, and environmental sensors. *Immune Netw.* 21, 1–18. doi: 10.4110/in.2021.21.e20
- Hazan, S. (2020). Rapid improvement in Alzheimer's disease symptoms following fecal microbiota transplantation: A case report. *J. Int. Med. Res.* 48:300060520925930. doi: 10.1177/0300060520925930
- Herman, J. P., McKlveen, J. M., Ghosal, S., Kopp, B., Wulsin, A., Makinson, R., et al. (2016). Regulation of the hypothalamic-pituitary-adrenocortical stress response. *Compr. Physiol.* 6, 603–621. doi: 10.1002/cphy.c150015
- Holzer, P., and Farzi, A. (2014). Neuropeptides and the microbiota-gut-brain axis. *Adv. Exp. Med. Biol.* 817, 195–219. doi: 10.1007/978-1-4939-0897-4\_9
- Hooper, L. V., Littman, D. R., and Macpherson, A. J. (2012). Interactions between the microbiota and the immune system. *Science* 336, 1268–1273. doi: 10.1126/science.1223490

- Hosoi, T., Okuma, Y., Matsuda, T., and Nomura, Y. (2005). Novel pathway for LPS-induced afferent vagus nerve activation: Possible role of nodose ganglion. *Auton. Neurosci.* 120, 104–107. doi: 10.1016/j.autneu.2004.11.012
- Iebba, V., Totino, V., Gagliardi, A., Santangelo, F., Cacciotti, F., Trancassini, M., et al. (2016). Eubiosis and dysbiosis: The two sides of the microbiota. *New Microbiol.* 39, 1–12.
- Jameson, K. G., and Hsiao, E. Y. (2018). Linking the gut microbiota to a brain neurotransmitter. *Trends Neurosci.* 41, 413–414. doi: 10.1016/j.tins.2018.04.001
- Jedema, H. P., and Grace, A. A. (2004). Corticotropin-releasing hormone directly activates noradrenergic neurons of the locus ceruleus recorded in vitro. *J. Neurosci.* 24, 9703–9713. doi: 10.1523/JNEUROSCI.2830-04.2004
- Kang, D., Adams, J., Gregory, A., Borody, T., Chittick, L., Fasano, A., et al. (2017). Microbiota transfer therapy alters gut ecosystem and improves gastrointestinal and autism symptoms: An open-label study. *Microbiome* 5:10. doi: 10.1186/s40168-016-0225-7
- Kho, Z. Y., and Lal, S. K. (2018). The human gut microbiome – a potential controller of wellness and disease. *Front. Microbiol.* 9:1835. doi: 10.3389/fmicb.2018.01835
- Korecka, A., and Arulampalam, V. (2012). The gut microbiome: Scourge, sentinel or spectator? *J. Oral Microbiol.* 4. doi: 10.3402/jom.v4i0.9367
- Kovacs, A., Ben-Jacob, N., Tayem, H., Halperin, E., Iraqi, F. A., and Gophna, U. (2011). Genotype is a stronger determinant than sex of the mouse gut microbiota. *Microb. Ecol.* 61, 423–428. doi: 10.1007/s00248-010-9787-2
- Lal, S., Kirkup, A. J., Brunson, A. M., Thompson, D. G., and Grundy, D. (2001). Vagal afferent responses to fatty acids of different chain length in the rat. *Am. J. Physiol. Gastrointest. Liver Physiol.* 281, G907–G915. doi: 10.1152/ajpgi.2001.281.4.G907
- Lathrop, S. K., Bloom, S. M., Rao, S. M., Nutsch, K., Lio, C.-W., Santacruz, N., et al. (2011). Peripheral education of the immune system by colonic commensal microbiota. *Nature* 478, 250–254. doi: 10.1038/nature10434
- Lee, N., and Kim, W. U. (2017). Microbiota in T-cell homeostasis and inflammatory diseases. *Exp. Mol. Med.* 49:e340. doi: 10.1038/emmm.2017.36
- Lerner, A., Neidhöfer, S., and Matthias, T. (2017). The gut microbiome feelings of the brain: A perspective for non-microbiologists. *Microorganisms* 5:66. doi: 10.3390/microorganisms5040066
- Li, P., Gan, Y., Sun, B. L., Zhang, F., Lu, B., Gao, Y., et al. (2013). Adoptive regulatory T-cell therapy protects against cerebral ischemia. *Ann. Neurol.* 74, 458–471. doi: 10.1002/ana.23815
- Li, R., Wang, R., Zhong, S., Asghar, F., Li, T., Zhu, L., et al. (2021). TGF- $\beta$ 1-overexpressing mesenchymal stem cells reciprocally regulate Th17/Treg cells by regulating the expression of IFN- $\gamma$ . *Open Life Sci.* 16, 1193–1202. doi: 10.1515/biol-2021-0118
- Li, Y., Hao, Y., Zhu, J., and Owyang, C. (2000). Serotonin released from intestinal enterochromaffin cells mediates luminal non-cholecystokinin-stimulated pancreatic secretion in rats. *Gastroenterology* 118, 1197–1207. doi: 10.1016/S0016-5085(00)70373-8
- Liesz, A., Suri-Payer, E., Veltkamp, C., Doerr, H., Sommer, C., Rivest, S., et al. (2009). Regulatory T cells are key cerebroprotective immunomodulators in acute experimental stroke. *Nat. Med.* 15, 192–199. doi: 10.1038/nm.1927
- Liu, H., Wang, J., He, T., Becker, S., Zhang, G., Li, D., et al. (2018). Butyrate: A double-edged sword for health? *Adv. Nutr.* 9, 21–29. doi: 10.1093/advances/nmx009
- Liu, Y., Sanderson, D., Mian, M. F., McVey Neufeld, K.-A., and Forsythe, P. (2021). Loss of vagal integrity disrupts immune components of the microbiota-gut-brain axis and inhibits the effect of *Lactobacillus rhamnosus* on behavior and the corticosterone stress response. *Neuropharmacology* 195:108682. doi: 10.1016/j.neuropharm.2021.108682
- Lobionda, S., Sittipo, P., Kwon, H. Y., and Lee, Y. K. (2019). The Role of gut microbiota in intestinal inflammation with respect to diet and extrinsic stressors. *Microorganisms* 7:271. doi: 10.3390/microorganisms7080271
- Luu, M., Steinhoff, U., and Visekruna, A. (2017). Functional heterogeneity of gut-resident regulatory T cells. *Clin. Transl. Immunol.* 6:e156. doi: 10.1038/cti.2017.39
- Lyte, M., and Ernst, S. (1992). Catecholamine induced growth of gram negative bacteria. *Life Sci.* 50, 203–212. doi: 10.1016/0024-3205(92)90273-r
- Makris, A. P., Karianaki, M., Tsamis, K. I., and Paschou, S. A. (2021). The role of the gut-brain axis in depression: Endocrine, neural, and immune pathways. *Hormones* 20, 1–12. doi: 10.1007/s42000-020-00236-4
- Mawe, G. M., and Hoffman, J. M. (2013). Serotonin signalling in the gut—functions, dysfunctions and therapeutic targets. *Nat. Rev. Gastroenterol. Hepatol.* 10, 473–486. doi: 10.1038/nrgastro.2013.105
- McCusker, R. H., and Kelley, K. W. (2013). Immune-neural connections: How the immune system's response to infectious agents influences behavior. *J. Exp. Biol.* 216, 84–98. doi: 10.1242/jeb.073411
- Metta, V., Leta, V., Mrudula, K., Prashanth, L., Goyal, V., Borgohain, R., et al. (2022). Gastrointestinal dysfunction in Parkinson's disease: Molecular pathology and implications of gut microbiome, probiotics, and fecal microbiota transplantation. *J. Neurol.* 269, 1154–1163. doi: 10.1007/s00415-021-10567-w
- Mingomataj, E. Ç., and Bakiri, A. H. (2016). Regulator versus effector paradigm: Interleukin-10 as Indicator of the switching response. *Clin. Rev. Allergy Immunol.* 50, 97–113. doi: 10.1007/s12016-015-8514-7
- Misiak, B., Loniewski, I., Marlicz, W., Frydecka, D., Szulc, A., Rudzki, L., et al. (2020). The HPA axis dysregulation in severe mental illness: Can we shift the blame to gut microbiota? *Prog. Neuropsychopharmacol. Biol. Psychiatry* 102:109951. doi: 10.1016/j.pnpbp.2020.109951
- Moloney, R. D., Johnson, A. C., O'Mahony, S. M., Dinan, T. G., Greenwood-Van Meerveld, B., and Cryan, J. F. (2016). Stress and the microbiota-gut-brain axis in visceral pain: Relevance to irritable bowel syndrome. *CNS Neurosci. Ther.* 22, 102–117. doi: 10.1111/cns.12490
- Mörbe, U. M., Jørgensen, P. B., Fenton, T. M., von Burg, N., Riis, L. B., Spencer, J., et al. (2021). Human gut-associated lymphoid tissues (GALT); diversity, structure, and function. *Mucosal Immunol.* 14, 793–802. doi: 10.1038/s41385-021-00389-4
- Moro-Sibilot, L., This, S., Blanc, P., Sanlaville, A., Sisirak, V., Bardel, E., et al. (2016). Plasmacytoid dendritic cells are dispensable for noninfectious intestinal IgA responses in vivo. *Eur. J. Immunol.* 46, 354–359. doi: 10.1002/eji.201545977
- Morris, D. J., and Ridlon, J. M. (2017). Glucocorticoids and gut bacteria: “The GALF hypothesis” in the metagenomic era. *Steroids* 125, 1–13. doi: 10.1016/j.steroids.2017.06.002
- Müller, A., and Daya, S. (2008). Acyclovir inhibits rat liver tryptophan-2,3-dioxygenase and induces a concomitant rise in brain serotonin and 5-hydroxyindole acetic acid levels. *Metab. Brain Dis.* 23, 351–360. doi: 10.1007/s11011-008-9095-4
- Nankova, B. B., Agarwal, R., MacFabe, D. F., and La Gamma, E. F. (2014). Enteric bacterial metabolites propionic and butyric acid modulate gene expression, including CREB-dependent catecholaminergic neurotransmission, in PC12 cells—possible relevance to autism spectrum disorders. *PLoS One* 9:e103740. doi: 10.1371/journal.pone.0103740
- Näslund, E., and Hellström, P. M. (2007). Appetite signaling: From gut peptides and enteric nerves to brain. *Physiol. Behav.* 92, 256–262. doi: 10.1016/j.physbeh.2007.05.017
- Nicholson, J. K., Holmes, E., Kinross, J., Burcelin, R., Gibson, G., Jia, W., et al. (2012). Host-gut microbiota metabolic interactions. *Science* 336, 1262–1267. doi: 10.1126/science.1223813
- Obata, Y., and Pachnis, V. (2016). The effect of microbiota and the immune system on the development and organization of the enteric nervous system. *Gastroenterology* 151, 836–844. doi: 10.1053/j.gastro.2016.07.044
- Park, S., Lee, J., Shin, J., Kim, J., Cha, B., Lee, S., et al. (2021). Cognitive function improvement after fecal microbiota transplantation in Alzheimer's dementia patient: A case report. *Curr. Med. Res. Opin.* 37, 1739–1744. doi: 10.1080/03007995.2021.1957807
- Pathak, M., Padghan, P., and Halder, N. (2020). CCR9 signaling in dendritic cells drives the differentiation of Foxp3 + Tregs and suppresses the allergic IgE response in the gut. *Eur. J. Immunol.* 417, 404–417. doi: 10.1002/eji.201948327
- Patnala, R., Arumugam, T. V., Gupta, N., and Dheen, S. T. (2017). HDAC inhibitor sodium butyrate-mediated epigenetic regulation enhances neuroprotective function of microglia during ischemic stroke. *Mol. Neurobiol.* 54, 6391–6411. doi: 10.1007/s12035-016-0149-z
- Paton, J. F., Li, Y. W., Deuchars, J., and Kasparov, S. (2000). Properties of solitary tract neurons receiving inputs from the sub-diaphragmatic vagus nerve. *Neuroscience* 95, 141–153. doi: 10.1016/S0306-4522(99)00416-9
- Pellissier, S., and Bonaz, B. (2017). The place of stress and emotions in the irritable bowel syndrome. *Vitam. Horm.* 103, 327–354. doi: 10.1016/bs.vh.2016.09.005
- Peng, H., Yu, S., Zhang, Y., Yin, Y., and Zhou, J. (2022). Intestinal dopamine receptor D2 is required for neuroprotection against 1-Methyl-4-phenyl-1,2,3,6-tetrahydropyridine-induced dopaminergic neurodegeneration. *Neurosci. Bull.* 38, 871–886. doi: 10.1007/s12264-022-00848-3
- Perez-Burgos, A., Wang, B., Mao, Y.-K., Mistry, B., McVey Neufeld, K.-A., Bienenstock, J., et al. (2013). Psychoactive bacteria *Lactobacillus rhamnosus* (JB-1) elicits rapid frequency facilitation in vagal afferents. *Am. J. Physiol. Gastrointest. Liver Physiol.* 304, G211–G220. doi: 10.1152/ajpgi.00128.2012
- Powley, T. L., Spaulding, R. A., and Haglof, S. A. (2011). Vagal afferent innervation of the proximal gastrointestinal tract mucosa: Chemoreceptor and mechanoreceptor architecture. *J. Comp. Neurol.* 519, 644–660. doi: 10.1002/cne.22541
- Quigley, E. M. M. (2017). Microbiota-brain-gut axis and neurodegenerative diseases. *Curr. Neurol. Neurosci. Rep.* 17:94. doi: 10.1007/s11910-017-0802-6
- Rackers, H. S., Thomas, S., Williamson, K., Posey, R., and Kimmel, M. C. (2018). Emerging literature in the microbiota-brain axis and perinatal mood and anxiety disorders. *Psychoneuroendocrinology* 95, 86–96. doi: 10.1016/j.psyneuen.2018.05.020
- Rahman, Z., and Dandekar, M. P. (2021). Crosstalk between gut microbiome and immunology in the management of ischemic brain injury. *J. Neuroimmunol.* 353:577498. doi: 10.1016/j.jneuroim.2021.577498
- Raybould, H. E. (2010). Gut chemosensing: Interactions between gut endocrine cells and visceral afferents. *Auton. Neurosci.* 153, 41–46. doi: 10.1016/j.autneu.2009.07.007
- Sajdel-Sulkowska, E., Makowska-Zubrycka, M., Czarzasta, K., Kasarello, K., Aggarwal, V., Bialy, M., et al. (2019). Common genetic variants link the abnormalities in the gut-brain axis in prematurity and autism. *Cerebellum* 18, 255–265. doi: 10.1007/s12311-018-0970-1
- Schächtle, M. A., and Rosshart, S. P. (2021). The microbiota-gut-brain axis in health and disease and its implications for translational research. *Front. Cell. Neurosci.* 15:698172. doi: 10.3389/fncel.2021.698172
- Schroeder, B. O., and Bäckhed, F. (2016). Signals from the gut microbiota to distant organs in physiology and disease. *Nat. Med.* 22, 1079–1089. doi: 10.1038/nm.4185



- Sharma, K. K., Singh, D., and Rawat, S. (2018). Molecular dynamics simulation studies suggest unconventional roles of non-secretory laccases from enteropathogenic gut bacteria and *Cryptococcus neoformans* serotype D. *Comput. Biol. Chem.* 73, 41–48. doi: 10.1016/j.compbiolchem.2018.01.010
- Shaw, W. (2010). Increased urinary excretion of a 3-(3-hydroxyphenyl)-3-hydroxypropionic acid (HPPHA), an abnormal phenylalanine metabolite of *Clostridia* spp. in the gastrointestinal tract, in urine samples from patients with autism and schizophrenia. *Nutr. Neurosci.* 13, 135–143. doi: 10.1179/147683010X12611460763968
- Shichita, T., Sugiyama, Y., Ooboshi, H., Sugimori, H., Nakagawa, R., Takada, I., et al. (2009). Pivotal role of cerebral interleukin-17-producing gammadeltaT cells in the delayed phase of ischemic brain injury. *Nat. Med.* 15, 946–950. doi: 10.1038/nm.1999
- Siddiqui, K. R. R., and Powrie, F. (2008). CD103 + GALT DCs promote Foxp3 + regulatory T cells. *Mucosal Immunol.* 1, 34–38. doi: 10.1038/mi.2008.43
- Silva, Y. P., Bernardi, A., and Frozza, R. L. (2020). The role of short-chain fatty acids from gut microbiota in gut-brain communication. *Front. Endocrinol.* 11:25. doi: 10.3389/fendo.2020.00025
- Singh, S. K., Yamashita, A., and Gouaux, E. (2007). Antidepressant binding site in a bacterial homologue of neurotransmitter transporters. *Nature* 448, 952–956. doi: 10.1038/nature06038
- Sobrinho Crespo, C., PerianesCachero, A., Puebla Jiménez, L., Barrios, V., and ArillaFerreiro, E. (2014). Peptides and food intake. *Front. Endocrinol.* 5:58. doi: 10.3389/fendo.2014.00058
- Song, J., Ma, W., Gu, X., Zhao, L., Jiang, J., Xu, Y., et al. (2019). Metabolomic signatures and microbial community profiling of depressive rat model induced by adrenocorticotrophic hormone. *J. Transl. Med.* 17:224. doi: 10.1186/s12967-019-1970-8
- Stilling, R. M., van de Wouw, M., Clarke, G., Stanton, C., Dinan, T. G., and Cryan, J. F. (2016). The neuropharmacology of butyrate: The bread and butter of the microbiota-gut-brain axis? *Neurochem. Int.* 99, 110–132. doi: 10.1016/j.neuint.2016.06.011
- Strader, A. D., and Woods, S. C. (2005). Gastrointestinal hormones and food intake. *Gastroenterology* 128, 175–191. doi: 10.1053/j.gastro.2004.10.043
- Strandwitz, P. (2018). Neurotransmitter modulation by the gut microbiota. *Brain Res.* 1693, 128–133. doi: 10.1016/j.brainres.2018.03.015
- Sudo, N., Chida, Y., Aiba, Y., Sonoda, J., Oyama, N., Yu, X.-N., et al. (2004). Postnatal microbial colonization programs the hypothalamic-pituitary-adrenal system for stress response in mice. *J. Physiol.* 558, 263–275. doi: 10.1113/jphysiol.2004.063388
- Takeuchi, O., and Akira, S. (2010). Pattern recognition receptors and inflammation. *Cell* 140, 805–820. doi: 10.1016/j.cell.2010.01.022
- Tanida, M., Yamano, T., Maeda, K., Okumura, N., Fukushima, Y., and Nagai, K. (2005). Effects of intraduodenal injection of *Lactobacillus johnsonii* La1 on renal sympathetic nerve activity and blood pressure in urethane-anesthetized rats. *Neurosci. Lett.* 389, 109–114. doi: 10.1016/j.neulet.2005.07.036
- Taniya, M., Chung, H., Al Mamun, A., Alam, S., Aziz, M., Emon, N., et al. (2022). Role of gut microbiome in autism spectrum disorder and its therapeutic regulation. *Front. Cell. Infect. Microbiol.* 12:915701. doi: 10.3389/fcimb.2022.915701
- Tashtush, A. A., Reed, D., and Lomax, A. E. (2022). Excitation of vagal afferent neurons by fecal supernatant from inflammatory bowel disease patients. *FASEB J.* 36. doi: 10.1096/fasebj.2022.36.S1.R2894
- Thursby, E., and Juge, N. (2017). Introduction to the human gut microbiota. *Biochem. J.* 474, 1823–1836. doi: 10.1042/BCJ20160510
- Turnbull, A. V., and Rivier, C. (1995). Regulation of the HPA axis by cytokines. *Brain Behav. Immun.* 9, 253–275. doi: 10.1006/brbi.1995.1026
- Vagnerová, K., Vodička, M., Hermanová, P., Ergang, P., Šrůtková, D., Klusová, P., et al. (2019). Interactions between gut microbiota and acute restraint stress in peripheral structures of the hypothalamic-pituitary-adrenal axis and the intestine of male mice. *Front. Immunol.* 10:2655. doi: 10.3389/fimmu.2019.02655
- van de Wouw, M., Boehme, M., Lyte, J. M., Wiley, N., Strain, C., O'Sullivan, O., et al. (2018). Short-chain fatty acids: Microbial metabolites that alleviate stress-induced brain-gut axis alterations. *J. Physiol.* 596, 4923–4944. doi: 10.1113/JP276431
- Vanamelbeke, M., and Vermeire, S. (2017). The intestinal barrier: A fundamental role in health and disease. *Exp. Rev. Gastroenterol. Hepatol.* 11, 821–834. doi: 10.1080/17474124.2017.1343143
- Vanuytsel, T., van Wanrooy, S., Vanheel, H., Vanormelingen, C., Verschueren, S., Houben, E., et al. (2014). Psychological stress and corticotropin-releasing hormone increase intestinal permeability in humans by a mast cell-dependent mechanism. *Gut* 63, 1293–1299. doi: 10.1136/gutjnl-2013-305690
- Varesi, A., Pierella, E., Romeo, M., Piccini, G., Alfano, C., Björklund, G., et al. (2022). The potential role of gut microbiota in Alzheimer's disease: From diagnosis to treatment. *Nutrients* 14:668. doi: 10.3390/nu14030668
- Vicario, M., Alonso, C., Guilarte, M., Serra, J., Martínez, C., González-Castro, A. M., et al. (2012). Chronic psychosocial stress induces reversible mitochondrial damage and corticotropin-releasing factor receptor type-1 upregulation in the rat intestine and IBS-like gut dysfunction. *Psychoneuroendocrinology* 37, 65–77. doi: 10.1016/j.psyneuen.2011.05.005
- Vogt, N. M., Kerby, R. L., Dill-McFarland, K. A., Harding, S. J., Merluzzi, A. P., Johnson, S. C., et al. (2017). Gut microbiome alterations in Alzheimer's disease. *Sci. Rep.* 7:13537. doi: 10.1038/s41598-017-13601-y
- Wang, F.-B., and Powley, T. L. (2007). Vagal innervation of intestines: Afferent pathways mapped with new en bloc horseradish peroxidase adaptation. *Cell Tissue Res.* 329, 221–230. doi: 10.1007/s00441-007-0413-7
- Wang, H.-X., and Wang, Y.-P. (2016). Gut microbiota-brain Axis. *Chin. Med. J.* 129, 2373–2380. doi: 10.4103/0366-6999.190667
- Weiner, H. L., and Wu, H. Y. (2011). Oral tolerance. *Immunol. Res.* 241, 241–259. doi: 10.1385/IR:28:3:265
- Weltens, N., Iven, J., Van Oudenhove, L., and Kano, M. (2018). The gut-brain axis in health neuroscience: Implications for functional gastrointestinal disorders and appetite regulation. *Ann. N. Y. Acad. Sci.* 1428, 129–150. doi: 10.1111/nyas.13969
- Williams, C. L., Garcia-Reyero, N., Martyniuk, C. J., Tubbs, C. W., and Bisesi, J. H. J. (2020). Regulation of endocrine systems by the microbiome: Perspectives from comparative animal models. *Gen. Comp. Endocrinol.* 292:113437. doi: 10.1016/j.ygcen.2020.113437
- Wirlitner, B., Neurauter, G., Schröcksnadel, K., Frick, B., and Fuchs, D. (2003). Interferon-gamma-induced conversion of tryptophan: Immunologic and neuropsychiatric aspects. *Curr. Med. Chem.* 10, 1581–1591. doi: 10.2174/0929867033457179
- Wu, Q., Xu, Z., Song, S., Zhang, H., Zhang, W., Liu, L., et al. (2020). Gut microbiota modulates stress-induced hypertension through the HPA axis. *Brain Res. Bull.* 162, 49–58. doi: 10.1016/j.brainresbull.2020.05.014
- Wu, T., Rayner, C. K., Young, R. L., and Horowitz, M. (2013). Gut motility and enteroendocrine secretion. *Curr. Opin. Pharmacol.* 13, 928–934. doi: 10.1016/j.coph.2013.09.002
- Yang, H.-L., Li, M.-M., Zhou, M.-F., Xu, H.-S., Huan, F., Liu, N., et al. (2021). Links Between gut dysbiosis and neurotransmitter disturbance in chronic restraint stress-induced depressive behaviours: The role of inflammation. *Inflammation* 44, 2448–2462. doi: 10.1007/s10753-021-01514-y
- Zhang, Y., Wang, Z., Peng, J., Gerner, S. T., Yin, S., and Jiang, Y. (2021). Gut microbiota-brain interaction: An emerging immunotherapy for traumatic brain injury. *Exp. Neurol.* 337:113585. doi: 10.1016/j.expneurol.2020.113585
- Zhao, L., Xiong, Q., Stary, C. M., Mahgoub, O. K., Ye, Y., Gu, L., et al. (2018). Bidirectional gut-brain-microbiota axis as a potential link between inflammatory bowel disease and ischemic stroke. *J. Neuroinflammation* 15:339. doi: 10.1186/s12974-018-1382-3
- Zhao, Q., and Elson, C. O. (2018). Adaptive immune education by gut microbiota antigens. *Immunology* 154, 28–37. doi: 10.1111/imm.12896
- Zhao, Y., Jaber, V., and Lukiw, W. J. (2021). Gastrointestinal tract microbiome-derived pro-inflammatory neurotoxins in Alzheimer's disease. *J. Aging Sci.* 9:002.





## OPEN ACCESS

EDITED BY  
Weiqi He,  
Soochow University,  
China

REVIEWED BY  
Yunyan Zhou,  
Zhejiang University of Technology, China  
Zhang Xinzhuan,  
Inner Mongolia Agricultural University,  
China

\*CORRESPONDENCE  
Changfa Wang  
✉ wangcf1967@163.com

SPECIALTY SECTION  
This article was submitted to  
Microorganisms in Vertebrate Digestive  
Systems,  
a section of the journal  
Frontiers in Microbiology

RECEIVED 22 November 2022  
ACCEPTED 12 January 2023  
PUBLISHED 27 January 2023

CITATION  
Zhang Z, Huang B, Gao X, Shi X, Wang X,  
Wang T, Wang Y, Liu G and Wang C (2023)  
Dynamic changes in fecal microbiota in donkey  
foals during weaning: From pre-weaning to  
post-weaning.  
*Front. Microbiol.* 14:1105330.  
doi: 10.3389/fmicb.2023.1105330

COPYRIGHT  
© 2023 Zhang, Huang, Gao, Shi, Wang, Wang,  
Wang, Liu and Wang. This is an open-access  
article distributed under the terms of the  
Creative Commons Attribution License (CC  
BY). The use, distribution or reproduction in  
other forums is permitted, provided the original  
author(s) and the copyright owner(s) are  
credited and that the original publication in this  
journal is cited, in accordance with accepted  
academic practice. No use, distribution or  
reproduction is permitted which does not  
comply with these terms.

# Dynamic changes in fecal microbiota in donkey foals during weaning: From pre-weaning to post-weaning

Zhenwei Zhang, Bingjian Huang, Xu Gao, Xiaoyuan Shi,  
Xinrui Wang, Tianqi Wang, Yonghui Wang, Guiqin Liu and  
Changfa Wang\*

Liaocheng Research Institute of Donkey High-Efficiency Breeding and Ecological Feeding, Agricultural Science and Engineering School, Liaocheng University, Liaocheng, China

**Introduction:** A better understanding of the microbiota community in donkey foals during the weaning transition is a prerequisite to optimize gut function and improve feed efficiency. The objective of the present study was to investigate the dynamic changes in fecal microbiota in donkey foals from pre-to post-weaning period.

**Methods:** A total of 27 fecal samples of donkey foals were collected in the rectum before morning feeding at pre-weaning (30days of age, PreW group,  $n=9$ ), during weaning (100days of age, DurW group,  $n=9$ ) and post-weaning (170days of age, PostW group,  $n=9$ ) period. The 16S rRNA amplicon sequencing were employed to indicate the microbial changes during the weaning period.

**Results:** In the present study, the cessation of breastfeeding gradually and weaning onto plant-based feeds increased the microbial diversity and richness, with a higher Shannon, Ace, Chao and Sobs index in DurW and PostW than in PreW ( $p<0.05$ ). The predominant bacterial phyla in donkey foal feces were Firmicutes (>50.5%) and Bacteroidota (>29.5%), and the predominant anaerobic fungi and archaea were Neocallimastigomycota and Euryarchaeota. The cellulolytic related bacteria including phylum Firmicutes, Spirochaetota and Fibrobacterota and genus norank\_f\_F082, *Treponema*, NK4A214\_group, *Lachnospiraceae*\_AC2044\_group and *Streptococcus* were increased from pre-to post-weaning donkey foals ( $p<0.05$ ). Meanwhile, the functions related to the fatty acid biosynthesis, carbohydrate metabolism and amino acid biosynthesis were significantly enriched in the fecal microbiome in the DurW and PostW donkeys. Furthermore, the present study provided the first direct evidence that the initial colonization and establishment of anaerobic fungi and archaea in donkey foals began prior to weaning. The relative abundance of *Orpinomyces* were the highest in DurW donkey foals among the three groups ( $p<0.01$ ). In terms of archaea, the abundance of *Methanobrevibacter* were higher in PreW than in DurW and PostW ( $p<0.01$ ), but the abundance of *Methanocorpusculum* were significantly increased in DurW and PostW compared to PreW donkey foals ( $p<0.01$ ).

**Discussion:** Altogether, the current study contributes to a comprehensive understanding of the development of the microbiota community in donkey foals from pre-to post-weaning period, which may eventually result in an improvement of the digestion and feed efficiency in donkeys.

## KEYWORDS

weaning, fecal microbiota, bacteria, anaerobic fungi, archaea, donkey foal

## 1. Introduction

Donkey hindgut is vastly developed and consists of the cecum, colon and rectum (Julliand and Grimm, 2016). It's a complex microbial ecosystem and is inhabited by highly dense and diverse microbiota, with bacteria, anaerobic fungi, methanogenic archaea, and ciliate protozoa involved (Edwards et al., 2020). Intestinal microbiota and their hosts have developed a complex and mutually adapted micro-ecological system (Santos et al., 2011). This steady microbiome-host balance is essential for the maintenance and ideal physiological function of intestine (Lindenberg et al., 2019).

Donkeys rely on the resident microbiota in hindgut to degrade dietary plant fiber to provide energy to support their growth and development (Dougal et al., 2012; Liu et al., 2020). A better understanding of the donkey hindgut microbiota is essential for the manipulation of the intestinal microbiota to optimize intestinal function and improve feed efficiency. In recent years, information is available in characterizing the hindgut microbiota in adult donkeys using high throughput sequencing of fecal samples (Liu et al., 2020; Li et al., 2022; Zhang et al., 2022a). As a suitable representation of the hindgut, feces are often used for microbial investigation in adult donkeys (Grimm et al., 2017). However, the fecal microbial population in donkey foal has never been studied during the weaning period. Weaning in donkey foals typically happens between 5 and 6 months of age in China, but the change from breast-feeding to plant-based feeds is gradual, as most donkey foals will have started ingesting plant-based solid feeds before weaning (Lindenberg et al., 2019).

From pre-weaning to post-weaning, donkey foals are subjected to a variety of stressors that include the separation from their dam, exposure to unfamiliar pens or novel pasture environments, and especially the switch from easily digestible milk to a more complicated adult-type feed (Zhang et al., 2022b). The cessation of milk and the subsequent shift in diet composition has a profound influence on the intestinal microbiota, as shown in other mammals, such as the calf (Luo et al., 2022), lamb (Li et al., 2018), deer Li et al., 2022), and piglet (Meng et al., 2020). Several studies have demonstrated that the development of the microbial ecosystem during weaning period may have an important impact on the microbial community structure in the adult and, consequently, the digestive efficiency and production performance (Zhang et al., 2017; Salem et al., 2018). The introduction of solid food leads to a new phase in the development of the microbiota, characterized by a significant increase in microbial abundance and diversity, and evolution toward a composition that is associated with adult individuals (Frese et al., 2015). Among the physiological and gastrointestinal factors influenced by the weaning transition, the microbiota alteration is likely to be considered as one of the keys leading to weaning stress (Weary et al., 2008). In addition, weaning stress usually causes intestinal microbiota related-disorders (Meng et al., 2020). Therefore, an in-depth understanding of foal gut microbiota during weaning transition is essential to optimize care of donkey foals and improve the health conditions.

However, to the very best of our knowledge, no work has reported on the dynamics of intestinal microbiota in donkey foals during weaning. An integrated investigation of the compositions and abundances of fecal bacteria, fungi, and archaea in donkey foals during weaning could be used to help develop microbial interventions to improve animal health and production performance. Therefore, the present study aimed at monitoring weaning-related changes in the microbial community structure in foal feces from pre-to post-weaning period using high-throughput MiSeq sequencing technique.

## 2. Materials and methods

### 2.1. Animals and sample collection

In the present study, 9 donkey foals (vaginal delivery) with the similar body weight and similar time of birth (from June 12, 2021 to July 4, 2021) were enrolled from the provincial Dezhou donkey original breeding farm. During the sampling period, donkey foals were clinically healthy and present no behavioral abnormalities. Following the practices commonly applied by Chinese equine breeders, donkey foal raising can be divided into three stages from pre-to post-weaning period.

From birth to day 50, donkey foals were maintained with their respective mares in the individual pens with straw bedding in a sandy paddock. Donkey foals had no access to concentrate and hay, but they received donkey milk and fresh water *ad libitum* during this pre-weaning period. From day 50 to day 150, donkey foals were still kept with their dams in a large sandy paddock and were not fed separately. In addition to the donkey milk, donkey foals had access to the mares feed bucket with wheat hay and supplemented concentrate *ad libitum* in the dur-weaning period. Donkey foals were abruptly weaned at 150 days of age. From day 150, foals were kept in one sand-bedded barn with wood shelters and were allowed access to wheat hay *ad libitum* and 1 kg/d concentrate diet (Hekangyuan Co., Ltd., Dezhou, Shandong Province, China). Donkey foals were fed twice daily at 08:00 and 18:00 in the post-weaning period. Water and a salt block were offered free access to all donkey foals.

Fecal samples of donkey foals were collected in the rectum using single-use gloves before morning feeding at pre-weaning (30 days of age), dur-weaning (100 days of age) and post-weaning (170 days of age) period. Each fecal sample was then put into sterile centrifuge tubes and kept in liquid nitrogen. All samples were transported to Liaocheng University laboratory immediately and stored at  $-80^{\circ}\text{C}$  until DNA extraction. In addition, the body height (BH), body length (BL), thoracic girth (TG), thoracic depth (TD), thoracic width (TW), rump height (RH), rump length (RL), rump width (RW), and cannon bone circumference (CB) of donkey foals were determined before morning feeding by using a measuring stick or a tape.

### 2.2. The DNA extraction, PCR amplification, and 16S rRNA sequencing

Following the manufacturer's protocol, microbial DNA of the fecal samples was extracted with the EZNA<sup>®</sup> Stool DNA Kit (Omega Bio-tek, Norcross, GA, United States). The extracted DNA purity and concentrations were determined using the NanoDrop 2000 UV-vis spectrophotometer (Thermo Scientific, Wilmington, United States).

The genomic DNA was then subjected to PCR amplification with the ABI GeneAmp<sup>®</sup> 9,700 PCR thermocycler (ABI, Foster City, CA, United States). For bacterial analysis, the V3-V4 hyper-variable region of the 16S rRNA gene was amplified with primers 338F (5'-ACTC CTAC GGA GGCA GCAG-3') and 806R (5'-GGAC TACH VGGG TWTC TAAT-3') (Zhang et al., 2022a). The PCR amplification was performed in triplicate using the TransStart Fastpfu DNA polymerase in a volume of 20  $\mu\text{L}$  containing 4  $\mu\text{L}$  of 5  $\times$  FastPfu buffer, 2  $\mu\text{L}$  of dNTPs (2.5 mM), 0.8  $\mu\text{L}$  of forward and reverse primers (5  $\mu\text{M}$ ), 0.2  $\mu\text{L}$  of BSA (bovine serum albumin), 0.4  $\mu\text{L}$  of FastPfu polymerase, 10 ng of template DNA and ddH<sub>2</sub>O. For anaerobic fungi analysis, the 28S rRNA gene was amplified using primers GGNLIF (5'-CATA GAGG GTGA GAAT

CCCG TA-3') and GGNL4R (5'-TCAA CATC CTAA GCGT AGGT A-3') (Nagler et al., 2019). For total archaea analysis, the 16S rDNA V4-V5 regions of the methanogen was amplified using primers 524F (5'-TGYC AGCC GCCG CGGT AA-3') (Wei et al., 2013) and Arch958R (5'-YCCG GCGT TGAV TCCA ATT-3') (Ma et al., 2018). The fungal and archaeal PCR amplifications were conducted with Pro Taq in a volume of 20  $\mu$ L containing 10  $\mu$ L of 2 $\times$  Pro Taq, 0.8  $\mu$ L of forward and reverse primers (5  $\mu$ M), 10 ng of template DNA and ddH<sub>2</sub>O. All PCR products were extracted from 2% agarose gel and further purified with DNA gel extraction kit (Axygen Bioscience, Union City, CA, United States) according to the manufacturer's instructions and quantified by Quantus<sup>TM</sup> Fluorometer (Promega, United States).

Purified amplicons were ultimately pooled together in equimolar concentrations and high-throughput sequenced (paired-end, 2 $\times$  300 bp) on an Illumina MiSeq platform (Illumina, San Diego, United States) at Majorbio Bio-Pharm Technology Co. Ltd (Shanghai, China) following standard protocols (Zhang et al., 2017).

### 2.3. Sequencing data processing and bioinformatic analysis

The raw data of sequencing reads were quality-filtered by Trimmomatic and merged by FLASH with the criteria as described by previous study (Zhang et al., 2017). To eliminate the influence of sequencing depth on microbial diversity and composition measurement, the number of reads from bacterial, fungal and archaeal sample was rarefied to 40,921, 30,469, and 34,214, respectively. Operational taxonomic units (OTUs) based on 97% identity were clustered with UPARSE (version 11.0),<sup>1</sup> and chimeric sequences were removed. The taxonomy of specific OTU representative sequence (bacteria, fungi, and archaea) was analyzed by RDP Classifier (version 2.13)<sup>2</sup> against the SILVA bacterial database (version 138) (Pruesse et al., 2007), UNITE fungi ITS database (version nt\_v20210917) (Kõljalg et al., 2005), and SILVA archaea database (version 138/16S\_archaea) through PYNAST (Caporaso et al., 2010) with the confidence threshold of 0.7 using QIIME.

Alpha diversity indices (Sobs, Chao, Shannon, and Simpson index) were measured by the MOTHUR (version 1.30.2). The Venn diagram and bar graphs were visualized by the R software (version 3.3.1). Beta diversity was determined by calculating the bray-curtis distance by QIIME (version 1.9.1) and showed by principal component analysis (PCA), principal coordinate analysis (PCoA) and non-metric multi-dimensional scaling (NMDS) plots. The microbial alterations among experimental groups were analyzed using partial least squares discriminant analysis (PLS-DA), and the results were plotted using R software (version 3.3.1). The Kruskal-Wallis H test and the One-way ANOVA was used to determine the phyla and genera that presented significant differences in abundance among groups using the sciply package in PYTHON and the stats package in R software (version 3.3.1). The linear discriminant analysis effect size (LEfSe) was used to determine statistically significant taxa in pre-, dur-, and post-weaning groups based on LDA scores >3.5 and  $p < 0.05$ . The co-abundant topological network of microbial genus was constructed using Networkx software. The PICRUST (phylogenetic investigation of

communities by reconstruction of unobserved states) transforms OTUs aligned against the SILVA, UNITE fungi and SILVA archaea database into the KEGG pathways (Kyoto Encyclopedia of Genes and Genomes).

All raw sequences after assembling and filtering were ultimately submitted to the NCBI Sequence Read Archive (SRA) with the accession number PRJNA903673.

### 2.4. Statistical analysis

Body measurements of donkey foals were conducted using PROC MEANS procedures in SAS 9.4 software (Statistical Analysis for Windows, SAS Institute Inc., Cary, NC, United States), and the data were expressed as Mean  $\pm$  SD. Significant differences of alpha diversity index, microbial abundance at phylum- and genus-level, enriched KEGG Module pathways and COG functions among PreW, DurW, and PostW groups were determined using Wilcoxon rank-sum test in R software (version 4.0.3). The presented data are expressed as least-squares means (SEM) with their standard errors. Statistical significance was set at  $p < 0.05$  and a trend was declared at  $p < 0.1$ . The correlations between donkey fecal microbiota and donkey body measurements were evaluated via Pearson's correlation analysis using the pheatmap package (version 3.3.1) in R.

## 3. Results

### 3.1. Body measurements of donkey foals

As shown in Table 1, with the age increasing, the body measurements including BH, BL, TG, TD, TW, RH, RL, RW, and CB linearly increased from pre-weaning to post-weaning period.

### 3.2. Fecal bacteria changes in donkey foals from pre- to post-weaning period

The Shannon, Ace, Chao and Sobs index of PreW group was lower than that of DurW and PostW group (Table 2,  $p < 0.01$ ), which indicated that the PreW group had lower bacterial diversity and richness in comparison with DurW and PostW groups.

The UpSet Venn diagram (Figure 1A) showed the distribution of bacterial community OTUs. There were 1,442, 2,559 and 2,625 OTUs observed in the PreW, DurW and PostW groups, respectively. The PreW donkey foals shared a bacterial community, including 959 OTUs, with DurW and PostW.

The results of PCoA and NMDS for bacteria with weighted uniFrac distances showed that the PreW group were obviously separated from DurW and PostW groups at the OTU level (Figures 2A,B, ANOSIM:  $R = 0.51$ ,  $p = 0.001$ ).

The relative abundance of bacterial phyla accounting for  $\geq 0.01\%$  of the total sequences in at least one samples were presented in Figure 3A. Among these phyla, Firmicutes and Bacteroidota had relatively high abundance, at mean abundance levels of 50.5 and 29.5%, respectively (Figure 3A). The relative abundance of Firmicutes, Spirochaetota and Fibrobacterota in PreW group were lower than that in DurW and PostW groups (Figure 4,  $p < 0.01$ ). However, the relative abundance of Fusobacteriota and Proteobacteria in PreW donkey foals were higher in comparison with DurW and PostW donkey foals ( $p < 0.01$ ).

1 <http://drive5.com/uparse/>

2 <https://sourceforge.net/projects/rdp-classifier/>

TABLE 1 Descriptive values for donkey foals are shown related to body measurement.

Items	BH	BL	TG	TD	TW	RH	RL	RW	CB
PreW	89 ± 1.3 <sup>c</sup>	60 ± 1.4 <sup>c</sup>	73 ± 1.8 <sup>c</sup>	33 ± 0.6 <sup>b</sup>	17 ± 0.5 <sup>c</sup>	90 ± 1.5 <sup>c</sup>	24 ± 0.6 <sup>c</sup>	21 ± 0.8 <sup>c</sup>	10 ± 0.2 <sup>c</sup>
DurW	102 ± 1.1 <sup>b</sup>	90 ± 2.2 <sup>b</sup>	94 ± 1.9 <sup>b</sup>	33 ± 0.8 <sup>b</sup>	22.1 ± 0.8 <sup>b</sup>	104 ± 1.1 <sup>b</sup>	30 ± 0.4 <sup>b</sup>	25 ± 0.6 <sup>b</sup>	13.2 ± 0.3 <sup>b</sup>
PostW	117 ± 3.1 <sup>a</sup>	117 ± 2.7 <sup>a</sup>	119 ± 3.2 <sup>a</sup>	44 ± 1.2 <sup>a</sup>	28 ± 0.9 <sup>a</sup>	121 ± 2.8 <sup>a</sup>	37 ± 1.1 <sup>a</sup>	32 ± 1.0 <sup>a</sup>	14 ± 0.3 <sup>a</sup>

<sup>a,b,c</sup>Different superscript letters within a row represents values with significantly different at  $P < 0.05$ . PreW, pre-weaning donkeys; DurW, during weaning donkeys; PostW, post-weaning donkeys; BH, body height (cm); BL, body length (cm); TG, thoracic girth (cm); TD, thoracic depth (cm); TW, thoracic width (cm); RH, rump height (cm); RL, rump length (cm); RW, rump width (cm); CB, circumference of cannon bone (cm); data expressed as Mean ± SEM.

TABLE 2 Alpha diversity indices of bacteria, anaerobic fungi, and archaea among different groups.

Items		PreW	DurW	PostW	SEM	P-value
Bacteria	Shannon	3.1 <sup>b</sup>	5.9 <sup>a</sup>	5.6 <sup>a</sup>	0.23	<0.01
	Ace	453.2 <sup>b</sup>	1840.6 <sup>a</sup>	1677.7 <sup>a</sup>	82.9	<0.01
	Chao	453.7 <sup>b</sup>	1853.3 <sup>a</sup>	1686.3 <sup>a</sup>	86.1	<0.01
	Sobs	343.4 <sup>b</sup>	1521.1 <sup>a</sup>	1375.2 <sup>a</sup>	69.6	<0.01
Anaerobic fungi	Shannon	1.0	1.0	1.0	0.09	0.97
	Ace	6.8 <sup>b</sup>	30.9 <sup>ab</sup>	18.0 <sup>ab</sup>	5.05	0.02
	Chao	7.5 <sup>b</sup>	29.2 <sup>a</sup>	17.6 <sup>ab</sup>	4.86	0.03
	Sobs	7.5 <sup>b</sup>	27.0 <sup>a</sup>	14.9 <sup>ab</sup>	4.68	0.04
Archaea	Shannon	0.9 <sup>b</sup>	1.3 <sup>a</sup>	1.2 <sup>ab</sup>	0.11	0.06
	Ace	23.4 <sup>b</sup>	26.6 <sup>b</sup>	46.1 <sup>a</sup>	5.96	0.03
	Chao	22.8 <sup>b</sup>	24.4 <sup>b</sup>	32.7 <sup>a</sup>	2.79	0.04
	Sobs	22.3	22.8	26.9	2.71	0.44

<sup>a,b</sup>Different superscript letters within a row represents values with significantly different at  $P < 0.05$ . PreW, pre-weaning donkeys; DurW, during weaning donkeys; PostW, post-weaning donkeys; SEM, standard error of the mean.

The top 10 abundant bacterial genera of fecal microbiota in pre-, dur- and post-weaning donkey foals were unclassified\_f\_Lachnospiraceae, Rikenellaceae\_RC9\_gut\_group, Bacteroides, norank\_f\_F082, Fusobacterium, Treponema, NK4A214\_group, Lachnospiraceae\_AC2044\_group, Escherichia-Shigella and Streptococcus (Figure 3B). The relative abundance of Rikenellaceae\_RC9\_gut\_group, norank\_f\_F082, Treponema, NK4A214\_group, Lachnospiraceae\_AC2044\_group and Streptococcus in PreW donkey foals were significantly lower than that in DurW and PostW donkey foals (Figure 5A,  $p < 0.01$ ). In contrast, the relative abundance of Fusobacterium and Escherichia-Shigella in PreW group were obviously higher than in DurW and PostW groups ( $p < 0.01$ ).

### 3.3. Fecal anaerobic fungi changes in donkey foals from pre- to post-weaning period

Compared to the PreW group, both the DurW and PostW group had the higher Ace, Chao and Sobs index (Table 2,  $p < 0.05$ ). However, there was no significant difference among PreW, DurW and PostW groups for Shannon index ( $p > 0.05$ ).

The distribution of anaerobic fungi community OTUs were presented in Figure 1B. There were 19, 61 and 143 OTUs in the PreW, DurW, and PostW donkey foals, respectively. The PreW donkey foals shared an anaerobic fungi community, including 9 OTUs, with DurW and PostW.

The PCoA and NMDS based on unweighted UniFrac distance revealed that the fecal anaerobic fungi of donkey foals showed no obvious segregation from pre-weaning to post-weaning (Figures 2C,D, ANOSIM:  $R = 0.11$ ,  $p = 0.06$ ).

The anaerobic fungi sequences determined at the phylum level largely belonged to Neocallimastigomycota (>99.9%), and there was no significant difference among PreW, DurW, and PostW groups (Figure 3C,  $p > 0.05$ ). At genus level, Caecomyces, unclassified\_c\_Neocallimastigomycetes, Piromyces, unclassified\_o\_Neocallimastigales and Orpinomyces were the predominant genera in all samples (Figure 3D). The relative abundance of unclassified\_o\_Neocallimastigales in PreW and DurW donkey foals were significantly higher than in PostW donkey foals (Figure 5B,  $p < 0.01$ ). The relative abundance of Orpinomyces were the highest in DurW donkey foals among the three groups (Figure 5B,  $p < 0.01$ ), but there was no significant difference between PreW and PostW donkey foals ( $p > 0.05$ ).

### 3.4. Fecal archaea changes in donkey foals from pre- to post-weaning period

As shown in Table 2, the PreW group had lower Shannon index than that in the DurW and PostW group ( $p < 0.05$ ). In addition, the Ace and Chao index in PreW group was also lower than that in the DurW and PostW group ( $p < 0.05$ ).

There were 19, 61 and 143 archaeal community OTUs in the PreW, DurW, and PostW groups (Figure 1C). A total of 27 OTUs could be observed in all three groups and there were 6, 11, and 63 unique OTUs in the PreW, DurW, and PostW donkey foals, respectively.

In terms of beta diversity of archaea community at the OTU level in donkey foals, unweighted UniFrac PCoA and NMDS showed that the separation of PreW group from DurW and PostW occurred (Figures 2E,F, ANOSIM:  $R = 0.34$ ,  $p = 0.001$ ), but no obvious separation of the samples between DurW and PostW.

The sequences detected at archaeal phylum level mainly belonged to Euryarchaeota and Halobacterota (Figure 3E). The predominant genera detected in the present study were Methanobrevibacter, Methanocorpusculum, Methanimicrococcus and Halococcus (Figure 3F). As shown in Figure 5C, the relative abundance of Methanobrevibacter were significantly higher in PreW donkey foals than in DurW and PostW donkey foals ( $p < 0.01$ ), however, the relative abundance of Methanocorpusculum in PreW group was remarkably lower than in DurW and PostW groups ( $p < 0.01$ ).

### 3.5. Microbial biomarkers of different groups

To identify the differences in fecal microbiota of donkey foals among PreW, DurW and PostW groups, linear discriminant analysis effect size (LEfSe) analysis was performed from phylum to genus level (Figure 6).



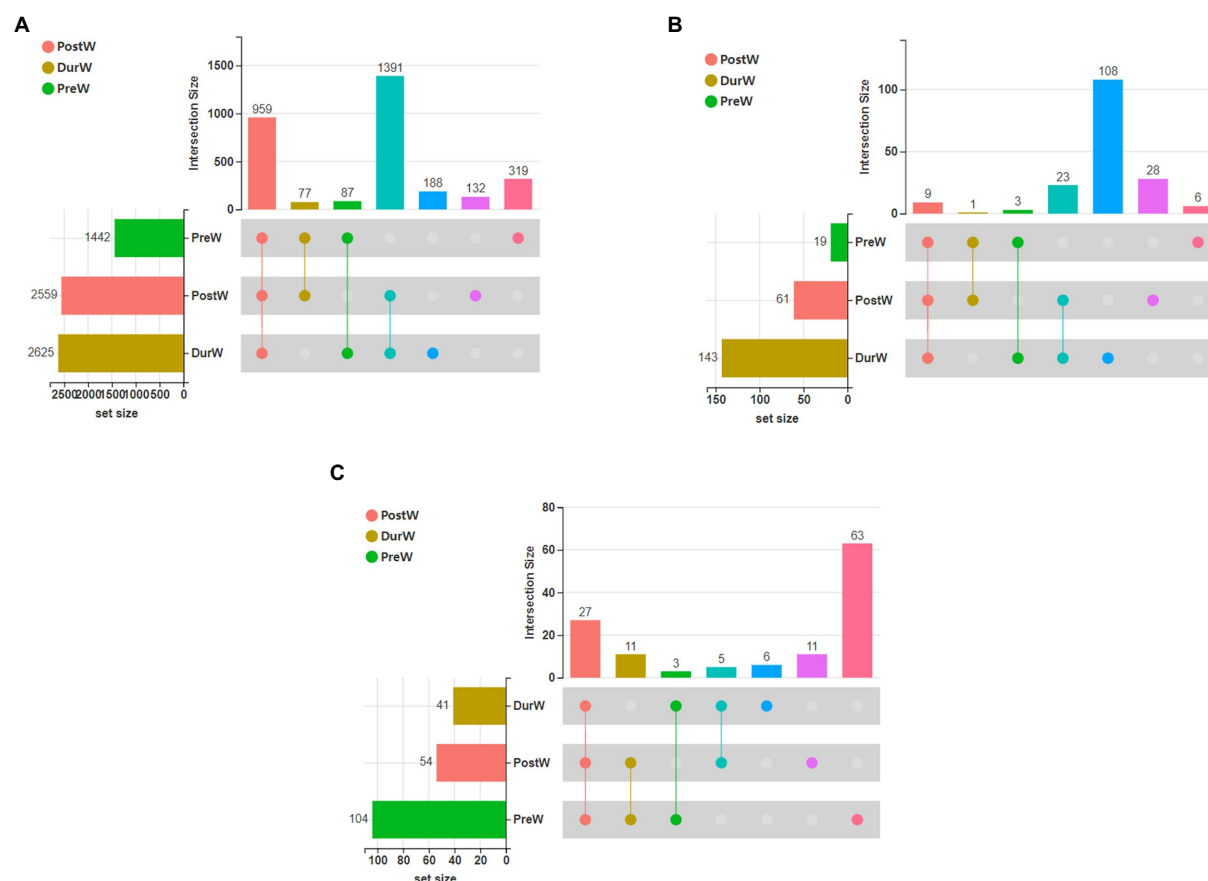


FIGURE 1

The UpSet Venn diagram presenting the distribution of microbial bacterial (A), anaerobic fungi (B), and archaeal (C) community OTUs among different groups. PreW, pre-weaning donkeys; DurW, during weaning donkeys; PostW, post-weaning donkeys.

The bacteria with significant differences in the PreW group were genus *g\_Bacteroides*, *g\_Fusobacterium*, *g\_Escherichia-Shigella* and *g\_Odoribacter*, the bacterial biomarkers for DurW group were genus *g\_Rikenellaceae\_RC9\_gut\_group*, *g\_Treponema*, *g\_NK4A214\_group*, *g\_norank\_f\_p-251-o5*, *g\_norank\_f\_Bacteroidales\_UCG-001*, *g\_norank\_f\_UCG-010* and *g\_Sarcina*; the bacterial biomarkers for PostW group were genus *g\_Streptococcus*, *g\_Lachnospiraceae\_AC2044\_group*, *g\_Lachnospiraceae\_XPB1014\_group*, *g\_norank\_f\_F082* and *g\_Fibrobacter* (Figures 6A,B).

For anaerobic fungi, only 5 biomarkers with statistical differences between PreW and DurW were determined using LEfSe (2 in the PreW, 3 in the DurW), as shown in Figures 6C,D. *Unclassified\_o\_Neocallimastigales* and *g\_unclassified\_o\_Neocallimastigales* was significantly enriched in the PreW group, and the DurW group was significantly enriched in genus *g\_Orpinomyces*.

A total of 16 biomarkers of archaea with statistical differences between PreW and DurW were observed by LEfSe analysis (11 in the PreW, 5 in the DurW; Figures 5E,F). The dominant archaea from the fecal samples in the PreW group were mainly from the genus *g\_Methanobrevibacter*, *g\_Halalkalicoccus*, *g\_Candidatus\_Methanoplasma* and *g\_Methanosarcina*, while the archaeal biomarkers for DurW group were genus *g\_Methanocorpusculum* and class *c\_Methanomicrobia*.

### 3.6. The co-occurrence network analysis on microbiota

The co-occurrence network analysis highlighted the differences among different weaning periods. There were more strongly bacterial and archaeal networks of DurW-PostW than the network of PreW-DurW and PreW-PostW (Figures 7A,C). The anaerobic fungi networks of DurW-PostW were weaker, and there were similarly networks of PreW-DurW and PreW-PostW (Figure 7B).

### 3.7. Correlation of differentially donkey fecal microbiota and body measurements

The possible correlations between the differentially donkey fecal microbiota and body measurements were determined based on Spearman's correlation (Figure 8). At phylum level, the bacterial Firmicutes, Spirochaetota, and Fibrobacterota were positively correlated with donkey BH, BL, TG, TW, RH, RL, RW, and CB (Figure 8A,  $p < 0.05$ ), but the bacterial Fusobacteriota and Proteobacteria was negatively related with donkey body measurements ( $p < 0.05$ ). At genus level, the bacterial *Rikenellaceae\_RC9\_gut\_group*, *norank\_f\_F082*, *Treponema*, *NK4A214\_group*, *Lachnospiraceae\_AC2044\_group* and *Streptococcus* were positively

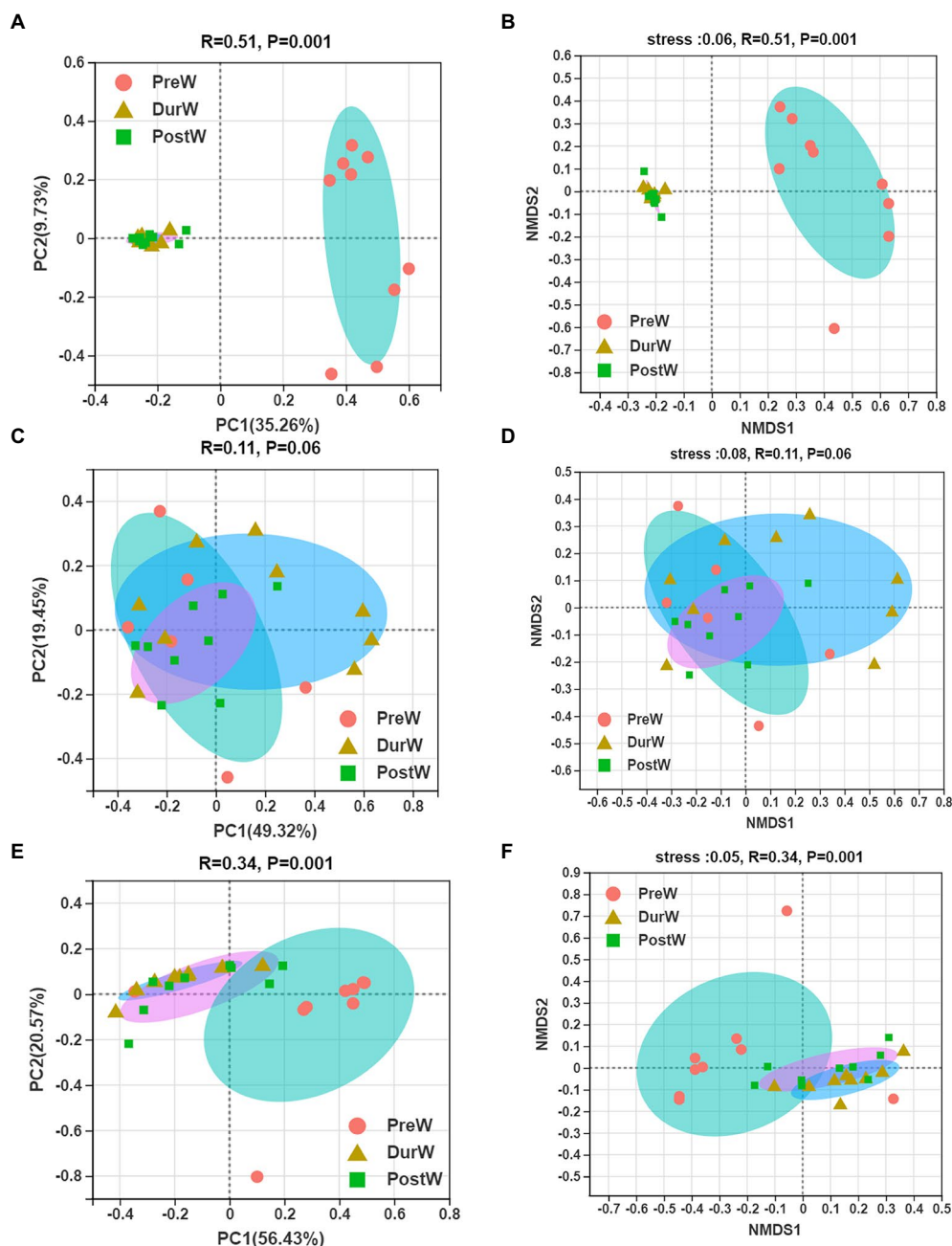


FIGURE 2

Principal co-ordinates analysis (PCoA) and Nonmetric multidimensional scaling analysis (NMDS) of microbial community composition among different groups. (A) The PCoA analysis of bacteria. (B) The NMDS analysis of bacteria. (C) The PCoA analysis of anaerobic fungi. (D) The NMDS analysis of anaerobic fungi. (E) The PCoA analysis of archaea. (F) The NMDS analysis of archaea; PreW, pre-weaning donkeys; DurW, during weaning donkeys; PostW, post-weaning donkeys.

correlated with donkey body measurements (Figure 8B,  $p < 0.05$ ). Conversely, the donkey body measurements were negatively correlated with the bacterial *Bacteroides*, *Fusobacterium* and *Escherichia-Shigella* ( $p < 0.05$ ). For fecal archaea, there was a significantly positive correlation between donkey body measurements and phylum Halobacterota (Figure 8C,  $p < 0.05$ ), but donkey body measurements were negatively correlated with Euryarchaeota ( $p < 0.05$ ). At genus level of archaea, the *Methanocorpusculum* were positively correlated with BH, BL, TG, TW, RH, RL, RW, and CB, however, the donkey body measurements were negatively correlated with *Methanobrevibacter* (Figure 8D,  $p < 0.05$ ). For anaerobic fungi, no obvious correlation was observed between donkey body measurements and Neocallimastigomycota ( $p > 0.05$ ). But at genus

level, there was a positive correlation between *Orpinomyces* and TW, CB, BL, TG and RH (Figure 8E,  $p < 0.05$ ). In addition, there was a negative correlation between unclassified\_o\_Neocallimastigales and donkey body measurements including BH, TG, RH, TD and RW ( $p < 0.05$ ).

### 3.8. Differences of microbial function in donkey foals from pre- to post-weaning period

The potential functional capacity of fecal bacteria of donkey foals were inferred by PICRUSt using the 16S rRNA data. A total of 178

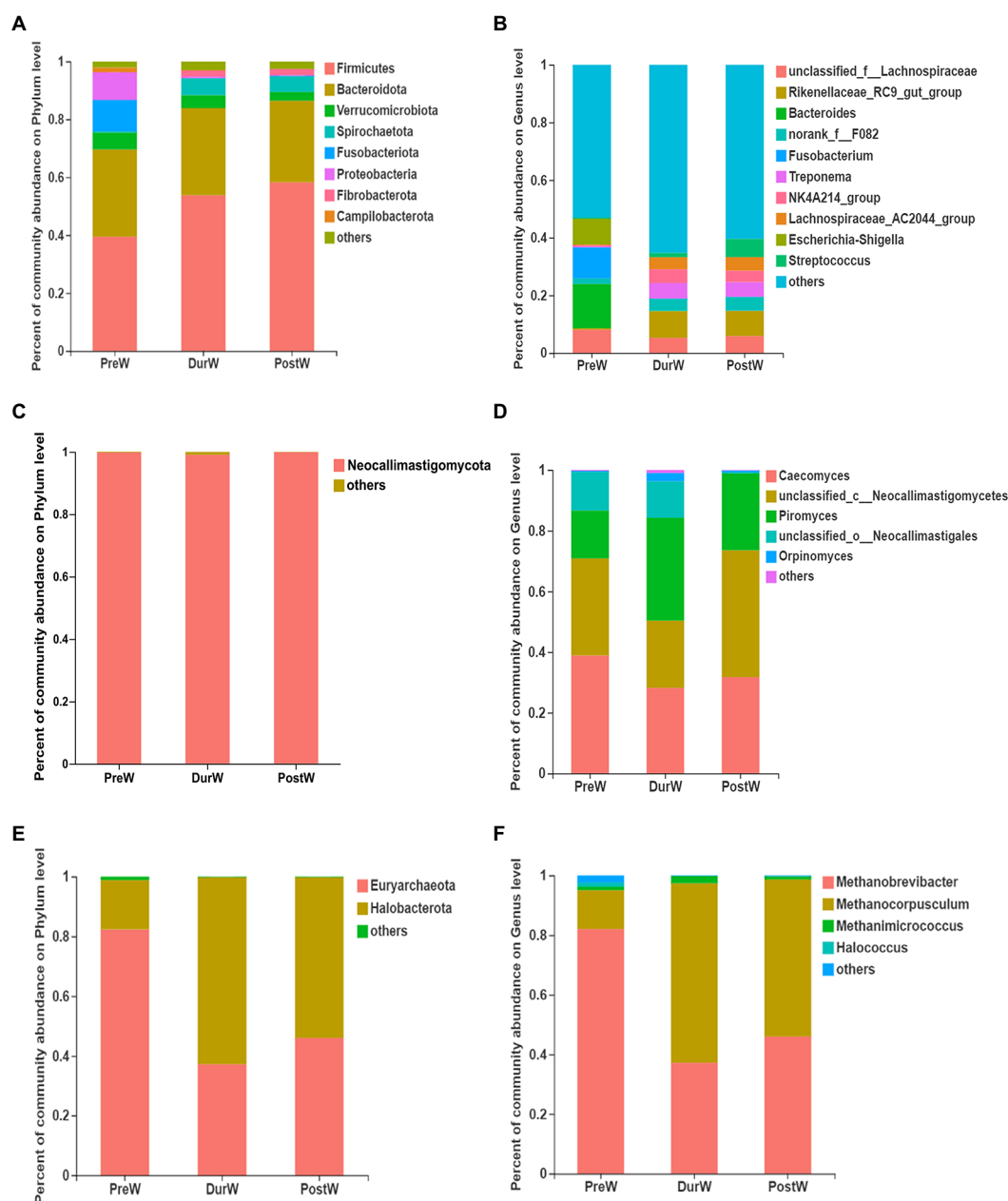


FIGURE 3

Composition of the predominant microbiota among different groups (accounting for  $\geq 0.01\%$  of the total sequences in at least one samples). (A) The predominant bacteria at phylum level. (B) The predominant bacteria at genus level. (C) The predominant anaerobic fungi at phylum level. (D) The predominant anaerobic fungi at genus level. (E) The predominant archaea at phylum level. (F) The predominant archaea at genus level; PreW, pre-weaning donkeys; DurW, during weaning donkeys; PostW, post-weaning donkeys.

differential KEGG metabolic pathways (level 3) were detected, and 9 differential KEGG metabolic pathways among PreW, DurW, and PostW groups are presented in Figure 9. The relative abundance of pathways including fatty acid biosynthesis (Figure 9A), biosynthesis of secondary metabolites (Figure 9B), Valine, leucine, and isoleucine biosynthesis (Figure 9C), phenylalanine tyrosine and tryptophan biosynthesis (Figure 9D), peptidoglycan biosynthesis (Figure 9E) and biosynthesis of amino acids (Figure 9F) in PreW donkey foals were significantly lower than that in DurW and PostW donkey foals ( $p < 0.05$ ). Conversely, the relative abundance of pathways including steroid hormone biosynthesis (Figure 9G), metabolic pathways (Figure 9H) and microbial metabolism in diverse environments (Figure 9I) in PreW

group were remarkably higher than in DurW and PostW groups ( $p < 0.05$ ).

The potential functional abundance of fecal anaerobic fungi of donkey foals were characterized by FUNGuild using the 28S rRNA data (Figure 10). There was no significant difference among PreW, DurW, and PostW groups for anaerobic fungi functional abundance ( $p > 0.05$ ).

## 4. Discussion

Weaning is one of the most important events in the early life of donkey foals. The large-scale donkey farms in China often use gradual

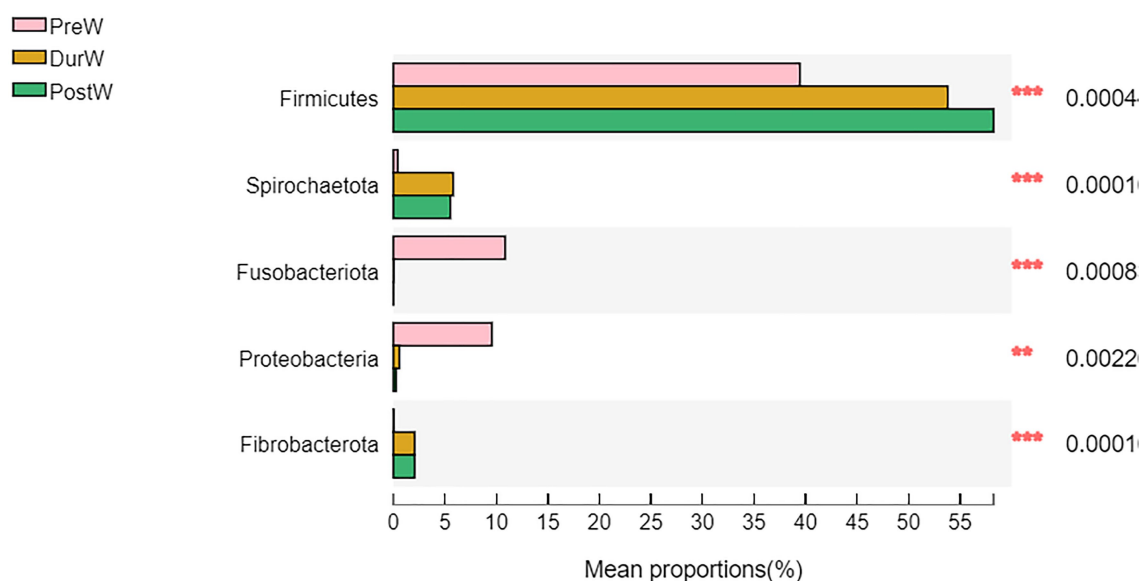


FIGURE 4

Difference of the predominant microbiota at phylum level among different groups (abundance of the microbiota is expressed as a percentage). PreW, pre-weaning donkeys; DurW, during weaning donkeys; PostW, post-weaning donkeys; \*\* $p < 0.05$ ; \*\*\* $p < 0.01$ .

weaning, allowing donkey foals to suckle the colostrum and then slowly reducing the amount of the breastfeed. From pre-weaning to post-weaning period, the gut microbiota composition of donkey foals was not immutable, but rather a dynamic alteration process (Lindenberg et al., 2019). During the weaning period, the diet of donkey foals gradually changes from a high-fat, low-fiber milk to a plant-based solid feed. The diet alteration was usually considered to be one of the important driving forces in the development and changes of gut microbiota in animals (Guevarra et al., 2018). Moreover, the process of microbial establishment in the gastrointestinal tract of donkey foals plays an important role for host health and nutrition (Lindenberg et al., 2019). However, few studies have focused on the development of the gut microbiome in donkey foals during the weaning period. To our best of knowledge, the present study is novel in being the first study to investigate the fecal microbiota (including bacteria, anaerobic fungi, and archaea) of donkey foals over a whole weaning period.

Microbial diversity and richness are usually applied to evaluate the stability of gut ecosystem in animals. Konopka (2009) noted that the high microbial diversity and richness could help to maintain the stability and resistance of ecosystem under environmental pressure. The high microbial diversity and richness is regarded as a sign of matured gut microbiota and it is also believed beneficial for host health (Turnbaugh et al., 2009; Li et al., 2020). In terms of present diversity and richness of donkey foal feces, the microbial Shannon, Ace, Chao and Sobs index in donkey foals were all increased with the changes in donkey foals' breast milk and starter intake from pre- to post-weaning period. This result indicated that the gut microbiota of donkey foals may be established more completely after weaning to better adapt to the digestion of plant-based feed. In addition, the bacterial, anaerobic fungi and archaeal complexity before weaning was lower than the post-weaning stage, which was consistent with previous studies using other animals like swine, horse, and lamb (Kim et al., 2012; Mach et al., 2017; Wang et al., 2022).

Regarding the beta diversity, the PcoA and NMDS analysis showed that there were obvious differences in donkey foal fecal

microbiota composition from pre-weaning to post-weaning period. However, no significant difference occurred between dur-weaning and post-weaning donkey foals. The cessation of breastfeeding may result in the microbial community changes due to the decreasing influence of specific milk components on the bacteria, anaerobic fungi and archaea (Lindenberg et al., 2019). As donkey foals at weaning have had a subtle intake of plant-based feed for at least several months, a microbial composition associated with this diet is to be expected.

#### 4.1. Fecal bacteria changes in donkey foals

Consistent with the previous reports on donkeys (Zhang et al., 2022a), Firmicutes and Bacteroidetes were the most predominant bacteria (represented >80% of all sequences). From pre-weaning to post weaning, the proportion of Firmicutes, Spirochaetota and Fibrobacterota increased, whereas the proportion of Fusobacteriota and Proteobacteria decreased. Both Proteobacteria and Fusobacteria have been found in the feces of newborn animals prior weaning, which act as stains to promote the development of the gut microbiome in the subsequent growth stages (Shao et al., 2021). In the present study, Fusobacteriota and Proteobacteria were higher bacterial phyla in the pre-weaning donkey foal feces than in post-weaning donkey foals, which is common in other animal species (Shao et al., 2021). Gharechahi et al. (2021) observed that the Firmicutes and Fibrobacterota were mainly enriched for genes related to the degradation of lignocellulosic polymers and the fermentation of degraded products into short chain volatile fatty acids (VFA). Firmicutes have the potential to degrade a wide range of carbohydrate polymers, which have also been reported in numerous ruminants such as moose (Svartström et al., 2017), camel (Gharechahi and Salekdeh, 2018), and cattle (Stewart et al., 2019). Fibrobacterota were particularly adapted to degrade glucan, cellulose, arabinan, xylan, and xyloglucan (Gharechahi et al., 2021).



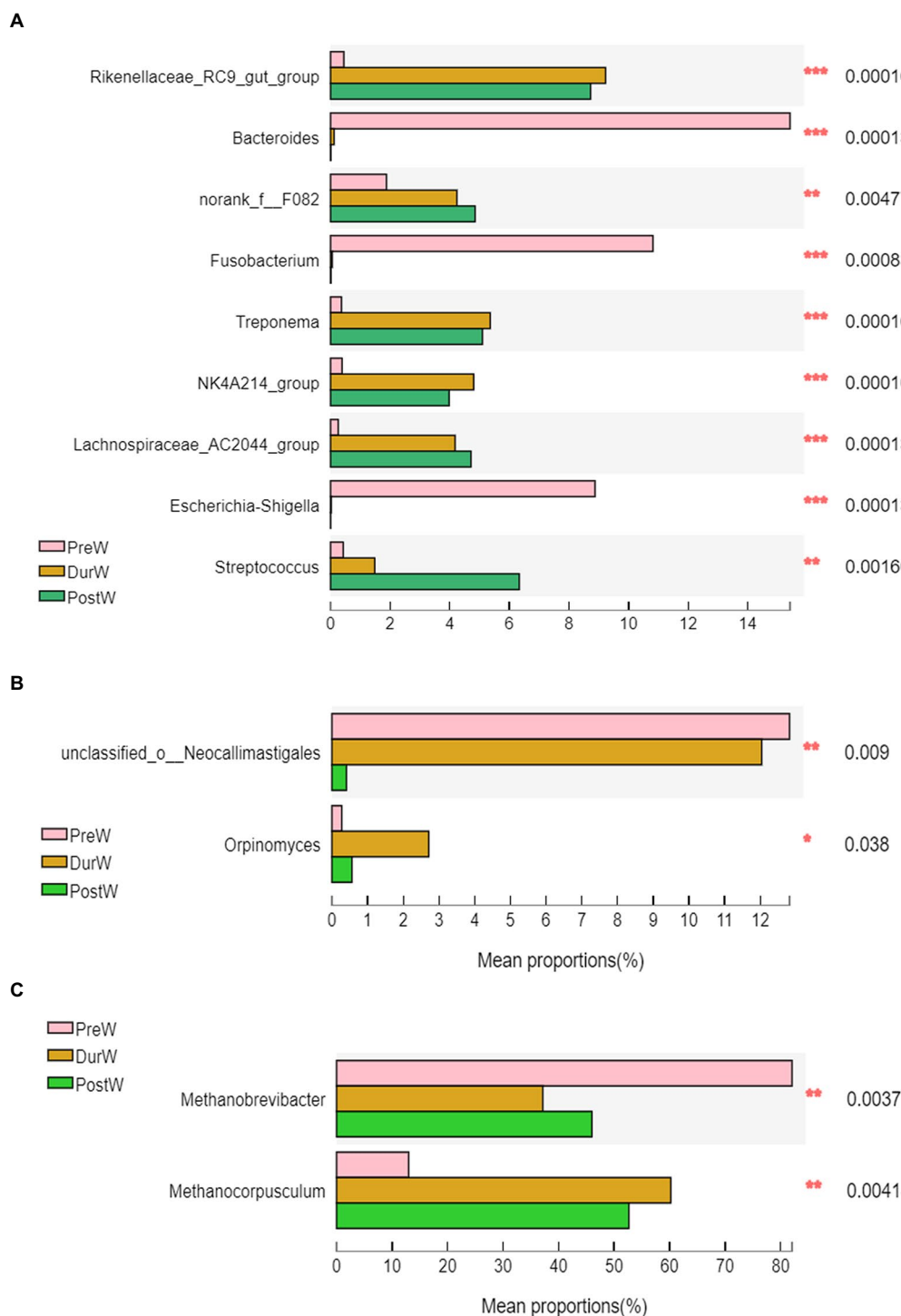
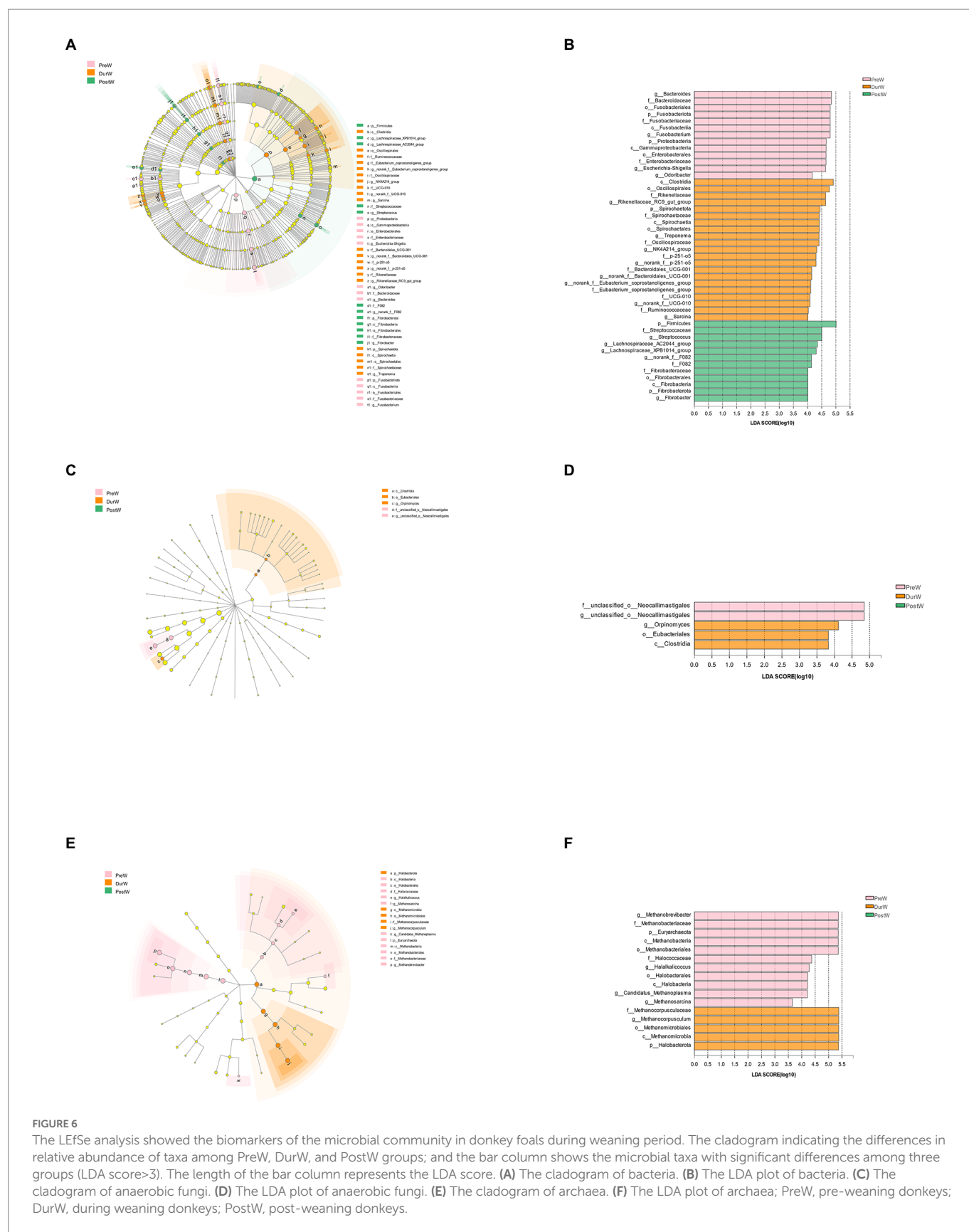


FIGURE 5

Difference of the predominant microbiota at genus level among different groups (abundance of the microbiota is expressed as a percentage). (A) The different bacteria. (B) The different anaerobic fungi. (C) The different archaea; PreW, pre-weaning donkeys; DurW, during weaning donkeys; PostW, post-weaning donkeys; \* $p < 0.05$ ; \*\* $p < 0.01$ ; \*\*\* $p < 0.001$ .

Spirochaetota also demonstrated a high ability for lignocellulose degradation (Svartström et al., 2017). Due to their ability to target cellulose-xyloglucan polysaccharide complexes through genes, Spirochaetota have been reported to play a significant role in the hemicellulose breakdown in termite hindgut microbiota (Tokuda et al., 2018; Liu N. et al., 2019). With respect to donkey foals in this study, the degradation of fibre probably enhanced the establishment

of the Firmicutes, Spirochaetota and Fibrobacterota colonization, as donkey foals no longer consume breast milk after weaning, but mainly feed on plant-based feeds. In addition, the gut microbiota has been linked with donkey body measurements. With the donkey body measurements increasing, the bacterial Firmicutes, Spirochaetota and Fibrobacterota were also increased. This result may indicate that the Firmicutes, Spirochaetota and Fibrobacterota promoted energy



acquisition and body fat accumulation in donkey foals as cellulose and hemicellulose decomposition capacity increased in donkey foals from pre- to post-weaning period.

At genus level, the abundance of *Fusobacterium* and *Escherichia-Shigella* in pre-weaning donkey foals were higher than in dur- and post-weaning groups. It has been reported that fecal microbiota of neonates is age and

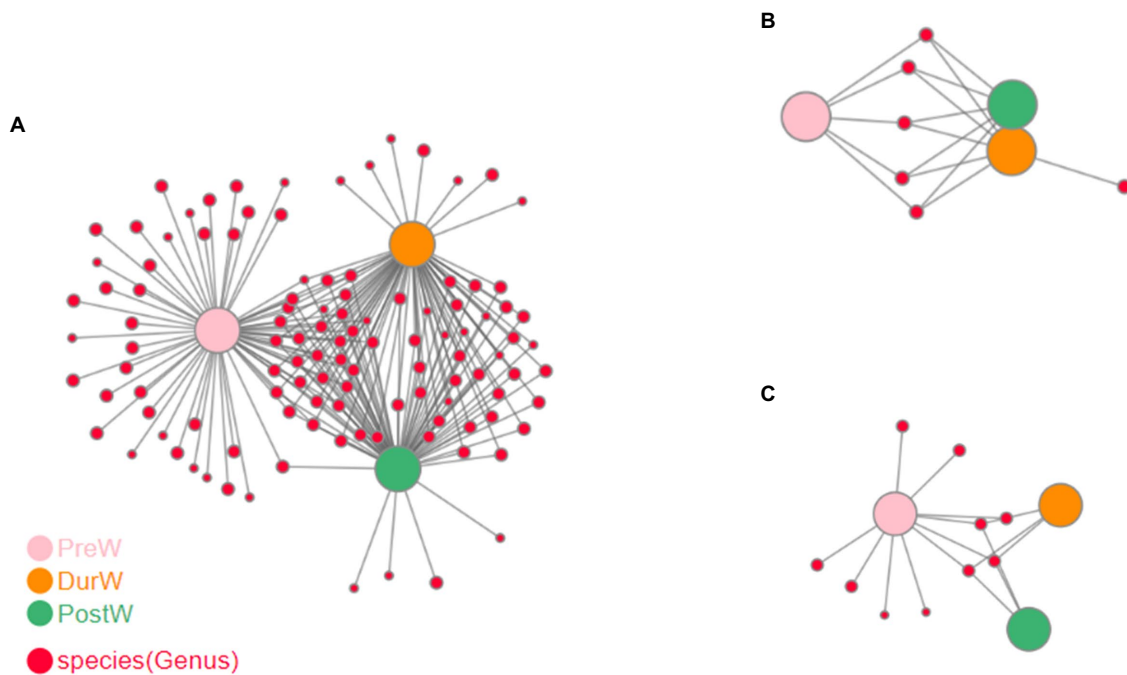


FIGURE 7

Co-occurrence network analysis on microbiota among different groups. (A) The network analysis of bacteria. (B) The network analysis of anaerobic fungi. (C) The network analysis of archaea; PreW, pre-weaning donkeys; DurW, during weaning donkeys; PostW, post-weaning donkeys.

growth dependent and its composition is closely related to pre-weaned animal health (Song et al., 2019). The *Fusobacterium* and *Escherichia-Shigella* presumably contribute to immunity development in the gut due to their capability to consume colostral oligosaccharides (Liu Y. et al., 2019). *Escherichia-Shigella* have also formed symbiotic relationships with anaerobes that require mono- and disaccharides (Maltby et al., 2013). Furthermore, *Escherichia-Shigella* participate in oxygen scavenging to contribute to an anaerobic environment (Jones et al., 2011). These activities could explain why *Escherichia-Shigella* is so prevalent in the pre-weaning donkey foal gut. In addition, *Escherichia-shigella* genus are usually associated with animal diarrhea in other species, such as pig and calf (Chanter et al., 1986; Song et al., 2019). Therefore, the lower abundance of this genus in the dur- and post-weaning groups compared to pre-weaning donkey foals suggests that donkey foals after weaning may have less prevalence of diarrhea caused by these opportunistic pathogens.

Conversely, the proportion of *Rikenellaceae\_RC9\_gut\_group*, *norank\_f\_F082*, *Treponema*, *NK4A214\_group*, *Lachnospiraceae\_AC2044\_group* and *Streptococcus* in PreW donkey foals were higher in DurW and PostW than in PreW donkey foals. Cui et al. (2022) noted that the *Rikenellaceae\_RC9\_gut\_group* may play an important role in the biosynthesis of VFAs and energy utilization due to it was positively correlated with VFA production. Yi et al. (2022) reported that the abundance of *norank\_f\_F082* was positively correlated with the proportion of concentrate. Therefore, the enriched *norank\_f\_F082* genera in dur- and post-weaning groups may play an important role in the digestion of plant-based solid feed containing a lot of non-structural carbohydrates. *Treponema* has been reported to be cellulolytic bacteria in previous study (Evans et al., 2011). The increasing abundance of *Treponema* in donkey foals from pre-weaning to post-weaning period may be attributed to their capability to degrade plant celluloses (Li et al., 2020). The *NK4A214\_group* belongs to the *Ruminococcus* family (Yi et al., 2022), and the high abundance in dur- and post-weaning groups may be related to its ability to digest plant fiber,

because diets after weaning feature more plant fiber. In addition, they also produce pili involved in the bacterium's adhesion to cellulose (Yi et al., 2022). *Lachnospiraceae\_AC2044\_group* was usually correlated with the propionate, and they ferment glucose to produce lactic acid (Han et al., 2021). The introduction of plant-based diets in dur- and post-weaning donkey foals may provide a large amount of fermentable carbohydrates that favored the growth of *Lachnospiraceae\_AC2044\_group*. Moreover, the easy availability of glucans in the substrate after weaning in donkey foals presumably promoted the colonization of fast-growing *Streptococcus*. Recently, Gharechahi et al. (2021) demonstrated that a high proportion of *Streptococcus* is observed when animals are offered concentrate. In accordance with the changes in bacterial genus during weaning period, the bacterial *Rikenellaceae\_RC9\_gut\_group*, *norank\_f\_F082*, *Treponema*, *NK4A214\_group*, *Lachnospiraceae\_AC2044\_group* and *Streptococcus* were positively correlated with donkey body measurements. By observing the body size of donkey foals from pre- to post-weaning period, we speculated that the large body size of post-weaning donkey foals might be related to the high cellulolytic bacteria content in their intestinal microbiota. After weaning, a high input of plant material in donkey foal hindgut may be hydrolyzed by these bacteria to produce more energy for bodily processes, which increased the body size of donkey foals.

Until now, little studies explored the bacterial function of the fecal microbiome in donkey foals during weaning transition. In the current study, we used PICRUSt software to determine the potential functional capacity of fecal bacteria of donkey foals from pre-weaning to post-weaning period. From pre-weaning to post-weaning period in donkey foals, the amounts and types of carbohydrates in breast and plant-based solid feeds are different, as well as the fermentation capacity of microbiota. The bacterial functions related to microbial metabolism and steroid hormone biosynthesis were significantly enriched in the fecal microbiome in the pre-weaning donkey foals. While the microbial gene functions, including the fatty acid

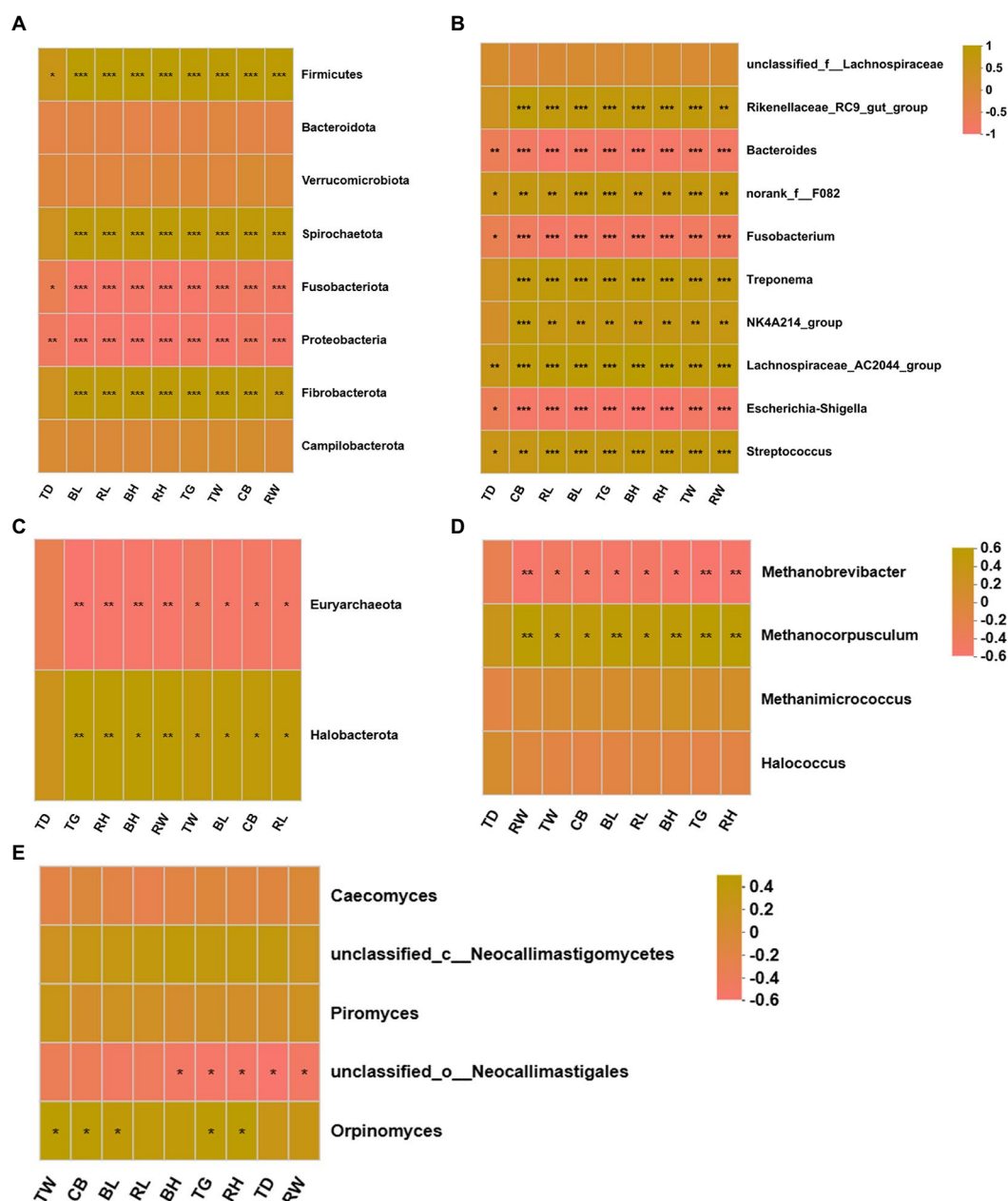


FIGURE 8

Correlation heatmap of differentially donkey fecal microbiota and body measurements. Each row in the graph represents a microbiota phylum/genus, each column represents a body measurement, the color in the graph indicates the Pearson coefficient between the microbial phylum/genus and donkey body measurements, and the brick yellow indicates positive correlation. The pale pink is representative negative correlation. The darker color indicate the greater the correlation. (A) Between donkey body measurements and bacteria at phylum level. (B) Between donkey body measurements and bacteria at genus level. (C) Between donkey body measurements and anaerobic fungi at phylum level. (D) Between donkey body measurements and anaerobic fungi at genus level. (E) Between donkey body measurements and archaea at genus level. \* $p < 0.05$ ; \*\* $p < 0.01$ ; \*\*\* $p < 0.001$ . BH, body height; BL, body length; TG, thoracic girth; TD, thoracic depth; TW, thoracic width; RH, rump height; RL, rump length; RW, rump width; CB, circumference of cannon bone.

biosynthesis, biosynthesis of secondary metabolites, Valine, leucine, and isoleucine biosynthesis, phenylalanine tyrosine and tryptophan biosynthesis, peptidoglycan biosynthesis and biosynthesis of amino acids, were mainly enriched in the pre-weaning donkey foals, and were linked with the carbohydrate metabolism and amino acid biosynthesis. These results indicated that the potential functions of bacteria in donkey foal feces are synergistic with host functions. The microbiota resident in the pre-weaning donkey foals were more inclined to have functions in the microbial metabolism and breast milk utilization, while microbiota resident in the dur- and post-weaning donkeys were more inclined to have functions such as fatty

acid biosynthesis, secondary metabolites biosynthesis and amino acid biosynthesis. However, further studies are still required to characterize the microbial functions of gut bacteria in donkey foals during weaning transition.

## 4.2. Fecal anaerobic fungi changes in donkey foals

Anaerobic fungi have been most extensively studied in ruminants, but they have been found in both domesticated and wild equine



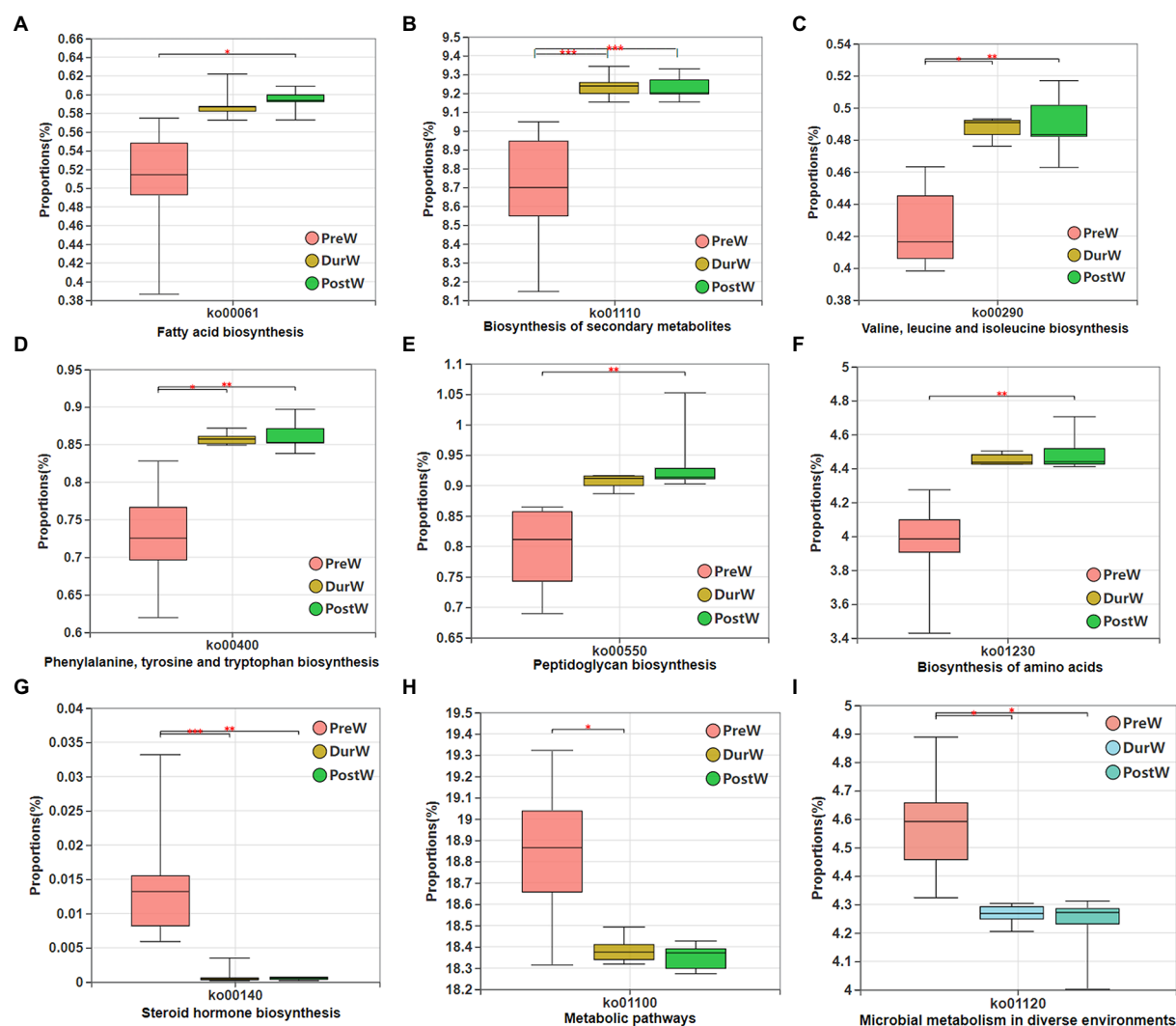
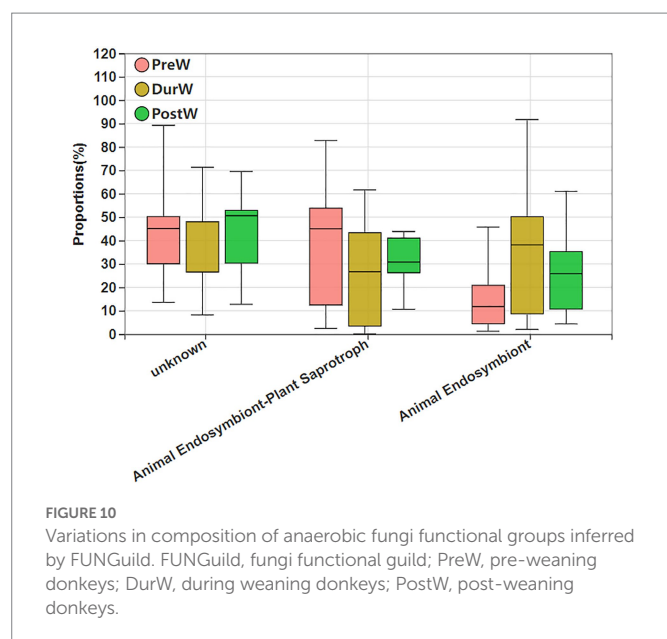


FIGURE 9

Variations in composition of bacterial KEGG metabolic pathways inferred by PICRUSt. KEGG, Kyoto Encyclopedia of Genes and Genomes; PICRUSt, the phylogenetic investigation of communities by reconstruction of unobserved states; PreW, pre-weaning donkeys; DurW, during weaning donkeys; PostW, post-weaning donkeys. \* $p < 0.05$ ; \*\* $p < 0.01$ ; \*\*\* $p < 0.001$ .

species (Hess et al., 2020). In the present study, Neocallimastigomycota was found to be the most predominant fungal phylum in donkey foal feces, which is consistent with previous studies in goats and heifers (Mao et al., 2016; Zhang et al., 2017). Neocallimastigomycota play an essential role in the degradation of fibrous plant materials in herbivores (Gruninger et al., 2014). At genus level, the *Caecomyces*, *unclassified\_c\_\_Neocallimastigomycetes*, *Piromyces*, *unclassified\_o\_\_Neocallimastigales* and *Orpinomyces* were the predominant fungi genera in donkey foal feces. The predominated *Caecomyces* genera has previously been reported to occur in the equine feces and pony caecum (Liggenstoffer et al., 2010; Hanafy et al., 2020), and they have also been cultured from equines (Edwards et al., 2020). Metabolic profiles have previously been investigated for equine and rumen strains of *Piromyces*, with equine *Piromyces* possessing higher fiber degradation capacity in comparison with rumen isolates (Julliand et al., 1998). The *Orpinomyces* are also powerful fiber degraders due to their highly effective plant degrading enzymes, which including cellulase and xylanase activities (Youssef et al., 2013). From pre-weaning to post weaning, the anaerobic fungi composition in

donkey foal feces were unchanged dramatically. Only the relative abundance of *unclassified\_o\_\_Neocallimastigales* were gradually decreased, and the proportion of *Orpinomyces* were the highest in DurW groups. The anaerobic fungus *Orpinomyces* is capable of growth on a variety of lignocellulosic materials and has a large reservoir of carbohydrate active enzymes (Morrison et al., 2016). Weaning of donkey foals usually occur between 5 to 6 months of age, but the shifts from milk to plant-based feeds is gradual. In the DurW group, donkey foals will have started ingesting forage and concentrates before weaning, which will promote the maturation of the digestive tract in preparation for the eventual change to forage-based feeds. Therefore, the forage-based feed with large quantity of fiber and lignocellulose may increase the abundance of *Orpinomyces* in the DurW donkey foals. A positive correlation between fungus *Orpinomyces* and body measurements of donkey foals was observed in the present study. This result means that the *Orpinomyces* may be associated with body size in donkey foals. The anaerobic fungi have been reported to be the primary degraders of fiber in herbivores (Edwards et al., 2020). The higher abundance of *Orpinomyces* in



post-weaning donkey foals may promoted the VFA production, which ultimately promoted the body measurements in donkey foals.

To data, rare study was performed on the potential functional abundance of anaerobic fungi within donkey foals. In this study, FUNGuild was applied to infer the metabolic functional variations in anaerobic fungi among pre-, dur-, and post-weaning donkey foal feces. FUNGuild is a tool for assigning fungi trait information based on matching to a taxonomic classification using the FUNGuild database (Xie et al., 2021). The results showed that there were no obvious differences for anaerobic fungi functional abundance in donkey foals from pre-weaning to post-weaning period. This result might indicate that the fungal colonization of the foal gut commences in pre-weaning period. However, the role of these anaerobic fungi in the pre-weaning donkey foal hindgut ecosystem is currently unclear. Further studies will be required to understand why there were anaerobic fungi in the donkey foal gut before weaning without plant materials.

### 4.3. Fecal archaea changes in donkey foals

Similarly to the rumen, the donkey hindgut also accommodates a number of archaea that work symbiotically with bacteria and anaerobic fungi to degrade and ferment the feeds ingested by the host (Edwards et al., 2020). Many studies have been focused on the bacterial and anaerobic fungi diversity in the hindgut of adult equine (Liu et al., 2020; Zhang et al., 2022a,c). However, only limited investigation is available on the archaeal composition in donkey foals. The sequences detected at archaeal phylum in our study clustered into the Euryarchaeota, which is in accordance with the previous study of Murrúa et al. (2018) in horse. The current PCoA of the methanogen community structure showed that in donkey foal feces there was a significant gap between the communities before and post weaning, but no obvious differences were observed between DurW and PostW groups. This finding suggested that weaning stress had a significant influence on the composition of the donkey foal methanogenic archaeal community.

Until now, the initial colonization of methanogens in the donkey foals has not yet been studied. In ruminants, Skillman et al. (2004)

reported that the *Methanobrevibacter* were detected in the rumen liquid of lambs at the age of 3 days. In the present study, the predominant archaeal genera in donkey foal feces before weaning were also *Methanobrevibacter*, thereby implying that the initial colonization and establishment of methanogens in donkey foals began prior to weaning. Before weaning, H<sub>2</sub> could be produced during carbohydrate fermentation. Methanogens use H<sub>2</sub> as a source of energy to convert CO<sub>2</sub> or acetate to CH<sub>4</sub> during methanogenesis (Wang et al., 2017). Guzman et al. (2015) noted that the *Proteobacteria*, *Ruminococcus flavefaciens*, or other species are thought to provide methanogens with the necessary H<sub>2</sub> and electrons for methanogenesis during the early stages prior to forage ingestion. After weaning, the relative abundance of *Methanocorpusculum* in donkey foals increased remarkably. Besides the change of diet structure and components, weaning transition also involves both psychological and physiological stress as the donkey foals were no longer raised alongside the dams. Therefore, the weaning may be a major event responsible for reshaping of the gut archaea in donkey foals. In the feces of adult horses, Lwin and Matsui (2014) identified the *Methanomicrobiales*, represented by *Methanocorpusculum*, as the predominate order and the *Methanobrevibacter* as the less common species. In addition, the *Methanocorpusculum* has also been reported in adult donkey feces (Liu et al., 2014). Both the *Methanobrevibacter* and the *Methanocorpusculum* are hydrogenotrophic methanogens, which can also use formate, but their preference of different ecological niches is evident. The *Methanocorpusculum* are demonstrated as endosymbionts of anaerobic ciliates (Murrúa et al., 2018). The abundance of methanogens related to the *Methanocorpusculum* in the equus species may be associated with the symbiotic relationship with the hydrogen producing “equine” anaerobic fungi and ciliates (Liggenstoffer et al., 2010). After weaning, plant feed particles may provide anaerobic fungi and ciliates with an abundant ecological niche. As a result, the increase abundance of anaerobic fungi and ciliates might encourage the growth of *Methanocorpusculum*.

For the anaerobic fermentation processes, the CH<sub>4</sub> is released by donkeys as a by-product of enteric food digestion to maintain hydrogen at low partial pressures (Murrúa et al., 2018). However, information regarding the loss of feed energy for a host animal and the composition of methanogenic microbial community in donkeys is limited. In the present study, there was a negative correlation between donkey body measurements and Euryarchaeota, and the BH, BL, TG, TW, RH, RL, RW, and CB of donkey foals were negatively correlated with *Methanobrevibacter*. The lower abundance of archaea means less loss of feed energy, thus, the decrease of methanogens in post-weaning donkey foals may enhance the body measurements of donkey foals by the improvement of feed efficiency. But in this study, there was also a positive correlation between donkey body measurements and *Methanocorpusculum* abundance. The composition of the archaea in the hindgut of equine could depend on the hindgut capacity as a reflection of body size (Lwin and Matsui, 2014). More investigation is needed in the future to understand the diversity and abundance of methanogens in the donkey foals for reducing CH<sub>4</sub> emission.

In summary, the present study provides integrative information on the global fecal microbiota of healthy donkey foals undergoing the weaning transition. From pre-weaning to post-weaning, the cessation of breastfeeding gradually and weaning onto plant-based feeds increased the microbial diversity and richness. The cellulolytic related bacteria including phylum Firmicutes, Spirochaetota, and Fibrobacterota and genus norank\_f\_F082, *Treponema*, NK4A214\_group, *Lachnospiraceae*\_AC2044\_group and *Streptococcus* increased. Meanwhile, the functions

related to the carbohydrate metabolism and amino acid biosynthesis were obviously enriched in the fecal microbiome in the dur- and post-weaning donkeys. In terms of anaerobic fungi and archaea, the present study provided the first direct evidence that the initial colonization and establishment of anaerobic fungi and archaea in donkey foals began prior to weaning. In addition, the changes in the composition of the anaerobic fungi and archaea occurred during the weaning period. Altogether, the current study contributes to a better understanding of the development of the microbiota community in donkey foals from the pre-weaning to the post-weaning period. Future research should focus on the interactions of the metabolome, microbiome, and the gut functional development, as well as the long-term impact of manipulation during the weaning period on donkey production.

## Data availability statement

The datasets presented in this study can be found in online repositories. The names of the repository/repositories and accession number(s) can be found at: <https://www.ncbi.nlm.nih.gov/>, PRJNA903673.

## Ethics statement

The animal study was reviewed and approved by the Animal Welfare Committee of Liaocheng University.

## Author contributions

ZZ contributed to the manuscript writing, editing, data generation and analysis, revision, and general ideas of the manuscript. ZZ, BH, XS, XW, TW, and YW contributed to all the sample collection, results discussion, and collection of literature. GL and CW contributed to the

conceptualization of the study, study fund support, results discussion, and draft revision. All authors read and approved the manuscript.

## Funding

This study was funded by the Shandong Province Modern Agricultural Technology System Donkey Industrial Innovation Team (grant number SDAIT-27), Livestock and Poultry Breeding Industry Project of the Ministry of Agriculture and Rural Affairs (grant number 19211162), Shandong Rural Revitalization Science and Technology Innovation Action Plan (Key Technology Innovation and Demonstration of Integrated Development of Dong-E Black Donkey Industry, grant number 2021TZXD012), Open Project of Liaocheng University Animal Husbandry Discipline (grant number 319312101-14), Open Project of Shandong Collaborative Innovation Center for Donkey Industry Technology (grant number 3193308), Research on Donkey Pregnancy Improvement (grant number K20LC0901), and Liaocheng University Scientific Research Fund (grant number 318052025).

## Conflict of interest

The authors declare that the research was conducted in the absence of any commercial or financial relationships that could be construed as a potential conflict of interest.

## Publisher's note

All claims expressed in this article are solely those of the authors and do not necessarily represent those of their affiliated organizations, or those of the publisher, the editors and the reviewers. Any product that may be evaluated in this article, or claim that may be made by its manufacturer, is not guaranteed or endorsed by the publisher.

## References

- Caporaso, J. G., Bittinger, K., Bushman, F. D., DeSantis, T. Z., Andersen, G. L., and Knight, R. (2010). PYNAST: a flexible tool for aligning sequences to a template alignment. *Bioinformatics* 26, 266–267. doi: 10.1093/bioinformatics/btp636
- Chanter, N., Hall, G. A., Bland, A. P., Hayle, A. J., and Parsons, K. R. (1986). Dysentery in calves caused by an atypical strain of *Escherichia coli* (S102-9). *Vet. Microbiol.* 12, 241–253. doi: 10.1016/0378-1135(86)90053-2
- Cui, Y., Liu, H., Gao, Z., Xu, J., Liu, B., Guo, M., et al. (2022). Whole-plant corn silage improves rumen fermentation and growth performance of beef cattle by altering rumen microbiota. *Appl. Microbiol. Biotechnol.* 106, 4187–4198. doi: 10.1007/s00253-022-11956-5
- Dougal, K., Harris, P. A., Edwards, A., Pachebat, J. A., Blackmore, T. M., Worgan, H. J., et al. (2012). A comparison of the microbiome and the metabolome of different regions of the equine hindgut. *FEMS Microbiol. Ecol.* 82, 642–652. doi: 10.1111/j.1574-6941.2012.01441.x
- Edwards, J. E., Shetty, S. A., van den Berg, P., Burden, F., van Doorn, D. A., Pellikaan, W. F., et al. (2020). Multi-kingdom characterization of the core equine fecal microbiota based on multiple equine (sub) species. *Anim. Microbiome* 2:6. doi: 10.1186/s42523-020-0023-1
- Evans, N. J., Brown, J. M., Murray, R. D., Getty, B., Birtles, R. J., Hart, C. A., et al. (2011). Characterization of novel bovine gastrointestinal tract *Treponema* isolates and comparison with bovine digital dermatitis treponemes. *Appl. Environ. Microbiol.* 77, 138–147. doi: 10.1128/AEM.00993-10
- Frese, S. A., Parker, K., Calvert, C. C., and Mills, D. A. (2015). Diet shapes the gut microbiome of pigs during nursing and weaning. *Microbiome* 3:28. doi: 10.1186/s40168-015-0091-8
- Gharechahi, J., and Salekdeh, G. H. (2018). A metagenomic analysis of the camel rumen's microbiome identifies the major microbes responsible for lignocellulose degradation and fermentation. *Biotechnol. Biofuels* 11:216. doi: 10.1186/s13068-018-1214-9
- Gharechahi, J., Vahidi, M. F., Bahram, M., Han, J. L., Ding, X. Z., and Salekdeh, G. H. (2021). Metagenomic analysis reveals a dynamic microbiome with diversified adaptive functions to utilize high lignocellulosic forages in the cattle rumen. *ISME J.* 15, 1108–1120. doi: 10.1038/s41396-020-00837-2
- Grimm, P., Philippeau, C., and Jullian, V. (2017). Fecal parameters as biomarkers of the equine hindgut microbial ecosystem under dietary change. *Animal* 11, 1136–1145. doi: 10.1017/S1751731116002779
- Gruninger, R. J., Puniya, A. K., Callaghan, T. M., Edwards, J. E., Youssef, N., Dagar, S. S., et al. (2014). Anaerobic fungi (phylum Neocallimastigomycota): advances in understanding their taxonomy, life cycle, ecology, role and biotechnological potential. *FEMS Microbiol. Ecol.* 90, 1–17. doi: 10.1111/1574-6941.12383
- Guevarra, R. B., Hong, S. H., Cho, J. H., Kim, B. R., Shin, J., Lee, J. H., et al. (2018). The dynamics of the piglet gut microbiome during the weaning transition in association with health and nutrition. *J. Anim. Sci. Biotechnol.* 9:54. doi: 10.1186/s40104-018-0269-6
- Guzman, C. E., Bereza-Malcolm, L. T., De Groef, B., and Franks, A. E. (2015). Presence of selected methanogens, fibrolytic bacteria, and proteobacteria in the gastrointestinal tract of neonatal dairy calves from birth to 72 hours. *PLoS One* 10:e0133048. doi: 10.1371/journal.pone.0133048
- Han, L., Xue, W., Cao, H., Chen, X., Qi, F., Ma, T., et al. (2021). Comparison of rumen fermentation parameters and microbiota of yaks from different altitude regions in Tibet China. *Front. Microbiol.* 12:807512. doi: 10.3389/fmicb.2021.807512
- Hanafy, R. A., Lanjekar, V. B., Dhakephalkar, P. K., Callaghan, T. M., Dagar, S. S., Griffith, G. W., et al. (2020). Seven new Neocallimastigomycota genera from wild, zoo-housed, and domesticated herbivores greatly expand the taxonomic diversity of the phylum. *Mycologia* 112, 1212–1239. doi: 10.1080/00275514.2019.1696619



- Hess, M., Paul, S. S., Puniya, A. K., van der Giezen, M., Shaw, C., Edwards, J. E., et al. (2020). Anaerobic fungi: past, present, and future. *Front. Microbiol.* 11:584893. doi: 10.3389/fmicb.2020.584893
- Jones, S. A., Gibson, T., Maltby, R. C., Chowdhury, F. Z., Stewart, V., Cohen, P. S., et al. (2011). Anaerobic respiration of *Escherichia coli* in the mouse intestine. *Infect. Immun.* 79, 4218–4226. doi: 10.1128/IAI.05395-11
- Julliand, V., and Grimm, P. (2016). Horse species symposium: the microbiome of the horse hindgut: history and current knowledge. *J. Anim. Sci.* 94, 2262–2274. doi: 10.2527/jas.2015-0198
- Julliand, V., Riondet, C., De Vaux, A., Alcaraz, G., and Fonty, G. (1998). Comparison of metabolic activities between *Piromyces citronii*, an equine fungal species, and *Piromyces communis*, a ruminal species. *Anim. Feed Sci. Technol.* 70, 161–168. doi: 10.1016/S0377-8401(97)00043-6
- Kim, H. B., Borewicz, K., White, B. A., Singer, R. S., Sreevatsan, S., Tu, Z. J., et al. (2012). Microbial shifts in the swine distal gut in response to the treatment with antimicrobial growth promoter, tylosin. *Proc. Natl. Acad. Sci. U. S. A.* 109, 15485–15490. doi: 10.1073/pnas.1205147109
- Köljal, U., Larsson, K. H., Abarenkov, K., Nilsson, R. H., Alexander, I. J., Eberhardt, U., et al. (2005). UNITE: a database providing web-based methods for the molecular identification of ectomycorrhizal fungi. *New Phytol.* 166, 1063–1068. doi: 10.1111/j.1469-8137.2005.01376.x
- Konopka, A. (2009). What is microbial community ecology? *ISME J.* 3, 1223–1230. doi: 10.1038/ismej.2009.88
- Li, Y., Ma, Q. S., Liu, G. Q., Zhang, Z. W., Zhan, Y. D., Zhu, M. X., et al. (2022). Metabolic alterations during gestation in Dezhou donkeys and the link to the gut microbiota. *Front. Microbiol.* 13:801976. doi: 10.3389/fmicb.2022.801976
- Li, Y., Shi, M., Zhang, T., Hu, X., Zhang, B., Xu, S., et al. (2020). Dynamic changes in intestinal microbiota in young forest musk deer during weaning. *PeerJ* 8:e8923. doi: 10.7717/peerj.8923
- Li, C., Wang, W., Liu, T., Zhang, Q., Wang, G., Li, F., et al. (2018). Effect of early weaning on the intestinal microbiota and expression of genes related to barrier function in lambs. *Front. Microbiol.* 9:1431. doi: 10.3389/fmicb.2018.01431
- Liggenstoffer, A. S., Youssef, N. H., Couger, M. B., and Elshahed, M. S. (2010). Phylogenetic diversity and community structure of anaerobic gut fungi (phylum Neocallimastigomycota) in ruminant and non-ruminant herbivores. *ISME J.* 4, 1225–1235. doi: 10.1038/ismej.2010.49
- Lindenberg, F., Krych, L., Kot, W., Fielden, J., Frøkiær, H., van Galen, G., et al. (2019). Development of the equine gut microbiota. *Sci. Rep.* 9:14427. doi: 10.1038/s41598-019-50563-9
- Liu, X., Fan, H., Ding, X., Hong, Z., Nei, Y., Liu, Z., et al. (2014). Analysis of the gut microbiota by high-throughput sequencing of the V5-V6 regions of the 16S rRNA gene in donkey. *Curr. Microbiol.* 68, 657–662. doi: 10.1007/s00284-014-0528-5
- Liu, N., Li, H., Chevrete, M. G., Zhang, L., Cao, L., Zhou, H., et al. (2019). Functional metagenomics reveals abundant polysaccharide-degrading gene clusters and cellobiose utilization pathways within gut microbiota of a wood-feeding higher termite. *ISME J.* 13, 104–117. doi: 10.1038/s41396-018-0255-1
- Liu, H., Zhao, X., Han, X., Xu, S., Zhao, L., Hu, L., et al. (2020). Comparative study of gut microbiota in Tibetan wild asses (*Equus kiang*) and domestic donkeys (*Equus asinus*) on the Qinghai Tibet plateau. *PeerJ* 8:e9032. doi: 10.7717/peerj.9032
- Liu, Y., Zheng, Z., Yu, L., Wu, S., Sun, L., Wu, S., et al. (2019). Examination of the temporal and spatial dynamics of the gut microbiome in newborn piglets reveals distinct microbial communities in six intestinal segments. *Sci. Rep.* 9:3453. doi: 10.1038/s41598-019-40235-z
- Luo, Z., Ma, L., Zhou, T., Huang, Y., Zhang, L., Du, Z., et al. (2022). Beta-glucan alters gut microbiota and plasma metabolites in pre-weaning dairy calves. *Meta* 12:687. doi: 10.3390/metabo12080687
- Lwin, K. O., and Matsui, H. (2014). Comparative analysis of the methanogen diversity in horse and pony by using mcrA gene and archaeal 16S rRNA gene clone libraries. *Archaea* 2014:483574. doi: 10.1155/2014/483574
- Ma, Z., Wang, R., Wang, M., Zhang, X., Mao, H., and Tan, Z. (2018). Short communication: variability in fermentation end-products and methanogen communities in different rumen sites of dairy cows. *J. Dairy Sci.* 101, 5153–5158. doi: 10.3168/jds.2017-14096
- Mach, N., Foury, A., Kittelmann, S., Reigner, F., Moroldo, M., Ballester, M., et al. (2017). The effects of weaning methods on gut microbiota composition and horse physiology. *Front. Physiol.* 8:535. doi: 10.3389/fphys.2017.00535
- Maltby, R., Leatham-Jensen, M. P., Gibson, T., Cohen, P. S., and Conway, T. (2013). Nutritional basis for colonization resistance by human commensal *Escherichia coli* strains HS and Nissle 1917 against *E. coli* O157:H7 in the mouse intestine. *PLoS One* 8:e53957. doi: 10.1371/journal.pone.0053957
- Mao, S. Y., Huo, W. J., and Zhu, W. Y. (2016). Microbiome-metabolome analysis reveals unhealthy alterations in the composition and metabolism of ruminal microbiota with increasing dietary grain in a goat model. *Environ. Microbiol.* 18, 525–541. doi: 10.1111/1462-2920.12724
- Meng, Q., Luo, Z., Cao, C., Sun, S., Ma, Q., Li, Z., et al. (2020). Weaning alters intestinal gene expression involved in nutrient metabolism by shaping gut microbiota in pigs. *Front. Microbiol.* 11:694. doi: 10.3389/fmicb.2020.00694
- Morrison, J. M., Elshahed, M. S., and Youssef, N. H. (2016). Defined enzyme cocktail from the anaerobic fungus *Orpinomyces* sp. strain C1A effectively releases sugars from pretreated corn Stover and switchgrass. *Sci. Rep.* 6:29217. doi: 10.1038/srep29217
- Murrua, F., Fliegerova, K., Mura, E., Mrázek, J., Kopečný, J., and Monielloa, G. (2018). A comparison of methanogens of different regions of the equine hindgut. *Anaerobe* 54, 104–110. doi: 10.1016/j.anaerobe.2018.08.009
- Nagler, M., Kozjek, K., Etemadi, M., Insam, H., and Podmirseg, S. M. (2019). Simple yet effective: microbial and biotechnological benefits of rumen liquid addition to lignocellulose-degrading biogas plants. *J. Biotechnol.* 300, 1–10. doi: 10.1016/j.jbiotec.2019.05.004
- Pruesse, E., Quast, C., Knittel, K., Fuchs, B. M., Ludwig, W., Peplies, J., et al. (2007). SILVA: a comprehensive online resource for quality checked and aligned ribosomal RNA sequence data compatible with ARB. *Nucleic Acids Res.* 35, 7188–7196. doi: 10.1093/nar/gkm864
- Salem, S. E., Maddox, T. W., Berg, A., Antczak, P., Ketley, J. M., Williams, N. J., et al. (2018). Variation in fecal microbiota in a group of horses managed at pasture over a 12-month period. *Sci. Rep.* 8:8510. doi: 10.1038/s41598-018-26930-3
- Santos, A. S., Rodrigues, M. A. M., Bessa, R. J. B., Ferreira, L. M., and Martin-Rosset, W. (2011). Understanding the equine cecum-colon ecosystem: current knowledge and future perspectives. *Animal* 5, 48–56. doi: 10.1017/S1751731110001588
- Shao, M., Wang, Z., He, Y., Tan, Z., and Zhang, J. (2021). Fecal microbial composition and functional diversity of Wuzhishan pigs at different growth stages. *AMB Express* 11:88. doi: 10.1186/s13568-021-01249-x
- Skillman, L. C., Evans, P. N., Naylor, G. E., Morvan, B., Jarvis, G. N., and Joblin, K. N. (2004). 16S ribosomal DNA-directed PCR primers for ruminal methanogens and identification of methanogens colonizing young lambs. *Anaerobe* 10, 277–285. doi: 10.1016/j.anaerobe.2004.05.003
- Song, Y., Malmuthuge, N., Li, F., and Guan, L. L. (2019). Colostrum feeding shapes the hindgut microbiota of dairy calves during the first 12 h of life. *FEMS Microbiol. Ecol.* 95:10. doi: 10.1093/femsec/fiy203
- Stewart, R. D., Auffret, M. D., Warr, A., Walker, A. W., Roehe, R., and Watson, M. (2019). Compendium of 4,941 rumen metagenome-assembled genomes for rumen microbiome biology and enzyme discovery. *Nat. Biotechnol.* 37, 953–961. doi: 10.1038/s41587-019-0202-3
- Svartström, O., Alneberg, J., Terrapon, N., Lombard, V., de Bruijn, I., Malmsten, J., et al. (2017). Ninety-nine de novo assembled genomes from the moose (*Alces alces*) rumen microbiome provide new insights into microbial plant biomass degradation. *ISME J.* 11, 2538–2551. doi: 10.1038/ismej.2017.108
- Tokuda, G., Mikaelyan, A., Fukui, C., Matsuura, Y., Watanabe, H., Fujishima, M., et al. (2018). Fiber-associated spirochetes are major agents of hemicellulose degradation in the hindgut of wood-feeding higher termites. *PNAS* 115, 11996–12004. doi: 10.1073/pnas.1810550115
- Turnbaugh, P. J., Hamady, M., Yatsunenko, T., Cantarel, B. L., Duncan, A., Ley, R. E., et al. (2009). A core gut microbiome in obese and lean twins. *Nature* 457, 480–484. doi: 10.1038/nature07540
- Wang, S., Chai, J., Zhao, G., Zhang, N., Cui, K., Bi, Y., et al. (2022). The temporal dynamics of rumen microbiota in early weaned lambs. *Microorganisms* 2022 10:144. doi: 10.3390/microorganisms10010144
- Wang, Z., Elekhwachi, C. O., Jiao, J., Wang, M., Tang, S., Zhou, C., et al. (2017). Investigation and manipulation of metabolically active methanogen community composition during rumen development in black goats. *Sci. Rep.* 7:422. doi: 10.1038/s41598-017-00500-5
- Wei, M., Zhang, R., Wang, Y., Ji, H., Zheng, J., Chen, X., et al. (2013). Microbial community structure and diversity in deep-sea hydrothermal vent sediments along the Eastern Lau Spreading Centre. *Acta Oceanol. Sin.* 32:42–51.
- Weary, D. M., Jasper, J., and Hotzel, M. J. (2008). Understanding weaning distress. *Appl. Anim. Behav. Sci.* 110, 24–41. doi: 10.1016/j.applanim.2007.03.025
- Xie, G., Kong, X., Kang, J., Su, N., Fei, J., and Luo, G. (2021). Fungal community succession contributes to product maturity during the co-composting of chicken manure and crop residues. *Bioresour. Technol.* 328:124845. doi: 10.1016/j.biortech.2021.124845
- Yi, S., Dai, D., Wu, H., Chai, S., Liu, S., Meng, Q., et al. (2022). Dietary concentrate-to-forage ratio affects rumen bacterial community composition and metabolome of yaks. *Front. Nutr.* 9:927206. doi: 10.3389/fnut.2022.927206
- Youssef, N. H., Couger, M. B., Struchtemeyer, C. G., Liggenstoffer, A. S., Prade, R. A., Najjar, F. Z., et al. (2013). The genome of the anaerobic fungus *Orpinomyces* sp. strain C1A reveals the unique evolutionary history of a remarkable plant biomass degrader. *Appl. Environ. Microbiol.* 79, 4620–4634. doi: 10.1128/AEM.00821-13
- Zhang, Z., Huang, B., Wang, Y., Zhan, Y., Zhu, M., and Wang, C. (2022a). Dynamic alterations in the donkey fecal bacteria community and metabolome characteristics during gestation. *Front. Microbiol.* 13:927561. doi: 10.3389/fmicb.2022.927561
- Zhang, Z., Huang, B., Wang, Y., Zhu, M., and Wang, C. (2022b). Could weaning remodel the oral microbiota composition in donkeys? An exploratory study. *Animals* 12:2024. doi: 10.3390/ani12162024
- Zhang, J., Shi, H., Wang, Y., Li, S., Cao, Z., Ji, S., et al. (2017). Effect of dietary forage to concentrate ratios on dynamic profile changes and interactions of ruminal microbiota and metabolites in Holstein heifers. *Front. Microbiol.* 8:2206. doi: 10.3389/fmicb.2017.02206
- Zhang, Z., Wang, Y., Huang, B., Zhu, M., and Wang, C. (2022c). The fibrolytic enzyme profiles and the composition of fungal communities in donkey cecum-colon ecosystem. *Animals* 12:412. doi: 10.3390/ani12040412





## OPEN ACCESS

## EDITED BY

Wei Qi He,  
Soochow University,  
China

## REVIEWED BY

Bini Wang,  
Shaanxi Normal University,  
China  
Ping Xu,  
Zhejiang University,  
China

## \*CORRESPONDENCE

Jiayong Zheng  
✉ zjy821212@zjut.edu.cn

## SPECIALTY SECTION

This article was submitted to  
Microorganisms in Vertebrate Digestive  
Systems,  
a section of the journal  
Frontiers in Microbiology

RECEIVED 08 November 2022

ACCEPTED 16 January 2023

PUBLISHED 02 February 2023

## CITATION

Pan L, Ye H, Pi X, Liu W, Wang Z, Zhang Y and  
Zheng J (2023) Effects of several flavonoids on  
human gut microbiota and its metabolism by *in vitro* simulated fermentation.  
*Front. Microbiol.* 14:1092729.  
doi: 10.3389/fmicb.2023.1092729

## COPYRIGHT

© 2023 Pan, Ye, Pi, Liu, Wang, Zhang and  
Zheng. This is an open-access article  
distributed under the terms of the [Creative Commons Attribution License \(CC BY\)](#). The  
use, distribution or reproduction in other  
forums is permitted, provided the original  
author(s) and the copyright owner(s) are  
credited and that the original publication in this  
journal is cited, in accordance with accepted  
academic practice. No use, distribution or  
reproduction is permitted which does not  
comply with these terms.

# Effects of several flavonoids on human gut microbiota and its metabolism by *in vitro* simulated fermentation

Lixia Pan<sup>1</sup>, Hangyu Ye<sup>1</sup>, Xiong Pi<sup>2</sup>, Wei Liu<sup>2</sup>, Zhao Wang<sup>1</sup>,  
Yinjun Zhang<sup>1</sup> and Jiayong Zheng<sup>1\*</sup>

<sup>1</sup>College of Biotechnology and Bioengineering, Zhejiang University of Technology, Hangzhou, China,

<sup>2</sup>Institute of Plant Protection and Microbiology, Zhejiang Academy of Agricultural Sciences, Hangzhou, China

**Introduction:** Flavonoids have antiviral, antitumor, anti-inflammatory, and other biological activities. They have high market value and are widely used in food and medicine fields. They also can regulate gut microbiota and promote human health. However, only a few flavonoids have been reported for their regulatory effects on human gut microbiota.

**Methods:** The effects of hesperidin, hesperetin-7-O-glucoside, hesperetin, naringin, prunin, naringenin, rutin, isoquercitrin, and quercetin on gut microbiota structural and metabolic differences in healthy subjects were studied by means of *in vitro* simulated fermentation technology.

**Results:** Results showed that the nine kinds of flavonoids mentioned above, especially hesperetin-7-O-glucoside, prunin, and isoquercitrin, were found to have more effect on the structure of human gut microbiota, and they could significantly enhance *Bifidobacterium* ( $p < 0.05$ ). After 24h of *in vitro* simulated fermentation, the relative abundance of intestinal probiotics (e.g., *Lactobacillus*) was increased by the three flavonoids and rutin. Furthermore, the relative abundance of potential pathogenic bacteria was decreased by the addition of hesperetin-7-O-glucoside, naringin, prunin, rutin, and isoquercitrin (e.g., *Lachnoclostridium* and *Bilophila*). Notably, prunin could also markedly decrease the content of H<sub>2</sub>S, NH<sub>3</sub>, and short-chain fatty acids. This performance fully demonstrated its broad-spectrum antibacterial activity.

**Discussion:** This study demonstrates that flavonoids can regulate the imbalance of gut microbiota, and some differences in the regulatory effect are observed due to different structures. This work provides a theoretical basis for the wide application of flavonoids for food and medicine.

## KEYWORDS

flavonoids, gut microbiota, gas, short-chain fatty acids, *in vitro* simulated fermentation

## 1. Introduction

In recent years, the important impact of gut microbiota on human health and disease has attracted widespread attention (Sarkar et al., 2021; Ling et al., 2022). Increasing evidence shows that changes in the gut microbiota not only cause various gastrointestinal diseases (Guinane and Cotter, 2013), but also are associated with other chronic diseases, such as metabolic syndrome (Lim et al., 2017), Parkinson's disease (Castelli et al., 2021), and certain cancers (Li and Chen, 2022). The structure and function of the gut microbiota are influenced by endogenous and exogenous factors. Among the many influential factors, dietary regulation is considered a critical factor (Tremaroli and Bäckhed, 2012; Nie et al., 2018). The gut microbiota fully utilizes its metabolic capacity to

catabolize and employ dietary factors, and the metabolites it produces can affect the host directly or indirectly (Trakman et al., 2022). The gut microbiota produces a variety of metabolites, including gases and short-chain fatty acids (SCFAs). Gases are primarily produced by anaerobic bacteria in the gut microbiota (Triantafyllou et al., 2014). Beneficial bacteria in the gut microbiota produce SCFAs, and SCFAs can mediate the interaction between the gut microbiota and the body (Serino, 2019). The type and amount of SCFAs and gases produced by the gut microbiota play an important role in maintaining its homeostasis (Kalantar-Zadeh et al., 2019). Flavonoids, which are widely distributed in plants, are dietary polyphenols with anti-oxidation and anti-inflammation biological activities (Kumar and Pandey, 2013). Most natural flavonoids are in the form of glycosides, which cannot be absorbed by the body as effectively as aglycones. Except for a small portion of the flavonoid glycosides in the daily diet, which are hydrolyzed into aglycones by enzymes in the digestive tract, most of them are transformed into aglycones by the gut microbiota in the colon and combined with the body's own function (Sandoval et al., 2020). They are further metabolized into various metabolites and small-molecule phenolic acids that can be absorbed by the intestinal cells (Liu et al., 2018). Consequently, this biotransformation process of flavonoids mediated by gut microbiota can effectively improve the bioavailability of flavonoid glycosides.

Flavonoids are a class of compounds with 2-phenyl chromogenic ketones as the parent nucleus and can be divided into the subclasses of flavones, flavonols, flavanones, flavan-3-ols, anthocyanins, dihydroflavonols, isoflavones, and chalconoids (Santos-Buelga and Feliciano, 2017). Flavanones mainly include hesperetin, naringenin, erodcyol, and etc., meanwhile quercetin is one of the most common flavonols (Jiang et al., 2020). Hesperetin-7-O-glucoside, prunin, and isoquercitrin are flavonoid monoglucoside forms of hesperetin, naringenin, and quercetin, respectively. Hesperidin, naringin, and rutin are their corresponding flavonoid diglycosides. The structural formulae and related information of the nine flavonoids are shown in Table 1. Naringenin and quercetin have inhibitory effects on some common bacteria in the gastrointestinal tract, including *Lactobacillus rhamnosus* (probiotics), *Staphylococcus aureus* and *Salmonella typhimurium* (enteropathogens), and *Escherichia coli* (commensal bacteria; Parkar et al., 2008). Duda-Jodak assessed the impacts of various polyphenols on the gut microbiota representatives (*Lactobacillus*, *Bacteroides galacturonicus*, and *Ruminococcus gauvreauii*), and then concluded that concentration more than 250 µg/mL of hesperetin, naringenin, and 4–50 µg/mL of quercetin inhibited their growth (Duda-Chodak, 2012). Gwiazdowska et al. (2015) found that *Bifidobacterium adolescentis* and *Bifidobacterium bifidum* were sustained inhibited by hesperidin and quercetin. In addition to broad-spectrum antibacterial activity, flavonoids have the effect of increasing the proportion of beneficial bacteria in the intestinal tract. *In vivo* studies found that hesperidin increased the *Lactobacillus/Enterococcus* ratio, and decreased the *Clostridium coccoides/Eubacterium rectale* ratio in the Lewis rat gut microbiota, which displayed prebiotic-like activity (Estruel-Amades et al., 2019). Quercetin affected the composition of the gut microbiota in high-fat fed rats, and decreased the ratio of Firmicutes/Bacteroidetes, which indicated that quercetin exerted a mitigating effect on obesity (Ettxeberria et al., 2015). In summary, flavonoids can regulate and balance the disordered gut microbiota. Nowadays, various new food, nutraceuticals, and pharmaceuticals have been developed in the market to perform their functional activities.

However, little is known about the impacts of most flavonoids on gut microbiota. Based on the antibacterial activity of flavonoids and the fact that hesperetin, naringenin, and quercetin are typical representatives of different subclasses of flavonoids, their effects on gut microbiota are worth exploring. In addition, the differences in the effects of flavonoid aglycones and their corresponding flavonoid monoglucosides and flavonoid diglycosides on the regulation of gut microbiota due to their different structures are also need to be investigated. In this work, the effects of hesperidin, hesperetin-7-O-glucoside, hesperetin, naringin, prunin, naringenin, rutin, isoquercitrin, and quercetin on healthy Chinese volunteers were studied by *in vitro* simulated fermentation technology. The theoretical basis of the differences caused by flavonoids on the structure and metabolism of gut microbiota enables the probable use of flavonoids as a functional food.

## 2. Materials and methods

### 2.1. Materials and reagents

Hesperetin-7-O-glucoside, prunin, and isoquercitrin were prepared in our laboratory (Ye H. et al., 2022; Hangzhou, China). Hesperidin, hesperetin, naringin, naringenin, rutin, and quercetin were obtained from Aladdin Reagent Co., Ltd. (Shanghai, China). Yeast extract powder, tryptone, crotonic acid,  $\text{KH}_2\text{PO}_4$ ,  $\text{K}_2\text{HPO}_4$ , heme,  $\text{MgSO}_4$ , NaCl,  $\text{CaCl}_2$ , and L-cysteine were purchased from Sigma (Missouri, United States).

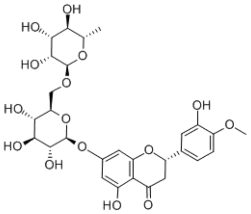
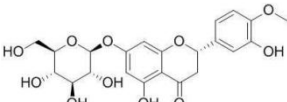
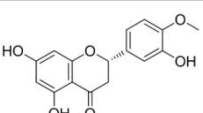
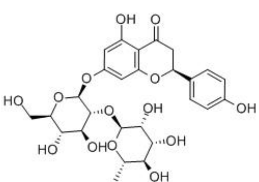
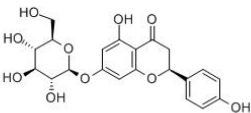
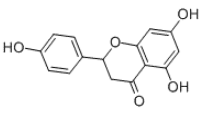
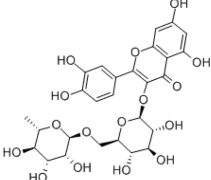
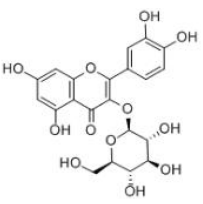
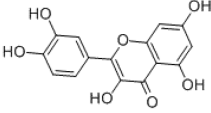
### 2.2. Fecal sample collection

Ten volunteers, five men and five women, aged 20–30 years old (people without no gastrointestinal diseases and not taking antibiotics, prebiotics, probiotics, and other drugs in recent 1 month) were selected from the local healthy population in Hangzhou, Zhejiang Province. All 10 volunteers personally signed the consent form and knew that this was for experimental use. This study was approved by the Ethical Committee of the Hangzhou Center for Disease Control and Prevention (no. 202047). To ensure that the fecal samples collected had little food residue while minimizing contact with oxygen, these volunteers were required to use a sterile fecal sampling box, the stool located in the middle was quickly collected at the time of defecation, and the sample could not be <3 g. Then, the name, age, and date of sampling of the volunteer corresponding to each sample were marked. The fecal samples were kept at 4°C and used in this experiment within 4 h.

### 2.3. Fecal sample pretreatment

Fresh fecal samples of about 0.3 g each were weighed three times from the stool sampling box, and each was placed in a 1.5 mL sterilized centrifuge tubes. Then, these original fecal samples were stored in the refrigerator at –80°C. Thereafter, the fecal samples of 0.8 g were weighed and placed in a 10 mL sterile centrifuge tube and then added with 8 mL of sterile PBS buffer solution. An oscillator was utilized to mix the stool and buffer solution thoroughly, and a sterile filter was used to sieve away large particles. Ultimately, a 10% fecal suspension inoculum was prepared.

TABLE 1 Structural formulae and related information of the nine flavonoids.

Substance	Structural formula	CAS number	Experimental purity
Hesperidin		520-26-3	97%
Hesperetin-7-O-glucoside		31712-49-9	95.38%
Hesperetin		520-33-2	97%
Naringin		4493-40-7	98%
Prunin		529-55-5	96.78%
Naringenin		480-41-1	97%
Rutin		153-18-4	98%
Isoquercitrin		482-35-9	96.51%
Quercetin		117-39-5	95%

## 2.4. Configuration of relevant media

*In vitro* fermentation followed the method of [Zhao et al. \(2021\)](#). The composition of the control medium (Con) was as follows: 10 g tryptone, 2.5 g yeast extract, 2 mL heme solution (5 mg/mL), 1 g L-cysteine, 0.9 g NaCl, 0.45 g K<sub>2</sub>HPO<sub>4</sub>, 0.45 g KH<sub>2</sub>PO<sub>4</sub>, 0.09 g MgSO<sub>4</sub>, and 0.09 g CaCl<sub>2</sub>,

which were dissolved in 1 L of deionized water. Immediately after boiling, nitrogen was added to keep the medium level anaerobic. The peristaltic pump dispensed 5 mL into vials, which were sealed up well and sterilized 30 min with high-pressure steam sterilizer at 115°C before use.

Flavonoid medium was prepared by adding hesperidin (S1), hesperetin-7-O-glucoside (S2), hesperetin (S3), naringin (S4), prunin

(S5), naringenin (S6), rutin (S7), isoquercitrin (S8), and quercetin (S9) to the control medium. Their final concentration was 4 mg/mL.

## 2.5. *In vitro* fermentation and gas analysis after the fermentation

Each of the nine flavonoids was used as a substrate for *in vitro* fermentation. A blank medium without additional substrate was also added as a control. Fecal samples from 10 donors were added to each of the media mentioned above individually, and three replicate experiments were performed on each media for each donor's fecal sample. 500  $\mu$ L of treated 10% fecal suspension inoculum from 10 volunteers was separately inoculated into the above-mentioned medium supplemented with different flavonoids (S1–S9) and control medium (Con) using a disposable sterile syringe in an anaerobic workstation. Each medium was shaken gently, and incubated in an incubator at 37°C for 24 h. The gases produced by *in vitro* anaerobic fermentation of gut microbiota were accumulated in sample vials. According to the method of Ye X. et al. (2022), the total amount of gases and gas composition ( $\text{CH}_4/\text{NH}_3/\text{H}_2/\text{H}_2\text{S}/\text{CO}_2$ ) were measured with a gas analyzer after cooling to room temperature. The injection needle of the gas analyzer delivered the accumulated gases in sample vials to this instrument for analysis, and the highest value of each gas was recorded. And then the gases were re-delivered to vials by the outlet needle, so that the air pressure in sample vials was kept constant. After the gas measurement, the sample vials were opened and the fermentation broth was packed into 1.5 mL centrifuge tubes. Then, each sample was centrifuged at 10,000 rpm for 5 min. The supernatant and precipitate were separated, placed into 1.5 mL centrifuge tubes, and frozen at  $-80^\circ\text{C}$  for storage.

## 2.6. Determination of short-chain fatty acids

Based on a previous method (Pi et al., 2022; Tian et al., 2022), metaphosphoric acid of 2.5 g was added to ddH<sub>2</sub>O at constant volume to 100 mL, and the mass-to-volume ratio (W/V) of the prepared metaphosphoric acid solution was 2.5%. Then, 0.6464 g of crotonic acid was weighed and added to the metaphosphate solution at constant volume to 100 mL, and the crotonic acid–metaphosphoric acid solution was obtained after even mixing. A total of 100  $\mu$ L of crotonic acid–metaphosphoric acid solutions was added to 500  $\mu$ L of fermentation supernatant, followed by fully mixing and acidification for 24 h at  $-80^\circ\text{C}$ . After acidification, the mixture was centrifuged for 3 min at 10,000 rpm and  $4^\circ\text{C}$ . The supernatant was filtered with a 0.22  $\mu$ m aqueous microporous membrane, and 150  $\mu$ L of the filtrate was pipetted into the injection vial. It was shaken to expel air bubbles at the bottom of the internal tube for preventing empty aspiration during sample loading.

When the gas chromatograph was ready to sample, the aging process was conducted. The column temperature heating procedure was as follows: the column temperature was  $80^\circ\text{C}$  for 1 min,  $10^\circ\text{C}/\text{min}$ , rising to  $190^\circ\text{C}$ , and maintained for 0.50 min. Then, it reached  $240^\circ\text{C}$  at the rate of  $40^\circ\text{C}/\text{min}$  for 5 min. FID detector:  $240^\circ\text{C}$ ; gasification chamber:  $240^\circ\text{C}$ ; carrier gas: nitrogen flow rate of 20 mL/min, hydrogen flow rate of 40 mL/min, and air flow rate of 400 mL/min. The editing program started to test the content of different SCFAs.

## 2.7. 16S rRNA gene sequencing of gut microbiota and bioinformatic analysis

Genomic DNA extraction was completed from fecal fermentation broth sediment samples obtained by centrifugation as described above. Genomic DNA was extracted from 10 samples in each experimental group, and the total number of samples tested was 110 when including the control and raw fecal groups. With these extracted genomes verified by electrophoresis as a template, and 341F (5'-CCTAYGGGRBGCASCAG-3)/806R (5'-GGACTACNNGGGTATCTAAT-3) as upstream and downstream primers, the V3–V4 regions of bacterial 16S rRNA gene were obtained. Purified amplicons were commissioned to Shanghai Meiji Biomedical Technology Co., Ltd. for paired-end sequencing on the Illumina MiSeq PE250 platform. During the use of QIIME2, the optimized sequences were denoised by the sequence noise reduction plugin DADA2 (Callahan et al., 2016; Bolyen et al., 2019). The taxonomic assignment of ASVs was achieved with reference to the resources in the SILVA 16S rRNA gene database (v138). All consensus sequence data of raw fecal and fermentation samples were submitted to the National Center for Biotechnology Information Short Read Archive under accession no. PRJNA874892. The obtained data were further subjected to bioinformatic analysis, and modeling analysis was performed on the microflora and related metabolic data. Bioinformatic analysis was performed on the online platform of Shanghai Meiji Biomedical Technology Co., Ltd.<sup>1</sup>  $\alpha$ -diversity relied on the Ace, Chao, Shannon, and Simpson index assessed at the ASV level.  $\beta$ -diversity was assessed based on Bray–Curtis distance, and expressed using principal coordinate analysis (PCoA). The relative abundance of different groups at the phylum and genus levels was represented by Bar plots. At the genus level, the number of species common and unique to multiple groups was counted using Venn plots. The correlations of the different genera of bacteria contained in the samples with the gases and SCFAs were evaluated using Spearman correlation coefficients, and they were presented in the correlation heatmap.

## 2.8. Statistics and analysis

Results were presented as mean  $\pm$  SEM (10 independent experiments  $\times$  3 parallel experiments). 16S rRNA gene sequencing of gut microbiota included 11 independent experiments. The experimental data were statistically analyzed and plotted by SPSS 26.0 and Origin 2021 software. The Shapiro–Wilk test was used to check whether the data obeyed a normal distribution. For data that obeyed a normal distribution, one-way ANOVA followed by Duncan's multiple range test was conducted between multiple groups. For data that did not obey a normal distribution, the Kruskal–Wallis test was conducted between multiple groups.  $p < 0.05$  indicated statistical significance.

## 3. Results

### 3.1. Effects of flavonoids *in vitro* simulated fermentation on gas production

The results of gas production after 24 h of *in vitro* fermentation with the addition of nine flavonoids are shown in Figure 1. The control and experimental media produced a large amount of  $\text{CO}_2$  and  $\text{H}_2$  and a small

<sup>1</sup> www.Majorbio.com



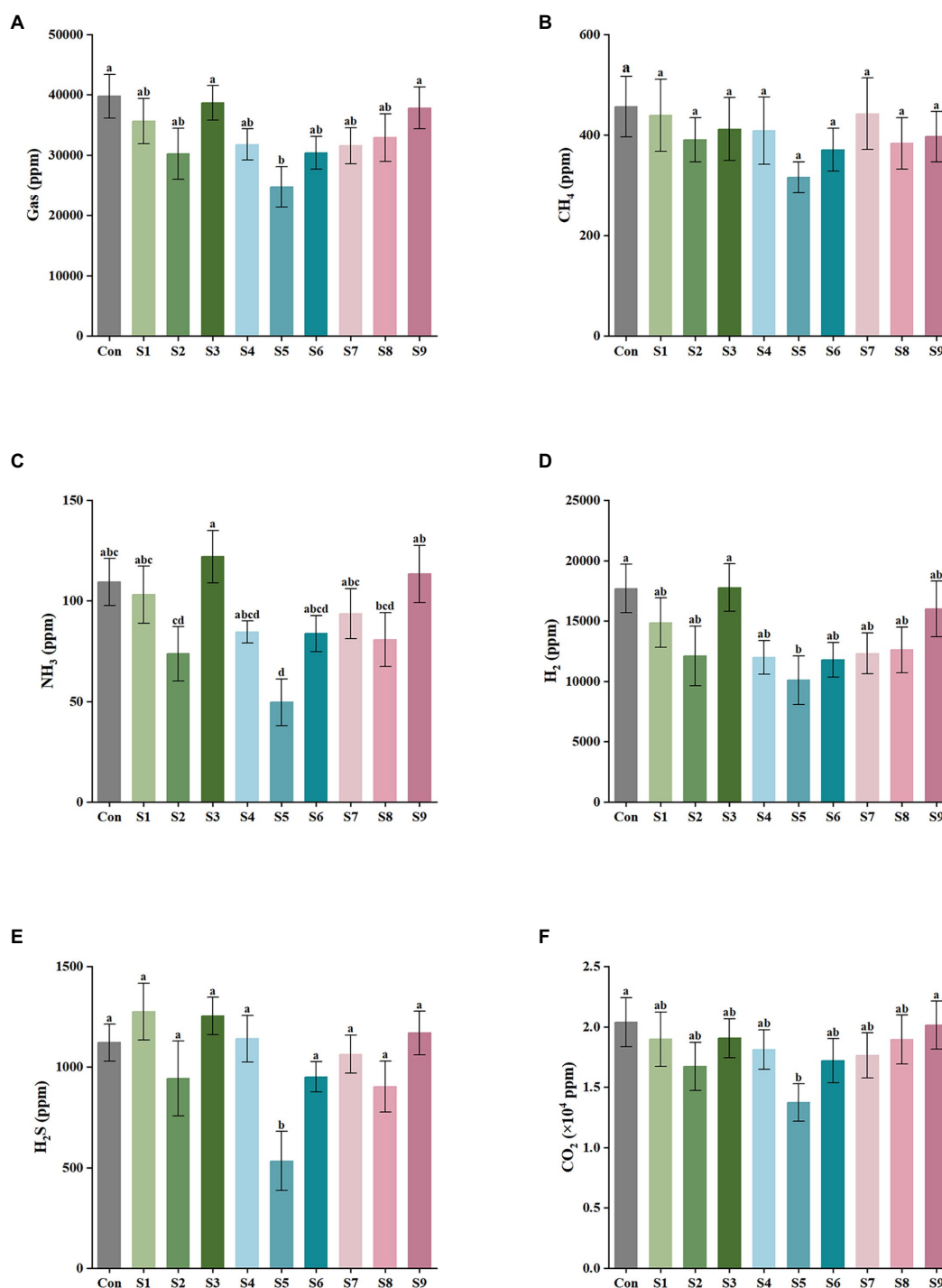


FIGURE 1

Gas composition and content of external fermentation of fecal microbiota under different substrate conditions. (A) The total amount of the five gases, (B)  $\text{CH}_4$ , (C)  $\text{NH}_3$ , (D)  $\text{H}_2$ , (E)  $\text{H}_2\text{S}$ , and (F)  $\text{CO}_2$ . Data are means  $\pm$  SEM (10 independent experiments  $\times$  3 replication experiments). Different lowercase letters indicate significant differences ( $p < 0.05$ ).

amount of  $\text{H}_2\text{S}$ ,  $\text{CH}_4$ , and  $\text{NH}_3$  after fecal bacteria fermentation for 24h. As illustrated in Figure 1A, the addition of hesperitin-7-O-glucoside, prunin, and isoquercitrin greatly reduced the total gas production compared with the control, and prunin had a statistically significant effect ( $p < 0.05$ ). Meanwhile, the hesperetin and quercetin groups had no significant difference ( $p > 0.05$ ). As shown in Figures 1B–F, the corresponding decreasing trends of  $\text{CH}_4$ ,  $\text{NH}_3$ ,  $\text{H}_2$ ,  $\text{H}_2\text{S}$ , and  $\text{CO}_2$  after 24h of simulated fermentation were also similar to the total, and the decrease in each gas was significant after the addition of prunin ( $p < 0.05$ ).

### 3.2. Effects of flavonoids *in vitro* simulated fermentation on short-chain fatty acid production

The variations in the content of the six SCFAs in the fermentation liquor in this study were measured, as shown in Figure 2. The highest content of acetic acid was found in the fermentation liquor of fecal samples, followed by those in propionic and butyric acids. The production of isobutyric, isovaleric, and

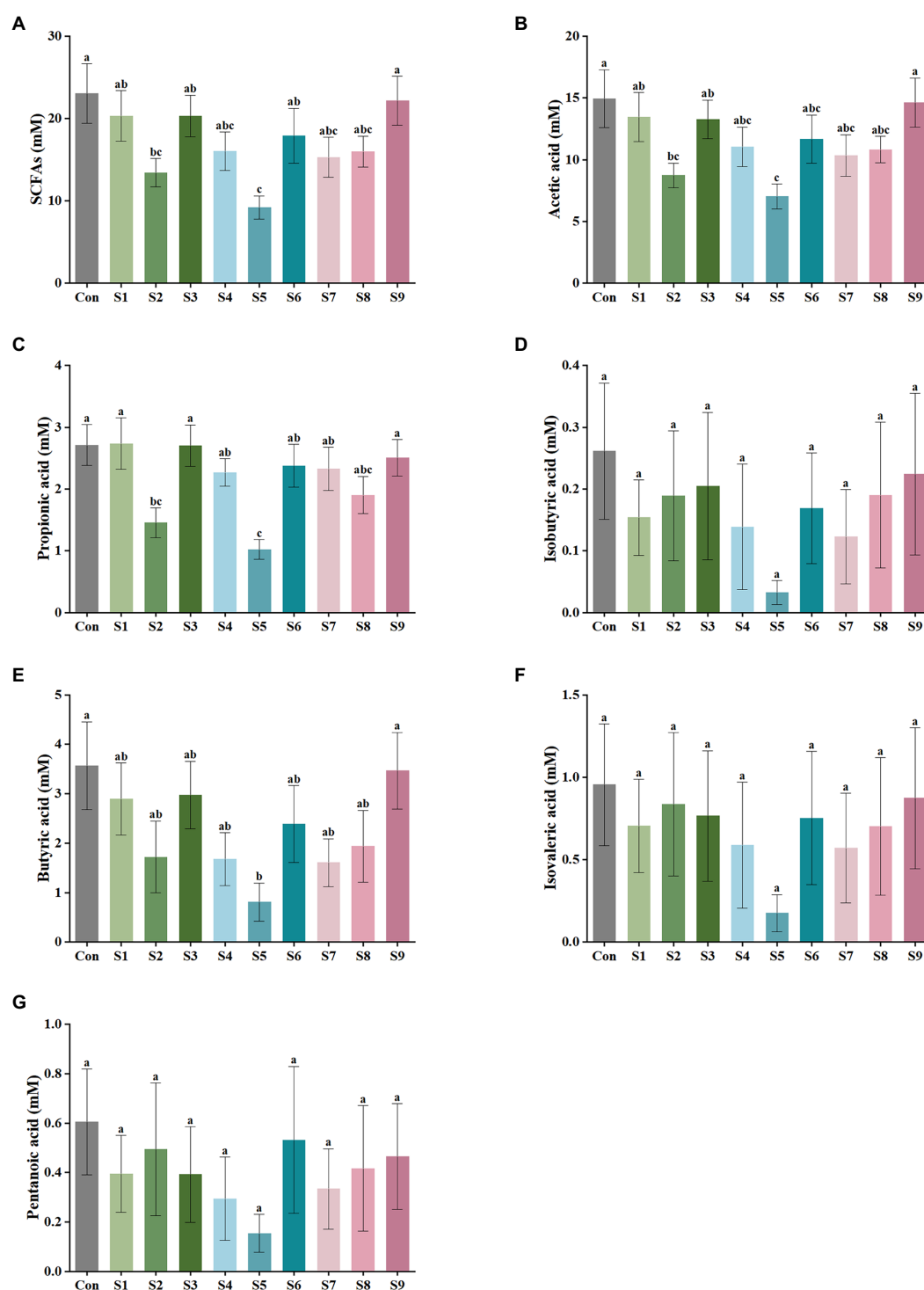


**FIGURE 2**  
SCFA output of external fermentation of fecal microbiota under different substrate conditions. **(A)** Total SCFA yield, **(B)** Acetic acid, **(C)** Propionic acid, **(D)** Isobutyric acid, **(E)** Butyric acid, **(F)** Isovaleric acid, and **(G)** Pentanoic acid. Data are means  $\pm$  SEM (10 independent experiments  $\times$  3 replication experiments). Different lowercase letters indicate significant differences ( $p < 0.05$ ).

pentanoic acids was the lowest. According to the data of total SCFA production in Figure 2A, the total SCFA content was decreased to 15 mmol/L or even lower by the addition of hesperitin-7-O-glucoside, prunin, rutin, and isoquercitrin compared with the total SCFA content of 23 mmol/L in the control group. The decrease degree of hesperitin-7-O-glucoside and prunin groups was statistically significant ( $p < 0.05$ ). This decreasing trend

corresponds to the effect on gas content described above. As displayed in Figures 2B–G, the impact of hesperitin-7-O-glucoside and prunin on the decrease in the content of acetic and propionic acids was significant ( $p < 0.05$ ), and prunin also caused a notable decrease in the level of butyric acid ( $p < 0.05$ ). The effects of the remaining six flavonoids on the production of the three SCFAs were insignificantly different from those of the control group.

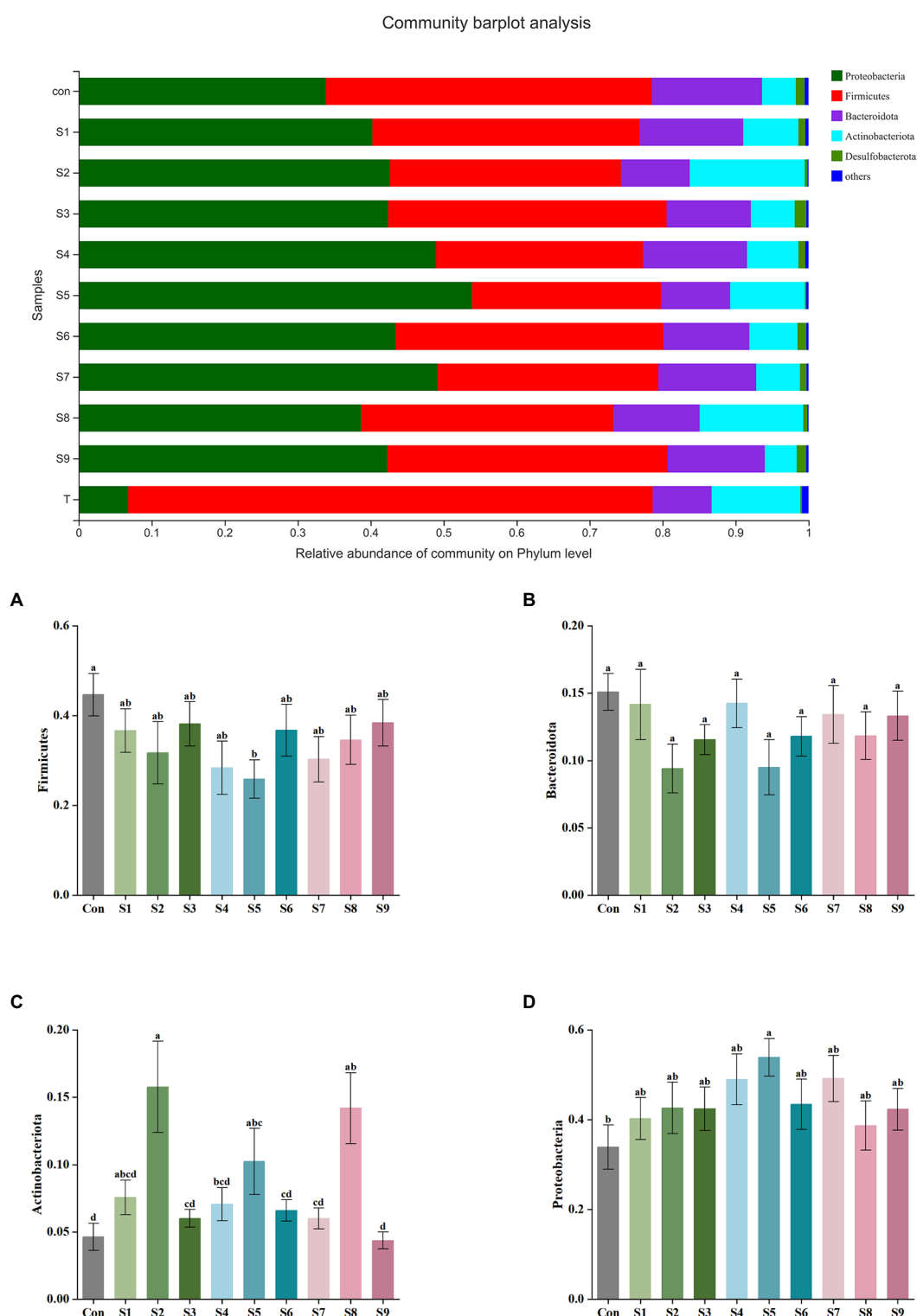


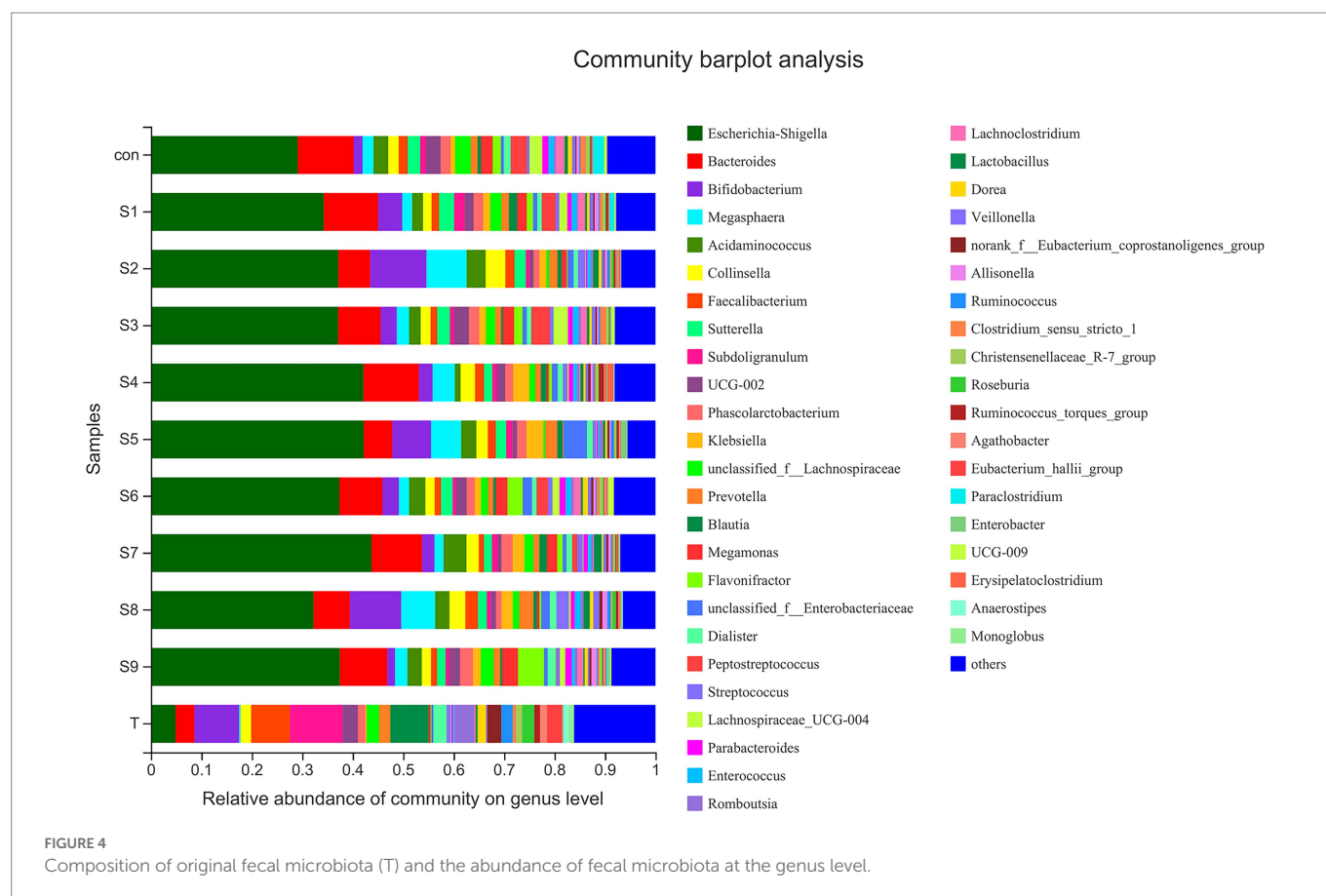
FIGURE 3

Composition of original fecal microbiota (T) and the abundance of fecal microbiota at the phylum level. Relative abundance of Firmicutes (A), Bacteroidota (B), Actinobacteriota (C), and Proteobacteria (D) in fecal microbiota after fermentation. Data are means  $\pm$  SEM (10 independent experiments). Different lowercase letters indicate significant differences ( $p < 0.05$ ).

### 3.3. Analysis of fecal microbiota composition before and after fermentation

The changes in fecal microbiota before and after fermentation were determined by 16S rRNA gene sequencing. The abundance of fecal

microbiota at the phylum level is shown in Figure 3. The Firmicutes were the most abundant phylum in the raw fecal T-samples, but the abundance of Firmicutes decreased substantially after fermentation, and this abundance in the prunin group was obviously lower ( $p < 0.05$ ). The abundance of Proteobacteria showed an increase in all groups after



fermentation, and the abundance of Proteobacteria increased significantly in the prunin group compared to the control group ( $p < 0.05$ ). After fermentation, the abundance of Actinobacteriota in each group except the quercetin group was higher than that in the control group, especially in the hesperetin-7-O-glucoside, prunin, and isoquercitrin groups ( $p < 0.05$ ). The results in Figure 4 show that, compared with after *in vitro* fermentation, *Subdoligranulum* was the most abundant genus in the raw fecal T-samples, followed by *Bifidobacterium*, *Faecalibacterium*, and *Blautia*. At the genus level, we performed analysis focusing on microorganisms with an abundance of more than 1%. After 24 h of fermentation, the abundance of *Bifidobacterium* in the control group was lower than that of raw fecal. Compared with the control group, Figure 5 also shows that the abundance of the probiotics *Bifidobacterium* was improved after the addition of the abovementioned flavonoids, except the quercetin group. Among them, the improvement effect of hesperetin-7-O-glucoside, prunin, and isoquercitrin groups was very significant ( $p < 0.05$ ). Meanwhile, hesperetin-7-O-glucoside, rutin, and isoquercitrin groups all increased the abundance of *Lactobacillus*. Prunin and isoquercitrin groups also enhanced the abundance of *Prevotella* to a greater extent. By contrast, the addition of all nine flavonoids decreased the abundance of *Lachnospiraceae*, and its abundance was significantly low in the hesperetin-7-O-glucoside, naringin, prunin, rutin, and isoquercitrin compared with that in the control group. Adding hesperetin-7-O-glucoside, naringin, and prunin also reduced the relative abundance of *Bifidobacterium*. In addition, adding hesperetin-7-O-glucoside, prunin, and isoquercitrin caused the relative abundance of *Bacteroides* to reduce.

The  $\alpha$ -diversity of fecal microbiota was analyzed, and the results are shown in Figure 6. After fermentation with the addition of flavonoids, the Ace index, Chao index, and Shannon index of each group were lower

than those of the control group, but all were insignificant ( $p > 0.05$ ). On the contrary, the Simpson index was increased slightly, but the increase was also insignificant ( $p > 0.05$ ). The  $\beta$ -diversity of the gut microbiota and the species Venn diagram were analyzed at the genus level to compare the overall differences in fecal microbiota composition among groups after adding different substrates. As shown in Figure 7, a significant difference existed between the fecal microbiota before and after fermentation ( $p = 0.001$ ). Compared with the group without additional substrate, a certain difference in fecal microbiota with flavonoids was observed after fermentation, but it was insignificant. A total of 79 species of the same bacteria before and after fermentation were found, and the microbiota after fermentation and the raw fecal microbiota differed in eight species.

### 3.4. Correlation analysis between fecal microbiota and metabolites

In this experiment, the relationship of gut microbiota with gas and SCFAs was analyzed with heatmaps and Spearman correlation coefficients, and the results are displayed in Figure 8. The bacteria with the top 15 abundance at genus level were screened. All gases and SCFAs were collectively influenced by a large number of bacteria, and the bacteria significantly affected  $\text{CO}_2$  production, followed by  $\text{CH}_4$ . In terms of individual bacteria, *Bifidobacterium* was the genus of bacteria that significantly affected production of all gases and SCFAs, and all were negatively correlated. *Prevotella* was strikingly negatively correlated with  $\text{NH}_3$ ,  $\text{H}_2$ ,  $\text{H}_2\text{S}$ , acetic acid, and propionic acid. *Flavonifractor* then exhibited a significant positive correlation with  $\text{NH}_3$ ,  $\text{H}_2\text{S}$ , acetic acid, propionic acid, and butyric acid. A remarkable



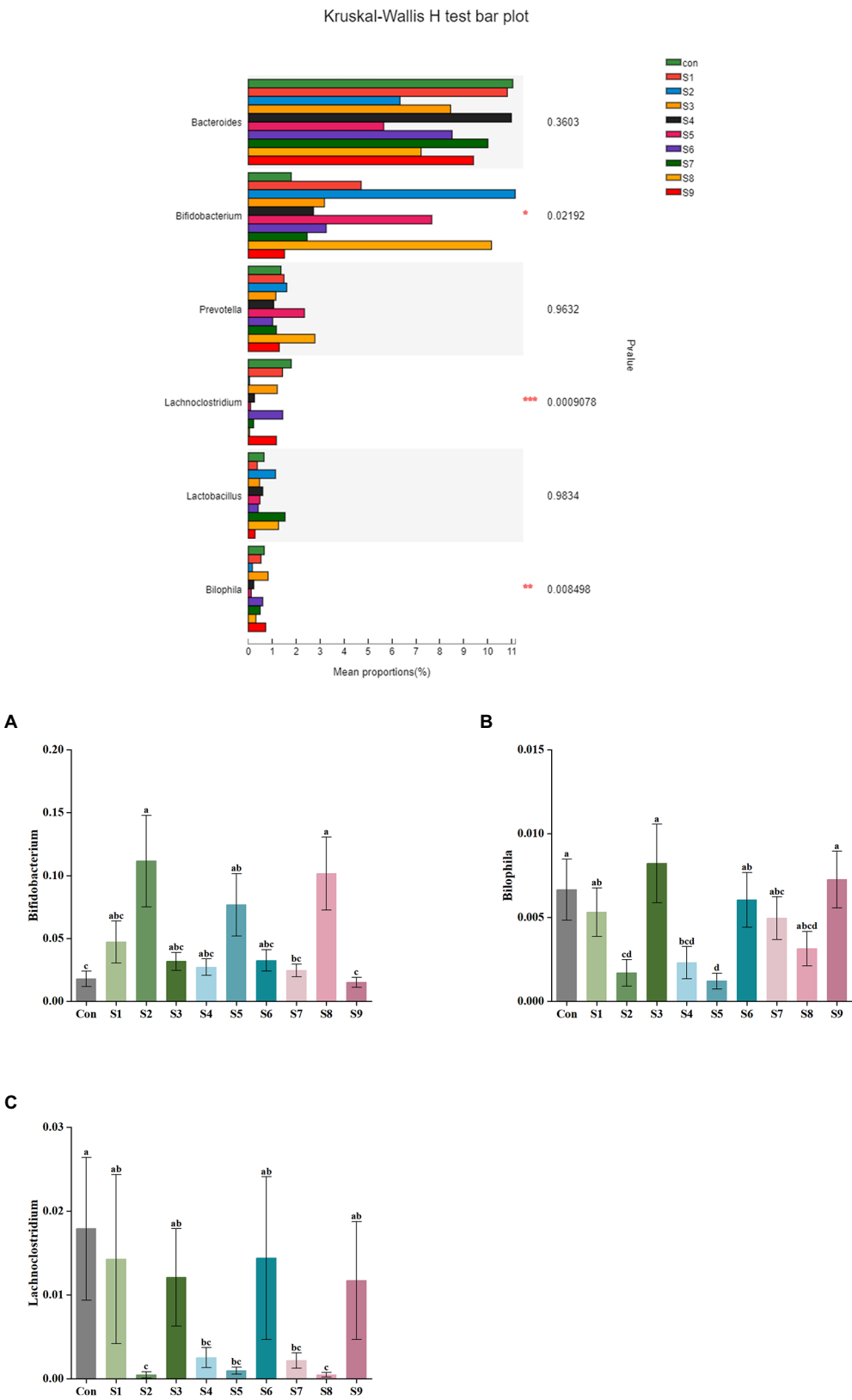
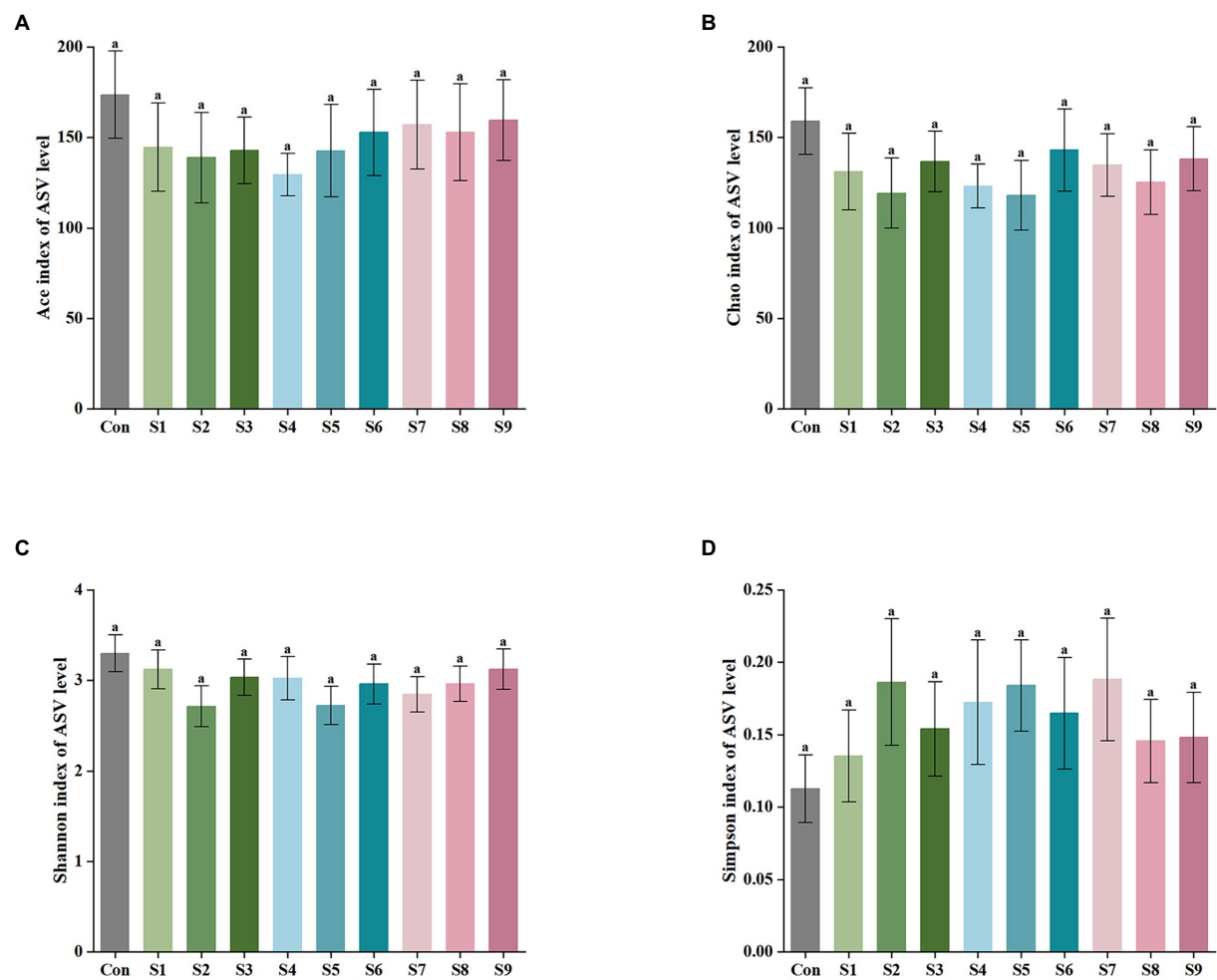
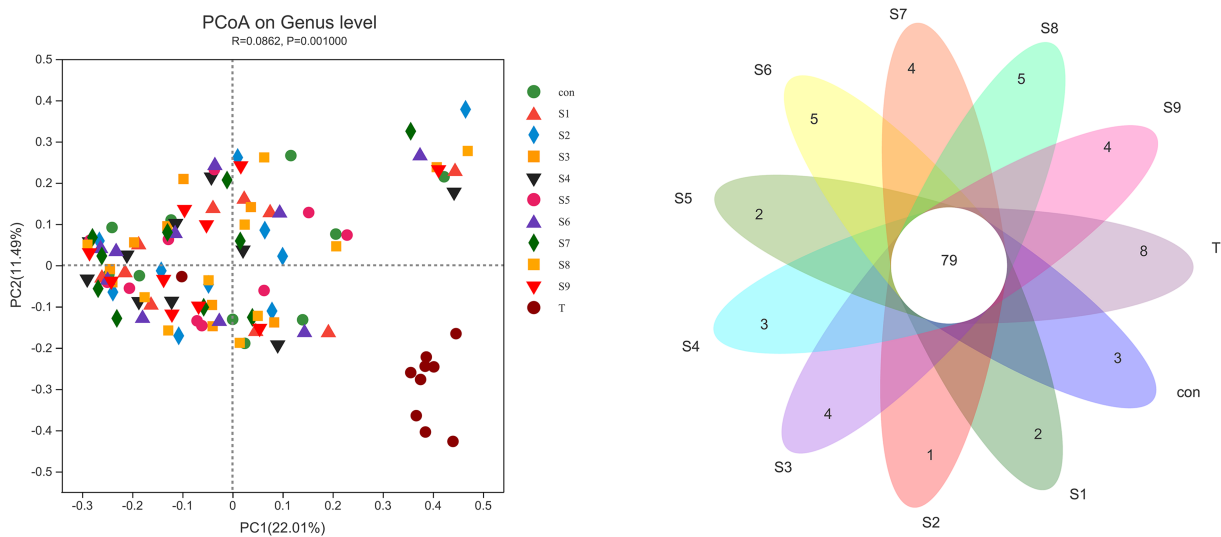


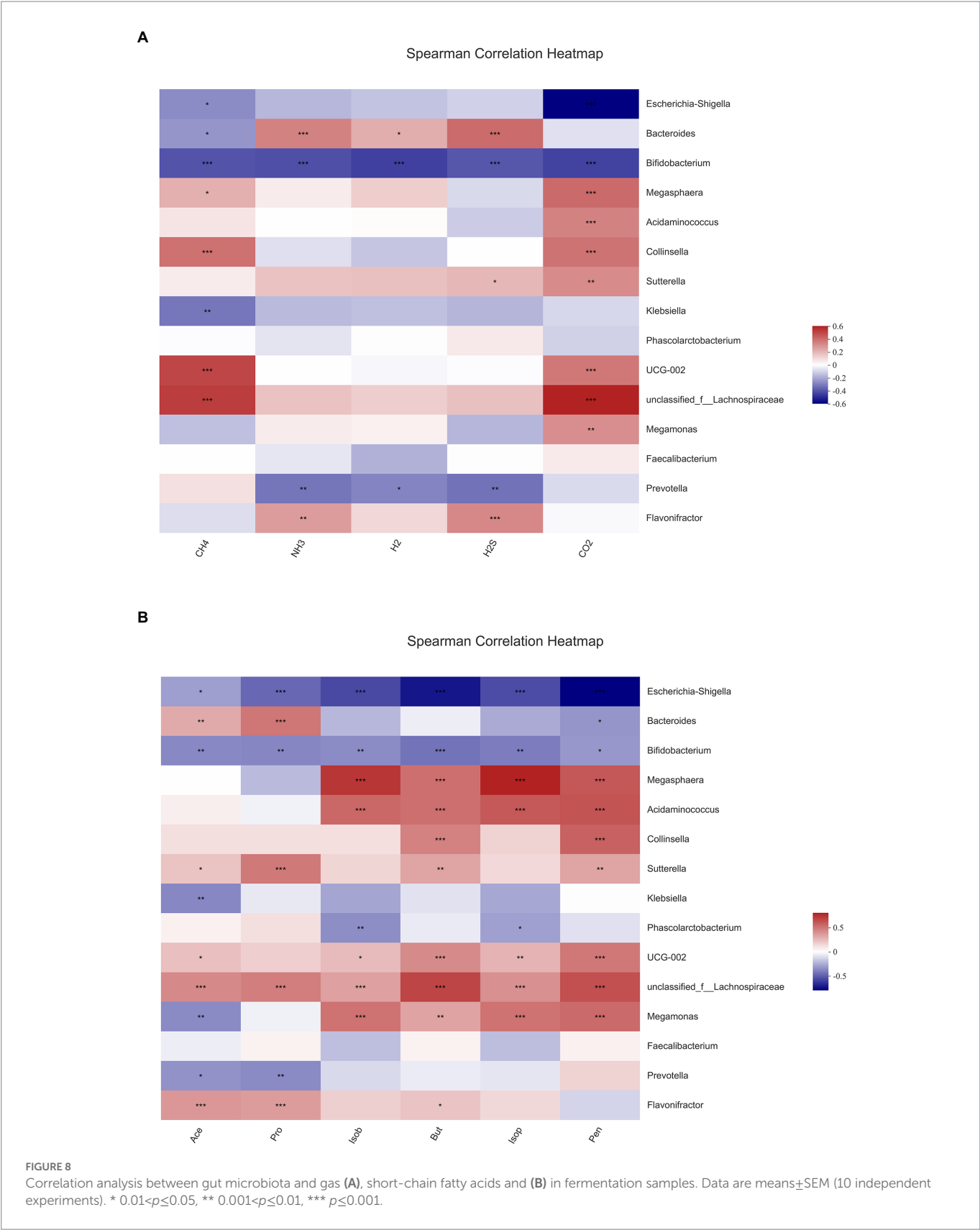
FIGURE 5  
Comparison of fecal microbiota under different substrate conditions at the genus level. Relative abundance of *Bifidobacterium* (A), *Bilophila* (B), and *Lachnospirillum* (C) in fecal microbiota after fermentation. Data are means±SEM (10 independent experiments). Different lowercase letters indicate significant differences ( $p<0.05$ ). \*  $0.01<p\leq0.05$ , \*\*  $0.001<p\leq0.01$ , \*\*\*  $p\leq0.001$ .



**FIGURE 6**  
 $\alpha$ -Diversity analysis of fecal microbiota after fermentation. (A) Ace index of ASV level, (B) Chao index, (C) Shannon index, and (D) Simpson index. Data are means  $\pm$  SEM (10 independent experiments). Different lowercase letters indicate significant differences ( $p < 0.05$ ).



**FIGURE 7**  
 $\beta$ -Diversity PCoA analysis and Venn diagram analysis of microbiota differences before and after fermentation.  $p < 0.05$  indicates a significant difference between groups.



positive correlation was observed between *Bacteroidetes* and NH<sub>3</sub>, H<sub>2</sub>, H<sub>2</sub>S, acetic acid, and propionic acid, and a negative correlation was found with CH<sub>4</sub> and pentanoic acid. *Escherichia-Shigella* had the highest abundance, and it was significantly negatively correlated with CH<sub>4</sub>, CO<sub>2</sub>, and all six SCFAs. However, *Faecalibacterium* had no significant correlation with any gases or SCFAs.

## 4. Discussion

The type and content of intestinal gases, as an important metabolite of intestinal bacteria, play a key part in the host, which are principally affected by flora and diet (Kalantar-Zadeh et al., 2019). Excessive amounts of gas produced in the intestine can cause discomfort such as bowel sounds and abdominal distension (Chang et al., 2020). Thus, in this experiment, the similarities and differences in the metabolic gas production of different flavonoids such as hesperidin (S1), hesperetin-7-O-glucoside (S2), hesperetin (S3), naringin (S4), prunin (S5), naringenin (S6), rutin (S7), isoquercitrin (S8), and quercetin (S9) at a same final concentration (4mg/mL) were investigated by *in vitro* simulated fermentation technology. As observed, all the nine flavonoids above could reduce the total gas production, and the reduction effect of hesperetin-7-O-glucoside, prunin, and isoquercitrin was obvious; especially, the prunin group statistically reduced the total gas production ( $p < 0.05$ ), and the reduction effect of CO<sub>2</sub>, NH<sub>3</sub>, H<sub>2</sub>S, and CH<sub>4</sub> ( $p < 0.05$ ) were also all significant (Figure 1). Relevant studies have shown that NH<sub>3</sub> and H<sub>2</sub>S produced by fermentation of gut microbiota is related to gastrointestinal disorders, including Crohn's disease and ulcerative colitis (Singh and Lin, 2015). Furthermore, a close correlation existed between the decrease in gas content and the changes in gut microbiota. The results demonstrate that the nine flavonoids above (particularly hesperetin-7-O-glucoside, prunin, and isoquercitrin) could regulate the gut microbiota, which could further adjust intestinal gas composition. In addition, the modulating effect of prunin should not be underestimated.

SCFAs are another vital metabolite of intestinal bacteria, and they are derived from carbohydrates that the body cannot digest on its own. The effect of flavonoids on SCFA production is mainly due to the direct effect of flavonoids on the gut microbiota which produces SCFAs. For example, baicalin treatment could increase the abundance of *Bifidobacterium* and *Ruminococcaceae* in the intestine of hypertensive rats, and both bacteria could produce different SCFAs (Wu et al., 2019). These SCFAs not only can be directly used by the body to play important physiological regulatory roles, such as influencing energy balance and glucose homeostasis directly through the central pathway or by the gut-brain axis, but also can be used as energy sources (Luo et al., 2022). Current studies have shown that SCFAs are critical for the metabolism of host and the activity of gut microbiota (Serino, 2019). Thus, in this research, the content of six common SCFAs was quantified, and the results of the assay focused on the three SCFAs with high contents above (Figure 2). The decrease in the content of SCFAs was also inextricably correlated with the changes in the gut microbiota structure. The addition of hesperetin-7-O-glucoside, prunin, and isoquercitrin resulted in a greater decrease in the total SCFA production. This finding implies that the number and abundance of intestinal flora had been regulated by these substrates, and the flavonoids hesperetin-7-O-glucoside, prunin, and isoquercitrin had various physiological activities such as bactericidal, antiviral, and anti-inflammatory. The production of acetic, propionic, and butyric acids was significantly decreased by the addition of prunin ( $p < 0.05$ ). These results suggest that prunin had excellent antibacterial and anti-inflammatory effects. Many studies have proven that flavonoids have broad-spectrum antibacterial effects; for example, high-flavonoid apple would inhibit the growth of *Lactobacillus* (Espley et al., 2014), and ellagitannins had inhibitory effects on *Bacillus cereus* and *Candida albicans* (Nohynek et al., 2006). *Smilax china* L. flavonoid could

reduce SCFAs in obese mice (Li et al., 2021), and this result is consistent with the fact that nine flavonoids reduced the total SCFAs to different degrees in this study. However, in many studies, flavonoids have been reported to increase the concentration of SCFAs due to the increase in the abundance of beneficial bacteria (Wu et al., 2019; Xuan et al., 2020). In contrast, the decrease in the content of SCFAs in the present study is attributed to the broad-spectrum inhibition of flavonoids. That means, flavonoids have certain inhibitory effects on all intestinal bacteria, including causing a decrease in the abundance of SCFA-producing bacteria (Espley et al., 2014; Gwiazdowska et al., 2015). This reason ultimately led to an overall decrease in the content of SCFAs.

Gut microbiota ferments human dietary intake of various nutrients to promote nutrient absorption and significantly influence the biotransformation and metabolic processes of the ingested active substances; thus, it regulates human health (Cotillard et al., 2013). In the digestive tract from stomach to colon, the colon contains the highest number and activity of gut microbiota (Rooks and Garrett, 2016). Meanwhile, flavonoids have a long residence time in the colon and can interact with a wide variety of intestinal flora therein; thus, they modulate the structure of the flora (Braune and Blaut, 2016). The regulatory action of flavonoids on the gut microbiota can be divided into two main aspects. On the one hand, flavonoids can be metabolized by the gut microbiota, and the flavonoids act as substrates in a series of catalytic reactions with various enzyme systems produced by the gut microbiota; as a result, the bacteria involved in these reactions will exhibit a tendency to grow (Lu et al., 2018). On the other hand, flavonoids can affect the cell membranes of some bacteria such as *Escherichia coli* and *Staphylococcus aureus*; for example, they directly disrupt the lipid bilayer of the cell membrane or alter the cell membrane permeability; ultimately, the reproduction of these bacteria is inhibited (Xie et al., 2015). We analyzed the differences in the taxonomic profiles of fecal microbiota before and after fermentation to clarify the modulation of gut microbiota structure by the nine flavonoids above. At the phylum level, this phenomenon was mainly reflected by the addition of the nine flavonoids that caused, to varying degrees, a reduction in the abundance of Firmicutes and an enhancement in the abundance of Actinobacteriota (Figure 3). This finding is consistent with that of previous studies in which the combined intervention of quercetin and resveratrol in rats markedly lowered the abundance of Firmicutes (Zhao et al., 2017). Among the bacteria involved in the metabolic transformation of flavonoids, Actinobacteriota accounted for a large proportion (Braune and Blaut, 2016). The remarkable rise in the abundance of Actinobacteriota in the hesperetin-7-O-glucoside and isoquercitrin groups may indicate that the two substrates have been more fully metabolized. Also, the addition of flavonoids increased the abundance of Proteobacteria. This phenomenon suggests that flavonoids promote the growth of Proteobacteria, which contains most of the harmful bacteria (Shin et al., 2015). This result supports the previous finding that supplementation with mulberry leaf flavonoids promoted an increase in the abundance of Proteobacteria in the gut microbiota of calves, and the specific promotion mechanism needs to be further investigated (Bi et al., 2017). However, the final conclusion of this study showed that mulberry leaf flavonoids could improve the gut health of calves. The main reason is that the researchers took into account the changes induced by mulberry leaf



flavonoids at the genus level. Therefore, we also need further analysis at the genus level to determine more comprehensively whether the addition of flavonoids is beneficial to the gut microbiota.

An increasing number of studies have shown that diversity of intestinal flora tends to be positively associated with human health and high levels of beneficial bacteria are more conducive to health. Consequently, in this study, the analysis of fecal microbiota composition at the genus level focused on the abundance of beneficial bacteria. The abundance of *Bifidobacterium*, *Lactobacillus*, and *Prevotella* was relatively enhanced after fermentation with the addition of hesperetin-7-O-glucoside, prunin, and isoquercitrin (Figure 5). *Bifidobacterium*, *Lactobacillus*, and *Prevotella* are all probiotics in human intestinal tract, and they have the functions of promoting absorption and digestion in the gastrointestinal tract, biological barrier function, and regulation of immunity (Odamaki et al., 2016; Milani et al., 2017). Currently, many studies have demonstrated that flavonoids can contribute to the increase in the abundance of these beneficial bacteria. The reason is mainly the involvement of these beneficial bacteria in the metabolism of flavonoids, particularly flavonoid monoglucosides. Icariside I is also a flavonoid monoglucoside. Oral administration of icaric acid to tumor-bearing mice has been reported to significantly enhance the abundance of *Lactobacillus* and *Bifidobacterium* in the cecal contents (Chen et al., 2021). *Bifidobacterium* and *Lactobacillus* have been reported to prove  $\beta$ -glycosidase activity, so they can perform hydrolysis reaction on flavonoid monoglucosides (Ávila et al., 2009). These studies fully explain the substantial increase in the abundance of *Bifidobacterium* and *Lactobacillus* in the three flavonoid monoglucoside groups, hesperetin-7-O-glucoside, prunin, and isoquercitrin. In addition to beneficial bacterial changes, we noted the effect of the nine flavonoids on some harmful bacteria. *Bilophila*, which can produce lipopolysaccharide, not only fails to promote host health but also aggravates inflammation and eventually leads to metabolic disorders (Lu et al., 2021). The results show that hesperetin-7-O-glucoside, naringin, and prunin significantly decreased the abundance of *Bilophila*, which indicates that the three flavonoids might possess better effects on anti-inflammation. Moreover, the addition of flavonoids resulted in a relative reduced abundance of *Bacteroides* and *Lachnospirillum*. Certain strains of *Bacteroides* have been shown that they can produce harmful metabolites, such as *Bacteroides fragilis* and *Bacteroides thetaiotaomicron* (Onoue et al., 1997). The present study also supported previous related studies *in vivo* and *in vitro* that flavonoids inhibited the growth of *Bacteroides* (Zhang et al., 2013; Wang et al., 2020). Due to their ability to regulate the gut-liver axis, flavonoids have an antihyperlipidemic effect. For example, hyperlipemia in mice was alleviated by the intake of flavonoids, while *Lachnospirillum* was also significantly reduced (Duan et al., 2021). The significant decrease in *Lachnospirillum* abundance in the current study is also consistent with this result. In conclusion, on the one hand, the nine flavonoid compounds above, especially hesperetin-7-O-glucoside, prunin, and isoquercitrin, can induce beneficial intestinal bacteria to become abundant while decreasing the percentage of harmful intestinal bacteria. On the other hand, they possessed the function of improving the imbalance of intestinal flora and could reduce the influence of other factors on intestinal flora. It needed to be particularly emphasized that the effects of hesperetin-7-O-glucoside, prunin, and isoquercitrin on the gut microbiota were

more pronounced than those of the remaining six flavonoids. It is still mainly because these three substrates belong to flavonoid monoglucosides, which are structurally characterized by containing only a single glucose group. In the studies by Makino et al., direct oral administration of quercetin and its various O-glycoside derivatives to rats showed that the bioavailability of isoquercitrin was higher than that of quercetin, whereas the bioavailability of rutin was lower than that of quercetin (Makino et al., 2009, 2013). Combined with the findings that flavonoid monoglucosides, such as puerarin-7-O-glucoside and calycosin-7-O- $\beta$ -D-Glucoside, had a longer residence time in the blood plasma than their corresponding flavonoid aglycones (Jiang et al., 2008; Ruan et al., 2015), we presumed that the bioavailability of flavonoid monoglucosides might be generally higher. Many studies have confirmed that one of the factors affecting the bioavailability of flavonoids is the interaction between flavonoids and gut microbiota (Hanske et al., 2009; Zhang et al., 2021; Baky et al., 2022). We thus suggest that the single glucose group contained in the structures of hesperetin-7-O-glucoside, prunin, and isoquercitrin make their interaction with gut microbiota more pronounced than the corresponding flavonoid aglycones and flavonoid diglycosides. However, neither  $\alpha$ -diversity nor  $\beta$ -diversity of the fecal microbiota composition showed significant differences in each group after fermentation. Therefore, the addition of the nine flavonoids did not result in significant differences in community distribution among the groups, and the richness and diversity of species in the community did not change significantly. In several previous *in vivo* studies, flavonoids were found to increase the  $\alpha$ -diversity and  $\beta$ -diversity of gut microbiota in mice (Peng et al., 2020; Xuan et al., 2020). However, the results of this study showed no significant effect of the nine flavonoids on the diversity of gut microbiota. We speculate that the main reason for this is the effect of the broad-spectrum inhibition of flavonoids during the *in vitro* study, and their antibacterial effects depend on the concentration of flavonoids.

Different fecal bacteria produce different metabolites when fermenting different substrates, and the similarities and differences of metabolites can affect the differences in bacterial abundance. The fermentation substrate affects the composition of bacterial communities after fecal bacteria fermentation, which leads to the similarities and differences of metabolites such as gases and SCFAs. We made a correlation analysis between fecal flora and metabolites to account for the changes in the two major metabolite groups of intestinal flora. All six SCFAs were obviously negatively associated with *Bifidobacterium*. Acetic and propionic acids also showed a significant negative relationship with *Prevotella* and a significant positive relationship with *Bacteroides* and *Flavonifractor*. After fermentation with the addition of nine flavonoids, the abundance of *Bifidobacterium* and *Prevotella* were relatively rose, while the abundance of *Bacteroides* and *Flavonifractor* were reduced, especially in the hesperetin-7-O-glucoside, prunin, and isoquercitrin groups. Thus, the concentration of SCFAs was decreased in all the groups with the addition of nine flavonoids, and the decrease was higher in the three groups. All gases were also significantly and negatively correlated with *Bifidobacterium*. Meanwhile,  $\text{NH}_3$ ,  $\text{H}_2$ , and  $\text{H}_2\text{S}$  were significantly negatively correlated with *Prevotella* and with *Bacteroides*. This finding correlates with the decrease in gas content after the addition of flavonoids. In summary, the community structure analysis also explains the decrease in gas and SCFA content after fermentation with the addition of the nine flavonoids mentioned above.

## 5. Conclusion

In this study, we investigated the similarities and differences in metabolic gas and SCFA production of different flavonoids (hesperidin, hesperetin-7-O-glucoside, hesperetin, naringin, prunin, naringenin, rutin, isoquercitrin, and quercetin) at 4 mg/mL in the fecal microbiota of 10 healthy Chinese individuals using an *in vitro* simulated fermentation technology. The results reveal that hesperetin-7-O-glucoside, prunin, and isoquercitrin can noticeably increase the relative abundance of intestinal probiotics, among which the increase in *Bifidobacterium* is the most significant, and they can decrease the relative abundance of *Lachnospirillum* and *Bilophila*. A certain amount of SCFAs and metabolic gases are produced, and these metabolites are intimately connected with the gut microbiota composition. This work provides a theoretical reference for the use of flavonoids to be a functional food.

## Data availability statement

The datasets presented in this study can be found in online repositories. The names of the repository/repositories and accession number(s) can be found in the article/supplementary material.

## Ethics statement

The studies involving human participants were reviewed and approved by the Ethics Committee of the Hangzhou Center for Disease Control and Prevention (no. 202047). The patients/participants provided their written informed consent to participate in this study. Written informed consent was obtained from the individual(s) for the publication of any potentially identifiable images or data included in this article.

## References

- Ávila, M., Hidalgo, M., Sánchez-Moreno, C., Pelaez, C., Requena, T., and De Pascual-Teresa, S. (2009). Bioconversion of anthocyanin glycosides by *Bifidobacterium* and *Lactobacillus*. *Food Res. Int.* 42, 1453–1461. doi: 10.1016/j.foodres.2009.07.026
- Baky, M. H., Elshahed, M., Wessjohann, L., and Farag, M. A. (2022). Interactions between dietary flavonoids and the gut microbiome: a comprehensive review. *Brit. J. Nutr.* 128, 577–591. doi: 10.1017/S0007114521003627
- Bi, Y., Yang, C., Diao, Q., and Tu, Y. (2017). Effects of dietary supplementation with two alternatives to antibiotics on intestinal microbiota of preweaned calves challenged with *Escherichia coli* K99. *Sci. Rep.* 7, 5439. doi: 10.1038/s41598-017-05376-z
- Bolyen, E., Rideout, J. R., Dillon, M. R., Bokulich, N. A., Abnet, C. C., Al-Ghalith, G. A., et al. (2019). Reproducible, interactive, scalable and extensible microbiome data science using QIIME 2. *Nat. Biotechnol.* 37, 852–857. doi: 10.1038/s41587-019-0209-9
- Braune, A., and Blaut, M. (2016). Bacterial species involved in the conversion of dietary flavonoids in the human gut. *Gut Microbes* 7, 216–234. doi: 10.1080/19490976.2016.1158395
- Callahan, B. J., McMurdie, P. J., Rosen, M. J., Han, A. W., Johnson, A. J., and Holmes, S. P. (2016). DADA2: high-resolution sample inference from Illumina amplicon data. *Nat. Methods* 13, 581–583. doi: 10.1038/nmeth.3869
- Castelli, V., D'Angelo, M., Quintiliani, M., Benedetti, E., Cifone, M. G., and Cimini, A. (2021). The emerging role of probiotics in neurodegenerative diseases: new hope for Parkinson's disease? *Neural Regen. Res.* 16, 628–634. doi: 10.4103/1673-5374.295270
- Chang, C. W., Chen, M. J., Shih, S. C., Chang, C. W., Chiau, J. C., Lee, H. C., et al. (2020). *Bacillus coagulans* (PROBACI) in treating constipation-dominant functional bowel disorders. *Medicine* 99:e20098. doi: 10.1097/MD.00000000000020098
- Chen, G., Cao, Z., Shi, Z., Lei, H., Chen, C., Yuan, P., et al. (2021). Microbiome analysis combined with targeted metabolomics reveal immunological anti-tumor activity of icariside I in a melanoma mouse model. *Biomed. Pharmacother.* 140:111542. doi: 10.1016/j.biopha.2021.111542
- Cotillard, A., Kennedy, S. P., Kong, L. C., Prifti, E., Pons, N., Le Chatelier, E., et al. (2013). Dietary intervention impact on gut microbial gene richness. *Nature* 500, 585–588. doi: 10.1038/nature12480
- Duan, R., Guan, X., Huang, K., Zhang, Y., Li, S., Xia, J., et al. (2021). Flavonoids from whole-grain oat alleviated high-fat diet-induced hyperlipidemia via regulating bile acid metabolism and gut microbiota in mice. *J. Agric. Food Chem.* 69, 7629–7640. doi: 10.1021/acs.jafc.1c01813
- Duda-Chodak, A. (2012). The inhibitory effect of polyphenols on human gut microbiota. *J. Physiol. Pharmacol.* 63, 497–503.
- Espley, R. V., Butts, C. A., Laing, W. A., Martell, S., Smith, H., McGhie, T. K., et al. (2014). Dietary flavonoids from modified apple reduce inflammation markers and modulate gut microbiota in mice. *J. Nutr.* 144, 146–154. doi: 10.3945/jn.113.182659
- Estruel-Amades, S., Massot-Cladera, M., Perez-Cano, F. J., Franch, A., Castell, M., and Camps-Bossacoma, M. (2019). Hesperidin effects on gut microbiota and gut-associated lymphoid tissue in healthy rats. *Nutrients* 11:324. doi: 10.3390/nu11020324
- Etzeberria, U., Arias, N., Boque, N., Macarulla, M. T., Portillo, M. P., Martinez, J. A., et al. (2015). Reshaping faecal gut microbiota composition by the intake of *trans*-resveratrol and quercetin in high-fat sucrose diet-fed rats. *J. Nutr. Biochem.* 26, 651–660. doi: 10.1016/j.jnutbio.2015.01.002
- Guinane, C. M., and Cotter, P. D. (2013). Role of the gut microbiota in health and chronic gastrointestinal disease: understanding a hidden metabolic organ. *Ther. Adv. Gastroenterol.* 6, 295–308. doi: 10.1177/1756283X13482996
- Gwiazdowska, D., Jus, K., Jasnowska-Malecka, J., and Kluczynska, K. (2015). The impact of polyphenols on *Bifidobacterium* growth. *Acta Biochim. Pol.* 62, 895–901. doi: 10.18388/abp.2015.1154
- Hanske, L., Loh, G., Szczesny, S., Blaut, M., and Braune, A. (2009). The bioavailability of apigenin-7-glucoside is influenced by human intestinal microbiota in rats. *J. Nutr.* 139, 1095–1102. doi: 10.3945/jn.108.102814
- Jiang, X., Shi, Y., Fu, Z., Li, W. W., Lai, S., Wu, Y., et al. (2020). Functional characterization of three flavonol synthase genes from *Camellia sinensis*: roles in flavonol accumulation. *Plant Sci.* 300:110632. doi: 10.1016/j.plantsci.2020.110632
- Jiang, J. R., Yuan, S., Ding, J. F., Zhu, S. C., Xu, H. D., Chen, T., et al. (2008). Conversion of puerarin into its 7-O-glucoside derivatives by *microbacterium oxydans* (CGMCC 1788)

## Author contributions

LP: data curation, formal analysis, investigation, and writing-original draft. HY: data curation, formal analysis, validation, and visualization. XP: methodology and conceptualization. WL: software and resources. ZW: supervision. YZ: funding acquisition. JZ: methodology, project administration, and review. All authors contributed to the article and approved the submitted version.

## Funding

This work was supported by the National Natural Science Foundation of China (grant no. 31600639) and Key Research and Development Program of Zhejiang Province (2019C01082).

## Conflict of interest

The authors declare that the research was conducted in the absence of any commercial or financial relationships that could be construed as a potential conflict of interest.

## Publisher's note

All claims expressed in this article are solely those of the authors and do not necessarily represent those of their affiliated organizations, or those of the publisher, the editors and the reviewers. Any product that may be evaluated in this article, or claim that may be made by its manufacturer, is not guaranteed or endorsed by the publisher.

- to improve its water solubility and pharmacokinetic properties. *Appl. Microbiol. Biotechnol.* 81, 647–657. doi: 10.1007/s00253-008-1683-z
- Kalantar-Zadeh, K., Berean, K. J., Burgell, R. E., Muir, J. G., and Gibson, P. R. (2019). Intestinal gases: influence on gut disorders and the role of dietary manipulations. *Nat. Rev. Gastroenterol. Hepatol.* 16, 733–747. doi: 10.1038/s41575-019-0193-z
- Kumar, S., and Pandey, A. K. (2013). Chemistry and biological activities of flavonoids: an overview. *Sci. World J.* 2013:162750. doi: 10.1155/2013/162750
- Li, W., and Chen, T. (2022). An insight into the clinical application of gut microbiota during anticancer therapy. *Adv. Gut. Microbiome Res.* 2022, 1–7. doi: 10.1155/2022/8183993
- Li, X., Yang, L. C., Li, J. E., Lin, L. Z., and Zheng, G. D. (2021). A flavonoid-rich *Smilax China* L. extract prevents obesity by upregulating the adiponectin-receptor/AMPK signalling pathway and modulating the gut microbiota in mice. *Food Funct.* 12, 5862–5875. doi: 10.1039/d1fo00282a
- Lim, M. Y., You, H. J., Yoon, H. S., Kwon, B., Lee, J. Y., Lee, S., et al. (2017). The effect of heritability and host genetics on the gut microbiota and metabolic syndrome. *Gut* 66, 1031–1038. doi: 10.1136/gutjnl-2015-311326
- Ling, Z., Xiao, H., and Chen, W. (2022). Gut microbiome: the cornerstone of life and health. *Adv. Gut. Microbiome Res.* 2022, 1–3. doi: 10.1155/2022/9894812
- Liu, Z., Bruins, M. E., Ni, L., and Vincken, J. P. (2018). Green and black tea phenolics: bioavailability, transformation by colonic microbiota, and modulation of colonic microbiota. *J. Agr. Food Chem.* 66, 8469–8477. doi: 10.1021/acs.jafc.8b02233
- Lu, F., Liao, X., Hu, X., and Zhang, Y. (2018). Research advances in the effect of polyphenols on the gut microbes and the discuss about microbes which will appear as polyphenols. *J. Food Sci. Technol.* 39, 330–335. doi: 10.13386/j.issn1002-0306.2018.16.059
- Lu, H. Q., You, Y. T., Zhou, X. H., He, Q. X., Wang, M., Chen, L. Q., et al. (2021). Citrus reticulatae pericarpium extract decreases the susceptibility to HFD-induced glycolipid metabolism disorder in mice exposed to azithromycin in early life. *Front. Immunol.* 12:774433. doi: 10.3389/fimmu.2021.774433
- Luo, P., Lednovich, K., Xu, K., Nnyamah, C., Layden, B. T., and Xu, P. W. (2022). Central and peripheral regulations mediated by short-chain fatty acids on energy homeostasis. *Transl. Res.* 248, 128–150. doi: 10.1016/j.trsl.2022.06.003
- Makino, T., Kanemaru, M., Okuyama, S., Shimizu, R., Tanaka, H., and Mizukami, H. (2013). Anti-allergic effects of enzymatically modified isoquercitrin ( $\alpha$ -oligoglucosyl quercetin 3-O-glucoside), quercetin 3-O-glucoside,  $\alpha$ -oligoglucosyl rutin, and quercetin, when administered orally to mice. *J. Nat. Med.* 67, 881–886. doi: 10.1007/s11418-013-0760-5
- Makino, T., Shimizu, R., Kanemaru, M., Suzuki, Y., Moriwaki, M., and Mizukami, H. (2009). Enzymatically modified isoquercitrin,  $\alpha$ -oligoglucosyl quercetin 3-O-glucoside, is absorbed more easily than other quercetin glycosides or aglycone after oral administration in rats. *Biol. Pharm. Bull.* 32, 2034–2040. doi: 10.1248/bpb.32.2034
- Milani, C., Mangifesta, M., Mancabelli, L., Lugli, G. A., James, K., Duranti, S., et al. (2017). Unveiling bifidobacterial biogeography across the mammalian branch of the tree of life. *ISME J.* 11, 2834–2847. doi: 10.1038/ismej.2017.138
- Nie, Y., Luo, F., and Lin, Q. (2018). Dietary nutrition and gut microflora: a promising target for treating diseases. *Trends Food Sci. Technol.* 75, 72–80. doi: 10.1016/j.tifs.2018.03.002
- Nohynek, L. J., Alakomi, H. L., Kahkonen, M. P., Heinonen, M., Helander, I. M., Oksman-Caldentey, K. M., et al. (2006). Berry phenolics: antimicrobial properties and mechanisms of action against severe human pathogens. *Nutr. Cancer* 54, 18–32. doi: 10.1207/s15327914nc5401\_4
- Odamaki, T., Kato, K., Sugahara, H., Xiao, J. Z., Abe, F., and Benno, Y. (2016). Effect of probiotic yoghurt on animal-based diet-induced change in gut microbiota: an open, randomised, parallel-group study. *Benef. Microbes* 7, 473–484. doi: 10.3920/BM2015.0173
- Onoue, M., Kado, S., Sakaitani, Y., Uchida, K., and Morotomi, M. (1997). Specific species of intestinal bacteria influence the induction of aberrant crypt foci by 1,2-dimethylhydrazine in rats. *Cancer Lett.* 113, 179–186. doi: 10.1016/s0304-3835(97)04698-3
- Parkar, S. G., Stevenson, D. E., and Skinner, M. A. (2008). The potential influence of fruit polyphenols on colonic microflora and human gut health. *Int. J. Food Microbiol.* 124, 295–298. doi: 10.1016/j.ijfoodmicro.2008.03.017
- Peng, Y., Yan, Y., Wan, P., Dong, W., Huang, K., Ran, L., et al. (2020). Effects of long-term intake of anthocyanins from *Lycium ruthenicum* Murray on the organism health and gut microbiota *in vivo*. *Food Res. Int.* 130:108952. doi: 10.1016/j.foodres.2019.108952
- Pi, X., Yu, Z., Yang, X., Du, Z., and Liu, W. (2022). Effects of zymosan on short-chain fatty acid and gas production in *in vitro* fermentation models of the human intestinal microbiota. *Front. Nutr.* 9:921137. doi: 10.3389/fnut.2022.921137
- Rooks, M. G., and Garrett, W. S. (2016). Gut microbiota, metabolites and host immunity. *Nat. Rev. Immunol.* 16, 341–352. doi: 10.1038/nri.2016.42
- Ruan, J. Q., Li, S., Li, Y. P., Wu, W. J., Lee, S. M., and Yan, R. (2015). The presystemic interplay between gut microbiota and orally administered calyosin-7-O- $\beta$ -D-glucoside. *Drug Metab. Dispos.* 43, 1601–1611. doi: 10.1124/dmd.115.065094
- Sandoval, V., Sanz-Lamora, H., Arias, G., Marrero, P. F., Haro, D., and Relat, J. (2020). Metabolic impact of flavonoids consumption in obesity: from central to peripheral. *Nutrients* 12:2393. doi: 10.3390/nu12082393
- Santos-Buelga, C., and Feliciano, A. S. (2017). Flavonoids: from structure to health issues. *Molecules* 22:477. doi: 10.3390/molecules22030477
- Sarkar, A., Yoo, J. Y., Valeria Ozorio Dutra, S., Morgan, K. H., and Groer, M. (2021). The association between early-life gut microbiota and long-term health and diseases. *J. Clin. Med.* 10:459. doi: 10.3390/jcm10030459
- Serino, M. (2019). SCFAs – the thin microbial metabolic line between good and bad. *Nat. Rev. Endocrinol.* 15, 318–319. doi: 10.1038/s41574-019-0205-7
- Shin, N. R., Whon, T. W., and Bae, J. W. (2015). Proteobacteria: microbial signature of dysbiosis in gut microbiota. *Trends Biotechnol.* 33, 496–503. doi: 10.1016/j.tibtech.2015.06.011
- Singh, S. B., and Lin, H. C. (2015). Hydrogen sulfide in physiology and diseases of the digestive tract. *Microorganisms* 3, 866–889. doi: 10.3390/microorganisms3040866
- Tian, B., Geng, Y., Xu, T., Zou, X., Mao, R., Pi, X., et al. (2022). Digestive characteristics of *Herichium erinaceus* polysaccharides and their positive effects on fecal microbiota of male and female volunteers during *in vitro* fermentation. *Front. Nutr.* 9:858585. doi: 10.3389/fnut.2022.858585
- Trakman, G. L., Fehily, S., Basnayake, C., Hamilton, A. L., Russell, E., Wilson-O'Brien, A., et al. (2022). Diet and gut microbiome in gastrointestinal disease. *J. Gastroenterol. Hepatol.* 37, 237–245. doi: 10.1111/jgh.15728
- Tremaroli, V., and Bäckhed, F. (2012). Functional interactions between the gut microbiota and host metabolism. *Nature* 489, 242–249. doi: 10.1038/nature11552
- Triantafyllou, K., Chang, C., and Pimentel, M. (2014). Methanogens, methane and gastrointestinal motility. *J. Neurogastroenterol. Motil.* 20, 31–40. doi: 10.5056/jnm.2014.20.1.31
- Wang, R., Wang, L., Wei, G., Liu, N., Zhang, L., Wang, S., et al. (2020). The effect and mechanism of baicalin on regulating gut microbiota and improving chemotherapy-induced intestinal mucositis in mice. *Acta Pharm. Sin. B* 55, 868–876. doi: 10.16438/j.0513-4870.2019-0933
- Wu, D., Ding, L., Tang, X., Wang, W., Chen, Y., and Zhang, T. (2019). Baicalin protects against hypertension-associated intestinal barrier impairment in part through enhanced microbial production of short-chain fatty acids. *Front. Pharmacol.* 10:1271. doi: 10.3389/fphar.2019.01271
- Xie, Y., Yang, W., Tang, F., Chen, X., and Ren, L. (2015). Antibacterial activities of flavonoids: structure-activity relationship and mechanism. *Curr. Med. Chem.* 22, 132–149. doi: 10.2174/0929867321666140916113443
- Xuan, H., Ou, A., Hao, S., Shi, J., and Jin, X. (2020). Galangin protects against symptoms of dextran sodium sulfate-induced acute colitis by activating autophagy and modulating the gut microbiota. *Nutrients* 12:347. doi: 10.3390/nu12020347
- Ye, H., Li, X., Li, L., Zhang, Y., and Zheng, J. (2022). Homologous expression and characterization of  $\alpha$ -L-rhamnosidase from *aspergillus Niger* for the transformation of flavonoids. *Appl. Biochem. Biotechnol.* 194, 3453–3467. doi: 10.1007/s12010-022-03894-9
- Ye, X., Pi, X., Zheng, W., Cen, Y., Ni, J., Xu, L., et al. (2022). The methanol extract of *Polygonatum odoratum* ameliorates colitis by improving intestinal short-chain fatty acids and gas production to regulate microbiota dysbiosis in mice. *Front. Nutr.* 9:899421. doi: 10.3389/fnut.2022.899421
- Zhang, X., Zhu, X., Sun, Y., Hu, B., Sun, Y., Jabbar, S., et al. (2013). Fermentation *in vitro* of EGCG, GCG and EGCG3 me isolated from oolong tea by human intestinal microbiota. *Food Res. Int.* 54, 1589–1595. doi: 10.1016/j.foodres.2013.10.005
- Zhang, M., Zhu, S., Yang, W., Huang, Q., and Ho, C. T. (2021). The biological fate and bioefficacy of citrus flavonoids: bioavailability, biotransformation, and delivery systems. *Food Funct.* 12, 3307–3323. doi: 10.1039/d0fo03403g
- Zhao, Z., Liu, W., and Pi, X. (2021). *In vitro* effects of stachyose on the human gut microbiota. *Starch* 73, 2100029–2100028. doi: 10.1002/star.202100029
- Zhao, L., Zhang, Q., Ma, W., Tian, F., Shen, H., and Zhou, M. (2017). A combination of quercetin and resveratrol reduces obesity in high-fat diet-fed rats by modulation of gut microbiota. *Food Funct.* 8, 4644–4656. doi: 10.1039/c7fo01383c





## OPEN ACCESS

## EDITED BY

Wei Qi He,  
Soochow University, China

## REVIEWED BY

Zhaolai Dai,  
China Agricultural University, China  
Haijun Zhang,  
Feed Research Institute (CAAS), China

## \*CORRESPONDENCE

Xiaoou Su  
✉ [suxiaoou@caas.cn](mailto:suxiaoou@caas.cn)

## SPECIALTY SECTION

This article was submitted to  
Microorganisms in Vertebrate Digestive  
Systems,  
a section of the journal  
Frontiers in Microbiology

RECEIVED 16 November 2022

ACCEPTED 06 February 2023

PUBLISHED 03 March 2023

## CITATION

Zhao W, Huang Y, Cui N, Wang R, Xiao Z and  
Su X (2023) Glucose oxidase as an alternative to  
antibiotic growth promoters improves the  
immunity function, antioxidative status, and  
cecal microbiota environment in  
white-feathered broilers.  
*Front. Microbiol.* 14:1100465.  
doi: 10.3389/fmicb.2023.1100465

## COPYRIGHT

© 2023 Zhao, Huang, Cui, Wang, Xiao and Su.  
This is an open-access article distributed under  
the terms of the [Creative Commons Attribution  
License \(CC BY\)](https://creativecommons.org/licenses/by/4.0/). The use, distribution or  
reproduction in other forums is permitted,  
provided the original author(s) and the  
copyright owner(s) are credited and that the  
original publication in this journal is cited, in  
accordance with accepted academic practice.  
No use, distribution or reproduction is  
permitted which does not comply with these  
terms.

# Glucose oxidase as an alternative to antibiotic growth promoters improves the immunity function, antioxidative status, and cecal microbiota environment in white-feathered broilers

Wenyu Zhao, Yuan Huang, Na Cui, Ruiguo Wang, Zhiming Xiao and Xiaoou Su\*

Key Laboratory of Agro-Product Quality and Safety of the Ministry of Agriculture, Institute of Quality Standards and Testing Technology for Agro-Products, Chinese Academy of Agricultural Sciences, Beijing, China

This study aimed to demonstrate the effects of glucose oxidase (GOD) on broilers as a potential antibiotic substitute. A total of four hundred twenty 1-day-old male Cobb500 broilers were randomly assigned into five dietary treatments, each with six replicates (12 chicks per replicate). The treatments included two control groups (a basal diet and a basal diet with 50 mg/kg aureomycin) and three GOD-additive groups involving three different concentrations of GOD. Analysis after the *t*-test showed that, on day 21, the feed:gain ratio significantly decreased in the 1,200 U/kg GOD-supplied group (GOD1200) compared to the antibiotic group (Ant). The same effect was also observed in GOD1200 during days 22–42 and in the 600 U/kg GOD-supplied group (GOD600) when compared to the control group (Ctr). The serum tests indicated that, on day 21, the TGF- $\beta$  cytokine was significantly decreased in both GOD600 and GOD1200 when compared with Ctr. A decrease in malondialdehyde and an increase in superoxide dismutase in GOD1200 were observed, which is similar to the effects seen in Ant. On day 42, the D-lactate and glutathione peroxidase activity changed remarkably in GOD1200 and surpassed Ant. Furthermore, GOD upregulated the expression of the jejunal barrier genes (MUC-2 and ZO-1) in two phases relative to Ctr. In the aureomycin-supplied group, the secretory immunoglobulin A significantly decreased in the jejunum at 42 days. Changes in microbial genera were also discovered in the cecum by sequencing 16S rRNA genes at 42 days. The biomarkers for GOD supplementation were identified as *Colidextribacter*, *Oscillibacter*, *Flavonifractor*, *Oscillospira*, and *Shuttleworthia*. Except for *Shuttleworthia*, all the abovementioned genera were n-butyrate producers known for imparting their various benefits to broilers. The PICRUSt prediction of microbial communities revealed 11 pathways that were enriched in both the control and GOD-supplied groups. GOD1200 accounted for an increased number of metabolic pathways, demonstrating their potential in aiding nutrient absorption and digestion. In conclusion, a diet containing GOD can be beneficial to broiler health, particularly at a GOD concentration of 1,200 U/kg. The improved feed conversion ratio, immunity, antioxidative capacity, and intestinal condition demonstrated that GOD could be a valuable alternative to antibiotics in broiler breeding.

## KEYWORDS

glucose oxidase, broiler, antibiotic, healthy condition, microbiota



## Introduction

Antibiotics have been playing a vital role in commercial poultry production since their first use in the 1940s (Castanon, 2007). They greatly improve the production efficiency of the breeding industry and satisfy the increasing human demand for animal-derived foods. However, their continued use has had negative impacts. The issue of antibiotic resistance has attracted a great amount of attention because of the existing and potential threats antibiotics pose to public health (Laxminarayan et al., 2014). Many countries, such as those in the European Union and the USA, started to restrict or even forbid the use of antibiotics in industrial-scale animal production (Marshall and Levy, 2011). From 1 January 2020, the Ministry of Agriculture of China also issued regulations prohibiting the use of any growth-promoting antibiotics. Thus, it is essential to find effective in-feed antibiotic alternatives in animal production without compromising human health. Accordingly, novel products, including plant essential oils (Brenes and Roura, 2010), probiotics (Kabir et al., 2005), organic acids (Adil et al., 2010), antibacterial peptides (Wang et al., 2016), and feed enzymes (Askelson et al., 2018), were investigated.

Glucose oxidase (GOD), as one of the feed enzymes, could specifically catalyze the oxidation of  $\beta$ -D-glucose to gluconic acid and hydrogen peroxide (Bankar et al., 2009).

This enzyme has been gradually accepted by the feed industry due to several verified advantages, including growth promotion, feed quality improvement, intestinal health regulation, and toxic reaction reduction, with non-toxic, low-residue characteristics (Dang et al., 2021, 2022; Hoque et al., 2022; Sun et al., 2022). In animals, particularly poultry, intestinal barrier and microbiota compositions are critical, since they are closely related to the immune system and health (Robinson et al., 2015; Awad et al., 2017; Pandit et al., 2018). The gastrointestinal tract's microbiota flora is linked to "intestinal" or "non-intestinal" functions ranging from nutrient absorption to immune response and even the gut-brain axis (Gao et al., 2017; Borda-Molina et al., 2018). Therefore, animal nutrition research mainly focuses on the host gut which correlates with optimal health and productivity. GOD has been known to help animals avoid intestinal dysfunction or other gut problems based on its reaction mechanism (Qu and Liu, 2021). The GOD-catalyzed glucose products can act on the gut of broilers, gluconic acid can produce the short-chain fatty acids (SCFAs) and further create a weakly acidic intestinal tract environment (Mortensen et al., 1988; Biagi et al., 2006), and hydrogen peroxide can participate in the oxidative stress response and regulate gut microbiota through its bactericidal and antimicrobial properties (Vatansever et al., 2013; Belambri et al., 2018). Though some researchers recently elucidated the effects of GOD with a sequencing-based technique (Wu et al., 2020; Meng et al., 2021), it is still ambiguous how GOD improves gut health and immunity function and why antibiotics can be replaced by it in broiler production (Liang et al., 2022). Some voids, such as how the additive, defense function, and growth performance interact with each other, still remain.

Therefore, this study aimed to determine the impact of glucose oxidase on the growth performance, immunity, antioxidative stage, and intestinal function of white-feathered broilers and attempted to explain it from the perspective of intestinal microorganisms. These findings may contribute to expanding the knowledge concerning

the application of glucose oxidase. Furthermore, the comparison between the GOD and aureomycin-supplemented groups can further illustrate the role of GOD in feed as a substitute for antibiotic growth promoters (AGPs).

## Materials and methods

### Birds, diet, and management

A total of four hundred twenty 1-day-old male Cobb500 white-feathered broiler chicks obtained from Beijing Poultry Breeding Co., Ltd. were randomly assigned into five dietary treatments, each in six replicates (12 chicks/replicate) by cage-rearing, and the original average weight of every replicate had no remarkable difference. The control group (Ctr) was fed with a basal diet formulated to meet the nutrient requirements of poultry as per the National Research Council 1994, and other treatment groups were based on the basal diet with the addition of various feed additives. The antibiotic group (Ant) was supplied with 50 mg/kg aureomycin (Chia Tai Co., Ltd., Henan, China). Different concentrations of GODs (300, 600, and 1,200 U per kilogram of diet) were determined from the doses recommended by the manufacturer (VTR Biotech Co., Ltd., Zhuhai, Guangdong, China) and from massive references for their effective applications in the poultry industry, and named as GOD300, GOD600, and GOD1200. Table 1 details the diet compositions and nutrient contents of the basal diet for the entire study's starting (day 0–21) and growing (day 21–42) phases. All the chickens were exposed to incandescent light for a 24-h photoperiod instead of daylight, and the birds were allowed *ad libitum* access to drinking water from nipple drinkers. The diets for the chickens were mash feed for the first 12 days and then gradually transitioned to pellet diets. For temperature, ventilation, and other types of ventilation management for the birds in this research, one is referred to the guidelines for raising meat-type broilers (National Technical Committee for Animal Agriculture Standardization, 2005). Feed consumption and body weight were recorded every week and the mortality of the birds was checked daily. These data were used to calculate the feed intake, body weight gain, and feed conversion ratio.

### Sample collection

One chicken with an average weight from each replicate was chosen for sample collection after a 12-h fast at the end of the two phases (days 21 and 42). The blood samples were drawn from the wing vein and dropped into tubes without anticoagulants. The serum used in further research was received after the blood samples were centrifuged at 3,500  $\times$  g for 10 min (4°C) and stored at  $-80^{\circ}\text{C}$ . Birds were killed and shortly dissected after collecting blood samples. Immune organs (the thymus, the spleen, and the bursa of Fabricius) were taken out from the dead body individually, following the rinsing, blotting, and weighting procedures. The segments ( $\sim 2$  cm) in the middle of the jejunum were collected, washed with physiological saline, and then dropped into 10% neutral-buffered formalin for immobilization. Meanwhile, the remaining segments of the jejunum were gently scraped to sample

**TABLE 1** Composition and nutrient levels of basal diet in the two phases of trial (% as fed basis).

Items	Contents (%)	
	1–21 d of age	22–42 d of age
<b>Ingredients</b>		
Corn	56.59	59.96
Soybean meal	25.95	20.00
Cottonseed meal	4.50	4.42
Corn gluten meal	4.00	5.00
Wheat middling	2.00	2.00
Soybean oil	2.49	4.50
Calcium hydrogen phosphate	1.82	1.58
Limestone	1.35	1.27
Salt	0.35	0.35
<i>L</i> -Lysine-HCl	0.35	0.35
<i>DL</i> -Methionine	0.23	0.21
Threonine	0.05	0.04
Mineral Premix <sup>a</sup>	0.20	0.20
Vitamin Premix <sup>b</sup>	0.02	0.02
Choline chloride	0.10	0.10
Total	100.00	100.00
<b>Nutrients</b>		
ME (kcal/kg)	2,980.00	3,160.00
Crude protein	21.95	19.95
Ca	1.00	0.90
Non-phytate P	0.45	0.40
Lysine	1.30	1.15
Methionine	0.58	0.54
Methionine + cystine	0.94	0.87
Threonine	0.84	0.75
Tryptophan	0.23	0.20

<sup>a</sup>The Mineral Premix supplied the following (per kilogram of complete feed): Cu, 8 mg; Zn, 75 mg; Fe, 80 mg; Mn, 100 mg; I, 0.35 mg; and Se, 0.15 mg.

<sup>b</sup>The Vitamin Premix supplied the following (per kilogram of complete feed): vitamin A, 12,500 IU, vitamin D<sub>3</sub>, 2,500 IU, vitamin E, 18.75 mg, vitamin K<sub>3</sub>, 2.65 mg, vitamin B<sub>1</sub>, 2 mg, vitamin B<sub>2</sub>, 6 mg, vitamin B<sub>12</sub>, 0.025 mg, biotin, 0.0325 mg, folic acid, 1.25 mg, pantothenic acid, 12 mg, and niacin, 50 mg.

the mucous membrane, snap-frozen in liquid nitrogen, and stored at  $-80^{\circ}\text{C}$  for gene expression analysis. Then, under the condition of being germ-free, the cecal part of the bird was gathered. Its contents were speedily squeezed into sterile cryopreservation tubes and then stored in liquid nitrogen as described previously.

## Biochemical index and enzyme activity analysis

Biochemical index and enzyme activity were measured after the collected, frozen serum samples finished the two-step gradient

thawing. Alanine aminotransferase (ALT), aspartate transaminase (AST), total protein (TP), alkaline phosphatase (ALP), and urea were all determined by a Cobas 6000 automatic biochemical analyzer (Roche Diagnostics Co., Ltd., Shanghai, China). The enzyme activities of glutathione peroxidase (GSH-Px), diamine oxidase (DAO), and also the malonaldehyde (MDA) concentration of serum were measured by colorimetric methods with a T9CS+ spectrophotometer (Purkinje General Instrument Co., Ltd., Beijing, China). A microplate reader detected the total antioxidant capacity (T-AOC) and superoxide dismutase (SOD). All the antioxidant indexes aforementioned were conducted according to the manufacturer's instructions.

## ELISA

Transforming growth factor- $\beta$  (TGF- $\beta$ ), D-lactate (D-Lac), diamine oxidase (DAO), and 8-hydroxy-2'-deoxyguanosine (8-OH-dG) in the serum were measured through enzyme-linked immunosorbent assay kits (Nanjing Jiancheng Institute of Bioengineering, Nanjing, China).

## Immunohistochemical observations of jejunal secretory immunoglobulin A

Jejunum samples fixed in 10% neutral-buffered formalin for over 24 h were embedded in paraffin. The 4- $\mu\text{m}$  tissue slices were prepared by Leica RM2255 (Leica Biosystems, Wetzlar, Germany). Afterward, dewaxing and dehydration of the samples were executed and 3% H<sub>2</sub>O<sub>2</sub> was used to remove the endogenous peroxidase activity in slices. Next, the primary antibody (SouthernBiotech, Birmingham, AL, USA) and secondary antibody (Thermo Fisher Scientific, Fremont, CA, USA) were applied for incubation of the samples accordingly, the former left overnight at  $4^{\circ}\text{C}$  and the latter for 10 min at room temperature, along with the color reaction visualized by the DAB chromogen. The SIgA-positive cells were stained prominently brown in contrast to the surrounding tissue, which was counterstained for identifying host cells. Finally, the slides were observed under the microscope (Olympus Corporation, Tokyo, Japan).

## Total RNA extraction and gene expression in the jejunum

The total RNA was extracted from collected jejunal mucosa using the RNA Easy Fast Tissue Kit (Tiangen Biotech Co., Ltd., Beijing, China) following the standard operating procedure. Nanodrop 2000 spectrophotometer (Thermo Fisher Scientific, Waltham, MA, USA) and agarose-ethidium bromide electrophoresis were applied to determine the concentration, purity, and integrity of the RNA. The synthesis of complementary DNA (cDNA) and further real-time PCRs in duplicate were all performed with the One Step TB Green<sup>®</sup> PrimeScript<sup>™</sup> RT-PCR Kit II (TaKaRa, Dalian, China) and the ABI 7500 Fast Real-Time PCR system (Applied Biosystems, Waltham, MA, USA). The

information on primer sequences of *Claudin-1*, *Occludin*, *ZO-1*, *MUC-2*, and  $\beta$ -*actin* is given in Table 2. The eukaryotic reference gene  $\beta$ -*actin* was used to normalize the relative gene quantification by the  $2^{-\Delta\Delta C_t}$  method (Livak and Schmittgen, 2001).

## 16srRNA amplification and illumina sequences

The cecal contents at the end of 42 day were extracted using the E.Z.N.A.<sup>®</sup> Stool DNA Kit (Omega Bio-tek, Norcross, GA, USA) for microbial DNA as per the manufacturer's instructions. The DNA extract's quality was checked similarly to that of RNA. Hypervariable region V3–V4 of the bacterial 16S rRNA gene was amplified by the primer pair 338F (5'-ACTCCTACGGGAGGCAGCAG-3') and 806R (5'-GGACTACHVGGGTWTCTAAT-3') with an ABI GeneAmp<sup>®</sup> 9700 PCR thermocycler (Applied Biosystems, Waltham, MA, USA). The specific program for the PCR amplification of 16srRNA was conducted as follows: denaturation at 95°C for 3 min, then followed by 27 cycles at 95°C for 30 s, annealing at 55°C for 30 s, then extension at 72°C for 45 s, and a final extension at 72°C for 10 min, and the final temperature was 4°C. The PCR was conducted in triplicate with a 20- $\mu$ L mixture for one. The mixture was composed of 4  $\mu$ L of 5  $\times$  FastPfu buffer, 2  $\mu$ L of 2.5 mM dNTPs, 0.8  $\mu$ L each of forward and reverse primers (5  $\mu$ M), 0.4  $\mu$ L of FastPfu DNA Polymerase, 10 ng of template DNA, and the ddH<sub>2</sub>O. Two percent agarose gel and the AxyPrep DNA Gel Extraction Kit (Axygen Biosciences, Union City, CA, USA) were used to finish the extraction and purification of the PCR product, and they were then quantified by a Quantus<sup>™</sup> Fluorometer (Promega, Madison, WI, USA).

Purified amplicons were pooled in equal amounts and paired-end sequenced (2  $\times$  300 bp). All the analysis was finished by Majorbio Bio-Pharm Technology Co., Ltd. (Shanghai, China) on the Illumina MiSeq platform (Illumina, San Diego, CA, USA) in accordance with the standard protocol. Finally, the raw reads were deposited into the NCBI Sequence Read Archive (SRA) database (Accession Number: SRP392472).

The in-house Perl script was used to demultiplex the raw FASTQ files that were quality-filtered by fastp version 0.19.6 and merged by flash version 1.2.7 with the following criteria later:

(i) The bases whose quality value is below 20 bp at the end of the reads are filtered. A 50-bp window is set and the back-end bases under 20 of the average quality value are cut off, the reads containing *N* bases are filtered, and the quality control value should be below 50 bp; (ii) paired reads are merged into one sequence with the relationship of overlap between the PE reads. Furthermore, the length of the overlap should be longer than 10 bp; (iii) the overlap region of the spliced sequence with the allowable mismatch rate is screened out to be higher than 0.2; and (iv) the barcode and primers at both ends of the sequence are used to distinguish the samples and adjust their direction. The barcode should have no mismatched primers, and the maximum primer mismatch number is 2.

## Statistical analysis

The data were analyzed by SPSS 25.0 (SPSS Inc., Chicago, IL, USA). The Shapiro–Wilk test was initially used to assess the normality of data. The differences between samples were evaluated using the one-way analysis of variance (ANOVA) and Duncan's multiple comparisons test. Each control group was pairwise compared with GOD300, GOD600, and GOD1200 using the *t*-tests to assess the growth performance indexes. A tendency toward significance was considered at  $0.05 \leq P < 0.1$ , and the statistical significance was stated based on the value of *P* of  $<0.05$  (Granato et al., 2014).

For microbiota profiling, the processed effective reads were clustered into operational taxonomic units (OTUs) using UPARSE 7.1 (<http://drive5.com/uparse/>) with 97% sequence similarity. Each 16S rRNA gene sequence was analyzed by the RDP Classifier algorithm (<http://rdp.cme.msu.edu/>) at different taxonomic levels and then against the Silva (SSU128) 16S rRNA database using a confidence threshold of 70%.

Rarefaction curves and  $\alpha$ -diversity indices were calculated by Mothur v1.30.1 (Schloss et al., 2009). The similarity among the microbial communities in different samples was determined by the principal coordinate analysis (PCoA) based on Bray–Curtis dissimilarity using the Vegan v2.5-3 package. The species composition was obtained based on the taxonomic analysis. Analysis of similarities (ANOSIM) was applied to assess the significance of the microbial community differences among various treatments. The Kruskal–Wallis H test and the Wilcoxon rank-sum test were employed to explore the differences in the relative abundance of bacteria among multiple groups and then between every two groups, respectively.

Each OUT representative sequence's taxonomy level was analyzed by an RDP Classifier version 2.2 (Wang et al., 2007) using the confidence threshold of 0.7. The PICRUST2 (Phylogenetic Investigation of Communities by Reconstruction of Unobserved States) software was used to predict the microbiome function, based on these OUT sequences. All the data aforementioned were analyzed on the platform of Majorbio I-Sanger Cloud Platform ([www.i-sanger.com](http://www.i-sanger.com)).

## Results

### Growth performance and the immune organ indexes

There were no significant differences in the growth performance indexes after multiple comparisons in five treatments. The specific indexes, including average daily feed intake (ADFI), average daily-weight gain (ADG), and feed:gain ratio (F:G), are shown in Table 3. Furthermore, the *t*-test result in Supplementary Figure S1 indicated that, during 0–21 days, the antibiotic supplement showed a significantly higher ADFI value ( $P < 0.05$ ) and an F:G value ( $P < 0.05$ ) than GOD1200. For days 22–42, the F:G showed a significant increase in the basal diet group when compared to GOD600 ( $P < 0.05$ ) or GOD1200 ( $P < 0.05$ ). Additionally, GOD and the antibiotic-supplemented groups have no significant effect ( $P > 0.05$ ) on the immune organ indexes

TABLE 2 Sequences of target and reference genes used for the evaluation of intestinal function.

Gene name	Primers (5' to 3')	
	Forward	Reverse
<i>ZO-1</i>	CTTCAGGTGTTCTCTCTCCTCCTC	CTGTGGTTTCATGGCTGGATC
<i>Occludin</i>	GCAGATGTCCAGCGTTACTAC	CGAAGAAGCAGATGAGGCAGAG
<i>Claudin-1</i>	ACAACATCGTGACGGCCCA	CCCGTCACAGCAACAAACAC
<i>MUC-2</i>	AGGAATGGGCTGCAAGAGAC	GTGACATCAGGGCACACAGA
<i>β-actin</i>	GAGAAATTGTGCGTGACATCA	CCTGAACCTCTCATTGCCA

*ZO-1*, Zona occludens 1; *MUC-2*, Mucin 2.

TABLE 3 Effect of GOD on the growth performance of broilers (mean ± SEM, *n* = 6).

Variable	Ctr	Ant	GOD300	GOD600	GOD1200	SEM	<i>P</i> -value
<b>1–21 d</b>							
ADFI (g/d)	52.83	52.65	51.65	52.95	51.73	0.773	0.501
ADG (g/d)	39.53	39.27	39.65	39.26	40.60	0.252	0.410
F:G (g:g)	1.34	1.35	1.30	1.35	1.27	0.025	0.444
<b>22–42 d</b>							
ADFI (g/d)	128.77	122.76	123.94	121.09	125.98	1.871	0.762
ADG (g/d)	66.06	67.68	65.74	67.38	67.85	0.933	0.944
F:G (g:g)	1.95	1.82	1.89	1.80	1.86	0.022	0.136
<b>1–42 d</b>							
ADFI (g/d)	88.80	87.47	88.25	86.07	89.37	1.121	0.910
ADG (g/d)	52.55	54.59	53.00	51.44	53.48	0.771	0.793
F:G (g:g)	1.69	1.62	1.67	1.68	1.66	0.123	0.432

ADFI, feed intake; ADG, body weight gain; F:G, feed:gain ratio; Ctr, control group; Ant, aureomycin group; GOD300, GOD600, and GOD1200 groups represent different concentrations of GOD (300, 600, and 1,200 U/kg).

(organ weight:body weight) during the experimental periods (Table 4).

## Biochemical, cytokine, and antioxidant parameters in serum

The relevant parameters tested in serum are shown in Table 5. For biochemical parameters, ALP was significantly higher in GOD300 than in Ctr ( $P < 0.05$ ) on day 21. However, no effect was observed for ALT, AST, TP, and urea ( $P > 0.1$ ). For cytokines, the GOD supplementation gave rise to significant differences in TGF- $\beta$  in its moderate and higher dosage groups ( $P < 0.05$ ) on day 21, and the effect was also exerted in the indicator of D-Lac in GOD1200 on day 42 ( $P < 0.05$ ) (Table 6). There were no significant differences in the activity of DAO in both stages. For the antioxidant parameters (Table 7), GOD1200 significantly increased the SOD activity ( $P < 0.05$ ) and showed a trend toward a lower level of MDA content ( $0.05 \leq P < 0.1$ ) compared with Ctr on day 21. Moreover, it was noted that the GSH-Px activity was extremely significant ( $P < 0.01$ ) at the growth anaphase of broiler in GOD1200, and no differences were found among other GOD treatment groups and the two control groups ( $P > 0.05$ ).

## Jejunal secretory immunoglobulin A

The distribution of SIgA in the jejunum and the proportion of positive cell ratio on day 42 are given in Figure 1. The SIgA-positive cells were prominently stained brown compared with the surrounding tissues. Although no significant differences were observed in the basal diet and GOD-supplied groups, the positive cell ratio in aureomycin-supplied group was remarkably decreased among the whole treatments ( $P < 0.05$ ).

## Gene expressions in the jejunum related to intestinal tight junctions

Figure 2A shows that, compared with Ctr, GOD300, and GOD1200 showed a significant increase in the content of *Mucin-2* (*MUC-2*) ( $P < 0.05$ ) and the effect was the same as that of Ant during the first growth stage of broilers (0–21 days). There were no notable differences in the extra three jejunal junction protein genes (*ZO-1*, *Claudin-1*, and *Occludin*) during this period ( $P > 0.05$ ). During the late growth stage (Figure 2B), we found that the relative mRNA expression of *ZO-1* upregulated apparently in GOD600 and GOD1200 compared with Ctr or Ant ( $P < 0.05$ ). However, no other



TABLE 4 Effect of GOD on relative weights of immune organs of broilers (mean ± SEM, n = 6).

Variable	Ctr	Ant	GOD300	GOD600	GOD1200	SEM	P-value
Immune index							
d 21							
Spleen	0.66	0.72	0.67	0.69	0.74	0.021	0.761
Thymus	6.03	5.41	4.97	5.03	5.03	0.231	0.570
Bursa of fabricius	1.60	1.37	1.33	1.44	1.53	0.050	0.481
d 42							
Spleen	0.89	0.77	0.75	0.80	0.86	0.042	0.852
Thymus	3.03	2.82	3.13	3.26	2.92	0.113	0.743
Bursa of fabricius	1.18	1.27	1.18	1.07	1.229	0.042	0.621

Ctr, control group; Ant, aureomycin group; GOD300, GOD600, and GOD1200 groups represent different concentrations of GOD (300, 600, and 1,200 U/kg).

TABLE 5 Effect of GOD on the biochemical parameters of broilers in serum (mean ± SEM, n = 6).

Variable	Ctr	Ant	GOD300	GOD600	GOD1200	SEM	P-value
d 21							
ALT (U/L)	5.00	7.29	6.57	5.00	5.71	0.361	0.194
AST (U/L)	218.00	251.43	252.00	221.29	239.71	5.086	0.112
TP g/dL	2.50	2.43	2.53	2.36	2.40	0.044	0.747
ALP (10 <sup>3</sup> U/L)	13.52 <sup>a</sup>	13.26 <sup>a,b</sup>	8.84 <sup>b</sup>	12.74 <sup>a,b</sup>	11.75 <sup>a,b</sup>	65.042	0.041
UREA mg/dL	3.00	3.29	3.71	3.43	3.57	0.100	0.227
d 42							
ALT (U/L)	<5.00	<0.00	<5.00	<5.00	<5.00	–	–
AST (U/L)	323.00	350.43	378.43	295.57	482.86	21.680	0.131
TP g/dL	2.49	2.66	2.56	2.54	2.74	0.055	0.543
ALP (10 <sup>3</sup> U/L)	6.61	3.29	4.24	4.67	4.31	555.062	0.433
UREA mg/dL	2.14	2.43	2.14	2.00	2.00	0.437	0.347

<sup>a,b</sup>Mean values within a row with no common superscript differ significantly ( $P < 0.05$ ). ALT, alanine aminotransferase; AST, aspartate transaminase; TP, total protein; ALP, alkaline phosphatase; Ctr, control group; Ant, aureomycin group; GOD300, GOD600, and GOD1200 groups represent different concentrations of GOD (300, 600, and 1,200 U/kg).

significant differences were found in the expression of *Claudin-1*, *MUC-2*, and *Occludin*.

Microbiota analysis by 16SrDNA

After filtering, an average of 50,736 reads per sample was obtained. The rarefaction curves are plotted in [Supplementary Figure S2](#) to provide the complete evidence of adequate sequencing depth. As the result showed, every sample reached the plateau indicating an adequate sampling depth. The  $\alpha$ -diversity of intestinal microbiota was analyzed using the indices of Shannon, Simpson, ACE, and Chao 1. The result in [Table 8](#). The  $\beta$ -diversity analysis was performed to compare the overall microbial profiles and obtain the results shown in [Supplementary Figure S3](#) without a notable difference ( $P > 0.05$ ). To assess the role of the GOD in feed, the taxonomic compositions of cecal microbes were compared at phyla and genus levels among the treatments ([Figure 3](#)). At the phylum

level, it could be concluded from the relative abundance maps that Firmicutes, Bacteroidota, and Cyanobacteria are the main phyla in the cecal bacterial community of broilers. Firmicutes constituted nearly 63.32% of the whole sequences followed by ~35% Bacteroidota and ~0.68% Cyanobacteria. When compared to the positive control group, broiler-fed GOD had a higher relative abundance of Firmicutes and a lower relative abundance of Bacteroidetes. At the genus level, the distribution shown in [Figure 3B](#) was summarized to show that 28 dominant genera (*Alistipes*, *g\_norank\_f\_norank\_o\_Clostridia\_UCG-014*, *Lacto bacillus*, *Ruminococcus\_torques\_group*, *Barnesiella*, *norank\_f\_norank\_o\_Clostridia\_vadinBB60\_group*, *Lachnoclostridium*, *unclassified\_f\_Lachnospiraceae*, *Eisenbergiella*, *Faecalibacterium*, *Blautia*, *Bacteroides*, *Christensenellaceae\_R-7\_group*, *norank\_f\_Ruminococcaceae*, *Odoribacter*, *Subdoligranulum*, *Butyrivicoccus*, *norank\_f\_Eubacterium\_coprostanoligenes\_group*, *norank\_f\_norank\_o\_RF39*, *norank\_f\_Barnesiellaceae*, *unclassified\_f\_Oscillospiraceae*, *unclassified\_f\_Ruminococcaceae*,

TABLE 6 Effect of GOD on cytokine parameters and serum markers of broilers in serum (mean  $\pm$  SEM,  $n = 6$ ).

Variable	Ctr	Ant	GOD300	GOD600	GOD1200	SEM	P-value
<b>d 21</b>							
TGF- $\beta$ (ng/L)	321.76 <sup>a</sup>	271.34 <sup>a,b</sup>	197.14 <sup>a,b</sup>	173.56 <sup>b</sup>	154.18 <sup>b</sup>	20.891	0.062
<b>Serum enterotoxin markers</b>							
D-Lac (nmol/mL)	6.56	4.00	6.90	6.05	6.24	0.900	0.872
DAO (U/L)	17.37	18.85	19.61	15.22	14.45	0.841	0.201
<b>d 42</b>							
TGF- $\beta$ (ng/L)	203.76	226.80	203.17	202.88	199.87	13.084	0.971
<b>Serum enterotoxin markers</b>							
D-Lac (nmol/mL)	27.58 <sup>a</sup>	30.64 <sup>a</sup>	28.39 <sup>a</sup>	28.55 <sup>a</sup>	5.94 <sup>b</sup>	3.002	0.031
DAO (U/L)	24.23	25.84	24.06	23.54	18.74	1.046	0.231

<sup>a,b</sup>Means within a row with no common superscripts are significantly different ( $P < 0.05$ ).

TGF- $\beta$ , transforming growth factor- $\beta$ ; D-Lac, D-lactic acid; DAO, diamine oxidase; Ctr, control group; Ant, aureomycin group; GOD300, GOD600, and GOD1200 groups represent different concentrations of GOD (300, 600, and 1,200 U/kg).

TABLE 7 Antioxidant parameters in the serum of broilers (mean  $\pm$  SEM,  $n = 6$ ).

Variable	Ctr	Ant	GOD300	GOD600	GOD1200	SEM	P-value
<b>d 21</b>							
T-AOC (U/L)	1.17	1.21	1.23	1.23	1.26	0.033	0.932
SOD (U/ml)	108.57 <sup>a</sup>	113.89 <sup>a,b</sup>	110.83 <sup>a,b</sup>	105.30 <sup>a</sup>	119.92 <sup>b</sup>	1.612	0.041
GSH-Px (U/ml)	486.39	505.97	527.71	520.53	565.58	14.471	0.573
8-OH-dG (ng/mL)	25.22	29.21	25.17	27.41	25.99	1.056	0.721
MDA (nmol/ml)	3.17 <sup>a</sup>	2.31 <sup>b</sup>	2.83 <sup>a,b</sup>	2.79 <sup>a,b</sup>	2.61 <sup>b</sup>	0.100	0.090
<b>d 42</b>							
T-AOC (U/L)	0.67	0.72	0.76	0.75	0.77	0.031	0.795
SOD (U/ml)	123.19	127.45	123.42	124.13	128.12	1.072	0.467
GSH-Px (U/ml)	1,516.27 <sup>A</sup>	1,353.97 <sup>A</sup>	1,742.03 <sup>A</sup>	1,693.47 <sup>A</sup>	2,231.39 <sup>B</sup>	87.153	<0.01
8-OH-dG (ng/mL)	55.88	61.28	54.13	53.68	55.58	1.138	0.221
MDA (nmol/ml)	1.63	1.55	1.63	1.62	1.62	0.036	0.873

<sup>a,b</sup>Means within a row with no common superscripts are significantly different ( $P < 0.05$ ) or have a tendency toward significance ( $0.05 < P < 0.1$ ).

<sup>A,B</sup>Means within a row with no common superscripts are extremely significantly different ( $P < 0.01$ ).

T-AOC, total antioxidative capacity; SOD, superoxide dismutase; GSH-Px, glutathione peroxidase; MDA, malondialdehyde; 8-OH-dG, 8-hydroxy-2'-deoxyguanosine; Ctr, control group; Ant, aureomycin group; GOD300, GOD600, and GOD1200 groups represent different concentrations of GOD (300, 600, and 1,200 U/kg).

*norank\_f\_Oscillospiraceae*, *Colidextribacter*, *Phascolarctobacterium*, UCG-005, NK4A214\_group, and *norank\_f\_norank\_o\_Gastranaerophilales*.) changed among these groups after various supplementations were added to the basal diet. Specifically, after performing the Kruskal–Wallis H test, five significantly differential bacteria ( $P < 0.05$ ) were noticed at the genus level in the multiple-group comparisons test (Figure 4A). They were *Colidextribacter*, *Oscillibacter*, *Shuttleworthia*, *Flavonifractor*, and *Oscillospira*. Subsequently, the Wilcoxon rank-sum tests were employed for each of the five bacteria to implement a pairwise comparison, and the results can be seen in Figures 4B–F. Compared with the basal diet group, GOD600 and GOD1200 showed a significant increase in the relative abundance of *Oscillospira* ( $P < 0.05$ ). The abundance of

*Colidextribacter* was enriched significantly in GOD600 as well ( $P < 0.01$ ). More and varying degrees of effects were noticed when GOD-supplied groups were compared with Ant. All three GOD-supplemented diets caused a significant increase in the relative abundance ( $P < 0.05$ ) of *Oscillibacter*. GOD600 produced significant ( $P < 0.05$ ) and even extreme differences ( $P < 0.01$ ) in the genera of *Flavonifractor* and *Colidextribacter*, respectively. A noticeable increase in *Colidextribacter* also took place in GOD1200 in broilers' cecal microbiota ( $P < 0.05$ ). However, in contrast to the aforementioned conclusions, we noticed that *Shuttleworthia* exhibited different trends in the other four genera. The control group (negative and positive types) brought about a significant increase ( $P < 0.05$ ) in this genus regardless of whether it was compared with GOD600 or GOD1200. There was an extreme

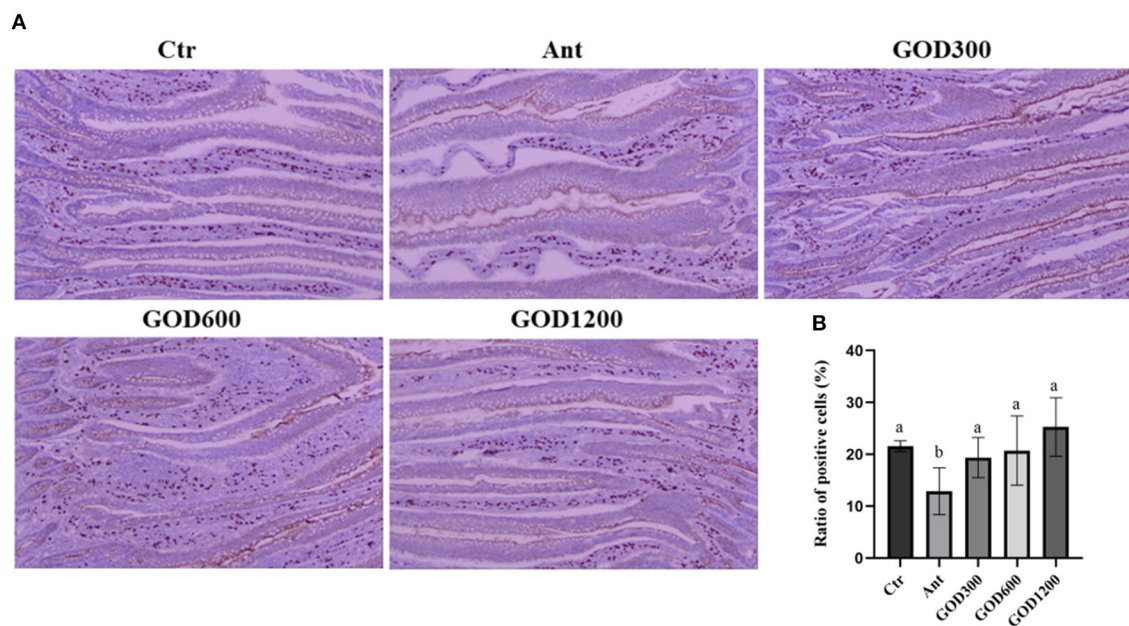


FIGURE 1

The effect of GOD-supplemented dietary on SIgA distribution in the jejunum of broilers on day 42 was examined by immunohistochemistry. SIgA-positive cells were stained prominently brown. The pictures were observed at 100× magnification ( $n = 6$ ) (A). The ratio of positive cells was calculated and analyzed among the five treatment groups (B) ( $P < 0.05$ ). Ctr, negative control fed with the basal diets; Ant, positive control fed with the basal diets added 50 mg/kg aureomycin; GOD300, GOD600, and GOD1200, the basal diets supplied with 300, 600, and 1,200 U/kg glucose oxidase, respectively. <sup>a,b</sup>Means within a row with no common superscripts are significantly different ( $P < 0.05$ ). Ctr, negative control group fed with the basal diets; Ant, positive control group fed with the basal diets added 50 mg/kg aureomycin.

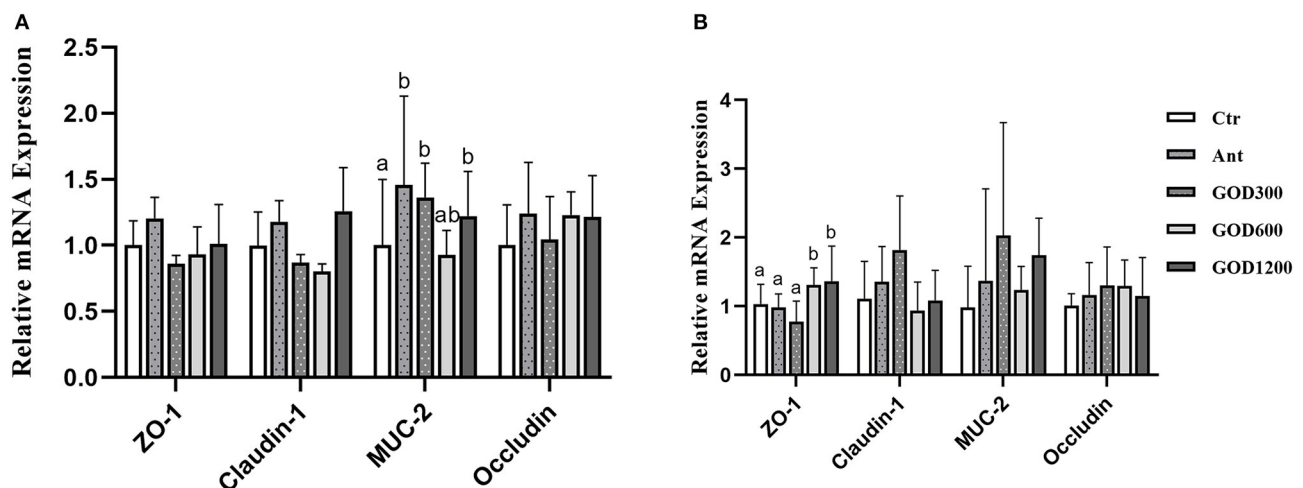


FIGURE 2

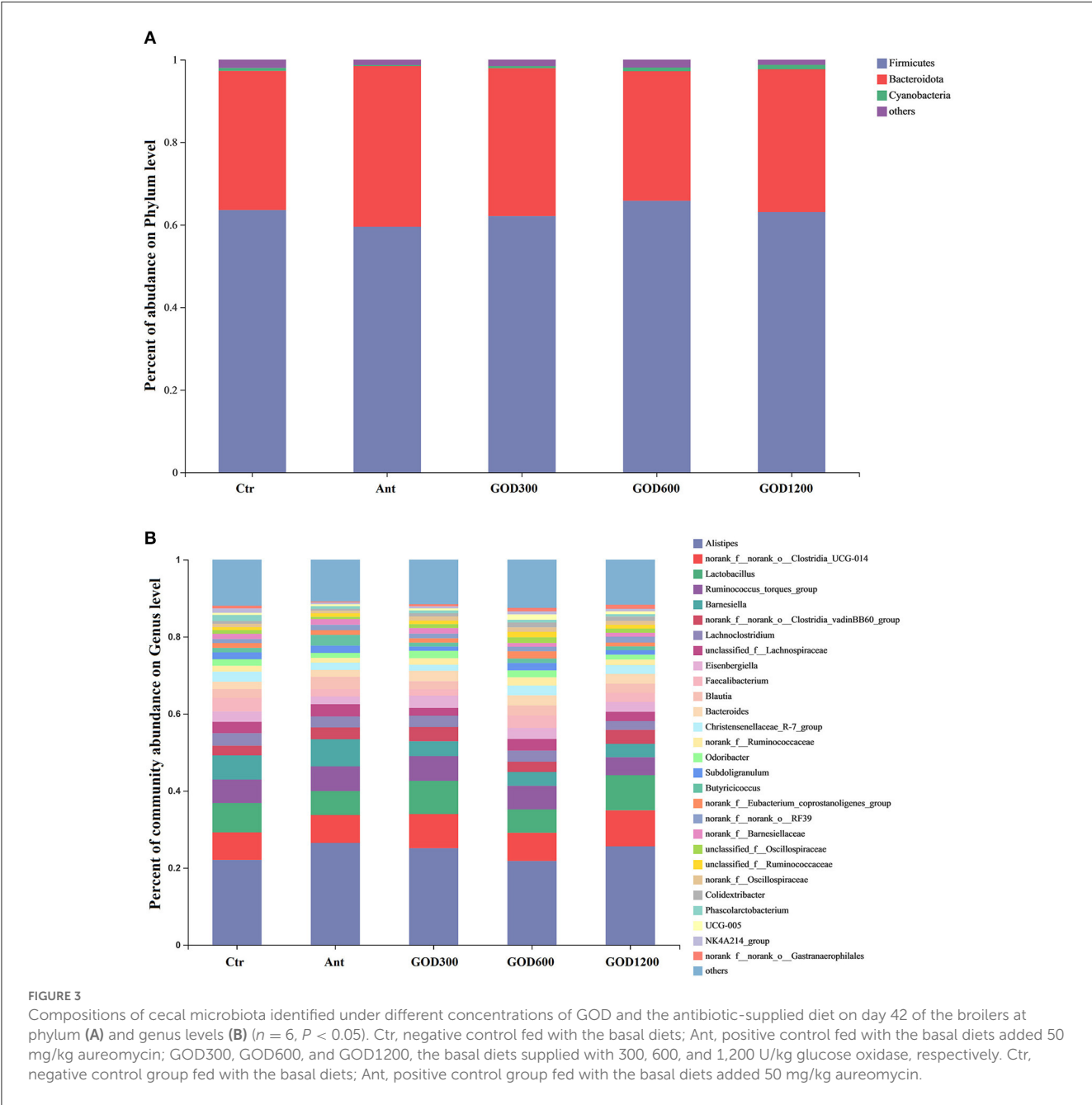
The effect of GOD-supplemented dietary on the relative mRNA expression of jejunal junction protein genes and the mucin gene of broilers during both days 0–21 (A) and 22–42 (B) growth phases. <sup>a,b</sup>Means within a row with no common superscripts are significantly different ( $n = 6$ ,  $P < 0.05$ ). Ctr, negative control fed with the basal diets; Ant, positive control fed with the basal diets added 50 mg/kg aureomycin; GOD300, GOD600, and GOD1200, the basal diets supplied with 300, 600, and 1,200 U/kg glucose oxidase, respectively. <sup>a,b</sup>Means within a row with no common superscripts are significantly different ( $P < 0.05$ ). Ctr, negative control group fed with the basal diets; Ant, positive control group fed with the basal diets added 50 mg/kg aureomycin.

increase in Ant when compared with GOD600 ( $P < 0.01$ ). Moreover, GOD300, which exerted a few impacts on the other four genera, significantly raised the content of this genus compared with GOD600 ( $P < 0.05$ ). Additionally, except for the comparisons of

control groups and the additive-supplied groups, we also noticed that the abundance of *Flavonifractor* and *Oscillibacter* genera in the basal diet group was significantly higher than that in the antibiotic control group.

TABLE 8 Effects of GOD-supplemented feed on the cecal  $\alpha$ -diversity of broilers.

Variable	Ctr	Ant	GOD300	GOD600	GOD1200	SEM	P-value
Shannon index	4.12	3.95	4.06	4.22	4.15	0.051	0.645
Simpson index	0.06	0.07	0.06	0.05	0.05	0.012	0.677
ACE index	479.84	480.83	488.62	485.16	491.68	5.485	0.953
Chao 1 index	487.36	484.55	497.91	490.66	498.19	5.772	0.899

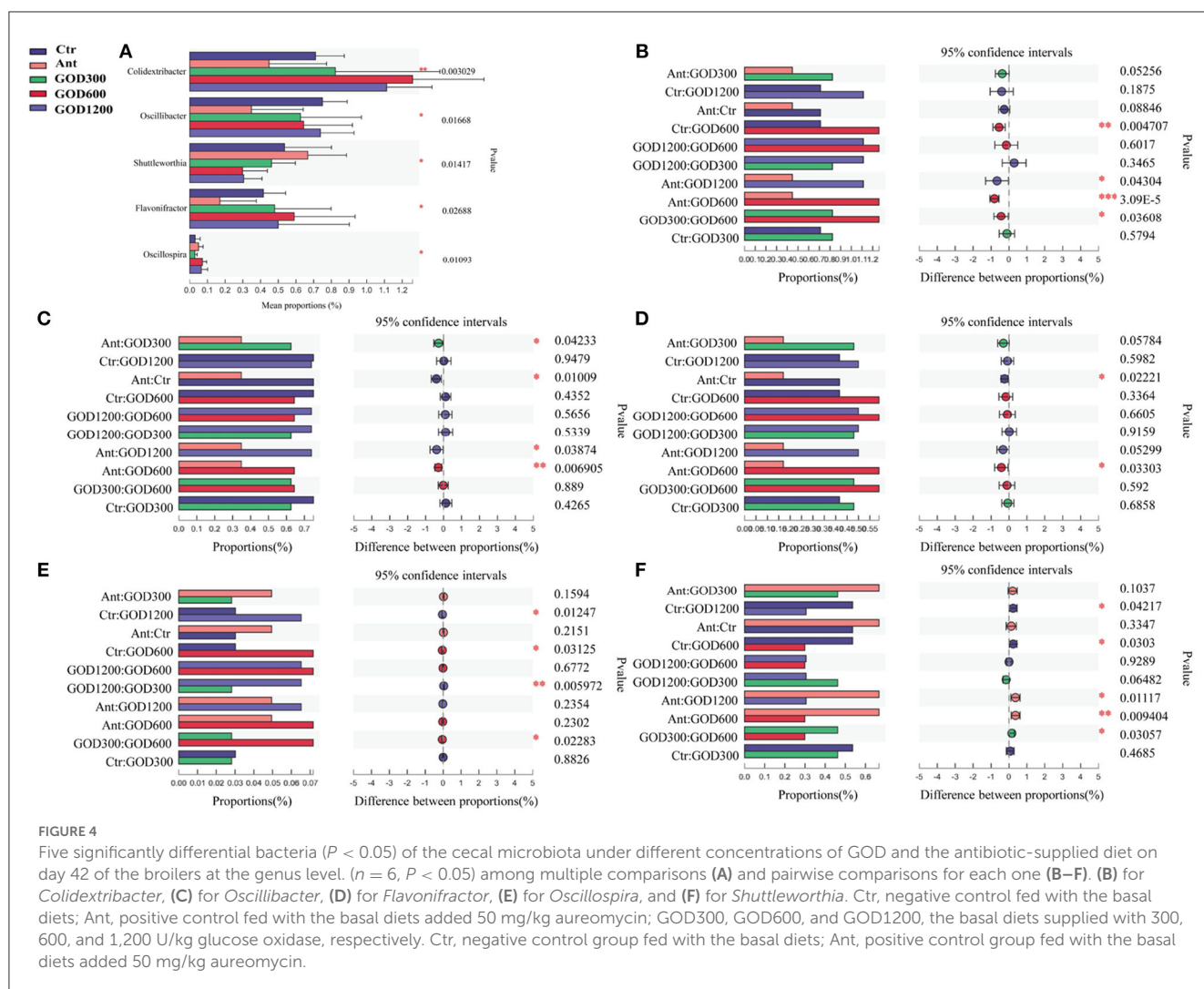


## Functional potential of cecal microbiota composition

All alterations in the presumptive function were evaluated using PICRUSt2 in the cecal microbiota at 42 days of the broilers.

There were 43 pathways predicted at level 2 of the KEGG pathways. However, no significant differences were found among them, and specific information was not shown here. Furthermore, it was found that some pathways were differentially enriched at level 3 among groups, and 289 KEGG categories were identified





in total. We conducted six pairwise comparisons between each of the control groups and each concentration of the GOD-supplied groups, that is, Ctr vs. GOD300, Ctr vs. GOD600, Ctr vs. GOD1200, and Ant vs. GOD300, Ant vs. GOD600, Ant vs. GOD1200, respectively. The results revealed in Figure 5 illustrated that, compared with the basal diet (i.e., negative control group), the GOD treatments significantly influenced the abundance of six functional pathways. Meanwhile, the abundance shifted remarkably in seven functional pathways when this comparison was made between the antibiotic-supplied group (i.e., positive control group) and the GOD treatments.

Specifically, the negative control group showed a significantly larger abundance of “Riboflavin metabolism” and “Proximal tubule bicarbonate reclamation” pathways against GOD600 ( $P < 0.05$ ). As for the “ABC transporters” and “Insect hormone biosynthesis” pathways, GOD1200 exerted a significant influence on making them decrease ( $P < 0.05$ ). In addition, the pathways of “Proximal tubule bicarbonate reclamation,” “Protein digestion and absorption,” and “Protein processing in endoplasmic reticulum” were all differentially enriched in GOD treatment groups ( $P < 0.05$ ). After the comparison between positive control and GOD groups, we observed that the former had a significantly

lower abundance of several functional pathways ( $P < 0.05$ ), including “Carbon fixation pathways in prokaryotes,” “Glycine, serine and threonine metabolism,” “Lysine degradation,” “Benzoate degradation,” and “Protein processing in endoplasmic reticulum.” Whereas, a significantly lower abundance of “Secondary bile acid biosynthesis” and “Riboflavin metabolism” existed in GOD ( $P < 0.05$ ). The details about how different concentrations of GOD interacted with both control groups are shown in Figure 5.

## Discussion

### Growth performance, immune organ indexes, and serum test results

Based on the aforementioned results, the antibiotic group showcased a relatively higher feed intake and a low weight gain against GOD1200 during the stage of starting phase (1–21 days). A few research types showed this tendency of the antibiotic (Khan et al., 2012; Elagib et al., 2013). However, it implied that the GOD1200 supplement could relatively improve the feed

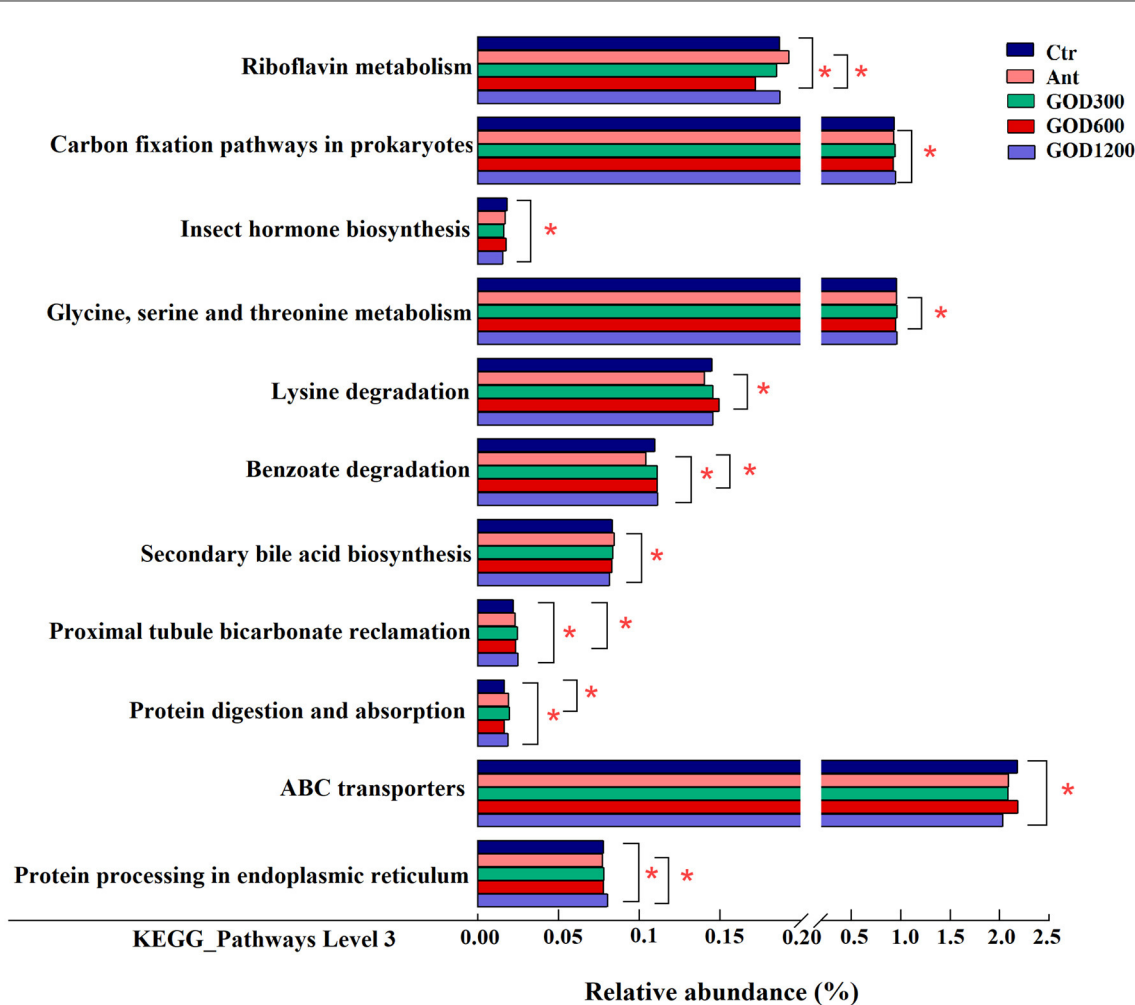


FIGURE 5

The mean proportion in predicted pathways grouped into level 3 functional categories of the cecal microbiota in various treatments on day 42 ( $n = 6$ ,  $P < 0.05$ ). Ctr, negative control fed with the basal diets; Ant, positive control fed with the basal diets added 50 mg/kg aureomycin; GOD300, GOD600, and GOD1200, the basal diets supplied with 300, 600, and 1,200 U/kg glucose oxidase, respectively. \*Means there are significant differences in the enrichment of this pathway between the two groups. Ctr, negative control group fed with the basal diets; Ant, positive control group fed with the basal diets added 50 mg/kg aureomycin.

conversion efficiency. For the same index, GOD600 and GOD1200 exerted a better efficiency than the basal diet group during the growing phase (22–42 days). These could serve as evidence for GOD in the role of a growth promoter. The F:G ratio were significantly affected by the dietary GOD supplied, especially in GOD1200, indicating that the dietary GOD-supplied could help cut costs and increase farming efficiency. Nevertheless, no other differences in growth indexes were observed, and we inferred that there were specific conditions that caused the disparity. A better feeding environment, various dosages of additives as well as the broiler's breed could result in this disparity (Hashemipour et al., 2013; Ahiwe et al., 2021). The unchanged relative weights of immune organs implied that additives or antibiotics may act to cause no significant shift in the immune organs under certain circumstances. It can be further conjectured that the three levels of GOD have no adverse effect on the development of the immune organ of the white-feathered broilers during their growth status.

Except for the relative weights of organs, some serum tests, such as biochemical, cytokines, and antioxidant indexes, could reflect the condition of the immune cells and the health level of the host medically as well. Several indexes changed significantly in the present study. A significant reduction in ALP, whose activity in blood was considered an essential indicator for assessing the adequacy of phosphorus (Li et al., 2020), was found in GOD300 on day 21 compared with the control group. Some experiments showed that the lower activity of ALP stood for a healthy broiler status (Skalicka et al., 2000), whereas we cannot draw a conclusion from this index alone. The immunity indicator, TGF- $\beta$  cytokine, significantly decreased when GOD (GOD600 or GOD1200) was compared with the basal diet group. Cytokines are mainly synthesized and secreted from various immune cells in the form of polypeptides or glycoproteins. Their existence can mediate the interaction between cells that perform various biological functions (Haddad, 2002). As a member of them, TGF- $\beta$  is regarded as a considerable enforcer of immune homeostasis

and tolerance, especially for regulating inflammatory processes (Batlle and Massagué, 2019; Fasina and Lillehoj, 2019) with a dual effect (Pickup et al., 2017; David and Massagué, 2018). The broiler growth stage of 1–21 days is typically associated with an immature immune system (Song et al., 2021). Based on the significant TGF- $\beta$  difference on day 21, we inferred that GOD- and Ant-supplied diets gave broilers a better ability toward stress stimulation at a specifically tested concentration. It could be further verified by the remarkable MDA increase and the SOD decrease in the basal diet group at 21 days, which was consistent with the former reports (Wang et al., 2018).

With the characteristic of high lipid content, broilers are easily induced to produce ROS (Bai et al., 2017). As for the results of this study, a higher content of MDA in Ctr represented attenuated antioxidant protection when the ROS increased (Yang et al., 2008). Correspondingly, SOD and GSH-Px, the two enzymes, were used to remove excess ROS (Ko et al., 2004) and showed a significant positive advantage in GOD1200. Meanwhile, the high GOD supplement exerted a similar and even better effect in contrast to the aureomycin-added diet on days 21 and 42, respectively. The changes in antioxidant parameters illustrated that the addition of GOD could reduce lipid peroxidation for broilers to a certain extent. In animals, the endogenous antioxidant defense system and immune system rely on external sources (Pamplona and Costantini, 2011). Both systems can facilitate the development of a robust antioxidant capacity. Herein, our results initially identified that the GOD could improve broilers' immune and antioxidant capacity, thereby further improving their health status.

## Immunohistochemical result and the gene expression of tight junctions in the jejunum

The gut is the most significant immune organ undertaking both the tolerance to dietary antigens and the immune defense for broilers. The organized gut-associated lymphoid tissues (GALT) in birds generate efficient responses with secretory IgA (Fagarasan et al., 2009), known as SIgA, to maintain mucosal homeostasis (Lammers et al., 2010; Curtis, 2017). For this experiment, the SIgA content showed a conspicuous decrease in the aureomycin-added group compared with all other groups. The reduction in SIgA could influence the pro-inflammatory downregulation ability of the host (Boullier et al., 2009), indicating that, after 42 days of feeding, the antibiotic did not give an advantage to the immunologic barrier. The results proved that GOD might be an advantageous alternative to antibiotics. Alongside the immunologic barrier, the mechanical barrier is the other primary component of intestinal mucosal immunity (Reynolds et al., 1996). Some studies reported that the intestinal mechanical barrier of chickens could be affected by the factor of dietary components' alteration (Fasina et al., 2006; Ma et al., 2021). In this study, the high-level GOD supplement increased the relative abundance of *MUC-2* and *ZO-1*. These two are the major components of adherence junctions (AJs) and tight junctions (TJs), respectively, which act as the crucial parts of the physical gut barrier (Ballard et al., 1995; Anderson et al., 2012). It was reported that *MUC-2* exerted a major role in protecting

the intestinal epithelium in preventing infection and maintaining the integrity of the intestinal mucosal barrier (McGuckin et al., 2011). As a member of the tight junctions, the *ZO-1* is negatively correlated with intestinal permeability (Alhotan et al., 2021). The results of this study indicated that the additive supplied could enhance the intestinal physical barrier of broilers. This inference can also be supported by the D-Lac's change in serum in this study, as the D-Lac is used to detect intestinal permeability and is an indirect indicator of the intestinal barrier (Fukudome et al., 2014; Wang J. et al., 2022). Taken together, GOD at a certain concentration can facilitate the integrity of the intestinal epithelium and enhance the mucosal immune capacity of broilers, thereby promoting their healthier living conditions.

## Intestinal microbiota comparison in the cecal contents and the functional prediction result

As the chief functional part in the distal intestine, the cecum has received increasing attention for its importance in chicken metabolism since it contains a vast majority of gut bacteria and has a significant fermentation ability with a lower passage rate (Pourabedin and Zhao, 2015). The cecal microbiota of chickens can influence the host health and productivity by regulating nutrient absorption and metabolism, immune response, and pathogen invasion (Stanley et al., 2014; Huang et al., 2018). There are a few reports on the main site of GOD's action in the intestinal segments. To the best of our knowledge, these reports include its biochemical features of oxygen consumption, gluconic acid production, and negative effects on certain pathogenic bacteria in broilers' gut (Liang et al., 2022). Therefore, to better understand and complement the current mechanism of GOD supplement in broilers and to evaluate its application effects at different concentrations, shifts in the cecal microbiota among five groups were observed in this study.

First, we noticed that the results of the data analysis for  $\alpha$ -diversity were not statistically significant after a 42-day feeding. These results are similar to the intestinal diversity results reported after certain additives were added to the feed (Ma et al., 2021; Liu C. et al., 2022). However, it is possible that rare numbers found in a small population could make a significant difference for the host (Shang et al., 2018). Therefore, the sequences were further analyzed at phylum and genus levels to identify the cecal differential bacteria. Similar to previous studies, Firmicutes, Bacteroidota, and Cyanobacteria are the dominant phyla in the broiler cecal bacterial community (Mohd Shaufi et al., 2015; Dai et al., 2021; Segura-Wang et al., 2021).

At the genus level, *Colidextribacter*, *Oscillibacter*, *Flavonifractor*, *Oscillospira*, and *Shuttleworthia* emerged after multiple comparisons and were identified as biomarkers to distinguish the groups for whether supplied with GOD. The former four genera showed a significant increase in GOD600 and GOD1200 compared with control groups. The first one, *Colidextribacter*, has been reported to promote the production of short-chain fatty acids (SCFAs) (Oakley et al., 2014; Wang Q. et al., 2022) and inosine (Lee et al., 2020; Guo et al., 2021). Studies on chickens

illustrated that SCFAs can reduce inflammation in the intestines (Wu et al., 2016). For example, butyrate can repress cell invasion in pathogenicity island caused by *Salmonella*, a pathogen of concern to the global poultry industry (Gantois et al., 2006), and the microbiota-derived butyrate could also effectively ameliorate certain immune system diseases (He et al., 2020). Correspondingly, substantial evidence highlighted that inosine has broad anti-inflammatory and immunomodulatory properties (Haskó et al., 2000, 2004; da Rocha Lapa et al., 2012). The second noticed genus, *Oscillibacter*, whose clade was regarded as a potential n-butyrate producer (Gophna et al., 2017; Contreras-Dávila et al., 2021), was placed in the family *Ruminococcaceae*. In recent studies, this family showed a high correlation with the increase in bodyweight and tight junction protein expression for birds (Dai et al., 2021; Farkas et al., 2022). *Oscillibacter* is considered a potentially beneficial microbe as it plays a crucial role in sugar fermentation (Ze et al., 2012) and starch degradation (Kim et al., 2014) and is positively associated with feed efficiency for broilers (Liu J. et al., 2021). One of its species, *Oscillibacter ruminantium*, was found to be negatively correlated to *Salmonella* (Pedroso et al., 2021) after the investigation of chickens' cecal content. Moreover, *Oscillibacter* was also demonstrated to reduce blood triglyceride concentration and the negative reaction to stress for research on humans (Jiang et al., 2015; Tong et al., 2020; Liu X. M. et al., 2022). *Flavonifractor* is also a butyrate-producing producer (Meng et al., 2019). It was positively correlated with ADG and could improve the growth performance of broilers (Zhang et al., 2021). Some of its clades were the key to catalyzing and initiating flavonoid metabolism. Currently, many studies on the flavonoid showed its marked effects on improving growth performance and the antioxidant capacity of broilers (Kamboh and Zhu, 2013). In light of the predominance of GOD in this study and the positive correlation between this genus and GOD in the cecum, we speculated that the combination of flavonoid and glucose oxidase might exert better anti-inflammatory, bacteriostatic, and immunity enhancement effects on animals as a novel feed additive (Wang et al., 2020; Yang G. et al., 2021). Along with *Oscillibacter*, the *Oscillospira* genus belongs to the family of *Ruminococcaceae* and is also regarded as a short-chain fatty acid butyrate producer. Accordingly, it could downregulate the expression of genes encoding pro-inflammatory cytokines and prevent inflammation in the host (Cushing et al., 2015; Gophna et al., 2017). *Ruminococcaceae* have been reported to be highly positively correlated with the gene expression of *ZO-1* (Dai et al., 2021). This can be confirmed in this study as the *Oscillibacter* and *Oscillospira* genera in GOD (GOD600 and GOD1200) were significantly higher than those in control groups, and the trend in *ZO-1* expression was the same between GOD and control groups. Moreover, based on human research, the significant *Oscillospira* decrease was associated with obesity-related chronic inflammatory and metabolic diseases (Yang J. et al., 2021). Hence, it may become a next-generation probiotic candidate for symptom relief in broilers. The genus of *Shuttleworthia* showed a noticeable increase in control groups, especially for GOD at the concentration of 600 or 1,200 U/kg. Compared with the former four genera, the tendency was the opposite. Combined with other parameters tested in the present study, although there were some benefits found in this genus for animals, we conjectured that its negative effects

played a leading role in the control groups (Liu Y. et al., 2021). These negative effects might be attenuated with the addition of glucose oxidase. The genera above all belong to the anaerobic genus, which could confirm that the GOD additive is conducive to creating a better anaerobic condition for the proliferation of beneficial bacteria into the gut. In addition, gluconic acid was rarely absorbed in the small intestine and primarily fermented by specific bacteria to produce SCFAs in the cecum (Biagi et al., 2006; Huyghebaert et al., 2011), which can be further verified. Furthermore, analysis of characteristic genera also provided a profound interpretation of the phenomenon of a higher F:G index in GOD.

According to the predicted functional profiles analyzed by PICRUSt, the microorganisms of broilers' cecum were mainly enriched in functions of metabolism, organismal systems, environmental information processing, and genetic information processing, of which the pathways associated with metabolism occupied the majority. Clearer differences were observed in level 3 KEGG pathways.

The metabolic pathways, such as riboflavin metabolism, insect hormone biosynthesis, and secondary bile acid biosynthesis, displayed varying degrees of benefits for broilers. The riboflavin metabolism was reported to be related to mitochondria-mediated apoptosis, and the flavoprotein participating in this metabolism may contribute to superoxide production along with mitochondrial energy metabolism (Balasubramaniam and Yapliito-Lee, 2020; Liao et al., 2021). It implied that this metabolism might play a part in oxidative stress. In our study, GOD supplementation of 600 U/kg significantly decreased this metabolic pathway in both control groups, indicating that the broilers were found to thrive in better living conditions after the GOD supply. The enrichment in the basal diet group of "insect hormone biosynthesis" may demonstrate that GOD1200 played a role in parasite removal, which contributed to a better intestinal condition and immune capacity for broilers. Moreover, the secondary bile acid biosynthesis enriched in Ant could provide a reasonable explanation for the phenomenon that the kind of biosynthesis always occurs in specific microbiota after antibiotic therapy to fight against pathogenic bacteria (Buffie et al., 2015; Koenigsknecht et al., 2015), similar to *Clostridium difficile* (Rupnik et al., 2009; Buffie et al., 2012). Notably, there were more differences in metabolic function pathways when comparing Ant and GOD. Among them, the amino acid, the energy, and the xenobiotic biodegradation and metabolism pathways were more abundant in the cecal flora in the medium and high concentration GOD. Combined with other indexes of the advantages displayed in this study, it was speculated that the aforementioned pathways mainly took effect in promoting nutrient absorption, digestion, and resistance to external disturbances. This could also be supported by significant enrichment of "protein digestion and absorption" in GOD compared with the basal diet group.

Meanwhile, the pathway of "proximal tubule bicarbonate reclamation" was reported to play an important role in maintaining the acid-base balance in host organisms (Guo et al., 2014). Since the acid-base balance can be easily disturbed by internal and external factors, such as diet, environmental conditions, and metabolism (Anrewaju et al., 2007), we inferred that the enrichment of certain genes in response to GOD (GOD600 and GOD1200) treatment may provide broilers with increased resistance to various stresses.



This is supported by our findings from the antioxidant analysis in this study.

Furthermore, two pathways involved in information processing drew our attention: “protein processing in endoplasmic reticulum” and “ABC transporters.” Previous research showed that the pathway of “protein processing in endoplasmic reticulum” can have different effects on chickens depending on the conditions they are exposed to. For example, the pathway might be enriched and participate in the apoptotic process in response to toxic substances (Sun et al., 2021) or environmental changes (Srikanth et al., 2019), however, it can also be downregulated in response to the infection by parasites (Li et al., 2019). A complicated process must exist in a broiler’s body in response to various conditions. The results of our study suggest that this pathway may have a positive effect on broilers treated with GOD1200, even though further research is needed for validation. Similarly, the “ABC transporters” accounting for a high abundance in the negative control group have been shown to play a role in both multidrug resistance and nutrition uptake (Rice et al., 2014; Hofmann et al., 2019). Based on the results aforementioned, we inferred that the 1,200 U/kg GOD-supplied group may help to reduce the microbial resistance in contrast to the control group.

Overall, evidence for all the pathways illustrated that specific GOD supplementations may have a beneficial effect on the health of birds, particularly in GOD1200, whereas the antibiotic additive may not. Even though the predictive tool of PICRUSt is well-used, it cannot confirm the functional capabilities of the metagenome with absolute certainty. Herein, further research is needed to validate our findings.

## Conclusion

In conclusion, our research showed that a diet supplemented with GOD resulted in a higher feed conversion efficiency and enhanced the internal body environment of broilers, and the concentration of 1,200 U/kg could be the recommended dosage based on the overall results. Unlike AGPs, which can disrupt the integrity of small intestinal epithelium and microbiota, GOD provides a non-pharmacological manner for strengthening the immunologic barrier and maintaining a healthy intestinal microecology. These findings deepen our understanding of the potential benefits of GOD as a feed additive and highlight its potential as a safe and effective substitute for AGPs as a growth promoter in poultry production.

## Data availability statement

The datasets presented in this study can be found in online repositories. The names of the repository/repositories

and accession number(s) can be found in the article/[Supplementary material](#).

## Ethics statement

The animal study was reviewed and approved by Animal Care and Use Committee of the Feed Research Institute of the Chinese Academy of Agricultural Science.

## Author contributions

WZ, RW, and ZX conceived and designed the experiments. WZ, YH, and NC performed the animal experiments. WZ analyzed the data and wrote the manuscript. XS supervised and provided continuous guidance for the experiments. All authors discussed the results and reviewed the manuscript. All authors contributed to the article and approved the submitted version.

## Funding

This study received funding from the National Natural Science Foundation of China 587 (Grant No. 31872394) and the Innovation Program of the Chinese Academy of Agricultural Sciences 588 (Feed Quality and Safety).

## Conflict of interest

The authors declare that the research was conducted in the absence of any commercial or financial relationships that could be construed as a potential conflict of interest.

## Publisher’s note

All claims expressed in this article are solely those of the authors and do not necessarily represent those of their affiliated organizations, or those of the publisher, the editors and the reviewers. Any product that may be evaluated in this article, or claim that may be made by its manufacturer, is not guaranteed or endorsed by the publisher.

## Supplementary material

The Supplementary Material for this article can be found online at: <https://www.frontiersin.org/articles/10.3389/fmicb.2023.1100465/full#supplementary-material>

## References

- Adil, S., Banday, T., Bhat, G. A., Mir, M. S., and Rehman, M. (2010). Effect of dietary supplementation of organic acids on performance, intestinal histomorphology, and serum biochemistry of broiler chicken. *Vet. Med. Int.* 2010, 479485–479485. doi: 10.4061/2010/479485
- Ahiwe, E. U., Dos Santos, T. T. T., Graham, H., and Iji, P. A. (2021). Can probiotic or prebiotic yeast (*Saccharomyces cerevisiae*) serve as alternatives to in-feed antibiotics for healthy or disease-challenged broiler chickens?: a review. *J. Appl. Poult. Res.* 30:100164. doi: 10.1016/j.japr.2021.100164

- Alhotan, R. A., Al Sulaiman, A. R., Alharthi, A. S., and Abudabos, A. M. (2021). Protective influence of betaine on intestinal health by regulating inflammation and improving barrier function in broilers under heat stress. *Poult. Sci.* 100:101337. doi: 10.1016/j.psj.2021.101337
- Anderson, R., Dalziel, J., Gopal, P., Bassett, S., Ellis, A., and Roy, N. J. C. (2012). *The Role of Intestinal Barrier Function in Early Life in the Development of Colitis*. Rijeka: InTech, 1–30.
- Annewaju, H. A., Thaxton, J. P., Dozier, W. A., and Branton, S. L. (2007). Electrolyte diets, stress, and acid-base balance in broiler chickens. *Poult. Sci.* 86, 1363–1371. doi: 10.1093/ps/86.7.1363
- Askelson, T. E., Flores, C. A., Dunn-Horrocks, S. L., Dersjant-Li, Y., Gibbs, K., Awati, A., et al. (2018). Effects of direct-fed microorganisms and enzyme blend co-administration on intestinal bacteria in broilers fed diets with or without antibiotics. *Poult. Sci.* 97, 54–63. doi: 10.3382/ps/pex270
- Awad, W. A., Hess, C., and Hess, M. (2017). Enteric pathogens and their toxin-induced disruption of the intestinal barrier through alteration of tight junctions in chickens. *Toxins* 9:60. doi: 10.3390/toxins9020060
- Bai, K., Huang, Q., Zhang, J., He, J., Zhang, L., and Wang, T. (2017). Supplemental effects of probiotic *Bacillus subtilis* fmbj on growth performance, antioxidant capacity, and meat quality of broiler chickens. *Poult. Sci.* 96, 74–82. doi: 10.3382/ps/pew246
- Balasubramaniam, S., and Yapito-Lee, J. (2020). Riboflavin metabolism: role in mitochondrial function. *J. Genet. Genom.* 4, 285–306. doi: 10.20517/jtgg.2020.34
- Ballard, S. T., Hunter, J. H., and Taylor, A. E. (1995). Regulation of tight-junction permeability during nutrient absorption across the intestinal epithelium. *Annu. Rev. Nutr.* 15, 35–55. doi: 10.1146/annurev.nu.15.070195.000343
- Bankar, S. B., Bule, M. V., Singhal, R. S., and Ananthanarayan, L. (2009). Glucose oxidase -- An overview. *Biotechnol. Adv.* 27, 489–501.
- Battle, E., and Massagué, J. (2019). Transforming growth factor- $\beta$  signaling in immunity and cancer. *Immunity* 50, 924–940. doi: 10.1016/j.immuni.2019.03.024
- Belambri, S. A., Rolas, L., Raad, H., Hurtado-Nedelec, M., Dang, P. M. C., and El-Benna, J. (2018). NADPH oxidase activation in neutrophils: role of the phosphorylation of its subunits. *Eur. J. Clin. Invest.* 48, e12951. doi: 10.1111/eci.12951
- Biagi, G., Piva, A., Moschini, M., Vezzali, E., and Roth, F. X. (2006). Effect of gluconic acid on piglet growth performance, intestinal microflora, and intestinal wall morphology. *J. Anim. Sci.* 84, 370–378. doi: 10.2527/2006.842370x
- Borda-Molina, D., Seifert, J., and Camarinha-Silva, A. (2018). Current perspectives of the chicken gastrointestinal tract and its microbiome. *Comput. Struct. Biotechnol.* 16, 131–139. doi: 10.1016/j.csbj.2018.03.002
- Boullier, S., Tanguy, M., Kadaoui, K. A., Caubet, C., Sansonetti, P., Corthésy, B., et al. (2009). Secretory IgA-mediated neutralization of *Shigella flexneri* prevents intestinal tissue destruction by down-regulating inflammatory circuits. *J. Immunol.* 183, 5879–5885. doi: 10.4049/jimmunol.0901838
- Brenes, A., and Roura, E. (2010). Essential oils in poultry nutrition: main effects and modes of action. *Anim. Feed Sci. Tech.* 158, 1–14. doi: 10.1016/j.anifeeds.2010.03.007
- Buffie, C. G., Bucci, V., Stein, R. R., McKenney, P. T., Ling, L., Goubourne, A., et al. (2015). Precision microbiome reconstitution restores bile acid mediated resistance to *Clostridium difficile*. *Nature* 517, U205–U207. doi: 10.1038/nature13828
- Buffie, C. G., Jarchum, I., Equinda, M., Lipuma, L., Goubourne, A., Viale, A., et al. (2012). Profound alterations of intestinal microbiota following a single dose of clindamycin results in sustained susceptibility to *Clostridium difficile*-induced colitis. *Infect. Immun.* 80, 62–73. doi: 10.1128/IAI.05496-11
- Castanon, J. I. R. (2007). History of the use of antibiotic as growth promoters in European poultry feeds. *Poult. Sci.* 86, 2466–2471. doi: 10.3382/ps.2007-00249
- Contreras-Dávila, C. A., Esveld, J., Buisman, C. J., and Strik, D. P. (2021). nZVI impacts substrate conversion and microbiome composition in chain elongation from D- and L-lactate substrates. *Front. Bioeng. Biotechnol.* 9, 508. doi: 10.3389/fbioe.2021.666582
- Curtis, J. L. (2017). A hairline crack in the levee: focal secretory IgA deficiency as a first step toward emphysema. *Am. J. Resp. Crit. Care* 195, 970–973. doi: 10.1164/rccm.201612-2509ED
- Cushing, K., Alvarado, D. M., and Ciorba, M. A. (2015). Butyrate and mucosal inflammation: new scientific evidence supports clinical observation. *Clin. Transl. Gastroenterol.* 6, e108. doi: 10.1038/ctg.2015.34
- da Rocha Lapa, F., da Silva, M. D., de Almeida Cabrini, D., and Santos, A. R. S. (2012). Anti-inflammatory effects of purine nucleosides, adenosine and inosine, in a mouse model of pleurisy: evidence for the role of adenosine A2 receptors. *Purinerg. Signal.* 8, 693–704. doi: 10.1007/s11302-012-9299-2
- Dai, D., Qiu, K., Zhang, H.-J., Wu, S.-G., Han, Y.-M., Wu, Y.-Y., et al. (2021). Organic acids as alternatives for antibiotic growth promoters alter the intestinal structure and microbiota and improve the growth performance in broilers. *Front. Microbiol.* 11, 618144. doi: 10.3389/fmicb.2020.618144
- Dang, D. X., Hoque, M. R., Liu, Y. J., Chen, N. B., and Kim, I. H. (2021). Dietary glucose oxidase supplementation improves growth performance, apparent nutrient digestibility, and serum antioxidant enzyme parameters in growing pigs. *Ital. J. Anim. Sci.* 20, 1568–1574. doi: 10.1080/1828051X.2021.1984853
- Dang, D. X., Liu, Y., Chen, N., and Kim, I. H. (2022). Dietary supplementation of *Aspergillus niger*-expressed glucose oxidase ameliorates weaning stress and improves growth performance in weaning pigs. *J. Anim. Physiol.* 106, 258–265. doi: 10.1111/jpn.13576
- David, C. J., and Massagué, J. (2018). Contextual determinants of TGF $\beta$  action in development, immunity and cancer. *Nat. Rev. Mol. Cell Biol.* 19, 419–435. doi: 10.1038/s41580-018-0007-0
- Elagib, H. A., Abbas, S. A., and Elamin, K. M. (2013). Effect of different natural feed additives compared to antibiotic on performance of broiler chicks under high temperature. *Bull. Env. Pharmacol. Life Sci.* 2, 139–144.
- Fagarasan, S., Kawamoto, S., Kanagawa, O., and Suzuki, K. (2009). Adaptive immune regulation in the gut: T cell-dependent and T cell-independent IgA synthesis. *Annu. Rev. Immunol.* 28, 243–273. doi: 10.1146/annurev-immunol-030409-101314
- Farkas, V., Csitari, G., Menyhart, L., Such, N., Pal, L., Husveth, F., et al. (2022). Microbiota composition of mucosa and interactions between the microbes of the different gut segments could be a factor to modulate the growth rate of broiler chickens. *Animals* 12:1296. doi: 10.3390/ani12101296
- Fasina, Y., Classen, H., Garlich, J., Black, B., Ferket, P., Uni, Z., et al. (2006). Response of turkey poults to soybean lectin levels typically encountered in commercial diets. 2. Effect on intestinal development and lymphoid organs. *Poult. Sci.* 85, 870–877. doi: 10.1093/ps/85.5.870
- Fasina, Y. O., and Lillehoj, H. S. (2019). Characterization of intestinal immune response to *Clostridium perfringens* infection in broiler chickens. *Poult. Sci.* 98, 188–198. doi: 10.3382/ps/pey390
- Fukudome, I., Kobayashi, M., Dabanaka, K., Maeda, H., Okamoto, K., Okabayashi, T., et al. (2014). Diamine oxidase as a marker of intestinal mucosal injury and the effect of soluble dietary fiber on gastrointestinal tract toxicity after intravenous 5-fluorouracil treatment in rats. *Med. Mol. Morphol.* 47, 100–107. doi: 10.1007/s00795-013-0055-7
- Gantois, I., Ducatelle, R., Pasmans, F., Haesebrouck, F., Hautefort, I., Thompson, A., et al. (2006). Butyrate specifically down-regulates *Salmonella* pathogenicity island 1 gene expression. *Appl. Environ. Microb.* 72, 946–949. doi: 10.1128/AEM.72.1.946-949.2006
- Gao, P., Ma, C., Sun, Z., Wang, L., Huang, S., Su, X., et al. (2017). Feed-additive probiotics accelerate yet antibiotics delay intestinal microbiota maturation in broiler chicken. *Microbiome* 5, 1–14. doi: 10.1186/s40168-017-0315-1
- Gophna, U., Konikoff, T., and Nielsen, H. B. (2017). Oscillospira and related bacteria—From metagenomic species to metabolic features. *Environ. Microbiol.* 19, 835–841. doi: 10.1111/1462-2920.13658
- Granato, D., de Araujo Calado, V. M., and Jarvis, B. (2014). Observations on the use of statistical methods in Food Science and Technology. *Food Res. Int.* 55, 137–149. doi: 10.1016/j.foodres.2013.10.024
- Guo, W., Xiang, Q., Mao, B., Tang, X., Cui, S., Li, X., et al. (2021). Protective effects of microbiome-derived inosine on lipopolysaccharide-induced acute liver damage and inflammation in mice via mediating the TLR4/NF- $\kappa$ B pathway. *J. Agric. Food Chem.* 69, 7619–7628. doi: 10.1021/acs.jafc.1c01781
- Guo, Y.-M., Liu, Y., and Chen, L.-M. (2014). Bicarbonate reabsorption in proximal renal tubule: molecular mechanisms and metabolic acidosis. *Acta Physiol. Sin.* 66, 398–414. doi: 10.13294/j.aps.2014.0047
- Haddad, J. J. (2002). Cytokines and related receptor-mediated signaling pathways. *Biochem. Biophys. Res. Co.* 297, 700–713. doi: 10.1016/S0006-291X(02)02287-8
- Hashemipour, H., Kermanshahi, H., Golian, A., and Veldkamp, T. (2013). Effect of thymol and carvacrol feed supplementation on performance, antioxidant enzyme activities, fatty acid composition, digestive enzyme activities, and immune response in broiler chickens. *Poult. Sci.* 92, 2059–2069. doi: 10.3382/ps.2012-02685
- Haskó, G., Kuhel, D. G., Németh, Z. H., Mabley, J. G., Stachlewitz, R. F., Virág, L., et al. (2000). Inosine inhibits inflammatory cytokine production by a posttranscriptional mechanism and protects against endotoxin-induced shock. *J. Immunol.* 164, 1013–1019. doi: 10.4049/jimmunol.164.2.1013
- Haskó, G., Sitkovsky, M. V., and Szabo, C. (2004). Immunomodulatory and neuroprotective effects of inosine. *Trends Pharmacol. Sci.* 25, 152–157. doi: 10.1016/j.tips.2004.01.006
- He, H., Xu, H., Xu, J., Zhao, H., Lin, Q., Zhou, Y., et al. (2020). Sodium butyrate ameliorates gut microbiota dysbiosis in lupus-like mice. *Front. Nutr.* 7, 604283. doi: 10.3389/fnut.2020.604283
- Hofmann, S., Janulien, D., Mehdipour, A. R., Thomas, C., Stefan, E., Brüchert, S., et al. (2019). Conformation space of a heterodimeric ABC exporter under turnover conditions. *Nature* 571, 580–583. doi: 10.1038/s41586-019-1391-0
- Hoque, M. R., Chen, N. B., Liu, Y. J., and Kim, I. H. (2022). Possibility of using glucose oxidase in the diet to improve selected indicators of blood antioxidant defense, digestibility and growth performance of broiler chicken. *Ital. J. Anim. Sci.* 21, 455–462. doi: 10.1080/1828051X.2021.2024457

- Huang, G., Tang, X., Bi, F., Hao, Z., Han, Z., Suo, J., et al. (2018). *Eimeria tenella* infection perturbs the chicken gut microbiota from the onset of oocyst shedding. *Vet. Parasitol.* 258, 30–37. doi: 10.1016/j.vetpar.2018.06.005
- Huyghebaert, G., Ducatelle, R., and Van Immerseel, F. (2011). An update on alternatives to antimicrobial growth promoters for broilers. *Vet. J.* 187, 182–188. doi: 10.1016/j.tvjl.2010.03.003
- Jiang, H., Ling, Z., Zhang, Y., Mao, H., Ma, Z., Yin, Y., et al. (2015). Altered fecal microbiota composition in patients with major depressive disorder. *Brain Behav. Immun.* 48, 186–194. doi: 10.1016/j.bbi.2015.03.016
- Kabir, S. M. L., Rahman, M. M., Rahman, M. B., Hosain, M. Z., Akand, M. S. I., and Das, S. K. (2005). Viability of probiotics in balancing intestinal flora and effecting histological changes of crop and caecal tissues of broilers. *Biotechnology* 4, 325–330. doi: 10.3923/biotech.2005.325.330
- Kamboh, A. A., and Zhu, W. Y. (2013). Individual and combined effects of genistein and hesperidin supplementation on meat quality in meat-type broiler chickens. *J. Sci. Food Agric.* 93, 3362–3367. doi: 10.1002/jsfa.6185
- Khan, S. H., Ansari, J., Haq, A. U., and Abbas, G. (2012). Black cumin seeds as phyto-genic product in broiler diets and its effects on performance, blood constituents, immunity and caecal microbial population. *Ital. J. Anim. Sci.* 11:e77. doi: 10.4081/ijas.2012.e77
- Kim, M., Kim, J., Kuehn, L., Bono, J., Berry, E., Kalchayanand, N., et al. (2014). Investigation of bacterial diversity in the feces of cattle fed different diets. *J. Anim. Sci.* 92, 683–694. doi: 10.2527/jas.2013-6841
- Ko, Y., Yang, H., and Jang, I. S. (2004). Effect of conjugated linoleic acid on intestinal and hepatic antioxidant enzyme activity and lipid peroxidation in broiler chickens. *Asian Aust. J. Anim.* 17, 1162–1167. doi: 10.5713/ajas.2004.1162
- Koenigsnecht, M. J., Theriot, C. M., Bergin, I. L., Schumacher, C. A., Schloss, P. D., Young, V. B., et al. (2015). Dynamics and establishment of *Clostridium difficile* infection in the murine gastrointestinal tract. *Infect. Immun.* 83, 934–941. doi: 10.1128/IAI.02768-14
- Lammers, A., Wieland, W. H., Kruijt, L., Jansma, A., Straetmans, T., Schots, A., et al. (2010). Successive immunoglobulin and cytokine expression in the small intestine of juvenile chicken. *Dev. Comp. Immunol.* 34, 1254–1262. doi: 10.1016/j.dci.2010.07.001
- Laxminarayan, R., Duse, A., and Wattal, A. (2014). Antibiotic resistance—the need for global solutions vol 13,pg 1057, 2013. *Lancet Infect. Dis.* 14, 675–675. doi: 10.1016/S1473-3099(13)70318-9
- Lee, J., Venna, V. R., Durgan, D. J., Shi, H., Hudobenko, J., Putluri, N., et al. (2020). Young versus aged microbiota transplants to germ-free mice: increased short-chain fatty acids and improved cognitive performance. *Gut Microbes* 12, 1814107. doi: 10.1080/19490976.2020.1814107
- Li, C., Yan, X. H., Lillehoj, H. S., Oh, S., Liu, L. H., Sun, Z. F., et al. (2019). *Eimeria maxima*-induced transcriptional changes in the cecal mucosa of broiler chickens. *Parasite Vect.* 12, 1–9. doi: 10.1186/s13071-019-3534-4
- Li, T. T., Xing, G. Z., Shao, Y. X., Zhang, L. Y., Li, S. F., Lu, L., et al. (2020). Dietary calcium or phosphorus deficiency impairs the bone development by regulating related calcium or phosphorus metabolic utilization parameters of broilers. *Poult. Sci.* 99, 3207–3214. doi: 10.1016/j.psj.2020.01.028
- Liang, Z. Q., Yan, Y. R., Zhang, W., Luo, H. Y., Yao, B., Huang, H. Q., et al. (2020). Review of glucose oxidase as a feed additive: production, engineering, applications, growth-promoting mechanisms, and outlook. *Crit. Rev. Biotechnol.* (2022) 2022, 1–18. doi: 10.1080/07388551.2022.2057275
- Liao, J., Yang, F., Bai, Y., Yu, W., Qiao, N., Han, Q., et al. (2021). Metabolomics analysis reveals the effects of copper on mitochondria-mediated apoptosis in kidney of broiler chicken (*Gallus gallus*). *J. Inorg. Biochem.* 224, 111581. doi: 10.1016/j.jinorgbio.2021.111581
- Liu, C., Radebe, S. M., Zhang, H., Jia, J., Xie, S., Shi, M., et al. (2022). Effect of *Bacillus coagulans* on maintaining the integrity intestinal mucosal barrier in broilers. *Vet. Microbiol.* 266. doi: 10.1016/j.vetmic.2022.109357
- Liu, J., Stewart, S. N., Robinson, K., Yang, Q., Lyu, W., Whitmore, M. A., et al. (2021a). Linkage between the intestinal microbiota and residual feed intake in broiler chickens. *J. Anim. Sci.* 12, 1–16. doi: 10.1186/s40104-020-00542-2
- Liu, X. M., Tong, X., Zou, Y. Q., Lin, X. Q., Zhao, H., Tian, L., et al. (2022b). Mendelian randomization analyses support causal relationships between blood metabolites and the gut microbiome. *Nat. Genet.* 54, 52–61. doi: 10.1038/s41588-021-00968-y
- Liu, Y., Li, S., Wang, X., Xing, T., Li, J., Zhu, X., et al. (2021b). Microbiota populations and short-chain fatty acids production in cecum of immunosuppressed broilers consuming diets containing  $\gamma$ -irradiated Astragalus polysaccharides. *Poult. Sci.* 100, 273–282. doi: 10.1016/j.psj.2020.09.089
- Livak, K. J., and Schmittgen, T. D. (2001). Analysis of relative gene expression data using real-time quantitative PCR and the 2(T)(-Delta Delta C) method. *Methods* 25, 402–408. doi: 10.1006/meth.2001.1262
- Ma, J., Mahfuz, S., Wang, J., and Piao, X. (2021). Effect of dietary supplementation with mixed organic acids on immune function, antioxidative characteristics, digestive enzymes activity, and intestinal health in broiler chickens. *Front. Nutr.* 8, 673316. doi: 10.3389/fnut.2021.673316
- Marshall, B. M., and Levy, S. B. (2011). Food animals and antimicrobials: impacts on human health. *Clin. Microbiol. Rev.* 24, 718. doi: 10.1128/CMR.00002-11
- McGuckin, M. A., Linden, S. K., Sutton, P., and Florin, T. H. (2011). Mucin dynamics and enteric pathogens. *Nat. Rev. Microbiol.* 9, 265–278. doi: 10.1038/nrmicro2538
- Meng, Q., Sun, S., Luo, Z., Shi, B., Shan, A., Cheng, B., et al. (2019). Maternal dietary resveratrol alleviates weaning-associated diarrhea and intestinal inflammation in pig offspring by changing intestinal gene expression and microbiota. *Food Funct.* 10, 5626–5643. doi: 10.1039/C9FO00637K
- Meng, Y., Huo, H. N., Zhang, Y., Bai, S. P., Wang, R. S., Zhang, K. Y., et al. (2021). Effects of dietary glucose oxidase supplementation on the performance, apparent ileal amino acids digestibility, and ileal microbiota of broiler chickens. *Animals* 11:2909. doi: 10.3390/ani11102909
- Mohd Shaufi, M. A., Sieo, C. C., Chong, C. W., Gan, H. M., and Ho, Y. W. (2015). Deciphering chicken gut microbial dynamics based on high-throughput 16S rRNA metagenomics analyses. *Gut Pathog.* 7, 1–12. doi: 10.1186/s13099-015-0051-7
- Mortensen, P. B., Holtug, K., and Rasmussen, H. S. (1988). Short-chain fatty acid production from mono- and disaccharides in a fecal incubation system: implications for colonic fermentation of dietary fiber in humans. *J. Nutr.* 118, 321–325. doi: 10.1093/jn/118.3.321
- National Technical Committee for Animal Agriculture Standardization (2005). *Production Technique Criterion for Commercial Broiler*. Beijing (in Chinese).
- Oakley, B. B., Buhr, R. J., Ritz, C. W., Kiepper, B. H., Berrang, M. E., Seal, B. S., et al. (2014). Successional changes in the chicken cecal microbiome during 42 days of growth are independent of organic acid feed additives. *BMC Vet. Res.* 10, 1–8. doi: 10.1186/s12917-014-0282-8
- Pamplona, R., and Costantini, D. (2011). Molecular and structural antioxidant defenses against oxidative stress in animals. *Am. J. Physiol. Reg. I* 301, R843–R863. doi: 10.1152/ajpregu.00034.2011
- Pandit, R. J., Hinsu, A. T., Patel, N. V., Koringa, P. G., Jakhesara, S. J., Thakkar, J. R., et al. (2018). Microbial diversity and community composition of caecal microbiota in commercial and indigenous Indian chickens determined using 16s rDNA amplicon sequencing. *Microbiome* 6, 1–13. doi: 10.1186/s40168-018-0501-9
- Pedroso, A. A., Lee, M. D., and Maurer, J. J. (2021). Strength lies in diversity: how community diversity limits salmonella abundance in the chicken intestine. *Front. Microbiol.* 12, 694215. doi: 10.3389/fmicb.2021.694215
- Pickup, M. W., Owens, P., and Moses, H. L. (2017). TGF- $\beta$ , bone morphogenetic protein, and activin signaling and the tumor microenvironment. *Csh Perspect. Biol.* 9, a022285. doi: 10.1101/cshperspect.a022285
- Pourabedin, M., and Zhao, X. (2015). Prebiotics and gut microbiota in chickens. *Fems Microbiol. Lett.* 362, fnv122. doi: 10.1093/femsle/fnv122
- Qu, W., and Liu, J. (2021). Effects of glucose oxidase supplementation on the growth performance, antioxidative and inflammatory status, gut function, and microbiota composition of broilers fed moldy corn. *Front. Physiol.* 685, 646393. doi: 10.3389/fphys.2021.646393
- Reynolds, J., O'farrelly, C., Feighery, C., Murchan, P., Leonard, N., Fulton, G., et al. (1996). Impaired gut barrier function in malnourished patients. *Br. J. Surg.* 83, 1288–1291. doi: 10.1046/j.1365-2168.1996.02330.x
- Rice, A. J., Park, A., and Pinkett, H. W. (2014). Diversity in ABC transporters: type I, II and III importers. *Crit. Rev. Biochem. Mol.* 49, 426–437. doi: 10.3109/10409238.2014.953626
- Robinson, K., Deng, Z., Hou, Y., and Zhang, G. (2015). Regulation of the intestinal barrier function by host defense peptides. *Front. Vet. Sci.* 2, 57. doi: 10.3389/fvets.2015.00057
- Rupnik, M., Wilcox, M. H., and Gerding, D. N. (2009). *Clostridium difficile* infection: new developments in epidemiology and pathogenesis. *Nat. Rev. Microbiol.* 7, 526–536. doi: 10.1038/nrmicro2164
- Schloss, P. D., Westcott, S. L., Ryabin, T., Hall, J. R., Hartmann, M., Hollister, E. B., et al. (2009). Introducing mothur: open-source, platform-independent, community-supported software for describing and comparing microbial communities. *Appl. Environ. Microb.* 75, 7537–7541. doi: 10.1128/AEM.01541-09
- Segura-Wang, M., Grabner, N., Koestelbauer, A., Klose, V., and Ghanbari, M. (2021). Genome-resolved metagenomics of the chicken gut microbiome. *Front. Microbiol.* 12, 726923. doi: 10.3389/fmicb.2021.726923
- Shang, Y., Kumar, S., Thippareddi, H., and Kim, W. K. (2018). Effect of dietary fructooligosaccharide (FOS) supplementation on ileal microbiota in broiler chickens. *Poult. Sci.* 97, 3622–3634. doi: 10.3382/ps/pey131
- Skalicka, M., Makoova, Z., and Korenekova, B. (2000). The influence of aflatoxin B-1 on activity of alkaline phosphatase and body weight of broiler chicks. *Trace Elem. Electroly.* 17, 142–146.
- Song, B., Tang, D., Yan, S., Fan, H., Li, G., Shahid, M. S., et al. (2021). Effects of age on immune function in broiler chickens. *J. Anim. Sci. Biotechnol.* 12, 1–12. doi: 10.1186/s40104-021-00559-1

- Srikanth, K., Kumar, H., Park, W., Byun, M., Lim, D., Kemp, S., et al. (2019). Cardiac and skeletal muscle transcriptome response to heat stress in kenyan chicken ecotypes adapted to low and high altitudes reveal differences in thermal tolerance and stress response. *Front. Genet.* 10, 993. doi: 10.3389/fgene.2019.00993
- Stanley, D., Hughes, R. J., Moore, R. J. (2014). Microbiota of the chicken gastrointestinal tract: influence on health, productivity and disease. *Appl. Microbiol. Biotechnol.* 98, 4301–4310. doi: 10.1007/s00253-014-5646-2
- Sun, C., Lin, S., Li, Z., Liu, H., Liu, Y., Wang, K., et al. (2021). iTRAQ-based quantitative proteomic analysis reveals the toxic mechanism of diclofenac sodium on the kidney of broiler chicken. *Comp. Biochem. Phys. C* 249, 109129. doi: 10.1016/j.cbpc.2021.109129
- Sun, X., Piao, L., Jin, H., Nogoy, K. M. C., Zhang, J., Sun, B., et al. (2022). Effects of dietary supplementation of glucose oxidase, catalase, or both on reproductive performance, oxidative stress, fecal microflora and apoptosis in multiparous sows. *Anim. Biosci.* 35, 75–86. doi: 10.5713/ab.20.0839
- Tong, A. J., Hu, R. K., Wu, L. X., Lv, X. C., Li, X., Zhao, L. N., et al. (2020). Ganoderma polysaccharide and chitosan synergistically ameliorate lipid metabolic disorders and modulate gut microbiota composition in high fat diet-fed golden hamsters. *J. Food Biochem.* 44, e13109. doi: 10.1111/jfbc.13109
- Vatansever, F., de Melo, W. C., Avci, P., Vecchio, D., Sadasivam, M., Gupta, A., et al. (2013). Antimicrobial strategies centered around reactive oxygen species–bactericidal antibiotics, photodynamic therapy, and beyond. *FEMS Microbiol. Rev.* 37, 955–989. doi: 10.1111/1574-6976.12026
- Wang, J., Li, G., Zhong, W., Zhang, H., Yang, Q., Chen, L., et al. (2022). Effect of dietary paeoniae radix alba extract on the growth performance, nutrient digestibility and metabolism, serum biochemistry, and small intestine histomorphology of Raccoon dog during the growing period. *Front. Vet. Sci.* 9, 839450. doi: 10.3389/fvets.2022.839450
- Wang, Q., Garrity, G. M., Tiedje, J. M., and Cole, J. R. (2007). Naive Bayesian classifier for rapid assignment of rRNA sequences into the new bacterial taxonomy. *Appl. Environ. Microb.* 73, 5261–5267. doi: 10.1128/AEM.00062-07
- Wang, Q., Wang, C., Abdullah, T., Tian, W., Qiu, Z., Song, M., et al. (2022). Hydroxytyrosol alleviates dextran sulfate sodium-induced colitis by modulating inflammatory responses, intestinal barrier, and microbiome. *J. Agric. Food Chem.* 70, 2241–2252. doi: 10.1021/acs.jafc.1c07568
- Wang, S., Zeng, X., Yang, Q., and Qiao, S. (2016). Antimicrobial peptides as potential alternatives to antibiotics in food animal industry. *Int. J. Mol. Sci.* 17:603. doi: 10.3390/ijms17050603
- Wang, Y., Ouyang, M., Gao, X., Wang, S., Fu, C., Zeng, J., et al. (2020). Phoceia, Pseudoflavonifractor and Lactobacillus intestinalis: three potential biomarkers of gut microbiota that affect progression and complications of obesity-induced type 2 diabetes mellitus. *Diabet. Metab. Syndr. Obesity* 13, 835. doi: 10.2147/DMSO.S240728
- Wang, Y., Wang, Y., Xu, H., Mei, X., Gong, L., Wang, B., et al. (2018). Direct-fed glucose oxidase and its combination with *B. amyloliquefaciens* SC06 on growth performance, meat quality, intestinal barrier, antioxidative status, and immunity of yellow-feathered broilers. *Poult. Sci.* 97, 3540–3549. doi: 10.3382/ps/pey216
- Wu, S., Chen, X., Li, T., Ren, H., Zheng, L., and Yang, X. (2020). Changes in the gut microbiota mediate the differential regulatory effects of two glucose oxidases produced by *Aspergillus niger* and *Penicillium amagasakiense* on the meat quality and growth performance of broilers. *J. Anim. Sci. Biotechnol.* 11, 1–13. doi: 10.1186/s40104-020-00480-z
- Wu, Y., Zhou, Y., Lu, C., Ahmad, H., Zhang, H., He, J., et al. (2016). Influence of butyrate loaded clinoptilolite dietary supplementation on growth performance, development of intestine and antioxidant capacity in broiler chickens. *PLoS ONE* 11, e0154410. doi: 10.1371/journal.pone.0154410
- Yang, G., Hong, S., Yang, P., Sun, Y., Wang, Y., Zhang, P., et al. (2021). Discovery of an ene-reductase for initiating flavone and flavonol catabolism in gut bacteria. *Nat. Commun.* 12, 1–15. doi: 10.1038/s41467-021-20974-2
- Yang, J., Li, Y., Wen, Z., Liu, W., Meng, L., and Huang, H. J. G. M. (2021). Oscillospira-a candidate for the next-generation probiotics. *Gut Microbes* 13, 1987783. doi: 10.1080/19490976.2021.1987783
- Yang, R. L., Li, W., Shi, Y. H., and Le, G. W. (2008). Lipoic acid prevents high-fat diet-induced dyslipidemia and oxidative stress: a microarray analysis. *Nutrition* 24, 582–588. doi: 10.1016/j.nut.2008.02.002
- Ze, X., Duncan, S. H., Louis, P., and Flint, H. J. (2012). Ruminococcus bromii is a keystone species for the degradation of resistant starch in the human colon. *ISME J.* 6, 1535–1543. doi: 10.1038/ismej.2012.4
- Zhang, S., Zhong, G., Shao, D., Wang, Q., Hu, Y., Wu, T., et al. (2021). Dietary supplementation with *Bacillus subtilis* promotes growth performance of broilers by altering the dominant microbial community. *Poult. Sci.* 100, 100935. doi: 10.1016/j.psj.2020.12.032





## OPEN ACCESS

## EDITED BY

Weiqi He,  
Soochow University,  
China

## REVIEWED BY

Susan Westfall,  
McGill University Health Center,  
Canada  
Mapitsi Thantsha,  
University of Pretoria,  
South Africa

## \*CORRESPONDENCE

Massimo Marzorati  
✉ massimo.marzorati@ugent.be

## PRESENT ADDRESS

Stef Deyaert and Pieter Van den Abbeele,  
Cryobiotix NV, Gent, Belgium

## SPECIALTY SECTION

This article was submitted to  
Microorganisms in Vertebrate Digestive  
Systems,  
a section of the journal  
Frontiers in Microbiology

RECEIVED 26 September 2022

ACCEPTED 14 December 2022

PUBLISHED 17 March 2023

## CITATION

Deyaert S, Moens F, Pirovano W,  
van den Bogert B, Klaassens ES,  
Marzorati M, Van de Wiele T,  
Kleerebezem M and Van den  
Abbeele P (2023) Development of a  
reproducible small intestinal microbiota  
model and its integration into the SHIME®-  
system, a dynamic *in vitro* gut model.  
*Front. Microbiol.* 13:1054061.  
doi: 10.3389/fmicb.2022.1054061

## COPYRIGHT

© 2023 Deyaert, Moens, Pirovano,  
van den Bogert, Klaassens, Marzorati, Van  
de Wiele, Kleerebezem and Van den  
Abbeele. This is an open-access article  
distributed under the terms of the [Creative  
Commons Attribution License \(CC BY\)](#). The  
use, distribution or reproduction in other  
forums is permitted, provided the original  
author(s) and the copyright owner(s) are  
credited and that the original publication in  
this journal is cited, in accordance with  
accepted academic practice. No use,  
distribution or reproduction is permitted  
which does not comply with these terms.

# Development of a reproducible small intestinal microbiota model and its integration into the SHIME®-system, a dynamic *in vitro* gut model

Stef Deyaert<sup>1†</sup>, Frédéric Moens<sup>1</sup>, Walter Pirovano<sup>2</sup>,  
Bartholomeus van den Bogert<sup>2</sup>, Eline Suzanne Klaassens<sup>2</sup>,  
Massimo Marzorati<sup>1,3\*</sup>, Tom Van de Wiele<sup>1,3</sup>, Michiel  
Kleerebezem<sup>4</sup> and Pieter Van den Abbeele<sup>1†</sup>

<sup>1</sup>ProDigest BV, Gent, Belgium, <sup>2</sup>Baseclear, Leiden, Netherlands, <sup>3</sup>Center of Microbial Ecology and Technology (CMET), Faculty of Bioscience Engineering, Ghent University, Ghent, Belgium, <sup>4</sup>Department of Animal Sciences, Wageningen University, Wageningen, Netherlands

The human gastrointestinal tract consists of different regions, each characterized by a distinct physiology, anatomy, and microbial community. While the colonic microbiota has received a lot of attention in recent research projects, little is known about the small intestinal microbiota and its interactions with ingested compounds, primarily due to the inaccessibility of this region *in vivo*. This study therefore aimed to develop and validate a dynamic, long-term simulation of the ileal microbiota using the SHIME®-technology. Essential parameters were identified and optimized from a screening experiment testing different inoculation strategies, nutritional media, and environmental parameters over an 18-day period. Subjecting a synthetic bacterial consortium to the selected conditions resulted in a stable microbiota that was representative in terms of abundance [ $8.81 \pm 0.12 \log$  (cells/ml)], composition and function. Indeed, the observed community mainly consisted of the genera *Streptococcus*, *Veillonella*, *Enterococcus*, *Lactobacillus*, and *Clostridium* (qPCR and 16S rRNA gene targeted Illumina sequencing), while nutrient administration boosted lactate production followed by cross-feeding interactions towards acetate and propionate. Furthermore, similarly as *in vivo*, bile salts were only partially deconjugated and only marginally converted into secondary bile salts. After confirming reproducibility of the small intestinal microbiota model, it was integrated into the established M-SHIME® where it further increased the compositional relevance of the colonic community. This long-term *in vitro* model provides a representative simulation of the ileal bacterial community, facilitating research of the ileum microbiota dynamics and activity when, for example, supplemented with microbial or diet components. Furthermore, integration of this present *in vitro* simulation increases the biological relevance of the current M-SHIME® technology.

## KEYWORDS

ileum, microbiota, *in vitro* model, short-chain fatty acid, small intestine, simulator of the human intestinal microbial ecosystem

## 1. Introduction

The human gastrointestinal tract (GIT) consists of distinct regions each comprising a unique physiology, anatomy, and microenvironment (Booijink et al., 2007; Donaldson et al., 2016; Ruan et al., 2020). The ecosystems of the stomach, small intestine and large intestine (or colon) together comprise hundreds of billions of bacteria, which are referred to as the gut microbiota (Bäckhed et al., 2005; Ley et al., 2006). This gut microbiota impacts human health through metabolizing undigested nutrients, producing health beneficial molecules, preventing pathogen colonization, and training the human immune system (Macfarlane and Macfarlane, 2011; Zoetendal et al., 2012; Arpaia et al., 2013; El Aidy et al., 2015; Marchesi et al., 2016). A key limitation for many studies that aim to investigate such interactions is the inaccessibility of the gastrointestinal tract, often resulting in the use of faecal samples which are only an approximation of what happens at the site of activity (Kastl et al., 2020). Therefore, a rather unexplored microbiota is the one that colonizes the small intestine. This microbiota is, nonetheless, of high interest since it is the first to encounter ingested food compounds and together with host physiology could have an important impact on stability and efficacy of ingested therapeutics (Zhang et al., 2018; van Kessel et al., 2019; van Kessel and El Aidy, 2019; Li et al., 2020).

The small intestine consists of the duodenum, jejunum, and ileum. Within these regions, microbial communities are shaped through distinct physiological parameters such as pH (Moore and Holdeman, 1974; Evans et al., 1988), transit time (Silvester et al., 1995), secretory products (Kitahara et al., 2004; Begley et al., 2005; O'May et al., 2005; Whitcomb and Lowe, 2007; Ridlon et al., 2014), and nutrient availability (Hao and Lee, 2004; reviewed in Booijink et al., 2007; Donaldson et al., 2016; Thursby and Juge, 2017). Furthermore, compared to the colon region, the small intestine comprises a higher surface area, thereby allowing intense

interactions with host epithelial cells and the immune system through, e.g., Peyer's patches (Stagg et al., 2004; Rakoff-Nahoum and Medzhitov, 2006). The intraluminal pH in the small intestine gradually increases from approximately 6 in the duodenum up to 7.4 in the terminal ileum (Evans et al., 1988; Booijink et al., 2007). Bile salts are typically present between 4 and 10 mM throughout the small intestine and can be toxic for bacteria through emulsification of their cell membranes (Islam et al., 2011; Kakiyama et al., 2013; Ridlon et al., 2014; Staley et al., 2017). Secretory products might comprise pancreatic enzymes among which trypsin, chymotrypsin, amylase and lipase are the most abundant ones (Whitcomb and Lowe, 2007). Furthermore, the small intestinal transit time is between  $3 \pm 1$  h (Davis et al., 1986), which is an order of magnitude shorter as compared to the colonic residence time ( $39 \pm 5$  h; Arhan et al., 1981). Unlike the colon – where complex fibers are the main carbon source for bacteria – small intestinal microbes rather ferment simple sugars that are unabsorbed leftovers from digestion along the upper GIT (Borgström et al., 1957; Booijink et al., 2007, 2010; Zoetendal et al., 2012).

Bacterial densities along the small intestine are largely affected by region-specific physiological conditions. While abundances in the duodenum ( $10^3$ – $10^5$  cells per gram) and jejunum ( $10^4$ – $10^5$  cells per gram) are rather low due to the initial acidity coming from the stomach and high concentrations of bile salts and pancreatic enzymes, the more alkaline environment of the ileum comprises substantial numbers of bacteria ( $10^7$ – $10^8$  cells per gram; Booijink et al., 2007). However, microbial loads and diversity are relatively small compared to that of the colon (Booijink et al., 2007; Zoetendal et al., 2012; Thursby and Juge, 2017; Kastl et al., 2020). In terms of microbial composition, there are considerable inter-study variations (Thadepalli et al., 1979; Bouhnik et al., 1999; Riordan et al., 2001; Hayashi et al., 2005; Wang et al., 2005; Ivanov et al., 2008; Hartman et al., 2009; Booijink et al., 2010; Zoetendal et al., 2012; van den Bogert et al., 2013; El Aidy et al., 2015; Seekatz et al., 2019; Kastl et al., 2020), which are likely due to differences in test population (healthy adults vs. ileostomy patients vs. sudden death victims), sampling procedures (ileostomy effluent vs. autopsy vs. biopsy), sampling regions (lumen vs. mucus and proximal ileum vs. terminal ileum), and methodology to analyze the microbiota. This further adds to noise generated by strong inter-individual and temporal variation inherent to the ileal microbiota (Booijink et al., 2010; Zoetendal et al., 2012). While the ileal microbiota is often dominated by Firmicutes members, mainly from the genera *Streptococcus*, *Veillonella*, *Lactobacillus*, *Enterococcus*, and *Clostridium*, the small

Abbreviations: BCFA, Branched-chain fatty acid; GIT, Gastrointestinal tract; SCFA, Short-chain fatty acid; M-SHIME, Mucosal Simulator of the Human Intestinal Microbial Ecosystem; ILE, Ileum; PC, Proximal colon; DC, Distal colon; SC, Synthetic consortium; FS, Faecal sample; IE, Ileostomy effluent; TSB, Tryptic soy broth; MRS, de Man, Rogosa and Sharpe medium; RCM, Reinforced clostridial medium; RT, Retention time; REF, Reference conditions; TCA, Taurocholic acid; GCA, Glycocholic acid; TDCA, Taurodeoxycholic acid; GDCA, Glycodeoxycholic acid; OTU, Operational taxonomic unit; LOQ, Limit of quantification; DAD, Diode array detector; FDR, False discovery rate; PTFE, Polytetrafluorethene; RP-HPLC, Reversed phase high pressure liquid chromatography; PCA, Principal component analysis; BSH, Bile salt hydrolase.

intestine from some individuals is distinct with high relative abundances of Proteobacteria and Actinobacteria, and specific genera such as *Fusobacterium*, *Faecalibacterium*, *Bacteroides*, *Ruminococcus*, *Blautia*, and *Prevotella* (Booijink et al., 2010; Zoetendal et al., 2012; van den Bogert et al., 2013; El Aidy et al., 2015; Cieplak et al., 2018; Seekatz et al., 2019). Furthermore, there seems to be consistency in metabolic functionality. Each elucidated ileal community comprises primary fermenters (e.g., *Streptococcus*, *Enterococcus*, and *Lactobacillus*) which metabolize simple carbohydrates into, e.g., lactate that supports growth of secondary fermenters (e.g., *Veillonella*). The latter consume lactate to produce short-chain fatty acids (SCFA; mainly acetate and propionate in the case of *Veillonella*) in a process termed cross-feeding (Foubert and Douglas, 1948; Egland et al., 2004; Hosseini et al., 2011; Scott et al., 2013; Kastl et al., 2020).

Due to interindividual variations, longitudinal dynamics, and inaccessibility of the ileal microbiota *in vivo*, development of robust *in vitro* models of the ileal microbiota could be useful to better understand the processes that drive the small intestinal microbiota (Booijink et al., 2010). Most of the currently available *in vitro* models of the small intestine focus on host physiology and lack representation of its colonizing microbiota (Guerra et al., 2012). In contrast, models that incorporate the ileal microbiota are rather short-term and include, e.g., dosing a mixture of ileum-specific bacterial strains which are then immediately investigated, thus being unsure whether they thrive well in the applied environment (Cieplak et al., 2018). Other models have also tried to simulate the ileal microbiota over longer periods of time, but the emerged communities appeared to resemble more colon-like communities with high abundances of either Bacteroidetes (Stolaki et al., 2019) or Enterobacteriaceae (Roussel et al., 2020), or showed strong temporal fluctuations (Roussel et al., 2020). Finally, miniaturized *in vitro* models such as gut-on-a-chip have been designed that can even recreate the anoxic–oxic interface defining the mucosal–bacteria microenvironment (Bein et al., 2018). However, establishing a stable gut microbiota in such a system for long-term studies is nearly impossible due to the very small handling volumes. Although these models present their own advantages, a dynamic, long-term *in vitro* model of the ileal microbial community would enable more mechanistic research, such as studying changes in microbial interactions or metabolic shifts upon administration of a compound of interest. To the best of our knowledge, there is no such model available yet.

Therefore, the aim of the current study was to develop a novel *in vitro* model which – with properly optimized environmental conditions – supports a microbiota that is representative in function and composition to the *in vivo* ileal microbiota during a period of multiple weeks. A second goal was to integrate this small intestinal microbiota model in the established Mucosal Simulator of the Human Intestinal Microbial Ecosystem (M-SHIME®) which already allows biorelevant simulation of the colon microbiota (Molly et al., 1993; Van den Abbeele et al., 2012).

## 2. Materials and methods

### 2.1. Chemicals

Chemicals were obtained from Alfa Aesar (Kandel, Germany), Carl Roth (Karlsruhe, Germany), Chem-Lab (Zedelgem, Belgium), Keyser & Mackay (Brussels, Belgium), Merck (Overijse, Belgium), Oxoid (Merelbeke, Belgium), Sigma-Aldrich (Overijse, Belgium), and VWR (Leuven, Belgium), as elaborated below.

### 2.2. Microbial inocula

During the present study, several inoculation strategies were compared. This involved the use of faecal inocula from healthy human adults collected and prepared as a 20% (w/v) solution of the fecal sample in anaerobic phosphate buffer as previously described (Molly et al., 1993), ileostomy effluents and a synthetic consortium comprising 12 bacterial species (Table 1). Samples derived from human donors were collected according to the ethical approval of the University Hospital Ghent with reference number B670201836585.

TABLE 1 Bacterial strains, their source and applied growth conditions.

Species	Strain source	Growth medium	Growth condition
<i>Streptococcus bovis</i>	LMG 8518	TSB	Aerobic
<i>Streptococcus intermedius</i>	LMG 17840	TSB	Aerobic
<i>Ligilactobacillus salivarius</i>	LMG 9477	MRS + 0.1% Tween*80	Aerobic
<i>Limosilactobacillus reuteri</i>	LMG 9213	MRS + 0.1% Tween*80	Aerobic
<i>Enterococcus faecalis</i>	LMG 7937	MRS	Aerobic
<i>Enterococcus faecium</i>	DSM 20477	MRS	Aerobic
<i>Veillonella parvula</i>	LMG 30945	Veillonella medium	Anaerobic
<i>Veillonella dispar</i>	DSM 20735	Veillonella medium	Anaerobic
<i>Blautia obeum</i>	DSM 25238	RCM + 0.01% mucin	Anaerobic
<i>Faecalibacterium prausnitzii</i>	DSM 17677	RCM	Anaerobic
<i>Clostridium nexile</i>	LMG 28906	RCM	Anaerobic
<i>Prevotella melaninogenica</i>	LMG 28911	RCM	Anaerobic

All species were incubated at 37°C. Species grown under aerobic conditions were shaken continuously at 90RPM, while species grown under anaerobic conditions were grown in a static fashion. Grown cultures were harvested during their exponential growth phase. TSB, tryptic soy broth (Oxoid); MRS, de Man, Rogosa and Sharpe broth (Oxoid); RCM, reinforced clostridial medium (Oxoid); Veillonella medium was prepared according to BCC/LMG medium 1,107 (BCC/LMG, Ghent, Belgium).

## 2.3. Preparation of glycerol stocks of strains selected for a small intestinal consortium

Glycerol stocks were prepared for each strain separately. Grown cultures were harvested during exponential growth and 0.5 ml culture was mixed with 0.5 ml glycerol-based cryoprotectant (50% v/v glycerol (86%) [Merck], 0.5 g L<sup>-1</sup> L-cysteine-HCl [Merck], 10 g L<sup>-1</sup> trehalose [Sigma-Aldrich], 3 g L<sup>-1</sup> tryptic soy broth (TSB) [Oxoid], 18 g L<sup>-1</sup> NaCl [Chem-Lab], 1 ml L<sup>-1</sup> resazurin [Alfa Aesar] stock solution (2% w/v) and 50% (v/v) dH<sub>2</sub>O). For strict anaerobic strains, the glycerol-based cryoprotectant was boiled for 1' to reduce oxygen content prior to autoclaving. Glycerol stocks were stored at -80°C until usage.

## 2.4. *In vitro* M-SHIME® technology

All experiments were performed through modification of the M-SHIME® technology previously described by [Van den Abbeele et al. \(2012\)](#). Setups were autoclaved prior to inoculation to assure sterility of the vessels. Furthermore, reactors were continuously homogenized through stirring, maintained at 37°C, and kept anaerobically by flushing with N<sub>2</sub> for 15 min, three times per day.

### 2.4.1. Nutritional media

Ileal nutritional medium (100%) was prepared by sterile addition (5% v/v) of a filter-sterilized stock solution containing (L<sup>-1</sup>) NaHCO<sub>3</sub> (50 g; Chem-Lab), NaH<sub>2</sub>PO<sub>4</sub> (10 g; VWR), K<sub>2</sub>HPO<sub>4</sub> (10 g; Chem-Lab), MgSO<sub>4</sub>·7H<sub>2</sub>O (0.9 g; Chem-Lab), MnCl<sub>2</sub>·4H<sub>2</sub>O (0.5 g; VWR International Europe BVBA), CaCl<sub>2</sub>·2H<sub>2</sub>O (0.9 g; VWR), FeSO<sub>4</sub>·7H<sub>2</sub>O (0.05 g; Sigma-Aldrich), ZnSO<sub>4</sub>·7H<sub>2</sub>O (0.05 g; Sigma-Aldrich), hemin (0.05 g; Sigma-Aldrich), glucose (12 g; Merck), fructose (12 g; Sigma-Aldrich), sucrose (12 g; Sigma-Aldrich), maltose (12 g; Carl Roth), lactose (12 g; Oxoid), mannose (7.5 g; Carl Roth), and galactose (7.5 g; Sigma-Aldrich) to an autoclaved medium comprising (L<sup>-1</sup>) bile salts (1.9 g; BD Bioscience, Erembodegem, Belgium), special peptone (0.7 g; Oxoid), yeast extract (2.2 g; Oxoid), mucin (2.2 g; Carl Roth), L-cysteine-HCl (0.4 g; AXO Industry SA, Wavre, Belgium) and Tween®80 (1.1 ml; Sigma-Aldrich). Ileal nutritional medium (30%) was equal to ileal nutritional medium (100%) apart from a 70% reduction in simple sugars, special peptone, yeast extract, mucin and cysteine-HCl. Autoclaved colonic nutritional medium (set at pH 2 with 37% HCl) was added to proximal colon (PC) reactors and comprised (in g L<sup>-1</sup>) arabinogalactan (1.2; Keyser & Mackay), pectin (2.0; Keyser & Mackay), xylan (0.5; Carl Roth), starch (4.0; Carl Roth), glucose (0.4; Merck), yeast extract (3.0; Oxoid), peptone (1.0; Oxoid), mucin (2.0; Carl Roth), and L-cysteine-HCl (0.5; Merck). When preceded by an ileum reactor, PC reactors received 50 ml of fiber solution instead of nutritional colon medium. Fiber solution contained (in g L<sup>-1</sup>) arabinogalactan (3.4; Keyser & Mackay), pectin (5.6; Keyser &

Mackay), xylan (1.4; Carl Roth), starch (11.2; Carl Roth), glucose (1.12; Merck), peptone (2.1; Oxoid), yeast extract (6.3; Oxoid), mucin (4.2; Carl Roth) and L-cysteine-HCl (1.0; Merck). This resulted in the same influx of nutrients in the proximal colon, independent from the incorporation of an ileum reactor.

### 2.4.2. Simulation of mucosal microbiota

Mucin-alginate beads were used for small intestinal simulations and prepared by dripping a 5×-boiled mucin-alginate solution [50 g L<sup>-1</sup> mucin (Carl Roth), 12 g L<sup>-1</sup> agar (VWR), 12 g L<sup>-1</sup> alginate (Carl Roth) and 2.22 ml L<sup>-1</sup> 10 M NaOH (Chem-Lab)] into crosslinking solution containing 7.6 g L<sup>-1</sup> CaCl<sub>2</sub>·2H<sub>2</sub>O (VWR). This approach was implemented as the small alginate beads allowed for sterile sampling of colonized beads and addition of fresh beads *via* a 50 ml-syringe with catheter tip (Novolab) connected to an inlet port. Sterility of such handlings was a prerequisite as one worked with a synthetic consortium in multiple ileal simulations. In contrast, for the colonic microbiota, the conventional approach using mucin-covered microcosms was used as previously described by [Van den Abbeele et al. \(2012\)](#). A buffer comprising (g L<sup>-1</sup>) K<sub>2</sub>HPO<sub>4</sub> (8.8; Chem-Lab) and KH<sub>2</sub>PO<sub>4</sub> (6.8; Chem-Lab) was used to rinse luminal content from mucosal samples. Half of the mucus-alginate beads and mucin-covered microcosms were replaced every 2 days.

### 2.4.3. Experimental designs

#### 2.4.3.1. Screening experiment

In a first experiment, different conditions were compared for their potential to maintain an ileal-representative microbiota ([Figure 1A](#)). For this purpose, the SHIME® (ProDigest, Ghent, Belgium and Ghent University, Ghent, Belgium) was configured for comparison of four parallel ileal and one colon simulation. The ileal simulations differed in inoculation strategy, i.e., synthetic consortium (vessel 1 and 2; mixture containing equal volumes of glycerol stocks of 12 strains – [Table 1](#)), ileostomy effluent (vessel 3; 5 ml of a 1:5 dilution) and faecal slurry (vessel 4; 5 ml of a 1:5 dilution). Moreover, while the standard retention time of ileal simulations was 4 h, an additional condition with increased retention time of 8 h was evaluated (reactor 2). At the start, ileal reactors were filled with 100 ml ileal nutritional medium (100%) and 5 g sterile mucin-alginate beads, while the colon vessel was filled with 500 ml of colon nutritional medium and 32 mucin-covered microcosms ([Van den Abbeele et al., 2012](#)). The pH of ileal vessels was controlled at 7.05–7.35, while the pH of the colon vessel was set at 6.15–6.40 (and a colonic retention time of 20 h was mimicked). Fresh nutritional medium was administered three times per day. Samples were collected on days 14, 16, 17 and 18 for analysis of SCFA, lactate, branched chain fatty acids (BCFA), bile salts and microbial composition *via* qPCR. Additionally, on day 14, sampling was performed at 0, 0.5, 1, 2, 4, and 8 h after entrance of fresh nutritional medium to elucidate the kinetic metabolic profile in terms of SCFA and lactate production.



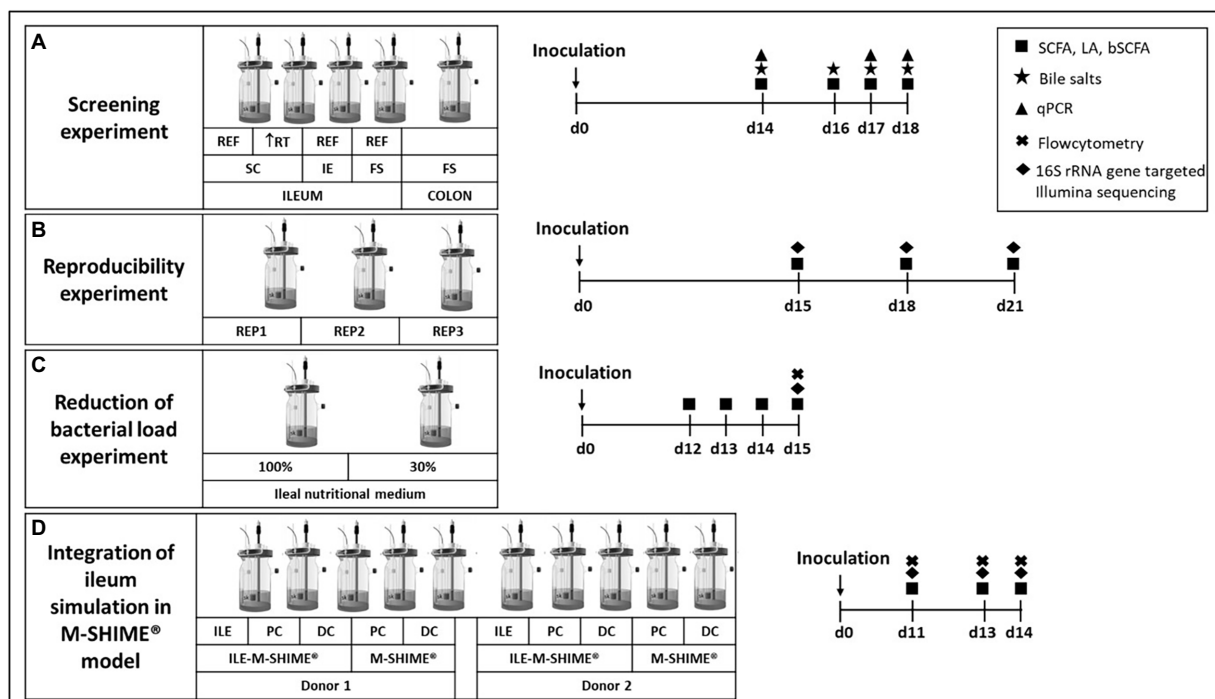


FIGURE 1

Experimental design for (A) screening experiment to compare different inoculation strategies (synthetic consortium, ileostomy effluent, or faecal slurry) under reference conditions (RT=4h) or upon doubled retention time (RT=8h) and a control colon simulation; (B) reproducibility experiment to confirm reproducibility of the synthetic consortium inoculation under reference conditions as selected from screening experiment; (C) reduction of bacterial load experiment to evaluate effect on bacterial levels upon feeding the simulation with a nutritional medium comprising reduced sugar levels; and (D) the validation experiment for integrating the ileum simulation in the M-SHIME® model. Numbers indicate the number of days after inoculation of the model. REF=reference conditions; RT=retention time; IE=ileostomy effluent; FS=faecal slurry.

#### 2.4.3.2. Reproducibility experiment

During a second experiment, observations from the screening experiment were validated by repeating test conditions of vessel 1 in triplicate (Figure 1B). Samples were collected on days 15, 18, and 21 for analysis of SCFA, lactate, BCFA and 16S rRNA gene targeted Illumina sequencing.

#### 2.4.3.3. Reduction of bacterial load

A third experiment aimed to reduce bacterial densities in the ileum simulation (Figure 1C). Therefore, two ileum simulations were performed in parallel. Parameters for both vessels were identical to the test conditions of vessel 1 from the screening experiment and vessels 1–3 from the reproducibility experiment, with the exception that the second vessel was fed with 30% ileal nutritional medium. Samples were collected on days 12, 13, 14, and 15 for analysis of SCFA, lactate and BCFA. On the final day, microbial composition was analyzed *via* 16S rRNA gene targeted Illumina sequencing coupled with flow cytometry.

#### 2.4.3.4. Integration of ileum simulation in M-SHIME® model

The final experiment evaluated integration of the ileum simulation in the M-SHIME® model as described by Šuligoj

et al. (2020; Figure 1D). The configuration was adapted to evaluate the impact of a preceding ileum onto the proximal colon (PC) and distal colon (DC) simulations. For this, the setup comprised of a first arm where the PC and DC were preceded by an ileum simulation (i.e., ILE-M-SHIME®), while a second arm comprised of a PC and DC without preceding ileum (i.e., M-SHIME®), and this for two donors. The ileum reactors were simulated under conditions identical to the reactor with decreased bacterial load, thus receiving ileal nutritional medium 30%. Regarding the colonic simulations, the pH was controlled between 5.70–5.90 for PC vessels, and between 6.60–6.90 for DC vessels. Pumping times were set so that retention times in the PC and DC vessels were 20 and 32 h, respectively. For ILE-M-SHIME® units, the proximal colons received both excess volume from the ileum vessels (approximately 150 ml) and 50 ml fiber solution. Instead, in M-SHIME® units, the proximal colon vessels received a mixture of colon nutritional medium, and pancreatic and bile liquid from the stomach vessel as described previously (Molly et al., 1993; Possemiers et al., 2004; Van den Abbeele et al., 2012, 2013; Ghyselinck et al., 2020; Šuligoj et al., 2020). Samples were collected on days 11, 13, and 14 for analysis of SCFA, lactate, BCFA and 16S rRNA gene targeted Illumina sequencing coupled with flow cytometry.

## 2.5. Metabolic activity analysis

Quantification of SCFAs, including acetate, propionate, butyrate, and branched SCFAs (BSCFA; i.e., isobutyrate, isovalerate, and isocaproate) was performed as previously reported by Ghyselinck et al. (2020). Lactate concentrations were determined on supernatant aliquots (centrifuged for 5 min at  $7,690\times g$ ) using a commercially available enzymatic assay kit according to the manufacturer's instructions. For the screening experiment and reproducibility experiment, the enzymatic assay kit of Roche was used (Roche Diagnostics, Machelen, Belgium) while the R-Biopharm kit was used for lactate quantification of the optimization experiment and incorporation experiment (R-Biopharm, Darmstadt, Germany). Concentrations of the bile salts taurocholic acid (TCA), glycocholic acid (GCA), taurodeoxycholic acid (TDCA), and glycodeoxycholic acid (GDCA) were determined through reversed-phase high pressure liquid chromatography (RP-HPLC; Hitachi Chromaster, Hitachi, Brussels, Belgium) with a diode array detector (DAD; VWR), using a reversed-phase C18 column (Hydro-RP, 4  $\mu$ m, 80 Å, 250  $\times$  4.6 mm, Synergi, Phenomenex BV, Utrecht, The Netherlands). The mobile phase at a flow rate of 0.7 ml/min consisted of acetonitrile (eluent A; VWR), and ultrapure HPLC-grade H<sub>2</sub>O at a pH of 2 (eluent B; VWR), with the following gradient: 0.0 min, 30% A and 70% B; 70 min, 90% A and 10% B; 71 min, 30% A and 70% B; and 75 min, 30% A and 70% B. The bile salts were detected through DAD at a wavelength of 210 nm. Sample preparation involved centrifugation of samples at  $7,690\times g$  for 5 min before storage at  $-20^{\circ}\text{C}$ . Afterwards, 500  $\mu$ l of supernatant was added to 500  $\mu$ l of methanol following centrifugation at  $7,690\times g$  for 5 min. Finally, the supernatant was filtered through a PTFE filter (0.2  $\mu$ m; VWR) prior to injection (50  $\mu$ l) onto the column. Quantification of samples was performed by using external standards.

## 2.6. Microbial community analysis

For bacterial community analysis, DNA was extracted as previously described by Boon et al. with some minor modifications (Boon et al., 2003). Homogenization was performed using a Beadblaster device (Benchmark Scientific, Edison, NJ, United States), which was conducted twice for 40 s at 6.00 m/s with a cooling period of 5 min between shakings. As an exception, DNA from samples of the final experiment was extracted *via* the ZymoBIOMICS 96 MagBead DNA Kit (Zymo Research, Irvine, CA, United States) at the KingFisher Flex Purification System (Thermo Fischer Scientific, Waltham, MA, United States) according to the manufacturer's instructions. Luminal DNA originated from pellets obtained from 1 ml sample, while mucosal DNA was extracted from 0.25 g mucin alginate agar (ileum) or mucin agar (colon).

Targeted microbial quantification was determined through quantitative polymerase chain reaction (qPCR) on a QuantStudio

5 Real-Time PCR system (Applied Biosystems, Forster City, CA, United States). Standard curves were generated from a 10-fold dilution series ranging from  $10^6$  gene copies/ $\mu$ l to 10 gene copies/ $\mu$ l. Except for qPCRs targeting Streptococcaceae and Veillonellaceae – which used PCR product –, plasmid DNA was used to generate standard curves. Each sample was run in technical triplicate and outliers were removed when standard deviation between replicates exceeded 0.5. qPCRs for following groups were performed as previously described: *Lactobacillus* spp. (Furet et al., 2009), *Bifidobacterium* spp. and *Eubacterium rectale/Clostridium coccoides* (Rinttilä et al., 2004), Bacteroidetes (Guo et al., 2008), *Faecalibacterium prausnitzii* (Sokol et al., 2009), Veillonellaceae (Rinttilä et al., 2004), Enterobacteriaceae (Nakano et al., 2003), Streptococcaceae (van den Bogert et al., 2011), Enterococcaceae (Rinttilä et al., 2004), and *Akkermansia muciniphila* (Collado et al., 2007). Illumina 16S rRNA gene amplicon libraries were generated and sequenced at BaseClear BV. In short, barcoded amplicons from the V3-V4 region of 16S rRNA genes were generated using a 2-step PCR. 10 ng genomic (g) DNA was used as template for the first PCR with a total volume of 50  $\mu$ l using the 341F (5'-CCTACGGGNGGCWGCAG-3') and the 785R (5'-GACTACHVGGGTATCTAATCC-3') primers appended with Illumina adaptor sequences. PCR products were purified, and the sizes of the PCR products were checked on Fragment analyzer (Agilent, Santa Clara, CA, United States) and quantified by fluorometric analysis. Purified PCR products were used for the second PCR in combination with sample-specific barcoded primers (Nextera XT index kit; Illumina, San Diego, CA, United States). Subsequently, PCR products were purified, checked on a Fragment analyzer (Agilent) and quantified, followed by multiplexing, clustering, and sequencing on an Illumina MiSeq with the paired-end (2 $\times$ ) 300 bp protocol and indexing. The sequencing run was analyzed with the Illumina CASAVA pipeline (v1.8.3) with demultiplexing based on sample-specific barcodes. The raw sequencing data was processed by removal of sequence reads of too low quality (only "passing filter" reads were selected) and discard of reads containing adaptor sequences or PhiX control with an in-house filtering protocol. A quality assessment on remaining reads was performed using the FASTQC quality control tool version 0.10.0. For data processing, Illumina-paired reads were merged into single reads (pseudoreads) through sequence overlap, after removal of the forward and reverse primers. Chimeric pseudoreads were removed and remaining reads were aligned to the RDP 16S gene databases. Based on the alignment scores of the pseudoreads, the taxonomic depth of the lineage is based on the identity threshold of the rank; Species 99%, Genus 97%, Family 95%, Order 90%, Class 85%, Phylum 80%.

Total bacterial cells were quantified *via* flow cytometry to convert proportional data obtained *via* 16S rRNA gene targeted Illumina sequencing to quantitative data (multiplication). Samples were 1:1-diluted in cryoprotectant and stored at  $-80^{\circ}\text{C}$  until analysis according to Hoefman et al. (2012). Upon staining with 0.01 mM SYTO24 (Life Technologies Europe NV, Merelbeke, Belgium) at room temperature for 15 min in the dark, samples

were analyzed on a BD FACSVerse (BDBiosciences, Merelbeke, Belgium) using the high flowrate setting and bacteria were separated from medium debris and signal noise by applying a threshold level of 200 on the SYTO channel. Flow cytometry data were analyzed using FlowJo, version 10.5.0.

## 2.7. Statistics

Statistically significant differences between acetate, propionate, butyrate, lactate, and bile salt concentrations were determined for each experiment separately. Significant differences on bacterial abundances were determined on absolute levels for luminal samples and relative levels for mucosal samples for the respective experiments. Statistical analysis was performed in Excel 2011 (Microsoft, Redmond, WA, United States). Two-sided t-tests were applied for comparisons between different vessels during statistical analysis of all experiments. Benjamini-Hochberg false discovery rate (FDR) was applied (with  $FDR = 0.05$ ) to correct for multiplicity issues as described previously (Lee and Lee, 2018). Principal component analysis (PCA) was performed with CLUSTVIS ([biit.cs.ut.ee/clustvis/](http://biit.cs.ut.ee/clustvis/)) using the proportional 16S rRNA gene targeted Illumina sequencing data of the 15 most abundant families in the lumen across all simulated communities supplemented with taxonomic families representing consortium genera but not being part of the top 15 most abundant families.

## 3. Results

### 3.1. Distinct environmental conditions strongly impacted bacterial composition and activity

During an initial screening experiment, four test conditions were evaluated in parallel and compared to a control colon simulation. Reactors 1 and 2 were inoculated with a synthetic consortium, while reactors 3 and 4 were inoculated with ileostomy effluent and faecal sample, respectively. Reactor 2 was distinguished from reactor 1 in that it was subjected to a longer retention time (8 h instead of 4 h). Both the inoculation strategies and retention time affected microbial colonization during the ileum simulations in terms of microbial composition and activity.

First, the validity of a qPCR panel in which 10 taxonomic groups were targeted was evaluated using an ileostomy effluent and faecal sample (Supplementary Table S1). This confirmed the presence of distinct microbial community compositions in both samples, in correspondence with literature, i.e., enrichment of Veillonellaceae, Streptococcaceae, and Enterococcaceae (and Lactobacillaceae depending on the intake of probiotics) in ileostomy samples in contrast to higher levels of Enterobacteriaceae, Akkermansiaceae, Bifidobacteriaceae, Bacteroidetes, Lachnospiraceae, and *F. prausnitzii* in the faecal sample (Supplementary Table S1), thus confirming that the qPCR

panel allowed to make representative statements on whether a microbial community is more ileum or colon-like.

This allowed to conclude that the steady-state communities of the screening experiments upon 2 weeks of colonization were largely affected by the inoculation strategy, with more ileum-like communities being obtained upon inoculation with the synthetic consortium. Indeed, the latter (upon applying a transit time of 4 h) resulted in a community dominated by Veillonellaceae [ $8.73 \pm \log(\text{copies/ml})$ ], Streptococcaceae [ $8.94 \log(\text{copies/ml})$ ], Enterococcaceae [ $9.16 \log(\text{copies/ml})$ ] and to a lesser extent, Lactobacillaceae [ $6.81 \log(\text{copies/ml})$ ] (Table 2). Strikingly, incubating the same consortium at increased retention time (8 h) induced dominance by Enterococcaceae [ $9.52 \log(\text{copies/ml})$ ] and Lactobacillaceae [ $7.53 \log(\text{copies/ml})$ ] at the expense of Veillonellaceae [ $3.50 \log(\text{copies/ml})$ ] and Streptococcaceae [ $3.46 \log(\text{copies/ml})$ ]. Further, inoculation with ileostomy effluent or faecal slurry increased abundances of colon-associated taxonomy groups such as Enterobacteriaceae [ $6.79$  and  $7.15 \log(\text{copies/ml})$ , respectively], Akkermansiaceae [ $4.45$  and  $4.38 \log(\text{copies/ml})$ , respectively], Bifidobacteriaceae [ $8.38$  and  $8.40 \log(\text{copies/ml})$ , respectively], Bacteroidetes [ $7.83$  and  $7.96 \log(\text{copies/ml})$ , respectively], *C. coccoides*/*E. rectale* [ $8.64$  and  $8.90 \log(\text{copies/ml})$ ], and *F. prausnitzii* [ $5.91$  and  $7.41 \log(\text{copies/ml})$ ]. The latter more closely resembled the stable community composition in the control colon vessel.

These drastic differences in microbiota composition significantly affected microbial activity. In a first aspect, inoculation with the synthetic consortium significantly lowered total SCFA levels in the reference condition ( $38.6 \pm 1.1 \text{ mM}$ ) and even further upon increased retention time ( $6.5 \pm 0.2 \text{ mM}$ ) as compared to the reference conditions inoculated with ileostomy effluent and faecal slurry ( $64.5 \pm 1.1 \text{ mM}$  and  $61.7 \pm 2.3 \text{ mM}$ , respectively), while total SCFA levels were the highest in the control colon ( $69.4 \pm 1.9 \text{ mM}$ ; Figure 2A). In a second aspect, steady-state lactate levels were similarly low among all reference conditions and control colon, which might indicate efficient cross-feeding of lactate to, e.g., propionate and/or butyrate. In contrast, the prolonged retention time significantly increased lactate, thereby suggesting impaired cross-feeding (Figure 2B). In addition, kinetic sampling during 8 h upon receiving fresh nutritional medium on day 14 of the experiment revealed an initial boost in lactate production followed by lactate consumption and a concomitant production of acetate and propionate for the reference consortium condition (Figure 3). Although to a lesser extent, this kinetic profile was also observed for the reference conditions inoculated with ileostomy effluent and faecal slurry. In contrast, entrance of nutritional medium into the condition with extended retention time increased lactate production but lacked the consequential consumption of lactate and concomitant acetate and propionate production (corresponding with the low Veillonellaceae levels upon increased retention time). The control colon showed a

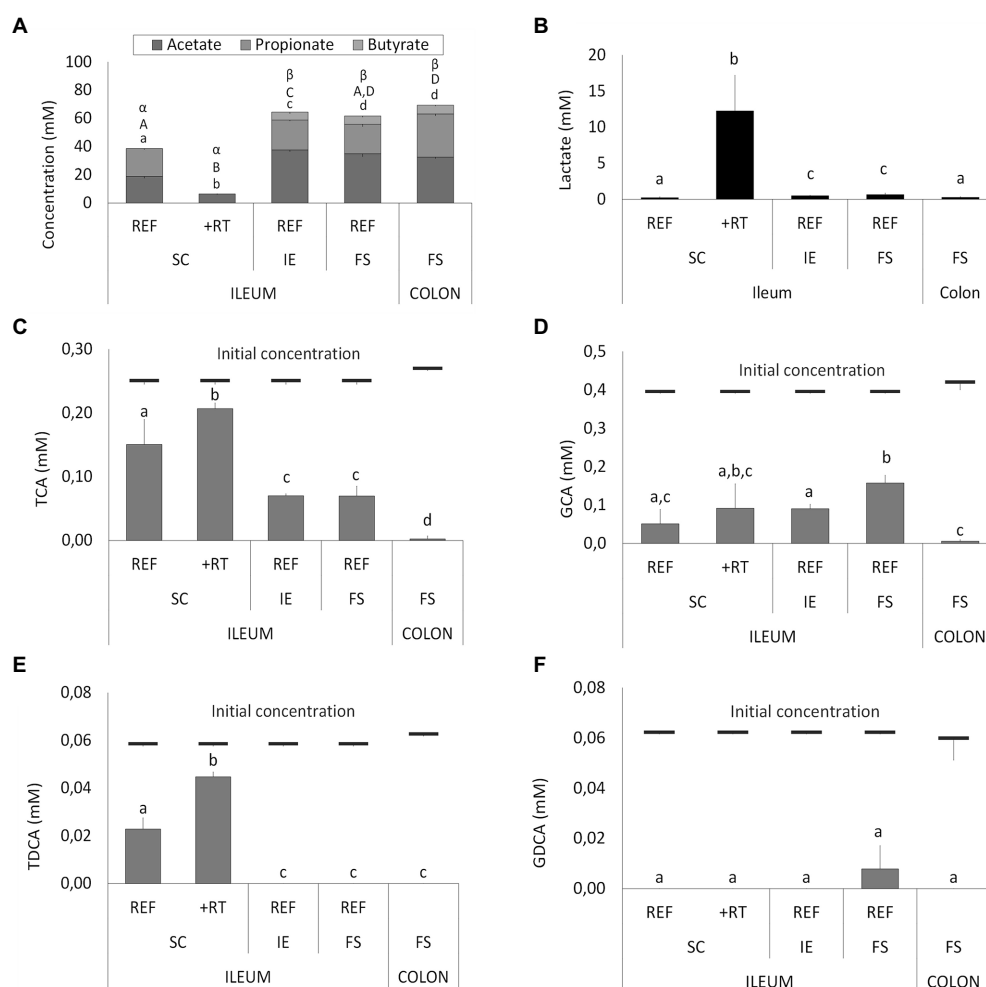


FIGURE 2

(A) Average short-chain fatty acids (SCFA) concentrations (mM) from days 14, 16, 17, and 18 in different ileum simulation test conditions. Values that significantly differ from each other are indicated with different letters (a, b, c, d for acetate; A, B, C, D for propionate, and  $\alpha$ ,  $\beta$  for butyrate). (B) Average lactate concentrations (mM) in different test conditions. Values that significantly differ from each other are indicated with different letters (a, b, c). (C–F) Average bile salt concentrations in different test conditions. Red bars indicate the initial concentration of the respective bile salt in the simulation upon administration of fresh nutritional medium. For ileum test conditions, either reference conditions (REF) or increased retention time (+RT) was tested with different inoculation strategies (SC, IE, and FS). For the colon, parameters from M-SHIME® technology were applied. SC=synthetic consortium; IE=ileostomy effluent; FS=faecal slurry; TCA=taurocholic acid; GCA=glycocholic acid; TDCA=taurodeoxycholic acid; GDCA=glycodeoxycholic acid.

modest increase in acetate, propionate, and butyrate concentrations over time while no increase in lactate level was observed.

Furthermore, different conditions affected bile salt metabolism both between the test conditions and as compared to the control colon (Figures 2C–F). The latter showed complete deconjugation of TCA, GCA, TDCA, and GDCA, while said bile salts were only partially deconjugated in the ileal vessels. Lowest bile salt conversions were observed upon inoculation with the synthetic consortium, and more specific, in combination with an increased retention time.

Overall, from all tested conditions, the synthetic consortium inoculation under reference conditions was selected as most closely representing the *in vivo* ileal community (Booijink et al.,

2010; Zoetendal et al., 2012; El Aidy et al., 2015; Cieplak et al., 2018; Seekatz et al., 2019).

### 3.2. The selected condition allows establishment of a stable and reproducible community

Next, the selected reference condition from the screening experiment was performed in triplicate to validate reproducibility of the simulation.

Luminal SCFA profiles were stable over time (87, 86, and 88% for replicates 1, 2, and 3, respectively) and highly reproducible (95%) across the multiple replicate vessels of the selected condition



(Figure 4A). Lactic acid levels were  $1.40 \pm 0.69$  mM on average and did not differ significantly between replicate simulations (data not shown). 16S rRNA gene targeted Illumina sequencing demonstrated a nearly identical community composition within the replicate vessels at different timepoints, thereby confirming both stability and reproducibility of the bacterial community (Figure 4B). Luminal communities were dominated by the genera *Streptococcus* ( $41.2 \pm 2.5\%$ ), *Veillonella* ( $30.7 \pm 2.0\%$ ), *Enterococcus* ( $11.2 \pm 2.7\%$ ), and *Clostridium* ( $8.4 \pm 1.3\%$ ). The genera *Lactobacillus* ( $2.6 \pm 0.8\%$ ), *Blautia* ( $1.6 \pm 0.4\%$ ), *Faecalibacterium* ( $0.7 \pm 0.2\%$ ), and *Prevotella* ( $0.1 \pm 0.1\%$ ) were present at lower abundances.

### 3.3. Reduction of bacterial concentration by adapting ileal nutritional medium

Total cell concentrations were estimated from qPCR measurements based on a post-hoc comparison between flow cytometry and qPCR analyses. Based on this correlation, qPCR analysis during the screening experiment pointed out that levels above  $10^9$  cells/ml in the ileum simulations were obtained, which was considered too high versus the *in vivo* situation where levels

in the range of  $10^8$  cells/ml have been reported (Booijink et al., 2007). Therefore, with the aim of reducing the bacterial load in the ileum simulation, adapted ileal nutritional medium (30%) was compared to the initial ileal nutritional medium (100%) in two identically configured vessels. Importantly, bacterial cell quantification through flow cytometry demonstrated an approximately 3-fold reduction in total bacterial density upon administration of the adapted ileal nutritional medium ( $2.53$  and  $7.58 \times 10^8$  cells/ml at the beginning and end of the feeding cycle, respectively) as compared to the initial ileal nutritional medium ( $6.65$  and  $19.95 \times 10^8$  cells/ml at beginning and end of the feeding cycle, respectively; Figure 5D).

This decreased cell density did not alter microbial activity or community composition. Indeed, while the adapted medium (30%) significantly ( $p = 2 \times 10^{-8}$ ) reduced total SCFA concentration, it did not alter the acetate/propionate/butyrate ratio (approximately 55/45/0; Figure 5A). Lactate was significantly ( $p < 10^{-5}$ ) higher – but still minimal – in the adapted medium ( $0.025 \pm 0.003$  mM) than the initial medium ( $0.007 \pm 0.002$  mM). 16S rRNA gene targeted Illumina sequencing revealed a similar microbial composition in both the luminal and mucosal regions between both nutritional media (Figures 5B,C). Lowered nutrient levels resulted in a mild proportional increase of *Clostridium*

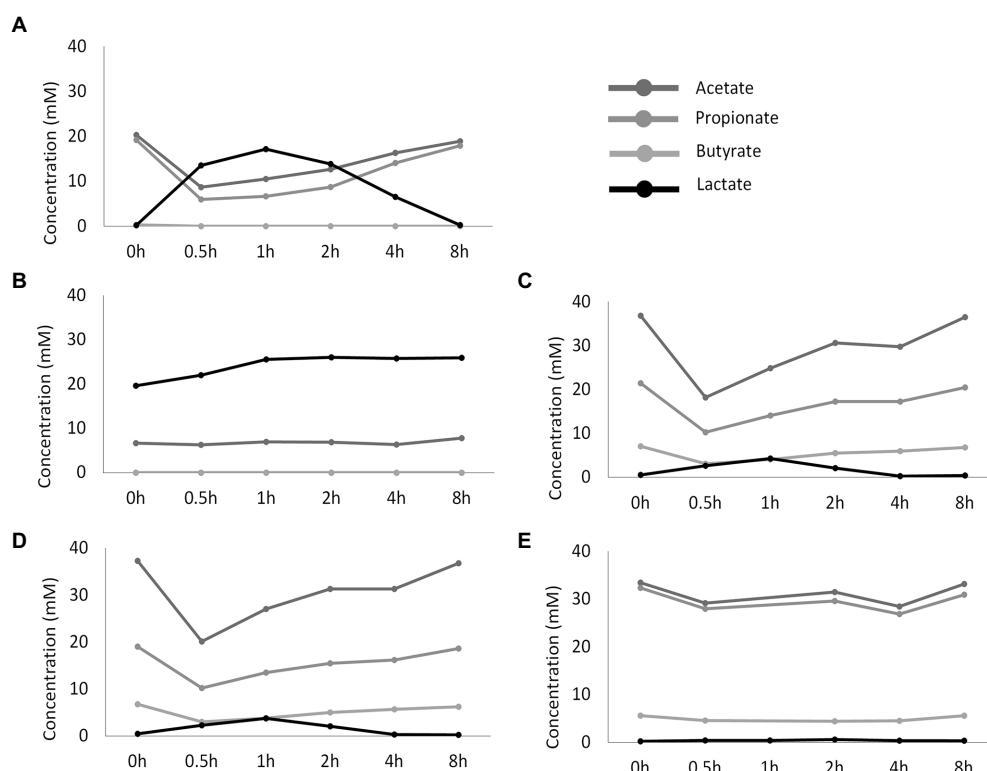


**FIGURE 3**  
Temporal profile of SCFA and lactate concentrations (mM) upon administration of fresh nutritional medium to different test conditions comprising a steady-state community: (A) reference conditions inoculated with synthetic consortium; (B) doubled retention time inoculated with synthetic consortium; (C) reference conditions inoculated with ileostomy effluent; (D) reference conditions inoculated with faecal slurry; (E) M-SHIME® proximal colon simulation.

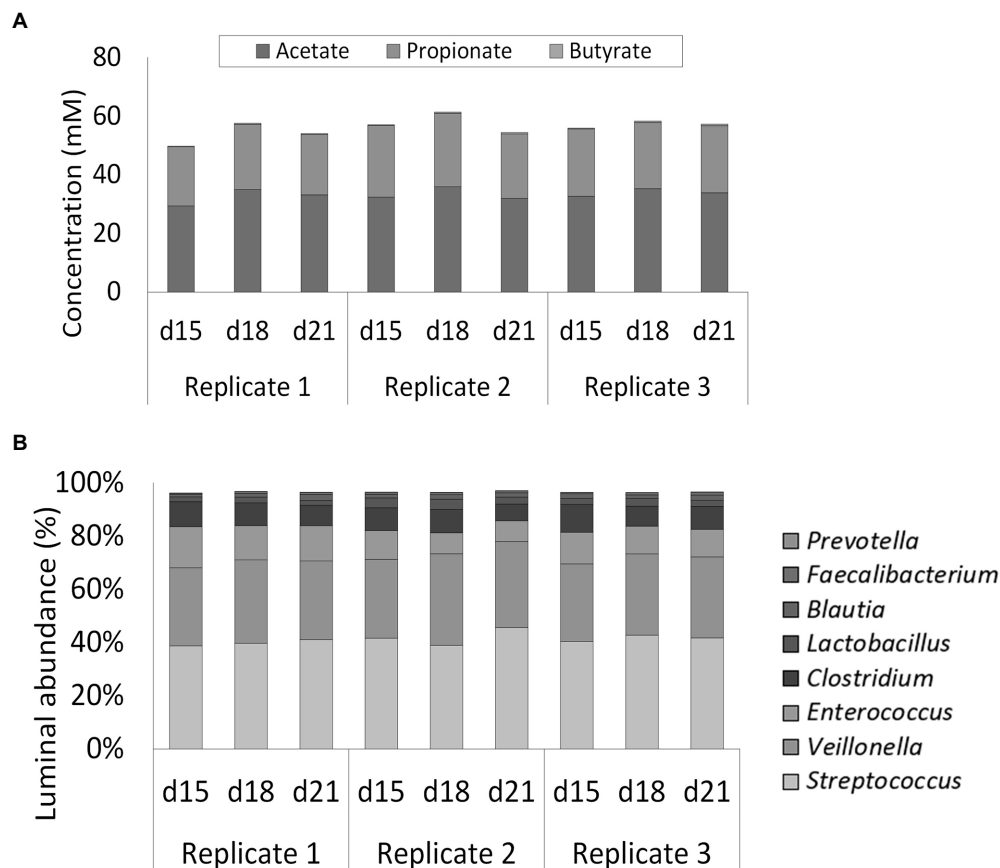


FIGURE 4

(A) Short-chain fatty acids (SCFA) concentrations (mM) in three replicate ileum simulations at three different timepoints (days 15, 18, and 21 after inoculation). All replicates represented the reference conditions inoculated with synthetic consortium. (B) Average genus level relative microbial community composition of three ileum simulation replicates incubated under reference conditions after inoculation with synthetic consortium at three different timepoints (days 15, 18, and 21 after inoculation). Genera included in the consortium account for nearly 100% of the steady-state community. The reference *Lactobacillus* is considered to include both the genera *Limosilactobacillus* and *Ligolactobacillus*.

(12.5% vs. 6.8%) and *Enterococcus* (16.7% vs. 8.7%) at the expense of *Streptococcus* (46.7% vs. 55.6%) and *Veillonella* (21.8% vs. 26.7%). Hence, where streptococci and *Veillonellae* accounted for more than 80% of the total community in the vessel receiving the 100% nutritional medium, these taxonomic groups represented approximately 65% of the community in the vessel receiving the adapted ileal nutritional medium (30%). Furthermore, *Lactobacillus* (0.2% vs. 0.2%), *Blautia* (0.1% vs. 0.1%), *Faecalibacterium* (<0.1% vs. <0.1%) and *Prevotella* (<0.1% vs. <0.1%) were not impacted. Together, genera comprised in the synthetic consortium accounted for more than 98% of the simulated community (98.0 and 98.2% for adjusted and initial nutritional medium, respectively). The missing approximately 2% relative abundance is represented by *Lactococcus* (1.2% vs. 1.3% for adjusted and initial nutritional medium, respectively), *Hungatella* (0.20% vs. 0.15%, for adjusted and initial nutritional medium, respectively) and a myriad of low-abundant genera (<0.1%; data not shown).

### 3.4. Integration of ileum simulation in M-SHIME® model

During the final experiment, the ileal simulation was integrated into the established M-SHIME® model which simulates colonic microbiota. For this, two arms for each of two donors were run in parallel. Per donor, one arm comprised of an ileum, proximal colon, and distal colon, whereas the second arm consisted of a proximal and distal colon only.

As illustrated by a PCA, based on the 15 most abundant families across the lumen of all reactors combined with families to which the genera of the ileal consortium belong but are not within the top 15 most abundant families, colon-region specific communities colonize the M-SHIME® model (Figure 6). Integration of an ileum simulation in the M-SHIME® maintained this colon-region specificity, thereby indicating that a preceding ileum does not disturb subsequent simulated colonic

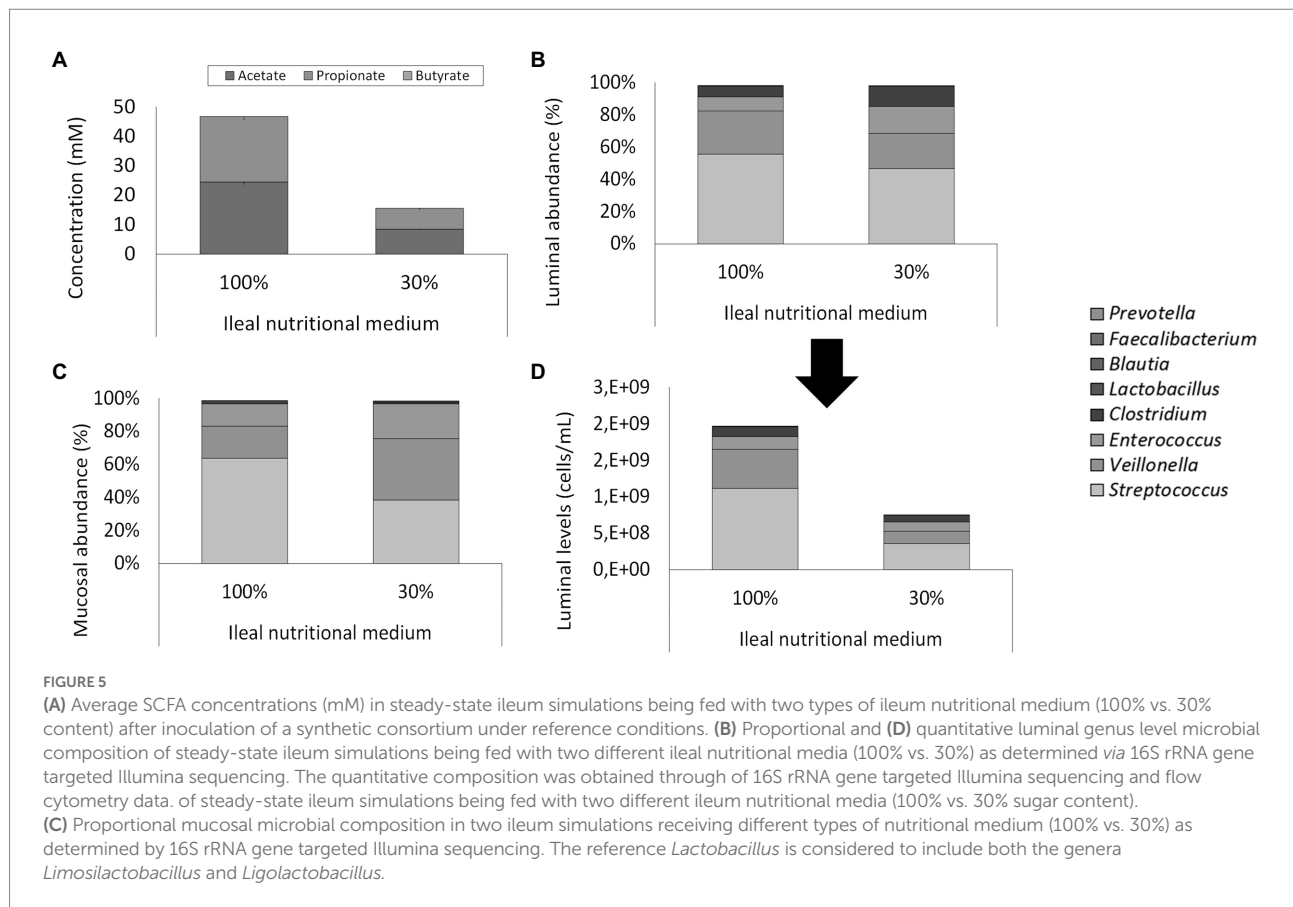


**TABLE 2** Average absolute levels [ $^{10}\log(16S\text{ rRNA copies/ml})$ ] of 10 different taxonomic groups (as determined with group-specific qPCR protocols) that, according to literature, colonize the small intestine and/or colon, when incubated in reactors under ileal or colonic conditions.

Region of colonization according to literature	Microbial group	Ileum				Colon
		Consortium		Ileostomy effluent	Faecal slurry	Faecal slurry
		REF	↑ RT			
Small intestine	Veillonellaceae	<b>8.73<sup>a</sup></b>	3.50 <sup>c</sup>	3.97 <sup>b,c</sup>	<LOQ <sup>c</sup>	4.84 <sup>b</sup>
	Streptococcaceae	<b>8.94<sup>a</sup></b>	3.46 <sup>c</sup>	7.81 <sup>b</sup>	6.94 <sup>c</sup>	5.19 <sup>d</sup>
	Enterococcaceae	<b>9.16<sup>a</sup></b>	<b>9.52<sup>a</sup></b>	7.76 <sup>b</sup>	7.03 <sup>b</sup>	5.42 <sup>c</sup>
	Lactobacillaceae	6.81 <sup>b</sup>	<b>7.53<sup>a</sup></b>	3.49 <sup>c</sup>	3.51 <sup>c</sup>	3.71 <sup>c</sup>
Small intestine – colon	Enterobacteriaceae	<LOQ <sup>c</sup>	<LOQ <sup>c</sup>	<b>6.79<sup>a,b</sup></b>	<b>7.15<sup>a</sup></b>	6.31 <sup>b</sup>
Colon	Akkermansiaceae	<LOQ <sup>c</sup>	<LOQ <sup>c</sup>	<b>4.45<sup>a,b</sup></b>	<b>4.38<sup>a</sup></b>	3.93 <sup>b</sup>
	Bifidobacteriaceae	<LOQ <sup>c</sup>	<LOQ <sup>c</sup>	<b>8.38<sup>a</sup></b>	<b>8.40<sup>a,b</sup></b>	7.65 <sup>b</sup>
	Bacteroidetes	4.70 <sup>c</sup>	<LOQ <sup>c</sup>	7.83 <sup>b</sup>	7.96 <sup>b</sup>	<b>8.42<sup>a</sup></b>
	<i>C. coccoides</i> / <i>E. rectale</i>	<LOQ <sup>b</sup>	3.47 <sup>b</sup>	<b>8.64<sup>a</sup></b>	<b>8.90<sup>a</sup></b>	<b>8.76<sup>a</sup></b>
	<i>F. prausnitzii</i>	<LOQ <sup>c</sup>	<LOQ <sup>c</sup>	5.91 <sup>b</sup>	<b>7.41<sup>a</sup></b>	5.12 <sup>b</sup>

While the colonic simulations started with a faecal inoculation, the ileal simulations involved inoculation of a consortium, ileostomy effluent or faecal slurry. While the standard residence time (RT) was 4 h for the ileal simulations, one condition involved an increased residence time of 8 h. Values that are significantly different from one another are indicated with a different letter (a, b, c, d, e). Values for the condition(s) that resulted in the highest levels measured for a given taxonomic group are indicated in bold. LOQ =  $3.31 \times 10^3 \log(\text{cells/ml})$ . REF, reference conditions.

communities. Moreover, inclusion of the ileum microbiota contributed to an increased diversity (Figure 7) as well as an increased species richness (data not shown) in the *in vitro* gut

model for both donors, reflecting more what has been reported happening *in vivo*. Furthermore, it was observed that distal colons more closely resembled the faecal inocula when preceded by an

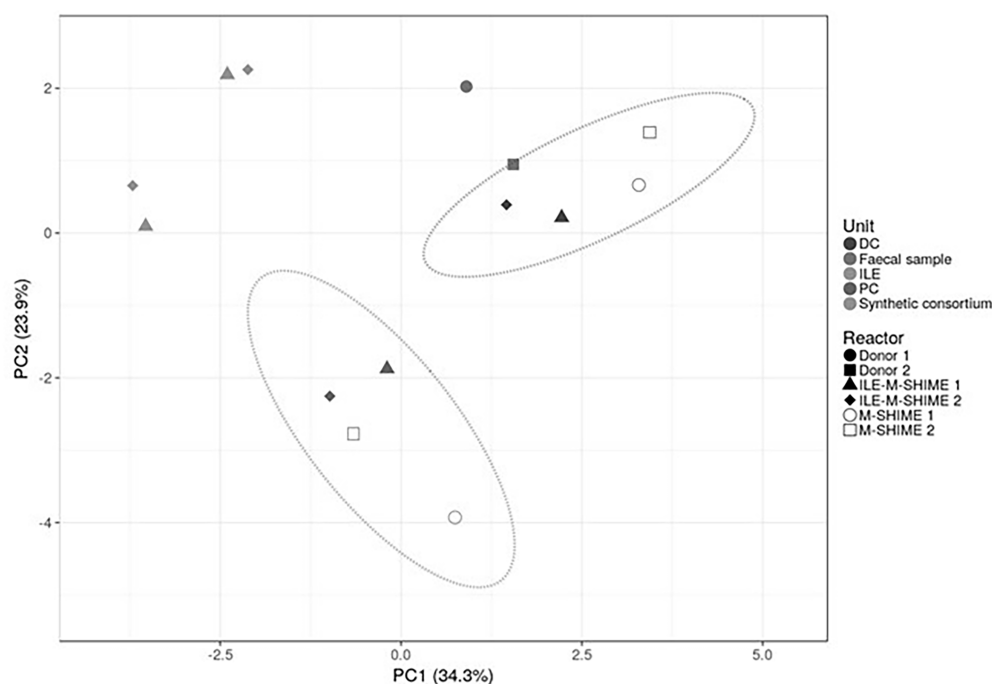


FIGURE 6

Principal component analysis (PCA) of microbiota based on proportional 16S rRNA gene targeted Illumina sequencing data. A total of 16 taxonomic families was considered, i.e., the 15 most abundant families supplemented with taxonomic families representing consortium genera not being part of the top 15 most abundant families. Percentage values at the axes indicate contribution of the principal components to the explanation of total variance in the data set. The impact of integrating an ileum before the PC and DC (ILE-M-SHIME®) was compared to the standard M-SHIME® for two donors.

ileum as compared to distal colons without preceding ileum (Figure 6).

Although integration of an ileum reactor increased initial lactate levels in the proximal ( $0.84 \pm 0.14$  mM to  $2.20 \pm 0.06$  mM) and distal ( $0.22 \pm 0.04$  mM to  $0.32 \pm 0.01$  mM) colons, lactate was more rapidly consumed in ileum-preceded colon reactors. SCFA analysis confirmed both ileum simulations to show nearly identical SCFA profiles (Figure 8). The total SCFA concentrations were  $13.5 \pm 0.7$  mM and  $13.9 \pm 0.5$  mM, and the acetate/propionate/butyrate ratios were 50/49/1 and 54/45/2 in the ileum vessels of reactor units 1 and 2, respectively. Incorporation of an ileum vessel did not impact the total SCFA concentration in proximal ( $54.8 \pm 3.8$  mM vs.  $53.1 \pm 6.3$  mM with or without preceding ileum, respectively) or distal colon vessels ( $73.0 \pm 4.2$  mM vs.  $72.5 \pm 2.1$  mM with and without preceding ileum, respectively). However, preceding ileum simulations impacted the proportional SCFA profiles in the subsequent colon compartments. For donor 1, the preceding ileum increased butyrate concentration in both colon vessels at the expense of acetate and propionate (SCFA ratios changed from 58/22/21 to 51/17/32 for the PC, and from 67/21/12 to 62/18/19 for the DC). Nonetheless, for donor 2, SCFA ratios remained constant (from 52/14/34 to 54/11/35 for the PC, and from 63/17/20 to 64/16/20 for the DC).

Regarding microbial composition, steady-state communities in the lumen and mucus of both ileum simulations consisted

nearly entirely of genera included in the synthetic consortium ( $98.8 \pm 0.4\%$  and  $99.3 \pm 0.2\%$ , and  $97.3 \pm 0.3\%$  and  $98.8 \pm 0.2\%$  for the lumen and mucus of ileum vessel of unit 1 and 2, respectively), indicating absence of colonization by contaminating strains (Figures 9A–C). In the ileum vessels of reactor units 1 and 2, stable luminal communities were dominated by the genera *Veillonella* ( $30.6 \pm 4.6\%$  and  $24.3 \pm 6.8\%$ , respectively), *Streptococcus* ( $13.0 \pm 5.0\%$  and  $27.8 \pm 7.0\%$ , respectively), and *Enterococcus* ( $55.1 \pm 1.6\%$  and  $38.5 \pm 1.1\%$ , respectively).

Integration of an ileum simulation into the M-SHIME® technology did not affect bacterial densities in subsequent proximal and distal colon reactors. Moreover, incorporation of the ileum simulation did not majorly affect the luminal bacterial community composition in neither the proximal nor distal colon (Supplementary Table S1). Minor changes included, for donor 1, a reduction in Bacteroidaceae (PC), Selenomonadaceae (PC), Synergistaceae (DC), and Akkermansiaceae (DC), while the levels of Enterococcaceae (PC and DC) and Streptococcaceae (PC and DC) were increased. Although not significantly, Ruminococcaceae levels were increased in the PC upon incorporation of an ileum simulation. For donor 2, Streptococcaceae and Enterococcaceae were increased in both the PC and DC, while the Ruminococcaceae were significantly increased in the PC and significantly decreased in the



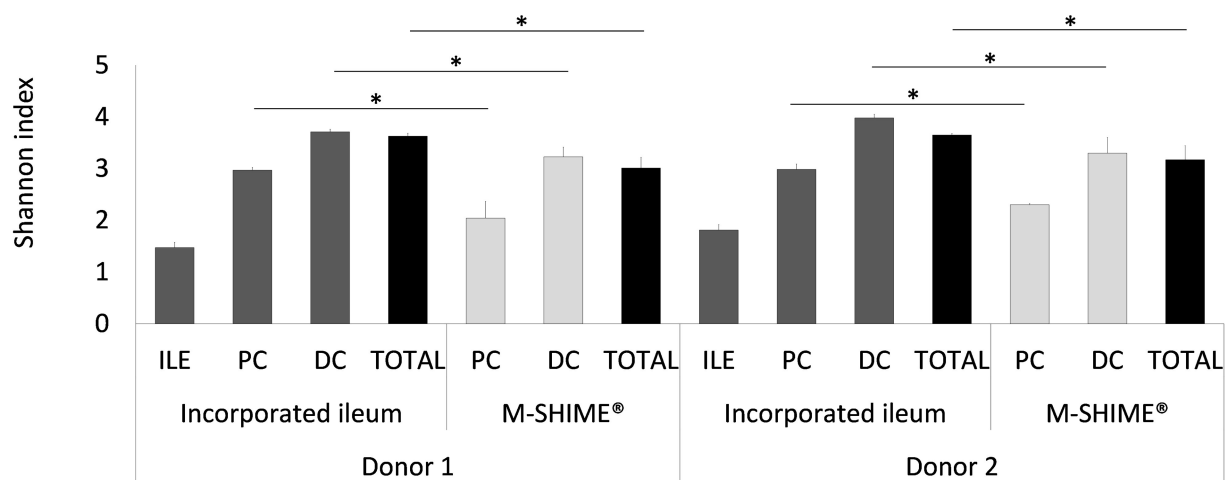


FIGURE 7

Shannon diversity indices based on (OUT's) in ileum simulation, and colon vessels whether or not preceded by an ileum simulation (ILE-M-SHIME® vs. M-SHIME®) as calculated from 16S rRNA gene targeted Illumina sequencing data. Diversity estimates were determined for separate vessels and total reactor units for two donors at three different timepoints (days 11, 13, and 14 after inoculation). Total diversity indices that were significantly different from each other, are indicated with an asterisk (\*). Only OTU's with >25 reads were considered.

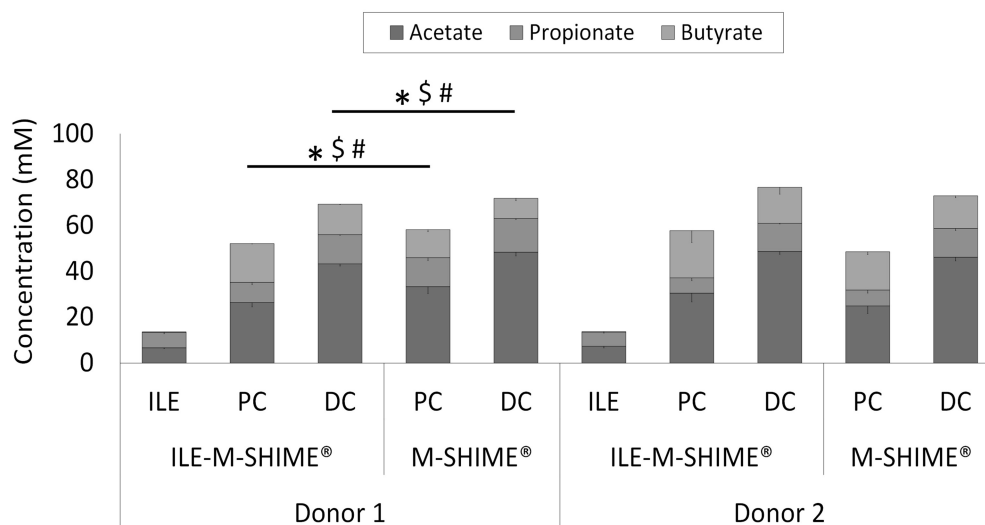


FIGURE 8

Average SCFA concentrations (mM) in steady-state colon vessels whether or not preceded by an ileum simulation (ILE-M-SHIME® vs. M-SHIME®, respectively). Symbols indicate significant differences in acetate (\*), propionate (\$) or butyrate (#) between corresponding region simulations of the same donor. ILE=ileum; PC=proximal colon; DC=distal colon.

DC. Changes in mucosal community compositions were less pronounced.

## 4. Discussion

The present study focused on the development of a stable and reproducible long-term *in vitro* model of the ileal microbiota that is representative for the *in vivo* situation. After its successful

development as a stand-alone model, the simulation was integrated in the M-SHIME® model that simulated up till now only the colonic microbiota, thereby further increasing the relevance of the latter model.

First, the established simulated ileal bacterial community after 2 weeks of incubation under reference conditions, involving amongst other factors inoculation with a synthetic consortium, application of a short retention time (4h) and a nutritional medium rich in simple sugars, was relevant for the *in vivo* situation

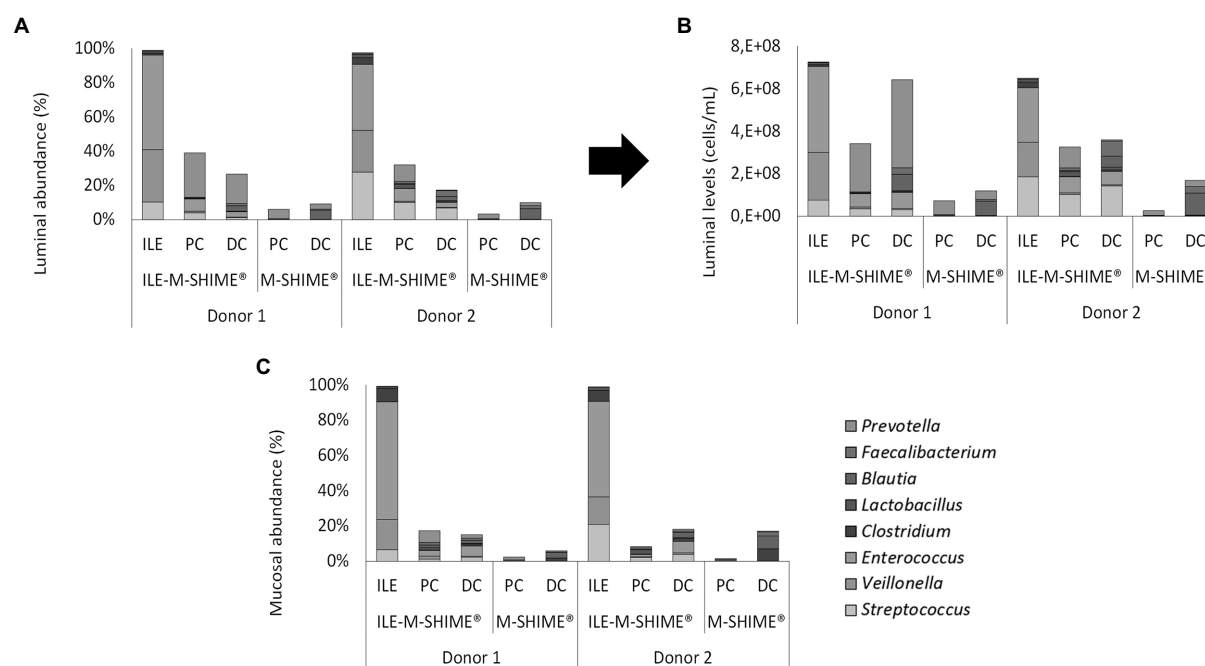


FIGURE 9

(A) Proportional and (B) quantitative composition of the luminal and mucosal (C) community in steady-state colon simulations whether or not preceded by an ileum simulation (ILE-M-SHIME® vs. M-SHIME®, respectively) as determined by 16S rRNA gene targeted Illumina sequencing. Ileum vessels were inoculated with a synthetic consortium under reference conditions. Quantitative compositions were obtained through combination of 16S rRNA gene targeted Illumina with flow cytometry data. Only genera included in the synthetic consortium are presented. The reference *Lactobacillus* is considered to include both the genera *Limosilactobacillus* and *Ligolactobacillus*.

with the genera *Streptococcus*, *Veillonella*, and *Enterococcus* prevailing in the model. Enrichment of these genera is in line with literature regarding microbial composition of ileostomy effluent which has often been used as a proxy for investigating the ileal community (Collado et al., 2007; Booiijink et al., 2010; van den Bogert et al., 2011, 2013; Zoetendal et al., 2012; Dlugosz et al., 2015; El Aidy et al., 2015; Chung et al., 2016). Abundances of selected consortium members well-above detection limit after 2 weeks of incubation confirmed the relevance of the applied environmental conditions. The observation that increasing the retention time to 8 h impaired colonization of *Veillonella* and *Streptococcus* members, shows the complexity of identifying the correct environmental conditions. It is hypothesized that this community shift can be attributed to prolonged metabolism of less favorable sugars when retention time is increased to 8 h, thereby promoting colonization of specific consortium members and potentially stimulating build-up of inhibitory metabolites and associated product inhibition. This would be in contrast with the reference conditions where a retention time of 4 h is potentially too short for fermentation of less favorable sugars, thereby stimulating consortium members that thrive on the most-favored carbon source (e.g., glucose). On the other hand, the reference condition did not prevent colonization of colon-like microbial groups upon inoculation with a faecal sample or ileostomy effluent, suggesting further potential for finetuning the environmental conditions by, e.g., inclusion of a fill-and-draw mechanism or incorporating

colon-to-ileum reflux simulations as attempted recently (Roussel et al., 2020). Nonetheless, the current model enabled the establishment and maintenance of a representative bacterial community in terms of composition and, importantly, quantity.

The microbial composition showed an ileum-relevant microbial activity. More specific, upon entrance of fresh nutritional medium, lactate levels rapidly increased during the first 30 min, after which acetate and propionate levels increased while lactate was consumed, thus suggesting bacterial cross-feeding interactions. The initial boost in lactate production was likely attributed to the *Streptococcus*, *Enterococcus*, and *Lactobacillus* species which are known to produce lactate upon consumption of simple sugars (Hoefman et al., 2012; Lee and Lee, 2018). In turn, successive cross-feeding of lactate into acetate and propionate was likely ascribed to high abundances of *Veillonella* species (Distler and Kröncke, 1981; Arif et al., 2008). The relatively short retention time (4 h) is thought to prevent substantial butyrate production in the ileum, as is supported by low abundances of slow-growing *Faecalibacterium* and *Clostridium*. Increased retention time strongly increased lactate production and prevented cross-feeding interactions. The latter might be explained by a prolonged utilization of less-favorable carbohydrates upon glucose depletion. Genera such as *Enterococcus* and *Lactobacillus* are known to be more flexible in carbohydrate fermentation, thereby being favored by an increased retention time. Higher abundances of these genera could result in a boosted production of inhibiting metabolites such as lactate and

ethanol, which might hamper the proliferation of, e.g., *Streptococcus* and *Veillonella*. Nonetheless, further investigation of this hypothesis is crucial for unraveling the mechanisms through which the increased retention time impacts the simulated community. In turn, inoculation with ileostomy effluent or faecal slurry prevented substantial buildup of lactate concentrations, which is likely explained by higher cross-feeding efficiency and lower lactate-producing capacity of the colon-like communities in these vessels. Furthermore, the established community under selected reference conditions and the condition with increased retention time only partially deconjugated the bile salts TCA, TDCA, GCA, and GDCA in the model. *In vivo*, most of the bile salts are reabsorbed in the ileum (enterohepatic circulation) but some are biotransformed by the gut microbiota. This biotransformation involves a first step of deconjugation (ileum), after which the deconjugated bile acid can be dehydroxylated and/or reconstituted in the colon. These bioconversions facilitate transport and improve functionalities and signaling properties of the bile salts. Hence, what observed corresponds to what happens *in vivo*, where unabsorbed bile salts are converted and/or deconjugated only partially in the ileum region (Hofmann, 1999; Martinez-Augustin and Sanchez de Medina, 2008). Opposed thereto, conditions inoculated with ileostomy effluent or faecal slurry more closely resembled the bile salt metabolism as observed in the control colon, i.e., nearly complete deconjugation and conversion of primary bile salts. Although not confirmed in the present study, these observations are likely to be linked to a limited presence of genes encoding for bile salt hydrolase and 7- $\alpha$ -dehydroxylase in the gene pool of the established ileum community as compared to the colon community. Overall, the optimized ileum simulation allowed mimicking of metabolic cross-feeding interactions between key members of the consortium while revealing a representative bile salt metabolism, thus suggesting that the model might be a useful tool in future research to study the microbial metabolite fluxes in the highly dynamic small intestinal environment (Seekatz et al., 2019).

The selected simulation strategy allowed the recreation of a highly reproducible microbial composition and activity within independent experiments. Nevertheless, between different experiments, minor shifts in relative bacterial profiles were detected although these did not appear to impact metabolic functionality. For instance, the genera *Streptococcus*, *Enterococcus*, and *Veillonella* accounted for approximately 85% of the ileal community (41, 11, and 31%, respectively) during the reproducibility experiment, while during the final experiment, combined relative abundances of the *Streptococcus*, *Enterococcus*, and *Veillonella* genera accounted for roughly 95% with *Streptococcus* being less abundant than *Enterococcus* (on average, 19, 47, and 28%, respectively). It is hypothesized that these compositional differences could follow from the reduced sugar concentration in the nutritional medium which was only 30% of the sugar content from the reproducibility experiment. In particular, reduced glucose administration might have expedited the diauxic shift towards less favorable sugars, thereby relatively

stimulating consortium members that more efficiently metabolize such less-favorable sugars (e.g., *Enterococcus*). Nonetheless, further research is necessary in order to confirm these hypotheses.

Reducing bacterial densities in the ileum simulation increased biological relevance of the simulation and enabled integration of the ileum into the M-SHIME® technology. Feeding the ileum vessel with adapted ileal nutritional medium (30%) reduced the total bacterial load 3-fold as compared to the model fed with the initial ileal nutritional medium (100%). On average, the bacterial load comprised 2.53 and  $7.58 \times 10^8$  cells/ml (at beginning and end of the feeding cycle, respectively) which is slightly higher than the *in vivo* levels of  $10^7$ – $10^8$  cells/ml being reported (Kastl et al., 2020). However, it was already hypothesized that actual *in vivo* levels are substantially higher than what is being reported due to the bias of the fasted state of patients upon sampling (Zoetendal et al., 2012; El Aidy et al., 2015; Villmones et al., 2018, 2020). This is illustrated by the observation of higher bacterial densities in samples from ileostomists after intake of carbohydrate-rich food. As such, it was hypothesized that ileal bacterial levels might fluctuate locally upon passage of nutrients, with bacterial loads increasing upon prolonged interaction between nutrient rich chyme and bacteria. Nonetheless, the optimized bacterial load in the current model allows studying metabolic shifts and community dynamics, whereas lower bacterial levels would likely result in shifts that are too close to the limit of quantification to allow proper investigation of induced changes. Overall, after optimization of the bacterial load, the latter more closely mimicked *in vivo* levels of  $10^7$ – $10^8$  cells/g and facilitated integration of the ileum simulation into the M-SHIME® technology.

Although the M-SHIME® model has been thoroughly validated and is known to reliably represent *in vivo* communities of both proximal and distal colon communities (Van den Abbeele et al., 2010), incorporation of the ileum model into the M-SHIME® seemed to further increase its biological relevance. First, inclusion of a bacterial community resembling the ileal microbiota according to criteria elaborated above, as such already mimics the *in vivo* situation more closely. Second, a preceding ileum tended to increase the observed number of species and diversity. Presumably, the preceding ileum incubation provides metabolites and substrates to the colon regions that support growth of otherwise washed-out species. Despite high recovery rates of bacterial strains between faecal samples and stabilized communities using the M-SHIME®, some taxonomic groups appear to be less effective at colonizing the conventional SHIME® model. For instance, Ruminococcaceae are often targeted as a health marker since they encompass health-promoting species like *F. prausnitzii*. However, Ruminococcaceae are typically underrepresented in especially the proximal (or ascending) colon of the M-SHIME® as compared to the faecal sample used as inoculum (Van den Abbeele et al., 2010). Inclusion of the ileum model increased the abundance of Ruminococcaceae in the proximal colon of both donor 1 and 2 as compared to the respective simulations without preceding ileum microbiota. This could be attributed to the influx of specific metabolic products (e.g., acetate) originating from the ileum, thereby creating a

stimulating niche for Ruminococcaceae. Such metabolic interactions might have contributed to the observation that samples derived from the distal colon of the SHIME® with preceding ileum clustered more closely to the faecal inocula than samples from the distal colon from the SHIME® without preceding ileum. Development of the ILE-M-SHIME® model can therefore further increase the relevance of long-term *in vitro* simulations of the colonic microbiota using the SHIME® technology.

## 5. Conclusion

In conclusion, the present study describes the development of a stable, reproducible, and representative long-term *in vitro* simulation of a human ileal microbial community that can be incorporated in the established M-SHIME® technology for the human colonic microbiota. Further studies will be needed to elucidate the role of this specific microbial community in influencing digestibility, drug stability and nutrient absorption. Although not replacing *in vivo* experimental studies, it is suggested that this model can serve as a primary screening method to reveal insights into the ileal microbiota, its interaction with therapeutics, and stimulate development of more efficient treatment methods.

## Data availability statement

The data presented in the study are deposited in the NCBI repository, accession number PRJNA940490 (link: <https://www.ncbi.nlm.nih.gov/bioproject/PRJNA940490>).

## Author contributions

SD, FM, Bv, MM, TV, MK, and PV developed the study concept. SD carried out the experiment and collected the data, except for the sequencing data that were generated by WP, Bv, and EK. SD, FM, and PA evaluated the data and wrote the manuscript, which was then proofread and approved by Bv, MM, TW, and MK. All authors contributed to the article and approved the submitted version.

## References

- Arhan, P., Devroede, G., Jehannin, B., Lanza, M., Faverdin, C., Dornic, C., et al. (1981). Segmental colonic transit time. *Dis. Colon Rectum* 24, 625–629. doi: 10.1007/BF02605761
- Arif, N., Do, T., Byun, R., Sheehy, E., Clark, D., Gilbert, S. C., et al. (2008). *Veillonella rogosae* sp. nov., an anaerobic, gram-negative coccus isolated from dental plaque. *Int. J. Syst. Evol. Microbiol.* 58, 581–584. doi: 10.1099/ijs.0.65093-0
- Arpaia, N., Campbell, C., Fan, X., Dikiy, S., van der Veeken, J., deRoos, P., et al. (2013). Metabolites produced by commensal bacteria promote peripheral regulatory T-cell generation. *Nature* 504, 451–455. doi: 10.1038/nature12726
- Bäckhed, F., Ley, R. E., Sonnenburg, J. L., Peterson, D. A., and Gordon, J. I. (2005). Host-bacterial mutualism in the human intestine. *Science* 307, 1915–1920. doi: 10.1126/science.1104816
- Begley, M., Gahan, C. G. M., and Hill, C. (2005). The interaction between bacteria and bile. *FEMS Microbiol. Rev.* 29, 625–651. doi: 10.1016/j.femsre.2004.09.003
- Bein, A., Shin, W., Jalili-Firoozinezhad, S., Park, M. H., Sontheimer-Phelps, A., Tovaglieri, A., et al. (2018). Microfluidic organ-on-a-chip models of human intestine. *Cell. Mol. Gastroenterol. Hepatol.* 5, 659–668. doi: 10.1016/j.jcmgh.2017.12.010
- Booijink, C. C. G. M., El-Aidy, S., Rajilić-Stojanović, M., Heilig, H. G. H. J., Troost, F. J., Smidt, H., et al. (2010). High temporal and inter-individual variation detected in the human ileal microbiota. *Environ. Microbiol.* 12, 3213–3227. doi: 10.1111/j.1462-2920.2010.02294.x
- Booijink, C. C. G. M., Zoetendal, E. G., Kleerebezem, M., and De Vos, W. M. (2007). Microbial communities in the human small intestine – coupling diversity to metagenomics. *Future Microbiol.* 2, 285–295. doi: 10.2217/17460913.2.3.285
- Boon, N., Top, E. M., Verstraete, W., and Siciliano, S. D. (2003). Bioaugmentation as a tool to protect the structure and function of an activated-sludge microbial community against a 3-chloroaniline shock load. *Appl. Environ. Microbiol.* 69, 1511–1520. doi: 10.1128/AEM.69.3.1511-1520.2003

## Funding

This work was financially supported by the Eurostars project Promise (E12091).

## Acknowledgments

We want to specifically thank Stoma Ilco VZW for providing us with ileostomy effluent samples.

## Conflict of interest

FM, MM, and TW are employees of ProDigest, that provides services to other companies using the model developed in this study. SD and PA were employees of ProDigest when this project was conducted. During the current project WP, Bv, and EK were employed by BaseClear, the company providing NGS services throughout the study.

The remaining authors declare that the research was conducted in the absence of any commercial or financial relationships that could be construed as a potential conflict of interest.

## Publisher's note

All claims expressed in this article are solely those of the authors and do not necessarily represent those of their affiliated organizations, or those of the publisher, the editors and the reviewers. Any product that may be evaluated in this article, or claim that may be made by its manufacturer, is not guaranteed or endorsed by the publisher.

## Supplementary material

The supplementary material for this article can be found online at: <https://www.frontiersin.org/articles/10.3389/fmicb.2022.1054061/full#supplementary-material>



- Borgström, B., Dahlqvist, A., Lundh, G., and Sjövall, J. (1957). Studies of intestinal digestion and absorption in the human. *J. Clin. Invest.* 36, 1521–1536. doi: 10.1172/JCI103549
- Bouhnik, Y., Alain, S., Attar, A., Flourie, B., Raskine, L., Sanson-Le Pors, M. J., et al. (1999). Bacterial populations contaminating the upper gut in patients with small intestinal bacterial overgrowth syndrome. *Am. J. Gastroenterol.* 94, 1327–1331. doi: 10.1016/S0002-9270(99)00071-4
- Chung, C.-S., Chang, P.-F., Liao, C.-H., Lee, T.-H., Chen, Y., Lee, Y.-C., et al. (2016). Differences of microbiota in small bowel and faeces between irritable bowel syndrome patients and healthy subjects. *Scand. J. Gastroenterol.* 51, 410–419. doi: 10.3109/00365521.2015.1116107
- Cieplak, T., Wiese, M., Nielsen, S., Van de Wiele, T., van den Berg, F., and Nielsen, D. S. (2018). The smallest intestine (TSI)—a low volume in vitro model of the small intestine with increased throughput. *FEMS Microbiol. Lett.* 365. doi: 10.1093/femsle/fny231
- Collado, M. C., Derrien, M., Isolauri, E., de Vos, W. M., and Salminen, S. (2007). Intestinal integrity and *Akkermansia muciniphila*, a mucin-degrading member of the intestinal microbiota present in infants, adults, and the elderly. *Appl. Environ. Microbiol.* 73, 7767–7770. doi: 10.1128/AEM.01477-07
- Davis, S. S., Hardy, J. G., and Fara, J. W. (1986). Transit of pharmaceutical dosage forms through the small intestine. *Gut* 27, 886–892. doi: 10.1136/gut.27.8.886
- Distler, W., and Kröncke, A. (1981). The lactate metabolism of the oral bacterium *Veillonella* from human saliva. *Arch. Oral Biol.* 26, 657–661. doi: 10.1016/0003-9969(81)90162-X
- Dlugosz, A., Winckler, B., Lundin, E., Zakikhany, K., Sandström, G., Ye, W., et al. (2015). No difference in small bowel microbiota between patients with irritable bowel syndrome and healthy controls. *Sci. Rep.* 5:8508. doi: 10.1038/srep08508
- Donaldson, G. P., Lee, S. M., and Mazmanian, S. K. (2016). Gut biogeography of the bacterial microbiota. *Nat. Rev. Microbiol.* 14, 20–32. doi: 10.1038/nrmicro3552
- Egland, P. G., Palmer, R. J., and Kolenbrander, P. E. (2004). Interspecies communication in *Streptococcus gordonii*-*Veillonella atypica* biofilms: signaling in flow conditions requires juxtaposition. *Proc. Natl. Acad. Sci. U. S. A.* 101, 16917–16922. doi: 10.1073/pnas.0407457101
- El Aidy, S., van den Bogert, B., and Kleerebezem, M. (2015). The small intestine microbiota, nutritional modulation and relevance for health. *Curr. Opin. Biotechnol.* 32, 14–20. doi: 10.1016/j.copbio.2014.09.005
- Evans, D. F., Pye, G., Bramley, R., Clark, A. G., Dyson, T. J., and Hardcastle, J. D. (1988). Measurement of gastrointestinal pH profiles in normal ambulant human subjects. *Gut* 29, 1035–1041. doi: 10.1136/gut.29.8.1035
- Foubert, E. L., and Douglas, H. C. (1948). Studies on the anaerobic micrococci; the fermentation of lactate by *Micrococcus lactilyticus*. *J. Bacteriol.* 56, 35–36. doi: 10.1128/JB.56.1.35-36.1948
- Furet, J.-P., Firmesse, O., Gourmelon, M., Bridonneau, C., Tap, J., Mondot, S., et al. (2009). Comparative assessment of human and farm animal faecal microbiota using real-time quantitative PCR. *FEMS Microbiol.* 68, 351–362. doi: 10.1111/j.1574-6941.2009.00671.x
- Ghyselinck, J., Verstreppe, L., Moens, F., Van den Abbeele, P., Said, J., Smith, B., et al. (2020). A 4-strain probiotic supplement influences gut microbiota composition and gut wall function in patients with ulcerative colitis. *Int. J. Pharm.* 587:119648. doi: 10.1016/j.ijpharm.2020.119648
- Guerra, A., Etienne-Mesmin, L., Livrelli, V., Denis, S., Blanquet-Diot, S., and Alric, M. (2012). Relevance and challenges in modeling human gastric and small intestinal digestion. *Trends Biotechnol.* 30, 591–600. doi: 10.1016/j.tibtech.2012.08.001
- Guo, X., Xia, X., Tang, R., Zhou, J., Zhao, H., and Wang, K. (2008). Development of a real-time PCR method for Firmicutes and Bacteroidetes in faeces and its application to quantify intestinal population of obese and lean pigs. *Lett. Appl. Microbiol.* 47, 367–373. doi: 10.1111/j.1472-765X.2008.02408.x
- Hao, W.-L., and Lee, Y.-K. (2004). Microflora of the gastrointestinal tract: a review. *Methods Mol. Biol.* 268, 491–502. doi: 10.1385/1-59259-766-1:491
- Hartman, A. L., Lough, D. M., Barupal, D. K., Fiehn, O., Fishbein, T., Zasloff, M., et al. (2009). Human gut microbiome adopts an alternative state following small bowel transplantation. *Proc. Natl. Acad. Sci. U. S. A.* 106, 17187–17192. doi: 10.1073/pnas.0904847106
- Hayashi, H., Takahashi, R., Nishi, T., Sakamoto, M., and Benno, Y. (2005). Molecular analysis of jejunal, ileal, caecal and recto-sigmoidal human colonic microbiota using 16S rRNA gene libraries and terminal restriction fragment length polymorphism. *J. Med. Microbiol.* 54, 1093–1101. doi: 10.1099/jmm.0.45935-0
- Hoefman, S., Hoorde, K. V., Boon, N., Vandamme, P., Vos, P. D., and Heylen, K. (2012). Survival or revival: long-term preservation induces a reversible viable but non-Culturable state in methane-oxidizing bacteria. *PLoS One* 7:e34196. doi: 10.1371/journal.pone.0034196
- Hofmann, A. F. (1999). The continuing importance of bile acids in liver and intestinal disease. *Arch. Intern. Med.* 159, 2647–2658. doi: 10.1001/archinte.159.22.2647
- Hosseini, E., Grootaert, C., Verstraete, W., and Van de Wiele, T. (2011). Propionate as a health-promoting microbial metabolite in the human gut. *Nutr. Rev.* 69, 245–258. doi: 10.1111/j.1753-4887.2011.00388.x
- Islam, K. B. M. S., Fukiya, S., Hagio, M., Fujii, N., Ishizuka, S., Ooka, T., et al. (2011). Bile acid is a host factor that regulates the composition of the cecal microbiota in rats. *Gastroenterology* 141, 1773–1781. doi: 10.1053/j.gastro.2011.07.046
- Ivanov, I. I., Frutos, R. D. L., Manel, N., Yoshinaga, K., Rifkin, D. B., Sartor, R. B., et al. (2008). Specific microbiota direct the differentiation of IL-17-producing T-helper cells in the mucosa of the small intestine. *Cell Host Microbe* 4, 337–349. doi: 10.1016/j.chom.2008.09.009
- Kakiyama, G., Pandak, W. M., Gillevet, P. M., Hylemon, P. B., Heuman, D. M., Daita, K., et al. (2013). Modulation of the fecal bile acid profile by gut microbiota in cirrhosis. *J. Hepatol.* 58, 949–955. doi: 10.1016/j.jhep.2013.01.003
- Kastl, A. J., Terry, N. A., Wu, G. D., and Albenberg, L. G. (2020). The structure and function of the human small intestinal microbiota: current understanding and future directions. *Cell. Mol. Gastroenterol. Hepatol.* 9, 33–45. doi: 10.1016/j.jcmgh.2019.07.006
- Kitahara, M., Sakata, S., Sakamoto, M., and Benno, Y. (2004). Comparison among fecal secondary bile acid levels, fecal microbiota and *Clostridium scindens* cell numbers in Japanese. *Microbiol. Immunol.* 48, 367–375. doi: 10.1111/j.1348-0421.2004.tb03526.x
- Lee, S., and Lee, D. K. (2018). What is the proper way to apply the multiple comparison test? *Korean J. Anesthesiol.* 71, 353–360. doi: 10.4097/kja.d.18.00242
- Ley, R. E., Peterson, D. A., and Gordon, J. I. (2006). Ecological and evolutionary forces shaping microbial diversity in the human intestine. *Cells* 124, 837–848. doi: 10.1016/j.cell.2006.02.017
- Li, X., Liu, L., Cao, Z., Li, W., Li, H., Lu, C., et al. (2020). Gut microbiota as an “invisible organ” that modulates the function of drugs. *Biomed. Pharmacother.* 121:109653. doi: 10.1016/j.biopha.2019.109653
- Macfarlane, G. T., and Macfarlane, S. (2011). Fermentation in the human large intestine: its physiologic consequences and the potential contribution of prebiotics. *J. Clin. Gastroenterol.* 45, S120–S127. doi: 10.1097/MCG.0b013e31822fecfe
- Marchesi, J. R., Adams, D. H., Fava, F., Hermes, G. D. A., Hirschfield, G. M., Hold, G., et al. (2016). The gut microbiota and host health: a new clinical frontier. *Gut* 65, 330–339. doi: 10.1136/gutjnl-2015-309990
- Martinez-Augustin, O., and Sanchez de Medina, F. (2008). Intestinal bile acid physiology and pathophysiology. *World J. Gastroenterol.* 14, 5630–5640. doi: 10.3748/wjg.14.5630
- Molly, K., Vande Woestyne, M., and Verstraete, W. (1993). Development of a 5-step multi-chamber reactor as a simulation of the human intestinal microbial ecosystem. *Appl. Microbiol. Biotechnol.* 39, 254–258. doi: 10.1007/BF00228615
- Moore, W. E., and Holdeman, L. V. (1974). Human fecal flora: the normal flora of 20 Japanese-Hawaiians. *Appl. Microbiol.* 27, 961–979. doi: 10.1128/am.27.5.961-979.1974
- Nakano, S., Kobayashi, T., Funabiki, K., Matsumura, A., Nagao, Y., and Yamada, T. (2003). Development of a PCR assay for detection of Enterobacteriaceae in foods. *J. Food Prot.* 66, 1798–1804. doi: 10.4315/0362-028X-66.10.1798
- O'May, G. A., Reynolds, N., and Macfarlane, G. T. (2005). Effect of pH on an in vitro model of gastric microbiota in enteric nutrition patients. *Appl. Environ. Microbiol.* 71, 4777–4783. doi: 10.1128/AEM.71.8.4777-4783.2005
- Possemiers, S., Verthé, K., Uyttendaele, S., and Verstraete, W. (2004). PCR-DGGE-based quantification of stability of the microbial community in a simulator of the human intestinal microbial ecosystem. *FEMS Microbiol.* 49, 495–507. doi: 10.1016/j.femsec.2004.05.002
- Rakoff-Nahoum, S., and Medzhitov, R. (2006). Role of the innate immune system and host-commensal mutualism. *Curr. Top. Microbiol. Immunol.* 308, 1–18. doi: 10.1007/3-540-30657-9\_1
- Ridlon, J. M., Kang, D. J., Hylemon, P. B., and Bajaj, J. S. (2014). Bile acids and the gut microbiome. *Curr. Opin. Gastroenterol.* 30, 332–338. doi: 10.1097/MOG.0000000000000057
- Rinttilä, T., Kassinen, A., Malinen, E., Krogius, L., and Palva, A. (2004). Development of an extensive set of 16S rRNA-targeted primers for quantification of pathogenic and indigenous bacteria in faecal samples by real-time PCR. *J. Appl. Microbiol.* 97, 1166–1177. doi: 10.1111/j.1365-2672.2004.02409.x
- Riordan, S. M., McIver, C. J., Wakefield, D., Duncombe, V. M., Thomas, M. C., and Bolin, T. D. (2001). Small intestinal mucosal immunity and morphometry in luminal overgrowth of indigenous gut flora. *Am. J. Gastroenterol.* 96, 494–500. doi: 10.1016/S0002-9270(00)02326-1
- Roussel, C., De Paepe, K., Galia, W., De Bodt, J., Chalancon, S., Leriche, F., et al. (2020). Spatial and temporal modulation of enterotoxigenic *E. coli* H10407 pathogenesis and interplay with microbiota in human gut models. *BMC Biol.* 18:141. doi: 10.1186/s12915-020-00860-x

- Ruan, W., Engevik, M. A., Spinler, J. K., and Versalovic, J. (2020). Healthy human gastrointestinal microbiome: composition and function after a decade of exploration. *Dig. Dis. Sci.* 65, 695–705. doi: 10.1007/s10620-020-06118-4
- Scott, K. P., Gratz, S. W., Sheridan, P. O., Flint, H. J., and Duncan, S. H. (2013). The influence of diet on the gut microbiota. *Pharmacol. Res.* 69, 52–60. doi: 10.1016/j.phrs.2012.10.020
- Seekatz, A. M., Schnitzlein, M. K., Koenigsnecht, M. J., Baker, J. R., Hasler, W. L., Bleske, B. E., et al. (2019). Spatial and temporal analysis of the stomach and small-intestinal microbiota in fasted healthy humans. *mSphere* 4:e00126-19. doi: 10.1128/mSphere.00126-19
- Silvester, K. R., Englyst, H. N., and Cummings, J. H. (1995). Ileal recovery of starch from whole diets containing resistant starch measured in vitro and fermentation of ileal effluent. *Am. J. Clin. Nutr.* 62, 403–411. doi: 10.1093/ajcn/62.2.403
- Sokol, H., Seksik, P., Furet, J. P., Firmesse, O., Nion-Larmurier, I., Beaugerie, L., et al. (2009). Low counts of *Faecalibacterium prausnitzii* in colitis microbiota. *Inflamm. Bowel Dis.* 15, 1183–1189. doi: 10.1002/ibd.20903
- Stagg, A. J., Hart, A. L., Knight, S. C., and Kamm, M. A. (2004). Microbial-gut interactions in health and disease. Interactions between dendritic cells and bacteria in the regulation of intestinal immunity. *Best Pract. Res. Clin. Gastroenterol.* 18, 255–270. doi: 10.1016/j.bpg.2003.10.004
- Staley, C., Weingarden, A. R., Khoruts, A., and Sadowsky, M. J. (2017). Interaction of gut microbiota with bile acid metabolism and its influence on disease states. *Appl. Microbiol. Biotechnol.* 101, 47–64. doi: 10.1007/s00253-016-8006-6
- Stolaki, M., Minekus, M., Venema, K., Lahti, L., Smid, E. J., Kleerebezem, M., et al. (2019). Microbial communities in a dynamic in vitro model for the human ileum resemble the human ileal microbiota. *FEMS Microbiol.* 95. doi: 10.1093/femsec/fiz096
- Šuligoj, T., Vigsnaes, L. K., den Abbeele, P. V., Apostolou, A., Karalis, K., Savva, G. M., et al. (2020). Effects of human milk oligosaccharides on the adult gut microbiota and barrier function. *Nutrients* 12. doi: 10.3390/nu12092808
- Thadepalli, H., Lou, S. M. A., Bach, V. T., Matsui, T. K., and Mandal, A. K. (1979). Microflora of the human small intestine. *Am. J. Surg.* 138, 845–850. doi: 10.1016/0002-9610(79)90309-X
- Thursby, E., and Juge, N. (2017). Introduction to the human gut microbiota. *Biochem. J.* 474, 1823–1836. doi: 10.1042/BCJ20160510
- Van den Abbeele, P., Belzer, C., Goossens, M., Kleerebezem, M., De Vos, W. M., Thas, O., et al. (2013). Butyrate-producing clostridium cluster XIVa species specifically colonize mucins in an in vitro gut model. *ISME J.* 7, 949–961. doi: 10.1038/ismej.2012.158
- Van den Abbeele, P., Grootaert, C., Marzorati, M., Possemiers, S., Verstraete, W., Gérard, P., et al. (2010). Microbial community development in a dynamic gut model is reproducible, colon region specific, and selective for Bacteroidetes and Clostridium cluster IX. *Appl. Environ. Microbiol.* 76, 5237–5246. doi: 10.1128/AEM.00759-10
- Van den Abbeele, P., Roos, S., Eeckhaut, V., MacKenzie, D. A., Derde, M., Verstraete, W., et al. (2012). Incorporating a mucosal environment in a dynamic gut model results in a more representative colonization by lactobacilli. *Microb. Biotechnol.* 5, 106–115. doi: 10.1111/j.1751-7915.2011.00308.x
- Van den Bogert, B., Boekhorst, J., Herrmann, R., Smid, E. J., Zoetendal, E. G., and Kleerebezem, M. (2013). Comparative genomics analysis of streptococcus isolates from the human small intestine reveals their adaptation to a highly dynamic ecosystem. *PLoS One* 8. doi: 10.1371/journal.pone.0083418
- Van den Bogert, B., de Vos, W. M., Zoetendal, E. G., and Kleerebezem, M. (2011). Microarray analysis and barcoded pyrosequencing provide consistent microbial profiles depending on the source of human intestinal samples. *Appl. Environ. Microbiol.* 77, 2071–2080. doi: 10.1128/AEM.02477-10
- van Kessel, S. P., and El Aidy, S. (2019). Contributions of gut bacteria and diet to drug pharmacokinetics in the treatment of parkinson's disease. *Front. Neurol.* 10:1087. doi: 10.3389/fneur.2019.01087
- Van Kessel, S. P., Frye, A. K., El-Gendy, A. O., Castejon, M., Keshavarzian, A., van Dijk, G., et al. (2019). Gut bacterial tyrosine decarboxylases restrict levels of levodopa in the treatment of Parkinson's disease. *Nat. Commun.* 10:310. doi: 10.1038/s41467-019-08294-y
- Villmones, H. C., Halland, A., Stenstad, T., Ulvestad, E., Weedon-Fekjær, H., and Kommedal, Ø. (2020). The cultivable microbiota of the human distal ileum. *Clin. Microbiol. Infect.* 27, 912.e7–912.e13. doi: 10.1016/j.cmi.2020.08.021
- Villmones, H. C., Haug, E. S., Ulvestad, E., Grude, N., Stenstad, T., Halland, A., et al. (2018). Species level description of the human ileal bacterial microbiota. *Sci. Rep.* 8:4736. doi: 10.1038/s41598-018-23198-5
- Wang, M., Ahrné, S., Jeppsson, B., and Molin, G. (2005). Comparison of bacterial diversity along the human intestinal tract by direct cloning and sequencing of 16S rRNA genes. *FEMS Microbiol. Ecol.* 54, 219–231. doi: 10.1016/j.femsec.2005.03.012
- Whitcomb, D. C., and Lowe, M. E. (2007). Human pancreatic digestive enzymes. *Dig. Dis. Sci.* 52, 1–17. doi: 10.1007/s10620-006-9589-z
- Zhang, J., Zhang, J., and Wang, R. (2018). Gut microbiota modulates drug pharmacokinetics. *Drug Metab. Rev.* 50, 357–368. doi: 10.1080/03602532.2018.1497647
- Zoetendal, E. G., Raes, J., van den Bogert, B., Arumugam, M., Booiijink, C. C., Troost, F. J., et al. (2012). The human small intestinal microbiota is driven by rapid uptake and conversion of simple carbohydrates. *ISME J.* 6, 1415–1426. doi: 10.1038/ismej.2011.212



## OPEN ACCESS

## EDITED BY

Wei Qi He,  
Soochow University,  
China

## REVIEWED BY

Prabhat Kumar Talukdar,  
Washington State University,  
United States  
Suhong Xia,  
Huazhong University of Science and  
Technology,  
China  
Ivan Šoša,  
University of Rijeka,  
Croatia

## \*CORRESPONDENCE

Yan Jun Liu  
✉ liuyanjun\_001@163.com  
Yi Li  
✉ lyi1980@126.com  
Tongtong Zhang  
✉ 163ztong@163.com

## SPECIALTY SECTION

This article was submitted to  
Microorganisms in Vertebrate Digestive  
Systems,  
a section of the journal  
Frontiers in Microbiology

RECEIVED 26 December 2022

ACCEPTED 03 March 2023

PUBLISHED 22 March 2023

## CITATION

Hu J, Tang J, Zhang X, Yang K, Zhong A,  
Yang Q, Liu Y, Li Y and Zhang T (2023)  
Landscape in the gallbladder mycobiome and  
bacteriome of patients undergoing  
cholelithiasis with chronic cholecystitis.  
*Front. Microbiol.* 14:1131694.  
doi: 10.3389/fmicb.2023.1131694

## COPYRIGHT

© 2023 Hu, Tang, Zhang, Yang, Zhong, Yang,  
Liu, Li and Zhang. This is an open-access article  
distributed under the terms of the [Creative  
Commons Attribution License \(CC BY\)](#). The  
use, distribution or reproduction in other  
forums is permitted, provided the original  
author(s) and the copyright owner(s) are  
credited and that the original publication in this  
journal is cited, in accordance with accepted  
academic practice. No use, distribution or  
reproduction is permitted which does not  
comply with these terms.

# Landscape in the gallbladder mycobiome and bacteriome of patients undergoing cholelithiasis with chronic cholecystitis

Junqing Hu<sup>1,2,3</sup>, Jichao Tang<sup>1,2,4</sup>, Xinpeng Zhang<sup>1,2,4</sup>,  
Kaijin Yang<sup>1,2,4</sup>, Ayan Zhong<sup>1,2,4</sup>, Qin Yang<sup>1,2,5</sup>, Yanjun Liu<sup>1,2\*</sup>,  
Yi Li<sup>1,2,4\*</sup> and Tongtong Zhang<sup>1,2,3\*</sup>

<sup>1</sup>Center of Gastrointestinal and Minimally Invasive Surgery, Department of General Surgery, The Third People's Hospital of Chengdu, Affiliated Hospital of Southwest Jiaotong University, The Second Affiliated Hospital of Chengdu, Chongqing Medical University, Chengdu, China, <sup>2</sup>The Center for Obesity and Metabolic Health, The Third People's Hospital of Chengdu, Affiliated Hospital of Southwest Jiaotong University, The Second Affiliated Hospital of Chengdu, Chongqing Medical University, Chengdu, China, <sup>3</sup>Medical Research Center, The Third People's Hospital of Chengdu, Affiliated Hospital of Southwest Jiaotong University, The Second Affiliated Hospital of Chengdu, Chongqing Medical University, Chengdu, China, <sup>4</sup>General Surgery Day Ward, Department of General Surgery, The Third People's Hospital of Chengdu, Affiliated Hospital of Southwest Jiaotong University, The Second Affiliated Hospital of Chengdu, Chongqing Medical University, Chengdu, China, <sup>5</sup>Section for Hepato-Pancreato-Biliary Surgery, Department of General Surgery, The Third People's Hospital of Chengdu, Affiliated Hospital of Southwest Jiaotong University, The Second Affiliated Hospital of Chengdu, Chongqing Medical University, Chengdu, China

Gallstone disease (GSD) is associated with changes in the gut and gallbladder bacterial composition, but there is limited information on the role of the fungal community (mycobiome) in disease development. This study aimed to characterize the gallbladder mycobiome profiles and their interactions with bacteriome in GSD. A total of 136 bile and gallstone samples (34 paired for bacteriome, and 33 paired and extra 2 bile samples for mycobiome) were obtained from calculi patients with chronic cholecystitis. Bile and gallstone bacteriome and mycobiome were profiled by 16S and internal transcribed spacer (ITS) rRNA gene sequencing, respectively. Gallbladder bacteriome, mycobiome, and interkingdom and intrakingdom interactions were compared between bile and gallstone. In general, microbial diversity was higher in bile than in gallstone, and distinct microbial community structures were observed among them. Deep Sea Euryarchaeotic Group, Rhodobacteraceae, and Rhodobacterales were microbial biomarkers of bile, while Clostridiales and *Eubacterium coprostanoligenes* were biomarkers of gallstone. Five fungal taxa, including *Colletotrichum*, *Colletotrichum sublineola*, and *Epicoccum*, were enriched in gallstone. Further ecologic analyses revealed that intensive transkingdom correlations between fungi and bacteria and intrakingdom correlations within them observed in gallstone were significantly decreased in bile. Large and complex fungal communities inhabit the gallbladder of patients with GSD. Gallstone, compared with bile, is characterized by significantly altered bacterial taxonomic composition and strengthened bacterial–bacterial, fungal–fungal, and bacterial–fungal correlations in the gallbladder of patients with GSD.

## KEYWORDS

gallstone disease, marker gene sequencing, microbiota, bile and gallstone, bacteria, fungi

## Introduction

Gallstone disease (GSD) has been prevalent worldwide, especially in Western countries and China in the last decades (Fan et al., 2017; Scherber et al., 2017). Most of the gallstones in the gallbladder are the cholesterol type (approximately two-thirds), and the remaining are mainly pigment stones (Portincasa and Wang, 2012). It was previously suggested that a healthy human biliary system is sterile; however, several years ago, it was recognized that the gallbladder has a complex microbiota in non-pathological conditions (Verdier et al., 2015; Warburton et al., 2017). Despite the high worldwide prevalence of GSD, the role of the biliary microbiota in gallstone pathogenesis remains unclear. To date, knowledge about the composition of the biliary microbiota and its influence on the development of biliary disease is limited. Previous studies have linked biliary infection with gallstone development and indicated that bacteria may act as the nucleating factor initiating the formation of both pigment and cholesterol gallstones (Maki, 1966; Swidsinski and Lee, 2001; Stewart et al., 2002; Begley et al., 2005; Stewart et al., 2006). The presence of living bacteria in gallstones has been demonstrated using multiple methods (Swidsinski et al., 1995; Lee et al., 1999; Hazrah et al., 2004; Ramana Ramya et al., 2017). Moreover, several studies have shown that the alterations of bacteria in bile were linked to biliary diseases, such as cholelithiasis (Petrov et al., 2020), cholangiocarcinoma (Chen B. et al., 2019), common bile duct stones (Choe et al., 2021; Kim et al., 2021), biliary injury (Ying Liu et al., 2018), and primary sclerosing cholangitis (Pereira et al., 2017; Timur Liwinski et al., 2019). While works have reported that bacteria could be detected in gallstones, the bacterial spectrum remains unclear in cholelithiasis.

Fungi, as eukaryotes, are ancestrally and ecologically intrinsic to terrestrial life with multiple roles, extending to the regulobiotic. Notably, fungal species have been reported to colonize as commensals in many niches in healthy humans (Cui et al., 2013). Alterations within the fungi are associated with different diseases. The association between fungi and gastrointestinal disease has been well documented, with a special focus on candidiasis (Mukherjee et al., 2015). Studies performed in the past decade have demonstrated that fungi have a complex, multifaceted role in the gastrointestinal tract and actively and directly influence health and disease. A recent retrospective study found that *Candida* presented in bile at a low level (1.3%) by culture (Serra et al., 2021). However, the fungal organisms in bile and gallstone

remain largely unclear. Fungi may have the potential to manipulate neighboring bacterial communities or vice versa. Therefore, interactions between the mycobiome and the bacteriome may also play a role in GSD.

In light of the above, we investigated both the fungal and bacterial profiles in paired bile and gallstone samples from patients with cholelithiasis using ITS and 16S rRNA gene high-throughput sequencing. To the best of our knowledge, this is the first study to uncover the fungal spectrum and its interaction with bacteria in both bile and gallstone. Thus, the current study provides insights into mycobiome in GSD. Importantly, the bile origin of the gallstone microbiota and fungal–bacterial interactions might contribute to the stone formation of cholelithiasis.

## Materials and methods

### Sample collection and processing

The stone and bile samples from gallbladder-stone patients were obtained during laparoscopic cholecystectomy. In total, 136 samples, 68 (34 paired bile and gallstone samples) for bacterial analysis and 68 (33 paired bile and gallstone samples, and 2 bile samples only) for fungal analysis, were acquired from 35 patients (Table 1, Supplementary Table S1). The gallstones were classified as cholesterol gallstones based on their physical characteristics (smooth, round to ovoid and yellow-white and laminated or crystalline cut surface).

### Extraction of microbial DNA from bile and gallstone

The total microbial genomic DNA extraction from bile samples (200 µL) was performed by QIAamp DNA Mini Kit (QIAGEN, Germany) following the manufacturer's instructions. Similarly, microbial DNA from gallstone (approximately 200 mg) was collected using QIAamp Fast DNA Stool Mini Kit (QIAGEN, Germany) according to the handbook. DNA concentrations were detected using a NanoDrop 2000 (Thermo Fisher Scientific, Waltham, MA, USA). DNA samples were stored at –80°C until required for experiments.

TABLE 1 Demographic and Clinical Details of GSD Subjects.

Data	Factor	Bile	Gallstone	#Paired
16S of bacteria	Sample size	34	34	34
	Age, <sup>a</sup> year	43 ± 14	43 ± 14	
	Male <sup>b</sup>	11 (32.4%)	11 (32.4%)	
	Cholesterol <sup>b</sup>	29 (85.3%)	29 (85.3%)	
ITS of fungi	Sample size	35	33	33
	Age, <sup>a</sup> year	43 ± 14	42 ± 13	
	Male <sup>b</sup>	11 (31.4%)	11 (33.3%)	
	Cholesterol <sup>b</sup>	30 (85.7%)	28 (84.8%)	

<sup>a</sup>Mean ± standard deviation (SD).

<sup>b</sup>Count (percentage).



## Determination of bacterial and fungal profiles by amplicon sequencing

The V3–V4 region of the bacterial 16S rRNA gene was amplified from extracted DNA using the 341F (CCTAYGGGRBGCASCAG) and 806R (GGACTACNNGGTATCTAAT) primer sets. For fungal analysis, ITS1 variable region was amplified with universal primers ITS1F (CTTGGTCATTTAGAGGAAGTAA) and ITS2 (GCTGCGTTCTTCATCGATGC). 16S amplicon sequencing was performed on the Illumina MiSeq platform (Applied Protein Technology Co., Ltd., Shanghai, China). ITS amplicon sequencing was conducted by OE Biotech Co., Ltd. (Shanghai, China).

## Data processing

The sequencing data of bacteria and fungi were imported into QIIME 2 (v2022.2) for preprocessing, denoising, diversity analyses and taxonomy classification (Bolyen et al., 2019). The amplicon sequence variants (ASVs) < 0.005% were finally removed from the analysis of both bacterial and fungal data. For the taxonomic assignment, the SILVA 138 and UNITE v8.3 datasets were used for bacteria and fungi, respectively. The QIIME artifacts were inputted into R by the file2meco package<sup>1</sup>, followed by the analysis and plotting using the microeco package (v0.9.0) in R 4.1.0 (Liu et al., 2021). FUNGuild database was used for fungal data to identify fungal guilds by microeco. The Tax4Fun2 (v1.1.5) workflow was applied for the prediction of metagenome functions of bacteria (Wemheuer et al., 2020).

## Co-occurrence network analysis

The general networks of bacteria–bacteria and fungi–fungi in gallbladder were constructed using SparCC correlation through microeco in R. The global network of bacteria–fungi in the gallbladder was generated using SparCC correlation by integrated Network Analysis Pipeline [iNAP, (Feng et al., 2022)]. Networks were also constructed for bacteria–bacteria, fungi–fungi, and bacteria–fungi in bile and gallstone separately by using this platform. Correlated genus pairs were selected when the absolute values of sparse correlation were  $|r| > 0.1$  and  $p < 0.05$ . Visualization and analysis of the network were conducted using Gephi (v0.9.2) (Bastian et al., 2009).

## Statistical analysis

The nonparametric Kruskal Wallis and Permutational multivariate analysis of variance (PERMANOVA, 999 permutations) were used to test the difference among groups of microbial alpha and beta diversity separately. Differentially abundant taxa were identified by linear discriminant analysis (LDA) effect size (LEfSe). In network analysis, pseudo  $p$ -values were calculated via a bootstrap procedure. First, shuffled (w. replacement) datasets were created, and then the SparCC

correlation for each dataset was computed. Finally, the two-sided  $p$ -values were computed based on the correlation results. A chi-square ( $\chi^2$ ) test was used to compare the difference in the number of correlations between bile and gallstone. Two-sided  $t$  test was applied to compare the difference in the relative abundance of taxa between bile and gallstone. The differences in predicted function outcomes of bacteria among the groups were compared using the STAMP software v2.1.3.<sup>2</sup>

## Results

### Clinical characteristics of study subjects

The study included 35 subjects: 29 cholesterol subjects and 6 pigment subjects (Table 1, Supplementary Table S1). For bacteriological analysis, the median age was 43 years for subjects from both the bile and gallstone groups. For mycological analysis, the median age was 43 years for the bile group and 42 years for the gallstone group. Other clinical characteristics (sex and type of stone) were comparable between subjects of bile and gallstone groups. In total, 4,518 features were obtained using the bacterial 16S rRNA metagenomic sequencing and 2,431 features were obtained using fungal ITS1 metagenomic sequencing.

### Largely different bacterial community in bile and gallstone of GSD

First, we compared the bacterial diversity and composition between bile and gallstone. Although bile and gallstone showed similar Shannon diversity and Observed features (ASVs) (Supplementary Figure S1), the Faith phylogenetic diversity (Faith PD,  $p = 0.028$ ) of bile was markedly higher than that of gallstone (Figure 1A). Principal coordinates analysis (PCoA) of unweighted Unifrac distance showed distinct clustering of bile and gallstone samples (Figure 1B; Supplementary Figure S2). Furthermore, it is known that age and sex have an effect on the human microbiota. Thus, we explored the age, sex as well as the gallstone type whether affect the microbial diversity in this study. There was no significant correlation between age and alpha diversity indices (Supplementary Figures S3A,B). In addition, no significant difference in alpha diversity between men and women (Supplementary Figures S3C,D), cholesterol and pigment stones (Supplementary Figures S3E,F) in this study was observed. These results suggest that age, sex, and stone type have negligible effects on the gallbladder bacteriome profile. These results suggest that age, sex, and stone type have negligible effects on the gallbladder bacteriome profile.

Based on 16S rRNA gene sequencing, the relative abundance of bacteria fluctuated largely in bile samples (27.55–98.50%), whereas it accounted for 66.53 to 100% in gallstone samples. Among the bacterial phyla, Firmicutes, Bacteroidetes, Actinobacteria, and Proteobacteria were the four dominant bacterial phyla in the gallbladder bacteriome (Figure 1C; Supplementary Figure S4A). At the genus level,

<sup>1</sup> <https://github.com/ChiLiubio/file2meco>

<sup>2</sup> <https://beikolab.cs.dal.ca/software/STAMP>

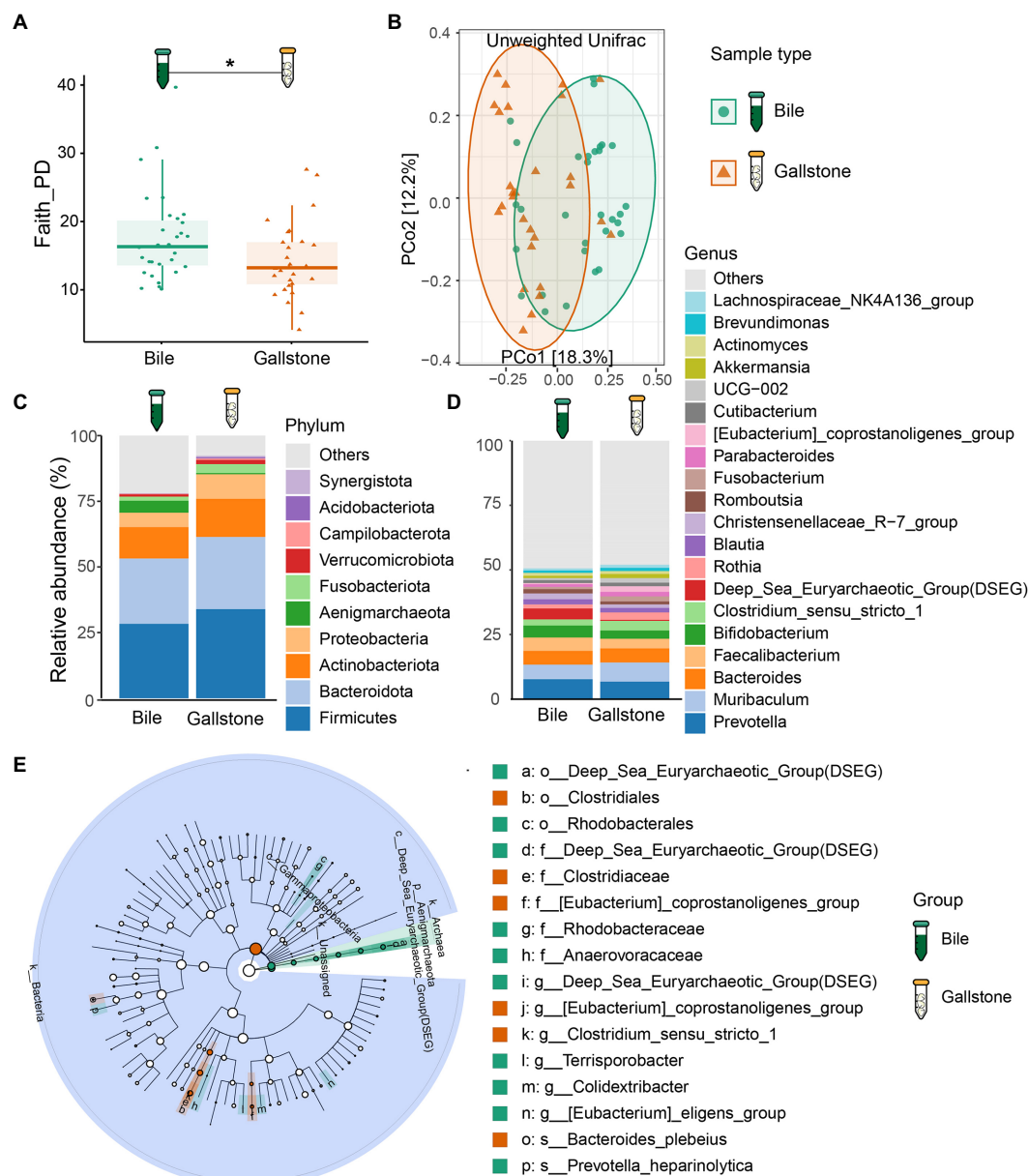


FIGURE 1

Bacteriome signature of bile and gallstone from GSD patients with chronic cholecystitis. (A) Boxplot showed the bacterial phylogenetic diversity (Faith PD) between bile ( $n=31$ ) and gallstone ( $n=28$ ). Statistic was performed by a Kruskal-Wallis (pairwise) test.  $*P (= 0.028) < 0.05$ . (B) Principal coordinate analysis (PCoA) of the unweighted UniFrac distance between bile ( $n=31$ ) and gallstone ( $n=28$ ). Statistic was performed by a pairwise PERMANOVA test (999 permutations;  $p=0.001$ ,  $q=0.001$ ). (C,D) Bar plot depicted the bacterial mean relative abundance at the phylum (C) and genus (D) levels in both bile and gallstone samples. (E) LefSe cladogram showed the different abundance of bacteria between bile and gallstone. The diameter of each circle was proportional to its abundance (LDA score  $> 3.0$ ).

*Muribaculum*, *Bacteroides*, *Prevotella*, *Faecalibacterium*, and *Bifidobacterium* were the dominant bacterial genera in gallbladder bacteriome (Figure 1D; Supplementary Figure S4B). Furthermore, the archaea also accounted for a large proportion. An unknown archaea phylum and Aenigmarchaeota were the major dominant archaea.

We further accessed the bacterial signatures associated with gallstone by LefSe and random forest (RF). After setting the LDA cutoff score at 3.0, we identified 10 and 6 taxa to be enriched in bile and gallstone, respectively. The Aenigmarchaeota presented a pronounced growth in bile samples (Figure 1E; Supplementary Figure S5). Deep Sea

Euryarchaeotic Group (DSEG), Rhodobacteraceae, and Rhodobacterales were microbial biomarker in bile samples, whereas *Eubacterium coprostanoligenes* was a biomarker in gallstone samples, as indicated by both LefSe and RF outcomes (Figure 1E; Supplementary Figure S5). Additionally, *Clostridiales*, *Clostridiaceae*, and *Bacteroides plebeius* was enriched in gallstone, whereas *Prevotella heparinolytica* was enriched in bile (Figures 1E, 2B; Supplementary Figure S5A).

As presented in Figure 2A, the detected bacterial sequences between bile and gallstone were almost completely different, only sharing 0.1%. Then, we explored the difference in bacterial composition

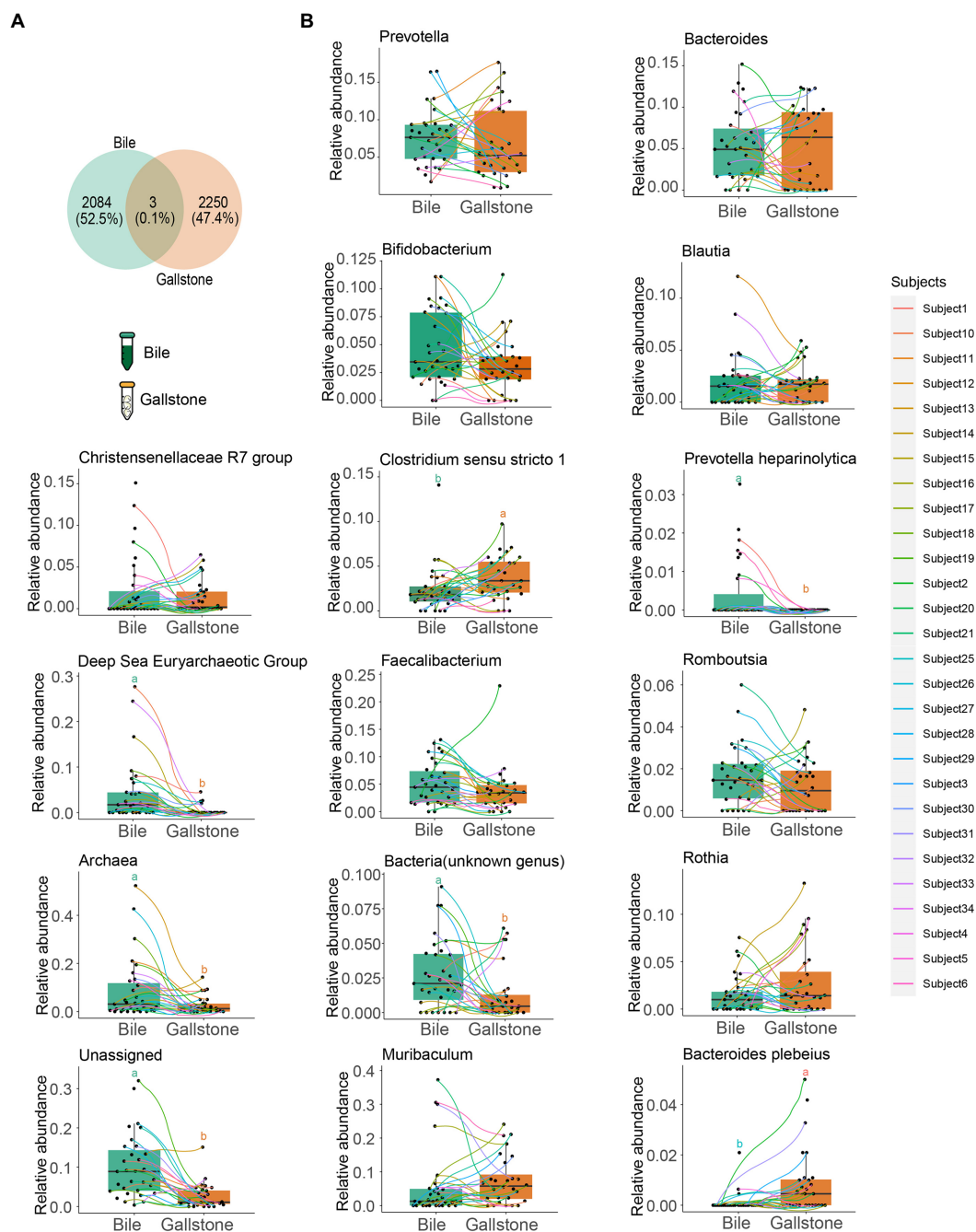


FIGURE 2

Comparison of the bacterial taxonomic composition between bile and gallstone from GSD patients with chronic cholecystitis. (A) Venn diagram of unique and shared ASVs among bile and gallstone samples. The percentage data is the sequence number/total sequence number. (B) Relative abundance of microbiota between bile (n=31) and gallstone (n=28) samples at multiple levels. Statistic was performed by a two-sided t test. Different lowercase letters indicated significant differences (p < 0.05).

in paired bile and gallstone samples (Figure 2B). The highest relative abundance of genus *Muribaculum* was increased from bile to gallstone. *Prevotella* was lower, and *Bacteroides* was higher in the gallstone than in bile. *Faecalibacterium* and *Bifidobacterium* were decreased in gallstone. The *Clostridium sensu stricto* 1, an unknown genus, Archaea, and unassigned bacteria also had a significant change from bile to gallstone. Taken together, these results suggest different bacterial phylogenetic diversity and taxonomic composition between bile and gallstone.

## Similar fungal community in bile and gallstone of GSD

To study the difference in gallbladder mycobiome in bile and gallstone, we first explored fungal alpha diversity indices between them. We found decreased evenness (Pielou's e) of the gallbladder mycobiome in gallstone samples compared with bile samples (p = 0.0018, Figure 3A). However, there were no changes in fungal

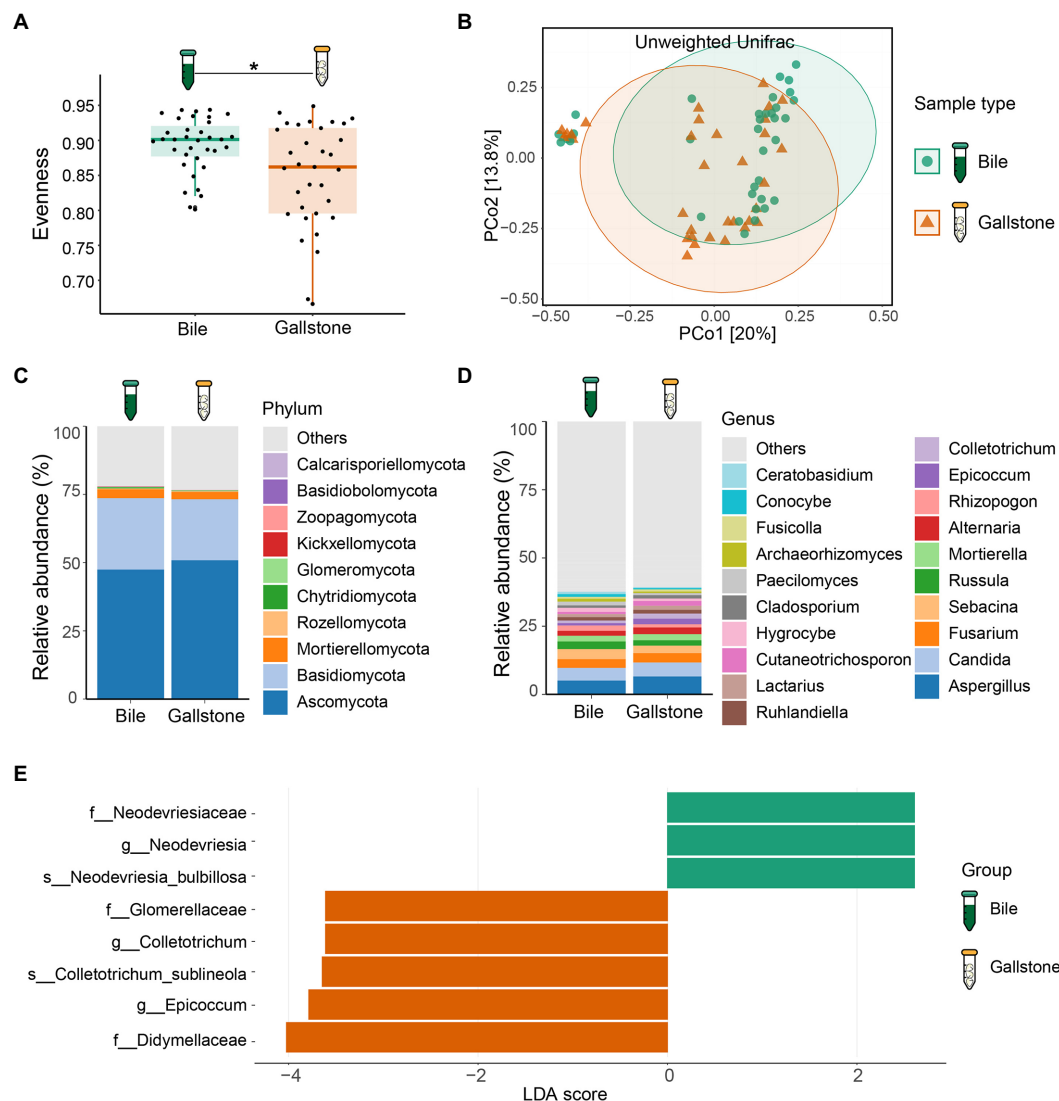


FIGURE 3

Mycobiome profile of bile and gallstone from GSD patients with chronic cholecystitis. **(A)** Boxplot presented the fungal community evenness between bile ( $n=35$ ) and gallstone ( $n=33$ ). Statistic was performed by a Kruskal-Wallis (pairwise) test.  $*P (= 0.018) < 0.05$ . **(B)** Principal coordinate analysis (PCoA) of the unweighted Unifrac distance between bile ( $n=35$ ) and gallstone ( $n=33$ ). Statistic was performed by a pairwise PERMANOVA test (999 permutations;  $p=0.038$ ,  $q=0.038$ ). **(C,D)** Bar plot depicted the fungal mean relative abundance at the phylum **(C)** and genus **(D)** levels in both bile and gallstone samples. **(E)** LefSe barplot showed the different abundance of fungi between bile and gallstone (LDA score  $> 2.0$ ).

diversity (Shannon) and richness (Observed ASVs) between the gallstone and bile samples (Supplementary Figure S6). PCoA based on the unweighted Unifrac distance between individual mycobiome revealed that the gallbladder mycobiome composition of bile and gallstone samples was separated into two distinct clusters, suggesting a different trend of gallbladder mycobiome profiles between bile and stone ( $p=0.038$ ; Figure 3B; Supplementary Figure S7). Similarly, there was no significant correlation/difference between age, sex, and stone type and alpha diversity indices (Supplementary Figure S8), suggesting that age, sex, and stone type have negligible effects on the gallbladder bacteriome profile.

At the phylum level, Ascomycota, Basidiomycota and Mortierellomycota dominated the gallbladder mycobiome (Figure 3C; Supplementary Figure S9A). Among the genera, *Aspergillus*, *Candida*,

*Fusarium*, *Sebacina*, *Russula*, *Mortierella*, *Alternaria*, *Rhizopogon*, *Epicoccum*, and *Colletotrichum* were the dominant fungal genera in the gallbladder mycobiome (Figure 3D; Supplementary Figure S9B). Furthermore, LefSe (LDA = 2.0) identified five fungal signatures associated with gallstone (Figure 3E). Among the differential taxa, *Colletotrichum* and *Epicoccum* had very small relative abundance (Figure 4B). The species *Colletotrichum sublineola* was also enriched in gallstone.

We also further explored the similarity of fungal composition between bile and gallstone. More than 70% (72.4%) shared fungal ASVs between bile and gallstone were observed (Figure 4A). In addition, phylum Ascomycota, the largest relative abundance genera *Candida*, *Sebacina*, an unknown genus, *Mortierella*, *Aspergillus*, *Fusarium*, and *Russula*, and species *Candida albicans* had no difference between bile and gallstone (Figure 4B). These



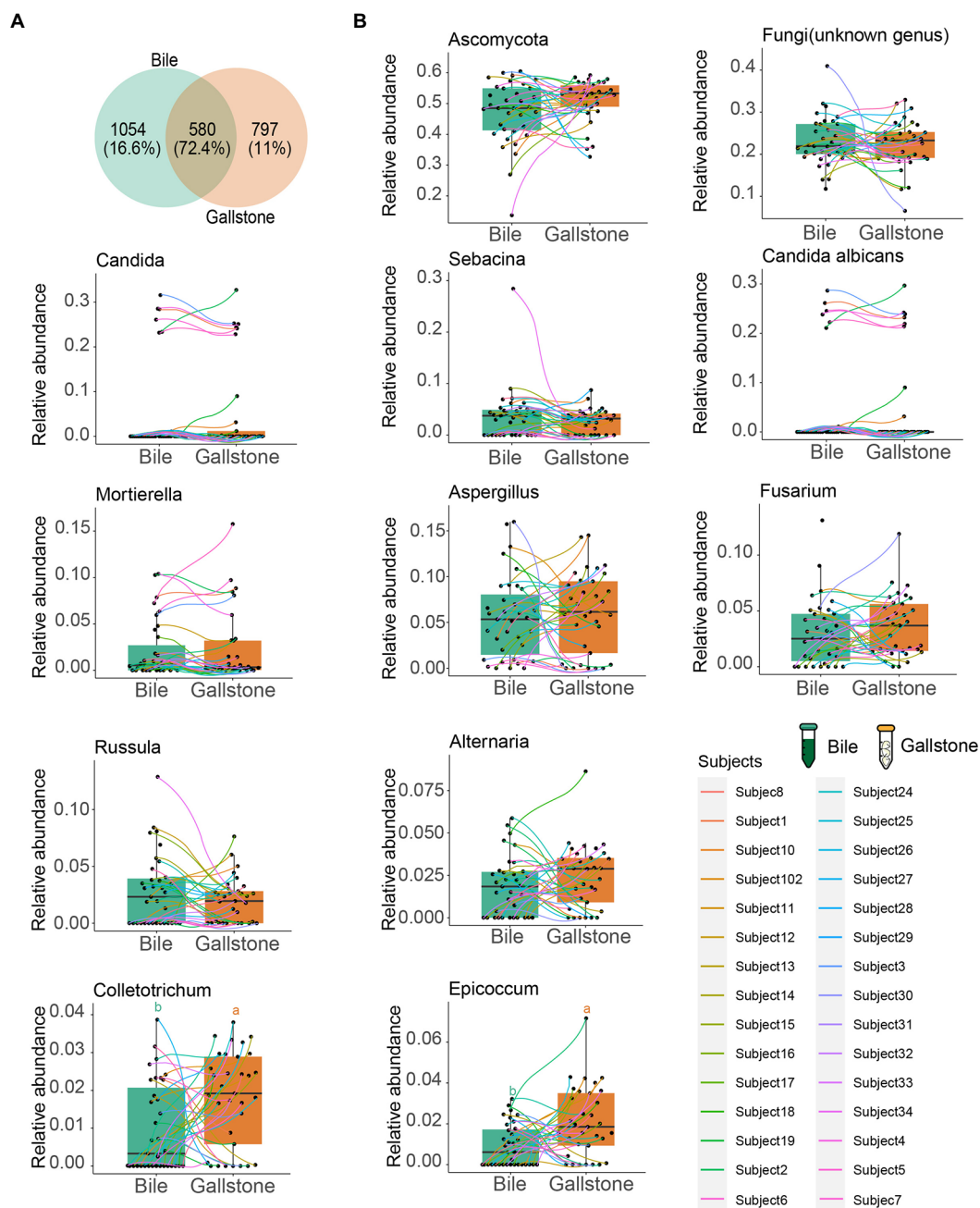


FIGURE 4

Comparison of the fungal taxonomic composition between bile and gallstone from GSD patients with chronic cholecystitis. (A) Venn diagram of unique and shared ASVs among bile and gallstone samples. The percentage data is the sequence number/total sequence number. (B) Relative abundance of microbiota between bile ( $n=35$ ) and gallstone ( $n=33$ ) samples at multiple levels. Statistic was performed by a two-sided  $t$  test. Different lowercase letters indicated significant differences ( $p<0.05$ ).

results imply a similar fungal diversity and taxonomic composition between bile and gallstone.

## Co-occurrence of bacteria, fungi and bacteria–fungi in the gallbladder of GSD

To explore the microbial keystone taxa in the gallbladder, we constructed microbial co-occurrence networks using

significant pairwise correlations between microbial taxa, bacteria–bacteria, fungi–fungi and bacteria–fungi. In general, we found 6 modules (M1–6) and four key communities (keystone taxa: *Muribaculum*, *Clostridium sensu stricto* 1, *Prevotella*, and *DSEG*) in bacteria of the gallbladder (Supplementary Figure S10A); six modules (M1–6) included four independent communities in fungi of the gallbladder (Supplementary Figure S10B). For the bacteria–fungi network (Supplementary Figure S10C; Supplementary Table S2), we obtained a network of four

modules consisting of both bacteria (17 taxa) and fungi (23 taxa).

To understand the network complexity and keystone taxa in gallstone, we compared the bacteria–bacteria, fungi–fungi, and bacteria–fungi co-occurrence networks between bile and gallstone. Although there were four modules of bacterial network found in both bile and gallstone, the network in gallstone had more correlations than that in bile (37 vs. 28;  $\chi^2$  test,  $p=0.047$ ; Figure 5A; Table 2; Supplementary Tables S3, S4). The keystone taxa were *Muribaculum*, *Faecalibacterium*, *Bifidobacterium*, *Bacteroides*, *Rothia*, and *Cutibacterium* in bile whereas *Bacteroides*, *Muribaculum*, *Archaea*, *Rothia*, *Fusobacterium*, *Prevotella*, and *Lachnospiraceae* in gallstone (Figure 5A). For fungi–fungi interactions, five modules (keystone

taxa: *Paecilomyces*, *Ascomycota*, *Epicoccum*, *Sebacina*, and *Archaeorhizomyces*) were observed in bile, whereas only three modules (keystone taxa: *Ascomycota*, *Fusarium*, and *Russula*) were found in gallstone. However, the correlations of the network in gallstone were more than three times those in bile, primarily driven by an increased number of nodes (94 vs. 28;  $\chi^2$  test,  $p=1.50E-37$ ; Figure 5B; Table 2; Supplementary Tables S5, S6).

Similarly, the network of bacteria–fungi interactions in gallstone was also greater than in bile, despite that they both had four modules (267 vs. 94;  $\chi^2$  test,  $p=3.88E-72$ ; Figures 6A,B; Table 2; Supplementary Tables S7, S8). Bacteria *Faecalibacterium*, *Prevotella*, *Bacteroides*, *Romboutsia*, and *Unassigned*, and fungi *Sebacina*, *Ascomycota*, *Archaeorhizomyces*, *Epicoccum*, and others were key taxa

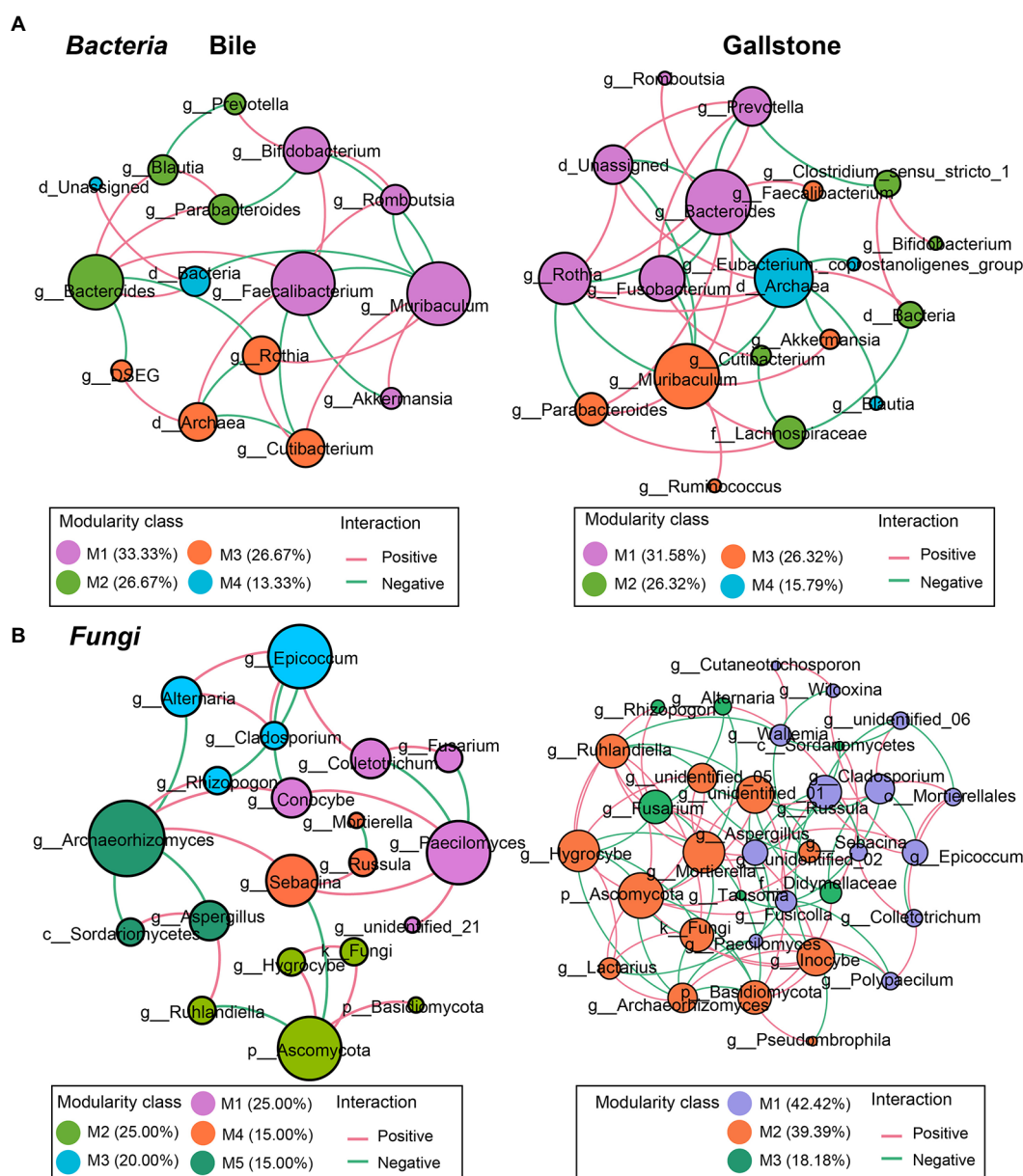
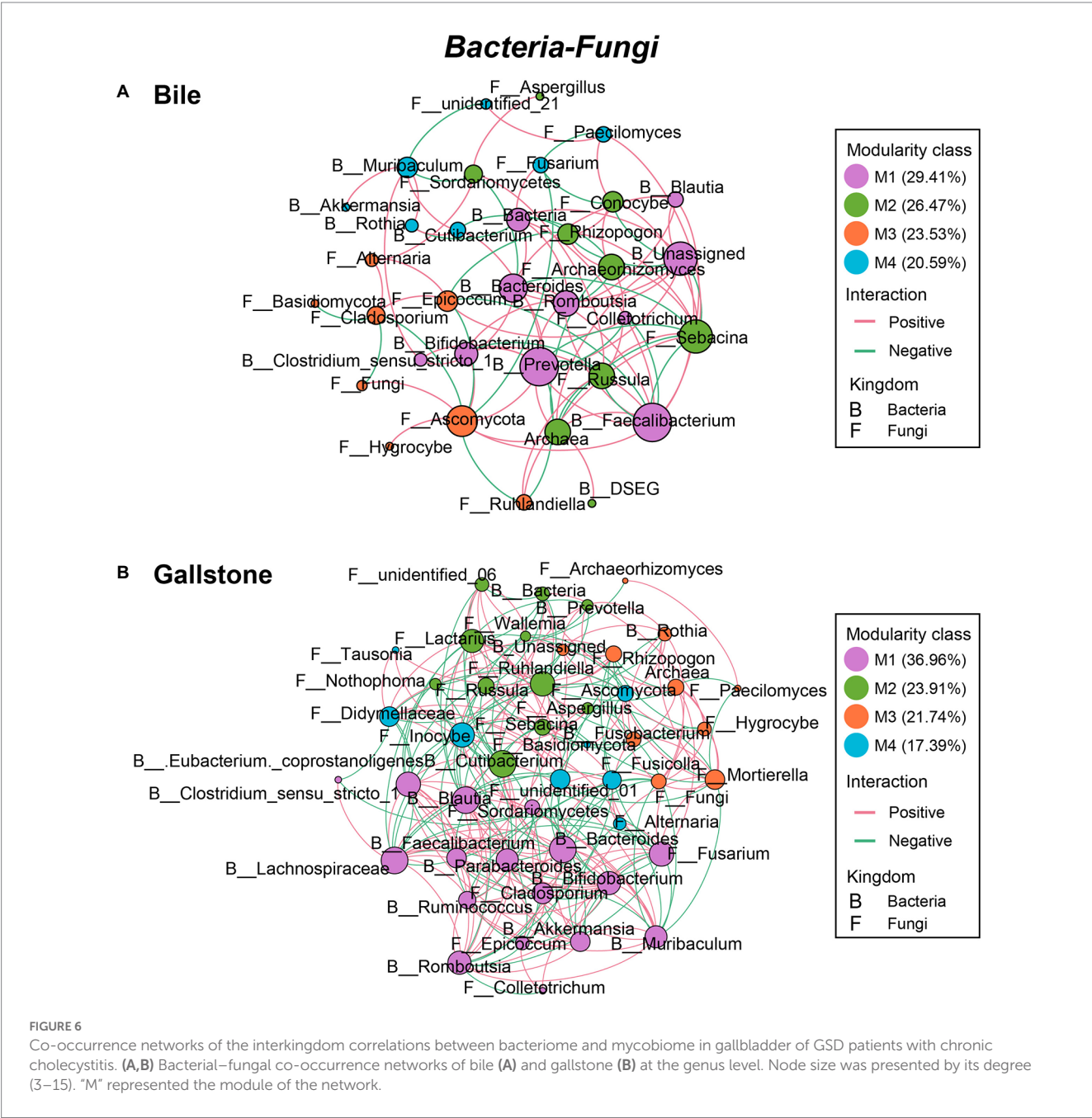


FIGURE 5

Co-occurrence networks of the intrakingdom correlations of bacteriome and mycobiome in gallbladder of GSD patients with chronic cholecystitis. (A,B) Bacterial–bacterial (A) and fungal–fungal (B) co-occurrence networks of bile (left) and gallstone (right) at the genus level. Node size was presented by its degree (3–15). “M” represented the module of the network.

TABLE 2 Summary of bacterial-bacterial, fungal-fungal and bacterial-fungal co-occurrence networks in bile and gallstone.

Network	Sample	#Node	#Edge	Positive (%)	Negative (%)	$\chi^2$ for #edge	Positive/Negative
Bacteria–Bacteria	Bile	15	28	57.14	42.86	0.047	1.33
	Gallstone	19	37	56.76	43.24		1.31
Fungi–Fungi	Bile	20	28	64.29	35.71	1.50E-37	1.80
	Gallstone	33	94	51.06	48.94		1.04
Bacteria–Fungi	Bile	34	94	64.89	35.11	3.88E-72	1.85
	Gallstone	46	267	55.81	44.19		1.26



in bile (Figure 6A). Bacteria *Lachnospiraceae*, *Muribaculum*, *Bacteroides*, *Blautia*, *Cutibacterium*, and *Clostridium sensu stricto* 1, and fungi *Fusarium*, *Ruhlandiella*, *Lactarius*, *Inocybe*, *Mortierella*, *Fusicolla*, *Didymellaceae*, and *Cladosporium* were keystone in

gallstone (Figure 6B). Altogether, these results indicate more diverse and complex microbial interactions in gallstone than bile in the gallbladder, and the fungi and its interactions with bacteria might play a key role in the formation of gallstone.

# Potential functions of bacteria and fungi in the gallbladder of GSD

To understand the potential functions of the gallbladder microbiome, we further compared the predicted outcomes of bacteria between bile and gallstone (Figure 7A) and analyzed the fungal trophic mode and guild in the gallbladder (Figure 7B). Vitamin B6 metabolism and carbapenem biosynthesis of bacteria were higher in bile than gallstone (Figure 7A). Conversely, bacterial sulfur metabolism, lipopolysaccharide biosynthesis, thyroid hormone

synthesis, and amoebiasis were significantly enriched in gallstones (Figure 7A).

For fungi, we used the FUNGuild database to identify species guilds (Figure 7B). Saprotroph was the most abundant trophic mode, followed by modes symbiotroph and pathotroph. Endophyte and animal pathogen were the two dominant guilds. Additionally, fungal parasite, ectomycorrhizal, wood saprotroph, plant pathogen, lichen parasite, litter saprotroph, and soil saprotroph were also observed in the gallbladder mycobiome. Collectively, these results demonstrated that bacterial sulfur metabolism and fungal saprotroph and animal

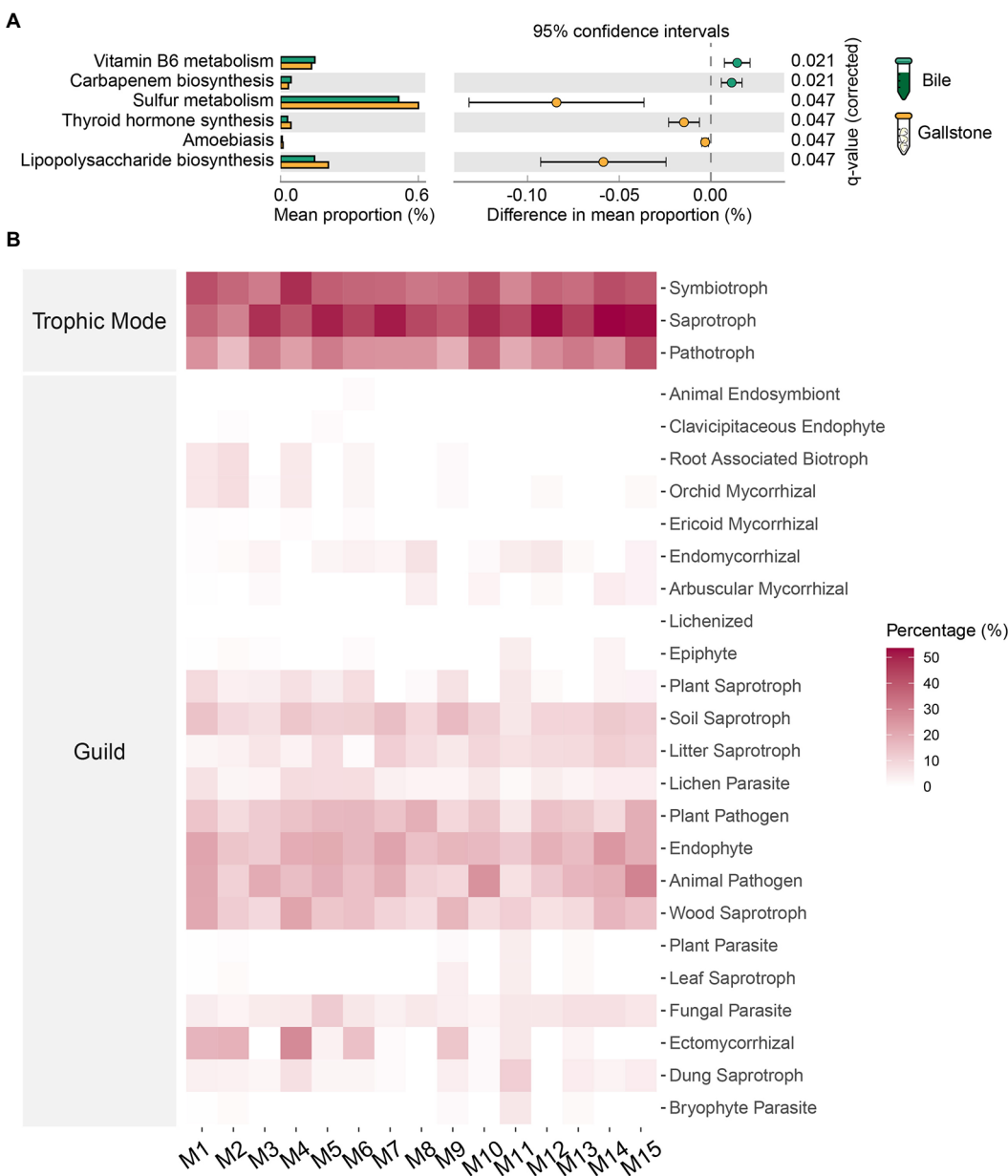


**FIGURE 7** Predicted potential functions of microbiota in gallbladder of GSD patients with chronic cholecystitis. **(A)** Extended error bar of differential bacterial pathways between bile and gallstone. Statistic was performed by a two-sided *t* test (equal variance) with Storey False Discovery Rate (FDR) in STAMP. **(B)** Heatmap of fungal traits (trophic modes and guilds) in gallbladder. "M" represented the module of constructed network performed by microeco package.



pathogen in the gallbladder might contribute to the formation of gallstones.

## Discussion

Increasing evidence has demonstrated the importance of microbiota in the development of many diseases. GSD is a major type of gallbladder disease, which affects 10–20% of the global adult population (Grigor'eva and Romanova, 2020). Multikingdom gallbladder microbiome analysis by metagenomic sequencing provides a new opportunity to explore the gallbladder mycobiome landscape in GSD. Accordingly, we used metagenomic sequencing to show for the first time that the gallbladder gallstone mycobiome in GSD subjects is similar to paired bile mycobiome, characterized by the same diversity and richness and a few differential gallstone-related fungal species. However, the interkingdom correlations between the mycobiome and bacteriome and the intrakingdom correlations within them were marked as more gallstone-related correlations. In addition, we first found that archaea (such as DSEG) were significantly thriving in bile, indicating the association thereof with gallbladder microbiome dysbiosis in GSD. These data fill an important gap in our current understanding of the potential role of gallbladder microbiome profile in GSD.

Research on the bile and gallstone microbiota and their role in biliary disease is quite rare. To our knowledge, no previous studies have described changes in the diversity of the human gallbladder mycobiome in GSD, although the fungus *Candida* in bile was recently reported by Serra et al. based on the culture method (Serra et al., 2021). To identify consistent gallbladder fungal signatures for bile and gallstone, we first combined both sex and types of gallstones to generally observe the changes. Our data showed a significant difference in evenness between bile and gallstone but not in the Shannon diversity and richness. One explanation could be that the species distribution was more uniform in gallstone than in bile (Supplementary Figure S9), which may have led to a more significant difference in the evenness of the samples. In addition, our PCoA results also suggest different trends of mycobiome between bile and gallstone samples. However, the pseudo-*F* values obtained in the PCoA remained low (1.81), indicating that larger unknown factors may contribute to variations between the subjects.

In this exploratory study to identify more potential taxa that might be associated with bile and gallstone, we included fungal species with a relative abundance of >0.005%. As a result, we found markedly differential fungal species, including taxa with lower abundance in gallstone samples. To date, limited information is available about the role of these differential fungal species in GSD, especially for the taxa with very low abundance (such as *C. sublineola*). Further functional research on the fungal markers might help understand the role of the mycobiome in gallbladder diseases.

Ascomycota and Basidiomycota constitute the major phyla of the kingdom fungi in the gallbladder. It was previously revealed that the Ascomycota:Basidiomycota ratio in the gut could represent a fungal dysbiosis index to differentiate diseases (Sokol et al., 2017; Cao et al., 2021). We found that it was higher in gallstone than in bile, implying a dysbiosis in bile, thus leading to stone formation in the gallbladder. Genera *Aspergillus* and *Candida* are two of the predominant members in the gallbladder mycobiome, some of which are widely reported to be pathogenic to humans and animals. One reason for the phenomena

might be that members of *Aspergillus* can survive in both highly acidic and mildly basic conditions and at a wide range of temperatures in addition to producing secondary metabolites mycotoxins that are capable of causing disease and death in humans (Bennett and Klich, 2003). Importantly, *Candida* spp. are commonly associated with humans. The genus *Candida* comprises over 10 species that are known to induce opportunistic infections in humans, especially *C. albicans* (Yapar, 2014; Kapitan et al., 2019). In line with that, *C. albicans* was the most abundant species in both bile and gallstone.

Numerous studies have identified bile bacterial alterations in biliary diseases, but there is limited evidence to compare gallbladder microbiome differences between bile and gallstone. Our results are consistent with those of previous studies, demonstrating that phyla, Firmicutes, Bacteroidetes, Actinobacteria, and Proteobacteria, predominate in the bile bacteriome (Shen et al., 2015; Molinero et al., 2019). We found that GSD subjects were associated with significant alterations in bacterial composition between bile and gallstone samples. Notably, kingdom bacteria was significantly enriched in gallstone, demonstrating that bacteria could be a key factor contributing to stone formation. Proteobacteria which include many pathogenic species was enriched in gallstone, implying its potential role contributing to the formation of stone (Timur Liwinski et al., 2019). A recent study demonstrated that bile acid and cholesterol metabolism dysfunction contributed to cholesterol gallstone formation (Hu et al., 2022). We observed a significant increase in the cholesterol-reducing anaerobic genus *E. coprostanoligenes* in gallstone of patients with GSD (Ren et al., 1996; Le et al., 2022). One possible explanation could be that the gallstones obtained in this study were mostly cholesterol stones (85.3%). In addition, *B. plebeius*, which was found in the human gut and could become an opportunistic pathogen if it escapes the gut, was thriving in gallstone.<sup>3</sup> *Clostridium sensu stricto* 1, referring to the *Clostridium* cluster I, which has a potential causative capacity, was associated with gallstone (Lopetuso et al., 2013). In addition, *Clostridiales* which can produce trimethylamine (TMA), the precursor of trimethylamine N-oxide (TMAO), was a biomarker in gallstone (Wang et al., 2015). Consistent with this, Chen Y. et al. (2019) found that high TMAO levels were positively associated with the presence of gallstone disease in humans. These results indicate that *Clostridiales* may contribute to GSD by a mechanism based on its metabolite TMA/TMAO signaling.

Archaea are widespread microorganisms that live in a variety of natural and host-associated ecosystems (Baker et al., 2020). Several aquatic microbiota types such as DSEG and Rhodobacteraceae were dominant in bile, which might be because of bile's liquid environment, indicating that the archaea are a major group that thrives in extreme environments. However, it should be noted that we assigned the Archaea according to data of 16S rRNA genes for bacteria and not the archaea-specific genes in this study. Further research on the archaeal markers and functions might help uncover the role of the archaeome in gallbladder diseases.

It should be noted that understanding the microbial interactions are of particular significance in human health and disease. Indeed, both positive and negative connections between bacteria and fungi in the gut have been reported (Richard and Sokol, 2019). Thus, we analyzed the bacterial and fungal interkingdom and intrakingdom

<sup>3</sup> <https://www.ncbi.nlm.nih.gov/genome/?term=txid310297>

interactions in gallbladder. In general, our data indicate a complex microbial ecologic community in gallstones and further demonstrate that the unique environment of gallstones promotes microbial interactions; in turn, the complex interactions may boost the formation and growth of gallstones in the gallbladder.

In addition, we found a reconstruction of microbial co-occurrence network in gallstone. First, the number of nodes increased in the network of gallstones. Second, the key modules changed within a network of gallstones. Third, the relationships altered between the taxa, and even in the same two taxa, such as the *Muribaculum* and *Rothia* (positive in bile, but negative in gallstone; Figures 5A,B; Supplementary Tables S3, S4). Interestingly, the ratio of positive and negative correlations seems to maintain a “relative balance” (positive/negative = 1.3) in the bacteria–bacteria network in both bile and gallstone. The ratio is close to 2 (1.8) in the networks of fungi–fungi and bacteria–fungi in bile, whereas it is close to 1 in these networks in gallstone. This suggests that (1) microbial interactions tend to affect homeostasis in the gallbladder, and that (2) fungal disorder in bile might play a vital role in GSD.

Importantly, in this study, we found that the bacterial communities are largely different, while the fungal colonies are similar between bile and gallstone in GSD. This interesting phenomenon could be explained by three points. First, the bacteria were indeed the most major members of microorganisms in bile while fungi were a smaller group than bacteria. Moreover, we detected a group of archaea accounting for a large proportion in bile which hardly were detected in gallstone in bacterial analysis (such as DSEG, Figure 2). Second, the number of negative interactions (e.g., resource competition) of bacteria–bacteria network was more than those of fungi–fungi in bile and gallstone (Table 2). Therefore, this might cause a large change of bacteria not fungi. Last, there are distinct types of environments between bile and gallstone—liquid for bile whereas solid for gallstone, as well as disparate environmental factors, mainly water, bile acids/salts, and inorganic ions for bile but cholesterol, calcium salts, and bilirubin for gallstone. Thus, there are more room and resource of bile than gallstone to survive for microbes so that bacteria altered largely for surviving. Altogether, it is implied that most fungi and a small part bacteria detected in current study might contribute to the formation of gallstone.

Hu et al. identified the gut bacterial *Desulfovibrionales* as a key taxon contributing to cholesterol gallstone formation (Hu et al., 2022). Furthermore, *Desulfovibrionales* are responsible for metabolizing dietary and host-derived sulfur-containing compounds (Peck et al., 2019). In line with this, bacterial sulfur metabolism was significantly active in gallstone according to function prediction analysis in this study. Lipopolysaccharide (LPS) is an endotoxin derived from the outer membrane of Gram-negative bacteria. LPS can cause many health problems, particularly in people who have thyroid and autoimmune thyroid disorders. Indeed, we found high thyroid hormone synthesis activity of bacteria in gallstones. In addition, LPS can cause an acute inflammatory response by triggering the release of a great number of inflammatory cytokines (Lopes, 2016). One possible interpretation is that the subjects recruited in this study have chronic cholecystitis complications.

Notably, this study had some limitations. First, because of ethical and social issues, we could not obtain healthy bile samples as the control group. Accordingly, collecting bile samples from the gallbladders of subjects without hepatobiliary disease from liver transplant donors for the control or reference bile microbiota group may be an alternative method (Molinero et al., 2019).

Second, we used the marker gene (16S/ITS) amplicon sequencing technology for microbial analysis, which did not provide the functional information of microbiota in the gallbladder. Meanwhile, we used the reference database approach for bacterial and fungal reads classification, which may allow the loss of a considerable part of novel microbiota owing to the absence of a reference data. As such, shotgun metagenomic sequencing is an alternative solution. In addition, an archaea-specific analysis method is further required.

Third, the gut microbiome community is also likely to be linked with the formation of gallstones (Hu et al., 2022; Zhao et al., 2022). Our study did not excavate the spectrum of the gut microbiome. Thus, the location difference of gut not only the feces need to be further explored. Moreover, the microbial metabolites (such as secondary bile acids) are now suggested to be very important in health and disease (de Vos et al., 2022; Hu et al., 2022). Metabonomics may be a useful approach to uncover the GSD-related microbial metabolites in the future.

Fourth, because we did not include patients with longitudinal follow-up and prognosis, we were unable to study the possibility of preventing GSD by evaluating the risk of GSD before its progression. Future studies should recruit individuals with prognoses to validate the value of predicting full-blown GSD by gallbladder microbial profiles.

Lastly, other external factors, including diet and lifestyle changes—which are known to affect the microbiome (David et al., 2014; Strasser et al., 2021)—were not assessed in this study. Nonetheless, these findings provided new insights into our understanding of the role of bacteriome and mycobiome alterations in bile and gallstone. Further larger-scale studies are needed to explore the confounding factors and cause–effect between microbiome and GSD.

## Conclusion

This study demonstrated that large and complex bacteria and fungi inhabited in the gallbladder of patients with GSD, and gallstone was characterized by significantly altered bacterial taxonomic composition. In addition, the bacterial–bacterial, fungal–fungal and bacterial–fungal correlations were strengthened compared to bile in the gallbladder of patients with GSD. As such, mycobiome, bacteriome, and even archaeome and their interactions might contribute to the formation of gallstone. We believe that our first paired bile–gallstone microbiome study has taken an important step in this field.

## Data availability statement

The data presented in the study are deposited in the Genome Sequence Archive (<https://ngdc.cnpc.ac.cn/gsa>) repository in the National Genomics Data Center (NGDC), accession numbers CRA008937 and CRA008920.

## Ethics statement

The studies involving human participants were reviewed and approved by the Institutional Ethics Review Board of the Third People's Hospital of Chengdu. The patients/participants provided their written informed consent to participate in this study.

## Author contributions

YL, TZ, and JH designed the study. YJL and QY obtained the grants. JH analyzed the data and obtained plots. JT, XZ, KY, AZ, and YL enrolled the patients and participated in the clinical part of the study. JH and TZ wrote the draft of the manuscript. All the authors participated in the discussion and reviewed the manuscript.

## Funding

This work was supported by the National Natural Science Foundation of China (82170887), the Chengdu High-level Key Clinical Specialty Construction Project, and the Science and Technology Project of The Health Planning Committee of Sichuan Municipality (20PJ211).

## Acknowledgments

We respectfully acknowledge our participants, who selflessly helped to complete this project.

## References

- Baker, B. J., De Anda, V., Seitz, K. W., Dombrowski, N., Santoro, A. E., and Lloyd, K. G. (2020). Diversity, ecology and evolution of Archaea. *Nat. Microbiol.* 5, 887–900. doi: 10.1038/s41564-020-0715-z
- Bastian, M., Heymann, S., and Jacomy, M. (2009). Gephi: an open source software for exploring and manipulating networks. *Int. AAAI Conf. Weblogs Soc. Med.* 3, 361–362. doi: 10.1609/icwsm.v3i1.13937
- Begley, M., Gahan, C. G., and Hill, C. (2005). The interaction between bacteria and bile. *FEMS Microbiol. Rev.* 29, 625–651. doi: 10.1016/j.femsre.2004.09.003
- Bennett, J. W., and Klich, M. (2003). Mycotoxins. *Clin. Microbiol. Rev.* 16, 497–516. doi: 10.1128/cmr.16.3.497-516.2003
- Bolyen, E., Rideout, J. R., Dillon, M. R., Bokulich, N. A., Abnet, C. C., Al-Ghalith, G. A., et al. (2019). Reproducible, interactive, scalable and extensible microbiome data science using QIIME 2. *Nat. Biotechnol.* 37, 852–857. doi: 10.1038/s41587-019-0209-9
- Cao, Y., Wang, L., Ke, S., Villafuerte Galvez, J. A., Pollock, N. R., Barrett, C., et al. (2021). Fecal microbiota combined with host immune factors distinguish *Clostridioides difficile* infection from asymptomatic carriage. *Gastroenterology* 160, 2328–2339.e6. doi: 10.1053/j.gastro.2021.02.069
- Chen, B., Fu, S. W., Lu, L., and Zhao, H. (2019). A preliminary study of biliary microbiota in patients with bile duct stones or distal Cholangiocarcinoma. *Biomed. Res. Int.* 2019, –1092512. doi: 10.1155/2019/1092563
- Chen, Y., Weng, Z., Liu, Q., Shao, W., Guo, W., Chen, C., et al. (2019). FMO3 and its metabolite TMAO contribute to the formation of gallstones. *Biochim. Biophys. Acta Mol. basis Dis.* 1865, 2576–2585. doi: 10.1016/j.bbdis.2019.06.016
- Choe, J. W., Lee, J. M., Hyun, J. J., and Lee, H. S. (2021). Analysis on microbial profiles & components of bile in patients with recurrent CBD stones after endoscopic CBD stone removal: a preliminary study. *J. Clin. Med.* 10:3303. doi: 10.3390/jcm10153303
- Cui, L., Morris, A., and Ghedin, E. (2013). The human mycobiome in health and disease. *Genome Med.* 5:63. doi: 10.1186/gm467
- David, L. A., Maurice, C. F., Carmody, R. N., Gootenberg, D. B., Button, J. E., Wolfe, B. E., et al. (2014). Diet rapidly and reproducibly alters the human gut microbiome. *Nature* 505, 559–563. doi: 10.1038/nature12820
- de Vos, W. M., Tilg, H., Van Hul, M., and Cani, P. D. (2022). Gut microbiome and health: mechanistic insights. *Gut* 71, 1020–1032. doi: 10.1136/gutjnl-2021-326789
- Fan, L. L., Chen, B. H., and Dai, Z. J. (2017). The relation between gallstone disease and cardiovascular disease. *Sci. Rep.* 7:15104. doi: 10.1038/s41598-017-15430-5
- Feng, K., Peng, X., Zhang, Z., Gu, S. S., He, Q., Shen, W. L., et al. (2022). iNAP: an integrated network analysis pipeline for microbiome studies. *iMeta* 1:e13. doi: 10.1002/imt2.13
- Grigor'eva, I. N., and Romanova, T. I. (2020). Gallstone disease and microbiome. *Microorganisms* 8:835. doi: 10.3390/microorganisms8060835
- Hazrah, P., Oahn, K. T., Tewari, M., Pandey, A. K., Kumar, K., Mohapatra, T. M., et al. (2004). The frequency of live bacteria in gallstones. *HPB (Oxford)* 6, 28–32. doi: 10.1080/13651820310025192
- Hu, H., Shao, W., Liu, Q., Liu, N., Wang, Q., Xu, J., et al. (2022). Gut microbiota promotes cholesterol gallstone formation by modulating bile acid composition and biliary cholesterol secretion. *Nat. Commun.* 13:252. doi: 10.1038/s41467-021-27758-8
- Kapitan, M., Niemiec, M. J., Steimle, A., Frick, J. S., and Jacobsen, I. D. (2019). Fungi as part of the microbiota and interactions with intestinal bacteria. *Curr. Top. Microbiol. Immunol.* 422, 265–301. doi: 10.1007/82\_2018\_117
- Kim, B., Park, J. S., Bae, J., and Hwang, N. (2021). Bile microbiota in patients with pigment common bile duct stones. *J. Korean Med. Sci.* 36:e94. doi: 10.3346/jkms.2021.36.e94
- Le, H. H., Lee, M. T., Besler, K. R., Comrie, J. M. C., and Johnson, E. L. (2022). Characterization of interactions of dietary cholesterol with the murine and human gut microbiome. *Nat. Microbiol.* 7, 1390–1403. doi: 10.1038/s41564-022-01195-9
- Lee, D. K., Tarr, P. I., Haigh, W. G., and Lee, S. P. (1999). Bacterial DNA in mixed cholesterol gallstones. *Am. J. Gastroenterol.* 94, 3502–3506. doi: 10.1111/j.1572-0241.1999.01614.x
- Liu, C., Cui, Y., Li, X., and Yao, M. (2021). microeco: an R package for data mining in microbial community ecology. *FEMS Microbiol. Ecol.* 97:fiaa255. doi: 10.1093/femsec/fiaa255
- Lopes, P. C. (2016). LPS and neuroinflammation: a matter of timing. *Inflammopharmacology* 24, 291–293. doi: 10.1007/s10787-016-0283-2
- Lopetuso, L. R., Scaldaferrri, F., Petito, V., and Gasbarrini, A. (2013). Commensal clostridia: leading players in the maintenance of gut homeostasis. *Gut Pathog.* 5:23. doi: 10.1186/1757-4749-5-23
- Maki, T. (1966). Pathogenesis of calcium bilirubinate gallstone: role of *E. coli*, beta-glucuronidase and coagulation by inorganic ions, polyelectrolytes and agitation. *Ann. Surg.* 164, 90–100. doi: 10.1097/0000658-196607000-00010
- Molinero, N., Ruiz, L., Milani, C., Gutierrez-Diaz, I., Sanchez, B., Mangifesta, M., et al. (2019). The human gallbladder microbiome is related to the physiological state and the biliary metabolic profile. *Microbiome* 7:100. doi: 10.1186/s40168-019-0712-8
- Mukherjee, P. K., Sendid, B., Hoarau, G., Colombel, J. F., Poulain, D., and Ghannoum, M. A. (2015). Mycobiota in gastrointestinal diseases. *Nat. Rev. Gastroenterol. Hepatol.* 12, 77–87. doi: 10.1038/nrgastro.2014.188
- Peck, S. C., Denger, K., Burrichter, A., Irwin, S. M., Balskus, E. P., and Schleheck, D. (2019). A glycol radical enzyme enables hydrogen sulfide production by the human intestinal bacterium *Bifidobacterium wadsworthia*. *Proc. Natl. Acad. Sci. U. S. A.* 116, 3171–3176. doi: 10.1073/pnas.1815661116
- Pereira, P., Aho, V., Arola, J., Boyd, S., Jokelainen, K., Paulin, L., et al. (2017). Bile microbiota in primary sclerosing cholangitis: impact on disease progression and development of biliary dysplasia. *PLoS One* 12:e0182924. doi: 10.1371/journal.pone.0182924
- Petrov, V. A., Fernandez-Peralbo, M. A., Derks, R., Knyazeva, E. M., Merzlikin, N. V., Sazonov, A. E., et al. (2020). Biliary microbiota and bile acid composition in cholelithiasis. *Biomed. Res. Int.* 2020, 1–8. doi: 10.1155/2020/1242364
- Portincasa, P., and Wang, D. Q. (2012). Intestinal absorption, hepatic synthesis, and biliary secretion of cholesterol: where are we for cholesterol gallstone formation? *Hepatology* 55, 1313–1316. doi: 10.1002/hep.25604

## Conflict of interest

The authors declare that the research was conducted in the absence of any commercial or financial relationships that could be construed as a potential conflict of interest.

## Publisher's note

All claims expressed in this article are solely those of the authors and do not necessarily represent those of their affiliated organizations, or those of the publisher, the editors and the reviewers. Any product that may be evaluated in this article, or claim that may be made by its manufacturer, is not guaranteed or endorsed by the publisher.

## Supplementary material

The Supplementary material for this article can be found online at: <https://www.frontiersin.org/articles/10.3389/fmicb.2023.1131694/full#supplementary-material>

- Ramana Ramya, J., Thanigai Arul, K., Epple, M., Giebel, U., Guendel-Graber, J., Jayanthi, V., et al. (2017). Chemical and structural analysis of gallstones from the Indian subcontinent. *Mater. Sci. Eng. C Mater. Biol. Appl.* 78, 878–885. doi: 10.1016/j.msec.2017.04.004
- Ren, D., Li, L., Schwabacher, A. W., Young, J. W., and Beitz, D. C. (1996). Mechanism of cholesterol reduction to coprostanol by *Eubacterium coprostanoligenes* ATCC 51222. *Steroids* 61, 33–40. doi: 10.1016/0039-128x(95)00173-n
- Richard, M. L., and Sokol, H. (2019). The gut mycobiota: insights into analysis, environmental interactions and role in gastrointestinal diseases. *Nat. Rev. Gastroenterol. Hepatol.* 16, 331–345. doi: 10.1038/s41575-019-0121-2
- Scherber, P. R., Lammert, F., and Glanemann, M. (2017). Gallstone disease: optimal timing of treatment. *J. Hepatol.* 67, 645–647. doi: 10.1016/j.jhep.2017.04.003
- Serra, N., Di Carlo, P., D'Arpa, F., Battaglia, E., Fasciana, T., Gulotta, G., et al. (2021). Human bile microbiota: a retrospective study focusing on age and gender. *J. Infect. Public Health* 14, 206–213. doi: 10.1016/j.jiph.2020.11.005
- Shen, H., Ye, F., Xie, L., Yang, J., Li, Z., Xu, P., et al. (2015). Metagenomic sequencing of bile from gallstone patients to identify different microbial community patterns and novel biliary bacteria. *Sci. Rep.* 5:17450. doi: 10.1038/srep17450
- Sokol, H., Leducq, V., Aschard, H., Pham, H. P., Jegou, S., Landman, C., et al. (2017). Fungal microbiota dysbiosis in IBD, Fungal microbiota dysbiosis in IBD. *Gut* 66, 1039–1048. doi: 10.1136/gutjnl-2015-310746
- Stewart, L., Griffiss, J. M., Jarvis, G. A., and Way, L. W. (2006). Biliary bacterial factors determine the path of gallstone formation. *Am. J. Surg.* 192, 598–603. doi: 10.1016/j.amjsurg.2006.08.001
- Stewart, L., Oesterle, A. L., Erdan, I., Griffiss, J. M., and Way, L. W. (2002). Pathogenesis of pigment gallstones in Western societies: the central role of bacteria. *J. Gastrointest. Surg.* 6:891-903; discussion 903-894. doi: 10.1016/s1091-255x(02)00035-5
- Strasser, B., Wolters, M., Weyh, C., Krüger, K., and Ticinesi, A. (2021). The effects of lifestyle and diet on gut microbiota composition, inflammation and muscle performance in our aging society. *Nutrients* 13:2045. doi: 10.3390/nu13062045
- Swidsinski, A., and Lee, S. P. (2001). The role of bacteria in gallstone pathogenesis. *Front. Biosci.* 6, E93–E103. doi: 10.2741/swidsinski
- Swidsinski, A., Ludwig, W., Pahlig, H., and Priem, F. (1995). Molecular genetic evidence of bacterial colonization of cholesterol gallstones. *Gastroenterology* 108, 860–864. doi: 10.1016/0016-5085(95)90461-1
- Timur Liwinski, R. Z., John, C., Ehlken, H., Rühlemann, M. C., Bang, C., Groth, S., et al. (2019). Alterations of the bile microbiome in primary sclerosing cholangitis. *Gut* 69, 665–672. doi: 10.1136/gutjnl-2019-318416
- Verdier, J., Luedde, T., and Sellge, G. (2015). Biliary mucosal barrier and microbiome. *Viszeralmedizin* 31, 156–161. doi: 10.1159/000431071
- Wang, Z., Roberts, A. B., Buffa, J. A., Levison, B. S., Zhu, W., Org, E., et al. (2015). Non-lethal inhibition of gut microbial trimethylamine production for the treatment of atherosclerosis. *Cells* 163, 1585–1595. doi: 10.1016/j.cell.2015.11.055
- Warburton, R. C., Harper, W. G. S., Rushbrook, S., and Narbad, A. (2017). Human bile retrieved from the normal biliary system is not sterile. *J. Hepatol.* 66:S65. doi: 10.1016/s0168-8278(17)30391-4
- Wemheuer, F., Taylor, J. A., Daniel, R., Johnston, E., Meinicke, P., Thomas, T., et al. (2020). Tax4Fun2: prediction of habitat-specific functional profiles and functional redundancy based on 16S rRNA gene sequences. *Environ. Microbiome* 15:11. doi: 10.1186/s40793-020-00358-7
- Yapar, N. (2014). Epidemiology and risk factors for invasive candidiasis. *Ther. Clin. Risk Manag.* 10, 95–105. doi: 10.2147/tcrm.s40160
- Ying Liu, J.-D. J., Sun, L.-Y., Zhu, Z.-J., Zhang, J.-R., Wei, L., Wei, Q., et al. (2018). Characteristics of bile microbiota in liver transplant recipients with biliary injury. *Int. J. Clin. Exp. Pathol.* 11, 481–489.
- Zhao, H. D., Gao, P., and Zhan, L. (2022). The mechanism of intestinal flora and its metabolites in the formation of cholesterol gallstones. *J. Clin. Hepatol.* 38, 947–950. doi: 10.3969/j.issn.1001-5256.2022.04.042





## OPEN ACCESS

EDITED BY  
Weiqi He,  
Soochow University, China

REVIEWED BY  
Jozsef Soki,  
University of Szeged, Hungary  
Zheng Sun,  
Harvard Medical School, United States

\*CORRESPONDENCE  
Yingzi Ming  
✉ mingyz\_china@csu.edu.cn

†These authors have contributed equally to this work and share first authorship

## SPECIALTY SECTION

This article was submitted to  
Microorganisms in Vertebrate Digestive  
Systems,  
a section of the journal  
Frontiers in Microbiology

RECEIVED 12 December 2022

ACCEPTED 07 March 2023

PUBLISHED 29 March 2023

## CITATION

Xiang X, Peng B, Liu K, Wang T, Ding P, Li H,  
Zhu Y and Ming Y (2023) Association between  
salivary microbiota and renal function in renal  
transplant patients during the perioperative  
period. *Front. Microbiol.* 14:1122101.  
doi: 10.3389/fmicb.2023.1122101

## COPYRIGHT

© 2023 Xiang, Peng, Liu, Wang, Ding, Li, Zhu  
and Ming. This is an open-access article  
distributed under the terms of the [Creative  
Commons Attribution License \(CC BY\)](#). The use,  
distribution or reproduction in other forums is  
permitted, provided the original author(s) and  
the copyright owner(s) are credited and that  
the original publication in this journal is cited, in  
accordance with accepted academic practice.  
No use, distribution or reproduction is  
permitted which does not comply with these  
terms.

# Association between salivary microbiota and renal function in renal transplant patients during the perioperative period

Xuyu Xiang<sup>1,2†</sup>, Bo Peng<sup>1,2†</sup>, Kai Liu<sup>1,2</sup>, Tianyin Wang<sup>1,2</sup>, Peng Ding<sup>1,2</sup>,  
Hao Li<sup>1,2</sup>, Yi Zhu<sup>1,2</sup> and Yingzi Ming<sup>1,2\*</sup>

<sup>1</sup>The Transplantation Center of the Third Xiangya Hospital, Central South University, Changsha, China,

<sup>2</sup>Engineering and Technology Research Center for Transplantation Medicine of National Health  
Commission, Changsha, China

**Introduction:** Renal transplantation is an effective treatment for the end stage renal disease (ESRD). However, how salivary microbiota changes during perioperative period of renal transplant recipients (RTRs) has not been elucidated.

**Methods:** Five healthy controls and 11 RTRs who had good recovery were enrolled. Saliva samples were collected before surgery and at 1, 3, 7, and 14 days after surgery. 16S rRNA gene sequencing was performed.

**Results:** There was no significant difference in the composition of salivary microbiota between ESRD patients and healthy controls. The salivary microbiota of RTRs showed higher operational taxonomic units (OTUs) amount and greater alpha and beta diversity than those of ESRD patients and healthy controls, but gradually stabilized over time. At the phylum level, the relative abundance of Actinobacteria, Tenericutes and Spirochaetes was about ten times different from ESRD patients or healthy controls for RTRs overall in time. The relative abundance of Bacteroidetes, Fusobacteria, Patensibacteria, Leptotrichiaceae and Streptococcaceae was correlated with serum creatinine (Scr) after renal transplantation.

**Discussion:** In short, salivary microbiota community altered in the perioperative period of renal transplantation and certain species of salivary microbiota had the potential to be a biomarker of postoperative recovery.

## KEYWORDS

salivary microbiota, renal function, renal transplantation, perioperative period, 16S rRNA

## 1. Introduction

End-stage renal disease (ESRD) represents a serious public health problem fueled by aging populations and a pandemic of chronic non-communicable diseases, which is characterized by high mortality and economic burden. Renal transplantation is one of the effective treatments, with the hope of recovery for patients to normal life. However, there is still a lack of highly sensitive and specific biomarkers with minimal invasion and cost to assess recovery or rejection during the perioperative period.

The oral cavity consists of teeth, gingival groove, tongue, soft and hard palates, buccal mucosa, and tonsils. All the above areas are inhabited by microbiota and soaked in saliva all the time. Each salivary gland is highly permeable and surrounded by capillaries, a feature that allows for a freer exchange of substances between the salivary glands and blood (Wilson et al., 2014). Therefore, the salivary microbiota has the potential to be a bridge between oral (Belström et al., 2018a) and systemic conditions.

Indeed, the relationship between chronic kidney disease (CKD) and gut microbiota has been widely investigated, both regarding changes in the floras of patients with CKD (Crespo-Salgado et al., 2016; Meijers et al., 2019; Ren et al., 2020) and regarding the mechanisms of gut microbiota in the development of CKD (Wang X. et al., 2020; Zhu et al., 2021; Wang et al., 2023). Saliva, one of the largest sources of gut microbiota, may play an important role in kidney disease that salivary microbiota ectopically colonizing the gut may be closely associated with the development of kidney disease and renal function. At the same time, several studies have discussed changes in salivary flora in patients with CKD (Hu et al., 2018; Duan et al., 2020; Guo et al., 2022; Liu et al., 2022). The overall composition of the salivary microbiota in CKD patients is significantly different from that of the healthy population, although the variation in individual flora or individual indicators is not entirely consistent across studies. Hence, the possibility of salivary microbiota functioning at CKD *in situ* cannot be ruled out. In summary, salivary microbiota has the potential as a diagnostic and therapeutic target for ESRDs or renal transplant recipients (RTRs).

Based on previous studies, we speculate that salivary microbiota in patients after renal transplantation will be significantly different from the preoperative flora and this change may be associated with renal function. Although the alteration of salivary floras in patients with ESRD has been studied, how salivary microbiota dynamic changes during the perioperative period of RTRs and the association between salivary microbiota and postoperative recovery have not been elucidated. Therefore, our study is the first to examine the variations of salivary microbiota during the perioperative period of renal transplantation and the relationship between salivary microbiota and renal function. We aimed to find some special floras associated with the return of renal function as clinical biomarkers.

## 2. Materials and methods

### 2.1. Subjects and sample collection

From 1 October 2022 to 18 October 2022, a total of 11 consecutive ESRD patients received renal transplantation in our center and were enrolled. Saliva samples were collected before surgery and at 1, 3, 7, and 14 days after surgery. Saliva samples from five healthy people were also collected as healthy controls. None of the above subjects had oral antibiotics, cortisol, smoking, or drinking history within 6 months.

Before collection, patients fasted for half an hour and rinsed their mouths. Patients spit the saliva into a sterile tube until it reaches 2 ml. Saliva was stored at  $-80^{\circ}\text{C}$  immediately after collection.

The study protocol was approved (22207) by the Ethics Committee of the Third Xiangya Hospital of Central South University (Changsha, China). Written informed consent was obtained from all study participants. Experiments were carried out in accordance with the ethical guidelines set by the Declaration of Helsinki 1964 and its later amendments.

### 2.2. Sequencing

#### 2.2.1. Sampling and DNA extraction

Total genome DNA from samples was extracted using the CTAB/SDS method. DNA concentration and purity were monitored on 1% agarose gel. According to the concentration, DNA was diluted to 1 ng/ $\mu\text{l}$  using sterile water.

#### 2.2.2. Amplicon generation

16S rRNA genes were amplified using the specific primer 341F (CCTAYGG-GRBGCASCAG) and 806R (GGACTACNNGGTATCTAAT) with the barcode. All PCR reactions were carried out in 30  $\mu\text{l}$  of reactions with 15  $\mu\text{l}$  of Phusion<sup>®</sup> High-Fidelity PCR Master Mix (New England Biolabs); 0.2  $\mu\text{M}$  of forward and reverse primers, and about 10 ng of template DNA. Thermal cycling consisted of initial denaturation at  $98^{\circ}\text{C}$  for 1 min, followed by 30 cycles of denaturation at  $98^{\circ}\text{C}$  for 10 s, annealing at  $50^{\circ}\text{C}$  for 30 s and elongation at  $72^{\circ}\text{C}$  for 60 s. And final extension at  $72^{\circ}\text{C}$  for 5 min.

#### 2.2.3. PCR products quantification and qualification

The same volume of 1X loading buffer (containing SYB green) with the PCR products and operate electrophoresis was mixed on a 2% agarose gel for detection. Samples with a bright main strip between 400 and 450 bp were chosen for further experiments.

#### 2.2.4. PCR products mixing and purification

PCR products were mixed in equidensity ratios. Then, the mixture of PCR products was purified with AxyPrep DNA Gel Extraction Kit (AXYGEN).

#### 2.2.5. Library preparation and sequencing

Sequencing libraries were generated using NEBNext<sup>®</sup> Ultra<sup>™</sup> DNA Library Prep Kit for Illumina (NEB, USA) following the manufacturer's recommendations, and index codes were added. The library quality was assessed on the Qubit<sup>®</sup> 2.0 Fluorometer (Thermo Scientific) and Agilent Bioanalyzer 2100 system. Finally, the library was sequenced on an Illumina NovaSeq 6000 platform, and 250 bp paired-end reads were generated. Sequences are deposited under SRA PRJNA904953.

### 2.3. Data analysis

#### 2.3.1. OTU cluster and species annotation

Paired-end reads from the original DNA fragments were merged using FLASH. Sequences analysis was performed by the UPARSE software package using the UPARSE-OTU and UPARSE-OTUref algorithms. In-house Perl scripts were used to analyze alpha (within samples) and beta (among samples) diversity. Sequences with  $\geq 97\%$  similarity were assigned to the same OTU. We picked a representative sequence for each OTUs and used the RDP classifier to annotate taxonomic information for each representative sequence based on Silva 132 database.

### 2.3.2. Phylogenetic distance and community distribution

Graphical representation of the relative abundance of bacterial diversity from phylum to species can be visualized using the Krona chart. Cluster analysis was preceded by principal component analysis (PCA), which was applied to reduce the dimension of the original variables using the QIIME software package. We used weighted UniFrac distance for principal coordinate analysis (PCoA) and Unweighted Pair Group Method with Arithmetic mean for the abbreviation (UPGMA) Clustering.

## 2.4. Statistical analysis

Linear discriminant analysis Effect Size (LEfSe) was used for the quantitative analysis of biomarkers within different groups. To identify differences in microbial communities between the two groups, ANOSIM and ADONIS were performed based on the Bray–Curtis dissimilarity distance matrices. A Wilcoxon rank-sum test and unpaired *t*-test were performed to evaluate differences between the two groups in alpha diversity, principal coordinates, and community difference analysis. Pearson correlation analysis was used to assess the correlation between microbiota and creatinine. A *p*-value of < 0.05 was required for the results to be considered statistically significant.

## 3. Results

### 3.1. Study population

The clinical information of RTRs (age  $44.8 \pm 12.2$  years; 63.6% males) is shown in Table 1. The mean body weight index (BMI) was  $20.5 \pm 3.8$  kg/m<sup>2</sup> for RTRs. All RTRs received antihuman thymocyte globulin (ATG) for induction, the same triple immunosuppressive therapy, FK506, mycophenolate mofetil (MMF) plus steroids, and meropenem as a primary antibiotic. The saliva samples were collected before surgery (ESRD, *n* = 11) and at 1 day (RTR1, *n* = 9), 3 days (RTR3, *n* = 11), 7 days (RTR7, *n* = 11), and 14 days (RTR14, *n* = 8) after surgery. Generally, the specimens were divided into two groups, namely the ESRD group and the RTR group.

Healthy controls (HCs, *n* = 5) ranged in age from 30 to 56 years and consisted of three men and two women. The mean BMI was  $24.0 \pm 3.1$  kg/m<sup>2</sup>, and the mean serum creatinine (Scr) was  $71.3 \pm 16.7$  μmol/L for HCs. We collected saliva samples (*n* = 9) from each of them two times, 7 days apart, to form the HC group. They all reported no history of chronic diseases or medication.

### 3.2. Impact of renal transplantation on salivary microbiota in individuals

First, according to the rarefaction curve, Shannon curve, and rank-abundance curve (Supplementary Figure 1), we found that the number of reads of most samples is reasonable. The curves tended to be flat, which indicated that the number of reads was relatively large enough to reflect species richness.

The Venn graph demonstrated the shared and unique OTUs between the three groups (Figure 1A). Overall, the RTR group has more OTUs. However, there was no significant difference in the number of OTUs in a single sample between the three groups. Figures 1B, C show the species composition of each group and individual samples at the phylum level. The ESRD and HC groups had relatively similar species composition, whereas the RTR group was quite different, especially in the relative abundance of Actinobacteria, Tenericutes, and Spirochaetes.

Alpha diversity, including Shannon, Simpson, and so on, provided a measurement of species diversity within a sample. The larger the Shannon index, the greater the diversity. The ESRD group was close to the HC group in alpha diversity. Group RTR always had larger intra-group differences (Figure 1D, RTR vs. ESRD: *p* < 0.05).

Beta diversity was used to study the intrinsic composition of the microbial structure. The closer the samples were to each other, the more similar the species' composition was. The PCoA was analyzed based on weighted UniFrac distance. According to the PCoA, the microbial composition of the RTR group was significantly different from those of the ESRD (Figure 1E) and HC (Supplementary Figure 2) groups, which was proved by the ADONIS analysis (RTR vs. ESRD: *p* = 0.001, RTR vs. HC: *p* = 0.001). On the contrary, the beta diversity of the ESRD group was not significantly different from that of the HC group (Figure 1F).

LEfSe analysis was used to describe differential species between different groups. When the LDA value was >2, the species was a statistically significant biomarker between groups. The results showed that when compared with the ESRD (Figure 2A) and HC (Figure 2B) groups, the relative abundances of Burkholderiaceae, Lautropia, and Actinobacteria of the RTR group were significantly increased, and Neisseriaceae and Neisseria were significantly decreased. The composition of OTU sequences was further transformed into KEGG orthodontics to analyze the differences in predicted function. The pathways related to membrane transport, carbohydrate metabolism, and signal transduction were significantly enriched in the RTR group (Figures 2C, D).

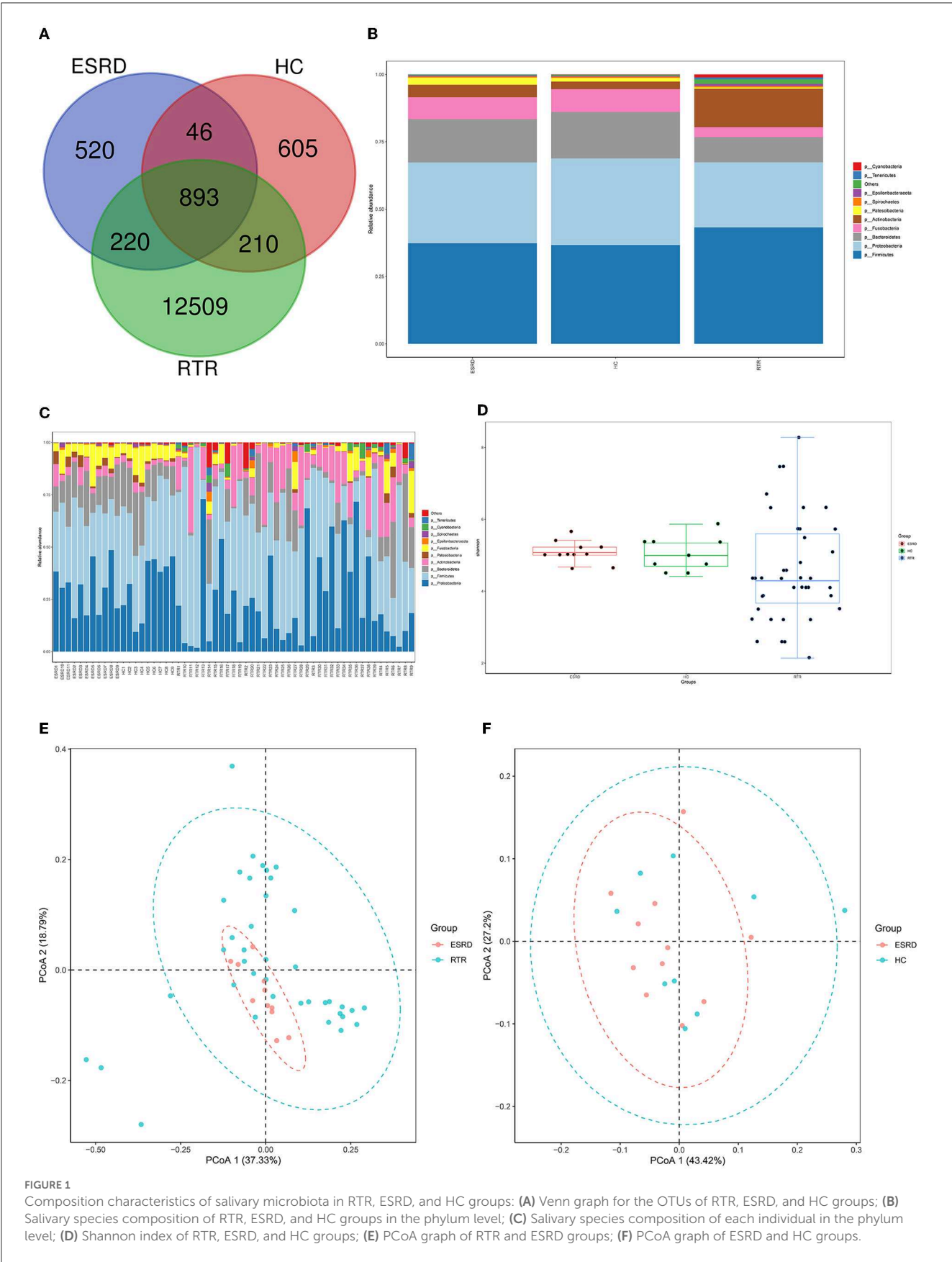
### 3.3. The dynamic change in salivary microbiota during the early stage post-renal transplantation

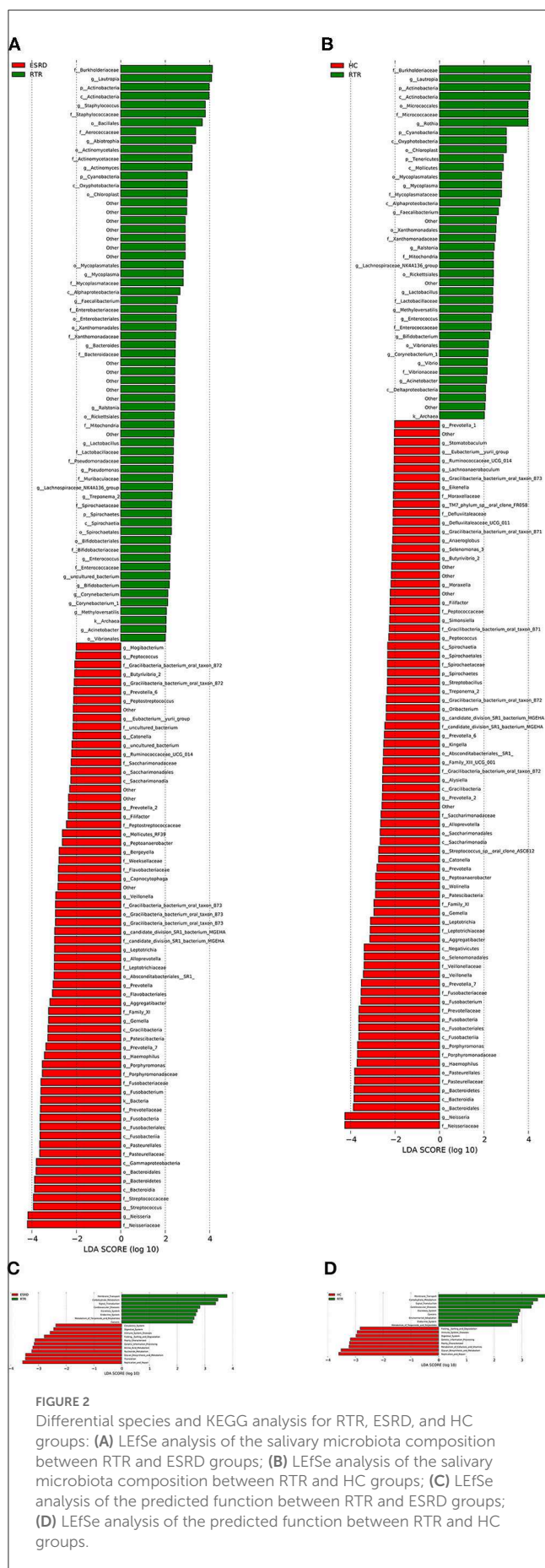
The unique community occupied most OTUs of the RTR1, RTR3, and RTR7 and differed between every two adjacent time points (Figure 3A, RTR1 vs. RTR14: *p* < 0.05). Over time, the OTUs of RTRs gradually decreased and the shared OTUs with ESRD or HC groups increased, and RTR1 or RTR7 was significantly different from ESRD or HC (Figure 3B, *p* < 0.05). Figures 3C, D show that the Ace index and intra-group differences of the RTR group descended and approached ESRD and HC groups over time (RTR1 vs. ESRD: *p* < 0.05, RTR1 vs. RTR14: *p* < 0.05). Other alpha diversity indexes also showed the same changes in the salivary microbiota of RTRs at different time points (Supplementary Figure 3). At the phylum level, the microbial composition of the RTR group was constantly changing (Figure 3E) but always differed from ESRD or HC groups (Figure 3F). From PCoA, the intrinsic microbial composition of RTR1 and RTR14

TABLE 1 Characteristics of renal transplant patients and control subjects.

Patient	Gender	Age (years)	Height (m)	Weight (kg)	Body mass index (kg/m <sup>2</sup> )	Induction therapy	Immunosuppressive therapy	Antibiotics	Dialysis type	Dialysis duration (months)	Cause of end stage renal disease	Scr before KT (umol /L)	eGFR before KT (mL/min /1.73 m <sup>2</sup> )	Scr 7 days after KT (umol /L)	Scr 14 days after KT (umol /L)
1	Female	45	1.58	51.5	20.63	ATG	FK506 + MMF +Steroids	Meropenem + Cefminox	HD	12	IgA Nephropathy	897	4.14	233	97
2	Male	53	1.62	67	25.53	ATG	FK506 + MMF +Steroids	Meropenem + Tikaolin	HD	8	Unknown	1,058	4.26	300	
3	Male	54	1.65	55.5	20.39	ATG	FK506 + MMF +Steroids	Meropenem + Carbofengin + Cefminol	HD	47	Unknown	753	6.37	204	136
4	Male	27	1.78	57.4	18.12	ATG	FK506 + MMF +Steroids	Meropenem + Colistin sulfate + Carbofengin + Cephalosporin	HD	13	Unknown	601	10.12	238	103
5	Male	64	1.5	65	28.89	ATG	FK506 + MMF +Steroids	Meropenem + Peracillin	HD	6	Unknown	623	7.47	135	114
6	Female	51	1.67	48.7	17.46	ATG	FK506 + MMF +Steroids	Meropenem	PD	60	Unknown	1,016	3.42	87	95
7	Male	31	1.76	66.6	21.50	ATG	FK506 + MMF +Steroids	Meropenem+ Peracillin	PD	19	Unknown	1,104	4.72	132	104
8	Female	32	1.63	47	17.70	ATG	FK506 + MMF +Steroids	Meropenem	PD	13	IgA Nephropathy	974	4.11	73	78
9	Male	51	1.71	48.1	16.45	ATG	FK506 + MMF +Steroids	Meropenem + Tikaolin + Peracillin	HD	3	Unknown	1,231	3.59	109	132
10	Female	53	1.45	44	20.93	ATG	FK506 + MMF +Steroids	Meropenem + Cefminox	HD	12	Unknown	999	3.44	65	87
11	Male	32	1.75	55	17.96	ATG	FK506 + MMF +Steroids	Meropenem	HD	29	Unknown	1,556	3.09	124	98
Control	Gender	Age (years)	Height (m)	Weight (kg)	Body mass index (kg/m <sup>2</sup> )	Scr (umol/L)	eGFR (mL/min/1.73 m <sup>2</sup> )								
1	Female	50	1.57	48.5	19.68	73	212.54								
2	Female	41	1.52	63	27.27										
3	Male	56	1.5	49.3	21.91	49.3	313.91								
4	Male	30	1.65	69	25.34	90	98.39								
5	Male	32	1.87	90	25.74	73	316.2								







groups significantly differed ( $p = 0.001$ ) from ESRD or HC groups (Figure 3H and Supplementary Figure 4) and the intrinsic microbial composition significantly changed between 3 and 7 days after surgery (Figure 3G and Supplementary Figure 4).

### 3.4. Certain species of salivary microbiota were associated with the recovery of renal function

The correlation between the predominant species of salivary microbiota in RTRs and ESRD and the corresponding Scr on the day of saliva collection was analyzed (Table 2 and Figure 4). In the RTRs group, Bacteroidetes, Fusobacteria, Patensibacteria, and Leptotrichiaceae were positively correlated with Scr, whereas Streptococcaceae was negatively correlated with Scr after renal transplantation. However, these floras were not significantly associated with Scr in the ESRD group.

## 4. Discussion

Salivary microbiota is more stable than gut microbiota, and factors that alter gut microbiota may not significantly alter salivary microbiota (David et al., 2014; Tuganbaev et al., 2022). ESRD patients have changes in the composition of their gut microbiota compared with healthy people (Rysz et al., 2021; Shivani et al., 2022). However, as shown in this research, the salivary microbiota of ESRD patients was similar to that of HCs in terms of the number of individual species, the relative abundance of dominant flora, alpha diversity, and beta diversity, and did not alter significantly due to chronic renal impairment, different long-term treatments, or accompanying changes in life habits. In contrast, the salivary microbiota of RTRs showed huge differences compared with ESRD and HC groups. RTRs contained nearly 10 times as many species of unique salivary microbiota. From both alpha diversity and beta diversity, the RTR group showed higher richness and intra-group differences than ESRD or HC groups. At the phylum level, the relative abundance of Actinobacteria, Tenericutes, and Spirochaetes was about 10 times higher than that of ESRD or HC groups. Actinobacteria is a ubiquitous gram-positive phylum, which has attracted much attention as a rich source of bioactive substances and a complex evolution and diversification process (Miao and Davies, 2010; Barka et al., 2016). As an oral bacterium, Actinobacteria may play a role in the etiology of diabetes (Long et al., 2017; Matsha et al., 2020). The Tenericutes were composed of bacteria that lack a peptidoglycan cell wall. The most well-studied branch of this phylum was Mollicutes, including Mycoplasma. To date, most studies had focused on pathogenic strains of the Mycoplasma order (Wang Y. et al., 2020). As reported, Mycoplasma was associated with oral leukoplakia (Mizuki et al., 2015, 2017), mucositis (Morand and Hatami, 2018), and Fanconi anemia-associated oral carcinoma (Henrich et al., 2014). Spirochaetes were important pathogenic bacteria in the clinic, but they were not well-understood. Some of these caused Lyme disease, leptospirosis, syphilis, and other human diseases. Moreover, Spirochaetes were

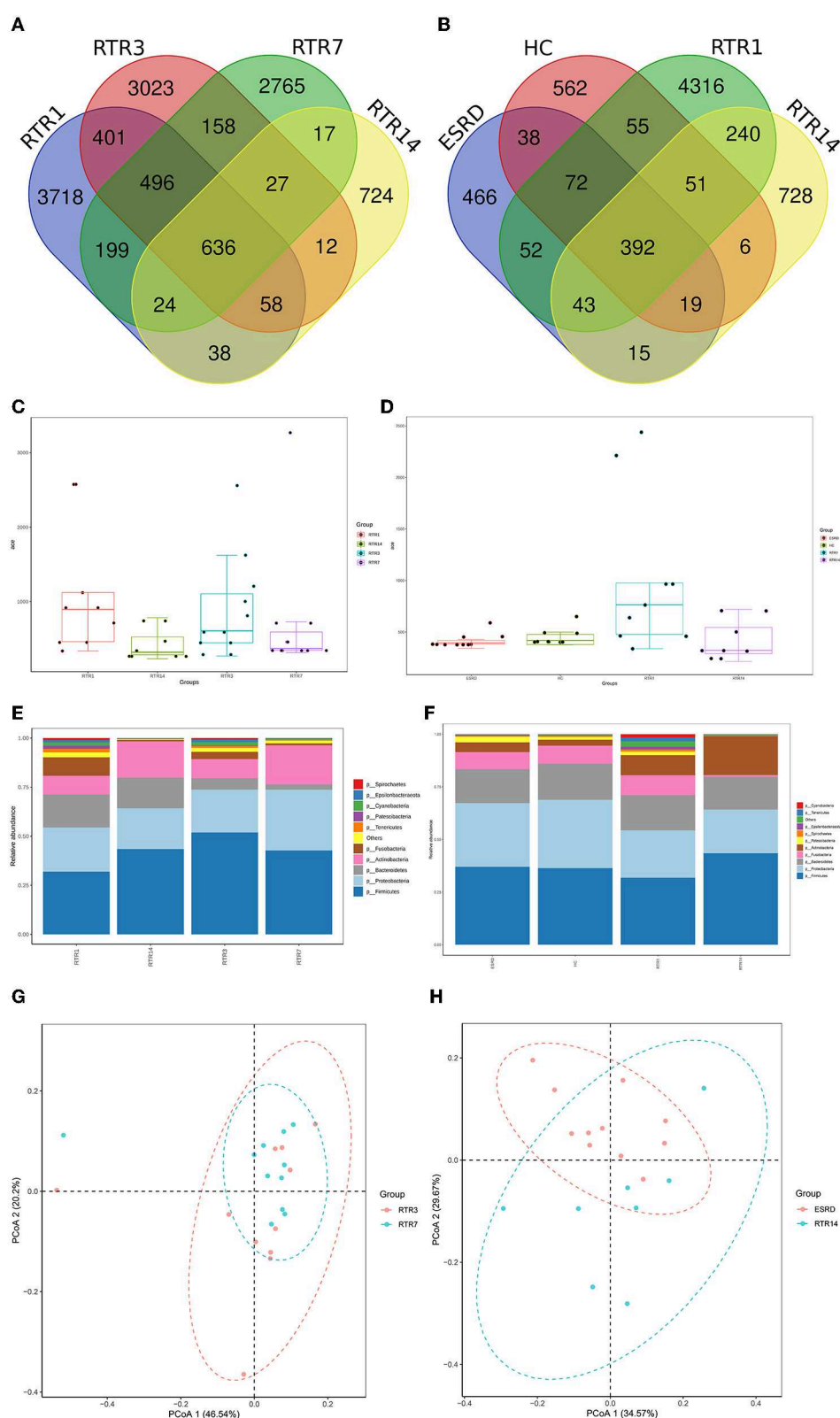


FIGURE 3

Composition characteristics of salivary microbiota at different time points and states: **(A)** the Venn graph for OTUs of the RTR group at different time points; **(B)** the Venn graph for OTUs of the RTR1, RTR14, ESRD, and HC; **(C)** the Ace index of the RTR group at different time points; **(D)** the Ace index of the RTR1, RTR14, ESRD, and HC; **(E)** salivary species composition of RTR group at different time points at the phylum level; **(F)** salivary species composition of RTR1, RTR14, ESRD, and HC at the phylum level; **(G)** PCoA graph of RTR3 and RTR7; **(H)** PCoA graph of RTR14 and ESRD.

**TABLE 2** Pearson correlation between the salivary microbiota and Scr after renal transplantation.

	RTR		ESRD	
	Pearson <i>r</i>	<i>P</i>	Pearson <i>r</i>	<i>P</i>
p__Bacteroidetes	0.3329	0.0384	0.4095	0.2111
p__Fusobacteria	0.3436	0.0322	−0.3558	0.2829
p__Patescibacteria	0.704	<0.0001	0.2271	0.5019
c__Bacteroidia	0.3321	0.0389	0.4095	0.2111
c__Fusobacteriia	0.3436	0.0322	−0.3558	0.2829
o__Fusobacteriales	0.3436	0.0322	−0.3558	0.2829
f__Streptococcaceae	−0.3166	0.0496	−0.0437	0.8984
f__Leptotrichiaceae	0.3409	0.0337	0.4137	0.2059
g__Streptococcus	−0.3166	0.0496	−0.0437	0.8984
g__Leptotrichia	0.3411	0.0336	0.4475	0.1675

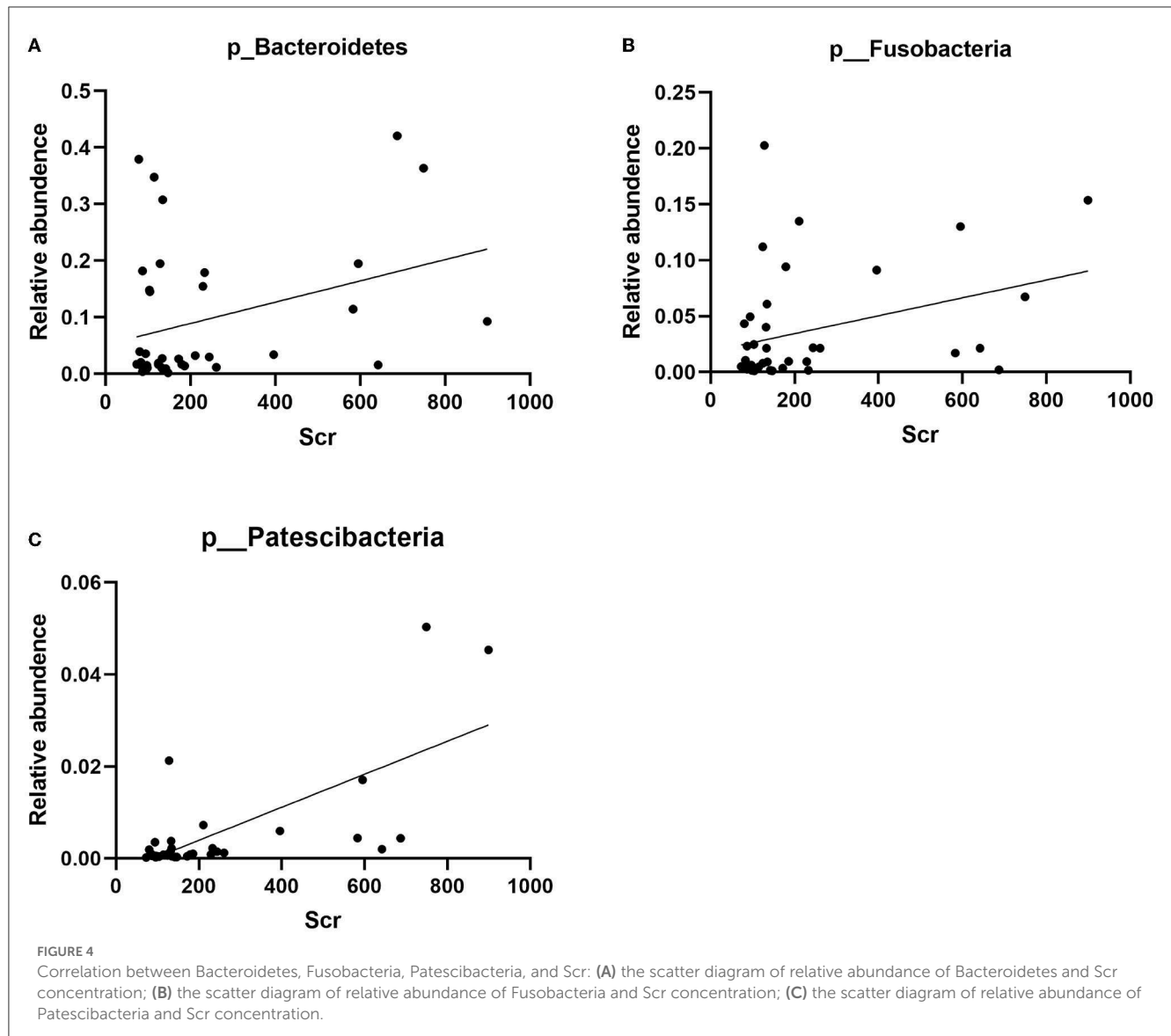
closely related to periodontal disease and gingivitis (Reed et al., 2018; Yousefi et al., 2020; Zeng et al., 2021), and, in turn, periodontal disease impacted the risk of systemic diseases such as diabetes (Deng et al., 2018). Taken together, these changes occurring in the salivary microbiota of RTRs appeared to be associated with the new onset diabetes, periodontal disease, and gingivitis after renal transplant.

During the early stage (<14 days) after surgery, the salivary microbiota of RTRs was not static. From the Venn graph, we could see that the total number of species decreased over time and most of the salivary microbiota were species unique at each time point. At the phylum level, the relative abundance of Actinobacteria, Cyanobacteria, Epsilonbacteraeota, Tenericutes, and Spirochaetes changed incrementally with time. Among them, Actinobacteria, Tenericutes, and Spirochaetes in RTRs had changed the most. From the point of alpha diversity, including kinds of evaluation indexes such as Ace, Chao1, Shannon, and Simpson, the composition of the salivary microbiota generally moved toward less richness and less variation within groups for each index. As shown in the PCoA figure, RTR1, RTR3, RTR7, and RTR14 groups all had different flora structures. However, the microbiota structure had significant differences only between RTR3 and RTR7 but not RTR1 and RTR3 or RTR7 and RTR14 which may be limited by the insufficient sample size. Moreover, the Chao1 and Ace, two alpha diversity evaluation indexes, described the distribution of bacteria with low abundances and decreased as the number of OTUs decreased during the perioperative period. Hence, we speculated that these low-abundance floras, which occurred in huge changes at different time points after renal transplant, occupy the majority of OTUs. As discussed, RTR14 was closer to HC in terms of OTU number and alpha diversity of salivary microbiota than RTR1. Hence, we considered that changes in the composition of the salivary microbiota of RTRs were a process of stabilization during the early stage after renal transplant.

All renal transplant patients received ATG preoperatively, a drug that inhibited thymocyte activity and helped patients fight

off rejection. ATG was also often used to treat severe aplastic anemia and altered patients' salivary microbiota but did not lead to a clear change in diversity over time (Ames et al., 2019). Similarly, RTRs were also all treated with FK506 and MMF which were related to oral cancer (Li et al., 2021) or oral ulcer (Asare and Gatzke, 2020), and these oral diseases were also related to salivary floras (Lin et al., 2021; Bai et al., 2022). Not only salivary microbiota but these immunosuppressants had been linked to the altered intestinal microbiota. Intaking a moderate dose of FK506 maintained immunosuppression, induced normal graft function of the liver, maintained gut barrier integrity, and low plasma endotoxin levels. In addition, it also led to increased species richness and rare species abundance which was consistent with our findings (Jiang et al., 2018). FK506 treatment significantly improved the relative abundance of Bacteroides (Zhang et al., 2018). In our study, the relative abundance of Bacteroides decreased than increased. As an ongoing drug, the effect of FK506 on the elevating relative abundance of Bacteroides may not manifest until the latter part of the early stage after kidney transplantation. MMF enhanced colonic integrity and decreased sympathetic drive in the gut which was associated with the improvement of gut dysbiosis, including the increased abundance of Proteobacteria and Bacteroidetes and decreased abundance of Firmicutes (Robles-Vera et al., 2021) such as the results of our study that the abundance of Firmicutes continuously reduced. MMF increased the alpha diversity of gut microbiota embodied in the first postoperative day of our research (Llorenç et al., 2022). Based on the induction therapy and immunosuppressive therapy, RTRs had immune dysfunction such as acquired immunodeficiency disease (AIDS) patients, according to which we speculated that salivary microbiota changes were similar to those in AIDS patients. In the research of Perez Rosero et al., the significant reduction in the frequency of oral neutrophils in the oral cavity of AIDS individuals was positively related to their CD4+ T cell count and observed OTUs indexes raised in AIDS individuals as alpha diversity of salivary microbiota (Perez Rosero et al., 2021). Interestingly, Alpha diversity altered as the disease progresses (Guo et al., 2021). Compared with healthy people, AIDS patients exhibited a lower abundance of salivary Fusobacteria resembles our study (Yang et al., 2020). For AIDS patients, antiretroviral therapy was an effective treatment. After the treatment, the patient's immune function would be restored to some extent, which was due to the changes in immune function during the perioperative period in RTRs as the gradual recovery of T cell abundance occurred (Bouteloup et al., 2017). These two statuses were all accompanied by decreased salivary alpha diversity (Imahashi et al., 2021). Although RTRs were essentially on constant antibiotics, previous studies had demonstrated that antibiotic use appears to have little effect on salivary flora composition (Tuganbaev et al., 2022). Coincidentally, some external factors which may affect salivary microbiota for patients, such as diet habits (Marsh et al., 2016), drinking water (Sinha et al., 2021), oral hygiene (Belström et al., 2018b), and living environment (David et al., 2014), changed between these time points of saliva collection. In conclusion, we speculated that the factors mentioned earlier functioned together and led to the alternation of salivary microbiota in RTRs like increasing and then gradually decreasing the number of OTUs and alpha diversity index and changing the





composition of species and relative abundance of dominant flora with various trends.

Finally, we analyzed the relationship between the dominant flora in saliva and Scr. We found that Bacteroidetes, Fusobacteria, Patescibacteria, and Leptotrichiaceae were positively correlated with Scr, and Streptococcaceae was negatively correlated with Scr after renal transplant. Therefore, these strains could be biomarkers of postoperative recovery of RTRs.

Although the presence of the floras Bacteroidetes, Fusobacteria, Patescibacteria, Leptotrichiaceae, and Streptococcaceae in saliva and their potential correlation with renal function have barely been researched, several studies have elucidated the relation of some of them in the gut and renal dysfunction. Studies have shown an increase in the relative abundance of gut Bacteroidetes in patients with stage 4–5 chronic kidney disease or patients with ESRD receiving hemodialysis (Crespo-Salgado et al., 2016; Wu et al., 2021). Although urinary stones are unlikely to

cause kidney damage, urolithiasis patients had significantly lower microbial abundance and higher proportions of Bacteroidetes (Zhou et al., 2020). In a study by Li et al., uremic clearance granules enhanced renal function and decreased levels of Scr, blood urea nitrogen, inflammatory responses, and NF- $\kappa$ B and MAPK expressions in renal tissues of ESRD rats. At the same time, the relative abundances of gut Bacteroidetes descended in response to uremic clearance granules (Li et al., 2022). As a prescription of traditional Chinese medicine for treating chronic kidney disease, the Shenyan Kangfu tablet alleviated renal dysfunction, glomerular and tubular damage, and renal inflammation and reduced the relative abundances of gut Bacteroidetes in the mouse with diabetic kidney disease (Chen et al., 2021). Accompanied by the fecal microbiota transplant, a significant increase of gut Bacteroidetes had the closest correlation with worse response to high salt of salt-sensitive rats, evidenced by increased albuminuria, systolic arterial pressure, and renal T-cell infiltration (Abais-Battad et al., 2021).

By contrast, SGL5213 and Daphnetin, two proven renoprotectants, saved kidney function in mice or rats with renal injury and elevated the relative abundances of gut Bacteroidetes (Ho et al., 2021; Zhou et al., 2022).

The relative abundance of Fusobacteria in patients with immunoglobulin A nephropathy or membranous nephropathy exhibited significant elevation when compared with healthy controls (Hu et al., 2020; Zhang et al., 2020; Sugurmar et al., 2021). The microbiota structure showed the same change in type 2 diabetes mellitus, chronic kidney disease, and renal uric acid stone patients (Salguero et al., 2019; Cao et al., 2022). Deltamethrin, as a widely used pyrethroid insecticide, had brought serious problems to the healthy breeding of aquatic animals. A high concentration of deltamethrin damaged the intestine and trunk kidney of goldfish or channel catfish in the early stage with a significant increase or decrease in the abundance of Fusobacteria (Zhou et al., 2021; Yang et al., 2022).

In summary, gastrointestinal Bacteroidetes and Fusobacteria in humans and mice were positively correlated with renal dysfunction which was consistent with our results. Hence, we speculated that these two floras and even more flora may have some connection with renal dysfunction. However, whether the changes in the digestive tract environment brought by renal dysfunction favored their colonization of the digestive tract or their colonization of the digestive tract promoted renal dysfunction remained to be proven.

## 5. Conclusion

This study has illustrated differences in salivary microbiota communities among RTRs, ESRD patients, and HCs, examining changes in the salivary microbiota community during the short period after renal transplantation. We speculated that changes in the salivary microbiota were a process of stabilization during the early stage after renal transplant, and certain species of salivary microbiota had the potential to be a biomarker of postoperative recovery. Our study first discussed the salivary microbiota variations associated with renal transplantation and the relationship between salivary microbiota and renal function.

## Data availability statement

The data presented in the study are deposited in the NCBI repository, accession number PRJNA904953, <https://www.ncbi.nlm.nih.gov/bioproject/PRJNA904953>.

## References

- Abais-Battad, J. M., Saravia, F. L., Lund, H., Dasinger, J. H., Fehrenbach, D. J., Alsheikh, A. J., et al. (2021). Dietary influences on the Dahl SS rat gut microbiota and its effects on salt-sensitive hypertension and renal damage. *Acta Physiol.* 232, e13662. doi: 10.1111/apha.13662
- Ames, N. J., Barb, J. J., Ranucci, A., Kim, H., Mudra, S. E., Cashion, A. K., et al. (2019). The oral microbiome of patients undergoing treatment for severe aplastic anemia: A pilot study. *Ann. Hematol.* 98, 1351–1365. doi: 10.1007/s00277-019-03599-w
- Asare, K., and Gatzke, C. B. (2020). Mycophenolate-induced oral ulcers: Case report and literature review. *Am. J. Health Syst. Pharm.* 77, 523–528. doi: 10.1093/ajhp/zxz358
- Bai, H., Yang, J., Meng, S., and Liu, C. (2022). Oral microbiota-driven cell migration in carcinogenesis and metastasis. *Front. Cell. Infect. Microbiol.* 12, 864479. doi: 10.3389/fcimb.2022.864479

## Ethics statement

The study protocol was approved (22207) by the Ethics Committee of the Third Xiangya Hospital of Central South University (Changsha, China). Written informed consent was obtained from all study participants. Experiments were carried out in accordance with the ethical guidelines set by the Declaration of Helsinki 1964 and its later amendments. The patients/participants provided their written informed consent to participate in this study.

## Author contributions

XX, BP, YZ, and YM conceived, designed, and directed the manuscript. XX, BP, and KL wrote and revised the manuscript. XX, PD, and HL participated in the performance of the research. XX, TW, and BP analyzed data. All authors contributed to the article and approved the submitted version.

## Funding

This study was supported by the National Natural Science Foundation of China (Grant Number: 81771722).

## Conflict of interest

The authors declare that the research was conducted in the absence of any commercial or financial relationships that could be construed as a potential conflict of interest.

## Publisher's note

All claims expressed in this article are solely those of the authors and do not necessarily represent those of their affiliated organizations, or those of the publisher, the editors and the reviewers. Any product that may be evaluated in this article, or claim that may be made by its manufacturer, is not guaranteed or endorsed by the publisher.

## Supplementary material

The Supplementary Material for this article can be found online at: <https://www.frontiersin.org/articles/10.3389/fmicb.2023.1122101/full#supplementary-material>

- Barka, E. A., Vatsa, P., Sanchez, L., Gaveau-Vaillant, N., Jacquard, C., Meier-Kolthoff, J. P., et al. (2016). Taxonomy, physiology, and natural products of actinobacteria. *Microbiol. Mol. Biol. Rev.* 80, 1–43. doi: 10.1128/MMBR.00019-15
- Belström, D., Grande, M. A., Sembler-Møller, M. L., Kirkby, N., Cotton, S. L., Paster, B. J., et al. (2018a). Influence of periodontal treatment on subgingival and salivary microbiotas. *J. Periodontol.* 89, 531–539. doi: 10.1002/JPER.17-0377
- Belström, D., Sembler-Møller, M. L., Grande, M. A., Kirkby, N., Cotton, S. L., Paster, B. J., et al. (2018b). Impact of oral hygiene discontinuation on supragingival and salivary microbiomes. *JDR Clin. Transl. Res.* 3, 57–64. doi: 10.1177/2380084417723625
- Bouteloup, V., Sabin, C., Mocroft, A., Gras, L., Pantazis, N., Le Moing, V., et al. (2017). Reference curves for CD4 T-cell count response to combination antiretroviral therapy in HIV-1-infected treatment-naïve patients. *HIV Med.* 18, 33–44. doi: 10.1111/hiv.12389
- Cao, C., Fan, B., Zhu, J., Zhu, N., Cao, J. Y., Yang, D. R., et al. (2022). Association of gut microbiota and biochemical features in a Chinese population with renal uric acid stone. *Front. Pharmacol.* 13, 888883. doi: 10.3389/fphar.2022.888883
- Chen, Q., Ren, D., Wu, J., Yu, H., Chen, X., Wang, J., et al. (2021). Shenyang Kangfu tablet alleviates diabetic kidney disease through attenuating inflammation and modulating the gut microbiota. *J. Nat. Med.* 75, 84–98. doi: 10.1007/s11418-020-01452-3
- Crespo-Salgado, J., Vehaskari, V. M., Stewart, T., Ferris, M., Zhang, Q., Wang, G., et al. (2016). Intestinal microbiota in pediatric patients with end stage renal disease: A Midwest Pediatric Nephrology Consortium study. *Microbiome* 4, 50. doi: 10.1186/s40168-016-0195-9
- David, L. A., Materna, A. C., Friedman, J., Campos-Baptista, M. I., Blackburn, M. C., Perrotta, A., et al. (2014). Host lifestyle affects human microbiota on daily timescales. *Genome Biol.* 15, R89. doi: 10.1186/gb-2014-15-7-r89
- Deng, Z. L., Sztajer, H., Jarek, M., Bhujji, S., and Wagner-Döbler, I. (2018). Worlds apart—Transcriptome profiles of key oral microbes in the periodontal pocket compared to single laboratory culture reflect synergistic interactions. *Front. Microbiol.* 9, 124. doi: 10.3389/fmicb.2018.00124
- Duan, X., Chen, X., Gupta, M., Seriwatanachai, D., Xue, H., Xiong, Q., et al. (2020). Salivary microbiome in patients undergoing hemodialysis and its associations with the duration of the dialysis. *BMC Nephrol.* 21, 414. doi: 10.1186/s12882-020-02009-y
- Guo, S., Wu, G., Liu, W., Fan, Y., Song, W., Wu, J., et al. (2022). Characteristics of human oral microbiome and its non-invasive diagnostic value in chronic kidney disease. *Biosci. Rep.* 42, 10694. doi: 10.1042/BSR20210694
- Guo, Y., Xia, W., Wei, F., Feng, W., Duan, J., Sun, X., et al. (2021). Salivary microbial diversity at different stages of human immunodeficiency virus infection. *Microbial Pathog.* 155, 104913. doi: 10.1016/j.micpath.2021.104913
- Henrich, B., Rummig, M., Sczyrba, A., Velleuer, E., Dietrich, R., Gerlach, W., et al. (2014). *Mycoplasma salivarium* as a dominant coloniser of Fanconi anaemia associated oral carcinoma. *PLoS ONE* 9, e92297. doi: 10.1371/journal.pone.0092297
- Ho, H. J., Kikuchi, K., Oikawa, D., Watanabe, S., Kanemitsu, Y., Saigusa, D., et al. (2021). SGLT-1-specific inhibition ameliorates renal failure and alters the gut microbial community in mice with adenine-induced renal failure. *Physiol. Rep.* 9, e15092. doi: 10.14814/phy2.15092
- Hu, J., Iragavarapu, S., Nadkarni, G. N., Huang, R., Erazo, M., Bao, X., et al. (2018). Location-specific oral microbiome possesses features associated with CKD. *Kidney Int. Rep.* 3, 193–204. doi: 10.1016/j.ekir.2017.08.018
- Hu, X., Du, J., Xie, Y., Huang, Q., Xiao, Y., Chen, J., et al. (2020). Fecal microbiota characteristics of Chinese patients with primary IgA nephropathy: A cross-sectional study. *BMC Nephrol.* 21, 97. doi: 10.1186/s12882-020-01741-9
- Imahashi, M., Ode, H., Kobayashi, A., Nemoto, M., Matsuda, M., Hashiba, C., et al. (2021). Impact of long-term antiretroviral therapy on gut and oral microbiotas in HIV-1-infected patients. *Sci. Rep.* 11, 960. doi: 10.1038/s41598-020-80247-8
- Jiang, J. W., Ren, Z. G., Lu, H. F., Zhang, H., Li, A., Cui, G. Y., et al. (2018). Optimal immunosuppressor induces stable gut microbiota after liver transplantation. *World J. Gastroenterol.* 24, 3871–3883. doi: 10.3748/wjg.v24.i34.3871
- Li, X., Zheng, J., Wang, J., Tang, X., Zhang, F., Liu, S., et al. (2022). Effects of uremic clearance granules on p38 MAPK/NF- $\kappa$ B signaling pathway, microbial and metabolic profiles in end-stage renal disease rats receiving peritoneal dialysis. *Drug Design Dev. Ther.* 16, 2529–2544. doi: 10.2147/DDDT.S364069
- Li, Y., Wang, Y., Li, J., Ling, Z., Chen, W., Zhang, L., et al. (2021). Tacrolimus inhibits oral carcinogenesis through cell cycle control. *Biomed. Pharmacother.* 139, 111545. doi: 10.1016/j.biopha.2021.111545
- Lin, D., Yang, L., Wen, L., Lu, H., Chen, Q., Wang, Z., et al. (2021). Crosstalk between the oral microbiota, mucosal immunity, and the epithelial barrier regulates oral mucosal disease pathogenesis. *Mucosal Immunol.* 14, 1247–1258. doi: 10.1038/s41385-021-00413-7
- Liu, F., Sheng, J., Hu, L., Zhang, B., Guo, W., Wang, Y., et al. (2022). Salivary microbiome in chronic kidney disease: What is its connection to diabetes, hypertension, and immunity? *J. Transl. Med.* 20, 387. doi: 10.1186/s12967-022-03602-5
- Llorenç, V., Nakamura, Y., Metea, C., Karstens, L., Molins, B., Lin, P., et al. (2022). Antimetabolite drugs exhibit distinctive immunomodulatory mechanisms and effects on the intestinal microbiota in experimental autoimmune uveitis. *Investig. Ophthalmol. Vis. Sci.* 63, 30. doi: 10.1167/iovs.63.3.30
- Long, J., Cai, Q., Steinwandel, M., Hargreaves, M. K., Bordenstein, S. R., Blot, W. J., et al. (2017). Association of oral microbiome with type 2 diabetes risk. *J. Periodontol. Res.* 52, 636–643. doi: 10.1111/jre.12432
- Marsh, P. D., Do, T., Beighton, D., and Devine, D. A. (2016). Influence of saliva on the oral microbiota. *Periodontology* 70, 80–92. doi: 10.1111/prd.12098
- Matsha, T. E., Prince, Y., Davids, S., Chikte, U., Erasmus, R. T., Kengne, A. P., et al. (2020). Oral microbiome signatures in diabetes mellitus and periodontal disease. *J. Dental Res.* 99, 658–665. doi: 10.1177/0022034520913818
- Meijers, B., Evenepoel, P., and Anders, H. J. (2019). Intestinal microbiome and fitness in kidney disease. *Nat. Rev. Nephrol.* 15, 531–545. doi: 10.1038/s41581-019-0172-1
- Miao, V., and Davies, J. (2010). Actinobacteria: the good, the bad, and the ugly. *Antonie van Leeuwenhoek* 98, 143–150. doi: 10.1007/s10482-010-9440-6
- Mizuki, H., Abe, R., and Mikami, T. (2017). Ultrastructural changes during the life cycle of *Mycoplasma salivarium* in oral biopsies from patients with oral leukoplakia. *Front. Cell. Infect. Microbiol.* 7, 403. doi: 10.3389/fcimb.2017.00403
- Mizuki, H., Kawamura, T., and Nagasawa, D. (2015). In situ immunohistochemical detection of intracellular *Mycoplasma salivarium* in the epithelial cells of oral leukoplakia. *J. Oral Pathol. Med.* 44, 134–144. doi: 10.1111/jop.12215
- Morand, M., and Hatami, A. (2018). Multiple superficial oral mucocoeles after *Mycoplasma*-induced mucositis. *Pediatr. Dermatol.* 35, e210–e1. doi: 10.1111/pde.13515
- Perez Rosero, E., Heron, S., Jovel, J., O'Neil, C. R., Turvey, S. L., Parashar, P., et al. (2021). Differential signature of the microbiome and neutrophils in the oral cavity of HIV-infected individuals. *Front. Immunol.* 12, 780910. doi: 10.3389/fimmu.2021.780910
- Reed, L. A., O'Bier, N. S., and Oliver, L. D. Jr., Hoffman, P. S., and Marconi, R. T. (2018). Antimicrobial activity of amoxicillin against *Treponema denticola* and other oral spirochetes associated with periodontal disease. *J. Periodontol.* 89, 1467–1474. doi: 10.1002/JPER.17-0185
- Ren, Z., Fan, Y., Li, A., Shen, Q., Wu, J., Ren, L., et al. (2020). Alterations of the human gut microbiome in chronic kidney disease. *Adv. Sci.* 7, 2001936. doi: 10.1002/adv.202001936
- Robles-Vera, I., de la Visitación, N., Toral, M., Sánchez, M., Gómez-Guzmán, M., Jiménez, R., et al. (2021). Mycophenolate mediated remodeling of gut microbiota and improvement of gut-brain axis in spontaneously hypertensive rats. *Biomed. Pharmacother.* 135, 111189. doi: 10.1016/j.biopha.2020.111189
- Rysz, J., Franczyk, B., Ławiński, J., Olszewski, R., Ciałkowska-Rysz, A., Gluba-Brzózka, A., et al. (2021). The impact of CKD on uremic toxins and gut microbiota. *Toxins* 13, 40252. doi: 10.3390/toxins13040252
- Salguero, M. V., Al-Obaide, M. A. I., Singh, R., Siepmann, T., and Vasylyeva, T. L. (2019). Dysbiosis of Gram-negative gut microbiota and the associated serum lipopolysaccharide exacerbates inflammation in type 2 diabetic patients with chronic kidney disease. *Exp. Therapeut. Med.* 18, 3461–3469. doi: 10.3892/etm.2019.7943
- Shivani, S., Kao, C. Y., Chattopadhyay, A., Chen, J. W., Lai, L. C., Lin, W. H., et al. (2022). Uremic toxin-producing bacteroides species prevail in the gut microbiota of Taiwanese CKD patients: An analysis using the new Taiwan microbiome baseline. *Front. Cell. Infect. Microbiol.* 12, 726256. doi: 10.3389/fcimb.2022.726256
- Sinha, R., Zhao, N., Goedert, J. J., Byrd, D. A., Wan, Y., Hua, X., et al. (2021). Effects of processed meat and drinking water nitrate on oral and fecal microbial populations in a controlled feeding study. *Environ. Res.* 197, 111084. doi: 10.1016/j.envres.2021.111084
- Sugumar, A. N. K., Mohd, R., Shah, S. A., Neoh, H. M., and Cader, R. A. (2021). Gut microbiota in immunoglobulin A nephropathy: A Malaysian perspective. *BMC Nephrol.* 22, 145. doi: 10.1186/s12882-021-02315-z
- Tuganbaev, T., Yoshida, K., and Honda, K. (2022). The effects of oral microbiota on health. *Science* 376, 934–936. doi: 10.1126/science.abn1890
- Wang, H., Ainiwaer, A., Song, Y., Qin, L., Peng, A., Bao, H., et al. (2023). Perturbed gut microbiome and fecal and serum metabolomes are associated with chronic kidney disease severity. *Microbiome* 11, 3. doi: 10.1186/s40168-022-01443-4
- Wang, X., Yang, S., Li, S., Zhao, L., Hao, Y., Qin, J., et al. (2020). Aberrant gut microbiota alters host metabolome and impacts renal failure in humans and rodents. *Gut* 69, 2131–2142. doi: 10.1136/gutjnl-2019-319766
- Wang, Y., Huang, J. M., Zhou, Y. L., Almeida, A., Finn, R. D., Danchin, A., et al. (2020). Phylogenomics of expanding uncultured environmental *Tenericutes* provides insights into their pathogenicity and evolutionary relationship with *Bacilli*. *BMC Genomics* 21, 408. doi: 10.1186/s12864-020-06807-4
- Wilson, K. F., Meier, J. D., and Ward, P. D. (2014). Salivary gland disorders. *Am. Fam. Physician* 89, 882–888. Available online at: <https://www.aafp.org/pubs/afp/issues/2014/0601/p882.html>

- Wu, R., Ruan, X. L., Ruan, D. D., Zhang, J. H., Wang, H. L., Zeng, Q. Z., et al. (2021). Differences in gut microbiota structure in patients with stages 4-5 chronic kidney disease. *Am. J. Transl. Res.* 13, 10056–10074.
- Yang, L., Dunlap, D. G., Qin, S., Fitch, A., Li, K., Koch, C. D., et al. (2020). Alterations in oral microbiota in HIV are related to decreased pulmonary function. *Am. J. Respirat. Crit. Care Med.* 201, 445–457. doi: 10.1164/rccm.201905-1016OC
- Yang, Y., Zhu, X., Huang, Y., Zhang, H., Liu, Y., Xu, N., et al. (2022). RNA-seq and 16S rRNA analysis revealed the effect of deltamethrin on channel catfish in the early stage of acute exposure. *Front. Immunol.* 13, 916100. doi: 10.3389/fimmu.2022.916100
- Yousefi, L., Leylabadlo, H. E., Pourlak, T., Eslami, H., Taghizadeh, S., Ganbarov, K., et al. (2020). Oral spirochetes: Pathogenic mechanisms in periodontal disease. *Microbial Pathog.* 144, 104193. doi: 10.1016/j.micpath.2020.104193
- Zeng, H., Chan, Y., Gao, W., Leung, W. K., and Watt, R. M. (2021). Diversity of *treponema denticola* and other oral treponeme lineages in subjects with periodontitis and gingivitis. *Microbiol. Spectr.* 9, e0070121. doi: 10.1128/Spectrum.00701-21
- Zhang, J., Luo, D., Lin, Z., Zhou, W., Rao, J., Li, Y., et al. (2020). Dysbiosis of gut microbiota in adult idiopathic membranous nephropathy with nephrotic syndrome. *Microbial Pathog.* 147, 104359. doi: 10.1016/j.micpath.2020.104359
- Zhang, Z., Liu, L., Tang, H., Jiao, W., Zeng, S., Xu, Y., et al. (2018). Immunosuppressive effect of the gut microbiome altered by high-dose tacrolimus in mice. *Am. J. Transplant.* 18, 1646–1656. doi: 10.1111/ajt.14661
- Zhou, C., Li, K., Zhao, L., Li, W., Guo, Z., Xu, J., et al. (2020). The relationship between urinary stones and gut microbiome by 16S sequencing. *BioMed Res. Int.* 2020, 1582187. doi: 10.1155/2020/1582187
- Zhou, R., Wen, W., Gong, X., Zhao, Y., and Zhang, W. (2022). Nephro-protective effect of Daphnetin in hyperoxaluria-induced rat renal injury via alterations of the gut microbiota. *J. Food Biochem.* 2022, e14377. doi: 10.1111/jfbc.14377
- Zhou, S., Dong, J., Liu, Y., Yang, Q., Xu, N., Yang, Y., et al. (2021). Effects of acute deltamethrin exposure on kidney transcriptome and intestinal microbiota in goldfish (*Carassius auratus*). *Ecotoxicol. Environ. Saf.* 225, 112716. doi: 10.1016/j.ecoenv.2021.112716
- Zhu, H., Cao, C., Wu, Z., Zhang, H., Sun, Z., Wang, M., et al. (2021). The probiotic *L. casei* Zhang slows the progression of acute and chronic kidney disease. *Cell Metabol.* 33, 1926–42.e8. doi: 10.1016/j.cmet.2021.06.014





## OPEN ACCESS

## EDITED BY

Wei Qi He,  
Soochow University, China

## REVIEWED BY

George Grant,  
University of Aberdeen, United Kingdom  
Yanzhen Bi,  
Hubei Academy of Agricultural Sciences, China

## \*CORRESPONDENCE

Pengju Zhao  
✉ zhaopengju2014@gmail.com  
Zhengguang Wang  
✉ wzhuang68@zju.edu.cn

## SPECIALTY SECTION

This article was submitted to  
Microorganisms in Vertebrate Digestive  
Systems,  
a section of the journal  
Frontiers in Microbiology

RECEIVED 06 February 2023

ACCEPTED 15 March 2023

PUBLISHED 20 April 2023

## CITATION

He J, Zhang Y, Li H, Xie Y, Huang G, Peng C,  
Zhao P and Wang Z (2023) Hybridization alters  
the gut microbial and metabolic profile  
concurrent with modifying intestinal functions  
in Tunchang pigs.  
*Front. Microbiol.* 14:1159653.  
doi: 10.3389/fmicb.2023.1159653

## COPYRIGHT

© 2023 He, Zhang, Li, Xie, Huang, Peng, Zhao  
and Wang. This is an open-access article  
distributed under the terms of the [Creative  
Commons Attribution License \(CC BY\)](#). The  
use, distribution or reproduction in other  
forums is permitted, provided the original  
author(s) and the copyright owner(s) are  
credited and that the original publication in this  
journal is cited, in accordance with accepted  
academic practice. No use, distribution or  
reproduction is permitted which does not  
comply with these terms.

# Hybridization alters the gut microbial and metabolic profile concurrent with modifying intestinal functions in Tunchang pigs

Jiayi He<sup>1,2</sup>, Yunchao Zhang<sup>1,2</sup>, Hui Li<sup>3</sup>, Yanshe Xie<sup>1,2</sup>, Guiqing Huang<sup>1,2</sup>,  
Chen Peng<sup>1,2</sup>, Pengju Zhao<sup>1,2\*</sup> and Zhengguang Wang<sup>1,2\*</sup>

<sup>1</sup>Hainan Institute of Zhejiang University, Sanya, China, <sup>2</sup>College of Animal Science, Zhejiang University, Hangzhou, China, <sup>3</sup>Long Jian Animal Husbandry Company, Haikou, China

**Introduction:** Hybridization has been widely used among Chinese wild boars to improve their growth performance and maintain meat quality. Most studies have focused on the genetic basis for such variation. However, the differences in the gut environment between hybrid and purebred boars, which can have significant impacts on their health and productivity, have been poorly understood.

**Methods:** In the current study, metagenomics was used to detect the gut microbial diversity and composition in hybrid Batun (BT, Berkshire × Tunchang) pigs and purebred Tunchang (TC) pigs. Additionally, untargeted metabolomic analysis was used to detect differences in gut metabolic pathways. Furthermore, multiple molecular experiments were conducted to demonstrate differences in intestinal functions.

**Results:** As a result of hybridization in TC pigs, a microbial change was observed, especially in *Prevotella* and *Lactobacillus*. Significant differences were found in gut metabolites, including fatty acyls, steroids, and steroid derivatives. Furthermore, the function of the intestinal barrier was decreased by hybridization, while the function of nutrient metabolism was increased.

**Discussion:** Evidences were shown that hybridization changed the gut microbiome, gut metabolome, and intestinal functions of TC pigs. These findings supported our hypothesis that hybridization altered the gut microbial composition, thereby modifying the intestinal functions, even the host phenotypes. Overall, our study highlights the importance of considering the gut microbiome as a key factor in the evaluation of animal health and productivity, particularly in the context of genetic selection and breeding programs.

## KEYWORDS

gut microbiome, gut metabolome, intestinal function, mammalian hybridization, wild boar

## 1. Introduction

Mammals have complicated intestinal microorganisms, which play a critical role in a variety of physiological processes, including nutrient metabolism and absorption (Meng et al., 2020), immune response (Ivanov et al., 2009), and growth performance (Zhou et al., 2021). Furthermore, many studies had shown that intestinal microorganisms were altered by host genome, breed age, sex, maternal effect, and diets (Adhikari et al., 2019; Bergamaschi et al., 2020). From a genetic point of view, the approximate Bayesian computation analysis of 103 genomes of Asian and European wild boar and domestic pigs demonstrated the existence of gene flow during and after domestication (Frantz et al.,

2015). Thus, it was feasible to suspect the hybridization would alter the intestinal environment of wild boar. The current study identified that BT pigs had greater growth performance than TC pigs, while the meat quality was maintained (Wang et al., 2011). However, the differential intestinal microbiome between TC pigs and BT pigs was still unknown, let alone the alteration of host–microbiota interaction by the hybridization.

Recent studies indicate that the intestinal microbiota plays a vital role in the adaptive evolution of mammal species (Moeller and Sanders, 2020). Furthermore, the mammalian intestinal metabolomes mirror microbiome composition and host phylogeny (Gregor et al., 2022). Therefore, a comprehensive analysis was needed in order to reflect the differences between purebred pigs and crossbred pigs. For instance, tracking the microbial and metabolic trends over time could clarify the colonization of bacteria and their effects (Wang et al., 2019). In addition, permutational multivariate analysis of variance was used to calculate whether interfering factors affect the microbiome and metabolome. Recent studies of correlation analysis also provided a perspective to understand the connection between microbiome and metabolome. Such analysis may explain how hybridization alters the intestinal microbiome. Finally, a variety of strategies were used to compare the intestinal functions between TC pigs and BT pigs. The expression of intestinal functional-related mRNAs was related to the intestinal state and reflected the main functions (Moran et al., 2010; Hartmann et al., 2016; Brooks II et al., 2021). On the other hand, intestinal histology indicated the capability of nutrient absorption (Wang et al., 2019), and serum LPS levels were used to reveal the intestinal barrier function (Ghosh et al., 2020) because serum LPS was now an accepted surrogate marker for assessing *in vivo* intestinal permeability.

To complement these blank studies, we designed an experimental approach that compares differential intestinal environments in certain aspects. First, a comparison with mRNA expression data, intestinal histology analysis, and serum lipopolysaccharide level revealed a significant difference in intestinal functions between TC pigs and BT pigs. In addition, collecting the intestinal content by rectum stimulus at the pre-weaning stage (PW, 30 days of age), weaned stage (WD, 60 days of age), and growth stage (90 days of age) to explore the colonization process of bacteria, and the changes of metabolic pathway. Moreover, the interfering factors, such as diet and pigpen, were strictly controlled, using a permutational multivariate analysis to calculate the influences of sex and maternal effect. Correlation analysis was also used to reflect the potential mechanism of host–microbiota interactions. In summary, the hybridization improved the nutrient metabolism and absorption functions but decreased the intestinal barrier function.

## 2. Materials and methods

### 2.1. Pigs and experimental design

A total of 18 healthy piglets (TC pigs,  $n=9$ ; BT pigs,  $n=9$ ) born from nine sows were selected and raised on a local commercial farm (Tunchang, China). Piglets lived with their mothers for 1 month of adaptation to solid feed and would imitate their mothers' behavior to eat solid feed; nevertheless, it was still hard to collect their intestinal content before 30 days old because they ate very little. Subsequently, piglets (30 days old) started weaning and housed by species. All pigs were provided with a commercial diet with *ad libitum* access to clean water. The growth performance parameters (body weight and average daily gain) were measured monthly from birth.

### 2.2. Sample collection

At the pre-weaning stage (PW, 30 days of age,  $n=18$ ), weaned stage (WD, 60 days of age,  $n=18$ ), and growing stage (GT, 90 days of age,  $n=18$ ), fresh intestinal content samples were collected by rectal stimulation of TC pigs and BT pigs. Each sample was stored in a 50 ml sterile centrifuge tube and kept on ice during transportation. The body weight was measured to the nearest 0.1 kg monthly since birth, and average daily gain was monitored. At 90 days of age, three pigs were randomly selected from TC pigs and BT pigs, respectively, and were slaughtered. Blood was drawn from the anterior vena cava and centrifuged at 3,000 rpm for 15 min at 4°C. Plasma was collected and immediately stored at  $-80^{\circ}\text{C}$  for further analysis. Tissue samples were collected from the midsection (4 cm) of the duodenum, jejunum, ileum, and colon. After that, all samples were stored in a  $-80^{\circ}\text{C}$  freezer for cryopreservation.

### 2.3. DNA extraction and whole-genome shotgun sequencing

DNA extraction and shotgun metagenomic sequencing were conducted at Personal Biotechnology Co., Ltd. (Shanghai, China). Total microbial genomic DNA in the intestinal content of 54 samples was extracted by a DNeasy PowerSoil Kit (QIAGEN, Hilden, Germany), following the manufacturer's instructions. The quality and quantity of the extracted DNA were assessed by agarose gel electrophoresis and a NanoDrop ND-1000 spectrophotometer (Thermo Fisher Scientific, Waltham, MA, United States). The qualified DNA was processed to construct the shotgun metagenomic sequencing library by a TruSeq DNA Nano High-Throughput Library Preparation Kit (Illumina, San Diego, CA, United States). The sequencing strategy was paired-end 150bp reads with an insert size of 400bp. A dual-indexed barcode structure was applied for multiplexing, and 1% PhiX Control v3 was added to the library for quality monitoring. The prepared libraries were stored at  $-20^{\circ}\text{C}$  before sequencing. The sequencing platform was Illumina NovaSeq (Illumina, San Diego, CA, United States). The cluster density was in the range of 1,255–1,412 K clusters/mm<sup>2</sup>, and the error rate was  $<0.05\%$  for the sequencing run.

### 2.4. Metagenomics data assembly and analyses

Raw sequenced reads were first processed to obtain high-quality clean reads. Adapter sequences were removed by Cutadapt (v1.2.1) (Martin, 2011), and raw reads were processed by a 5-bp sliding window to trim low-quality sequences ( $<Q20$ , read accuracy  $<99\%$ ). Trimmed reads with a length of  $>50\text{bp}$  and no ambiguous bases were kept for further analyses. Human reads were removed by KneadData (v0.9.0) and BMTagger (v3.101). The clean reads were assembled by MEGAHIT (v1.0.5) with a succinct de Bruijn graph approach (Li et al., 2015). The coding sequences (CDS,  $>300\text{bp}$ ) were predicted by MetaGeneMark (v3.25; Zhu et al., 2010). CDSs were clustered by CD-HIT (v4.8.1; Fu et al., 2012) at 90% amino acid sequence identity to obtain a non-redundant gene catalog. The abundance of genes was calculated as the number of aligned reads by SOAPdenovo2 (v1.0) (Luo et al., 2012). The taxonomy was annotated by searching against the NCBI-NT database by BLASTN (e-value  $<0.001$ ) and annotated by MEGAN with

the lowest common ancestor approach (Huson et al., 2007). The functional gene was annotated by searching the sequence of the non-redundant genes against the KEGG databases (release 90.0) by DIAMOND protein aligner (v2.0.4), with an e-value of <0.001 and coverage ratio of >40% (Buchfink et al., 2015). Microbial compositional variation (beta diversity) was calculated by Bray–Curtis distance metrics and visualized by principal coordinate analysis (PCoA) and non-metric multidimensional scaling (NMDS) hierarchical clustering (Bray and Curtis, 1957; Ramette, 2007). Permutation analysis (999 permutations) was conducted for microbial taxonomic composition between TC pig and BT pig samples by the Adonis function in R (v4.1.0). The bacterial co-correlation matrix was calculated by the R “igraph” package, and figures of the co-correlation network were plotted by Gephi. R (v4.1.0) was used throughout the study for data processing, analysis, and visualization (Caporaso et al., 2010).

## 2.5. Sample preparation for liquid chromatography–tandem mass spectrometry (LC–MS) analysis

The extraction of intestinal microbiota metabolites was performed with minor modifications, as described earlier (Turroni et al., 2016). In brief, approximately 1.0 g of intestinal content samples were mixed with 600  $\mu$ L of MeOH [stored at  $-20^{\circ}\text{C}$ , containing 2-Amino-3-(2-chloro-phenyl)-propionic acid (4 ppm)]. After vortex mixing for 30 s, samples were placed in a tissue grinder for 90 s at 60 Hz, with the addition of 100 mg of glass bead followed by ultrasound at room temperature for 10 min. Finally, the samples were centrifuged at 12,000 rpm for 10 min at  $4^{\circ}\text{C}$ , and the supernatant was collected for an LC–MS analysis after filtering through a 0.22  $\mu$ m filter.

## 2.6. LC–MS analysis

Untargeted intestinal metabolomics was performed using an LC–MS platform at Personal Bio Inc. (Shanghai, China). The LC analysis was performed on a Vanquish UHPLC System (Thermo Fisher Scientific, United States). Chromatography was carried out with an ACQUITY UPLC<sup>®</sup> HSS T3 (150  $\times$  2.1 mm, 1.8  $\mu$ m) (Waters, Milford, MA, United States). Mass spectrometric detection of metabolites was performed on Q Exactive HF-X (Thermo Fisher Scientific, United States) with an ESI ion source. Simultaneous MS1 and MS/MS (full MS–ddMS2 mode, data-dependent MS/MS) acquisition were used.

## 2.7. LC–MS data processing and multivariate analysis

The raw data were first converted to mzXML format by MSConvert in the ProteoWizard software package (v3.0.8789) and processed using XCMS (Sud et al., 2007) for feature detection, retention time correction, and alignment. The metabolites were identified by accuracy mass (< 30 ppm) and MS/MS data which were matched with HMDB (Abdelrazik et al., 2020),<sup>1</sup> MassBank (Gagnebin

et al., 2017),<sup>2</sup> LIPID MAPS (Thévenot et al., 2015),<sup>3</sup> mzCloud (Xia and Wishart, 2011),<sup>4</sup> and KEGG (Dunn et al., 2011).<sup>5</sup> QC robust LOESS signal correction (QC-RLSC; Want et al., 2013) was applied for data normalization to correct any systematic bias. After normalization, only ion peaks with relative standard deviations (RSDs) of less than 30% in QC were kept to ensure proper metabolite identification.

The ropls (Boulesteix and Strimmer, 2007) software was used for all multivariate data analyses and modelings. Data were mean-centered using scaling. Models were built on orthogonal partial least-square discriminant analysis (OPLS-DA) and partial least-square discriminant analysis (PLS-DA). The metabolic profiles could be visualized as a score plot, where each point represents a sample. The corresponding loading plot and S-plot were generated to provide information on the metabolites that influence the clustering of the samples. All the models evaluated were tested for overfitting with methods of permutation tests. The descriptive performance of the models was determined by R2X (cumulative) (perfect model: R2X (cum) = 1) and R2Y (cumulative) (perfect model: R2Y (cum) = 1) values, while their prediction performance was measured by Q2 (cumulative) (perfect model: Q2 (cum) = 1) and a permutation test. The permuted model should not be able to predict classes. The R2 and Q2 values at the Y-axis intercept should be lower than those obtained from the non-permuted model for Q2 and R2. OPLS-DA allowed the determination of discriminating metabolites using the variable importance in projection (VIP). The *p*-value, VIP produced by OPLS-DA, and fold change (FC) were applied to discover the contributable variable for classification. Finally, the *p*-value of <0.05 and the VIP values of >1 were considered to be statistically significant metabolites.

Differential metabolites were subjected to pathway analysis by MetaboAnalyst (Trygg and Wold, 2002), which combines results from powerful pathway enrichment analysis with the pathway topology analysis. The identified metabolites in metabolomics were then mapped to the KEGG pathway for biological interpretation of higher level systemic functions. The metabolites and corresponding pathways were visualized using the ggplot software.

## 2.8. Detection of mRNA expression

Total RNA Isolation Kit (SparkJade, China) was used to extract RNA from the jejunum, the ileum, and the colon tissues. A cDNA library was prepared by transcribing 2  $\mu$ g of RNA with the SPARK script II 1st Strand cDNA Synthesis Kit (SparkJade, China) and qPCR performed with specific primer pairs (Supplementary Table S6) and the 2  $\times$  SYBR Green qPCR Mix (SparkJade, China) on the CFX96 system (Bio-Rad, United States). Relative expression levels were calculated using the  $2^{-\Delta\Delta C_t}$  method, and  $\beta$ -actin was utilized to normalize the relative mRNA expression levels of the target genes. Student's *t*-test was used to evaluate the statistical difference of each target gene.

<sup>1</sup> <http://www.hmdb.ca>

<sup>2</sup> <http://www.massbank.jp/>

<sup>3</sup> <http://www.lipidmaps.org>

<sup>4</sup> <https://www.mzcloud.org>

<sup>5</sup> <http://www.genome.jp/kegg/>

## 2.9. Intestinal histology analysis

Approximately 4 cm of each sample was taken from the middle sections of the duodenum, jejunum, and ileum. These tissue samples were washed with cold sterile saline and immediately fixed in 4% paraformaldehyde solution (Biosharp, China) for 24 h followed by dehydrating and embedding in paraffin wax before transverse sections were cut. The preserved samples were stained with hematoxylin and eosin according to the manufacturer's guidelines of the Hematoxylin–Eosin (HE) Stain Kit (Solarbio, United States). A total of 12 well-orientated sections of villi and their adjoint crypts in each sample were performed using a Nikon A1 inverted laser scanning confocal microscope (Nikon, Japan). Images were analyzed using Image-Pro Plus software (version 6.0, Media Cybernetics, United States).

## 2.10. Serum lipopolysaccharide levels

Serum LPS levels were measured using ELISA Kit (JingMei Biotechnology, China), and the product was visualized at 450 nm in a microplate reader (BioTek Synergy HT microplate reader, United States). Student's *t*-test was used to evaluate the statistical difference.

## 2.11. Correlation analysis between microbiome and metabolome

Correlation analysis between the microbiome and metabolome was calculated by Spearman's correlation coefficient and *p*-value and plotted by the R “pheatmap” package. Bacteria were deduced from the top 20 genera which accounted for more than 80% of the microbial sequence reads, and metabolites were deduced from the differential KEGG metabolic pathways.

# 3. Results

## 3.1. Hybridization improves the nutrient metabolism of TC pigs

We confirmed that the hybridization significantly improved ( $p < 0.05$ ) the body weight of TC pigs (Figure 1A), which were healthy throughout the feeding trial period. The average daily gain and feed intake were increased as well (Figures 1B,D). In addition, the feed conversion rate was decreased (Figure 1C). Intestinal histology is critical to maintaining ecosystem stability and performance. However, only the histology of the duodenum was changed (Figures 2A–D) by hybridization, indicating the histology was similar in TC pigs and BT pigs overall. As a result, the differential growth performance may be caused by the intestinal functions and intestinal microbiota.

Then, we assayed mRNA expression in different intestine segments of TC pigs and BT pigs, to compare the differences in intestinal functions. We examined mRNA expression of intestinal development and proliferation was downregulated ( $p < 0.05$ ) in the colon after hybridization (Figure 3C), and it was related to the colonization of intestinal microbiota. In addition, the mRNA expression of nutrient metabolism and absorption was upregulated

( $p < 0.05$ ) in the small intestine by hybridization (Figures 3A,B), including zinc transporter1 (ZNT1) and glucose transporter 2 (GLUT2). These transporters may contribute to the greater growth performance of BT pigs.

## 3.2. Hybridization decreases the intestinal barrier function of TC pigs

The intestinal barrier plays an important role in mammalian metabolism and immunity. Remarkably, mRNA expression of the intestinal barrier was downregulated in the colon after hybridization, including regenerating family member 3 gamma (REG3G) and occludin (Figure 3C). Specifically, REG3G had both bacteriostatic and bactericidal activities, and occludin was positively correlated with intestinal permeability. Furthermore, the serum LPS concentration was higher after hybridization (Figure 4). This evidence showed that the ability of anti-inflammation was impaired by the hybridization of TC pigs.

## 3.3. Microbial community richness was similar, but the diversity was different between TC pigs and BT pigs

To achieve comprehensive comparisons, we detected the intestinal microbiota through microbial richness and diversity. The current metagenomic analysis included a total of 54 samples collected longitudinally from nine TC piglets and nine BT piglets, obtaining an average of 46,007,294.19 reads per sample. Herein, taxonomic alpha diversity was estimated using Simpson, Chao1, ACE, and Shannon indices (Figures 5A–D). These indices showed no difference ( $p > 0.05$ ) between TC pigs and BT pigs, reflecting that the numbers of observed taxa were similar. Principal coordinate analysis (PCoA, Figures 5E–G) based on the Bray–Curtis distance was performed to assess the beta diversity. Unlike alpha diversity, beta diversity demonstrated compositional differences in bacterial communities between TC pigs and BT pigs. Notably, the microbial compositional difference was most significant ( $p = 0.001$ ) at the weaned stage. These data indicated that the microbial abundance of different taxa would be different after hybridization.

## 3.4. Microbial community dynamics and dominant microbiota were altered by age in TC pigs and BT pigs

As shown in Figure 6A, the majority of phyla in all samples were *Firmicutes*, *Bacteroidetes*, and *Actinobacteria*. The detailed data are presented in Supplementary Table S1. Nevertheless, the abundance of *Bacteroides* was increased ( $p < 0.05$ ) after hybridization at weaned stage (Supplementary Table S2). At the genus level, consistent stepwise increases or decreases were seen for all samples in most of the taxa from the pre-weaning stage to the growth stage (Figure 6B). However, *Lactobacillus*, by far the most differential genus, showed obvious differences in TC pigs and BT pigs, not only in the tendency but also in the relative abundance. Existing species-level data revealed such difference was led by *Lactobacillus reuteri*, *Lactobacillus johnsonii*, and



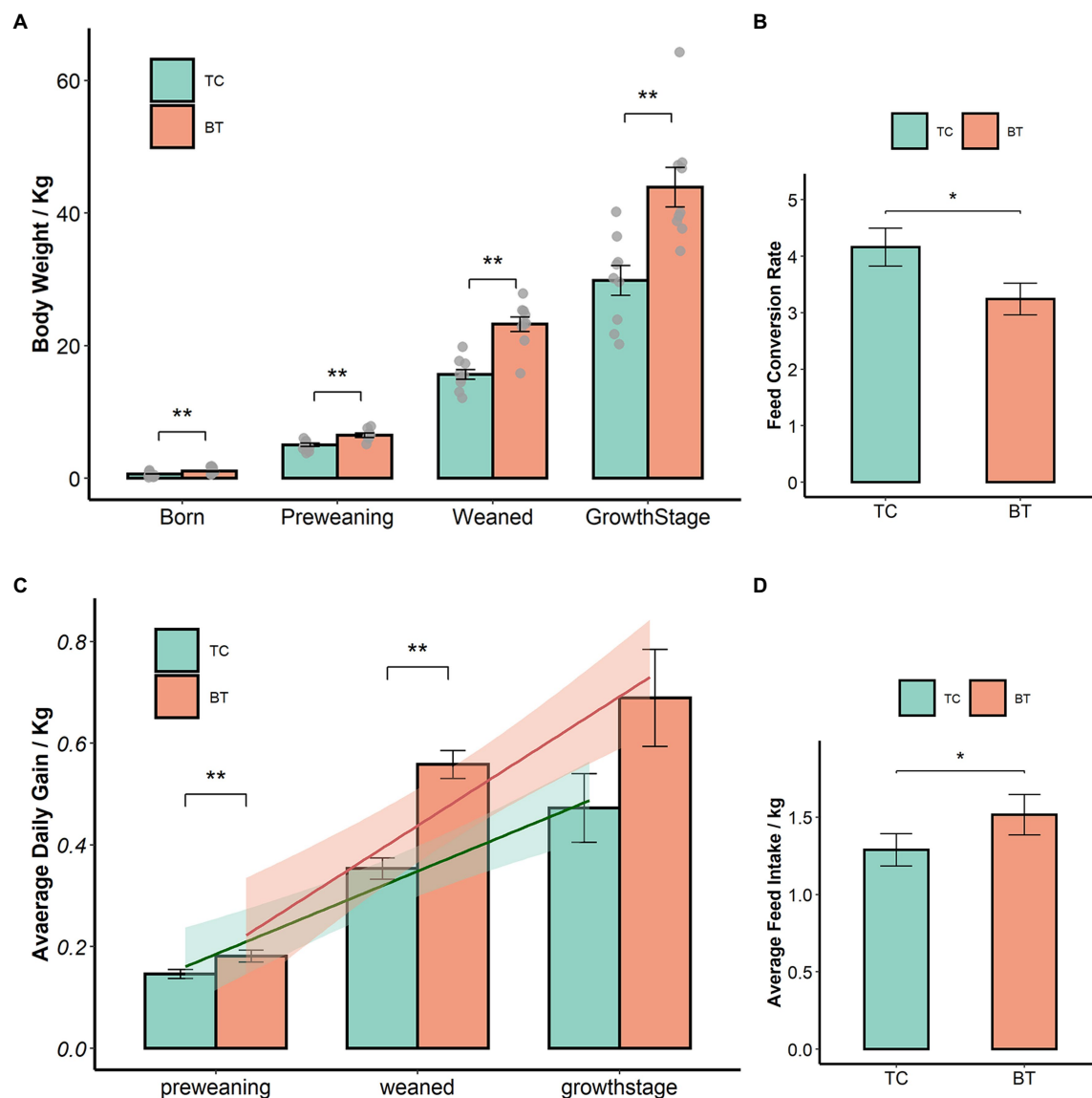


FIGURE 1

Hybridization improved the growth performance of TC pigs, the values showed in the bar presented as means  $\pm$  SEM, and differences in the figures were marked by "\*" and "\*\*" while  $p < 0.05$  and  $p < 0.01$ , respectively. (A) Body weight. (B) Average daily gain. (C) Feed conversion rate. (D) Feed intake.

*Lactobacillus amylovorus* (Figure 6C). Furthermore, the microbial composition was significantly different at the species level in TC pigs and BT pigs by stage (Supplementary Table S2), which was consistent with the beta diversity analysis.

The goal of network inference was to identify combinations of microorganisms that show significant co-correlation across species and to combine them into a network. Network analysis can also reveal why some microbial groups consistently occur together or whether certain microbial taxa are more important for maintaining network structure. Obviously, *Prevotella*, positively associated with many other bacteria, was the dominant and core genus at the pre-weaning stage (Figure 7A). Then, *Prevotella* and *Lactobacillus* showed numerous correlations at the weaned stage (Figure 7B), indicating their stability and importance under the weaning stress. Finally, the core genus of *Prevotella* was replaced by multiple genera at the growth stage as the network showed (Figure 7C),

indicating the relative stability of intestinal microbiota. Above all, hybridization changed not only the microbial composition but also the microbial connections as well.

### 3.5. Predicted functions through the intestinal metagenome of TC pigs and BT pigs

To compare the specific physiological properties between TC pigs and BT pigs, we next conducted KEGG analyses of the intestinal metagenome, which were identified from different stages. According to the KEGG analyses (Supplementary Table S3), hybridization improved the biosynthesis of many aromatic amino acids at the pre-weaning stage, such as phenylpropanoid, tyrosine, and tryptophan (Figure 8A). Intriguingly, these aromatic amino acids

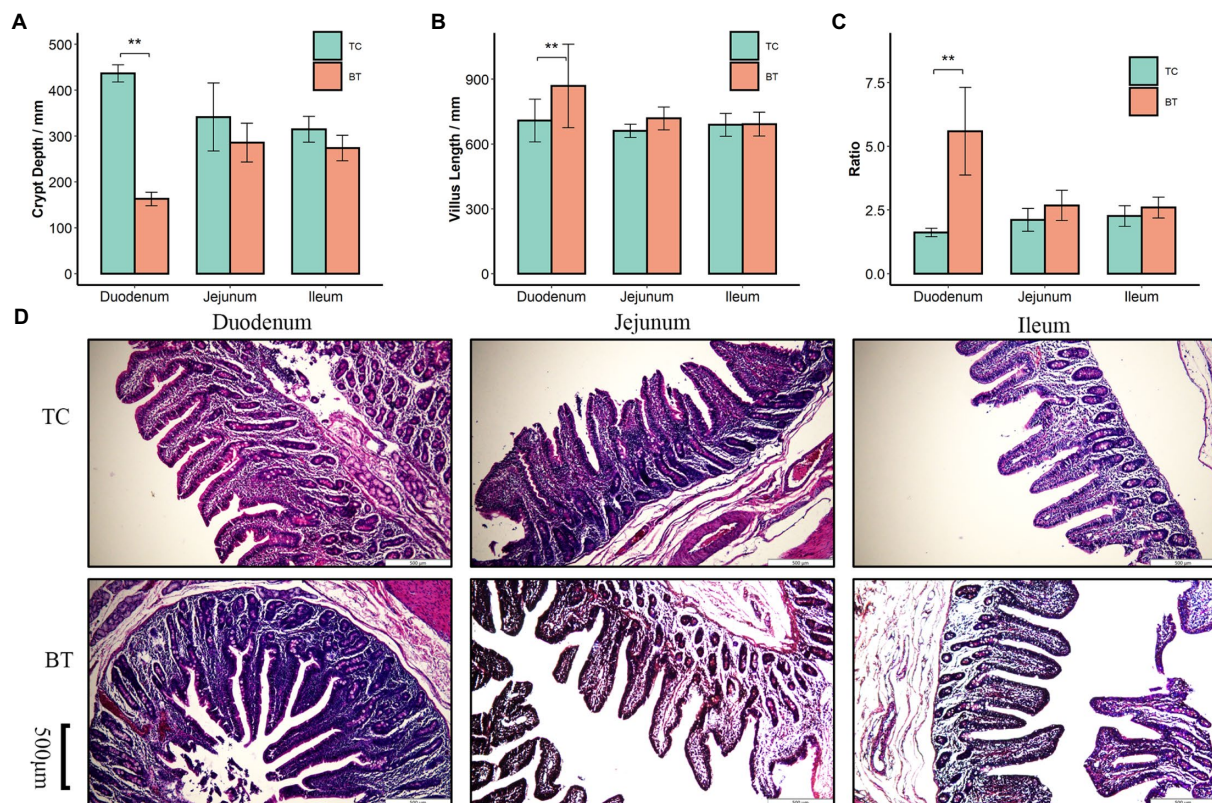


**FIGURE 2**  
Histological analysis of the duodenum, jejunum, and ileum in TC pigs and BT pigs, the values showed in the bar presented as means  $\pm$  SEM, and differences in the figures were marked by “\*\*” and “\*\*\*” while  $p < 0.05$  and  $p < 0.01$ , respectively. (A) Crypt depth. (B) Villus length. (C) The ratio of villus length to crypt depth. (D) HE staining for histological examination.

were involved in the biosynthesis of melanin. We suspected such aromatic amino acids affected the biosynthesis of melanin and coat color as the coat color of BT pigs with all-black while the coat color of TC pigs with piebald. Then, the enrichment of the ‘PPAR signaling pathway’ was detected to be decreased by hybridization (Figure 8B). The PPAR signaling was associated with lipid metabolism and adipocyte differentiation, but more evidence was needed to demonstrate its function. Finally, we detected that the ‘NOD-like receptor signaling pathway’ was enriched in BT pigs at the growth stage (Figure 8C), reflecting a bacterial infection caused by hybridization. At the same time, some pathways related to the construction of the intestinal barrier were decreased by hybridization. These data were consistent with the conclusion of intestinal functions.

### 3.6. Major metabolites of TC pigs and BT pigs at different stages

Metabolite composition, through untargeted metabolomics analysis (Supplementary Table S4), revealed significant pattern differences between TC pigs and BT pigs at various stages (Figures 9B–D), suggesting that the hybridization altered the metabolic processes of TC pigs. In addition, the class of carboxylic acids and derivatives presented the largest proportion of these primary metabolites (TCPW: 52.2%, BTPW: 51.4%, TCWD: 48.5%, BTWD:

40.2%, TCGT: 54.7%, and BTGT: 54.5%, Figure 9A). Moreover, the class of hydroxy acid and derivatives showed significant differences at the weaned stage and growth stage. However, the significantly different metabolites were fatty acids and steroids, including prostaglandins and short-chain fatty acid-related metabolites (Figures 10A–C). These data reflected that hybridization was associated with intestinal inflammation and development.

An important indication of microbial fermentation activity is the relative amount of acetate, propionate, and butyrate. They play an important role in maintaining intestinal function and integrity as well. Here, the proportions of acetate to propionate to butyrate in all the samples were in general close, and acetate had taken the most (Figure 11D). However, hybridization decreased the proportion of acetate (Figure 11A) and increased the proportion of butyrate (Figure 11C). Despite their similar intestinal histology, this indicates that the elevated acetate levels are more likely a function of the composition of the microbial community than that of intestinal histology.

### 3.7. Differences in the metabolic pathway between TC pigs and BT pigs over time

The functions of these changed metabolites were determined by the KEGG pathway analysis (Supplementary Table S5). The “arachidonic acid metabolism”, “intestinal immune network for IgA

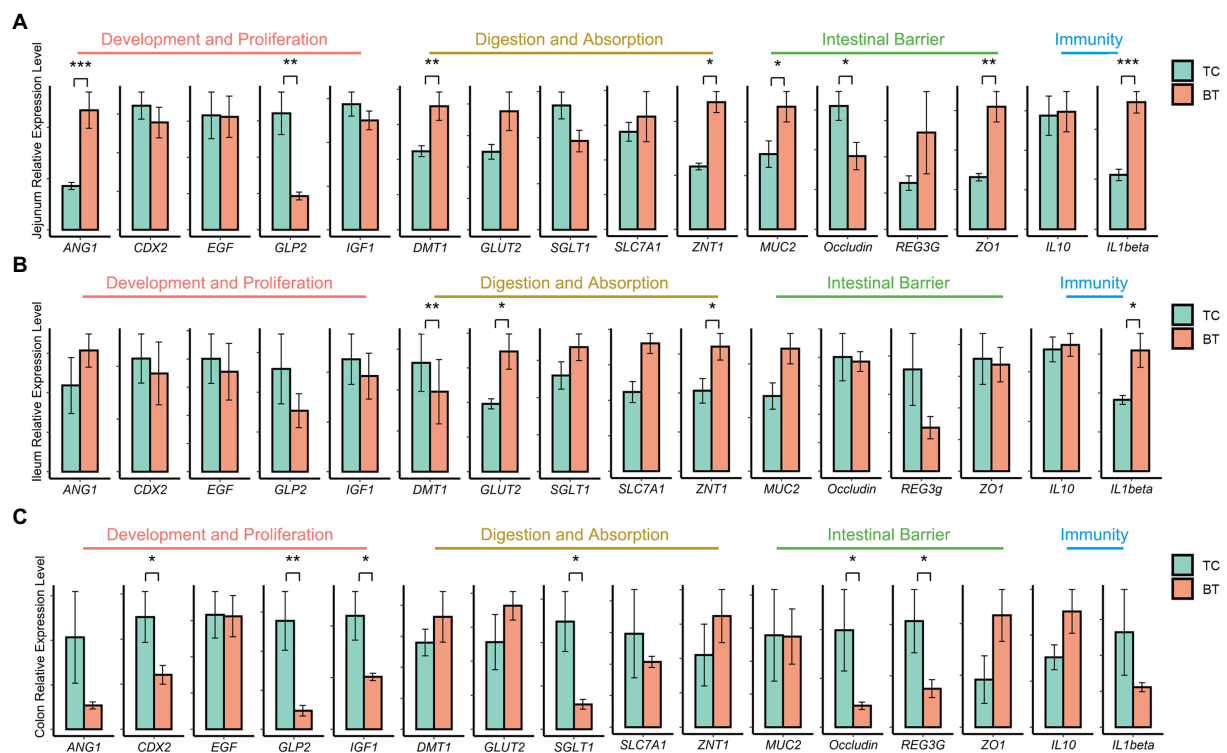


FIGURE 3

mRNA expression of genes related to intestinal functions was assessed by real-time PCR and normalized to beta-actin. The values showed in the bar are presented as means  $\pm$  SEM, and differences in the figures were marked by "\*" and "\*\*\*" while  $p < 0.05$  and  $p < 0.01$ , respectively. (A) mRNA expression in the jejunum tissue. (B) mRNA expression in the ileum tissue. (C) mRNA expression in the colon tissue.

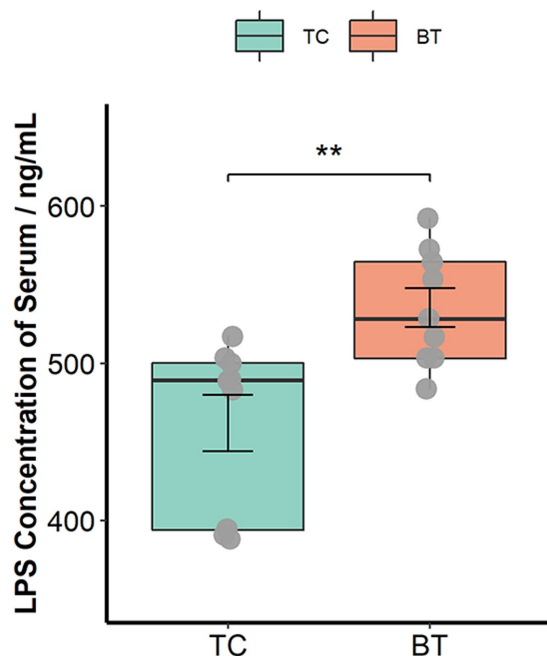


FIGURE 4

LPS concentration of serum was assessed by the ELISA Kit. The values showed in the boxplot presented as means  $\pm$  SEM, and differences in the figures were marked by "\*" and "\*\*\*" while  $p < 0.05$  and  $p < 0.01$ , respectively.

production", "linoleic acid metabolism", and "phenylalanine metabolism" were enriched after hybridization at the pre-weaning stage (Figure 10D). Similarly, the "PPAR signaling pathway" was also not enriched after hybridization at the weaned stage (Figure 10E), indicating that lipid metabolism and adipocyte differentiation may be downregulated by the hybridization. In addition, the pathway of "bile secretion" was impaired after hybridization at the weaned stage, which increased the risk of intestinal inflammation because bile acid was required for efficient lipid absorption and possessed powerful direct and indirect antimicrobial functions in the small intestine. Notably, many inflammation-related pathways were enriched after hybridization at the growth stage, including "eicosanoids", "linoleic acid metabolism", "arachidonic acid metabolism", "cortisol biosynthesis and secretion", and "steroid hormone biosynthesis" (Figure 10F). Nevertheless, "protein digestion and absorption" was still enriched in BT pigs of hybrid, reflecting its advantage on nutrient metabolism but potential inflammation.

The influences of maternal effect and gender on the microbiome and metabolome were tested using the permutational analysis of variance (PERMANOVA) implemented using the Adonis function in the R "vegan" package with the Bray-Curtis method to calculate pairwise distances and 9,999 permutations. As a result, microbiome was little influenced by gender and maternal effect in TC pigs and BT pigs (Table 1). But the maternal effect had influenced the metabolome at pre-weaning stage (Table 2). Overall, differences in microbiome and metabolome was mainly caused by the different species.

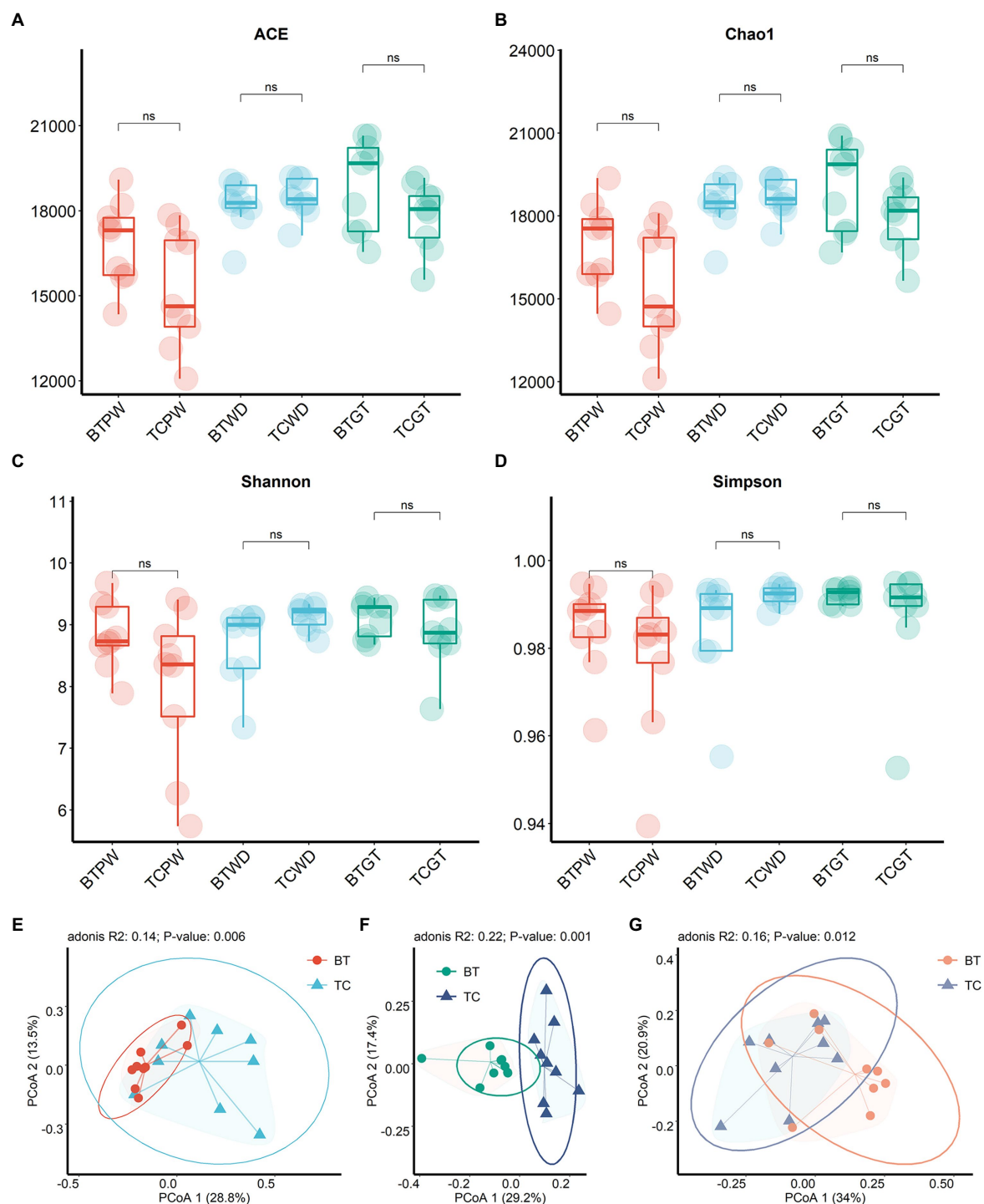


FIGURE 5

Microbial community richness and diversity between TC pigs and BT pigs at different stages. (A) ACE index. (B) Chao1 index. (C) Shannon index. (D) Simpson index. (E–G) Principal coordinate analysis (PCoA) was calculated from metagenome sequence data from individual samples, which showed the differences in microbiota composition over time.

### 3.8. Correlation analysis between microbiome and metabolism

We first verified that maternal effect and gender did not impact the selected metabolites through PERMANOVA (Table 3). The correlation analysis was performed by calculating Spearman's

correlation coefficient and *p*-value, reflecting the correlations between intestinal microbiota and metabolites. Furthermore, the metabolites were chosen from the different metabolic pathways. Here, the data suggested that *Prevotella*, the dominant bacteria at the pre-weaning stage, was positively correlated with the prostaglandin metabolites, including Prostaglandin E2, Prostaglandin D2, and



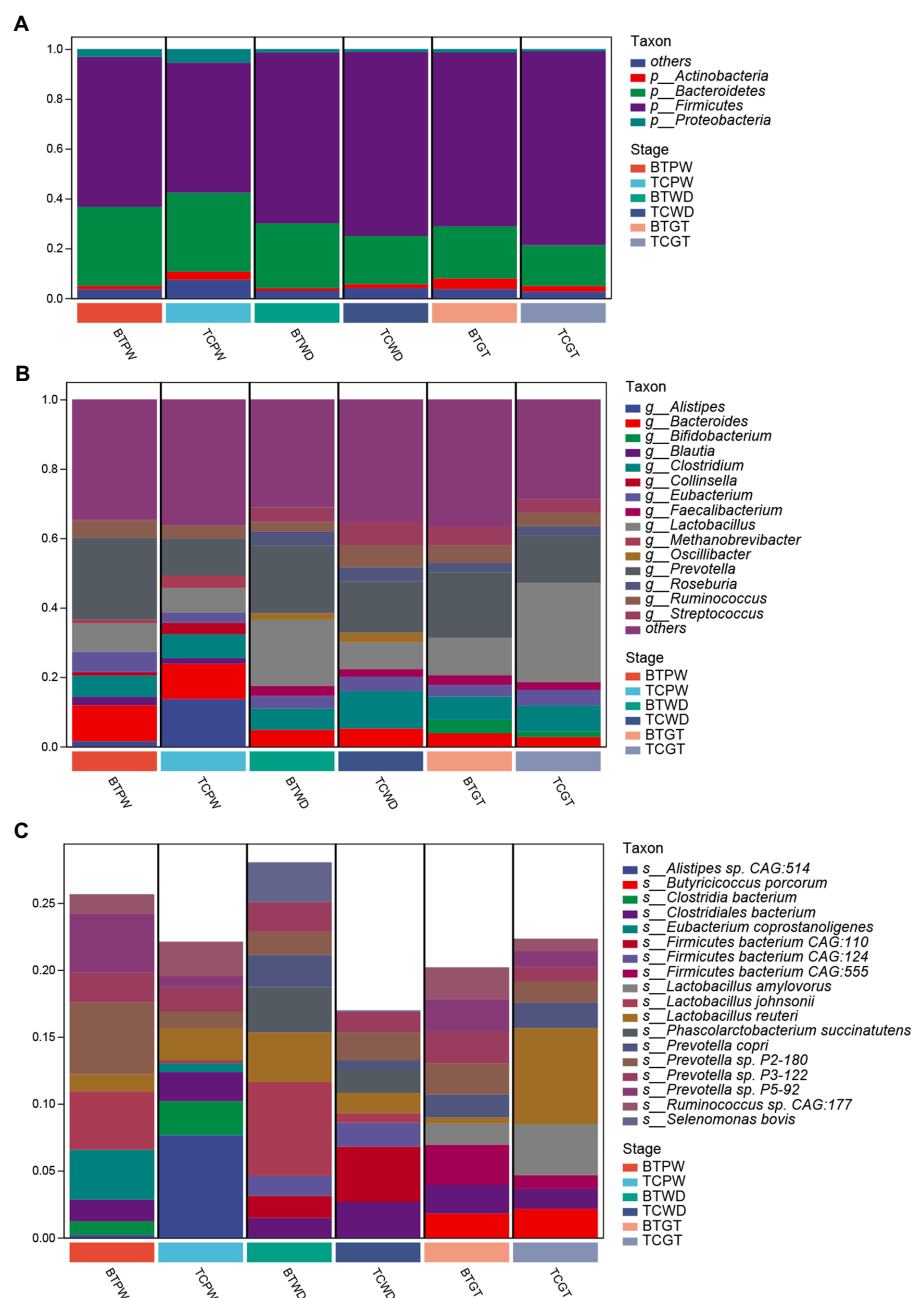


FIGURE 6

Composition and differences of the highly abundant microbial community at different stages in TC pigs and BT pigs. (A) Phylum-level, (B) genus-level, and (C) species-level composition of intestinal microbial communities; each bar shows the average relative abundance of the top 10 microbiota among the samples.

15-Deoxy-d-12,14-PGJ2 (Figure 12A). These metabolites were linked with chronic inflammation. We, then, found out that the majority of the differential metabolites were classified as fatty acyls and steroids and steroid derivatives at the weaned stage. Most of these metabolites were correlated with *Ruminococcus* and *Lactobacillus* (Figure 12B). Specifically, *Lactobacillus* was negatively correlated with the inflammation-related and steroid hormone biosynthesis-related metabolites, while *Ruminococcus* played the opposite role. Meanwhile, both *Lactobacillus* and *Ruminococcus* showed statistical differences in TC pigs and BT pigs at the weaned

stage, indicating that they may regulate the differential metabolic pathways. Finally, the classification showed that most differential metabolites were involved in fatty acyls and steroids and steroid derivatives at the growth stage. These metabolites were also related to the inflammatory pathways, including “arachidonic acid metabolism”, “linoleic acid metabolism”, and “steroid hormone biosynthesis”. Similarly, *Lactobacillus* showed a negative correlation with the inflammation-related metabolites, but *Oscillibacter* played the opposite role this time (Figure 12C). These results confirmed our suspicion that the intestinal environment between TC pigs and BT

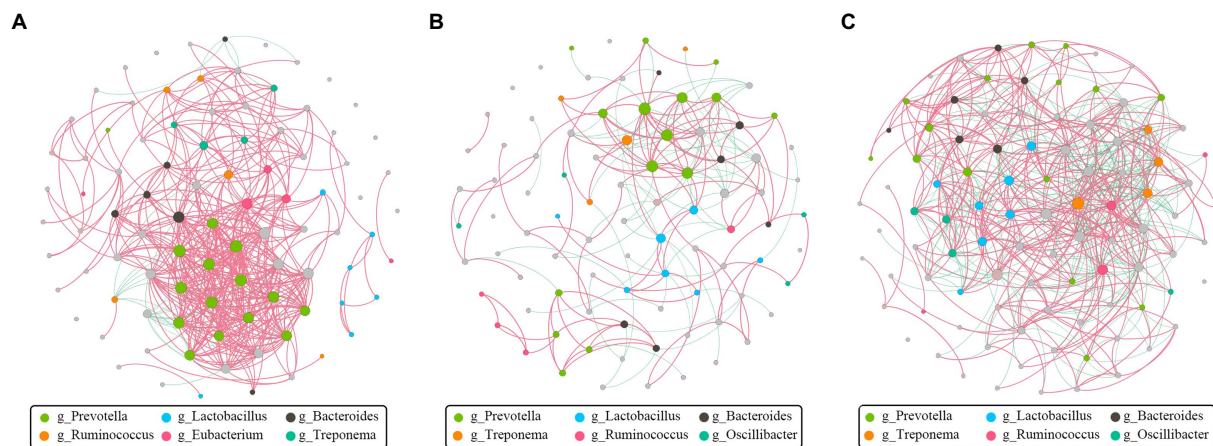


FIGURE 7

Co-correlation analysis of bacterial network by different stages. Each node represents a species, the size of each node is proportional to the relative abundance, and the color of the nodes indicates their taxonomic assignment. The red and green lines represent the positive and negative correlations, respectively. Only lines corresponding to correlations with a magnitude greater than 0.5 are shown. (A) Pre-weaning stage. (B) Weaned stage. (C) Growth stage.

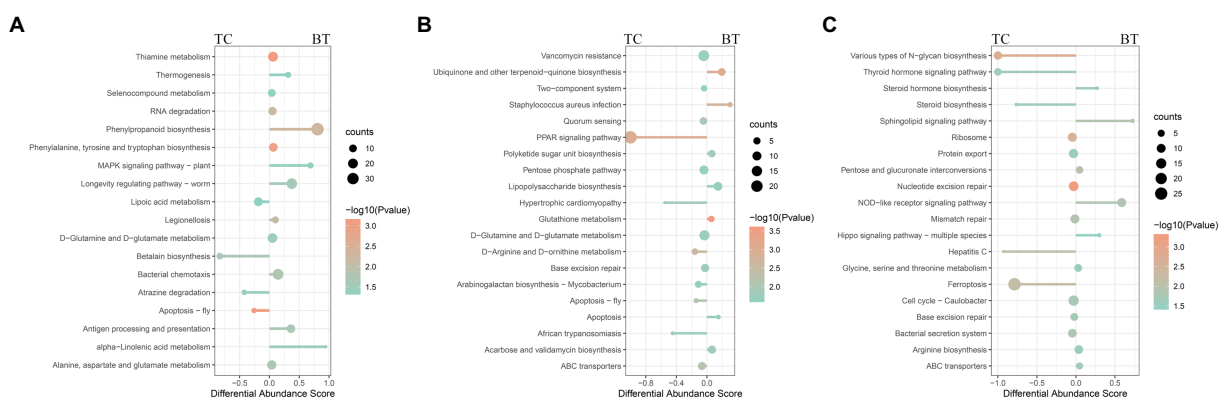


FIGURE 8

Enrichment analysis of KEGG pathway through the intestinal metagenome. Pathways were grouped by stages: (A) pre-weaning stage, (B) weaned stage, and (C) growth stage. Each point represents a pathway, the size of each point is proportional to the counts, and the color of the point indicates their  $p$ -values. The length of the line represents the differential abundance score (DAS) calculated by the relative gene ratio.

pigs was altered by microbial communities and revealed the anti-inflammatory effect of *Lactobacillus*.

## 4. Discussion

In the current study, we revealed several significant differences in intestinal functions and intestinal microbiome and metabolome between TC pigs and BT pigs. Furthermore, we verified that microbiota was significantly associated with many metabolites through correlation analysis. In conclusion, we identified that the hybridization increased the growth performance and the capability of nutrient absorption and metabolism of TC pigs but weakened the intestinal barrier function and development, especially in the colon.

Notably, significant differences were found in the intestinal microbiome and metabolome over time. We detected that the abundance of *Prevotella* was increased after hybridization, which may

benefit nutrient metabolism (Chen et al., 2021; Ren et al., 2021). On the other hand, *Lactobacillus*, as the most dominant genus in TC pigs at the growth stage, contributed to intestinal health (Moeller and Sanders, 2020), but its abundance was decreased by hybridization. Meanwhile, the variation tendency of *Lactobacillus* was changed as well. As for the short-chain fatty acid, the proportion of acetate to propionate to butyrate in all the samples was in general close, but hybridization increased the average molar of butyrate and decreased the average molar of acetate. We also found that, through correlation analysis, *Lactobacillus* was negatively correlated with several steroid hormone-related and inflammation-related metabolites. These metabolites included cortisol and leukotriene and prostaglandin, which participated in the differential KEGG pathways, such as “steroid hormone biosynthesis” and “arachidonic acid metabolism” (Samuelsson, 1991; Shin et al., 2019a; Wang et al., 2021; Del Castillo-Izquierdo et al., 2022). These observations support the potential regulation by the hybridization and the anti-inflammatory effect of

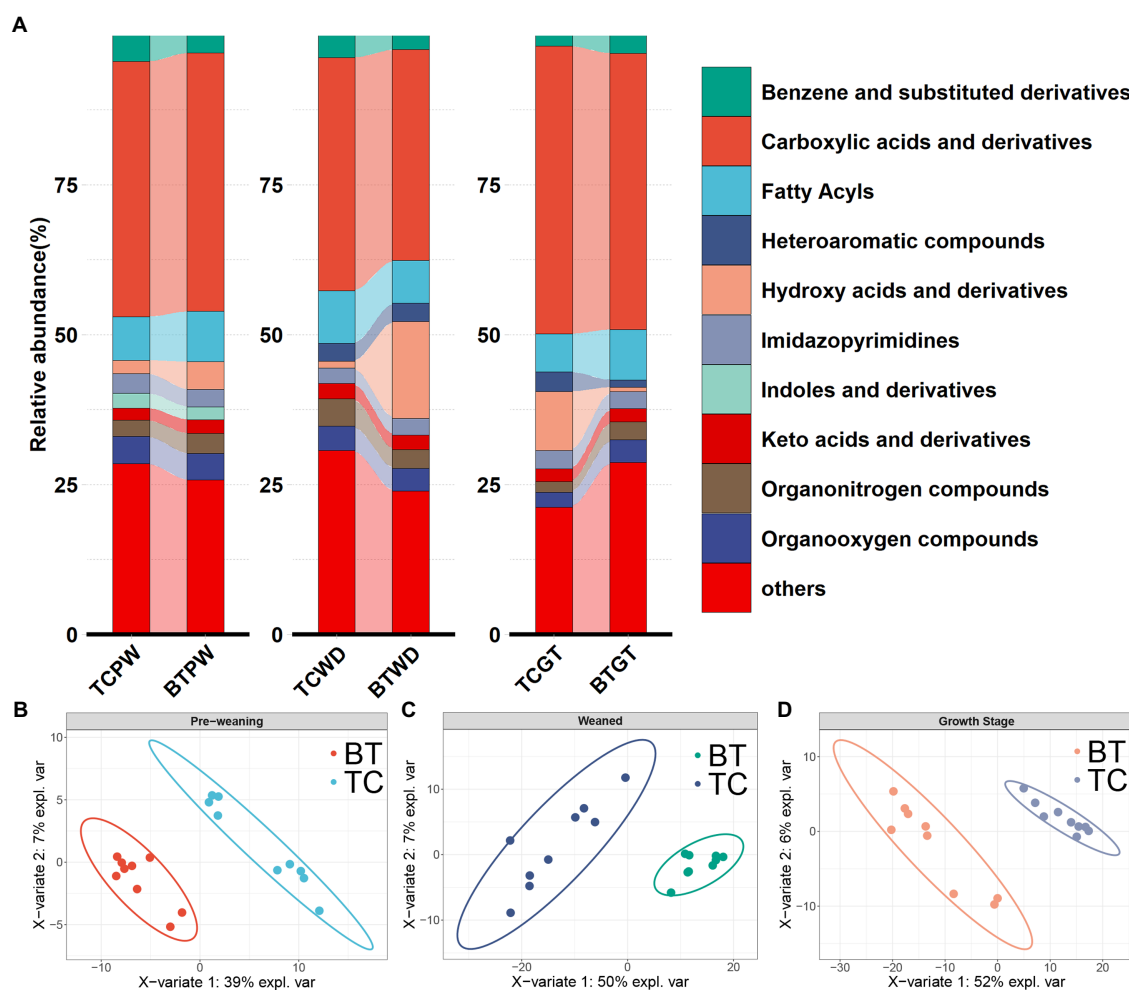


FIGURE 9

Metabolic composition and pattern were altered by hybridization. **(A)** Intestinal metabolite class composition according to relative metabolite masses (sum of standardized abundances), metabolites were deduced from the top 10 primary metabolites which accounted for more than 80% of the total metabolites. The PLS-DA model of intestinal metabolome analysis was performed on TC pigs and BT pigs at **(B)** the pre-weaning stage, **(C)** the weaned stage, and **(D)** the growth stage.

*Lactobacillus*. Histologically, it was similar before and after hybridization. In addition, the expression of several nutrient transporters, such as GLUT2 and ZNT1, was increased after hybridization, and the growth performance also confirmed that the capability of nutrient and absorption was better in BT pigs (Pluske et al., 2018; Quan et al., 2019; Yaqoob et al., 2021). As for the intestinal barrier, we detected the mRNA expression of occludin, REG3G, and IL10 was decreased after hybridization, while the LPS concentration of serum was increased. This evidence reflected that the hybridization impaired the intestinal barrier function of TC pigs (Tabung et al., 2017; Rohr et al., 2020; Engevik and Engevik, 2021). Furthermore, several intestinal development and proliferation-related mRNAs, such as CDX2 and IGF1 (Bonhomme et al., 2003; Van Landeghem et al., 2015; Sun et al., 2017), were decreased in colon tissues, which was unfavorable for bacterial colonization. In summary, our results reflected that hybridization reshaped the intestinal microbiome, metabolome, and functions.

Remarkably, *Prevotella* and *Lactobacillus* were the dominant genera during our studies. It was interesting that *Lactobacillus* was

abundant in both pigs, although hybridization decreased its relative abundance. Moreover, the role of *Lactobacillus* has been reported as gut protection (Reid, 1999; Wang et al., 2018; Zhang et al., 2018; Dawood et al., 2019; Mao et al., 2019), since its production of SCFAs contributes to intestinal permeability (Chen et al., 2018; Mao et al., 2019) and regulation of the microbial composition (Xia et al., 2020). On the other hand, multiple phenotypes of TC pigs were altered by the hybridization. Most studies used to explain such changes through genome (Fu et al., 2021; Wu et al., 2022). However, the intestinal microbiome and metabolome participated in a variety of pathophysiological processes as well (Pei et al., 2021). Herein, we detected *Prevotella*, which played a role in the metabolism of proteins, peptides, and amino acids (Chen et al., 2021; Ren et al., 2021), was abundant after hybridization and may explain its better growth performance. According to the correlation analysis, inflammation-related metabolites were negatively correlated with *Lactobacillus*. Therefore, we predicted that *Lactobacillus* decreased intestinal inflammation. This agrees with the fact that *Lactobacillus* regulated intestinal homeostasis and immunity (Foyssal et al., 2020;

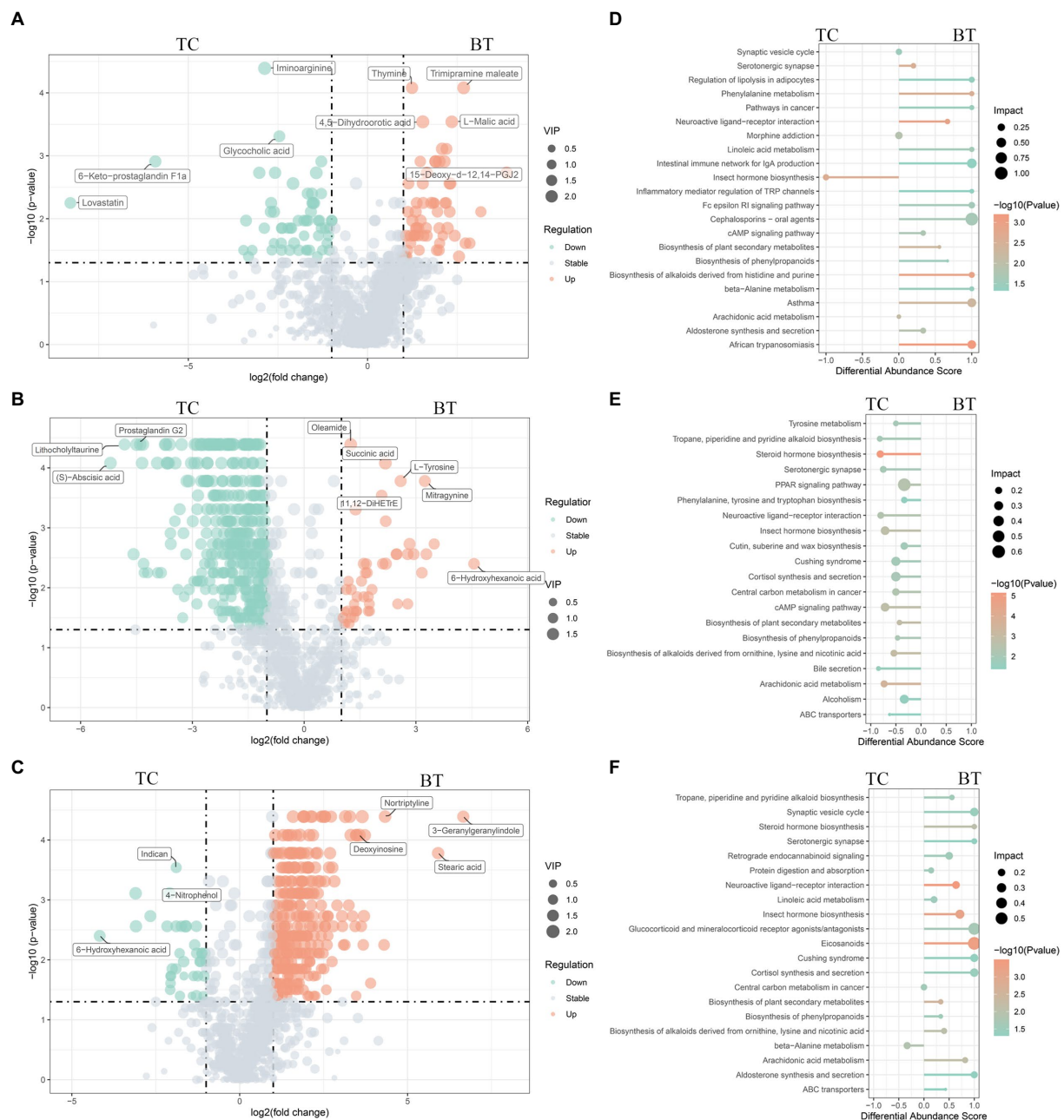


FIGURE 10

Different metabolites and metabolic pathways between TC pigs and BT pigs. Volcano plot of the differential metabolites at (A) the pre-weaning stage, (B) the weaned stage, and (C) the growth stage. Each point represents a metabolite, the points highlighted in green are enriched metabolites of TC pigs while those in red are enriched metabolites of BT pigs, and the size of the point represents the variable importance in projection. Differential metabolic pathways are grouped by (D) pre-weaning stage, (E) weaned stage, and (F) growth stage, the color represents the  $p$ , and the size of the point represents the impact value.

Xin et al., 2020). In addition, the relative amount of acetate was decreased by hybridization, which was negative for intestinal health. However, the intestinal function analysis also demonstrated a similar result that the intestinal barrier was impaired. This evidence displayed the advantages and disadvantages of hybridization in TC pigs. In addition, *Lactobacillus* still occupied a large proportion (TC pigs, 28.8%; BT pigs, 11.0%) in the total intestinal microbiota at the growth stage, compared to the other commercial pigs. These phenomena enticed us to investigate the

possible regulations of *Lactobacillus*. Here, we gave several conjectures to learn more about the alteration of the colonization of *Lactobacillus*. KEGG pathway of the metagenome showed that 'tetracycline biosynthesis' was enriched in TC pigs, such antibiotics affected microbial colonization, including *Prevotella* and *Lactobacillus* (Takahashi et al., 2006; Campedelli et al., 2019; Li et al., 2019; Greppi et al., 2020). On the other hand, several steroid-related metabolites were negatively correlated with *Lactobacillus*. Some studies confirmed that serum steroid hormone could alter the



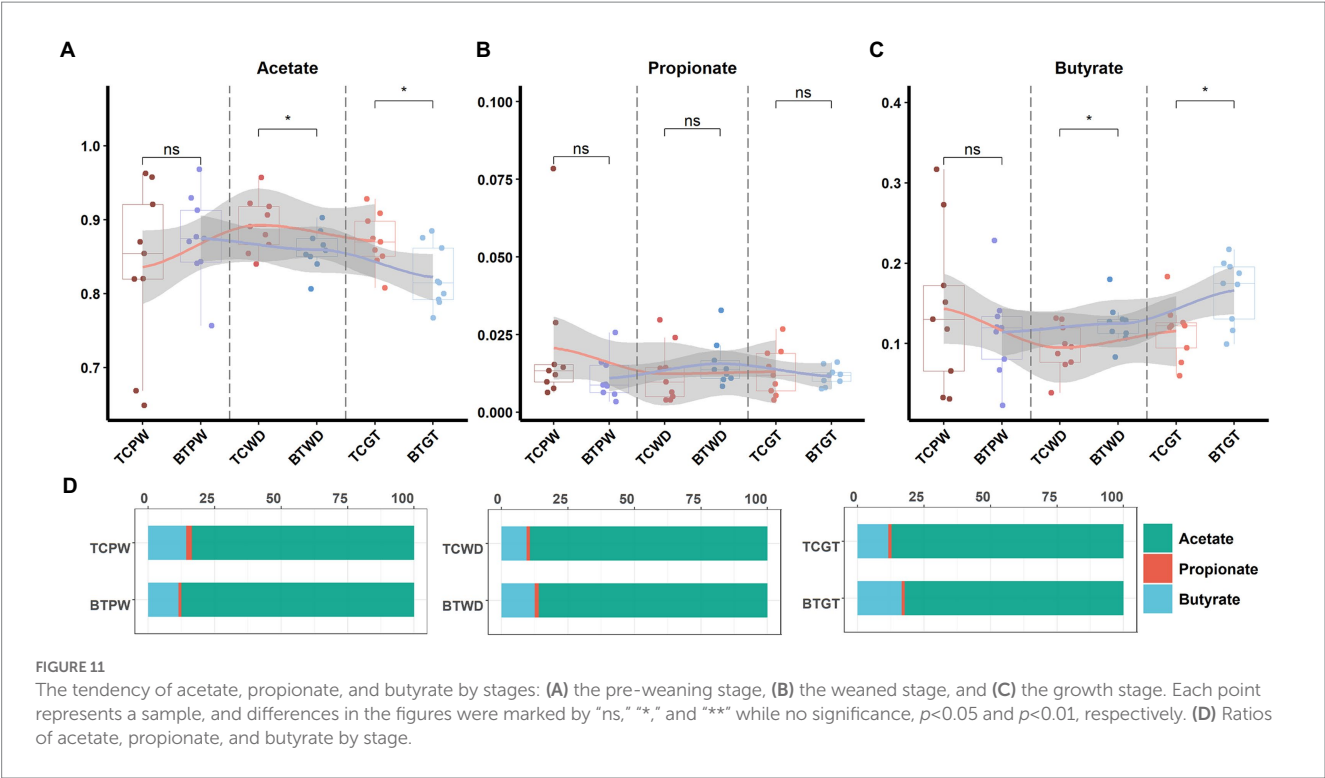


TABLE 1 Andonis results of the microbiome.

Factor	Pre-weaning		Weaned		Growth stage	
	$R^2$	$p$	$R^2$	$p$	$R^2$	$p$
Species	0.12949	0.0119 *	0.2137	0.0015 **	0.15189	0.035 *
Gender	0.07567	0.1729	0.03536	0.6829	0.02192	0.8529
Maternal effect	0.07114	0.1884	0.02275	0.8879	0.06399	0.3063

\* $p < 0.05$ ; \*\* $p < 0.01$ .

TABLE 2 Andonis results of the metabolome.

Factor	Pre-weaning		Weaned		Growth stage	
	$R^2$	$p$	$R^2$	$p$	$R^2$	$p$
Species	0.33864	0.0001**	0.39841	0.0006**	0.41957	0.0005**
Gender	0.03111	0.3794	0.01146	0.08790	0.02761	0.5096
Maternal effect	0.38491	0.0225*	0.25339	0.6373	0.2561	0.4993

\* $p < 0.05$ ; \*\* $p < 0.01$ .

TABLE 3 Andonis results of the differential metabolites.

Factor	Pre-weaning		Weaned		Growth Stage	
	$R^2$	$p$	$R^2$	$p$	$R^2$	$p$
Species	0.17555	0.0543	0.42717	0.0009**	0.44146	0.0002**
Gender	0.02382	0.6404	0.02463	0.5897	0.05959	0.1447
Maternal effect	0.41096	0.3216	0.21844	0.7439	0.23925	0.4338

\* $p < 0.05$ ; \*\* $p < 0.01$ .

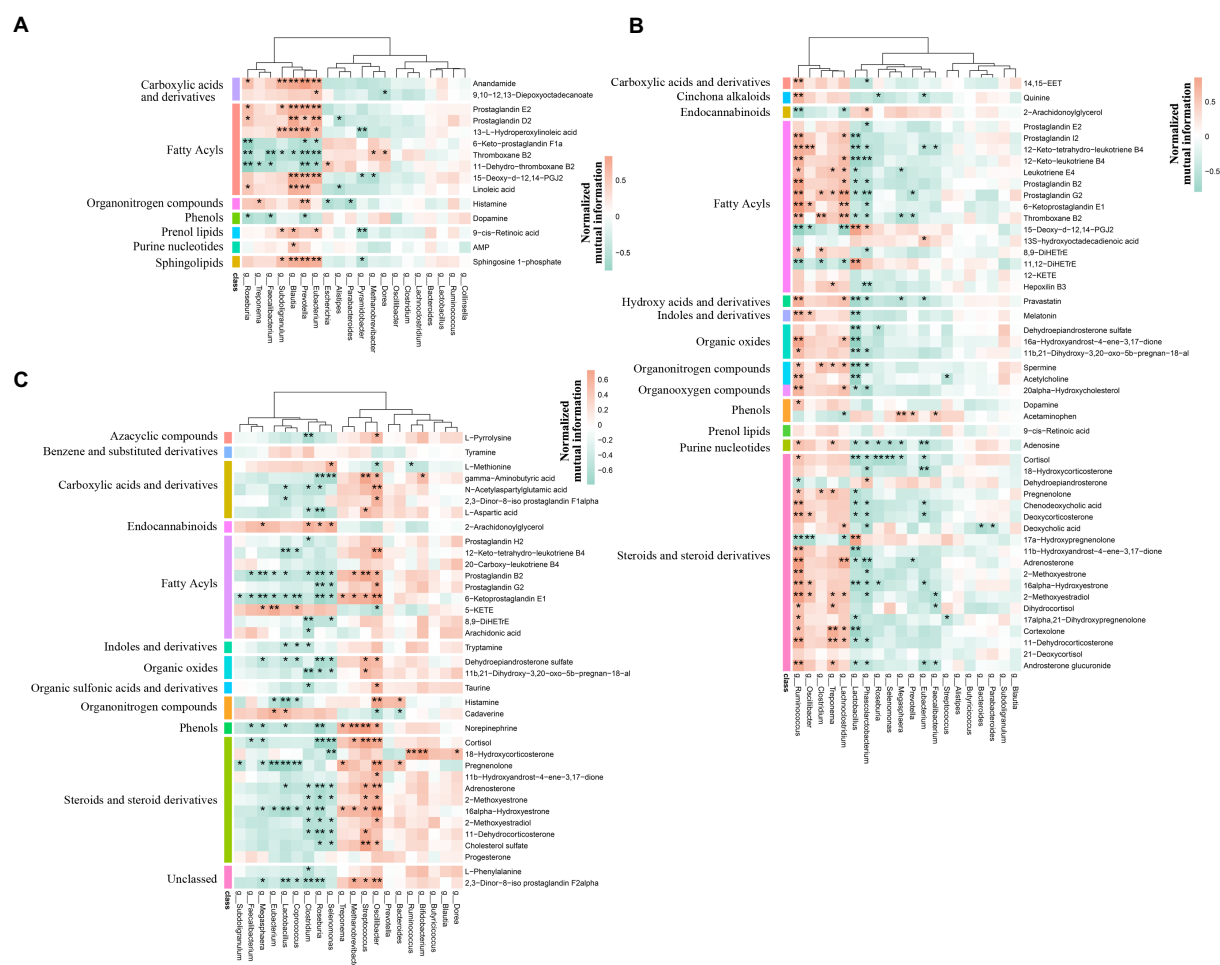


FIGURE 12

Spearman's correlation analysis of microbiome and metabolism. The correlation analysis was performed by stages, including (A) the pre-weaning stage, (B) the weaned stage, and (C) the growth stage. Bacteria were deduced from the top 20 genera which accounted for more than 80% of the microbial sequence reads, and metabolites were deduced from the different metabolic pathways by stages. The color represents the correlation coefficient. Only correlation coefficient beyond 0.6 and  $p$ -value below 0.05 were considered significant and displayed in bold in [Supplementary Tables](#); in figures, \*\* and \* denote, respectively,  $p$ -values below 0.01 and 0.05.

diversity of the intestinal microbiome as well (Tetel et al., 2018; Shin et al., 2019b). This evidence indicated that *Lactobacillus* may be medicated by steroid hormones. These conjectures reflected the potential mechanism of host–microbiome interactions which may be changed by hybridization.

Several reports have shown that hybridization improved the growth performance and lean percentage in Chinese native pigs (Yen et al., 1991; Hyun et al., 2001; Luo et al., 2018; Chen et al., 2021). Meanwhile, intestinal microbiota could spread stably through mother–infant interactions (Desselberger, 2018; Ferretti et al., 2018), which made the microbial composition special among species. However, seldom studies associated the intestinal microbiota with the hybridization effect, while microbiota plays a vital role in the host physiological process. This prompted us to explore the differences in intestinal environment between crossbred pigs and purebred pigs. The noteworthy observation was the abundance of *Lactobacillus* that occupied a very high proportion in TC pigs (28.8%) and BT pigs (11.0%) at the growth stage, which was significantly different from the western commercial pigs (Han et al.,

2018; Lim et al., 2019; Luo et al., 2022). In general, *Lactobacillus* was the dominant intestinal microbiota before weaning, and its abundance would decrease with age. We speculated that such a trait in TC pigs was caused by the coevolution between host and intestinal microbiota because evidence showed that *Lactobacillus* was positively correlated with the environmental temperature, but further evidence is still needed to confirm such host–microbiome interactions. In conclusion, our results shed light on the effect of hybridization on the intestinal environment in TC pigs and provide a novel perspective to the study of host–microbiome interaction between purebred pigs and crossbred pigs.

## 5. Conclusion

Given the findings that hybridization altered the gut microbiome, metabolome and intestinal functions, it is possible to explain how the intestinal microbiota may affect the traits of TC and BT pigs, including growth performance, nutrient digestion and

absorption, and immune response. Furthermore, we explored the potential mechanisms of host–microbiome interactions. Taken together, these findings presented new insights into the role of hybridization in the intestinal microbiome–metabolome correlation, providing a theoretical basis for future microbiota transplantation and pig breeding programs.

## Data availability statement

The data presented in the study are deposited in the Sequence Read Archive (SRA) database, accession number PRJNA951204.

## Ethics statement

The animal study was reviewed and approved by Institutional Animal Care and Use Committee of Zhejiang University. Written informed consent was obtained from the owners for the participation of their animals in this study.

## Author contributions

JH, YZ, and ZW contributed to conception and design of the study. HL contributed to the acquisition of the samples. JH organized the database and wrote the first draft of the manuscript. YX performed the statistical analysis. GH, CP, and PZ wrote sections of the manuscript. All authors contributed to manuscript revision, read, and approved the submitted version.

## References

- Abdelrazig, S., Safo, L., Rance, G. A., Fay, M. W., Theodosiou, E., Topham, P. D., et al. (2020). Metabolic characterisation of magnetospirillum gryphiswaldense msr-1 using lc-ms-based metabolite profiling. *RSC Adv.* 10, 32548–32560. doi: 10.1039/D0RA05326K
- Adhikari, B., Kim, S. W., and Kwon, Y. M. (2019). Characterization of microbiota associated with digesta and mucosa in different regions of gastrointestinal tract of nursery pigs. *Int. J. Mol. Sci.* 20:1630. doi: 10.3390/ijms20071630
- Bergamaschi, M., Tiezzi, F., Howard, J., Huang, Y. J., Gray, K. A., Schillebeeckx, C., et al. (2020). Gut microbiome composition differences among breeds impact feed efficiency in swine. *Microbiome* 8, 1–15. doi: 10.1186/s40168-020-00888-9
- Bonhomme, C., Duluc, I., Martin, E., Chawengsaksophak, K., Chenard, M. P., Kedinger, M., et al. (2003). The cdx2 homeobox gene has a tumour suppressor function in the distal colon in addition to a homeotic role during gut development. *Gut* 52, 1465–1471. doi: 10.1136/gut.52.10.1465
- Boulesteix, A., and Strimmer, K. (2007). Partial least squares: a versatile tool for the analysis of high-dimensional genomic data. *Brief. Bioinform.* 8, 32–44. doi: 10.1093/bib/bbl016
- Bray, J. R., and Curtis, J. T. (1957). An ordination of the upland forest communities of southern Wisconsin. *Ecol. Monogr.* 27, 325–349. doi: 10.2307/1942268
- Brooks, J. F. II, Behrendt, C. L., Ruhn, K. A., Lee, S., Raj, P., Takahashi, J. S., et al. (2021). The microbiota coordinates diurnal rhythms in innate immunity with the circadian clock. *Cells* 184, 4154–4167.e12. doi: 10.1016/j.cell.2021.07.001
- Buchfink, B., Xie, C., and Huson, D. H. (2015). Fast and sensitive protein alignment using diamond. *Nat. Methods* 12, 59–60. doi: 10.1038/nmeth.3176
- Campedelli, I., Mathur, H., Salvetti, E., Clarke, S., Rea, M. C., Torriani, S., et al. (2019). Genus-wide assessment of antibiotic resistance in lactobacillus spp. *Appl. Environ. Microbiol.* 85, e1718–e1738. doi: 10.1128/AEM.01738-18
- Caporaso, J. G., Kuczynski, J., Stombaugh, J., Bittinger, K., Bushman, F. D., Costello, E. K., et al. (2010). Qiime allows analysis of high-throughput community sequencing data. *Nat. Methods* 7, 335–336. doi: 10.1038/nmeth.f303
- Chen, C., Fang, S., Wei, H., He, M., Fu, H., Xiong, X., et al. (2021). Prevotella copri increases fat accumulation in pigs fed with formula diets. *Microbiome* 9, 1–21. doi: 10.1186/s40168-021-01110-0
- Chen, Y., Yang, N., Lin, Y., Ho, S., Li, K., Lin, J., et al. (2018). A combination of lactobacillus Mali aps1 and dieting improved the efficacy of obesity treatment via manipulating gut microbiome in mice. *Sci. Rep.* 8, 1–14. doi: 10.1038/s41598-018-23844-y
- Chen, C., Zhu, J., Ren, H., Deng, Y., Zhang, X., Liu, Y., et al. (2021). Growth performance, carcass characteristics, meat quality and chemical composition of the shaziling pig and its crossbreeds. *Livest. Sci.* 244:104342. doi: 10.1016/j.livsci.2020.104342
- Dawood, M. A., Magouz, F. I., Salem, M. F., and Abdel-Daim, H. A. (2019). Modulation of digestive enzyme activity, blood health, oxidative responses and growth-related gene expression in gift by heat-killed lactobacillus plantarum (l-137). *Aquaculture* 505, 127–136. doi: 10.1016/j.aquaculture.2019.02.053
- Del Castillo-Izquierdo, Á., Mayneris-Perxachs, J., and Fernández-Real, J. M. (2022). Bidirectional relationships between the gut microbiome and sexual traits. *Am. J. Physiol.-Cell Physiol.* 322, C1223–C1229. doi: 10.1152/ajpcell.00116.2022
- Desselberger, U. (2018). The mammalian intestinal microbiome: composition, interaction with the immune system, significance for vaccine efficacy, and potential for disease therapy. *Pathogens* 7:57. doi: 10.3390/pathogens7030057
- Dunn, W. B., Broadhurst, D., Begley, P., Zelena, E., Francis-McIntyre, S., Anderson, N., et al. (2011). Procedures for large-scale metabolic profiling of serum and plasma using gas chromatography and liquid chromatography coupled to mass spectrometry. *Nat. Protoc.* 6, 1060–1083. doi: 10.1038/nprot.2011.335
- Engelvik, A. C., and Engelvik, M. A. (2021). Exploring the impact of intestinal ion transport on the gut microbiota. *Comp. Struct. Biotechnol. J.* 19, 134–144. doi: 10.1016/j.csbj.2020.12.008
- Ferretti, P., Pasolli, E., Tett, A., Asnicar, F., Gorfer, V., Fedi, S., et al. (2018). Mother-to-infant microbial transmission from different body sites shapes the developing infant gut microbiome. *Cell Host Microbe* 24, 133–145.e5. doi: 10.1016/j.chom.2018.06.005
- Foysal, M. J., Fotadar, R., Siddik, M. A., and Tay, A. (2020). Lactobacillus acidophilus and l. Plantarum improve health status, modulate gut microbiota and innate immune response of marron (cherax cainii). *Sci. Rep.* 10, 1–13.

## Funding

The research was supported by the Hainan Province Science and Technology Special Fund (ZDYF2022XDNY238) and the Project of Sanya Yazhou Bay Science and Technology City (SCKJ-JYRC-2022-07 and SKJC-2020-02-007).

## Conflict of interest

HL was employed by Long Jian Animal Husbandry Company.

The remaining authors declare that the research was conducted in the absence of any commercial or financial relationships that could be construed as a potential conflict of interest.

## Publisher's note

All claims expressed in this article are solely those of the authors and do not necessarily represent those of their affiliated organizations, or those of the publisher, the editors and the reviewers. Any product that may be evaluated in this article, or claim that may be made by its manufacturer, is not guaranteed or endorsed by the publisher.

## Supplementary material

The Supplementary material for this article can be found online at: <https://www.frontiersin.org/articles/10.3389/fmicb.2023.1159653/full#supplementary-material>

- Frantz, L. A., Schraiber, J. G., Madsen, O., Megens, H., Cagan, A., Bosse, M., et al. (2015). Evidence of long-term gene flow and selection during domestication from analyses of Eurasian wild and domestic pig genomes. *Nature Genet.* 47, 1141–1148. doi: 10.1038/ng.3394
- Fu, H., He, M., Wu, J., Zhou, Y., Ke, S., Chen, Z., et al. (2021). Deep investigating the changes of gut microbiome and its correlation with the shifts of host serum metabolome around parturition in sows. *Front. Microbiol.* 12:2778. doi: 10.3389/fmicb.2021.729039
- Fu, L., Niu, B., Zhu, Z., Wu, S., and Li, W. (2012). Cd-hit: accelerated for clustering the next-generation sequencing data. *Bioinformatics* 28, 3150–3152. doi: 10.1093/bioinformatics/bts565
- Gagnebin, Y., Tonoli, D., Lescuyer, P., Ponte, B., de Seigneux, S., Martin, P., et al. (2017). Metabolomic analysis of urine samples by uhplc-qtof-ms: impact of normalization strategies. *Anal. Chim. Acta* 955, 27–35. doi: 10.1016/j.aca.2016.12.029
- Ghosh, S. S., Wang, J., Yannie, P. J., and Ghosh, S. (2020). Intestinal barrier dysfunction, lps translocation, and disease development. *J. Endocr. Soc.* 4:z39. doi: 10.1210/jendso/bvz039
- Gregor, R., Probst, M., Eyal, S., Aksenov, A., Sasson, G., Horovitz, I., et al. (2022). Mammalian gut metabolomes mirror microbiome composition and host phylogeny. *ISME J.* 16, 1262–1274. doi: 10.1038/s41396-021-01152-0
- Greppi, A., Asare, P. T., Schwab, C., Zemp, N., Stephan, R., and Lacroix, C. (2020). Isolation and comparative genomic analysis of reuterin-producing lactobacillus reuteri from the chicken gastrointestinal tract. *Front. Microbiol.* 11:1166. doi: 10.3389/fmicb.2020.01166
- Han, G. G., Lee, J., Jin, G., Park, J., Choi, Y. H., Kang, S., et al. (2018). Tracing of the fecal microbiota of commercial pigs at five growth stages from birth to shipment. *Sci. Rep.* 8:6012. doi: 10.1038/s41598-018-24508-7
- Hartmann, P., Seebauer, C. T., Mazagova, M., Horvath, A., Wang, L., Llorente, C., et al. (2016). Deficiency of intestinal mucin-2 protects mice from diet-induced fatty liver disease and obesity. *Am. J. Physiol.-Gastroint. Liver Physiol.* 310, G310–G322. doi: 10.1152/ajpgi.00094.2015
- Huson, D. H., Auch, A. F., Qi, J., and Schuster, S. C. (2007). Megan analysis of metagenomic data. *Genome Res.* 17, 377–386. doi: 10.1101/gr.5969107
- Hyun, Y., Wolter, B. F., and Ellis, M. (2001). Feed intake patterns and growth performance of purebred and crossbred Meishan and Yorkshire pigs. *Asian Australas. J. Anim. Sci.* 14, 837–843. doi: 10.5713/ajas.2001.837
- Ivanov, I. I., Atarashi, K., Manel, N., Brodie, E. L., Shima, T., Karaoz, U., et al. (2009). Induction of intestinal Th17 cells by segmented filamentous bacteria. *Cells* 139, 485–498. doi: 10.1016/j.cell.2009.09.033
- Li, Y., Li, L., Kromann, S., Chen, M., Shi, L., and Meng, H. (2019). Antibiotic resistance of lactobacillus spp. and streptococcus thermophilus isolated from Chinese fermented milk products. *Foodborne Pathog. Dis.* 16, 221–228. doi: 10.1089/fpd.2018.2516
- Li, D., Liu, C., Luo, R., Sadakane, K., and Lam, T. (2015). Megahit: an ultra-fast single-node solution for large and complex metagenomics assembly by succinct de Bruijn graph. *Bioinformatics* 31, 1674–1676. doi: 10.1093/bioinformatics/btv033
- Lim, M. Y., Song, E., Kang, K. S., and Nam, Y. (2019). Age-related compositional and functional changes in micro-pig gut microbiome. *Geroscience* 41, 935–944. doi: 10.1007/s11357-019-00121-y
- Luo, R., Liu, B., Xie, Y., Li, Z., Huang, W., Yuan, J., et al. (2012). Soapdenovo2: an empirically improved memory-efficient short-read de novo assembler. *Gigascience*. 1, 2047–2217. doi: 10.1186/2047-217X-1-18
- Luo, Y., Ren, W., Smidt, H., Wright, A. G., Yu, B., Schyns, G., et al. (2022). Dynamic distribution of gut microbiota in pigs at different growth stages: composition and contribution. *Microbiol. Spectr.* 10, e621–e688. doi: 10.1128/spectrum.00688-21
- Luo, J., Shen, L., Tan, Z., Cheng, X., Yang, D., Fan, Y., et al. (2018). Comparison reproductive, growth performance, carcass and meat quality of liangshan pig crossbred with duroc and berkshire genotypes and heterosis prediction. *Livest. Sci.* 212, 61–68. doi: 10.1016/j.livsci.2017.09.010
- Mao, G., Li, S., Orfila, C., Shen, X., Zhou, S., Linhardt, R. J., et al. (2019). Depolymerized rg-i-enriched pectin from citrus segment membranes modulates gut microbiota, increases scfa production, and promotes the growth of bifidobacterium spp., lactobacillus spp and faecalibaculum spp. *Food Funct.* 10, 7828–7843. doi: 10.1039/C9FO01534E
- Martin, M. (2011). Cutadapt removes adapter sequences from high-throughput sequencing reads. *EMBnet J.* 17, 10–12. doi: 10.14806/ej.17.1.200
- Meng, Q., Luo, Z., Cao, C., Sun, S., Ma, Q., Li, Z., et al. (2020). Weaning alters intestinal gene expression involved in nutrient metabolism by shaping gut microbiota in pigs. *Front. Microbiol.* 11:694. doi: 10.3389/fmicb.2020.00694
- Moeller, A. H., and Sanders, J. G. (2020). Roles of the gut microbiota in the adaptive evolution of mammalian species. *Philos. Trans. R. Soc. B* 375:20190597. doi: 10.1098/rstb.2019.0597
- Moran, A. W., Al-Rammahi, M. A., Arora, D. K., Batchelor, D. J., Coulter, E. A., Ionescu, C., et al. (2010). Expression of na+/glucose co-transporter 1 (sglt1) in the intestine of piglets weaned to different concentrations of dietary carbohydrate. *Br. J. Nutr.* 104, 647–655. doi: 10.1017/S0007114510000954
- Pei, Y., Chen, C., Mu, Y., Yang, Y., Feng, Z., Li, B., et al. (2021). Integrated microbiome and metabolome analysis reveals a positive change in the intestinal environment of myostatin edited large white pigs. *Front. Microbiol.* 12:628685. doi: 10.3389/fmicb.2021.628685
- Pluske, J. R., Turpin, D. L., and Kim, J. (2018). Gastrointestinal tract (gut) health in the young pig. *Anim. Nutr.* 4, 187–196. doi: 10.1016/j.aninu.2017.12.004
- Quan, J., Cai, G., Yang, M., Zeng, Z., Ding, R., Wang, X., et al. (2019). Exploring the fecal microbial composition and metagenomic functional capacities associated with feed efficiency in commercial dly pigs. *Front. Microbiol.* 10:52. doi: 10.3389/fmicb.2019.00052
- Ramette, A. (2007). Multivariate analyses in microbial ecology. *FEMS Microbiol. Ecol.* 62, 142–160. doi: 10.1111/j.1574-6941.2007.00375.x
- Reid, G. (1999). The scientific basis for probiotic strains of lactobacillus. *Appl. Environ. Microbiol.* 65, 3763–3766. doi: 10.1128/AEM.65.9.3763-3766.1999
- Ren, W., Yan, H., Yu, B., Walsh, M. C., Yu, J., Zheng, P., et al. (2021). Prevotella-rich enterotype may benefit gut health in finishing pigs fed diet with a high amylose-to-amylopectin ratio. *Anim. Nutr.* 7, 400–411. doi: 10.1016/j.aninu.2020.08.007
- Rohr, M. W., Narasimulu, C. A., Rudeski-Rohr, T. A., and Parthasarathy, S. (2020). Negative effects of a high-fat diet on intestinal permeability: a review. *Adv. Nutr.* 11, 77–91. doi: 10.1093/advances/nmz061
- Samuelsson, B. (1991). Arachidonic acid metabolism: role in inflammation. *Z. Rheumatol.* 50 Suppl 1, 3–6.
- Shin, J., Park, Y., Sim, M., Kim, S., Joung, H., and Shin, D. (2019a). Serum level of sex steroid hormone is associated with diversity and profiles of human gut microbiome. *Res. Microbiol.* 170, 192–201. doi: 10.1016/j.resmic.2019.03.003
- Shin, J., Park, Y., Sim, M., Kim, S., Joung, H., and Shin, D. (2019b). Serum level of sex steroid hormone is associated with diversity and profiles of human gut microbiome. *Res. Microbiol.* 170, 192–201. doi: 10.1016/j.resmic.2019.03.003
- Sud, M., Fahy, E., Cotter, D., Brown, A., Dennis, E. A., Glass, C. K., et al. (2007). Lmsd: lipid maps structure database. *Nucleic Acids Res.* 35, D527–D532. doi: 10.1093/nar/gkl838
- Sun, X., Yang, Q., Rogers, C. J., Du, M., and Zhu, M. (2017). Ampk improves gut epithelial differentiation and barrier function via regulating cdx2 expression. *Cell Death Differ.* 24, 819–831. doi: 10.1038/cdd.2017.14
- Tabung, F. K., Birmann, B. M., Epstein, M. M., Martínez-Maza, O., Breen, E. C., Wu, K., et al. (2017). Influence of dietary patterns on plasma soluble cd14, a surrogate marker of gut barrier dysfunction. *Curr. Dev. Nutr.* 1:e1396:e001396. doi: 10.3945/cdn.117.001396
- Takahashi, N., Ishihara, K., Kimizuka, R., Okuda, K., and Kato, T. (2006). The effects of tetracycline, minocycline, doxycycline and ofloxacin on prevotella intermedia biofilm. *Oral Microbiol. Immunol.* 21, 366–371. doi: 10.1111/j.1399-302X.2006.00305.x
- Tetel, M. J., De Vries, G. J., Melcangi, R. C., Panzica, G., and O'Mahony, S. M. (2018). Steroids, stress and the gut microbiome-brain axis. *J. Neuroendocrinol.* 30:e12548. doi: 10.1111/jne.12548
- Thévenot, E. A., Roux, A., Xu, Y., Ezan, E., and Junot, C. (2015). Analysis of the human adult urinary metabolome variations with age, body mass index, and gender by implementing a comprehensive workflow for univariate and opls statistical analyses. *J. Proteome Res.* 14, 3322–3335. doi: 10.1021/acs.jproteome.5b00354
- Trygg, J., and Wold, S. (2002). Orthogonal projections to latent structures (o-pls). *J. Chemom. J. Chemometr. Soc.* 16, 119–128. doi: 10.1002/cem.695
- Turrioni, S., Fiori, J., Rampelli, S., Schnorr, S. L., Consolandi, C., Barone, M., et al. (2016). Fecal metabolome of the hadza hunter-gatherers: a host-microbiome integrative view. *Sci. Rep.* 6, 1–9. doi: 10.1038/srep32826
- Van Landeghem, L., Santoro, M. A., Mah, A. T., Krebs, A. E., Dehmer, J. J., McNaughton, K. K., et al. (2015). Igfl stimulates crypt expansion via differential activation of 2 intestinal stem cell populations. *FASEB J.* 29, 2828–2842. doi: 10.1096/fj.14-264010
- Wang, J., Ji, H., Wang, S., Liu, H., Zhang, W., Zhang, D., et al. (2018). Probiotic lactobacillus plantarum promotes intestinal barrier function by strengthening the epithelium and modulating gut microbiota. *Front. Microbiol.* 9:1953. doi: 10.3389/fmicb.2018.01953
- Wang, X., Tsai, T., Deng, F., Wei, X., Chai, J., Knapp, J., et al. (2019). Longitudinal investigation of the swine gut microbiome from birth to market reveals stage and growth performance associated bacteria. *Microbiome* 7, 1–18. doi: 10.1186/s40168-019-0721-7
- Wang, L., Wang, A., Wang, L., Li, K., Yang, G., He, R., et al. (2011). “Animal genetic resources in China: pigs,” in *China National Commission of animal genetic resources*. eds. B. Zhang, W. Chen, J. Gu, C. Wu, N. Ma, Z. Wang, et al. (Beijing, China: China Agriculture Press).
- Wang, B., Wu, L., Chen, J., Dong, L., Chen, C., Wen, Z., et al. (2021). Metabolism pathways of arachidonic acids: mechanisms and potential therapeutic targets. *Signal Transduct. Target. Ther.* 6, 1–30. doi: 10.1038/s41392-020-00443-w
- Wang, L., Yan, S., Li, J., Li, Y., Ding, X., Yin, J., et al. (2019). Rapid communication: the relationship of enterocyte proliferation with intestinal morphology and



nutrient digestibility in weaning piglets. *J. Anim. Sci.* 97, 353–358. doi: 10.1093/jas/sky388

Want, E. J., Masson, P., Michopoulos, F., Wilson, I. D., Theodoridis, G., Plumb, R. S., et al. (2013). Global metabolic profiling of animal and human tissues via uplc-ms. *Nat. Protoc.* 8, 17–32. doi: 10.1038/nprot.2012.135

Wu, G., Tang, X., Fan, C., Wang, L., Shen, W., Ren, S., et al. (2022). Gastrointestinal tract and dietary fiber driven alterations of gut microbiota and metabolites in durcox bamei crossbred pigs. *Front. Nutr.* 8:806646. doi: 10.3389/fnut.2021.806646

Xia, Y., Chen, Y., Wang, G., Yang, Y., Song, X., Xiong, Z., et al. (2020). Lactobacillus plantarum ar113 alleviates dss-induced colitis by regulating the tlr4/myd88/nf-kb pathway and gut microbiota composition. *J. Funct. Food.* 67:103854. doi: 10.1016/j.jff.2020.103854

Xia, J., and Wishart, D. S. (2011). Web-based inference of biological patterns, functions and pathways from metabolomic data using metaboanalyst. *Nat. Protoc.* 6, 743–760. doi: 10.1038/nprot.2011.319

Xin, J., Zeng, D., Wang, H., Sun, N., Zhao, Y., Dan, Y., et al. (2020). Probiotic lactobacillus johnsonii bs15 promotes growth performance, intestinal immunity, and

gut microbiota in piglets. *Probiotics Antimicrob. Proteins.* 12, 184–193. doi: 10.1007/s12602-018-9511-y

Yaqoob, M. U., Abd El-Hack, M. E., Hassan, F., El-Saadony, M. T., Khafaga, A. F., Batiha, G. E., et al. (2021). The potential mechanistic insights and future implications for the effect of prebiotics on poultry performance, gut microbiome, and intestinal morphology. *Poult. Sci.* 100:101143. doi: 10.1016/j.psj.2021.101143

Yen, J. T., Nienaber, J. A., Klindt, J., and Crouse, J. D. (1991). Effect of ractopamine on growth, carcass traits, and fasting heat production of us contemporary crossbred and chinese Meishan pure-and crossbred pigs. *J. Anim. Sci.* 69, 4810–4822. doi: 10.2527/1991.69124810x

Zhang, Z., Lv, J., Pan, L., and Zhang, Y. (2018). Roles and applications of probiotic lactobacillus strains. *Appl. Microbiol. Biotechnol.* 102, 8135–8143. doi: 10.1007/s00253-018-9217-9

Zhou, H., Sun, J., Yu, B., Liu, Z., Chen, H., He, J., et al. (2021). Gut microbiota absence and transplantation affect growth and intestinal functions: an investigation in a germ-free pig model. *Anim. Nutr.* 7, 295–304. doi: 10.1016/j.aninu.2020.11.012

Zhu, W., Lomsadze, A., and Borodovsky, M. (2010). Ab initio gene identification in metagenomic sequences. *Nucleic Acids Res.* 38:e132. doi: 10.1093/nar/gkq275



## OPEN ACCESS

## EDITED BY

Wei Qi He,  
Soochow University, China

## REVIEWED BY

Piklu Roy Chowdhury,  
University of Technology Sydney, Australia  
Adriana Belas,  
Universidade Lusófona, Portugal

## \*CORRESPONDENCE

Guangneng Peng  
✉ pgn.sicau@163.com  
Xianmeng Qiu  
✉ 13008142361@126.com

<sup>†</sup>These authors have contributed equally to this work and share first authorship

RECEIVED 10 January 2023

ACCEPTED 20 April 2023

PUBLISHED 10 May 2023

## CITATION

Liu L, Dong Z, Ai S, Chen S, Dong M, Li Q, Zhou Z, Liu H, Zhong Z, Ma X, Hu Y, Ren Z, Fu H, Shu G, Qiu X and Peng G (2023) Virulence-related factors and antimicrobial resistance in *Proteus mirabilis* isolated from domestic and stray dogs. *Front. Microbiol.* 14:1141418. doi: 10.3389/fmicb.2023.1141418

## COPYRIGHT

© 2023 Liu, Dong, Ai, Chen, Dong, Li, Zhou, Liu, Zhong, Ma, Hu, Ren, Fu, Shu, Qiu and Peng. This is an open-access article distributed under the terms of the [Creative Commons Attribution License \(CC BY\)](https://creativecommons.org/licenses/by/4.0/). The use, distribution or reproduction in other forums is permitted, provided the original author(s) and the copyright owner(s) are credited and that the original publication in this journal is cited, in accordance with accepted academic practice. No use, distribution or reproduction is permitted which does not comply with these terms.

# Virulence-related factors and antimicrobial resistance in *Proteus mirabilis* isolated from domestic and stray dogs

Lijuan Liu<sup>1†</sup>, Zhiyou Dong<sup>1†</sup>, Shengquan Ai<sup>2†</sup>, Shanyu Chen<sup>1†</sup>, Mengyao Dong<sup>3</sup>, Qianlan Li<sup>1</sup>, Ziyao Zhou<sup>1</sup>, Haifeng Liu<sup>1</sup>, Zhijun Zhong<sup>1</sup>, Xiaoping Ma<sup>1</sup>, Yanchun Hu<sup>1</sup>, Zhihua Ren<sup>1</sup>, Hualin Fu<sup>1</sup>, Gang Shu<sup>1</sup>, Xianmeng Qiu<sup>2\*</sup> and Guangneng Peng<sup>1\*</sup>

<sup>1</sup>Key Laboratory of Animal Disease and Human Health of Sichuan, College of Veterinary Medicine, Sichuan Agricultural University, Chengdu, China, <sup>2</sup>New Ruipeng Pet Healthcare Group, Chengdu, China, <sup>3</sup>State Key Laboratory of Agricultural Microbiology, National Engineering Research Center of Microbial Pesticides, College of Life Science and Technology, Huazhong Agricultural University, Wuhan, China

**Introduction:** *Proteus mirabilis* is a multi-host pathogen that causes diseases of varying severity in a wide range of mammals, including humans. *Proteus mirabilis* is resistant to multiple antibiotics and has acquired the ability to produce expanded spectrum of  $\beta$ -lactamases, leading to serious public health problems. However, the available information on *P. mirabilis* isolated from feces of dogs, is still poorly understood, as is the correlation between its virulence-associated genes (VAGs) and antibiotic resistance genes (ARGs).

**Method:** In this study, we isolated 75 strains of *P. mirabilis* from 241 samples, and investigated the swarming motility, biofilm formation, antimicrobial resistance (AMR), distribution of VAGs and ARGs, as well as the presence of class 1, 2, and 3 integrons in these isolates.

**Results:** Our findings suggest a high prevalence of intensive swarming motility and strong biofilm formation ability among *P. mirabilis* isolates. Isolates were primarily resistant to cefazolin (70.67%) and imipenem (70.67%). These isolates were found to carry *ureC*, *FliL*, *ireA*, *zapA*, *ptA*, *hpmA*, *hpmB*, *pmfA*, *rsbA*, *mrpA*, and *ucaA* with varying prevalence levels of 100.00, 100.00, 100.00, 98.67, 98.67, 90.67, 90.67, 90.67, 89.33, and 70.67%, respectively. Additionally, the isolates were found to carry *aac(6)-Ib*, *qnrD*, *floR*, *bla*<sub>CTX-M</sub>, *bla*<sub>CTX-M-2</sub>, *bla*<sub>OXA-1</sub>, *bla*<sub>TEM</sub>, *tetA*, *tetB* and *tetM* with varying prevalence levels of 38.67, 32.00, 25.33, 17.33, 16.00, 10.67, 5.33, 2.67, 1.33, and 1.33%, respectively. Among 40 MDR strains, 14 (35.00%) were found to carry class 1 integrons, 12 (30.00%) strains carried class 2 integrons, while no class 3 integrons was detected. There was a significant positive correlation between the class 1 integrons and three ARGs: *bla*<sub>TEM</sub>, *bla*<sub>CTX-M</sub>, and *bla*<sub>CTX-M-2</sub>. This study revealed that *P. mirabilis* strains isolated from domestic dogs exhibited a higher prevalence of MDR, and carried fewer VAGs but more ARGs compared to those isolated from stray dogs. Furthermore, a negative correlation was observed between VAGs and ARGs.

**Discussion:** Given the increasing antimicrobial resistance of *P. mirabilis*, veterinarians should adopt a prudent approach towards antibiotics administration in dogs to mitigate the emergence and dissemination of MDR strains that pose a potential threat to public health.

## KEYWORDS

*Proteus mirabilis*, virulence-related factors, antimicrobial resistance, antibiotic resistance genes, virulence-associated genes, domestic and stray dogs

# 1. Introduction

*Proteus mirabilis*, a member of the *Enterobacteriaceae* family, as an opportunistic pathogen can cause skin infection, respiratory tract infection, urinary tract infection (UTI), and gastrointestinal tract infection, and it has been suggested that it may be related to Crohn's disease (Zhang J. W. et al., 2021). As a zoonotic bacteria, *P. mirabilis* can infect a variety of animals, such as chicken (Wong et al., 2013), ducks (Algammal et al., 2021), turtles (Pathirana et al., 2018), cattle (Sun et al., 2020), companion animals (Marques et al., 2019).

The virulence factors of *P. mirabilis* include flagella, pili, urease, hemolysin, metalloproteinase, which can help *P. mirabilis* to colonize, destroy tissues, and escape immunity (Coker et al., 2000). *Proteus mirabilis* is a model organism for urease<sup>+</sup> bacteria (Norsworthy and Pearson, 2017). The main functional subunit of urease, the alpha subunit, is encoded by *ureC*, which breaks down urea into one carbonic acid and two ammonia molecules (Armbruster et al., 2018). Ammonia produced by urease can increase the pH of urine above 7.2 and precipitates calcium and magnesium compounds into crystals of magnesium ammonium phosphate (struvite) and calcium phosphate (apatite) (Broomfield et al., 2009). Struvite and apatite crystals are deposited in biofilms to form crystalline biofilms (Armbruster et al., 2018). The presence of crystalline biofilms makes antibiotic treatment more difficult (Maszewska et al., 2021). *Proteus mirabilis* has peritrichous flagella, which can carry out the typical swarming motility, called the "bull-eye" (Aygül et al., 2019). The swarming motility of *P. mirabilis* is a process in which vegetative cells periodically differentiate into swarming cells on solid surfaces.

The swarming motility is important because it is coupled to the expression of virulence-associated genes (VAGs) and the ability to invade cells (Rather, 2005). It has been shown that there is a specific correlation between virulence factors and antimicrobial resistance (AMR) in *P. mirabilis* (Filipiak et al., 2020). The AMR of clinical *P. mirabilis* isolates is gradually increasing. Studies have shown that in addition to intrinsic resistance to tetracycline and polymyxin, *P. mirabilis* has acquired resistance to the  $\beta$ -lactams (Shelenkov et al., 2020). *Proteus mirabilis* is usually susceptible to fluoroquinolones (Girlich et al., 2020). Multidrug-resistant (MDR) was defined as acquired non-susceptibility to at least one agent in three or more antimicrobial categories (Magiorakos et al., 2012). MDR isolates of *P. mirabilis* have been identified in both human and veterinary medicine, emphasizing on the need for continuous surveillance (Decôme et al., 2020). MDR may be mediated by mutations in a resistance gene, or resistance genes may be acquired through horizontal transfer. These resistant genes are widely present on plasmids and integrons, leading to the problems of rapid transmission and treatment failure (Leverstein-van Hall et al., 2003). Recent studies have also shown that the prevalence of  $\beta$ -lactams resistance genes in *P. mirabilis* is gradually increasing (Wong et al., 2013; Algammal et al., 2021). The antibiotic resistance gene (ARG) is one of the many mechanisms by which bacteria can develop AMR (Hughes and Andersson, 2017). However, the presence of a specific ARG does not necessarily lead to the corresponding AMR, as other genetic and environmental factors can influence the expression and function of the gene (Hughes and Andersson, 2017). Previous studies in *Escherichia coli* have revealed both positive and negative associations between VAGs and ARGs, with predominance of positive correlations (Zhao et al., 2021; Zhang S. et al., 2021). But little is known about the

AMR, VAGs, and ARGs of *P. mirabilis* isolated from feces of dogs and the correlations among them.

Previous studies have shown that UTI in companion animals and humans may be caused by closely related *P. mirabilis* strains and that such strains from both origins share common ARGs and VAGs (Marques et al., 2019), which suggest that companion animals may serve as potential reservoirs of antibiotic-resistant bacteria in humans. *Proteus mirabilis* also was considered to be the host of storing ARGs and VAGs (Hu et al., 2020). With 50.85 million dogs living in Chinese cities as of 2018, dogs are the most popular companion animals in China (Yin et al., 2020). There have been some studies of *P. mirabilis* isolated from the urinary tract of dogs (Gaastra et al., 1996; Harada et al., 2014). Therefore, there is great significance in monitoring AMR, ARGs and VAGs carried by *P. mirabilis* isolates from dog feces for public health security. Additionally, prior studies overlooked *P. mirabilis* isolates carried by stray dogs. Therefore, this study aimed to determine the prevalence of *P. mirabilis* in the feces of domestic dogs and stray dogs. Furthermore, the swarming motility, biofilm formation, AMR, VAGs, and ARGs of *P. mirabilis* isolates were detected and their correlations were analyzed.

# 2. Materials and methods

## 2.1. Sample collection

From April 2021 to April 2022, we collected a total of 241 dog fecal swabs, comprising of 147 fecal swabs from domestic dogs obtained from 8 pet hospitals situated in Chengdu city, Sichuan province in southwestern China, as well as 94 fecal swabs from stray dogs sourced from the Center of Protect Beastie located in Sichuan Province. All stray dog fecal swabs were collected by laboratory staff and domestic dog fecal swabs were collected by veterinarians. To minimize the risk of contamination between samples, disinfection of hands and changing of disposable gloves were mandatory for staff involved in sample collection. The fecal swabs of the dogs were collected with sterile cotton swabs into sterile Eppendorf (EP) tubes and placed in a foam box with an ice pack, then sent to the laboratory by express as soon as possible for bacteriological examination.

## 2.2. *Proteus mirabilis* screening

The obtained samples were enriched in 1 mL of Luria-Bertani (LB) broth at 37°C, 120 r/min for 24 h. The bacteria suspension was streaked onto LB solid medium using an inoculation loop, and observed for colony morphology on LB agar medium after 24 h of static cultivation at 37°C. Suspected *P. mirabilis* colonies were selected and streaked on *Salmonella-Shigella* (SS) agar medium for further purification. The colony color on SS agar medium was observed, and then the single colony with a black center was selected for Gram staining and observed under microscope.

## 2.3. Identification of isolates

Firstly, biochemical tests such as gelatin liquefaction test, fermentation test of maltose, glucose, sucrose, lactose and mannose,

VP test, nitrate dynamic test, MR Test, indole test, iron triosaccharide test, hydrogen sulfide test and citrate utilization were carried out on all isolates using biochemical tubes and interpreted according to Berger's manual. Then, the 16S rRNA gene was amplified by polymerase chain reaction (PCR) and combined with biochemical result to identify *P. mirabilis* isolates (Gao et al., 2018). The PCR products were then sent to Beijing Tsingke Biotechnology Co., LTD for sequencing. BLAST (Basic Local Alignment Search Tool) was used to detect sequence homology between the sequencing results and GenBank accessions.

## 2.4. Hemolysin and urease production

The hemolysis properties of *P. mirabilis* isolates were determined by observing clear zones around bacterial colonies on blood agar supplemented with 5% defibrinated sheep blood after 24 or 48 h of static cultivation in 37°C. The bacterial suspension of *P. mirabilis* isolates was streaked on SS agar medium and incubated at 37°C for 24 h. A single colony was selected and streaked into the urease biochemical tubes and incubated at 37°C for 8–10 h to observe the color change. A change in color from orange to red observed in the biochemical tubes indicates the production of ureases by isolates.

## 2.5. Swarming motility testing

The swarming motility rates of *P. mirabilis* isolates were assessed by measuring the coverage scale of LB solid medium after incubating under the same conditions. LB solid medium with an agar concentration of 1.5% was prepared. After the medium was solidified, the plates were dried in an oven at 42°C for 60 min before use. The optical density of the bacterial suspension propagated to the logarithmic growth stage was measured at 600 nm and diluted to an optical density (OD) 600 of 0.4. 5 µL of the diluted bacterial suspension was inoculated into the center of LB solid plates. The plates were inverted and incubated at 37°C after the bacterial suspension was absorbed into the agar matrix (~5 min). Swarming motility of *P. mirabilis* isolates was observed and the coverage scale was measured after 9 h. The ability of swarming motility is divided into three categories: category 1, weak swarming (coverage ≤5%); category 2 medium swarming (5% < coverage ≤25%); category 3, dense swarming (coverage >25%; Filipiak et al., 2020). The assay was repeated three times for each strain.

## 2.6. Estimation of the biofilm formation

Biofilm formation was determined by using the crystal violet staining method in 96-well cell plates. After the OD<sub>600</sub> of the bacterial solution culture to the logarithmic growth stage was detected and adjusted to 0.1, 200 µL diluted bacterial suspension was added to a 96-well cell culture plate and incubated for 24 h at 37°C. The experiment was repeated with 3 wells for each strain. Wells containing only LB broth medium were used as negative controls. After 24 h, the biofilm formed in 96-well cell culture plates was stained by crystal violet staining according to the literature (Sun et al., 2020). After removing the medium and washing the cells with phosphate-buffered saline (PBS), the bacteria were stained with 200 µL crystal violet for

5 min. The crystal violet dye was solubilized by the addition of 200 µL of organic solvent (anhydrous ethanol: acetone = 70:30, v/v), and was quantified by measuring absorbance at 590 nm with a microplate reader. When OD value exceeds 1, dilute with 33% glacial acetic acid, and multiply the obtained value by dilution ratio.

The mean OD of the negative control plus three times its standard deviation (SD) was defined as the cut-off value (OD<sub>c</sub>). Based on the OD<sub>c</sub>, the biofilm-forming ability of isolates can be divided into the following four types: OD<sub>590</sub> ≤ OD<sub>c</sub> is a non-biofilm-forming strain (–), OD<sub>c</sub> < OD<sub>590</sub> ≤ 2OD<sub>c</sub> is a weak biofilm-forming strain (+), and 2OD<sub>c</sub> < OD<sub>590</sub> ≤ 4OD<sub>c</sub> is medium biofilm-forming strains (++), OD<sub>590</sub> > 4OD<sub>c</sub> is strong biofilm-forming strains (+++) (Khoramian et al., 2015).

## 2.7. Antimicrobial susceptibility testing

Kirby-Bauer disc diffusion method was used to evaluate the AR of 75 *P. mirabilis* isolates to 15 antibiotics in 7 categories. These antibiotics include ampicillin (AMP) (10 µg), amoxicillin/clavulanic acid (AUG) (20/10 µg), ampicillin/sulbactam (SAM) (10/10 µg), cefazolin (CZO) (30 µg), cefepime (FEP) (30 µg), cefotaxime (CTX) (30 µg), imipenem (IPM) (10 µg), meropenem (MEM) (10 µg), aztreonam (ATM) (30 µg), gentamicin (GEN) (10 µg), tetracycline (TET) (30 µg), ciprofloxacin (CIP) (5 µg), sulfamethoxazole/trimethoprim (SXT) (25 µg), fosfomycin (FOS) (200 µg) and chloramphenicol (C) (30 µg). In brief, bacterium suspension of 0.5 McFarland was uniformly spread onto Mueller-Hinton (MH) agar plates and incubated at 37°C for 18 h. *Escherichia coli* ATCC 25922 was used as the control microorganism. The inhibitory zone around each disc was measured, and the results were interpreted according to the guidelines provided by the manufacturer and the Clinical and Laboratory Standards Institute (CLSI; Clinical and Laboratory Standards Institute, 2020). Isolates were considered non-susceptible if they were intermediate or resistant to a certain antibiotic (Decôme et al., 2020). MDR was defined as acquired non-susceptibility to at least one agent in three or more antimicrobial categories (Magiorakos et al., 2012). Non-MDR was defined as resistance to none or up to two antimicrobial categories (Qi et al., 2016).

## 2.8. Detection of VAGs, ARGs, and integrons

The distribution of VAGs and ARGs in 75 *P. mirabilis* isolates was investigated through screening of 11 VAGs, 18 ARGs, and class 1, 2, and 3 integrons using conventional PCR. The details of VAGs, ARGs, and integrons (gene names, primer sequences, product lengths and annealing temperatures) are shown in Supplementary Tables 1, 2. The reaction system containing 12.5 µL of 2 × Taq Master Mix, 1 µL each of upstream/downstream primers, 2 µL of bacterial-DNA, and then sterile ddH<sub>2</sub>O was added up to 25 µL. The cycling conditions of VAGs were as follows: initial denaturation at 94°C for 2 min; followed by 30 cycles of denaturation at 94°C for 2 min, anneal for 1 min and extension at 72°C for 1 min; 72°C, 5 min. The cycling conditions of ARGs and integrons were as follows: initial denaturation at 93°C for 5 min; followed by 30 cycles of denaturation at 93°C for 30s, anneal for 30s and extension at 72°C for 1 min; 72°C 5 min. At the same time, negative controls without DNA were set. PCR products with positive



bands after electrophoresis screening were sent to Beijing Tsingke Biotechnology Co., Ltd. for sequencing. BLAST (Basic Local Alignment Search Tool) was used to detect sequence homology between the sequencing results and GenBank accessions.

## 2.9. Statistical analyses

The obtained data were analyzed using the Chi-square test (SPSS software, version 9.4; Significance-level;  $p < 0.05$ ). Comparisons between groups were conducted by Fisher's Exact test, with an alpha value of 0.05. The statistical analysis took into account standard deviations, and they are based on data obtained from repeated experiments.

## 3. Results

### 3.1. Prevalence of *Proteus mirabilis* in the examined samples

A total of 75 non-duplicate strains of *P. mirabilis* were isolated from 241 samples of dog feces, and the isolation rate was 31.12% (75/241). Among them, 41 strains of *P. mirabilis* isolates were from domestic dog feces collected from pet hospitals, and 34 strains of *P. mirabilis* isolates were from stray dog feces collected from the Center of Protect Beastie (Table 1). The detection rate of *P. mirabilis* in the feces of stray dogs was significantly higher than that of domestic dogs ( $p < 0.01$ ).

### 3.2. Hemolysin and urease production

On defibrinated sheep blood agar plates, all *P. mirabilis* isolates produced color changes, but none exhibited typical  $\beta$ -hemolysis. After 8–10 h of incubation, the urease biochemical tubes inoculated with *P. mirabilis* isolates changed from orange yellow to rose red, indicating that all 75 strains of *P. mirabilis* isolates could produce urease to decompose urea.

### 3.3. Swarming motility testing

In this experiment, all *P. mirabilis* isolates showed the ability of “fog creep” migration. The isolate with the strongest ability of swarming motility was PM55 with a velocity of 5.43 mm/h, while the isolate with the weakest ability of swarming motility was PM13, whose speed was only 0.125 mm/h. Additionally, 7 (6.67%) isolates of *P. mirabilis* exhibited weak swarming motility; 32 (42%) isolates

exhibited moderate swarming motility, and 38 (50.67%) isolates exhibited strong swarming motility. There was no significant difference in swarming motility between *P. mirabilis* isolated from domestic and stray dog feces ( $p > 0.05$ ).

## 3.4. Estimation of the biofilm formation

The test of biofilm formation showed that all *P. mirabilis* isolates could form biofilm. Only 7 strains (9.33%) of *P. mirabilis* isolates were medium biofilm producers ( $0.7 < OD_{590} \leq 1.4$ ), and 68 strains (90.67%) are intensive biofilm producers ( $OD_{590} > 1.4$ ; Supplementary Figure 3). There was no significant difference in biofilm formation between *P. mirabilis* isolated from domestic and stray dog feces ( $p > 0.05$ ).

## 3.5. Antimicrobial susceptibility

The AMR of the *P. mirabilis* isolates was assessed and is presented in Table 2. The results indicate that the resistance rate of these *P. mirabilis* isolates to tetracycline (TE) was the highest (75, 100%), followed by cefazolin (KZ) (53, 70.67%) and imipenem (IPM) (53, 70.67%), ampicillin (AMP) (27, 36.00%), fosfomycin (FOS) (26, 34.67%), sulfamethoxazole/trimethoprim (SXT) (23, 30.67%), meropenem (MEM) (22, 29.33%), chloramphenicol (C) (21, 28.00%), cefepime (FEP) (17, 22.67%), ciprofloxacin (CIP) (15, 20.00%), cefotaxime (CTX) (13, 17.33%), amoxicillin/clavulanic acid (AMC) (11, 14.67%), ampicillin/sulbactam (SAM) (11, 14.67%), gentamicin (CN) (9, 12%), aztreonam (ATM) (1, 1.33%). Moreover, the AMR of *P. mirabilis* isolates from the two sources was significantly different to different antibiotics ( $p < 0.05$ ; Supplementary Figure 4).

Out of 75 *P. mirabilis* isolates, 40 strains (53.33%) with MDR were identified, comprising of 30 strains sourced from domestic dogs and 10 from stray dogs (Table 3). *Proteus mirabilis* strains isolated from domestic dogs exhibited a significantly higher prevalence of MDR than those isolated from stray dogs ( $p < 0.001$ ).

## 3.6. Detection of VAGs, ARGs, and integrons

This study identified 11 VAGs in 75 *P. mirabilis* isolates. Figure 1 shows that *ureC*, *FlhL* and *ireA* were the universally present VAGs with a detection rate of 100%, followed by *zapA* (98.67%), *ptA* (98.67%), *hpmA* (90.67%), *hpmB* (90.67%), *pmfA* (90.67%), *rsbA* (90.67%), *mrpA* (89.33%) and *ucaA* (70.67%). The prevalence rates of VAGs (*hpmA*, *hpmB*, *pmfA*, *mrpA*, and *rsbA*) of *P. mirabilis* strains isolated from stray dogs were significantly higher than those isolated from domestic dogs ( $p < 0.05$ ). Furthermore, the prevalence rates of these VAGs in non-MDR strains were significantly higher than those in MDR strains ( $p < 0.05$ ).

In total, 10 out of 18 ARGs were identified in 75 *P. mirabilis* isolates. Among these, *aac*-(6')-Ib was the universally present ARG with a prevalence rate of 38.67%, followed by *qnrD* (32.00%), *floR* (25.33%), *bla*<sub>CTX-M</sub> (17.33%), *bla*<sub>CTX-M-2</sub> (16.00%), *bla*<sub>OXA-1</sub> (10.67%), *bla*<sub>TEM</sub> (5.33%), *tetA* (2.67%), *tetB* (1.33%) and *tetM* (1.33%; Figure 2). The detection rates of ARGs (*bla*<sub>OXA-1</sub>, *bla*<sub>CTX-M</sub>, *bla*<sub>CTX-M-2</sub>, *floR* and

TABLE 1 Prevalence of *Proteus mirabilis* in dog fecal samples (N=241).

Sources of samples	Prevalence of <i>P. mirabilis</i> (n)	p-value
Domestic dogs	27.89% (41/147)	0.004**
Stray dogs	36.17% (34/94)	
Total	30.71% (75/241)	

\*\* represents a highly significant difference.

TABLE 2 Antimicrobial resistance in *Proteus mirabilis* isolates.

Antimicrobial category		Antibiotics agents	Percentage of antibiotic resistant strains (n)	Percentage of antibiotic resistant strains from different sources		p-value
				Domestic dogs (n)	Stray dogs (n)	
β-lactams	Penicillins	Ampicillin (AMP)	36.00% (27/75)	58.54% (24/41)	8.82% (3/34)	<0.001***
	β-lactam compound	Amoxicillin/clavulanic acid (AMC)	14.67% (11/75)	26.83% (11/41)	0% (0/34)	<0.001***
		Ampicillin/sulbactam (SAM)	14.67% (11/75)	26.83% (11/41)	0% (0/34)	<0.001***
	Cephalosporins	Cefazolin (KZ)	70.67% (53/75)	87.80% (36/41)	50.00% (17/34)	<0.001***
		Cefepime (FEP)	22.67% (17/75)	29.27% (12/41)	14.71% (5/34)	0.134
		Cefotaxime (CTX)	17.33% (13/75)	31.71% (13/41)	0% (0/34)	<0.001***
	Carbapenems	Imipenem (IPM)	70.67% (53/75)	58.54% (24/41)	85.29% (29/34)	0.011*
		Meropenem (MEM)	29.33% (22/75)	21.95% (9/41)	38.24% (13/34)	0.123
	Monocyclic lactam	Aztreonam (ATM)	1.33% (1/75)	2.44% (1/41)	0% (0/34)	0.547
Aminoglycosides		Gentamicin (CN)	12.00% (9/75)	21.95% (9/41)	0% (0/34)	0.003**
Tetracyclines		Tetracycline (TE)	100% (75/75)	100% (41/41)	100% (34/34)	-
Quinolones		Ciprofloxacin (CIP)	20.00% (15/75)	36.59% (15/41)	0% (0/34)	<0.001***
Sulfonamides		Sulfamethoxazole/trimethoprim (SXT)	30.67% (23/75)	51.22% (21/41)	5.88% (2/34)	<0.001***
Polyphosphates		Fosfomycin (FOS)	34.67% (26/75)	34.15% (14/41)	35.29% (12/34)	0.917
Styrene acrylic alcohols		Chloramphenicol (C)	28.00% (21/75)	51.22% (21/41)	0% (0/34)	<0.001***

Specific antimicrobial resistance phenotypes of *P. mirabilis* isolates are shown in [Supplementary Table 1](#). \* represents a significant difference, \*\* represents a highly significant difference, and \*\*\* denotes an extremely significant difference.

TABLE 3 Percentage of MDR *Proteus mirabilis* isolates from two sources.

The sources of samples	MDR (N=40)	non-MDR (N=35)	p-value
Domestic dogs	75.00% (30/40)	31.43% (11/35)	<0.001***
Stray dogs	25.00% (10/40)	68.57% (24/35)	
Total	53.33% (40/75)	46.67% (35/75)	

\*\*\* denotes an extremely significant difference.

*aac*-(6')-Ib in *P. mirabilis* isolated from domestic dogs were significantly higher when compared to those isolated from stray dogs ( $p < 0.01$ ). Furthermore, the detection rates of these ARGs in MDR strains were significantly higher when compared to non-MDR strains ( $p < 0.01$ ). Out of 40 MDR strains, 14 (35.00%) were found to carry class 1 integrons, 12 (30.00%) strains carried class 2 integrons, while no class 3 integrons was detected. The abundance of the class 2 integrons was found to be significantly higher in *P. mirabilis* isolates from domestic dogs compared to that from stray dogs ( $p < 0.05$ ), while no significant difference in class 1 integrons was observed between stray and domestic dogs.

### 3.7. Correlations analysis

In this study, the correlation coefficient was utilized to evaluate the relationships between these factors. [Figure 3](#) illustrates the

intra-group and inter-group correlations of AMR, VAGs, and ARGs for 75 *P. mirabilis* isolates (excluding non-statistically significant data). There were 51 pairs of the 15 antibiotics that exhibited positive correlations, with the most significant positive correlation found between CIP and C ( $r = 0.80$ ,  $p < 0.001$ ). Negative correlations were shown between IPM and AMP ( $r = -0.25$ ,  $p < 0.05$ ), and between IPM and CTX ( $r = -0.32$ ,  $p < 0.01$ ). However, no significant association was observed between MEM and any of the other antibiotics. Analysis of the correlation between AMR and VAGs revealed that only AMP had a negative correlation with VAGs (*hpmA*, *hpmB*, *pmfA*, *mrpA* and *rsbA*), and the most significant correlation was found between AMP and *mrpA* ( $r = -0.46$ ,  $p < 0.001$ ). Meanwhile, there were 67 pairs of antimicrobial and ARGs positively correlated, and 3 pairs were negatively correlated. There was the most significant correlation between CTX of β-lactam and *bla*<sub>CTX-M</sub>, and between ATM and *tetM* ( $r = 1.00$ ,  $p < 0.001$ ).

Furthermore, 25 pairs of the 8 VAGs showed positive correlation with *hmpA*, *hpmB*, *pmfA* and *rsbA* exhibiting the strongest correlations ( $r = 1.00$ ,  $p < 0.001$ ). Similarly, 21 pairs of the 10 ARGs showed positive correlations, with the strongest correlation observed between *bla*<sub>CTX-M</sub> and *bla*<sub>CTX-M-2</sub> ( $r = 0.95$ ,  $p < 0.001$ ). Additionally, the correlation analysis between VAGs and ARGs revealed that 11 pairs of VAGs and ARGs exhibited negative correlations. Among them, *aac*-(6')-Ib had the strongest negative correlations with *hpmA*, *hpmB*, *pmfA*, and *rsbA* ( $r = -0.40$ ,  $p < 0.01$ ). Specific results of the correlation analysis can be found in [Figure 3](#). In the present study, we examined the correlation between ARGs and the integrons of 40 MDR strains

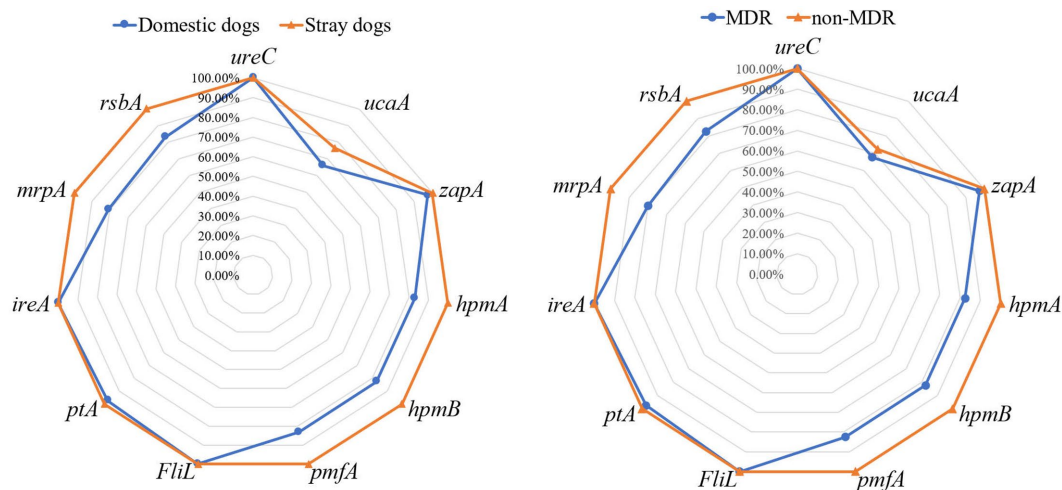


FIGURE 1

The prevalence of virulence-associated genes in *Proteus mirabilis* isolates. The radar map on the left shows the virulence-associated genes carried by *P. mirabilis* strains from domestic and stray dogs. The radar map on the right shows the virulence-associated genes carried by MDR and non-MDR strains.

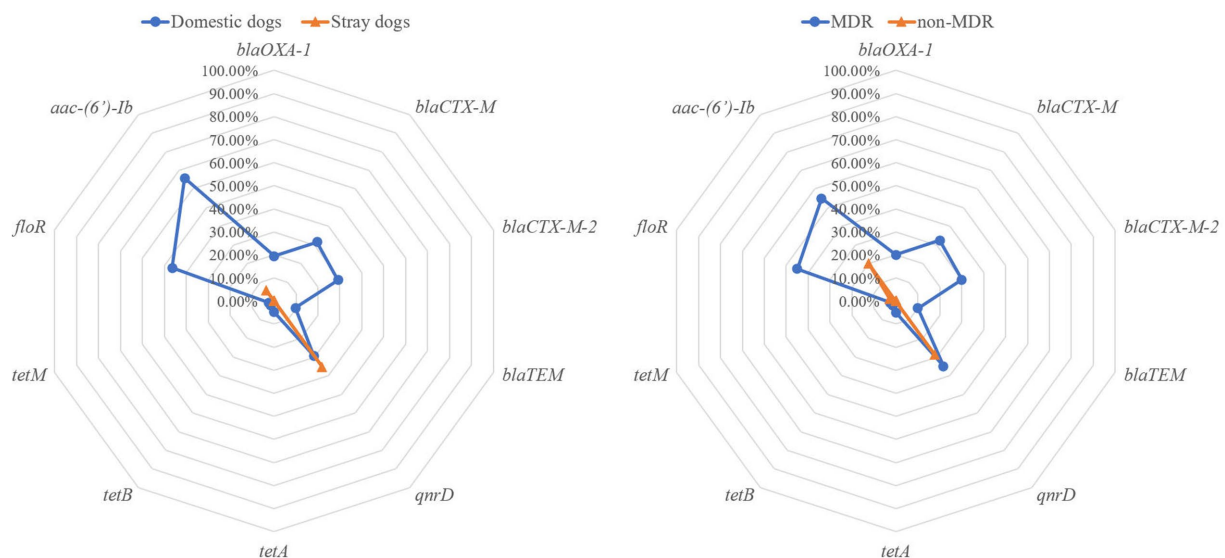


FIGURE 2

The prevalence of antibiotic resistance genes of the *Proteus mirabilis* isolates. The radar map on the left shows the antibiotic resistance genes carried by *P. mirabilis* strains from domestic and stray dogs. The radar map on the right shows the antibiotic resistance genes carried by MDR and non-MDR strains.

(Figure 4). Our results revealed a significant positive correlation between class 1 integrons and the  $\beta$ -lactam-resistant genes  $bla_{TEM}$  ( $r=0.31$ ,  $p<0.05$ ),  $bla_{CTX-M}$  ( $r=0.35$ ,  $p<0.05$ ), and  $bla_{CTX-M-2}$  ( $r=0.35$ ,  $p<0.05$ ). It is noteworthy that a significant negative correlation was observed between  $qnrD$  and the class 2 integrons.

## 4. Discussion

*Proteus mirabilis* has been extensively researched as a urinary tract pathogen in humans over the past decades (Durgadevi et al., 2020; Kot

et al., 2021; Wilks et al., 2021). However, there is limited research focusing on *P. mirabilis* isolated from dog feces. This study aims to investigate the prevalence and biological characteristics of *P. mirabilis* in the feces of domestic and stray dogs in Chengdu, southwestern China, to determine the potential threat it poses to public health.

Out of 241 samples of dog feces, a total of 75 non-duplicate *P. mirabilis* strains were isolated, with a prevalence of 31.12%. This prevalence is similar to that found in a study of dogs with diarrhea in Northeast China (Sun et al., 2020), where 76 out of 232 samples had *P. mirabilis* infection, accounting for 32.76%. In the same study, Sun et al. also investigated the presence of *P. mirabilis* in the feces of other

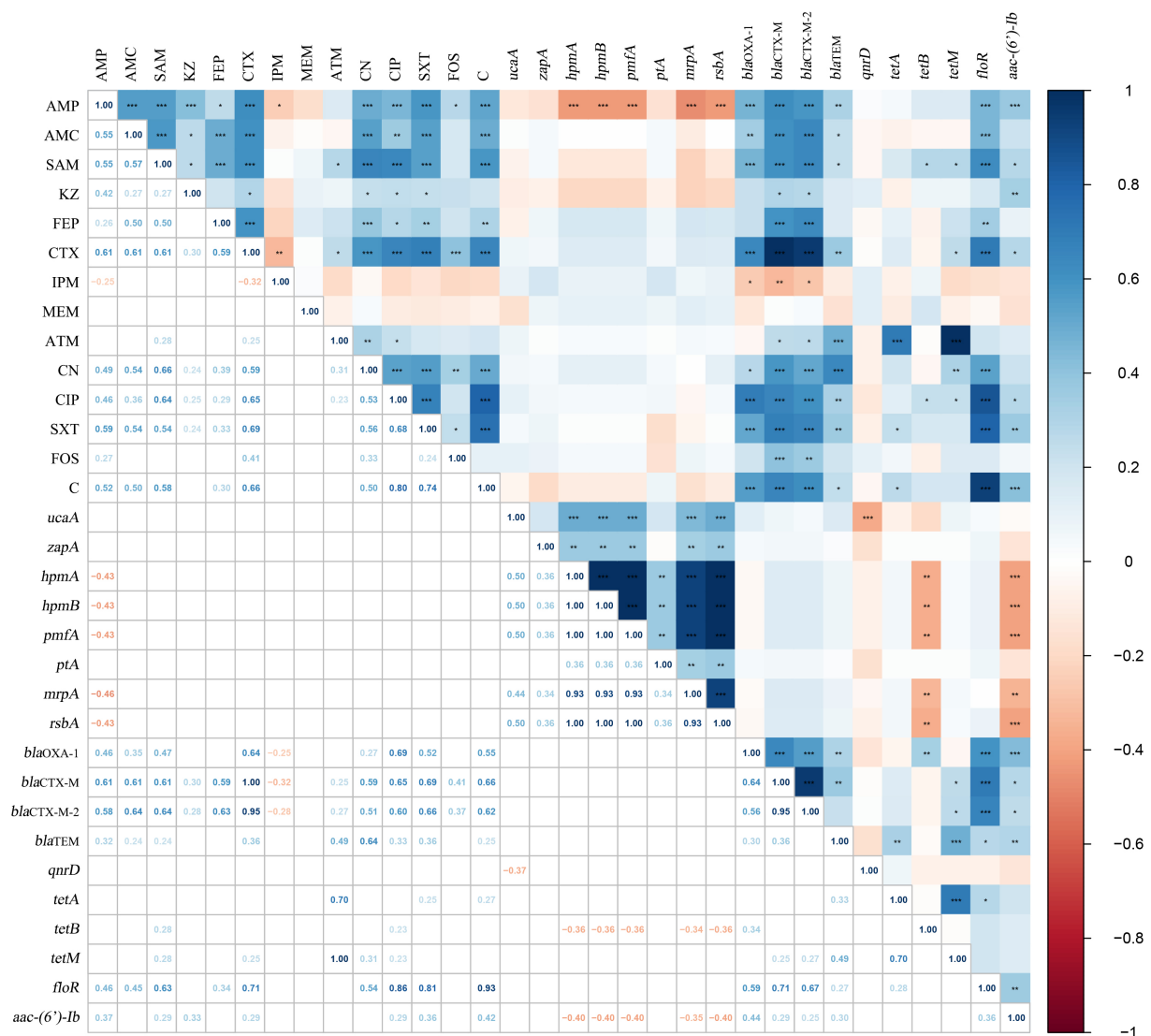


FIGURE 3

The correlations among AMR, VAGs and ARGs of *Proteus mirabilis* isolates. The numbers in the heat map represent the correlation coefficient ( $r$ ). Positive numbers (blue) show a positive correlation and negative numbers (red) show a negative correlation.

animals (mink, cattle, and fowl) with diarrhea. Notably, dogs had the highest infection rate among the animals tested. In our findings, the prevalence of *P. mirabilis* in the feces of stray dogs was significantly higher than that of domestic dogs ( $p < 0.01$ ). This may be attributed to the fact that *P. mirabilis* is commonly present in soil and sewage, and stray dogs are more susceptible to exposure to these contaminated sources, resulting in the infection of *P. mirabilis*. This agrees with previous studies conducted on non-human species, such as Namibian cheetahs and chimpanzees, suggesting that gut microbiota can be influenced by the living environment (Vilson et al., 2018; Reese et al., 2021).

The 75 *P. mirabilis* isolates from this study exhibited the abilities of swarming motility and biofilm formation. There was no significant difference in swarming motility and biofilm formation between MDR and non-MDR isolates. This finding contrasts with a study conducted by Filipiak et al., which reported that multi-drug sensitive (MDS) strains had weaker biofilm formation but stronger swarming motility

compared to MDR strains (Filipiak et al., 2020). Currently, AMR and MDR of bacteria derived from animals are the focus of attention. In this study, a high resistant rate was observed for most *P. mirabilis* isolates to KZ (70.67%) and IPM (70.67%). This resistance rate was higher than that reported in other studies, such as *P. mirabilis* isolated from dogs in Japan (Harada et al., 2014) and *P. mirabilis* isolated from dogs with bacterial urine (Decôme et al., 2020). Although current research on the AMR of *P. mirabilis* isolated from dogs reports varying results, a consistent trend across these studies is the gradual increase in AMR of *P. mirabilis* over time (Decôme et al., 2020). Furthermore, differences in AMR were observed among *P. mirabilis* strains from domestic and stray dogs. Except for natural resistance to tetracycline, the highest resistance to KZ (87.80%) was found in the *P. mirabilis* isolated from domestic dogs, followed by AMP (58.54%), IPM (58.54%), SXT (51.22%) and C (51.22%). There was no significant difference in AMR to FEP, MEM, ATM, F, and FOS between *P. mirabilis* isolated from domestic and stray dogs ( $p > 0.05$ ). For the



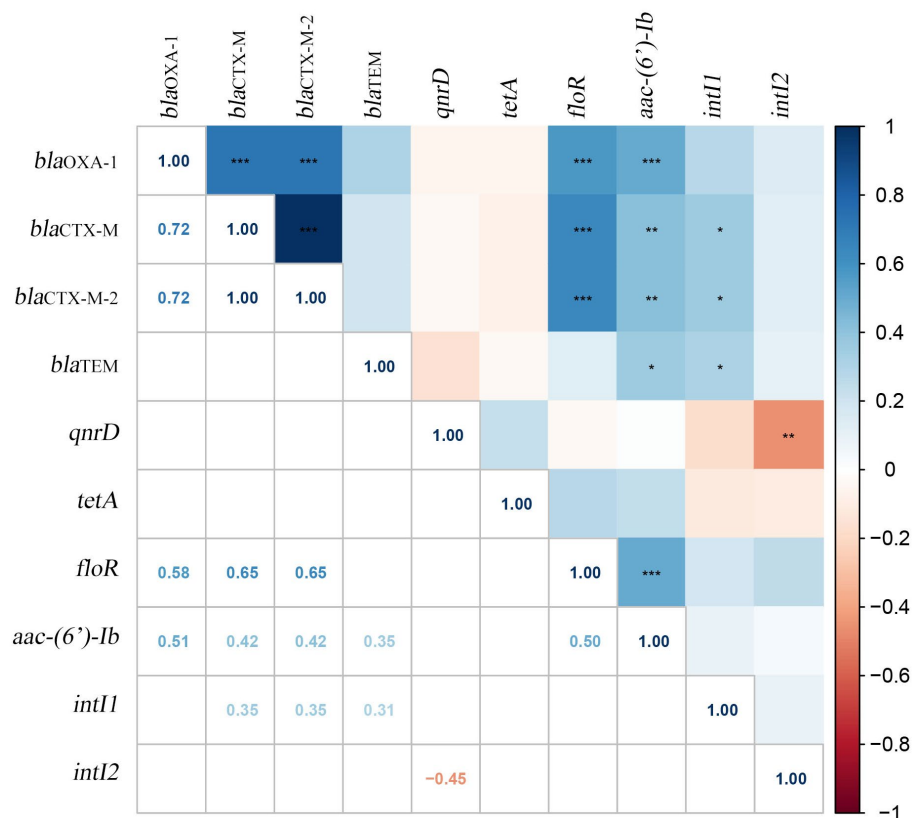


FIGURE 4

Correlation between ARGs and integrons in 40 MDR *Proteus mirabilis* strains. The numbers in the heat map represent the correlation coefficient ( $r$ ). Positive numbers (blue) show a positive correlation and negative numbers (red) show a negative correlation.

resistance to IPM, the AMR of *P. mirabilis* isolated from stray dogs was higher than that of domestic dogs. For the rest of the antibiotics, the opposite is true. The emergence of MDR bacteria is reflected as a risk factor for public health. A total of 30 (75.00%, 30/40) MDR strains were isolated from domestic dogs, which was significantly higher than 10 (25.00%, 10/40) MDR strains isolated from stray dogs. This phenomenon may be related to the widespread use (and frequent misuse) of antibiotics in clinical, and stray dogs rarely receive antibiotic treatment from veterinarians (Liu C. et al., 2021; Liu Y. et al., 2021).

Aside from antimicrobial resistance, virulence factors are also receiving considerable attention. The current investigation identified a total of 11 VAGs, with detection rates exceeding 90% for all except *mrpA* (89.33%) and *ucaA* (70.67%). Notably, the *ureC* gene was detected in 100% of isolates, which was consistent with the result that all isolates were capable of producing urease. The detection rates of VAGs in this study were found to be higher compared to a prior study conducted in Northeast China, which fecal swabs collected from diarrhea animals (dogs, mink, cattle and poultry) demonstrated *ureC* as the most prevalent VAG, observed in 90.91% of samples (Sun et al., 2020). Similar results were obtained in a study conducted on *P. mirabilis* isolated from ducks, where 100% detection rates of *ureC*, 94.3% for *rsbA*, and 91.4% for *zapA* were recorded, consistent with our findings (Algammal et al., 2021). Interestingly, a high detection rate of *ucaA* (76.47%) was observed in 34 *P. mirabilis* isolates from stray dogs was, with all other VAGs demonstrating 100% detection rates.

Comparatively, *P. mirabilis* strains isolated from stray dogs exhibited a greater number of VAGs when compared to those isolated from domestic dogs. Previous research has shown that the microbiota of captive animals harbors more VAGs in comparison to that of wild animals (Guo et al., 2019; Liu C. et al., 2021). Due to increased interactions between captive animals and humans, horizontal gene transfer from other bacteria in the environment (such as air and water) leads to virulence factor accumulation (Liu C. et al., 2021). Indeed, the environmental factors surrounding stray dogs, such as exposure to rotten food, sewage and other pollutants, along with inadequate living conditions, are likely to be contributing factors to the higher incidence of VAGs detected in *P. mirabilis* isolated from these animals. In contrast, wild animals and domestic dogs may have a broader range of dietary options and cleaner lifestyles, which might result in the reduced chance of acquisition of VAGs.

In addition, the present study also involved the examination of ARGs carried by *P. mirabilis* isolates. Out of the 18 screened ARGs, 10 were detected in the 75 isolates, with *aac-(6')-Ib* (38.67%), *qnrD* (32.00%), *floR* (25.33%), *bla<sub>CTX-M</sub>* (17.33%), and *bla<sub>CTX-M-2</sub>* (16.00%) being the top five ARGs detected. A Japanese study demonstrated that clinical isolates of *P. mirabilis* did not exhibit positivity for *qnrA*, *qnrB*, *qnrS*, and *aac (6')-Ib-cr*; however, 1.9% (2/105) of isolates were found to be positive for *qnrD* (Harada et al., 2014). Our study revealed higher rates of ARGs detection compared to a study from Brazil which detected only 4 ARGs (*bla<sub>TEM</sub>*, *bla<sub>SHV</sub>*, *bla<sub>CTX-M-1</sub>*, and *bla<sub>OXA-1</sub>*) in *P. mirabilis* isolated from dogs (Sfaciote et al., 2021). However, the

detection rates of ARGs in our study were lower than a previous study that detected 7 out of 14 ARGs in clinical isolates of *P. mirabilis* obtained from human in northern Taiwan (Lin et al., 2019). The integrons system possesses the capability to capture and express exogenous ARGs. Bacteria have the perceptive capacity to acquire and aggregate ARGs from their surrounding environment through the integrase mediated by *intI* within the system, allowing for the formation of extensive drug-resistant gene arrays. Consequently, integrons assume a crucial role in the evolution of MDR bacteria and horizontal diffusion of ARGs determinants. Class 1 integrons and Class 2 integrons were detected in the MDR strain in this study, which was higher than the detection rate in a previous study on cooked meat products in China, but lower than the detection rate in Chinese human isolates (Yu et al., 2017; Lu et al., 2022). Significantly, the *P. mirabilis* isolates from domestic dogs were found to carry a significantly more ARGs compared to those isolated from stray dogs ( $p < 0.05$ ). This observation is consistent with the result that *P. mirabilis* isolated from domestic dogs exhibited a more severe antimicrobial resistance phenotype than that isolated from stray dogs. In 2019, a study suggested that UTIs in companion animals (dogs and cats) and humans may be caused by closely related strains of *P. mirabilis*, sharing similar ARGs in both sources (Marques et al., 2019), indicating a potential public health risk. To mitigate this risk, veterinarians must use antibiotics judiciously and avoid overuse. Additionally, researchers can explore alternative therapies such as phages and lactobacillus to combat *P. mirabilis* infections (Melo Luís et al., 2016; Shaaban et al., 2020).

A previous study showed that the occurrence and the positive correlations of VAGs and ARGs can be used as a reference for the regulatory use of antibiotics to stop the direct or indirect transmission of these resistance and virulent microbes to the natural environment (Zhang S. et al., 2021). So, we further analyzed the correlation among AMR, VAGs, and ARGs of *P. mirabilis* isolates. In this study, there was a positive correlation between the resistance phenotypes of *P. mirabilis* isolates to various antibiotics. There was also a significant positive correlation between the ARGs they carried. In addition, there was a significant positive correlation between AMR and ARGs, which were consistent with the statement of Algammal et al. (2021). It is worth noting that there were only negative correlations between AMR and VAGs, which were also reflected in the correlations between ARGs and VAGs. A previous study showed that MDR strains of *P. mirabilis* isolated from ducks did not differ significantly from the VAGs carried by non-MDR strains (Algammal et al., 2021). Therefore, our results are different from previous studies. Moreover, class 1 integrons are positively correlated with  $\beta$ -lactam resistance genes (*bla*<sub>CTX-M</sub>, *bla*<sub>CTX-M-2</sub>, *bla*<sub>TEM</sub>), which means that these genes may be on class 1 integrons.

## 5. Conclusion

This study has shown that *P. mirabilis* strains isolated from domestic dogs carrying fewer VAGs but more ARGs compares to those isolated from stay dogs. In addition, we observed a negative correlation between VAGs and ARGs, which is different from previous studies and requires further study at a later stage. Increased antimicrobial resistance has been detected in MDR *P. mirabilis* isolates over the past 10 years, and therefore the need to control the use of antimicrobial agents in animals to minimize the emergence and

eventual spread of resistant pathogens is necessary to protect human and animal health.

## Data availability statement

The original contributions presented in the study are included in the article/Supplementary material, further inquiries can be directed to the corresponding authors.

## Author contributions

GP, LL, MD, SA, and XQ: conceptualization, methodology, and software. LL, ZD, SC, SA, and QL: data curation and writing-original draft preparation. ZZ, HL, XM, ZR, and XQ: visualization and investigation. YH, ZR, HF, and GS: supervision. LL, MD, SA, and ZZ: software and validation. LL, ZD, SC, MD, XQ, and GP: writing-reviewing and editing. All authors contributed to the article and approved the submitted version.

## Funding

This work was supported by “Research on Prevention and Control Technology and Regulation Products of Important Nutritional Metabolic Diseases of Pets,” a key Special project of “13th Five-Year Plan,” Ministry of Science and Technology (2016YFD0501009).

## Acknowledgments

The authors are grateful to the providing at the Center of Protect Beastie in Sichuan Province and the veterinaries at the pet hospitals for their help with collecting the samples.

## Conflict of interest

The authors declare that the research was conducted in the absence of any commercial or financial relationships that could be construed as a potential conflict of interest.

## Publisher's note

All claims expressed in this article are solely those of the authors and do not necessarily represent those of their affiliated organizations, or those of the publisher, the editors and the reviewers. Any product that may be evaluated in this article, or claim that may be made by its manufacturer, is not guaranteed or endorsed by the publisher.

## Supplementary material

The Supplementary material for this article can be found online at: <https://www.frontiersin.org/articles/10.3389/fmicb.2023.1141418/full#supplementary-material>

## References

- Algammal, A. M., Hashem, H. R., Alfifi, K. J., Hetta, H. F., Sheraba, N. S., Ramadan, H., et al. (2021). *atpD* gene sequencing, multidrug resistance traits, virulence-determinants, and antimicrobial resistance genes of emerging XDR and MDR-*Proteus mirabilis*. *Sci. Rep.* 11:9476. doi: 10.1038/s41598-021-88861-w
- Armbruster, C. E., Mobley, H. L. T., and Pearson, M. M. (2018). Pathogenesis of *Proteus mirabilis* infection. *EcoSal Plus* 8:ecosalplus. ESP-0009-2017. doi: 10.1128/ecosalplus.ESP-0009-2017
- Aygül, A., Öztürk, İ., Çilli, F. F., and Ermetcan, Ş. (2019). Quercetin inhibits swarming motility and activates biofilm production of *Proteus mirabilis* possibly by interacting with central regulators, metabolic status or active pump proteins. *Phytomedicine* 57, 65–71. doi: 10.1016/j.phymed.2018.12.014
- Broomfield, R. J., Morgan, S. D., Khan, A., and Stickler, D. J. (2009). Crystalline bacterial biofilm formation on urinary catheters by urease-producing urinary tract pathogens: a simple method of control. *J. Med. Microbiol.* 58, 1367–1375. doi: 10.1099/jmm.0.012419-0
- Clinical and Laboratory Standards Institute (2020). *Performance standards for antimicrobial disk and dilution susceptibility tests for Bacteria isolated from animals*, 5th ed, PA: Clinical and Laboratory Standards Institute (VET01SEd5E).
- Coker, C., Poore, C. A., Li, X., and Mobley, H. L. T. (2000). Pathogenesis of *Proteus mirabilis* urinary tract infection. *Microbes Infect.* 2, 1497–1505. doi: 10.1016/S1286-4579(00)01304-6
- Decôme, M., Cuq, B., Fairbrother, J.-H., Gatel, L., and Conversy, B. (2020). Clinical significance of *Proteus mirabilis* bacteriuria in dogs, risk factors and antimicrobial susceptibility. *Can. J. Vet. Res.* 84, 252–258.
- Durgadevi, R., Kaleeshwari, R., Swetha, T. K., Alexpandi, R., Pandian, S. K., and Ravi, A. V. (2020). Attenuation of *Proteus mirabilis* colonization and swarming motility on indwelling urinary catheter by antibiofilm impregnation: an in vitro study. *Colloids Surf. B: Biointerfaces* 194:111207. doi: 10.1016/j.colsurfb.2020.111207
- Filipiak, A., Chrapek, M., Literacka, E., Wawszczak, M., Gluszek, S., Majchrzak, M., et al. (2020). Pathogenic factors correlate with antimicrobial resistance among clinical *Proteus mirabilis* strains. *Front. Microbiol.* 11:579389. doi: 10.3389/fmicb.2020.579389
- Gaaster, W., Van Oosterom, R. A. A., Pieters, E. W. J., Bergmans, H. E. N., Van Dijk, L., Agnes, A., et al. (1996). Isolation and characterisation of dog uropathogenic *Proteus mirabilis* strains. *Vet. Microbiol.* 48, 57–71. doi: 10.1016/0378-1135(95)00133-6
- Gao, H., Gao, Y., Yang, C., Dong, D., Yang, J., Peng, G., et al. (2018). Influence of outer membrane vesicles of *Proteus mirabilis* isolated from boar semen on sperm function. *Vet. Microbiol.* 224, 34–42. doi: 10.1016/j.vetmic.2018.08.017
- Girlich, D., Bonnin, R. A., Dortet, L., and Naas, T. (2020). Genetics of acquired antimicrobial resistance genes in *Proteus* spp. *Front. Microbiol.* 11:256. doi: 10.3389/fmicb.2020.00256
- Guo, W., Mishra, S., Wang, C., Zhang, H., Ning, R., Kong, F., et al. (2019). Comparative study of gut microbiota in wild and captive Giant pandas (*Ailuropoda melanoleuca*). *Genes (Basel)* 10:E827. doi: 10.3390/genes10100827
- Harada, K., Niina, A., Shimizu, T., Mukai, Y., Kuwajima, K., Miyamoto, T., et al. (2014). Phenotypic and molecular characterization of antimicrobial resistance in *Proteus mirabilis* isolates from dogs. *J. Med. Microbiol.* 63, 1561–1567. doi: 10.1099/jmm.0.081539-0
- Hu, R., Wang, X., Muhamamd, I., Wang, Y., Dong, W., Zhang, H., et al. (2020). Biological characteristics and genetic analysis of a highly pathogenic *Proteus Mirabilis* strain isolated from dogs in China. *Front. Vet. Sci.* 7:589. doi: 10.3389/fvets.2020.00589
- Hughes, D., and Andersson, D. I. (2017). Environmental and genetic modulation of the phenotypic expression of antibiotic resistance. *FEMS Microbiol. Rev.* 41, 374–391. doi: 10.1093/femsre/fux004
- Khoramian, B., Jabalameli, F., Niasari-Naslaji, A., Taherikalani, M., and Emameini, M. (2015). Comparison of virulence factors and biofilm formation among *Staphylococcus aureus* strains isolated from human and bovine infections. *Microb. Pathog.* 88, 73–77. doi: 10.1016/j.micpath.2015.08.007
- Kot, B., Gruzewska, A., Szewda, P., Wicha, J., and Parulska, U. (2021). Antibiotic resistance of Uropathogens isolated from patients hospitalized in district Hospital in Central Poland in 2020. *Antibiotics* 10:447. doi: 10.3390/antibiotics10040447
- Leverstein-van Hall, M. A., Blok, H. E. M., Donders, A. R. T., Paaum, A., Fluit, A. C., and Verhoef, J. (2003). Multidrug resistance among *Enterobacteriaceae* is strongly associated with the presence of integrons and is independent of species or isolate origin. *J. Infect. Dis.* 187, 251–259. doi: 10.1086/345880
- Lin, M., Liou, M., Kuo, C., Lin, Y., Chen, J., and Kuo, H. (2019). Antimicrobial Susceptibility and Molecular Epidemiology of *Proteus mirabilis* Isolates from Three Hospitals in Northern Taiwan. *Microbial. Drug Resistance* 25, 1338–1346. doi: 10.1089/mdr.2019.0066
- Liu, C., Hu, J., Wu, Y., Irwin, D., Chen, W., Zhang, Z., et al. (2021). Comparative study of gut microbiota from captive and confiscated-rescued wild pangolins. *J. Genet. Genomics* 48, 825–835. doi: 10.1016/j.jgg.2021.07.009
- Liu, Y., Liu, B., Liu, C., Hu, Y., Liu, C., Li, X., et al. (2021). Differences in the gut microbiomes of dogs and wolves: roles of antibiotics and starch. *BMC Vet. Res.* 17:112. doi: 10.1186/s12917-021-02815-y
- Lu, W., Qiu, Q., Chen, K., Zhao, R., Li, Q., and Wu, Q. (2022). Distribution and molecular characterization of functional class 2 Integrons in clinical *Proteus mirabilis* isolates. *Infect. Drug Resist.* 15, 465–474. doi: 10.2147/IDR.S347119
- Magiorakos, A.-P., Srinivasan, A., Carey, R. B., Carmeli, Y., Falagas, M. E., Giske, C. G., et al. (2012). Multidrug-resistant, extensively drug-resistant and pandrug-resistant bacteria: an international expert proposal for interim standard definitions for acquired resistance. *Clin. Microbiol. Infect.* 18, 268–281. doi: 10.1111/j.1469-0691.2011.03570.x
- Marques, C., Belas, A., Aboim, C., Trigueiro, G., Cavaco-Silva, P., Gama, L. T., et al. (2019). Clonal relatedness of *Proteus mirabilis* strains causing urinary tract infections in companion animals and humans. *Vet. Microbiol.* 228, 77–82. doi: 10.1016/j.vetmic.2018.10.015
- Maszevska, A., Moryl, M., Wu, J., Liu, B., Feng, L., and Rozalski, A. (2021). Amikacin and bacteriophage treatment modulates outer membrane proteins composition in *Proteus mirabilis* biofilm. *Sci. Rep.* 11, 1522–1512. doi: 10.1038/s41598-020-80907-9
- Melo Luis, D. R., Veiga, P., Cerca, N., Kropinski, A. M., Almeida, C., Azeredo, J., et al. (2016). Development of a phage cocktail to control *Proteus mirabilis* catheter-associated urinary tract infections. *Front. Microbiol.* 7:1024. doi: 10.3389/fmicb.2016.01024
- Norsworthy, A. N., and Pearson, M. M. (2017). From catheter to kidney stone: the Uropathogenic lifestyle of *Proteus mirabilis*. *Trends Microbiol.* 25, 304–315. doi: 10.1016/j.tim.2016.11.015
- Pathirana, H. N. K. S., Silva, S. H. M. P., Hossain, S., and Heo, G. J. (2018). Comparison of virulence genes in *Proteus* species isolated from human and pet turtle. *Iran J. Vet. Res.* 19, 48–52.
- Qi, L., Li, H., Zhang, C., Liang, B., Li, J., Wang, L., et al. (2016). Relationship between antibiotic resistance, biofilm formation, and biofilm-specific resistance in *Acinetobacter baumannii*. *Front. Microbiol.* 7:483. doi: 10.3389/fmicb.2016.00483
- Rather, P. N. (2005). Swarmer cell differentiation in *Proteus mirabilis*. *Environ. Microbiol.* 7, 1065–1073. doi: 10.1111/j.1462-2920.2005.00806.x
- Reese, A. T., Chadaideh, K. S., Diggins, C. E., Schell, L. D., Beckel, M., Callahan, P., et al. (2021). Effects of domestication on the gut microbiota parallel those of human industrialization. *elife* 10:e60197. doi: 10.7554/eLife.60197
- Sfaiotote, R. A. P., Parussolo, L., Melo, F. D., Wildemann, P., Bordignon, G., Israel, N. D., et al. (2021). Identification and characterization of multidrug-resistant extended-Spectrum Beta-lactamase-producing Bacteria from healthy and diseased dogs and cats admitted to a veterinary Hospital in Brazil. *Microbiol. Drug Resist* 27, 855–864. doi: 10.1089/mdr.2020.0043
- Shaaban, M., EI-Rahman, O. A. A., AI-Qaidi, B., and Ashour, H. M. (2020). Antimicrobial and Antibiofilm activities of probiotic *Lactobacilli* on antibiotic-resistant *Proteus mirabilis*. *Microorganisms* 8:960. doi: 10.3390/microorganisms8060960
- Shelenkov, A., Petrova, L., Fomina, V., Zamyatin, M., Mikhaylova, Y., and Akimkin, V. (2020). Multidrug-resistant *Proteus mirabilis* strain with Cointegrate plasmid. *Microorganisms* 8:1775. doi: 10.3390/microorganisms8111775
- Sun, Y., Wen, S., Zhao, L., Xia, Q., Pan, Y., Liu, H., et al. (2020). Association among biofilm formation, virulence gene expression, and antibiotic resistance in *Proteus mirabilis* isolates from diarrhetic animals in Northeast China. *BMC Vet. Res.* 16:176. doi: 10.1186/s12917-020-02372-w
- Vilson, Å., Ramadan, Z., Li, Q., Hedhammar, Å., Reynolds, A., Spears, J., et al. (2018). Disentangling factors that shape the gut microbiota in German shepherd dogs. *PLoS One* 13:e0193507. doi: 10.1371/journal.pone.0193507
- Wilks, S. A., Koerfer, V. V., Prieto, J. A., Fader, M., and Keevil, C. W. (2021). Biofilm development on urinary catheters promotes the appearance of viable but Nonculturable Bacteria. *mBio* 12:e03584-20. doi: 10.1128/mBio.03584-20
- Wong, M. H. Y., Wan, H. Y., and Chen, S. (2013). Characterization of multidrug-resistant *Proteus mirabilis* isolated from chicken carcasses. *Foodborne Pathog. Dis.* 10, 177–181. doi: 10.1089/fpd.2012.1303
- Yin, D., Gao, Q., Zhu, H., and Li, J. (2020). Public perception of urban companion animals during the COVID-19 outbreak in China. *Health Place* 65:102399. doi: 10.1016/j.healthplace.2020.102399
- Yu, T., Jiang, X., Liang, Y., Zhu, Y., Tian, J., Wang, X., et al. (2017). Characterization and horizontal transfer of antimicrobial resistance genes and Integrons in Bacteria isolated from cooked meat products in China. *J. Food Prot.* 80, 2048–2055. doi: 10.4315/0362-028X.JFP-17-119
- Zhang, S., Chen, S., Rehman, M. U., Yang, H., Yang, Z., Wang, M., et al. (2021). Distribution and association of antimicrobial resistance and virulence traits in *Escherichia coli* isolates from healthy waterfowls in Hainan, China. *Ecotoxicol. Environ. Saf.* 220:112317. doi: 10.1016/j.ecoenv.2021.112317
- Zhang, J. W., Hoedt, E. C., Liu, Q., Berendsen, E., Teh, J. J., Hamilton, A., et al. (2021). Elucidation of *Proteus mirabilis* as a key bacterium in Crohn's disease inflammation. *Gastroenterology* 160, 317–330.e11. doi: 10.1053/j.gastro.2020.09.036
- Zhao, X., Lv, Y., Adam, F. E. A., Xie, Q., Wang, B., Bai, X., et al. (2021). Comparison of antimicrobial resistance, virulence genes, Phylogroups, and biofilm formation of *Escherichia coli* isolated from intensive farming and free-range sheep. *Front. Microbiol.* 12:699927. doi: 10.3389/fmicb.2021.699927



## OPEN ACCESS

## EDITED BY

WeiQi He,  
Soochow University, China

## REVIEWED BY

Minakshi Prasad,  
Lala Lajpat Rai University of Veterinary and  
Animal Sciences, India  
Houqiang Luo,  
Wenzhou Vocational College of Science and  
Technology, China

## \*CORRESPONDENCE

Qianfu Gan  
✉ ganning707@163.com  
Shaoming Fang  
✉ 15279156575@163.com

†These authors have contributed equally to this work

RECEIVED 16 December 2022

ACCEPTED 11 April 2023

PUBLISHED 12 May 2023

## CITATION

Li K, Pang S, Li Z, Ding X, Gan Y, Gan Q and  
Fang S (2023) House ammonia exposure causes  
alterations in microbiota, transcriptome, and  
metabolome of rabbits.  
*Front. Microbiol.* 14:1125195.  
doi: 10.3389/fmicb.2023.1125195

## COPYRIGHT

© 2023 Li, Pang, Li, Ding, Gan, Gan and Fang.  
This is an open-access article distributed under  
the terms of the [Creative Commons Attribution  
License \(CC BY\)](https://creativecommons.org/licenses/by/4.0/). The use, distribution or  
reproduction in other forums is permitted,  
provided the original author(s) and the  
copyright owner(s) are credited and that the  
original publication in this journal is cited, in  
accordance with accepted academic practice.  
No use, distribution or reproduction is  
permitted which does not comply with these  
terms.

# House ammonia exposure causes alterations in microbiota, transcriptome, and metabolome of rabbits

Keyao Li<sup>†</sup>, Shuo Pang<sup>†</sup>, Zhechen Li, Xiaoning Ding, Yating Gan,  
Qianfu Gan\* and Shaoming Fang\*

College of Animal Science (College of Bee Science), Fujian Agriculture and Forestry University, Fuzhou, China

**Introduction:** Pollutant gas emissions in the current production system of the livestock industry have negative influences on environment as well as the health of farm staffs and animals. Although ammonia (NH<sub>3</sub>) is considered as the primary and harmful gas pollutant in the rabbit farm, less investigation has performed to determine the toxic effects of house ammonia exposure on rabbit in the commercial confined barn.

**Methods:** In this study, we performed multi-omics analysis on rabbits exposed to high and low concentration of house ammonia under similar environmental conditions to unravel the alterations in nasal and colonic microbiota, pulmonary and colonic gene expression, and muscular metabolic profile.

**Results and discussion:** The results showed that house ammonia exposure notably affected microbial structure, composition, and functional capacity in both nasal and colon, which may impact on local immune responses and inflammatory processes. Transcriptome analysis indicated that genes related to cell death (*MCL1*, *TMBIM6*, *HSPB1*, and *CD74*) and immune response (*CDC42*, *LAMTOR5*, *VAMP8*, and *CTSB*) were differentially expressed in the lung, and colonic genes associated with redox state (*CAT*, *SELENBP1*, *GLUD1*, and *ALDH1A1*) were significantly up-regulated. Several key differentially abundant metabolites such as L-glutamic acid, L-glutamine, L-ornithine, oxoglutaric acid, and isocitric acid were identified in muscle metabolome, which could denote house ammonia exposure perturbed amino acids, nucleotides, and energy metabolism. In addition, the widespread and strong inter-system interplay were uncovered in the integrative correlation network, and central features were confirmed by in vitro experiments. Our findings disclose the comprehensive evidence for the deleterious effects of house ammonia exposure on rabbit and provide valuable information for understanding the underlying impairment mechanisms.

## KEYWORDS

house ammonia, microbiota, transcriptome, metabolome, rabbit

## Introduction

The current production system of the livestock industry is characterized by increasing numbers of animals raised in largely confined housing facilities (Alvarado and Predicala, 2019). Although this improves the industry's productivity and profitability, various environmental issues have been raised. Pollutant gas emissions from animal barns not only affect the surrounding environment but also threaten the health of farmers and the wellbeing of animals (Kilic et al., 2021). Among the main gases emitted from the livestock production



industry, ammonia is produced during manure management, and its concentration is typically high in confined livestock houses with bad ventilation.

Microbiota colonized in the respiratory and intestinal tracts of farm animals establish a symbiotic relationship with the host and exert crucial modulatory roles in immune processes, neural functions, and endocrine pathways, which have important implications for the health and welfare of farm animals (Chen S. et al., 2021). Numerous studies have been conducted on farm animals raised in respiration chambers to evaluate the microbial and physiological alterations induced by ammonia exposure. For instance, sustained exposure to ambient ammonia causes pulmonary microbial perturbation in chickens, which promotes the release of inflammatory cytokines and suppresses the production of neurotransmitters via the lung–brain axis (Wang et al., 2022). Ammonia exposure disrupts chicken gut microbial homeostasis, activating the TLR4/TNF- $\alpha$  signaling pathway and inducing intestinal inflammation (Zhou et al., 2021). Ammonia stress resulted in the increased presence of harmful bacteria in the nasal microbiota and decreased respiratory immunity, which is harmful to porcine growth performance (Wang et al., 2019). Inhalation of excessive ammonia contributes to the dysbiosis of the porcine gut-brain axis by interfering with the oxidative stress-inflammation-apoptosis interaction network (Li et al., 2021a). Although rabbits are particularly sensitive to ambient ammonia, to date, research focusing on the deleterious effects of ammonia on rabbits is limited (Cui et al., 2021). More importantly, the artificially ammoniated environments in the respiration chambers may fail to reflect the complicated air conditions of confined barns (Pokharel et al., 2017).

Thus, we selected rabbits raised in a commercial, confined barn as research subjects exposed to high- and low-level house ammonia under similar environmental conditions. Alterations in the microbiota, transcriptome, and metabolome of different tissues were investigated using multi-omics analysis. Our observations could provide valuable insights into the adverse role of house ammonia exposure in rabbits and lay the foundation for illustrating the underlying toxicity mechanism of house ammonia exposure.

## Materials and methods

### Experimental animals and environmental parameter measurements

A total of 648 weaned Ira rabbits (330 males and 318 females) were randomly assigned to 324 double-deck cages (two rabbits per cage) in a commercial, confined rabbit house of Laidewang Animal Husbandry Co., Ltd., Sanming, China. The rabbit house building is 57.7 m long, 6.6 m wide, and 3.8 m high and is equipped with mechanical ventilation and a cooling system (Supplementary Figure S1). During a 45-day experimental period in the summertime, a multi-gas analyzer (MultiRAE IR Lite, RAE Systems, USA) with electrochemical and NDIR sensors was used for NH<sub>3</sub>, H<sub>2</sub>S, and CO<sub>2</sub> concentration measurements. The device recorded concentrations for 12 h (6:00 a.m.–6:00 p.m.) on a daily basis. Indoor air temperature, relative humidity, and air velocity in the house were measured at 3-h intervals

throughout the experiment using a portable air velocity meter (PCE-VA 20, PCE, Spain). At the end of the experiment, each of the six rabbits (three male and three female) exposed to high and low levels ( $16.49 \pm 1.67$  vs.  $4.81 \pm 0.92$  ppm) of house ammonia, but with similar other environmental parameters, were selected for sampling (Supplementary Table S1). A commercial pellet diet (Supplementary Table S2) was provided to all rabbits two times a day. All rabbits were healthy and did not receive any antibiotic, anticoccidial drug, probiotic, or prebiotic treatment before sampling.

### Sample collection

Nasal swabs were collected from the nares of the selected rabbits and placed into sterile tubes. The swabs were transported to the laboratory, where they were resuspended in 300  $\mu$ l PBS and stored at  $-20^{\circ}\text{C}$  for further analysis. The rabbits were anesthetized using electric shock and euthanized using exsanguination from the carotid artery. The lung, longissimus dorsi muscle, colon, and colonic digesta were immediately sampled after euthanization and frozen in liquid nitrogen for transportation. In the laboratory, the tissue and digested samples were stored at  $-80^{\circ}\text{C}$  for further analysis. All animal experiments were conducted according to the guidelines for the care and use of experimental animals established by the Ministry of Agriculture and Rural Affairs of China. The project was specially approved by the Animal Care and Use Committee (ACUC) at Fujian Agriculture and Forestry University (NO. PZCASFAFU2020).

### 16S rRNA gene sequencing

According to the manufacturer's instructions, total microbial genomic DNA was extracted from nasal swabs and colonic digesta using a FastDNA SPIN Kit for Soil (MP Biomedicals, USA). DNA quantity and quality were detected using a Nanodrop ND-2000 spectrophotometer (Thermo Fisher Scientific, USA) and 1.5% agarose gel electrophoresis, respectively. The V3-V4 hypervariable regions of the 16S rRNA gene were amplified using the barcoded fusion primers 341F (5'-CCTACGGGNGGCWGCAG-3') and 806R (5'-GGACTACHVGGGTATCTAAT-3'). The protocols for 16S rRNA gene sequencing and bioinformatics analysis were described in our previous research (Fang et al., 2020).

### Transcriptome sequencing

The total RNA in lung and colon samples was isolated using TRIzol reagent (Invitrogen, USA). RNA concentration, purity, and integrity were measured using the Nanodrop ND-2000 spectrophotometer (Thermo Fisher Scientific, USA) and a Bioanalyzer 2100 system (Agilent Technologies, USA). Following the manufacturer's illustrations, the sequencing libraries were constructed using a NEBNext<sup>®</sup> UltraTM RNA Library Prep Kit for Illumina<sup>®</sup> (NEB, Beverly, MA, USA). The prepared

libraries were sequenced on an Illumina HiSeq 2500 platform using a 150-bp paired-end read strategy. Raw data generated from Illumina sequencing were subjected to quality control using FASTX-Toolkit software. After removing adaptor sequences and low-quality reads, the remaining clean data were aligned with the rabbit reference genome (*OryCun2.0.107*) using TopHat v2.0.14 software. HTSeq v0.6.0 was used to count the number of mapped reads to each gene, and the gene expression was calculated in fragments per kilobase of exon per million mapped fragments (FPKM) using Cufflinks v0.14.0 software. DESeq2 v1.16.1 software was used to identify the differentially expressed genes (DEGs) according to the thresholds of  $|\log_2(\text{fold change})| > 1$  and FDR-adjusted *P*-value of  $< 0.01$ . Gene ontology (GO) and Kyoto Encyclopedia of Genes and Genomes (KEGG) pathway enrichment analysis of DEGs was performed using the clusterProfiler R package.

## Muscle metabolomics profiling

Hundred milligram of muscle sample was homogenized in 1 ml of precooled extraction mixture (methanol: water, 1:1) using a high-throughput tissue grinder and ultrasonicated at room temperature for 25 min. After centrifugation at 13,000 rpm for 20 min at 4°C, 500 µL of supernatant was dried in a vacuum, resolved in 200 µL of 15% methanol, and filtered through a 0.2 µm membrane (Millipore, USA). The filtrate was collected for subsequent UPLC-QTOFMS analysis, and an aliquot of equal volume (20 µL) for each sample was mixed to make a quality control (QC) sample. An Acquity UPLC system (Waters, USA) equipped with an HSS T3 column (150 × 2.1 mm, 1.8 µm) was used for chromatographic separation. After separation by UPLC, a Q-TOF Premier (Waters, USA) equipped with an electrospray ionization (ESI) source operating in positive and negative modes with spray voltages of 3.5 and −2.5 kV was used for mass spectrometry analysis. System control and data acquisition were performed using MassLynx (Waters, USA). The raw data were processed using Progenesis QI (Waters, USA) for peak alignment to obtain a peak list consisting of the retention time, *m/z*, and peak area. The peaks were normalized to the QC sample using the MetNormalizer R package. The metabolites were identified by aligning against the HMDB database. Principal component analysis (PCA) and partial least squares discriminate analysis (OPLS-DA) were performed using the ropls R package. Differentially expressed metabolites were identified by variable importance in the projection (VIP)  $> 1$  and by an FDR-adjusted *P*-value of  $< 0.05$ . A KEGG pathway enrichment analysis of differentially expressed metabolites was performed using the MetaboAnalyst 4.0 web server.

## Validation of key features

To confirm the key differentially enriched microbes and differentially expressed genes, quantitative PCR analysis was performed using microbial genomic DNA and tissue RNA,

respectively. The PCR reactions were run in a 7500-Fast Real-Time PCR System (ABI, USA) using an SYBR<sup>®</sup> Premix Ex Taq<sup>™</sup> II Kit (TaKaRa, Japan). The PCR conditions comprised an initial denaturation at 95°C for 10 s, followed by 40 cycles of denaturation at 95°C for 5 s and annealing at 60°C for 30 s. The expression levels of microbes and genes were determined based on normalization to the 16S rRNA gene and β-actin using the  $2^{-\Delta\Delta C_t}$  method. The primer sequences are listed in [Supplementary Table S3](#). The centrally differentially abundant metabolites were verified using targeted quantitative metabolomics methodology on a GC-MS/MS platform (Agilent Technologies, USA), as previously described ([Shin et al., 2019](#)). In brief, proteins were precipitated using acetonitrile from each 100 mg muscle sample containing 3,4-dimethoxybenzoic acid (0.1 µg) as an internal standard for isocitric acid and norvaline (0.2 µg) as an internal standard for L-glutamic acid. After centrifugation, the supernatant was adjusted to a pH  $\geq 12$  with 5.0 M sodium hydroxide in dichloromethane (1.5 ml) containing ethyl chloroformate (30 µL), which was converted to the ethoxycarbonyl derivative and subsequently the methoxime derivative by reaction with methoxyamine hydrochloride at 60°C for 1 h. After washing with diethyl ether two times, the aqueous phase was acidified with 10% sulfuric acid (pH  $< 2.0$ ), saturated with sodium chloride, and sequentially extracted with diethyl ether (3 mL) and ethyl acetate (2 mL). The extracts were evaporated to dryness by nitrogen. Prior to GC-MS/MS analysis, dry residues containing isocitric acid and L-glutamic acid were reacted with TEA (5 µL) and toluene (10 µL) at 60°C for 30 min to produce TBDMS derivatives. The derivatives were transferred to GC-MS/MS and quantified by multiple reaction monitoring (MRM) modes.

## Statistical analysis

A Wilcoxon rank sum test with false discovery rate (FDR) correction was performed to detect differences in microbial diversity indices, relative abundances of microbes at the phylum and genus levels, and functional capacities. Nasal microbial principal coordinate analysis (PCoA) and colonic microbial hierarchical clustering analysis of the unweighted pair-group method with arithmetic means (UPGMA) were performed to reveal the structural variation using the ape and facto extra R packages, respectively. The nasal and colonic differentially enriched OTUs were visualized using linear discriminant analysis effect size (LEfSe) analysis and Interactive Tree of Life (iTOL), respectively. The nasal and colonic differentially enriched functional items were exhibited using ComplexHeatmap and the ggplot2 R package, respectively. A Spearman correlation network was first generated based on potential biomarkers identified in each omic dataset of high-level house ammonia-challenged rabbits, and the core community was defined by the Girvan-Newman algorithm ([Lv et al., 2019](#)). Subsequently, the features of the core community in each network were selected for constructing the integrated network, and key features were identified according to the maximal clique centrality ([Ke et al., 2019](#)).

## Results

### House ammonia affects the nasal microbial communities of rabbits

The microbial diversity of the nasal microbiota was first analyzed. Compared to low-level house ammonia-exposed rabbits, both the Shannon and ACE index values of rabbits exposed to a high concentration of house ammonia significantly declined ([Supplementary Figures S2A, B](#)). The PCoA analysis result based on unweighted and weighted UniFrac distances showed that the individuals were distinctively separated ([Supplementary Figures S2C, D](#)).

Alterations in nasal microbial composition were investigated at the phylum, genus, and OTU levels. As shown in [Figure 1A](#), *Proteobacteria*, *Firmicutes*, *Campilobacterota*, *Bacteroidetes*, and *Actinobacteriota* were the top five phyla in all samples, and they constituted over 95% of the total sequences. Among these, the relative abundance of *Proteobacteria* significantly increased in rabbits exposed to high concentrations of house ammonia, and significant reductions in the relative abundances of both *Firmicutes* and *Bacteroidetes* were also observed. At the genus level, 20 dominant genera, including *Moraxella*, *Pasteurella*, *Neisseria*, *Bordetella*, *Helicobacter*, *Staphylococcus*, *Akkermansia*, *Lactobacillus*, *Bifidobacterium*, and *Enterococcus*, comprised more than 85% of the total sequences ([Figure 1B](#)). Of these, *Moraxella*, *Escherichia-Shigella*, and *Mannheimia* were more abundant in rabbits exposed to high concentrations of house ammonia, while *Akkermansia*, *Lactobacillus*, and *Bifidobacterium* exhibited lower abundances. As shown in [Figure 1C](#), 12 OTUs were enriched in a high concentration of house ammonia-exposed rabbits, including one OTU annotated to the family *Neisseriaceae*, one OTU annotated to each of the genera *Enterococcus*, *Streptococcus*, *Fusicatenibacter*, *Helicobacter*, and *Mycoplasma*, and one OTU annotated to each of the species *Escherichia coli*, *Anaerostipes hadrus*, *Klebsiella quasipneumoniae*, *Dialister sp. Marseille-P5638*, and *Moraxella cuniculi*. The other eight OTUs were augmented in low concentrations of house ammonia-exposed rabbits, including one OTU annotated to the family *Lachnospiraceae*, one OTU annotated to each of the genera *Clostridium innocuum* group, *Ruminococcus gnavus* group, *Bifidobacterium*, and *Blautia*, and one OTU annotated to each of the species *Bifidobacterium longum*, *Bifidobacterium breve*, and *Faecalibaculum rodentium*.

To evaluate how the nasal microbial functional capacities altered as house ammonia levels varied, the predicted KOs and KEGG pathways were compared between the two groups of rabbits ([Figure 2](#); [Supplementary Table S4](#)). Sixty-four KOs were highly represented in rabbits exposed to high levels of house ammonia, of which most were assigned to ABC transporters, the phosphotransferase system (PTS), lipopolysaccharide biosynthesis, phenylpropanoid biosynthesis, and non-homologous end-joining. Moreover, 38 KOs were significantly enriched in rabbits exposed to low-level house ammonia, of which most were related to the lysosome, biosynthesis of siderophore group non-ribosomal peptides, inositol phosphate metabolism, mismatch repair, and nucleotide excision repair. KEGG pathway comparison analysis showed that seven functional categories, including

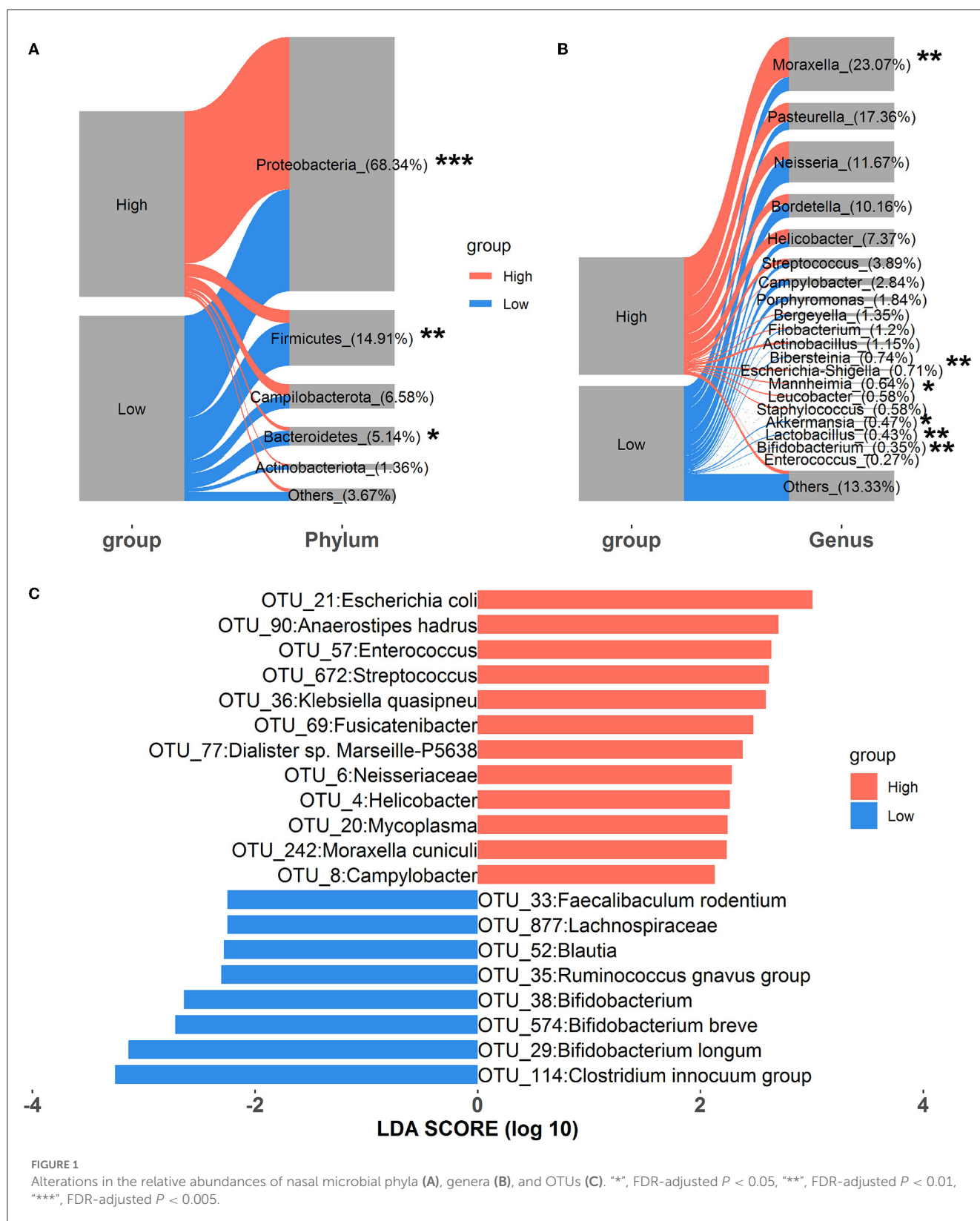
ABC transporters, the phosphotransferase system (PTS), and lipopolysaccharide biosynthesis, were more prevalent in rabbits exposed to high levels of house ammonia. In addition, 11 functional categories, such as the lysosome, nucleotide excision repair, biosynthesis of siderophore group non-ribosomal peptides, mismatch repair, and inositol phosphate metabolism, were more active in rabbits exposed to low-level household ammonia.

### House ammonia impacts the colonic microbiota of rabbits

Regarding the alpha diversity, the Shannon and ACE indices significantly declined in rabbits exposed to an increasing level of house ammonia ([Supplementary Figures S3A, B](#)). Additionally, hierarchical clustering analysis of UPGMA indicated that the colonic microbiota of rabbits exposed to high- and low-level house ammonia exhibited a clear separation ([Supplementary Figures S3C, D](#)).

The relative abundances of microbial taxa were assessed to investigate the alterations in colonic microbial compositions. At the phylum level, *Firmicutes*, *Bacteroidetes*, *Verrucomicrobiota*, *Actinobacteriota*, and *Proteobacteria* were predominant in all samples, comprising more than 95% of the total reads ([Figure 3A](#)). Compared to the low-level house ammonia-challenged rabbits, the relative abundances of *Firmicutes* and *Actinobacteriota* in the high-level house ammonia-challenged rabbits were remarkably decreased, but the relative abundance of *Bacteroidetes* was significantly increased. At the genus level, the top 12 genera accounted for ~50% of total reads ([Figure 3B](#)). While comparing the rabbits exposed to low concentrations of house ammonia with those exposed to high concentrations, it was observed that the latter had increased abundances of the *Christensenellaceae* R-7 group, *Akkermansia*, *Oscillospiraceae* V9D2013 group, and *Alistipes*, and decreased abundances of the *Oscillospiraceae* NK4A214 group, *Eubacterium siraeum* group, *Ruminococcus*, *Subdoligranulum*, and *Lachnospiraceae* NK4A136 group. As shown in [Figure 3C](#), 13 OTUs showed higher abundances in rabbits exposed to a high concentration of house ammonia, including four OTUs classified as *Muribaculaceae*, two classified as *Christensenellaceae* R-7 group, two as *Eggerthellaceae*, and one each classified as *Escherichia coli*, *Bacteroides fragilis*, *Bacteroides vulgatus*, *Defluviitaleaceae* UCG-011, and *Oscillospiraceae* V9D2013 group. Moreover, 12 OTUs possessed greater proportions in rabbits exposed to low-level house ammonia, including two OTUs classified as *Oscillospirales*\_UCG-010 and one each classified as *Enterococcus faecium*, *Eubacteriaceae*, *Lachnospiraceae* NK4B4 group, *Oscillospiraceae* NK4A214 group, *Clostridia vadinBB60* group, *Eubacterium siraeum* group, *Rikenellaceae*, *Subdoligranulum*, *Ruminococcus*, and *Monoglobus*.

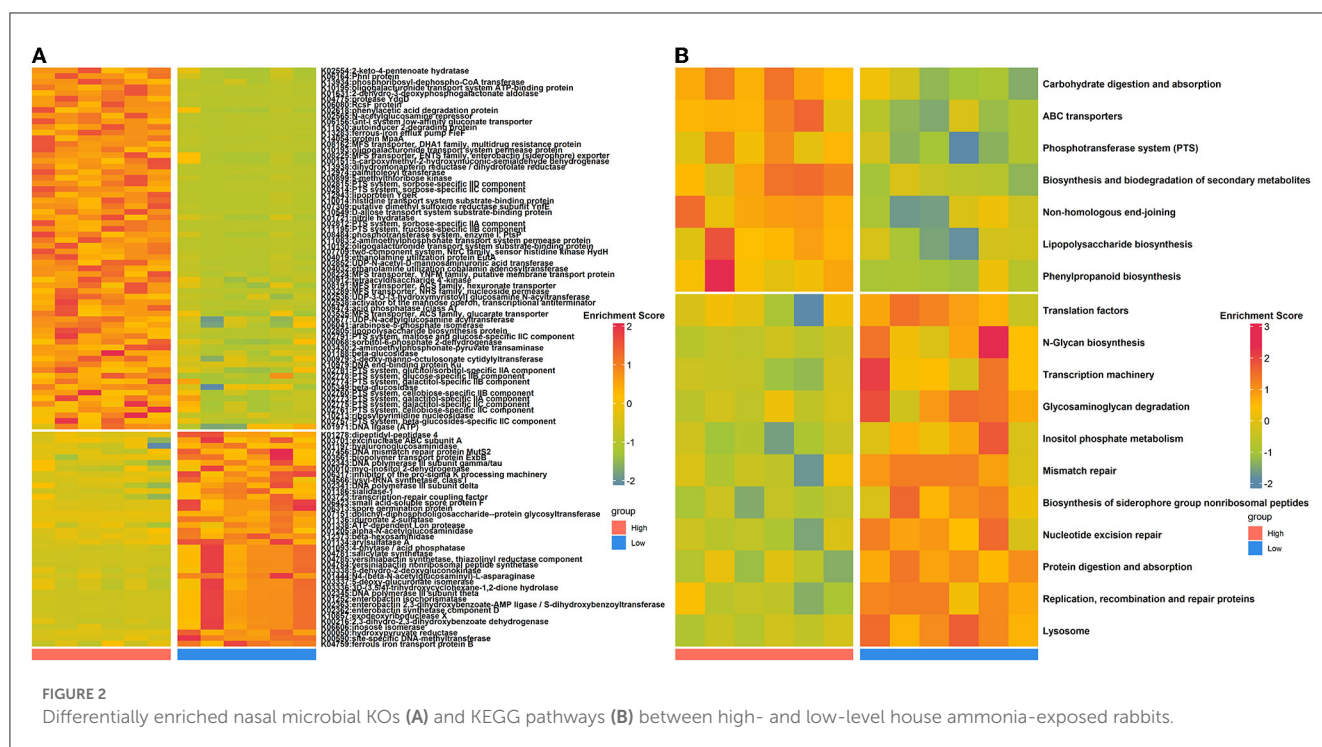
To gain insights into functional alterations of the colonic microbiota, the predicted gene catalog was aligned with the KEGG database. A total of 113 KOs were significantly different in abundance between high- and low-level house ammonia-challenged rabbits ([Figure 4A](#); [Supplementary Table S5](#)). The KOs were more abundant in rabbits exposed to a high concentration of house ammonia related to nitrogen metabolism, phenylalanine



metabolism, valine, leucine and isoleucine biosynthesis, glycerophospholipid metabolism, and thiamine metabolism. The KOs showed higher abundance in rabbits exposed to low concentrations of house ammonia and were associated with

peptidoglycan biosynthesis, cysteine and methionine metabolism, glyoxylate and dicarboxylate metabolism, base excision repair, and pentose and glucuronate interconversions. However, 18 KEGG pathways manifested significantly different abundances between





the two groups of rabbits (Figure 4B). Similar to KO analysis results, valine, leucine and isoleucine biosynthesis, nitrogen metabolism, glycerophospholipid metabolism, thiamine metabolism, and phenylalanine metabolism were more abundant in rabbits exposed to high concentrations of house ammonia, while cysteine and methionine metabolism, peptidoglycan biosynthesis, pentose and glucuronate interconversions, glyoxylate and dicarboxylate metabolism, and base excision repair were enhanced in rabbits exposed to low concentrations of household ammonia.

## House ammonia influences the lung and colon transcriptomes of rabbits

A total of 100 pulmonary differentially expressed genes (DEGs) were identified between the two groups of rabbits (Figure 5A). GO enrichment analysis showed that DEGs were enriched in nine categories of biological processes, nine categories of cellular components, and 11 categories of molecular function (Figure 5B; Supplementary Table S6). Among these, DEGs showed greater expression levels in rabbits exposed to a high concentration of house ammonia and are mainly involved in the regulation of the intrinsic apoptotic signaling pathway, autophagy, lytic vacuole, viral life cycle, neutrophil activation involved in immune response, and cytochrome-c oxidase activity. Additionally, upregulated DEGs in rabbits exposed to low concentrations of ammonia mainly contributed to oxidative phosphorylation, oxidoreductase complex, and NADH dehydrogenase activity. Similar results were observed in the KEGG enrichment analysis (Figure 5B). The DEGs derived from rabbits exposed to a high concentration of house ammonia engaged in lysosome and autophagy functions, while the DEGs from the rabbits exposed to a low concentration of house

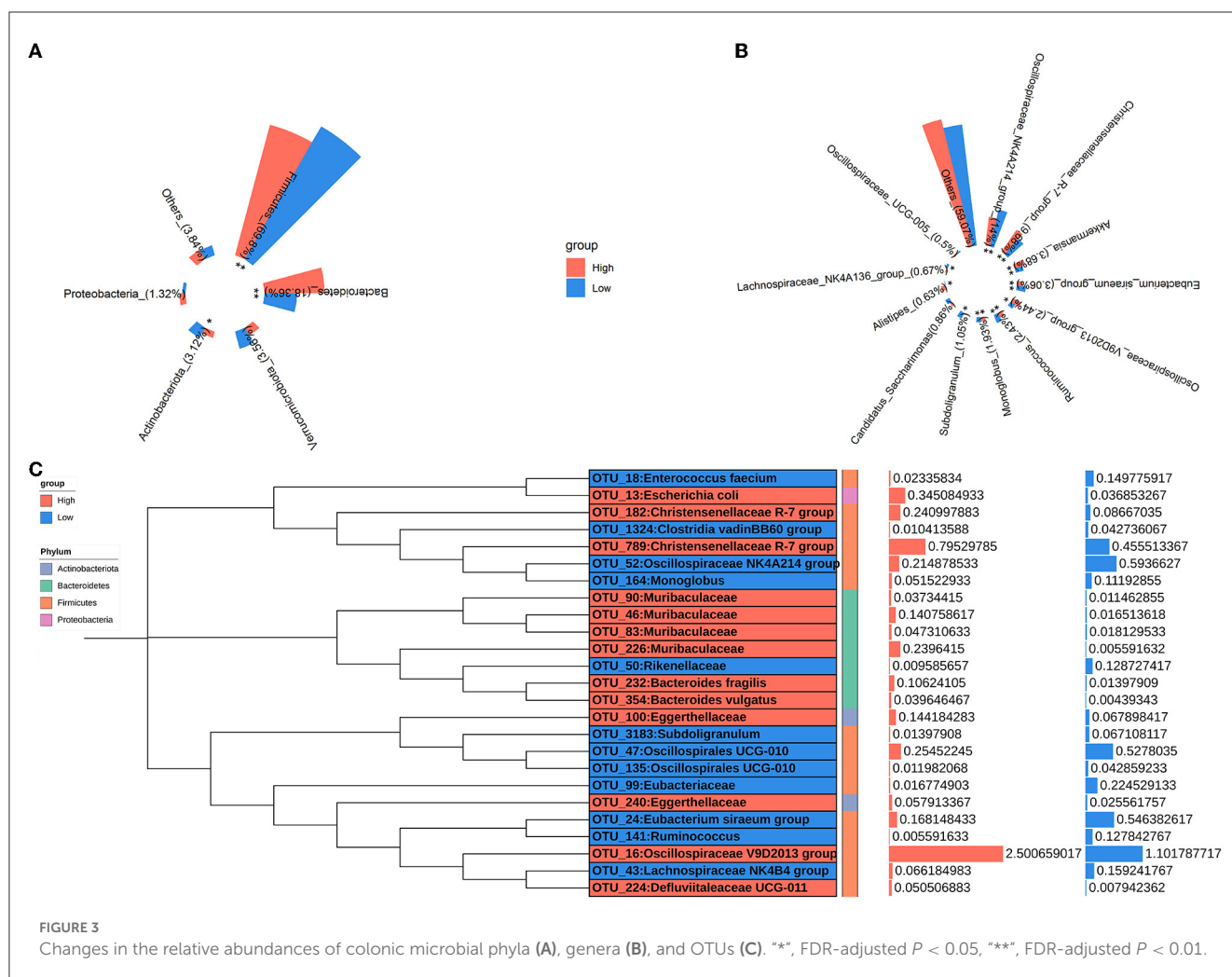
ammonia participated in oxidative phosphorylation, ECM-receptor interaction, and the relaxin signaling pathway.

In the colon, 89 genes were differentially expressed between the two groups of rabbits (Figure 6A). A total of 25 enriched GO functional terms were identified, including 11 terms of biological processes, seven terms of cellular components, and eight terms of molecular function (Figure 6B; Supplementary Table S7). Among them, the highly expressed DEGs of high-level house ammonia-challenged rabbits related to aerobic respiration, antibiotic metabolic process, oxidation-reduction process, cytosolic ribosome, and NAD binding. In addition, the enhanced DEGs of rabbits exposed to low-level house ammonia were associated with positive regulation of muscle structure development, adherens junctions, and ion channel binding. Furthermore, KEGG enrichment analysis indicated that DEGs were mainly enriched in carbon metabolism, proximal tubule bicarbonate reclamation, citrate cycle, and leukocyte transendothelial migration (Figure 6B).

## House ammonia perturbs the muscle metabolome of rabbits

A total of 515 metabolites were identified using UPLC-QTOFMS. Multivariate statistical analyses, including PCA and OPLS-DA, were performed to evaluate the variations in metabolic patterns between the two groups of rabbits. The results showed that high- and low-level house ammonia-challenged rabbits were clustered separately, which implied distinctive metabolic patterns (Supplementary Figure S4).

To further confirm the metabolic disruption effect of house ammonia, univariate analysis was performed on each

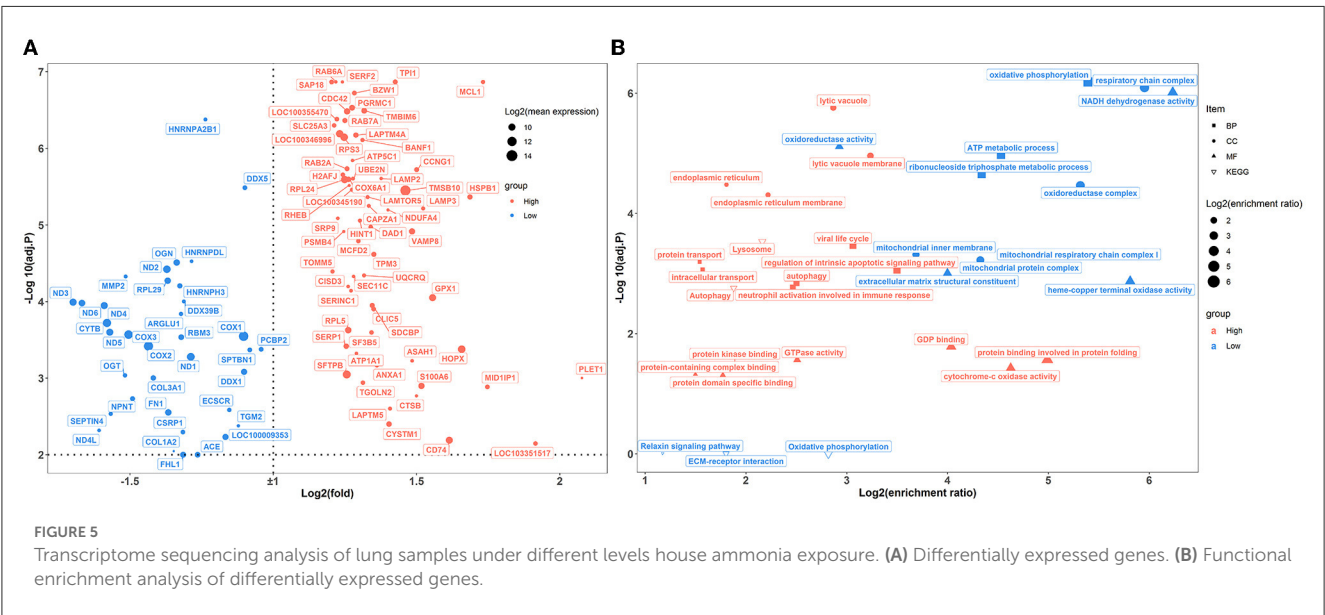
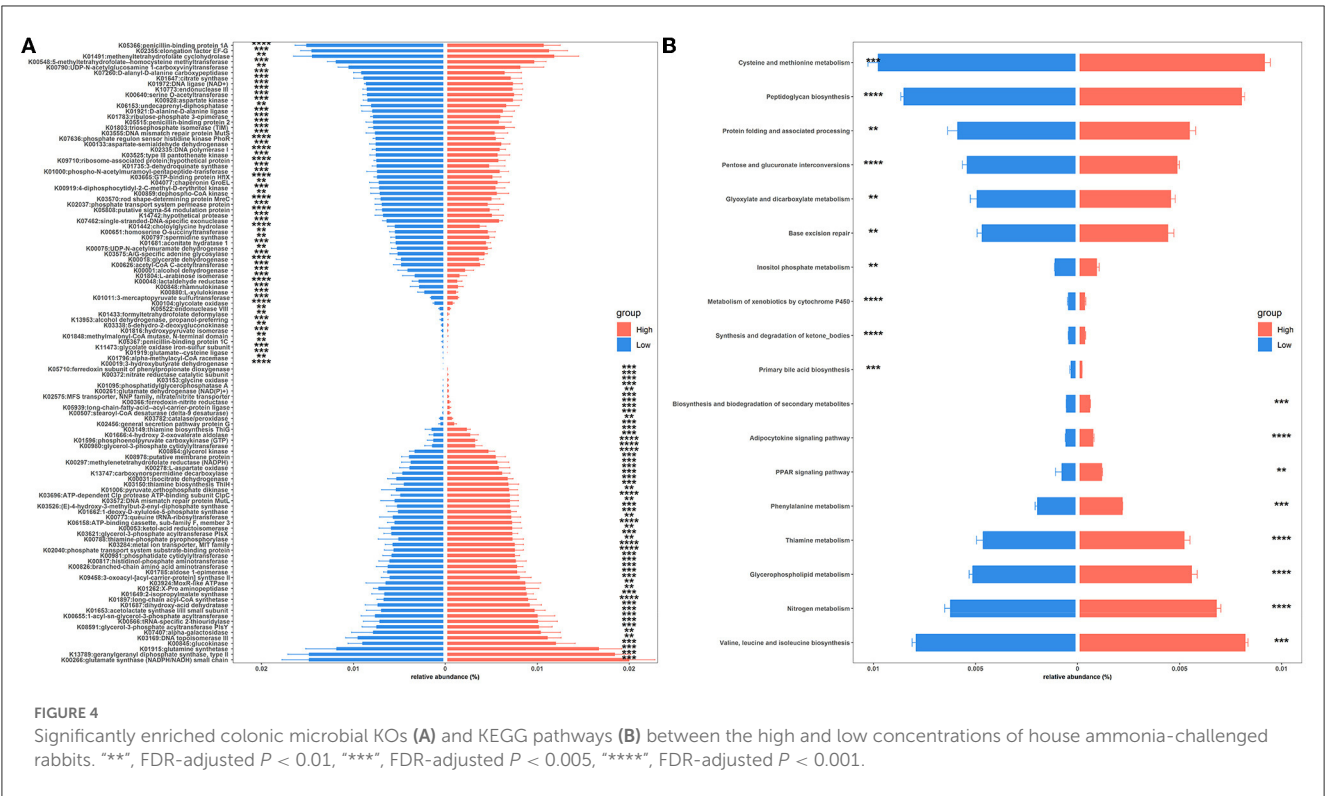


metabolite. As shown in Figure 7A, 70 metabolites were significantly affected by different levels of house ammonia exposure. Among them, 35 differentially abundant metabolites were enriched in rabbits exposed to high-level house ammonia exposure, with 10 amino acids and their derivatives (e.g., L-glutamic acid, beta-alanyl-L-lysine, L-phenylalanine, L-tyrosine, and L-ornithine), eight organic acids and their derivatives (e.g., o-toluate, methylselenopyruvate, isocitric acid, and oxoglutaric acid), three phenols (acetaminophen, dopamine, and phenol), three benzoyl derivatives (4-methylbenzaldehyde, phenylacetaldehyde, and benzaldehyde), three organic oxygen compounds (N-acetylmannosamine, N-acetyl-D-galactosamine, and 4-hydroxybenzaldehyde), and two fatty acids and derivatives (pimelate and 2-Isopropylmalic acid). The remaining 35 differentially abundant metabolites were concentrated in rabbits exposed to low concentrations of house ammonia, with seven fatty acids and their derivatives (e.g., prostaglandin F2a, prostaglandin H2, palmitic acid, and alcoholic acid), seven organic oxygen compounds (e.g., N-acetyl-D-glucosamine, D-glyceraldehyde 3-phosphate, quinate, and dihydroxyacetone phosphate), six amino acids and their derivatives (e.g., L-aspartic acid, L-glutamine, and L-lysine), five organic acids and their derivatives (e.g., 2-Keto-6-acetamidocaproate, folic acid, and

gentisic acid), and three pyrimidines and their derivatives (e.g., pentobarbital, thymidine, and 5-hydroxymethyluracil). KEGG enrichment analysis indicated that differentially abundant metabolites are involved in 12 metabolic processes (Figure 7B). It is intriguing to note that tyrosine metabolism, glyoxylate, and dicarboxylate metabolism, arginine and proline metabolism, and the citrate cycle (TCA cycle) were significantly increased in high-level house ammonia-challenged rabbits, while pyrimidine metabolism, purine metabolism, glycolysis/gluconeogenesis, the pentose phosphate pathway, and glycerolipid metabolism were highly active in low-level house ammonia-challenged rabbits.

## Integrated analysis of multi-omics data

To explore the systematically impairing action of house ammonia on rabbits, a correlation network was first generated based on potential biomarkers identified in each omic dataset of high-level house ammonia-challenged rabbits (Supplementary Figure S5), and then, the features in the core community in each network were selected for constructing



the integrated network. Finally, three main communities containing 70 interrelated features were detected (Figure 8), which suggested statistically robust interactions within and between each omic dataset. Importantly, 11 key features were identified in the integrated network. Among these, six features were presented in the light green community, including four lung genes (*LAMTOR5*, *VAMP8*, *CDC42*, and *HSPB1*) and two colon genes (*CAT* and *ALDH1A1*). Three features, including two muscle metabolites (L-glutamic acid and isocitric acid) and one colonic microbe

(OTU\_232:*Bacteroides fragilis*), were exhibited in the coral-red community. The colon gene *SELENBP1* and the nasal microbe OTU\_242:*Moraxella cuniculi* were recognized in the violet community.

To confirm the reliability of multi-omics data, key features were used for qPCR validation and quantitative metabolite assays. As shown in Figure 9A, the gene expression patterns of *HSPB1*, *VAMP8*, *LAMTOR5*, *CDC42*, *SELENBP1*, *ALDH1A1*, and *CAT* between RNA-Seq and qPCR were similar. Compared to rabbits exposed to low-level house ammonia,

**A**

Figure A is a volcano plot showing differentially expressed genes. The x-axis represents the Log2(fold) change, ranging from -2 to 2. The y-axis represents the negative log10 of the adjusted p-value, ranging from 2 to 6. Points are colored by group: red for 'High' and blue for 'Low'. The size of the points indicates the Log2(mean expression), with sizes corresponding to 10, 12, and 14. A horizontal dashed line is at y ≈ 2.5. A vertical dashed line is at x = 1.5. Labeled genes include: APM1A, WDR1, SNX3, RPS16, RPS11, NPC2, RPL4, RPL10A, CS, CAT, TST, COA3, PRDX6, TMEM45B, DHRS11, SLC5B1, SLC25A3, SLC6A1, SLC11A1, SLC11A2, SLC11A3, SLC11A4, SLC11A5, SLC11A6, SLC11A7, SLC11A8, SLC11A9, SLC11A10, SLC11A11, SLC11A12, SLC11A13, SLC11A14, SLC11A15, SLC11A16, SLC11A17, SLC11A18, SLC11A19, SLC11A20, SLC11A21, SLC11A22, SLC11A23, SLC11A24, SLC11A25, SLC11A26, SLC11A27, SLC11A28, SLC11A29, SLC11A30, SLC11A31, SLC11A32, SLC11A33, SLC11A34, SLC11A35, SLC11A36, SLC11A37, SLC11A38, SLC11A39, SLC11A40, SLC11A41, SLC11A42, SLC11A43, SLC11A44, SLC11A45, SLC11A46, SLC11A47, SLC11A48, SLC11A49, SLC11A50, SLC11A51, SLC11A52, SLC11A53, SLC11A54, SLC11A55, SLC11A56, SLC11A57, SLC11A58, SLC11A59, SLC11A60, SLC11A61, SLC11A62, SLC11A63, SLC11A64, SLC11A65, SLC11A66, SLC11A67, SLC11A68, SLC11A69, SLC11A70, SLC11A71, SLC11A72, SLC11A73, SLC11A74, SLC11A75, SLC11A76, SLC11A77, SLC11A78, SLC11A79, SLC11A80, SLC11A81, SLC11A82, SLC11A83, SLC11A84, SLC11A85, SLC11A86, SLC11A87, SLC11A88, SLC11A89, SLC11A90, SLC11A91, SLC11A92, SLC11A93, SLC11A94, SLC11A95, SLC11A96, SLC11A97, SLC11A98, SLC11A99, SLC11A100, SLC11A101, SLC11A102, SLC11A103, SLC11A104, SLC11A105, SLC11A106, SLC11A107, SLC11A108, SLC11A109, SLC11A110, SLC11A111, SLC11A112, SLC11A113, SLC11A114, SLC11A115, SLC11A116, SLC11A117, SLC11A118, SLC11A119, SLC11A120, SLC11A121, SLC11A122, SLC11A123, SLC11A124, SLC11A125, SLC11A126, SLC11A127, SLC11A128, SLC11A129, SLC11A130, SLC11A131, SLC11A132, SLC11A133, SLC11A134, SLC11A135, SLC11A136, SLC11A137, SLC11A138, SLC11A139, SLC11A140, SLC11A141, SLC11A142, SLC11A143, SLC11A144, SLC11A145, SLC11A146, SLC11A147, SLC11A148, SLC11A149, SLC11A150, SLC11A151, SLC11A152, SLC11A153, SLC11A154, SLC11A155, SLC11A156, SLC11A157, SLC11A158, SLC11A159, SLC11A160, SLC11A161, SLC11A162, SLC11A163, SLC11A164, SLC11A165, SLC11A166, SLC11A167, SLC11A168, SLC11A169, SLC11A170, SLC11A171, SLC11A172, SLC11A173, SLC11A174, SLC11A175, SLC11A176, SLC11A177, SLC11A178, SLC11A179, SLC11A180, SLC11A181, SLC11A182, SLC11A183, SLC11A184, SLC11A185, SLC11A186, SLC11A187, SLC11A188, SLC11A189, SLC11A190, SLC11A191, SLC11A192, SLC11A193, SLC11A194, SLC11A195, SLC11A196, SLC11A197, SLC11A198, SLC11A199, SLC11A200, SLC11A201, SLC11A202, SLC11A203, SLC11A204, SLC11A205, SLC11A206, SLC11A207, SLC11A208, SLC11A209, SLC11A210, SLC11A211, SLC11A212, SLC11A213, SLC11A214, SLC11A215, SLC11A216, SLC11A217, SLC11A218, SLC11A219, SLC11A220, SLC11A221, SLC11A222, SLC11A223, SLC11A224, SLC11A225, SLC11A226, SLC11A227, SLC11A228, SLC11A229, SLC11A230, SLC11A231, SLC11A232, SLC11A233, SLC11A234, SLC11A235, SLC11A236, SLC11A237, SLC11A238, SLC11A239, SLC11A240, SLC11A241, SLC11A242, SLC11A243, SLC11A244, SLC11A245, SLC11A246, SLC11A247, SLC11A248, SLC11A249, SLC11A250, SLC11A251, SLC11A252, SLC11A253, SLC11A254, SLC11A255, SLC11A256, SLC11A257, SLC11A258, SLC11A259, SLC11A260, SLC11A261, SLC11A262, SLC11A263, SLC11A264, SLC11A265, SLC11A266, SLC11A267, SLC11A268, SLC11A269, SLC11A270, SLC11A271, SLC11A272, SLC11A273, SLC11A274, SLC11A275, SLC11A276, SLC11A277, SLC11A278, SLC11A279, SLC11A280, SLC11A281, SLC11A282, SLC11A283, SLC11A284, SLC11A285, SLC11A286, SLC11A287, SLC11A288, SLC11A289, SLC11A290, SLC11A291, SLC11A292, SLC11A293, SLC11A294, SLC11A295, SLC11A296, SLC11A297, SLC11A298, SLC11A299, SLC11A300, SLC11A301, SLC11A302, SLC11A303, SLC11A304, SLC11A305, SLC11A306, SLC11A307, SLC11A308, SLC11A309, SLC11A310, SLC11A311, SLC11A312, SLC11A313, SLC11A314, SLC11A315, SLC11A316, SLC11A317, SLC11A318, SLC11A319, SLC11A320, SLC11A321, SLC11A322, SLC11A323, SLC11A324, SLC11A325, SLC11A326, SLC11A327, SLC11A328, SLC11A329, SLC11A330, SLC11A331, SLC11A332, SLC11A333, SLC11A334, SLC11A335, SLC11A336, SLC11A337, SLC11A338, SLC11A339, SLC11A340, SLC11A341, SLC11A342, SLC11A343, SLC11A344, SLC11A345, SLC11A346, SLC11A347, SLC11A348, SLC11A349, SLC11A350, SLC11A351, SLC11A352, SLC11A353, SLC11A354, SLC11A355, SLC11A356, SLC11A357, SLC11A358, SLC11A359, SLC11A360, SLC11A361, SLC11A362, SLC11A363, SLC11A364, SLC11A365, SLC11A366, SLC11A367, SLC11A368, SLC11A369, SLC11A370, SLC11A371, SLC11A372, SLC11A373, SLC11A374, SLC11A375, SLC11A376, SLC11A377, SLC11A378, SLC11A379, SLC11A380, SLC11A381, SLC11A382, SLC11A383, SLC11A384, SLC11A385, SLC11A386, SLC11A387, SLC11A388, SLC11A389, SLC11A390, SLC11A391, SLC11A392, SLC11A393, SLC11A394, SLC11A395, SLC11A396, SLC11A397, SLC11A398, SLC11A399, SLC11A400, SLC11A401, SLC11A402, SLC11A403, SLC11A404, SLC11A405, SLC11A406, SLC11A407, SLC11A408, SLC11A409, SLC11A410, SLC11A411, SLC11A412, SLC11A413, SLC11A414, SLC11A415, SLC11A416, SLC11A417, SLC11A418, SLC11A419, SLC11A420, SLC11A421, SLC11A422, SLC11A423, SLC11A424, SLC11A425, SLC11A426, SLC11A427, SLC11A428, SLC11A429, SLC11A430, SLC11A431, SLC11A432, SLC11A433, SLC11A434, SLC11A435, SLC11A436,

**Figure 7A: Volcano Plot of Differentially Metabolites**

This plot shows the relationship between the VIP value (Y-axis, 1.50 to 2.25) and the negative logarithm of the adjusted p-value (-Log<sub>10</sub>(adj.P), X-axis, 2 to 6). Metabolites are categorized into 'High' (red outline) and 'Low' (blue outline) groups. Key metabolites include o-Toluate, N-Acetyl-D-glucosamine, Pentobarbital, Cinchonidine, Adenine, Acetaminophen, Isocitric acid, 6-Hydroxynicotinate, 4-Methylbenzaldehyde, Methylselenopyruvate, S-Adenosylmethionine, L-Glutamic acid, Thymidine, Prostaglandin F2α, Folic acid, 2-Keto-6-acetamidocaproate, Phenylacetaldehyde, Spermine, Benzaldehyde, Aspartame, Quinate, Gentisic acid, N-methyl-L-glutamic acid, Ribose 1,5-bisphosphate, L-Phenylalanine, L-Glutamine, D-Glyceraldehyde, 4-Hydroxycinnamic acid, Dopamine, Methyl jasmonate, hydroxybenzaldehyde, L-lysine, Genistein, Prostaglandin H2, Undecanoic acid, Glycylleucine, L-Tyrosine, 2-Deoxyadenosine, Palmitic acid, Oxoglutaric acid, Terephthalic acid, L-Homoserine, Selenomethionine, 5-Hydroxymethyluracil, Pimelate, N6-Acetyl-L-lysine, D-Phenyllactic acid, Allicolic acid, Piperidine, L-Lysine, L-Aspartic acid, Prephenate, hydroxytestosterone, 3-Dehydro-scyllo-inosose, S-Adenosylhomocysteine, xyxinosine, N-Acetyl-L-phenylalanine, dAMP, Dihydroxyacetone phosphate, 2-Isopropylmalic acid, Adenosine, O-Phosphoethanolamine, Pyrimidodiazepine, N-Acetylmannosamine, Acetyl adenylate, N-Acetylglucosamine, Acetyl-D-galactosamine, and Antibiotic JI-20A.

**Figure 7B: KEGG Enrichment Analysis**

This bar chart shows the metabolites count (Y-axis, 0 to 6) for various KEGG pathways (X-axis). The pathways are color-coded by group: High (red outline) and Low (blue outline). The pathways and their counts are: Tyrosine metabolism (High: 3, Low: 1), Amino sugar and nucleotide sugar metabolism (High: 2, Low: 1), Pyrimidine metabolism (High: 2, Low: 1), Purine metabolism (High: 2, Low: 1), Glyoxylate and dicarboxylate metabolism (High: 2, Low: 1), Arginine and proline metabolism (High: 2, Low: 1), Cysteine and methionine metabolism (High: 2, Low: 1), Nitrogen metabolism (High: 2, Low: 1), Glycolysis / Gluconeogenesis (High: 2, Low: 1), Pentose phosphate pathway (High: 2, Low: 1), Glycerolipid metabolism (High: 2, Low: 1), and Citrate cycle (TCA cycle) (High: 2, Low: 1).

the OTU\_242:*Moraxella cuniculi* and OTU\_232:*Bacteroides fragilis* showed markedly increased abundances in rabbits exposed to high-level house ammonia, which is in line with the results of 16S rRNA gene sequencing analysis

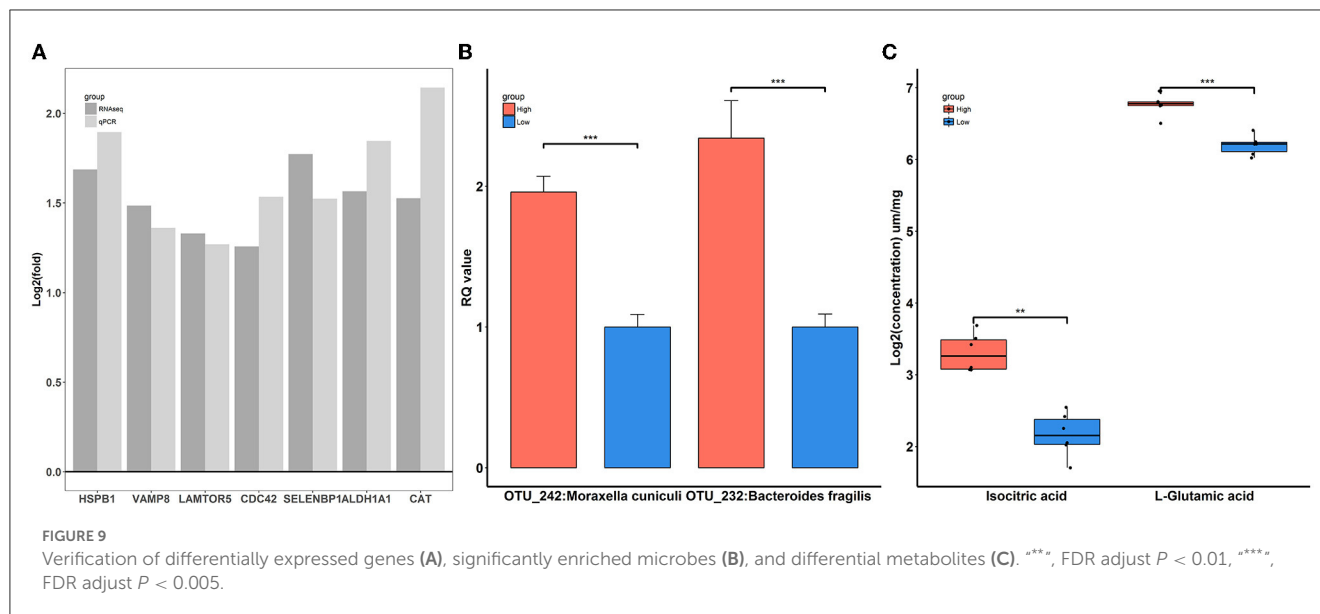
(Figure 9B). Additionally, the alterations in isocitric acid and L-glutamic acid between the two groups of rabbits were in accordance with muscle metabolic profile characterization (Figure 9C).





systematically and comprehensively understand the deleterious effects of house ammonia on rabbits reared in a commercial, confined barn.

The nose is the major interface between the internal body and the external environment, and tremendous changes in the



porcine nasal microbial community have been observed following different concentrations of house ammonia exposure (Wang et al., 2019). Similarly, we found that the nasal microbiota of rabbits was notably affected by different levels of house ammonia treatment. A remarkable reduction in nasal microbial alpha diversity was observed when rabbits were exposed to high levels of house ammonia, and beta diversity also exhibited significant differences between high- and low-level house ammonia-exposed rabbits (Supplementary Figure S1). Nasal cavity pH is regarded as an important factor that affects microbiota colonization, while ammonia exposure disrupts acid-base equilibrium and may result in nasal microbial biodiversity alterations (Morawska-Kochman et al., 2019).

In accordance with previous studies on nasal microbial phylogenetic composition (Qin et al., 2019; Gomez et al., 2021), our results indicated that *Proteobacteria*, *Firmicutes*, and *Bacteroidetes* were the most prevalent phyla in the nasal microbial community. Moreover, rabbits exposed to high levels of house ammonia presented a noticeable augmentation of *Proteobacteria* and a depletion of *Firmicutes* and *Bacteroidetes* (Figure 1A). *Proteobacteria* comprises several well-known opportunistic pathogens (e.g., *Pasteurella*, *Neisseria*, and *Campylobacter*), which showed increased abundance in conjunction with losses in *Firmicutes* and *Bacteroidetes*, as reported in the nasal microbial communities of humans with chronic rhinosinusitis and pigs with Glässer's disease (Choi et al., 2014; Correa-Fiz et al., 2016). This suggests that house ammonia exposure leads to variations in these predominant phyla in the nasal microbiota and may increase rabbits' susceptibility to respiratory tract infections and diseases. We also identified 20 abundant genera that accounted for over 85% of the total sequences (Figure 1B). Among these, it is worth noting that the relative abundance of *Moraxella*, *Escherichia-Shigella*, and *Mannheimia* significantly increased in high-level house ammonia-challenged rabbits, while *Akkermansia*, *Lactobacillus*, and *Bifidobacterium* distinctly declined. Although previous studies demonstrated that *Moraxella* was commonly present in the nasal

microbiota of animals and humans, its overgrowth was associated with an increased risk of respiratory illness due to its potential role in inducing epithelial damage and inflammatory cytokine expression (McCauley et al., 2019; Lopez-Serrano et al., 2020). This should be due to the synergistic effect of house ammonia exposure on nasal mucosal injuries, possibly promoting the proliferation of *Moraxella* and aggravating inflammatory responses (Urbain et al., 1996). In addition, nasal microbiota profiles dominated by both *Escherichia-Shigella* and *Mannheimia* were previously reported to have intimate relationships with respiratory disorders in broilers and steers (Cirone et al., 2019; Liu et al., 2020).

However, *Akkermansia*, *Lactobacillus*, and *Bifidobacterium* could regulate epithelial barrier function and immune response, and their absences were closely correlated with decreased respiratory tract immunity (Heintz-Buschart et al., 2018; Kim et al., 2019; Wang et al., 2019). Importantly, we found that several distinctly different OTUs annotated to the specific species belonged to the abovementioned genera, for example, OTU\_21:*Escherichia coli*, OTU\_242:*Moraxella cuniculi*, OTU\_29:*Bifidobacterium longum*, and OTU\_574:*Bifidobacterium breve* (Figure 1C). This implies that certain nasal microbial species should be regarded as potential indicators of house ammonia exposure detrimental to respiratory health in rabbits.

We also assessed the functional variations of the nasal microbiota under different levels of house ammonia exposure (Figure 2). As the level of exposure to house ammonia increased, functional processes, such as ABC transporters and lipopolysaccharide biosynthesis, which are capable of driving respiratory tract-cascaded inflammatory responses, were activated (Lee et al., 2019; Ma et al., 2021). Moreover, functional items that have regulatory roles in pathogens' invasion defense and epithelial cell injury repair, such as the lysosome and inositol phosphate metabolism, were inhibited (Cohen et al., 2016; Wu S. E. et al., 2020). These results suggested that a high concentration of house ammonia exposure may mediate the respiratory inflammatory processes by disturbing the nasal microbial functional homeostasis.

## Ammonia exposure induces colonic microbial changes

The symbiotic relationship between the host and gut microbiota ensures the appropriate development of the metabolic and immune systems, which is crucial for host health (Jandhyala et al., 2015). However, a growing body of evidence suggests that the inhalation of excessive ammonia causes gut microbial dysbiosis, which consequently influences the health and growth of farm animals (Li et al., 2021b; Zhou et al., 2021). Our results also showed that the colonic microbial communities of rabbits were continuously changed following house ammonia exposure. Gut microbial alpha diversity was notably decreased with exposure to an increased level of house ammonia, and beta diversity was dramatically altered under different concentrations of house ammonia (Supplementary Figure S2), which confirmed that ammonia exposure caused gut microbial dysbiosis in animals (Tao et al., 2019; Han H. et al., 2021).

The colonic microbial composition also exhibited noticeable variations under high-level exposure to house ammonia (Figure 3). At the phylum level, ammonia exposure increased the relative abundance of *Bacteroidetes* and decreased the relative abundance of *Firmicutes* and *Actinobacteriota*. This could be due to ammonia exposure promoting the production of urea that flows into the colon, which facilitates the preferential proliferation of urea metabolism bacteria derived from *Bacteroidetes* (Tang et al., 2020; Yin et al., 2022). Consistently, we found that the growth of the genus *Alistipes*, which belongs to the phylum *Bacteroidetes*, was promoted following high-level house ammonia exposure, while the growth of genera in the phylum *Firmicutes*, such as the *Eubacterium siraeum* group, *Ruminococcus*, and *Subdoligranulum*, was inhibited. Although *Alistipes* are commonly present in a relatively low proportion, it is highly relevant to intestinal dysbiosis and inflammation in humans and animals. For instance, the augmentation of *Alistipes* and the elevation of lipopolysaccharide biosynthesis were intimately associated with intestinal inflammation and permeability in hypertension patients (Kim et al., 2018). A metagenomic study in a mouse model of ileitis suggested that *Alistipes* showed a strong correlation with ileitis incidence (Rodriguez-Palacios et al., 2018).

In contrast, the *Eubacterium siraeum* group, *Ruminococcus*, and *Subdoligranulum* are butyric acid-producing bacteria that have beneficial effects on maintaining intestinal epithelial integrity and immune functions, and their elimination in inflammatory conditions will aggravate intestinal impairment (Zhu et al., 2020; Correa et al., 2021). Additionally, we noticed that the potentially beneficial bacteria *Akkermansia* was enriched by a high concentration of house ammonia exposure, which was different from the observation in the nasal microbiota. *Akkermansia* in the colon may act as scavengers, which clean the mucin produced by ammonia exposure (Duan et al., 2018).

Nonetheless, *Akkermansia* thrives in the gut microbiota and may be capable of inducing the incidence of epizootic rabbit enteropathy (Jin et al., 2018). At the OTU level, we further identified several important microbial species related to house ammonia exposure, such as *Bacteroides fragilis* (OTU232), *Bacteroides vulgatus* (OTU354), and *Enterococcus faecium*

(OTU18). As mentioned above, a high concentration of ammonia exposure led to an increase in colonic urea flux, and urea was eventually broken down into endogenous ammonia with the aid of bacterial urease. Coincidentally, *Bacteroides vulgatus* is an ureolytic bacterium, and *Bacteroides fragilis* can utilize endogenous ammonia as a primary nitrogen source to promote its growth and reproduction (Forsythe and Parker, 1985; Gibson and Macfarlane, 1988). However, a high proportion of *Bacteroides fragilis* is implicated in immune system dysfunction and colonic inflammatory conditions (Thiele Orberg et al., 2017; Chung et al., 2018). Moreover, the depletion of *Enterococcus faecium* caused by ammonia exposure has a negative impact on intestinal epithelial cell barrier function, increasing ammonia toxicity (Park et al., 2016).

In agreement with the results of recent studies on functional alterations of intestinal microbiota under ammonia exposure (Duan et al., 2021; Tang et al., 2021b), our functional capacity analysis demonstrated that colonic microbiota were more engaged in amino acid metabolism (e.g., valine, leucine, and isoleucine biosynthesis and phenylalanine metabolism) and lipid metabolism (e.g., glycerophospholipid metabolism) following high-level house ammonia exposure but less engaged in carbohydrate metabolism (e.g., peptidoglycan biosynthesis, pentose and glucuronate interconversions, and glyoxylate and dicarboxylate metabolism). A low intestinal pH and the presence of carbohydrates restrict amino acid metabolism (Louis and Flint, 2017), but increased pH caused by ammonia exposure could remove this inhibition. Furthermore, *in vitro* experiments indicated that microbes could modulate amino acid and lipid metabolic strategies to respond to environmental stress, which may help explain our observations (Stancik et al., 2002; Li et al., 2019).

## Ammonia exposure modulates pulmonary and colonic gene expression

Several studies have reported that ammonia exposure could regulate gene expression patterns in different tissues of farm animals (Wang et al., 2020; Li et al., 2021a). In the lung, our transcriptome sequencing results showed that house ammonia exposure led to remarkable alterations in gene expressions related to cell death (e.g., regulation of intrinsic apoptotic signaling pathway, autophagy, and lytic vacuole) and immune response (e.g., viral life cycle and neutrophil activation involved in the immune response) (Figure 5).

Cell death is an important modulator in response to a variety of environmental and internal stressors (Martins et al., 2011). We have identified several DEGs, including *MCL1*, *TMBIM6*, *HSPB1*, and *CD74*, that are associated with cell death processes. Myeloid cell leukemia 1 (*MCL1*) is a unique Bcl-2 family member with a significantly short half-life but an important anti-apoptotic function (Wu X. et al., 2020). A recent broiler study indicated that ammonia exposure can cause lung injury, which may be due to the increased expression level of *MCL1*, causing a delay in neutrophil apoptosis and leading to a disrupted immune response (Blomgran et al., 2012; Liu et al., 2020). Ammonia exposure has

been implicated in inducing endoplasmic reticulum stress, and the activation of cell autophagy and the apoptosis-related protein transmembrane BAX inhibitor motif containing 6 (*TMBIM6*) play a regulatory role in response to endoplasmic reticulum stress (Han Q. et al., 2021; Kim et al., 2021). Heat shock protein beta 1 (*HSPB1*) is another cell autophagy and apoptosis-associated protein that commonly participates in different types of stress resistance, and its expression was upregulated in this study, which may be related to the cellular response to stress caused by house ammonia exposure (Wu et al., 2016; D'Anna et al., 2017). *CD74* binds to specific cytokines and exerts important roles in orchestrating a variety of pathological processes, such as cell necroptosis and the inflammatory response, and an elevated expression level of *CD74* is positively associated with lung injury (Takahashi et al., 2009; Su et al., 2017).

The precise and targeted surveillance mechanisms at the lung-environment interface are essential for maintaining pulmonary homeostasis and functions; however, inhaled environmental irritants can stimulate and disrupt the immune response of the lung, leading to potentially pathological consequences (Guttenberg et al., 2021). Upon ammonia stimulation, the immune response associated DEGs such as *CDC42*, *LAMTOR5*, *VAMP8*, and *CTSB* were identified. Cell division cycle 42 (*CDC42*) is a Rho GTPase that affects T-cell differentiation and inflammatory cytokine production, and is capable of initiating airway inflammation responses (Chen L. et al., 2021). Although the late endosomal/lysosomal adaptor and MAPK and MTOR activator 5 (*LAMTOR5*) are characterized as indispensable components of the amino acid sensing machinery, their key role in modulating lung immunosuppression has recently been noted (Wang L. et al., 2021). Here, the upregulation of *CDC42* and *LAMTOR5* expression may be correlated with immune dysfunctions of the airways caused by ammonia exposure (Chen J. et al., 2021; Wang H. et al., 2021). Vesicle-associated membrane protein 8 (*VAMP8*) can be involved in antigen cross-presentation and activation of cytolytic T-cell immune responses (Dingjan et al., 2017). Cystatin B (*CSTB*) can modulate the immune response under pathological conditions by inhibiting cysteine proteases (Premachandra et al., 2013). Moreover, the increased expressions of both *CTSB* and *VAMP8* are associated with inflammatory and bacterial infection processes (Xia et al., 2019), which may indirectly reflect the dysbiosis of pulmonary immunity and microbiota triggered by ammonia exposure.

However, house ammonia exposure resulted in changes in colonic gene expression that were related to the redox state (e.g., oxidation-reduction process, aerobic respiration, oxidoreductase activity, and NAD binding) (Figure 6). Most environmental pollutants could activate the antioxidant defense system, thereby affecting the redox state (Zheng et al., 2020). This study presented redox state-related DEGs such as *CAT*, *SELENBP1*, *GLUD1*, and *ALDH1A1*. Catalase (*CAT*) is an important member of the antioxidant defense system that plays a vital role in maintaining redox balance. In line with our findings, the expression level of *CAT* in aquatic animals also increases with excessive exposure to ammonia (Sun et al., 2014; Hongxing et al., 2021). This can likely be attributed to the surplus production of reactive

oxygen species (ROS) that occurs at high concentrations of ammonia, leading to the upregulation of *CAT* expression (Zhang et al., 2008). Selenium binding protein 1 (*SELENBP1*) has been identified as a methanethiol oxidase in the colonic enterocytes, which catalyzes the conversion of methanethiol to redox signaling molecules hydrogen sulfide and hydrogen peroxide that engage in environmental stress responses (Sies and Jones, 2020; Philipp et al., 2021). In this study, the house ammonia challenge promotes the expression of *SELENBP1*, which may be linked to redox signaling molecule generation and transduction. Increased activity of glutamate dehydrogenase 1 (*GLUD1*) upon ammonia exposure has been observed in previous studies (Voss et al., 2021). It plays an important role in catalyzing the conversion of glutamate to alpha-ketoglutarate, which is known to maintain redox homeostasis and serve as a substrate for the detoxification of ammonia (Jin et al., 2015). Aldehyde dehydrogenase A1 (*ALDH1A1*) catalyzes the detoxification of toxic unsaturated aldehydes generated by lipid peroxidation during redox imbalance (Calleja et al., 2021). It is well-recognized that ammonia exposure could trigger lipid peroxidation to produce malondialdehyde (Li and Qi, 2019), which may further induce the expression of *ALDH1A1*.

## Ammonia exposure interferes with the muscular metabolic profile

Previous studies have demonstrated that ammonia exposure results in perturbations of amino acids, nucleotides, energy, and lipid metabolism in animals (Dong et al., 2020; Tang et al., 2020; Qin et al., 2022). We have consistently found that tyrosine metabolism, arginine and proline metabolism, pyrimidine metabolism, purine metabolism, citrate cycle (TCA cycle), glycolysis/gluconeogenesis, pentose phosphate pathway, and glycerolipid metabolism were influenced by house ammonia exposure (Figure 7). More importantly, we identified a variety of differentially abundant metabolites that should be regarded as signals for metabolic alterations under ammonia exposure. Glutamate (L-glutamic acid) is a key player in ammonia removal in a muscle, capturing ammonia to form glutamine. Glutamine is the major inter-organ carrier of ammonia that can transport ammonia in the muscle to the liver for detoxification (Hakvoort et al., 2017). However, high-level ammonia exposure could cause the initial ammonia condensation reaction to be less efficient (Dong et al., 2020). In addition, glutamine also serves as an important precursor for purine and pyrimidine synthesis, and the enhanced detoxification of ammonia could reduce nitrogen donors for nucleotide synthesis (Cory and Cory, 2006). Hence, glutamate accumulation, glutamine consumption, and nucleotide anabolism depletion were observed in this study. Notably, glutamate, as a central junction for the interchange of amino nitrogen, could facilitate L-ornithine synthesis (Blachier et al., 2009). L-ornithine participates in the urea cycle, leading to the excretion of excess ammonia and the generation of L-arginine and L-proline (Hoche et al., 2004). In addition, ammonia is utilized as a nitrogen source by aminotransferases for the *de novo* synthesis of aromatic amino acids



such as L-tyrosine and L-phenylalanine, which should be another effective way to reduce ammonia content in muscle (Wang S. et al., 2021). Therefore, the metabolic activities of tyrosine, arginine, and proline were also enhanced.

However, energy metabolism processes such as the TCA cycle and glycolysis were impaired by a high concentration of house ammonia exposure. This could be partially explained by ammonia being used as a substrate for catalyzing the  $\alpha$ -ketoglutarate (oxoglutaric acid) to glutamate conversion by glutamate dehydrogenase in muscle mitochondria and high-level ammonia stimulation enhancing the drain of  $\alpha$ -ketoglutarate from the TCA cycle adversely affects ATP generation (Davuluri et al., 2016). Additionally, isocitrate dehydrogenase has been reported to be inhibited by ammonia, resulting in the accumulation of isocitrate (isocitric acid), which could further interfere with the TCA cycle (Katunuma et al., 1966). The impairment of the TCA cycle will cause a reduction in glycolysis due to feedback inhibition (Drews et al., 2020).

## Integrated analysis and validation experiment

To gain insights into the interactive relationships between different biological layers concerning distinct features linked to house ammonia exposure, an integrative correlation network was constructed based on multi-omics data (Figure 8). The network modeling yielded three communities composed of intertwined microbes, genes, and metabolites, indicating close intersystem interactions that may allow for proposing certain hypotheses to be tested in further studies focusing on house ammonia impairment mechanisms. For instance, there are close immune and metabolic interactions between the respiratory and gastrointestinal tracts, which are commonly referred to as the gut–lung axis, and the important roles of the gut–lung axis in pathophysiological processes caused by air pollution exposure have been generally recognized (Keulers et al., 2022; Mousavi et al., 2022). Moreover, the existence of a gut–muscle axis has been suggested more recently, and the gut–muscle axis is increasingly implicated in endogenous ammonia and urea nitrogen metabolism (Ticinesi et al., 2019; Yeh et al., 2022). Moreover, the specific roles of highlighted features such as OTU\_242:*Moraxella cuniculi*, OTU\_232:*Bacteroides fragilis*, HSPB1, LAMTOR5, CDC42, CAT, and L-glutamic acid present in the network communities had been discussed above, and their alterations under house ammonia exposure were confirmed by different experimental measurements (Figure 9). This implies that these features should not be underestimated in dissecting the underlying mechanisms linked to the deleterious effects of house ammonia on rabbits.

## Limitations

Our study has several limitations. The first is that the small sample size within the single rabbit population limited our ability to detect more taxonomic and functional features related to house ammonia exposure. Investigations of larger and more diverse rabbit populations will probably help to identify

additional biomarkers. Due to the relatively limited taxonomic resolution of 16S rRNA sequencing, high-resolution shotgun metagenomic sequencing should be performed to uncover the specific microbial species associated with house ammonia exposure in future studies. In addition, our study was also limited to an episode of house ammonia exposure outcomes, and therefore, it would be particularly interesting to perform time series multi-omics analyses to capture the dynamic changes. Finally, *in vivo* experiments should be performed to explore how the cross-talk between different biological entities may exacerbate the detrimental roles of house ammonia exposure.

## Conclusions

In the present study, integrated analysis of the multi-omics data was performed to obtain overviews of changes in microbial communities, gene expressions, and metabolic profiles in rabbits exposed to house ammonia. The results indicated that house ammonia exposure caused dramatic variations in both nasal and intestinal microbial diversities, phylogenetic compositions, and functional capacities, which could potentially affect the immune responses and inflammatory processes of rabbits. Furthermore, house ammonia exposure led to genes being differentially expressed in the lung and colon and enriched functional terms related to cell death processes, immune responses, and redox state. A change in the muscular metabolic profile was also observed after house ammonia stimulation. Several crucial, differentially abundant metabolites, such as L-glutamic acid, L-glutamine, and L-ornithine, associated with amino acid and nucleotide metabolism, as well as oxoglutaric acid and isocitric acid, correlated with energy metabolism, were identified. Additionally, the widespread and strong inter-system cross-talk was outlined. Our findings provide valuable insights into the detrimental effects of house ammonia exposure on rabbits and pave the way for exploring the underlying impairment mechanisms.

## Data availability statement

The datasets presented in this study can be found in online repositories. The names of the repository/repositories and accession number(s) can be found below: <https://db.cngb.org/CNP0003860>.

## Ethics statement

The animal study was reviewed and approved by Animal Care and Use Committee (ACUC) in Fujian Agriculture and Forestry University.

## Author contributions

SF conceived and designed the experiments, supervised the experiment progress, and wrote and revised the manuscript. QG designed the experiments, analyzed the data, and wrote and revised the manuscript. KL and SP performed the experiments, analyzed

the data, and wrote the manuscript. ZL revised the manuscript. XD and YG performed the experiments. All authors contributed to the article and approved the submitted version.

## Funding

This work was supported in part by grants from the Natural Science Foundation of Fujian Province (2020J01537), the Agricultural Science and Technology Project of Fuzhou (2021-N-129), the Modern Agricultural Equipment Fujian University Engineering Research Center Open Fund (MAE-201903), the Rural Revitalization Service Team of Fujian Agriculture and Forestry University-Herbivore Industry Service Team (11899170139), and the Fujian Agriculture and Forestry University Science and Technology Innovation Special Fund Project (CXZX2020057A).

## Acknowledgments

We would like to thank Suzhou PANOMIX Biomedical Tech Co., Ltd. for providing muscle metabolome technical help.

## Conflict of interest

The authors declare that the research was conducted in the absence of any commercial or financial relationships that could be construed as a potential conflict of interest.

## Publisher's note

All claims expressed in this article are solely those of the authors and do not necessarily represent those of their affiliated organizations, or those of the publisher, the editors and the reviewers. Any product that may be evaluated in this article, or claim that may be made by its manufacturer, is not guaranteed or endorsed by the publisher.

## References

- Alvarado, A. C., and Predicala, B. Z. (2019). Occupational exposure risk for swine workers in confined housing facilities. *J. Agric. Saf. Health* 25, 37–50. doi: 10.13031/jash.12990
- Blachier, F., Boutry, C., Bos, C., and Tome, D. (2009). Metabolism and functions of L-glutamate in the epithelial cells of the small and large intestines. *Am. J. Clin. Nutr.* 90, 814S–21S. doi: 10.3945/ajcn.2009.27462S
- Blomgran, R., Patcha Brodin, V., Verma, D., Bergstrom, I., Soderkvist, P., Sjowall, C., et al. (2012). Common genetic variations in the Nalp3 inflammasome are associated with delayed apoptosis of human neutrophils. *PLoS ONE* 7, e31326. doi: 10.1371/journal.pone.0031326
- Calleja, L. F., Yoval-Sanchez, B., Hernandez-Esquivel, L., Gallardo-Perez, J. C., Sosa-Garrocho, M., Marin-Hernandez, A., et al. (2021). Activation of Aldh1a1 by omeprazole reduces cell oxidative stress damage. *FEBS J.* 288, 4064–4080. doi: 10.1111/febs.15698
- Chen, J., Jin, A., Huang, L., Zhao, Y., Li, Y., Zhang, H., et al. (2021). Dynamic changes in lung microbiota of broilers in response to aging and ammonia stress. *Front. Microbiol.* 12, 696913. doi: 10.3389/fmicb.2021.696913
- Chen, L., Collado, K., and Rastogi, D. (2021). Contribution of systemic and airway immune responses to pediatric obesity-related asthma. *Paediatr. Respir. Rev.* 37, 3–9. doi: 10.1016/j.prrv.2020.02.005
- Chen, S., Luo, S., and Yan, C. (2021). Gut microbiota implications for health and welfare in farm animals: a review. *Animals* 12:93. doi: 10.3390/ani12010093
- Choi, E. B., Hong, S. W., Kim, D. K., Jeon, S. G., Kim, K. R., Cho, S. H., et al. (2014). Decreased diversity of nasal microbiota and their secreted extracellular vesicles in patients with chronic rhinosinusitis based on a metagenomic analysis. *Allergy* 69, 517–526. doi: 10.1111/all.12374
- Chung, L., Orberg, E. T., Geis, A. L., Chan, J. L., Fu, K., DeStefano Shields, C. E., et al. (2018). *Bacteroides fragilis* toxin coordinates a pro-carcinogenic inflammatory cascade via targeting of colonic epithelial cells. *Cell Host Microbe* 23, 421. doi: 10.1016/j.chom.2018.02.004
- Cirone, F., Padalino, B., Tullio, D., Capozza, P., Lo Surdo, M., Lanave, G., et al. (2019). Prevalence of pathogens related to bovine respiratory disease before and after transportation in beef steers: preliminary results. *Animals* 9:1093. doi: 10.3390/ani9121093

## Supplementary material

The Supplementary Material for this article can be found online at: <https://www.frontiersin.org/articles/10.3389/fmicb.2023.1125195/full#supplementary-material>

### SUPPLEMENTARY FIGURE S1

Diagram of confined barn structural parameters and air quality measurement instrument distribution. A, B, C, and D represent four sets of double-deck cages, which were further divided evenly into three parts (1, 2, and 3).

### SUPPLEMENTARY FIGURE S2

House ammonia impacted the alpha (A, B) and beta (C, D) diversity of the nasal microbial community. \*\*\*, FDR-adjusted  $P < 0.005$ .

### SUPPLEMENTARY FIGURE S3

Colonic microbial alpha (A, B) and beta (C, D) diversity are altered by house ammonia. \*\*\*, FDR-adjusted  $P < 0.01$ .

### SUPPLEMENTARY FIGURE S4

PCA (A) and PLS-DA (B) analysis showing the effect of house ammonia on muscle metabolome.

### SUPPLEMENTARY FIGURE S5

Network analysis of the interplay between nasal microbes (A), colonic microbes (B), lung genes (C), colon genes (D), and muscle metabolites (E) enriched in high-level house ammonia-exposed rabbits.

### SUPPLEMENTARY TABLE S1

Air quality parameter measurements of high- and low-concentration ammonia-exposed rabbits.

### SUPPLEMENTARY TABLE S2

Nutrients in the commercial pellet diet.

### SUPPLEMENTARY TABLE S3

Primers used for qPCR analysis.

### SUPPLEMENTARY TABLE S4

Significantly enriched nasal microbial KO pathway assignment.

### SUPPLEMENTARY TABLE S5

Significantly enriched colonic microbial KO pathway assignment.

### SUPPLEMENTARY TABLE S6

Pulmonary differentially expressed genes functional enrichment analysis.

### SUPPLEMENTARY TABLE S7

Colonic differentially expressed genes functional enrichment analysis.

- Cohen, T. S., Hilliard, J. J., Jones-Nelson, O., Keller, A. E., O'Day, T., Tkaczyk, C., et al. (2016). *Staphylococcus aureus* alpha toxin potentiates opportunistic bacterial lung infections. *Sci. Transl. Med.* 8, 329ra31. doi: 10.1126/scitranslmed.aad9922
- Correa, P. S., Jimenez, C. R., Mendes, L. W., Rymer, C., Ray, P., Gerdes, L., et al. (2021). Taxonomy and functional diversity in the fecal microbiome of beef cattle reared in Brazilian traditional and semi-intensive production systems. *Front. Microbiol.* 12, 768480. doi: 10.3389/fmicb.2021.768480
- Correa-Fiz, F., Fraile, L., and Aragon, V. (2016). Piglet nasal microbiota at weaning may influence the development of glasser's disease during the rearing period. *BMC Genom.* 17, 404. doi: 10.1186/s12864-016-2700-8
- Cory, J. G., and Cory, A. H. (2006). Critical roles of glutamine as nitrogen donors in purine and pyrimidine nucleotide synthesis: asparaginase treatment in childhood acute lymphoblastic leukemia. *In Vivo* 20, 587–589.
- Cui, J., Wu, F., Yang, X., Liu, S., Han, S., Chen, B., et al. (2021). Effects of ammonia on hypothalamic-pituitary-ovarian axis in female rabbits. *Ecotoxicol. Environ. Saf.* 227, 112922. doi: 10.1016/j.ecoenv.2021.112922
- D'Anna, C., Cigna, D., Di Sano, C., Di Vincenzo, S., Dino, P., Ferraro, M., et al. (2017). Exposure to cigarette smoke extract and lipopolysaccharide modifies cytoskeleton organization in bronchial epithelial cells. *Exp. Lung Res.* 43, 347–358. doi: 10.1080/01902148.2017.1377784
- Davuluri, G., Allawy, A., Thapaliya, S., Rennison, J. H., Singh, D., Kumar, A., et al. (2016). Hyperammonaemia-induced skeletal muscle mitochondrial dysfunction results in cataplexis and oxidative stress. *J. Physiol.* 594, 7341–7360. doi: 10.1113/JP272796
- Dingjan, I., Paardekooper, L. M., Verboogen, D. R. J., von Mollard, G. F., Ter Beest, M., van den Bogaart, G., et al. (2017). Vamp8-mediated Nox2 recruitment to endosomes is necessary for antigen release. *Eur. J. Cell Biol.* 96, 705–714. doi: 10.1016/j.ejcb.2017.06.007
- Dong, X., Liu, Q., Kan, D., Zhao, W., Guo, H., Lv, L., et al. (2020). Effects of ammonia-N exposure on the growth, metabolizing enzymes, and metabolome of *Macrobrachium rosenbergii*. *Ecotoxicol. Environ. Saf.* 189, 110046. doi: 10.1016/j.ecoenv.2019.110046
- Drews, L., Zimmermann, M., Westhoff, P., Brilhaus, D., Poss, R. E., Bergmann, L., et al. (2020). Ammonia inhibits energy metabolism in astrocytes in a rapid and glutamate dehydrogenase 2-dependent manner. *Dis. Model. Mech.* 13, doi: 10.1242/dmm.047134
- Duan, Y., Liu, Q., Wang, Y., Zhang, J., and Xiong, D. (2018). Impairment of the intestine barrier function in *Litopenaeus vannamei* exposed to ammonia and nitrite stress. *Fish Shellfish Immunol.* 78, 279–288. doi: 10.1016/j.fsi.2018.04.050
- Duan, Y., Xiong, D., Wang, Y., Li, H., Dong, H., Zhang, J., et al. (2021). Toxic effects of ammonia and thermal stress on the intestinal microbiota and transcriptomic and metabolomic responses of *Litopenaeus vannamei*. *Sci. Total Environ.* 754, 141867. doi: 10.1016/j.scitotenv.2020.141867
- Fang, S., Chen, X., Ye, X., Zhou, L., Xue, S., Gan, Q., et al. (2020). Effects of gut microbiome and short-chain fatty acids (scfas) on finishing weight of meat rabbits. *Front. Microbiol.* 11, 1835. doi: 10.3389/fmicb.2020.01835
- Forsythe, S. J., and Parker, D. S. (1985). Nitrogen metabolism by the microbial flora of the rabbit caecum. *J. Appl. Bacteriol.* 58, 363–369. doi: 10.1111/j.1365-2672.1985.tb01475.x
- Gibson, S. A., and Macfarlane, G. T. (1988). Studies on the proteolytic activity of bacteroides fragilis. *J. Gen. Microbiol.* 134, 19–27. doi: 10.1099/00221287-134-1-19
- Gomez, D. E., Arroyo, L. G., Lillie, B., and Weese, J. S. (2021). Nasal bacterial microbiota during an outbreak of equine herpesvirus 1 at a farm in Southern Ontario. *Can. J. Vet. Res.* 85, 3–11.
- Guttenberg, M. A., Vose, A. T., and Tighe, R. M. (2021). Role of innate immune system in environmental lung diseases. *Curr. Allergy Asthma Rep.* 21, 34. doi: 10.1007/s11882-021-01011-0
- Hakvoort, T. B., He, Y., Kulik, W., Vermeulen, J. L., Duijst, S., Ruijter, J. M., et al. (2017). Pivotal role of glutamine synthetase in ammonia detoxification. *Hepatology* 65, 281–293. doi: 10.1002/hep.28852
- Han, H., Zhou, Y., Liu, Q., Wang, G., Feng, J., Zhang, M., et al. (2021). Effects of ammonia on gut microbiota and growth performance of broiler chickens. *Animals* 11:1716. doi: 10.3390/ani11061716
- Han, Q., Liu, H., Zhang, R., Yang, X., Bao, J., Xing, H., et al. (2021). Selenomethionine protects against ammonia-induced apoptosis through inhibition of endoplasmic reticulum stress in pig kidneys. *Ecotoxicol. Environ. Saf.* 223, 112596. doi: 10.1016/j.ecoenv.2021.112596
- Heintz-Buschart, A., Pandey, U., Wicke, T., Sixel-Doring, F., Janzen, A., Sittig-Wiegand, E., et al. (2018). The nasal and gut microbiome in Parkinson's disease and idiopathic rapid eye movement sleep behavior disorder. *Mov. Disord.* 33, 88–98. doi: 10.1002/mds.27105
- Hoche, F., Klapperstuck, T., and Wohlrab, J. (2004). Effects of L-ornithine on metabolic processes of the urea cycle in human keratinocytes. *Skin Pharmacol. Physiol.* 17, 283–288. doi: 10.1159/000081113
- Hongxing, G., Xiafei, L., Jialing, L., Zhenquan, C., Luoyu, G., Lei, L., et al. (2021). Effects of acute ammonia exposure on antioxidant and detoxification metabolism in clam *Cyclina sinensis*. *Ecotoxicol. Environ. Saf.* 211, 111895. doi: 10.1016/j.ecoenv.2021.111895
- Jandhyala, S. M., Talukdar, R., Subramanyam, C., Vuyyuru, H., Sasikala, M., Nageshwar Reddy, D., et al. (2015). Role of the normal gut microbiota. *World J. Gastroenterol.* 21, 8787–8803. doi: 10.3748/wjg.v21.i29.8787
- Jin, D. X., Zou, H. W., Liu, S. Q., Wang, L. Z., Xue, B., Wu, D., et al. (2018). The underlying microbial mechanism of epizootic rabbit enteropathy triggered by a low fiber diet. *Sci. Rep.* 8, 12489. doi: 10.1038/s41598-018-30178-2
- Jin, L., Li, D., Alesi, G. N., Fan, J., Kang, H. B., Lu, Z., et al. (2015). Glutamate dehydrogenase 1 signals through antioxidant glutathione peroxidase 1 to regulate redox homeostasis and tumor growth. *Cancer Cell* 27, 257–270. doi: 10.1016/j.ccr.2014.12.006
- Katunuma, N., Okada, M., and Nishii, Y. (1966). Regulation of the urea cycle and tca cycle by ammonia. *Adv. Enzyme Regul.* 4, 317–336. doi: 10.1016/0065-2571(66)90025-2
- Ke, S., Fang, S., He, M., Huang, X., Yang, H., Yang, B., et al. (2019). Age-based dynamic changes of phylogenetic composition and interaction networks of health pig gut microbiome feeding in a uniformed condition. *BMC Vet. Res.* 15, 172. doi: 10.1186/s12917-019-1918-5
- Keulers, L., Dehghani, A., Knippels, L., Garssen, J., Papadopoulos, N., Folkerts, G., et al. (2022). Probiotics, prebiotics, and synbiotics to prevent or combat air pollution consequences: the gut-lung axis. *Environ. Pollut.* 302, 119066. doi: 10.1016/j.envpol.2022.119066
- Kilic, I., Simsek, E., Yaslioglu, E., Heber, A., and Uguz, S. (2021). Air quality measurements in four sheep barns part II: pollutant gas emissions. *Environ. Sci. Pollut. Res. Int.* 28, 19064–19078. doi: 10.1007/s11356-020-12184-y
- Kim, H. K., Lee, G. H., Bhattarai, K. R., Lee, M. S., Back, S. H., Kim, H. R., et al. (2021). Tmbim6 (transmembrane bax inhibitor motif containing 6) enhances autophagy through regulation of lysosomal calcium. *Autophagy* 17, 761–778. doi: 10.1080/15548627.2020.1732161
- Kim, S., Goel, R., Kumar, A., Qi, Y., Lobaton, G., Hosaka, K., et al. (2018). Imbalance of gut microbiome and intestinal epithelial barrier dysfunction in patients with high blood pressure. *Clin. Sci.* 132, 701–718. doi: 10.1042/CS20180087
- Kim, W. G., Kang, G. D., Kim, H. I., Han, M. J., and Kim, D. H. (2019). *Bifidobacterium longum* Im55 and *Lactobacillus plantarum* Im76 alleviate allergic rhinitis in mice by restoring Th2/Treg imbalance and gut microbiota disturbance. *Benef. Microbes* 10, 55–67. doi: 10.3920/BM2017.0146
- Lee, J. J., Kim, S. H., Lee, M. J., Kim, B. K., Song, W. J., Park, H. W., et al. (2019). Different upper airway microbiome and their functional genes associated with asthma in young adults and elderly individuals. *Allergy* 74, 709–719. doi: 10.1111/all.13608
- Li, L. H., and Qi, H. X. (2019). Effect of acute ammonia exposure on the glutathione redox system in Ffrc strain common carp (*Cyprinus carpio*, L.). *Environ. Sci. Pollut. Res. Int.* 26, 27023–27031. doi: 10.1007/s11356-019-05895-4
- Li, Y., Pan, L., Zeng, X., Zhang, R., Li, X., Li, J., et al. (2021a). Ammonia exposure causes the imbalance of the gut-brain axis by altering gene networks associated with oxidative metabolism, inflammation and apoptosis. *Ecotoxicol. Environ. Saf.* 224, 112668. doi: 10.1016/j.ecoenv.2021.112668
- Li, Y., Yan, P., Lei, Q., Li, B., Sun, Y., Li, S., et al. (2019). Metabolic adaptability shifts of cell membrane fatty acids of *Komagataeibacter hansenii* Hdm1-3 improve acid stress resistance and survival in acidic environments. *J. Ind. Microbiol. Biotechnol.* 46, 1491–1503. doi: 10.1007/s10295-019-02225-y
- Li, Y., Zhang, R., Li, X., Li, J., Ji, W., Zeng, X., et al. (2021b). Exposure to the environmental pollutant ammonia causes changes in gut microbiota and inflammatory markers in fattening pigs. *Ecotoxicol. Environ. Saf.* 208, 111564. doi: 10.1016/j.ecoenv.2020.111564
- Liu, Q. X., Zhou, Y., Li, X. M., Ma, D. D., Xing, S., Feng, J. H., et al. (2020). Ammonia induce lung tissue injury in broilers by activating Nlrp3 inflammasome via Escherichia/Shigella. *Poult. Sci.* 99, 3402–3410. doi: 10.1016/j.psj.2020.03.019
- Lopez-Serrano, S., Galofre-Mila, N., Costa-Hurtado, M., Perez-de-Rozas, A. M., and Aragon, V. (2020). Heterogeneity of moraxella isolates found in the nasal cavities of piglets. *BMC Vet. Res.* 16, 28. doi: 10.1186/s12917-020-2250-9
- Louis, P., and Flint, H. J. (2017). Formation of propionate and butyrate by the human colonic microbiota. *Environ. Microbiol.* 19, 29–41. doi: 10.1111/1462-2920.13589
- Lv, X., Chai, J., Diao, Q., Huang, W., Zhuang, Y., Zhang, N., et al. (2019). The signature microbiota drive rumen function shifts in goat kids introduced to solid diet regimes. *Microorganisms* 7:516. doi: 10.3390/microorganisms7110516
- Ma, S., Zhang, F., Zhou, F., Li, H., Ge, W., Gan, R., et al. (2021). Metagenomic analysis reveals oropharyngeal microbiota alterations in patients with Covid-19. *Signal Transd. Target. Therapy* 6, 191. doi: 10.1038/s41392-021-00614-3
- Martins, I., Galluzzi, L., and Kroemer, G. (2011). Hormesis, cell death and aging. *Aging* 3, 821–828. doi: 10.18632/aging.100380
- McCauley, K., Durack, J., Valladares, R., Fadrosch, D. W., Lin, D. L., Calatroni, A., et al. (2019). Distinct nasal airway bacterial microbiotas differentially relate

- to exacerbation in pediatric patients with asthma. *J. Allergy Clin. Immunol.* 144, 1187–1197. doi: 10.1016/j.jaci.2019.05.035
- Morawska-Kochman, M., Jermakow, K., Nelke, K., Zub, K., Pawlak, W., Dudek, K., et al. (2019). The Ph value as a factor modifying bacterial colonization of sinonasal mucosa in healthy persons. *Ann. Otol. Rhinol. Laryngol.* 128, 819–828. doi: 10.1177/0003489419843143
- Mousavi, S. E., Delgado-Saborit, J. M., Adivi, A., Pauwels, S., and Godderis, L. (2022). Air pollution and endocrine disruptors induce human microbiome imbalances: a systematic review of recent evidence and possible biological mechanisms. *Sci. Total Environ.* 816, 151654. doi: 10.1016/j.scitotenv.2021.151654
- Park, J. W., Jeong, J. S., Lee, S. I., and Kim, I. H. (2016). Effect of dietary supplementation with a probiotic (*Enterococcus faecium*) on production performance, excreta microflora, ammonia emission, and nutrient utilization in isa brown laying hens. *Poult. Sci.* 95, 2829–2835. doi: 10.3382/ps/pew241
- Philipp, T. M., Will, A., Richter, H., Winterhalter, P. R., Pohnert, G., Steinbrenner, H., et al. (2021). A coupled enzyme assay for detection of selenium-binding protein 1 (Selenbp1) methanethiol oxidase (Mto) activity in mature enterocytes. *Redox Biol.* 43, 101972. doi: 10.1016/j.redox.2021.101972
- Pokharel, B. B., Dos Santos, V. M., Wood, D., Van Heyst, B., and Harlander-Matauschek, A. (2017). Laying hens behave differently in artificially and naturally sourced ammoniated environments. *Poult. Sci.* 96, 4151–4157. doi: 10.3382/ps/pex273
- Premachandra, H. K. A., Elvitigala, D. A. S., Whang, I., Kim, E., De Zoysa, M., Lim, B. S., et al. (2013). Expression profile of cystatin B ortholog from manila clam (*Ruditapes philippinarum*) in host pathology with respect to its structural and functional properties. *Fish Shellfish Immunol.* 34, 1505–1513. doi: 10.1016/j.fsi.2013.03.349
- Qin, T., Zhang, F., Zhou, H., Ren, H., Du, Y., Liang, S., et al. (2019). High-level Pm<sub>2.5</sub>/Pm<sub>10</sub> exposure is associated with alterations in the human pharyngeal microbiota composition. *Front. Microbiol.* 10, 54. doi: 10.3389/fmicb.2019.00054
- Qin, W., Shen, L., Wang, Q., Gao, Y., She, M., Li, X., et al. (2022). Chronic exposure to ammonia induces oxidative stress and enhanced glycolysis in lung of piglets. *Environ. Toxicol.* 37, 179–191. doi: 10.1002/tox.23382
- Rodríguez-Palacios, A., Harding, A., Menghini, P., Himmelman, C., Retuerto, M., Nickerson, K. P., et al. (2018). The artificial sweetener splenda promotes gut proteobacteria, dysbiosis, and myeloperoxidase reactivity in crohn's disease-like ileitis. *Inflamm. Bowel Dis.* 24, 1005–1020. doi: 10.1093/ibd/izy060
- Shin, T. H., Seo, C., Lee, D. Y., Ji, M., Manavalan, B., Basith, S., et al. (2019). Silica-coated magnetic nanoparticles induce glucose metabolic dysfunction *in vitro* via the generation of reactive oxygen species. *Arch. Toxicol.* 93, 1201–1212. doi: 10.1007/s00204-019-02402-z
- Sies, H., and Jones, D. P. (2020). Reactive oxygen species (ros) as pleiotropic physiological signalling agents. *Nat. Rev. Mol. Cell Biol.* 21, 363–383. doi: 10.1038/s41580-020-0230-3
- Stancik, L. M., Stancik, D. M., Schmidt, B., Barnhart, D. M., Yoncheva, Y. N., Slonczewski, J. L., et al. (2002). Ph-dependent expression of periplasmic proteins and amino acid catabolism in *Escherichia coli*. *J. Bacteriol.* 184, 4246–4258. doi: 10.1128/JB.184.15.4246-4258.2002
- Su, H., Na, N., Zhang, X., and Zhao, Y. (2017). The biological function and significance of Cd74 in immune diseases. *Inflamm. Res.* 66, 209–216. doi: 10.1007/s00011-016-0995-1
- Sun, H., Wang, W., Li, J., and Yang, Z. (2014). Growth, oxidative stress responses, and gene transcription of juvenile bighead carp (*Hypophthalmichthys nobilis*) under chronic-term exposure of ammonia. *Environ. Toxicol. Chem.* 33, 1726–1731. doi: 10.1002/etc.2613
- Takahashi, K., Koga, K., Lin, G. H., Zhang, Y., Lin, X., Metz, C. N., et al. (2009). Macrophage Cd74 contributes to mif-induced pulmonary inflammation. *Respir. Res.* 10, 33. doi: 10.1186/1465-9921-10-33
- Tang, S., Xie, J., Wu, W., Yi, B., Liu, L., Zhang, H., et al. (2020). High ammonia exposure regulates lipid metabolism in the pig skeletal muscle via mtor pathway. *Sci. Total Environ.* 740, 139917. doi: 10.1016/j.scitotenv.2020.139917
- Tang, S., Zhong, R., Yin, C., Su, D., Xie, J., Chen, L., et al. (2021b). Exposure to high aerial ammonia causes hindgut dysbiotic microbiota and alterations of microbiota-derived metabolites in growing pigs. *Front. Nutr.* 8, 689818. doi: 10.3389/fnut.2021.689818
- Tao, Z., Xu, W., Zhu, C., Zhang, S., Shi, Z., Song, W., et al. (2019). Effects of ammonia on intestinal microflora and productive performance of laying ducks. *Poult. Sci.* 98, 1947–1959. doi: 10.3382/ps/pey578
- Thiele Orberg, E., Fan, H., Tam, A. J., Dejea, C. M., Destefano Shields, C. E., Wu, S., et al. (2017). The myeloid immune signature of enterotoxigenic bacteroides fragilis-induced murine colon tumorigenesis. *Mucosal Immunol.* 10, 421–433. doi: 10.1038/mi.2016.53
- Ticinesi, A., Lauretani, F., Tana, C., Nouvenne, A., Ridolo, E., Meschi, T., et al. (2019). Exercise and immune system as modulators of intestinal microbiome: implications for the gut-muscle axis hypothesis. *Exerc. Immunol. Rev.* 25, 84–95.
- Urbain, B., Gustin, P., Charlier, G., Coignoul, F., Lambotte, J. L., Grignon, G., et al. (1996). A morphometric and functional study of the toxicity of atmospheric ammonia in the extrathoracic airways in pigs. *Vet. Res. Commun.* 20, 381–399. doi: 10.1007/BF00366545
- Voss, C. M., Arildsen, L., Nissen, J. D., Waagepetersen, H. S., Schousboe, A., Maechler, P., et al. (2021). Glutamate dehydrogenase is important for ammonia fixation and amino acid homeostasis in brain during hyperammonemia. *Front. Neurosci.* 15, 646291. doi: 10.3389/fnins.2021.646291
- Wang, G., Liu, Q., Zhou, Y., Feng, J., and Zhang, M. (2022). Effects of different ammonia concentrations on pulmonary microbial flora, lung tissue mucosal morphology, inflammatory cytokines, and neurotransmitters of broilers. *Animals* 12:261. doi: 10.3390/ani12030261
- Wang, H., Zeng, X., Zhang, X., Liu, H., and Xing, H. (2021). Ammonia exposure induces oxidative stress and inflammation by destroying the microtubule structures and the balance of solute carriers in the trachea of pigs. *Ecotoxicol. Environ. Saf.* 212, 111974. doi: 10.1016/j.ecoenv.2021.111974
- Wang, L., Sun, M., Lin, X., Lei, Y., Yin, Z., Zhou, W., et al. (2021). Down-regulation of Hbxip inhibits non-small cell lung cancer growth and enhances the anti-tumor immunity of mice by reducing Nrp-1. *Ann. Clin. Lab. Sci.* 51, 487–493.
- Wang, S., Li, X., Zhang, M., Jiang, H., Wang, R., Qian, Y., et al. (2021). Ammonia stress disrupts intestinal microbial community and amino acid metabolism of juvenile yellow catfish (*Pelteobagrus fulvidraco*). *Ecotoxicol. Environ. Saf.* 227, 112932. doi: 10.1016/j.ecoenv.2021.112932
- Wang, T., He, Q., Yao, W., Shao, Y., Li, J., Huang, F., et al. (2019). The variation of nasal microbiota caused by low levels of gaseous ammonia exposure in growing pigs. *Front. Microbiol.* 10, 1083. doi: 10.3389/fmicb.2019.01083
- Wang, X., Wang, M., Chen, S., Wei, B., Gao, Y., Huang, L., et al. (2020). Ammonia exposure causes lung injuries and disturbs pulmonary circadian clock gene network in a pig study. *Ecotoxicol. Environ. Saf.* 205, 111050. doi: 10.1016/j.ecoenv.2020.111050
- Wu, D., Zhang, M., Xu, J., Song, E., Lv, Y., Tang, S., et al. (2016). *In vitro* evaluation of aspirin-induced hspb1 against heat stress damage in chicken myocardial cells. *Cell Stress Chaper.* 21, 405–413. doi: 10.1007/s12192-016-0666-8
- Wu, S. E., Hashimoto-Hill, S., Woo, V., Eshleman, E. M., Whitt, J., Engleman, L., et al. (2020). Microbiota-derived metabolite promotes Hdac3 activity in the gut. *Nature* 586, 108–112. doi: 10.1038/s41586-020-2604-2
- Wu, X., Luo, Q., and Liu, Z. (2020). Ubiquitination and deubiquitination of mcl1 in cancer: deciphering chemoresistance mechanisms and providing potential therapeutic options. *Cell Death Dis.* 11, 556. doi: 10.1038/s41419-020-02760-y
- Xia, Y., Liu, N., Xie, X., Bi, G., Ba, H., Li, L., et al. (2019). The Macrophage-specific V-atpase subunit Atp6v0d2 restricts inflammasome activation and bacterial infection by facilitating autophagosome-lysosome fusion. *Autophagy* 15, 960–975. doi: 10.1080/15548627.2019.1569916
- Yeh, W. L., Hsu, Y. J., Ho, C. S., Ho, H. H., Kuo, Y. W., Tsai, S. Y., et al. (2022). *Lactobacillus plantarum* PL-02 supplementation combined with resistance training improved muscle mass, force, and exercise performance in mice. *Front. Nutr.* 9, 896503. doi: 10.3389/fnut.2022.896503
- Yin, H., Zhong, Y., Wang, H., Hu, J., Xia, S., Xiao, Y., et al. (2022). Short-term exposure to high relative humidity increases blood urea and influences colonic urea-nitrogen metabolism by altering the gut microbiota. *J. Adv. Res.* 35, 153–168. doi: 10.1016/j.jare.2021.03.004
- Zhang, X., Yang, F., Zhang, X., Xu, Y., Liao, T., Song, S., et al. (2008). Induction of hepatic enzymes and oxidative stress in Chinese rare minnow (*Gobiocypris rarus*) exposed to waterborne hexabromocyclodecane (Hbcbd). *Aquat. Toxicol.* 86, 4–11. doi: 10.1016/j.aquatox.2007.07.002
- Zheng, F., Gonçalves, F. M., Abiko, Y., Li, H., Kumagai, Y., Aschner, M., et al. (2020). Redox toxicology of environmental chemicals causing oxidative stress. *Redox Biol.* 34, 101475. doi: 10.1016/j.redox.2020.101475
- Zhou, Y., Zhang, M., Zhao, X., and Feng, J. (2021). Ammonia exposure induced intestinal inflammation injury mediated by intestinal microbiota in broiler chickens via Tlr4/Tnf- $\alpha$  signaling pathway. *Ecotoxicol. Environ. Saf.* 226, 112832. doi: 10.1016/j.ecoenv.2021.112832
- Zhu, L., Xu, L. Z., Zhao, S., Shen, Z. F., Shen, H., Zhan, L. B., et al. (2020). Protective effect of baicalin on the regulation of Treg/Th17 balance, gut microbiota and short-chain fatty acids in rats with ulcerative colitis. *Appl. Microbiol. Biotechnol.* 104, 5449–5460. doi: 10.1007/s00253-020-10527-w





## OPEN ACCESS

EDITED BY  
Weiqi He,  
Soochow University, China

REVIEWED BY  
Hangshu Xin,  
Northeast Agricultural University, China  
Anusorn Cherdthong,  
Khon Kaen University, Thailand

\*CORRESPONDENCE  
Miao Lin  
✉ linmiao@yzu.edu.cn

RECEIVED 10 February 2023

ACCEPTED 20 April 2023

PUBLISHED 18 May 2023

## CITATION

Ji H, Tan D, Chen Y, Cheng Z, Zhao J and Lin M (2023) Effects of different manganese sources on nutrient digestibility, fecal bacterial community, and mineral excretion of weaning dairy calves. *Front. Microbiol.* 14:1163468. doi: 10.3389/fmicb.2023.1163468

## COPYRIGHT

© 2023 Ji, Tan, Chen, Cheng, Zhao and Lin. This is an open-access article distributed under the terms of the [Creative Commons Attribution License \(CC BY\)](https://creativecommons.org/licenses/by/4.0/). The use, distribution or reproduction in other forums is permitted, provided the original author(s) and the copyright owner(s) are credited and that the original publication in this journal is cited, in accordance with accepted academic practice. No use, distribution or reproduction is permitted which does not comply with these terms.

# Effects of different manganese sources on nutrient digestibility, fecal bacterial community, and mineral excretion of weaning dairy calves

Huimin Ji<sup>1</sup>, Dejin Tan<sup>1</sup>, Yuhua Chen<sup>1</sup>, Zhiqiang Cheng<sup>1</sup>,  
Jingwen Zhao<sup>1,2,3</sup> and Miao Lin<sup>1,2,3\*</sup>

<sup>1</sup>Institute of Animal Culture Collection and Application, College of Animal Science and Technology, Yangzhou University, Yangzhou, China, <sup>2</sup>Institutes of Agricultural Science and Technology Development, Yangzhou University, Yangzhou, China, <sup>3</sup>Joint International Research Laboratory of Agriculture and Agri-Product Safety, The Ministry of Education of China, Yangzhou University, Yangzhou, China

**Introduction:** Mn, which is an essential trace mineral for all animals, has functions in skeletal system development, carbohydrate and lipid metabolism. The aim of this study was to clarify the effects of different manganese (Mn) sources in basal diets on nutrient apparent digestibility, fecal microbes, and mineral elements excretion before and after weaning.

**Methods:** A total of 15 Holstein heifer calves (6-week-old,  $82.71 \pm 1.35$ , mean  $\pm$  standard error) were randomly designed into three groups (five each): no extra Mn supplemented (CON), 20 mg Mn/kg (dry matter basis) in the form of chelates of lysine and glutamic acid in a mixture of 1:1 (LGM), and 20 mg Mn/kg (dry matter basis) in the form of  $MnSO_4$ . All calves were weaned at 8 weeks of age. The experiment lasted for 28 days (14 days before weaning and 14 days after weaning). Dry matter intake (DMI) was recorded daily. The animals were weighed by electronic walk-over, and body size indices were collected using tape on days -14, -1, and 14 of weaning. The feces of calves was collected to measure the apparent digestibility of nutrients (acid insoluble ash was an internal marker) and bacterial community on days -1, 1, 3, 7, and 14 of weaning. Fecal mineral concentration was determined by inductively coupled plasma emission spectroscopy on days -1, 1, 7, and 14 of weaning.

**Results:** The results showed that, compared with the CON group, adding LGM to diets containing 158.82 mg/kg Mn increased the apparent digestibility ( $P < 0.05$ ). The Chao 1 and Shannon index of fecal bacteria decreased at day 1 in the LGM and  $MnSO_4$  groups and increased after weaning. The PCoA results indicated that the LGM group was distinctly separate from the CON and  $MnSO_4$  groups during the whole experimental period. Significant differences ( $P < 0.05$ ) were observed in the relative abundance of two phyla (*Proteobacteria* and *Spirochaetota*) and eight genera (*Alloprevotella*, *Prevotellaceae\_UCG-001*, *Clostridia* UCG 014, RF39, UCG-010, *Pseudomonas*, *Ralstonia*, and *Treponema*) in three groups. Moreover, the LGM group showed less excretion of Fe, P, and Mn than the  $MnSO_4$  group.

**Discussion:** In summary, 20 mg Mn/kg diet supplementation improved nutrient digestibility, changed the fecal microbial community, and reduced mineral excretion. Organic Mn supplementation in the diet had more advantages over the sulfate forms in weaning calves.

## KEYWORDS

Holstein heifers weaning, digestibility, bacteria, mineral element, feces

## 1. Introduction

Effective feeding and management of calves are linked to the future productive performance of the dairy herd on intensive farms. Therefore, the healthy development of calves, along with good growth performance, is strongly associated with the future development and economic efficiency of the farm. The rumen of a newborn calf is more similar to the stomach of monogastric animals and starts developing after receiving a solid diet (Baldwin et al., 2004). Therefore, before the rumen is fully developed, the feed digestion in calves is more dependent on enzymatic digestion in the hindgut (Guilloteau et al., 2009). Gut microbial colonization occurs from the day of birth and stimulates the development of animal defense mechanisms (Yáñez-Ruiz et al., 2015). The gut microbiota community in early life has long-term impacts on host health (Malmuthuge and Guan, 2017), and different positions of the GIT contain various communities (Malmuthuge et al., 2014), i.e., microbial diversity and richness increase from the proximal small intestine to the distal colon (Malmuthuge et al., 2015). The strong gut microbiota can form a barrier of bacterial membrane on the surface of intestinal epithelial cells, protect the host from harmful foreign bacteria, and inhibit the invasion and reproduction of gut pathogens by competing for nutrients (Bibiloni et al., 2005). Additionally, microbial diversity is also influenced by several factors, such as age, diet, and intake (Guilloteau et al., 2009), and trace mineral source (i.e., solubility) is one of the known influencing factors (Faulkner et al., 2017).

Spears (1996) believed that the mineral form is more important than the quantity. Chelating minerals can produce stable soluble molecules with high bioavailability and are better absorbed than inorganic forms, due to the fact that chelated minerals are metal ions bound to organic substances such as amino acids, peptides, or polysaccharides and are then absorbed through the pathway of ion-bound organic ligands, avoiding their interaction with other molecules (Kratzer and Vohra, 1996). Manganese (Mn), an essential trace mineral for all animals, is absorbed in the GIT after ingestion and then transported to mitochondria-containing organs such as the liver, pancreas, and pituitary, where it is rapidly enriched (Deng et al., 2013). Mn has functions in skeletal system development, carbohydrate and lipid metabolism, and the innate immune response (Santamaria, 2008; Haase, 2018). Organic sources (glycine amino acid-chelated zinc, manganese, and copper) presented higher bioavailability compared with inorganic sources (zinc sulfate monohydrate, manganese sulfate monohydrate, and copper sulfate pentahydrate) in Murrah buffalo (Mudgal et al., 2019). In addition, previous studies have reported the application of Mn in sheep, poultry, and swine production. Wong-Valle et al. (1989) reported that Mn concentration of the liver, the kidney, and the bones of sheep based on the multiple linear regression slopes, and the relative bioavailability of Mn from MnO, MnO<sub>2</sub>, and MnCO<sub>3</sub> averaged 57.7%, 32.9%, and 27.8%, compared with 100% for MnSO<sub>4</sub>. Manganese methionine hydroxyl analog chelated (Mn-MHAC; 25, 50, 75, and 100 mg Mn/kg) had a positive effect on body weight and average daily gain compared with the control group (Meng et al., 2021). Mn requirements for reproduction in swine are substantially greater than requirements for growth, with a recommendation of 25 mg/kg for gestating

(Hurley and Keen, 1987). However, there are few reports about the application of manganese in calf production. Weaning impacts the trace mineral status of calves and likely influences health and productivity outcomes (Caramalac et al., 2017). Thus, adding trace elements to calf diets before and after weaning is a strategy to guarantee animal performance. Bampidis et al. (2021) reported that supplementing with Mn in the form of chelates of lysine and glutamic acid in a mixture of 1:1 (LGM) was an effective manganese source for animals and friendly to the environment. It is worth investigating in depth how the effect of LGM on microbiota and mineral elements of calves' feces pre-weaning and post-weaning, as compared with sulfate forms. It was hypothesized that supplementation with organic sources of Mn would improve nutrient digestion, increase the relative abundance of beneficial bacteria, and reduce the excretion of mineral elements to the environment during the pre-weaning and post-weaning. Thus, the present study assessed the influence of feeding organic or inorganic manganese on the apparent digestibility of nutrients, fecal bacteria, and mineral elements in feces in pre-weaning and post-weaning calves.

## 2. Materials and methods

### 2.1. Animals and experimental design

All animals were cared for according to protocols approved by the Yangzhou University Laboratory Animal Care and Use Committee.

A total of 15 healthy Holstein calves (6 weeks old, 82.71 ± 1.35 kg BW) were randomly assigned to three groups and five calves each. Calves were housed individually and had free access to concentrate and water throughout the study period. The experimental diets were as follows: (1) a basal diet without Mn supplementation (CON), (2) 20 mg Mn/kg (dry matter basis) in the form of chelates (lysine Mn: glutamic acid Mn = 1:1, LGM), (3) 20 mg Mn/kg (dry matter basis) in the form of Mn sulfate (MnSO<sub>4</sub>; Figure 1). LGM was purchased from Zinpro Co. LTD (United States), and Mn content is 15%. Mn sulfate monohydrate (MnSO<sub>4</sub>·H<sub>2</sub>O) was purchased from Sichuan Combell Biotechnology Co. LTD (China), and Mn content is 31.8%. The study was conducted over a period of 28 days (28 November 2021 to 3 January 2022). Milk was provided (2 kg/day), and concentrate plus oat hay was offered freely two times daily (08:00 h and 18:00 h). LGM and MnSO<sub>4</sub> were mixed in milk pre-weaning and concentrate post-weaning. The chemical composition of the concentrate, oat hay, and milk fed to calves is shown in Supplementary Table 1.

### 2.2. Sampling and measurements

#### 2.2.1. Growth measurements

The amount of concentrate and oat hay offered and the residues were weighed daily for the average dry matter intake (DMI) calculation [average DMI/kg, (feed offered – residual feed)/test days × DM%] of each calf. The calves were weighed at the beginning of the experiment (day –14), the last day before weaning

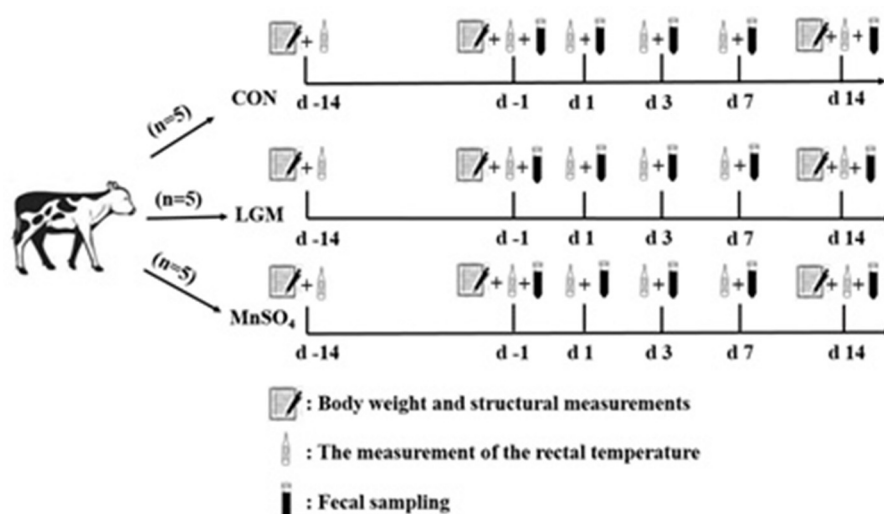


FIGURE 1

Diagram of the experimental design. LGM, in the form of chelates (lysine Mn: glutamic acid Mn = 1:1). MnSO<sub>4</sub>, in the form of sulfate Mn. days -14, -1, 1, 3, 7, and 14 represent calves at -14, -1, 1, 3, 7, and 14 days after weaning, respectively.

(day -1), and the final day of the experiment (day 14) by electronic walk-over weighing scale at 2–3 h after the morning feeding. The body height (vertical distance between the highest point of the withers and the ground), body length (distance between the points of the shoulder and pin bone), chest girth (body circumference immediately behind the front shoulder at the fourth rib, posterior to the front legs), cannon circumference (horizontal circumference of the thinnest point on the cannon bone of the left forelimb), hip height (vertical distance between the highest point of the hook bone and the ground), and hip width (distance between the points of hook bones) were measured using a tape. The average daily gain [ADG/kg, (final body weight – initial body weight)/28], feed/gain (F/G/%, average DMI/ADG), and body size growth (final body size – initial body size) of calves overall (day -14 to day 14), pre-weaning (day -14 to day -1), and post-weaning [first day before weaning (day -1) to day 14] were calculated from the above data. The rectal temperature of a calf was measured on days -14, -1, 1, 3 after weaning (day 3), 7th day after weaning (day 7), and day 14. The results are shown in [Supplementary Tables 2–4](#).

### 2.2.2. Collection and measurements of fecal samples

Fecal samples were collected aseptically from calves at days -1, 1, 3, 7, and 14. In total, 10% diluted sulfuric acid was mixed with a fecal sample (2 ml per 100 g sample) for nitrogen fixation. All feed and fecal samples were placed in a 65°C oven until dried and grounded through a 0.35 mm screen for later determination. The fecal dry matter (DM), ash, organic matter (OM), ether extract (EE), and crude protein (CP) were determined following the method described by [Silva and Queiroz \(2006\)](#). Neutral detergent fiber (NDF) and acid detergent fiber (ADF) were analyzed following the method described by [Soest \(1994\)](#). In addition, acid insoluble ash (AIA) was used as an internal marker to determine the nutrient digestibility of nutrients which was calculated using the equation

as follows:

$$\text{Nutrient digestibility (\%)} = [1 - (A1 \times F2) / (A2 \times F1)] \times 100 \text{ according to } \text{Álvarez-Rodríguez et al. (2017)}.$$

where A1 and A2 are the nutrient contents in feces and diet (%), respectively, F1 and F2 are the AIA contents in feces and diet (%), respectively.

For analyzing bacterial community, the fresh fecal sample was collected and measured by high-throughput sequencing by Beijing Novogene Biotechnology Co., LTD. In brief, total bacterial DNA was extracted using a TIANamp stool DNA kit (Tiangen Biotech Co., LTD). Then, the 16S rRNA V4 region gene was amplified by PCR using the primers 515F (5'-GTGCCAGCMGCCGCGGTAA-3') and 806R (5'-GGACTACHVGGGTWTCTAAT-3'). Alpha-diversity (observed OTUs and  $\alpha$  diversity index) and principal coordinate analysis (PCoA, unweighted Unifrac) were calculated using QIIME2.

For analyzing fecal minerals concentration, fresh samples at days -1, 1, 7, and 14 were placed in an oven at 45°C until dried. Then, 0.5 g samples were weighed into a 50 ml conical flask, digested (270°C) in the mixture of nitric acid and perchloric acid (6:1), and then diluted with deionized water to make a 25 ml solution. The minerals (iron, copper, calcium, phosphorus, manganese, and magnesium) were assayed by inductively coupled plasma emission spectroscopy (Optima 7300 DV, PerkinElmer Co., United States) ([Esaka, 2017](#)).

### 2.3. Statistical analysis

Data of apparent nutrient digestibility, fecal bacterial diversity indices, relative abundance of bacterial phylum and genus, and fecal mineral element concentrations were analyzed by PROC MIXED of

TABLE 1 Effects of different manganese sources on apparent digestibility of weaning calves.

Item	Group	Duration of treatment (days)					SEM	P-value		
		−1	1	3	7	14		D	T	D × T
DM	CON	57.31 <sup>Cb</sup>	69.92 <sup>Aa</sup>	45.26 <sup>Ce</sup>	47.13 <sup>Bd</sup>	54.13 <sup>Bc</sup>	7.19	<0.01	<0.01	<0.01
	LGM	64.89 <sup>Ba</sup>	64.60 <sup>Aa</sup>	56.61 <sup>Bb</sup>	57.61 <sup>Ab</sup>	54.91 <sup>Ab</sup>				
	MnSO <sub>4</sub>	68.05 <sup>Aa</sup>	53.77 <sup>Bcd</sup>	57.32 <sup>Abc</sup>	57.95 <sup>Ab</sup>	51.17 <sup>Bd</sup>				
OM	CON	63.89 <sup>Bb</sup>	73.08 <sup>Aa</sup>	51.42 <sup>Bc</sup>	50.19 <sup>Bc</sup>	59.32 <sup>b</sup>	6.92	<0.01	<0.01	<0.01
	LGM	69.34 <sup>Aa</sup>	67.25 <sup>Bb</sup>	62.48 <sup>Ac</sup>	62.75 <sup>Ac</sup>	60.14 <sup>d</sup>				
	MnSO <sub>4</sub>	72.54 <sup>Aa</sup>	52.40 <sup>Cd</sup>	62.50 <sup>Ab</sup>	63.58 <sup>Ab</sup>	56.89 <sup>c</sup>				
CP	CON	49.57 <sup>bc</sup>	67.55 <sup>Aa</sup>	51.78 <sup>Bbc</sup>	42.38 <sup>c</sup>	54.31 <sup>Ab</sup>	8.29	0.18	<0.01	<0.01
	LGM	63.05 <sup>a</sup>	53.65 <sup>Bb</sup>	53.64 <sup>Ab</sup>	56.51 <sup>b</sup>	56.26 <sup>Ab</sup>				
	MnSO <sub>4</sub>	54.62	40.05 <sup>C</sup>	52.50 <sup>A</sup>	50.87	45.92 <sup>B</sup>				
NDF	CON	43.74 <sup>Bb</sup>	55.80 <sup>Aa</sup>	33.22 <sup>Cc</sup>	33.25 <sup>Cc</sup>	38.69 <sup>bc</sup>	6.72	<0.01	<0.01	<0.01
	LGM	52.54 <sup>Aa</sup>	44.95 <sup>Bb</sup>	45.10 <sup>Ab</sup>	44.38 <sup>Ab</sup>	44.64 <sup>b</sup>				
	MnSO <sub>4</sub>	42.39 <sup>B</sup>	42.08 <sup>B</sup>	39.34 <sup>B</sup>	40.50 <sup>B</sup>	34.43				
ADF	CON	25.35 <sup>Bb</sup>	34.90 <sup>a</sup>	24.20 <sup>b</sup>	22.26 <sup>Bb</sup>	22.76 <sup>b</sup>	5.71	<0.01	<0.01	0.01
	LGM	36.89 <sup>Aa</sup>	32.00 <sup>ab</sup>	34.86 <sup>a</sup>	26.47 <sup>Ab</sup>	25.19 <sup>b</sup>				
	MnSO <sub>4</sub>	28.77 <sup>B</sup>	25.47	31.09	30.41 <sup>A</sup>	23.74				

Values in the same row (a–e) or in the same column (A–C) with different letters are significantly different ( $P < 0.05$ ). LGM, in the form of chelates (lysine Mn: glutamic acid Mn = 1:1). MnSO<sub>4</sub>, in the form of sulfate Mn. SEM, standard error of means. D, effect of day. T, effect of group. D × T, interaction between day and group.

SAS (version 9.4). The model used is as follows:

$$Y_{ijkl} = \mu + T_i + R_j + e_{ij} + e_{ijkl}$$

where  $Y_{ijkl}$  = observation,  $\mu$  = general mean,  $T_i$  = treatment effect,  $R_j$  = block effect,  $e_{ij}$  = experimental error (block × treatment), and  $e_{ijkl}$  = sampling error (cow × block × treatment × sample).

The statistical significance of the means of apparent nutrient digestibility, Chao1, Shannon and Simpson indexes, the analysis of PCoA results, the relative abundance of bacteria, and the concentration of fecal minerals were defined by  $P < 0.05$ . It is worth noting that correlation coefficients with absolute values  $>0.5$  are considered relevant. Significant differences were declared at  $P < 0.05$ , and  $P < 0.01$  was considered a highly significant difference.

## 3. Results

### 3.1. Effects of different manganese sources on apparent nutrient digestibility of weaning calves

Table 1 shows the apparent nutrient digestibility for days −1, 1, 3, 7, and 14. Mn supplementation and the interaction of day × treatment significantly affected the apparent digestibility of nutrients ( $P < 0.01$ ). Except for CP, there was a significant effect of days on the apparent nutrient digestibility ( $P < 0.05$ ). The nutrient digestibility was the highest on day −1 in the LGM group. The nutrient digestibility was the highest on day 1 in the

CON group ( $P < 0.01$ ), and then gradually decreased with time. Apparent nutrient digestibility was greater in the LGM and MnSO<sub>4</sub> groups than in the CON group on days 3 and 7 ( $P < 0.05$ ). The apparent digestibility of DM, OM, CP, NDF, and ADF in the CON group was 45.26%–69.92%, 50.19%–73.08%, 42.38%–67.55%, 33.22%–55.80%, and 22.26%–34.90%, respectively. The values in the LGM group were 54.91%–64.89%, 60.14%–69.34%, 53.64%–63.05%, 44.38%–52.54%, and 25.19%–36.89%, and in the MnSO<sub>4</sub> group, 51.17%–68.05%, 52.40%–72.54%, 40.05%–54.62%, 34.43–42.39%, and 23.74%–31.09%, respectively.

### 3.2. Effects of different manganese sources on fecal microbiota diversity of weaning calves

In this study, 16S rRNA was amplified, and its sequence was analyzed to study the effects of supplementation on the fecal microbiota of calves pre-weaning and post-weaning at five time points (days −1, 1, 3, 7, and 14), with an average of 61,544 sequences per fecal sample. These results reflect the interaction between treatment and day in three alpha diversity indices (Table 2,  $P < 0.05$ ). The Chao 1 index of CON is significantly higher than that of LGM and MnSO<sub>4</sub> on day −1 ( $P < 0.05$ ), and then gradually decreases. However, in the LGM and MnSO<sub>4</sub> groups, it was stabilized from days −1 to 14. The Shannon and Simpson index was significantly higher in the CON and LGM groups than the MnSO<sub>4</sub> group on day 1 ( $P < 0.05$ ).

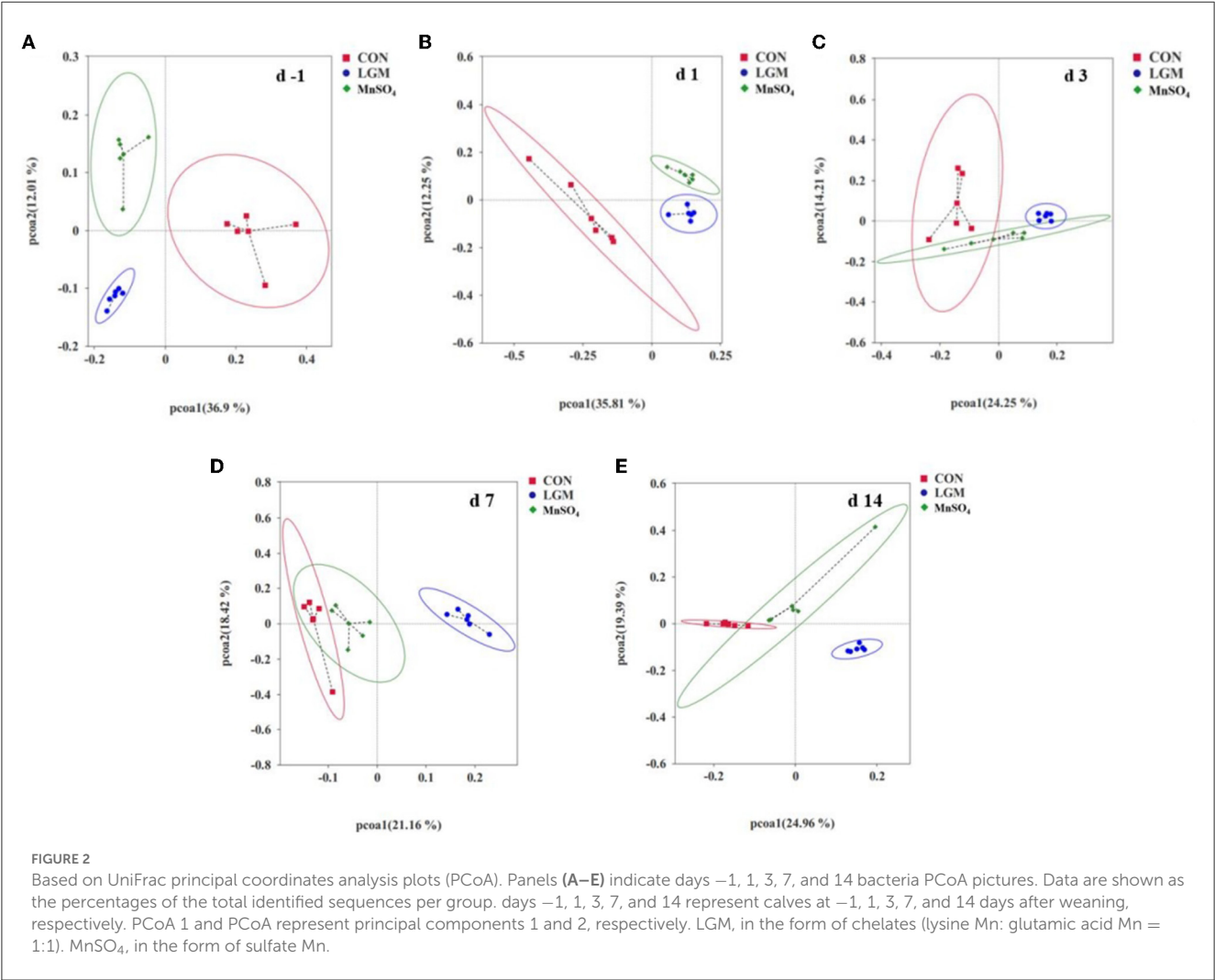
The principal coordinates analysis plot results showed that the fecal microbial community on day −1 was



TABLE 2 Effects of different manganese sources on fecal bacterial Chao1, Shannon, and Simpson indexes of weaning calves.

Item	Group	Duration of treatment (days)					SEM	P-value		
		−1	1	3	7	14		D	T	D × T
Chao1	CON	887.36 <sup>A</sup>	889.12	759.12	730.27	617.50	123.53	0.28	0.04	0.04
	LGM	696.57 <sup>B</sup>	681.35	737.62	717.54	707.20				
	MnSO <sub>4</sub>	704.88 <sup>B</sup>	653.97	714.67	735.71	699.50				
Shannon	CON	7.80	7.71 <sup>A</sup>	7.33	7.37	7.01	0.65	0.47	0.01	0.03
	LGM	7.55	7.54 <sup>A</sup>	7.49	7.12	7.44				
	MnSO <sub>4</sub>	7.20	6.19 <sup>B</sup>	6.91	7.49	7.15				
Simpson	CON	0.99	0.99 <sup>A</sup>	0.98	0.98	0.98	0.04	0.21	<0.01	0.01
	LGM	0.99	0.99 <sup>A</sup>	0.98	0.97	0.98				
	MnSO <sub>4</sub>	0.95	0.88 <sup>B</sup>	0.95	0.98	0.98				

Values in the same column (A, B) with different letters are significantly different ( $P < 0.05$ ). LGM, in the form of chelates (lysine Mn: glutamic acid Mn = 1:1). MnSO<sub>4</sub>, in the form of sulfate Mn. SEM, standard error of means. D, effect of day. T, effect of group. D × T, interaction between day and group.



significantly different among the three groups (Figure 2A). On day 1, the community of LGM and MnSO<sub>4</sub> was close (Figure 2B). By contrast, the community of MnSO<sub>4</sub> closed to CON on days 3, 7, and 14 after weaning, and that of LGM was kept more distance from the CON group (Figures 2C–E).

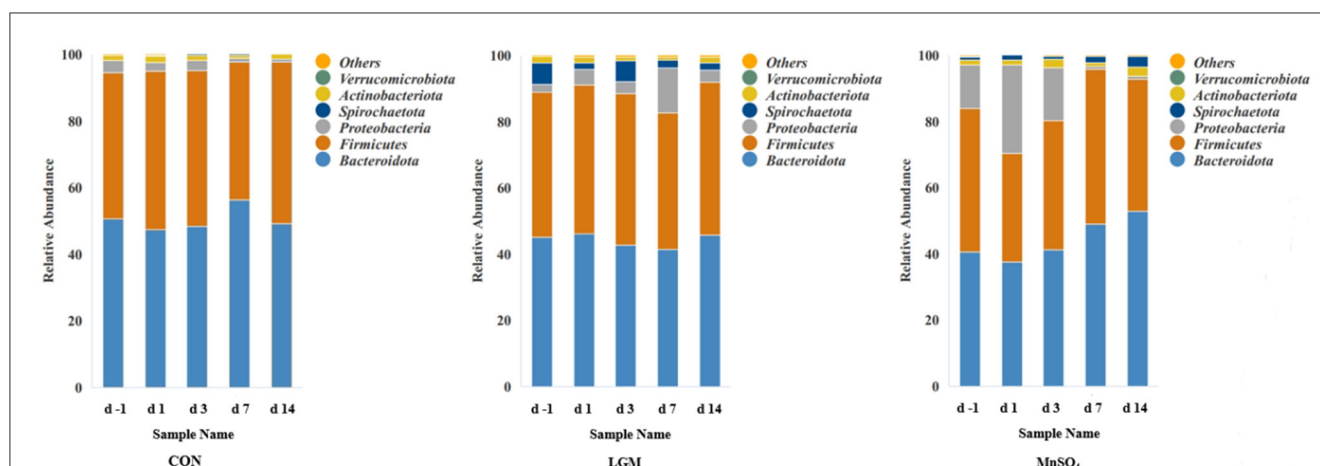


FIGURE 3

Relative abundances of the major phylum fecal bacterial. Data are shown as the percentages of the total identified sequences per group. days -1, 1, 3, 7, and 14 represent calves at -1, 1, 3, 7, and 14 days after weaning, respectively. LGM, in the form of chelates (lysine Mn: glutamic acid Mn = 1:1).  $\text{MnSO}_4$ , in the form of sulfate Mn.

### 3.3. Effects of different manganese sources on the relative abundance of fecal microbiota in weaning calves

The top six relative abundances of fecal bacteria at the phylum level were analyzed (Figure 3 and Supplementary Table 5). The predominant bacteria were *Bacteroidota* and *Firmicutes*. There was no significant difference in the relative abundance of *Bacteroidota* and *Actinobacteriota* according to Mn source or days. No day effect was observed in the relative abundance of *Firmicutes* and *Verrucomicrobiota*. Compared with CON, the relative abundance of *Firmicutes* in  $\text{MnSO}_4$  was lower on days -1, 7, and 14 ( $P < 0.01$ ), and that in LGM was lower on day 7 ( $P < 0.01$ ). The relative abundance of *Proteobacteria* was higher on day -1 in the  $\text{MnSO}_4$  group and day 14 in the LGM group ( $P < 0.01$ ). It decreased in the  $\text{MnSO}_4$  group on days 7 and 14 compared with days -1, 1, and 3 ( $P = 0.02$ ). The relative abundance of *Spirochaetota* in the LGM group was significantly higher than that of the CON and  $\text{MnSO}_4$  groups at days -1 and 3 ( $P < 0.05$ ).

The interaction of day  $\times$  treatment was significant ( $P < 0.05$ ) for the relative abundance of *Alloprevotella*, *Prevotellaceae\_UCG-001*, *Clostridia* UCG 014, RF39, UCG-010, *Pseudomonas*, *Ralstonia*, and *Treponema* ( $P < 0.05$ ; Table 3). Day effect was observed in the relative abundance of seven genera (*Prevotella*, *Alloprevotella*, *Alistipes*, UCG-005, *Clostridia* UCG 014, *Pseudomonas*, and *Ralstonia*;  $P < 0.05$ ). The treatment effect was observed in the relative abundance of all genera ( $P < 0.05$ ). The genus *Bacteroides*, which belongs to *Bacteroidota*, was the most abundant in the three groups.

### 3.4. Effects of different manganese sources on fecal minerals excretion of weaning calves

There was a significant difference in the concentration of minerals according to days (Table 4,  $P < 0.01$ ). No treatment

effect was observed in the Fe concentration. Moreover, the interaction of day  $\times$  treatment was shown in the concentrations of Cu, P, Mn, and Mg ( $P < 0.01$ ). The decrease in Fe, Ca, and P concentrations with days was observed in the two groups ( $P < 0.01$ ). The concentration of Cu and Mg was higher on day 1 in the LGM group and day -1 in the  $\text{MnSO}_4$  group ( $P < 0.01$ ). The Mn concentration was significantly lower on day -1 in the LGM and  $\text{MnSO}_4$  groups than at other time points ( $P = 0.01$ ).

### 3.5. Correlation analysis of fecal minerals and fecal major bacteria

Spearman's correlation analysis was performed to assess the relationship between fecal minerals and fecal microbiota structure in the presence of manganese sources. At the genus level, the relative abundance of *Bacteroides* was negatively correlated with the concentration of Cu ( $r = -0.40$ ,  $P < 0.01$ ) and Mg ( $r = -0.32$ ,  $P < 0.05$ ). The relative abundance of UCG-005 was negatively correlated with the concentrations of Fe ( $r = -0.38$ ,  $P < 0.01$ ), Cu ( $r = -0.40$ ,  $P < 0.01$ ), Mn ( $r = -0.44$ ,  $P < 0.01$ ), and Mg ( $r = -0.45$ ,  $P < 0.01$ ). The relative abundance of *Olsenella* was negatively correlated with the concentration of Mn ( $r = -0.40$ ,  $P < 0.01$ ) and Mg ( $r = -0.35$ ,  $P < 0.01$ ). The concentration of Fe was positively correlated with the relative abundance of the *Bacteroidales\_RF16\_group* ( $r = 0.28$ ,  $P < 0.05$ ). The concentration of Cu was positively correlated with the relative abundance of *Bacteroidales\_RF16\_group* ( $r = 0.55$ ,  $P < 0.001$ ), *Rikenellaceae\_RC9\_gut\_group* ( $r = 0.47$ ,  $P < 0.001$ ), *Prevotellaceae\_UCG-001* ( $r = 0.46$ ,  $P < 0.001$ ), *Sharpea* ( $r = 0.26$ ,  $P < 0.05$ ), *Treponema* ( $r = 0.61$ ,  $P < 0.001$ ), and *Akkermansia* ( $r = 0.51$ ,  $P < 0.001$ ). The concentration of Mn was positively correlated with the relative abundance of *Bacteroidales\_RF16\_group* ( $r = 0.55$ ,  $P < 0.001$ ), *Rikenellaceae\_RC9\_gut\_group* ( $r = 0.47$ ,  $P < 0.001$ ), *Clostridia\_UCG-014* ( $r = 0.46$ ,  $P < 0.001$ ), *Sharpea* ( $r = 0.56$ ,  $P < 0.001$ ), and *Treponema* ( $r = 0.55$ ,  $P < 0.001$ ). The

TABLE 3 Effects of different manganese sources on fecal bacteria of weaning calves at the genus level.

Phylum	Genus	Group	Duration of treatment (days)					SEM	P-value		
			−1	1	3	7	14		D	T	D × T
<i>Bacteroidota</i>	<i>Bacteroides</i>	CON	18.59 <sup>A</sup>	23.41 <sup>A</sup>	23.07	16.44 <sup>A</sup>	17.68	6.89	0.80	<0.01	0.15
		LGM	11.65 <sup>B</sup>	12.39 <sup>B</sup>	11.37	10.42 <sup>B</sup>	12.38				
		MnSO <sub>4</sub>	10.99 <sup>Bbc</sup>	9.57 <sup>Bc</sup>	12.58 <sup>abc</sup>	16.47 <sup>Aab</sup>	18.58 <sup>a</sup>				
	<i>Prevotella</i>	CON	1.40 <sup>Bb</sup>	2.22 <sup>Bb</sup>	3.11 <sup>b</sup>	3.13 <sup>b</sup>	5.92 <sup>Ba</sup>	2.28	<0.01	<0.01	0.77
		LGM	1.98 <sup>Bb</sup>	1.49 <sup>Bb</sup>	2.68 <sup>b</sup>	2.50 <sup>b</sup>	4.73 <sup>Ba</sup>				
		MnSO <sub>4</sub>	4.13 <sup>A</sup>	3.31 <sup>A</sup>	4.79	6.60	7.59 <sup>A</sup>				
	<i>Alloprevotella</i>	CON	2.24 <sup>Ab</sup>	2.56 <sup>Ab</sup>	2.19 <sup>Ab</sup>	2.78 <sup>Ab</sup>	5.03 <sup>Aa</sup>	1.32	<0.01	<0.01	<0.01
		LGM	0.40 <sup>B</sup>	0.39 <sup>B</sup>	0.39 <sup>B</sup>	0.55 <sup>B</sup>	0.81 <sup>C</sup>				
		MnSO <sub>4</sub>	0.57 <sup>Bb</sup>	0.32 <sup>Bb</sup>	1.60 <sup>ABa</sup>	2.30 <sup>Aa</sup>	2.48 <sup>Ba</sup>				
	<i>Alistipes</i>	CON	4.80 <sup>Aa</sup>	2.97 <sup>Ab</sup>	2.63 <sup>b</sup>	2.13 <sup>b</sup>	1.84 <sup>b</sup>	1.27	<0.01	<0.01	0.22
		LGM	4.33 <sup>A</sup>	3.83 <sup>A</sup>	2.75	3.10	2.58				
		MnSO <sub>4</sub>	2.91 <sup>B</sup>	1.50 <sup>B</sup>	1.81	1.76	2.18				
	<i>Bacteroidales RF16 group</i>	CON	0.26 <sup>B</sup>	0.27 <sup>B</sup>	0.15	0.35	0.15 <sup>B</sup>	1.41	0.90	<0.01	0.53
		LGM	1.74 <sup>A</sup>	1.37 <sup>A</sup>	1.68	1.58	2.60 <sup>A</sup>				
		MnSO <sub>4</sub>	1.56 <sup>A</sup>	2.75 <sup>A</sup>	1.35	2.26	1.28 <sup>AB</sup>				
	<i>Rikenellaceae RC9 gut group</i>	CON	1.00 <sup>B</sup>	1.02 <sup>C</sup>	1.00 <sup>B</sup>	1.31 <sup>B</sup>	1.99	1.92	0.22	<0.01	0.25
		LGM	3.48 <sup>A</sup>	4.05 <sup>A</sup>	4.61 <sup>A</sup>	5.05 <sup>A</sup>	3.76				
		MnSO <sub>4</sub>	2.77 <sup>AB</sup>	2.42 <sup>B</sup>	2.86 <sup>AB</sup>	2.38 <sup>B</sup>	4.98				
	<i>Prevotellaceae_UCG-001</i>	CON	0.28 <sup>B</sup>	0.53	0.43 <sup>B</sup>	0.59	0.45	0.56	0.17	<0.01	0.04
		LGM	1.93 <sup>A</sup>	0.88	0.78 <sup>A</sup>	0.89	0.71				
		MnSO <sub>4</sub>	0.67 <sup>B</sup>	0.65	0.57 <sup>AB</sup>	0.58	0.53				
<i>Firmicutes</i>	<i>UCG-005</i>	CON	8.53 <sup>A</sup>	9.09 <sup>A</sup>	8.35	12.93	7.55	3.61	0.05	<0.01	0.17
		LGM	7.18 <sup>A</sup>	6.30 <sup>B</sup>	7.40	5.65	4.87				
		MnSO <sub>4</sub>	4.35 <sup>Bb</sup>	3.41 <sup>Cb</sup>	3.83 <sup>b</sup>	8.63 <sup>a</sup>	5.50 <sup>b</sup>				
	<i>Clostridia UCG 014</i>	CON	3.05 <sup>Bc</sup>	3.34 <sup>Bc</sup>	4.20 <sup>Bbc</sup>	4.80 <sup>b</sup>	6.40 <sup>a</sup>	1.60	<0.01	<0.01	0.02
		LGM	4.36 <sup>Bb</sup>	5.33 <sup>Aab</sup>	3.92 <sup>Bb</sup>	4.50 <sup>ab</sup>	6.09 <sup>a</sup>				
		MnSO <sub>4</sub>	6.67 <sup>A</sup>	4.86 <sup>A</sup>	6.44 <sup>A</sup>	6.04	7.37				
	<i>RF39</i>	CON	2.81	2.80 <sup>AB</sup>	2.84	2.57	2.81	1.14	0.58	0.79	0.01
		LGM	3.60 <sup>ab</sup>	4.17 <sup>Aa</sup>	1.96 <sup>c</sup>	2.32 <sup>bc</sup>	2.45 <sup>bc</sup>				
		MnSO <sub>4</sub>	2.46 <sup>ab</sup>	1.62 <sup>Bb</sup>	2.99 <sup>ab</sup>	2.61 <sup>ab</sup>	3.82 <sup>a</sup>				
	<i>UCG-010</i>	CON	1.22	1.44 <sup>A</sup>	1.37 <sup>A</sup>	2.68 <sup>A</sup>	2.30 <sup>A</sup>	0.88	0.07	<0.01	0.05
		LGM	1.18	1.64 <sup>A</sup>	1.17 <sup>A</sup>	1.41 <sup>AB</sup>	0.56 <sup>B</sup>				
		MnSO <sub>4</sub>	0.57	0.37 <sup>B</sup>	0.42 <sup>B</sup>	0.90 <sup>B</sup>	1.00 <sup>B</sup>				
	<i>Sharpea</i>	CON	0.03	0.05	0.12	0.04 <sup>B</sup>	0.08	0.52	0.21	0.01	0.62
		LGM	0.07	0.08	0.06	0.14 <sup>B</sup>	0.27				
		MnSO <sub>4</sub>	0.29	0.07	0.40	0.49 <sup>A</sup>	1.07				
<i>Proteobacteria</i>	<i>Pseudomonas</i>	CON	0.13 <sup>C</sup>	0.24 <sup>C</sup>	0.11	0.16 <sup>B</sup>	0.30 <sup>B</sup>	1.85	0.03	<0.01	<0.01
		LGM	1.63 <sup>B</sup>	2.36 <sup>B</sup>	2.38	2.65 <sup>A</sup>	2.59 <sup>A</sup>				
		MnSO <sub>4</sub>	4.15 <sup>Aab</sup>	4.78 <sup>Aa</sup>	2.95 <sup>b</sup>	0.05 <sup>Bc</sup>	0.14 <sup>Bc</sup>				
	<i>Ralstonia</i>	CON	0.28	0.03 <sup>B</sup>	0.20	0.02 <sup>B</sup>	0.01 <sup>B</sup>	0.66	<0.01	<0.01	<0.01
		LGM	0.31	0.88 <sup>AB</sup>	0.52	0.63 <sup>A</sup>	0.46 <sup>A</sup>				
		MnSO <sub>4</sub>	0.88 <sup>b</sup>	1.85 <sup>Aa</sup>	0.62 <sup>b</sup>	0.06 <sup>Bb</sup>	0.03 <sup>Bb</sup>				

(Continued)

TABLE 3 (Continued)

Phylum	Genus	Group	Duration of treatment (days)					SEM	P-value		
			−1	1	3	7	14		D	T	D × T
<i>Spirochaetota</i>	<i>Treponema</i>	CON	0.02 <sup>B</sup>	0.09 <sup>A</sup>	0.07 <sup>B</sup>	0.07	0.06	2.50	0.11	<0.01	<0.01
		LGM	6.34 <sup>Aa</sup>	1.94 <sup>Ab</sup>	6.39 <sup>Aa</sup>	2.36 <sup>b</sup>	2.17 <sup>b</sup>				
		MnSO <sub>4</sub>	1.04 <sup>B</sup>	1.32 <sup>B</sup>	0.90 <sup>B</sup>	2.08	3.15				
<i>Actinobacteriota</i>	<i>Bifidobacterium</i>	CON	0.74	0.24	0.72 <sup>B</sup>	0.16	0.24	1.43	0.49	0.07	0.91
		LGM	0.19	0.07	0.21 <sup>B</sup>	0.18	0.95				
		MnSO <sub>4</sub>	0.77	0.96	1.76 <sup>A</sup>	0.44	2.13				
	<i>Olsenella</i>	CON	0.31 <sup>B</sup>	0.89	0.53	0.62	0.79	0.66	0.22	<0.01	0.15
		LGM	1.53 <sup>A</sup>	1.48	0.52	0.54	0.63				
		MnSO <sub>4</sub>	0.49 <sup>B</sup>	0.27	0.35	0.21	0.42				
<i>Verrucomicrobiota</i>	<i>Akkermansia</i>	CON	0.01 <sup>B</sup>	0.01	0.00	0.00 <sup>B</sup>	0.00	0.07	0.20	<0.01	0.65
		LGM	0.11 <sup>A</sup>	0.13	0.05	0.02 <sup>A</sup>	0.06				
		MnSO <sub>4</sub>	0.04 <sup>B</sup>	0.01	0.00	0.00 <sup>B</sup>	0.00				

Values in the same row (a–c) or in the same column (A–C) with different letters are significantly different ( $P < 0.05$ ). LGM, in the form of chelates (lysine Mn: glutamic acid Mn = 1:1). MnSO<sub>4</sub>, in the form of sulfate Mn. SEM, standard error of means. D, effect of day. T, effect of group. D × T, interaction between day and group.

TABLE 4 Effects of different manganese sources on fecal minerals excretion of weaning calves.

Item	Group	Duration of treatment (days)				SEM	P-value		
		−1	1	7	14		D	T	D × T
Fe	LGM	801.47 <sup>a</sup>	504.15 <sup>b</sup>	586.69 <sup>b</sup>	380.27 <sup>c</sup>	178.16	<0.01	0.12	0.12
(mg/kg)	MnSO <sub>4</sub>	849.46 <sup>a</sup>	591.63 <sup>b</sup>	508.63 <sup>b</sup>	552.70 <sup>b</sup>				
Cu	LGM	75.36 <sup>b</sup>	82.41 <sup>a</sup>	75.96 <sup>b</sup>	61.39 <sup>c</sup>	8.26	<0.01	<0.01	<0.01
(mg/kg)	MnSO <sub>4</sub>	73.90 <sup>a</sup>	66.17 <sup>b</sup>	67.46 <sup>b</sup>	59.09 <sup>c</sup>				
Ca	LGM	1.92	1.65	1.59	1.45	0.10	0.02	<0.01	0.22
(%)	MnSO <sub>4</sub>	1.92 <sup>a</sup>	1.71 <sup>a</sup>	0.68 <sup>b</sup>	0.76 <sup>b</sup>				
P	LGM	0.80	0.73	0.71	0.74	0.47	<0.01	<0.01	<0.01
(%)	MnSO <sub>4</sub>	1.02 <sup>a</sup>	0.87 <sup>b</sup>	0.81 <sup>b</sup>	0.77 <sup>b</sup>				
Mn	LGM	435.24 <sup>c</sup>	591.94 <sup>a</sup>	586.99 <sup>a</sup>	484.01 <sup>b</sup>	75.33	<0.01	0.01	<0.01
(mg/kg)	MnSO <sub>4</sub>	469.44 <sup>c</sup>	540.95 <sup>b</sup>	663.31 <sup>a</sup>	526.16 <sup>b</sup>				
Mg	LGM	4651.46 <sup>b</sup>	5218.06 <sup>a</sup>	4658.62 <sup>b</sup>	4196.49 <sup>c</sup>	368.52	<0.01	<0.01	<0.01
(mg/kg)	MnSO <sub>4</sub>	5322.88 <sup>a</sup>	5115.52 <sup>b</sup>	4998.34 <sup>bc</sup>	4848.35 <sup>c</sup>				

Values in the same row (a–c) with different letters are significantly different ( $P < 0.05$ ). LGM, in the form of chelates (lysine Mn: glutamic acid Mn = 1:1). MnSO<sub>4</sub>, in the form of sulfate Mn. SEM, standard error of means. D, effect of day. T, effect of group. D × T, interaction between day and group.

concentration of Mg was positively correlated with the relative abundance of *Bacteroidales\_RF16\_group* ( $r = 0.57$ ,  $P < 0.001$ ), *Rikenellaceae\_RC9\_gut\_group* ( $r = 0.36$ ,  $P < 0.01$ ), *Prevotellaceae\_UCG-001* ( $r = 0.29$ ,  $P < 0.05$ ), *Clostridia\_UCG-014* ( $r = 0.31$ ,  $P < 0.05$ ), *Sharpea* ( $r = 0.40$ ,  $P < 0.01$ ), and *Treponema* ( $r = 0.51$ ,  $P < 0.001$ ; Figure 4).

## 4. Discussion

This study was based on the laboratory's previous dietary addition of 40 mg Mn/kg to Holstein cows (milk yield: 39.64 ± 5.55 kg, body weight: ~668.0 kg), which promoted both feed intake

and milk production of dairy cows. In addition, the manganese absorption rate of calves is higher than that of adult animals. Therefore, 20 mg Mn/kg was selected to be added into calf diets to study the effects of this concentration on the apparent digestibility of nutrients, fecal microorganisms, and excretion of fecal mineral elements of calves.

### 4.1. Effects of different manganese sources on apparent digestibility of weaning calves

The digestibility of nutrients reflects the utilization of nutrients by animals, which is important for animal growth. Insufficient solid



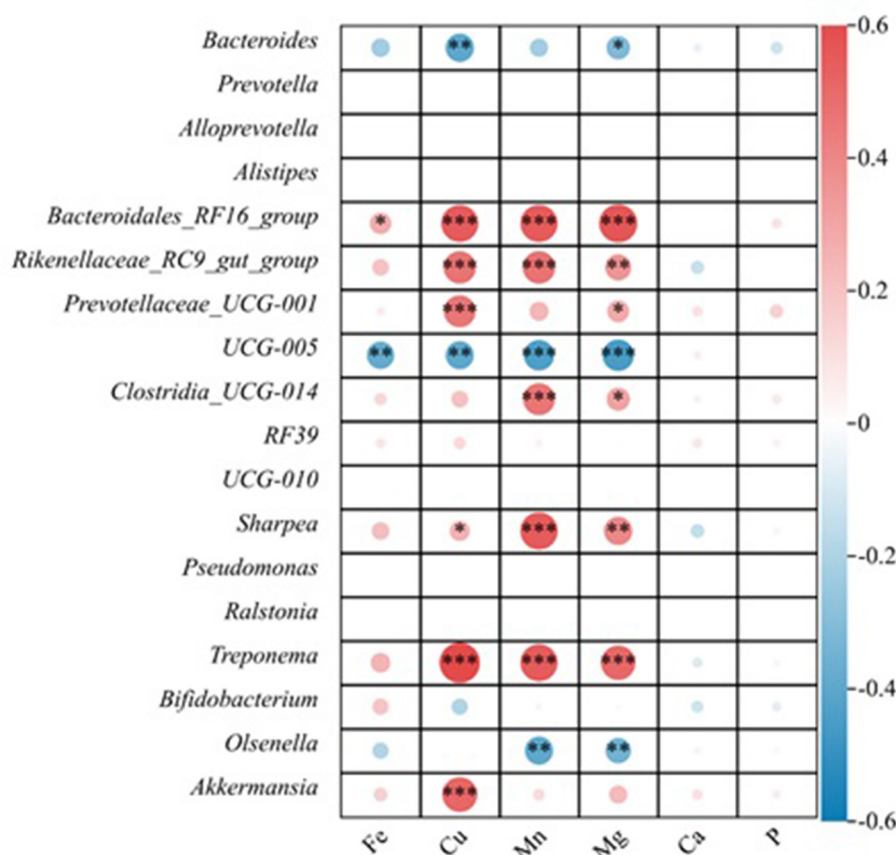


FIGURE 4

Spearman's correlation between fecal minerals and bacterial population. The area of the circle indicates the magnitude of the correlation, and the different colors indicate a positive correlation (red) or negative correlation (blue). \* indicates  $0.01 < P \leq 0.05$ , \*\* indicates  $P \leq 0.01$ , and \*\*\* indicates  $P \leq 0.001$ .

feed intake results in reduced apparent digestibility of nutrients, especially NDF and ADF, thus it is assumed that low solid feed intake may reduce the growth rate of calves post-weaning (Hill et al., 2010). In this study, the DMI of overall and post-weaning was significantly higher in the LGM and  $\text{MnSO}_4$  groups than in the CON group. Due to the low feed intake in the CON group, the apparent digestibility of DM in this group was lower than that of the LGM group except for day 1, indicating that the addition of LGM improved the nutrient utilization of calves. The diets supplemented with Mn, Zn, and Cu as methionine, glycine, and sulfate salts, respectively, had positive effects on DMI in dry cows (Roshanzamir et al., 2020). In the other study, sulfate sources reduced the total digestibility of NDF in cows compared with hydroxy sources in Cu, Mn, and Zn (Faulkner and Weiss, 2017). The results of this study are consistent with the study by Faulkner and Weiss (2017), and this may indicate stronger digestion and absorption of calves in the organic mineral-supplemented group. In addition, we observed a decrease in digestibility in calves post-weaning. Weaning stress was ruled out as it was not observed throughout the trial period. We speculated that the calves have an increased feed intake after weaning, and only solid feed was available.

#### 4.2. Effects of different manganese sources on the microbiota diversity and relative abundance of feces of weaning calves

The unique OTU number of the CON group in this study was higher than that of the LGM and  $\text{MnSO}_4$  groups at -1, 1, 3, and 7 days of weaning and decreased on day 14. The specific OTU number of the LGM and  $\text{MnSO}_4$  groups had been steadily increasing and exceeded the CON group on day 14. The analysis within-group revealed that the specific OTU number of the LGM and  $\text{MnSO}_4$  groups was proportional to the increase in age, but this was not found in the CON group. The Chao 1 index was numerically increased in the LGM and  $\text{MnSO}_4$  groups on days 3 and 7, which hinted that the bacterial richness of calves was disordered by weaning, but it could be quickly repaired by supplementation with Mn. The Shannon index was also not affected by time factors, but a lower Shannon index was observed in the LGM and  $\text{MnSO}_4$  groups. The Shannon index represented bacterial diversity and evenness (Shabat et al., 2016). Combining the digestibility and growth performance of calves, the lower the microbiota diversity in the rumen is accomplished by the higher metabolic efficiency (Tuomisto, 2010). However, calves fed

with extra manganese may provide more digestible fermentation products for animals in this study. According to previous reports, the stable equilibrium of microbial community lies in the ability as a whole to restore such changes to the original status when individual bacteria are disturbed or temporally damaged (Lozupone et al., 2012). A characteristic of the establishment of a healthy human gut microbiota is the increase in early diversity and stability of the microbiota (Palmer et al., 2007; Yatsunenko et al., 2012). In this study, the bacterial community of LGM did not coincide with that of CON and over the entire study, which indicated that organic Mn resulted in a more aggregated and stable bacterial community. The addition of LGM to the calf diet may have the function of maintaining the fecal microbiota during the weaning period.

Calves were fed solid feed pre-weaning, and there was no effect of time on the bacterial community at the phylum level, suggesting that the microbial community developed more maturely with the aging of calves (Li et al., 2012). Meale et al. (2016) also found that different weaning strategies (gradual vs. abrupt) did not affect the fecal microbiota of pre-weaning and post-weaning calves if they were fed solid feed before weaning. Research showed that the developing gut (1-day-old–2-month-old) and the more mature gut (2-year-old) contain the same dominant bacteria (*Bacteroidota*, *Firmicutes*, and *Proteobacteria*), but the relative abundance changes depending on the stage of development (Jami et al., 2013). Jami et al. (2013) reported that *Bacteroidota* was the predominant phylum of bacteria in 2-month-old calves, and the results obtained in this study are consistent with the study by Jami. According to published reports, *Prevotellaceae*\_UCG-001 has the ability to degrade non-cellulosic polysaccharides, pectins, and proteins (Flint et al., 2008; Kabel et al., 2011). The results of this study showed that the relative abundance of UCG-005 and UCG-010 was higher in the CON group. This may be the reason for the higher relative abundance of *Firmicutes* in the CON group than in the  $\text{MnSO}_4$  group on days 1, 7, and 14. It was found that *Ruminococcaceae* genera (UCG-005 and UCG-010) can convert complex polysaccharides into a variety of nutrients for the host (La Reau and Suen, 2018). *Sharpea* act as an important factor of lactate production and utilization (Kamke et al., 2016). In the present study, we observed an increase in the relative abundance of *Sharpea* in the  $\text{MnSO}_4$  group on day 7, although the relative abundance is not influenced by the time factor. Myer et al. (2015) detected that many genera in *Firmicutes* were associated with high ADG, consistent with the results of the present study.

The relative abundance of *Pseudomonas* and *Ralstonia* in the LGM group was higher than the other two groups. *Proteobacteria* is the dominant phylum in many environmental ecological niches (Lauber et al., 2009; Redford and Fierer, 2009) and play an important role in the colonization of the intestinal anaerobes of newborn calves. In this study, the relative abundance of *Proteobacteria* in the CON and  $\text{MnSO}_4$  groups was significantly higher than that of the LGM group on day –1 and then gradually decreased. However, in the LGM group, it was stabilized from days –1 to 14 and significantly higher on day 14 than the other two groups. In addition, the organic mineral-supplemented group had a significantly higher relative abundance of Spirochaetota than the CON and  $\text{MnSO}_4$  groups on days –1, 1, and 3. The richness of *Treponema*, a member of Spirochaetota, was significantly higher in the LGM group than that of the CON and  $\text{MnSO}_4$  groups at

–1, 1, and 3 days too. Gharechahi and Salekdeh (2018) performed metagenomic sequencing of rumen microorganisms of grazing camels and showed that Spirochaetota has significant potential to contribute to cellulose and hemicellulose degrading enzymes. Members of Spirochaetota, especially *Treponema*, are associated with the degradation of pectin in the rumen (Liu et al., 2015). The role played by Verrucomicrobiota in the rumen has been underappreciated due to its uncultured *in vitro* nature. It was found that Verrucomicrobiota is an organism known to code a variety of carbohydrate-degrading enzymes, peptidases, and sulfatase and is therefore considered well suited for degrading lignocellulose in the rumen (Martinez-Garcia et al., 2012). As observed in this study, the organic mineral group showed a more relative abundance of Verrucomicrobiota on day –1. In addition, the relative abundance of *Akkermansia*, which belonged to the Verrucomicrobiota phylum, was significantly higher in the LGM group on days –1 and 7. These results indicated that calves in the organic manganese group may have a stronger ability to degrade lignocellulose than those in the CON and  $\text{MnSO}_4$  groups. In addition, this also echoes the fact that calves in the LGM group had higher apparent digestibility of NDF and ADF.

### 4.3. Effects of different manganese sources on fecal trace minerals of weaning calves

In nature, trace minerals generally exist in the ionic state or in combination with certain molecular ligands (Weller et al., 2014), and this property is essential for animals, making them highly necessary components in animal diets. They excrete the excess supply through the circulation of animal organisms, and feces is one of the routes of excretion (Windisch, 2002). The concentrations of Fe, Cu, Ca, P, Mn, and Mg in the feces of lactating cows were 879 mg/kg, 75.7 mg/kg, 2.65%, 0.76%, 311 mg/kg, and 0.99%, respectively (Sheppard and Sanipelli, 2012). The results of this experiment were slightly lower than those of the Sheppard study except for Mn, which may be due to the lower intake of calves compared with lactating cows. Moreover, the concentration of trace minerals in feces was three times in the feed, which is consistent with the results of the present study (Sheppard et al., 2010). The absorption of Mn in cows is low (0.75% reported by NRC), and therefore, Mn is excreted in excess through the bile and small intestine (Ho et al., 1984). In the current study, the content of Mn in feces increased with the intake of calves, and as the Mn content in feces increased, the Fe content gradually decreased. Fe is the most important cofactor for oxygen transport and transfer in living organisms. Non-heme iron in the diet mainly exists as  $\text{Fe}^{3+}$ , which needs to be reduced to  $\text{Fe}^{2+}$  by ferredoxinase, and then transported across the intestinal epithelium by divalent metal ion transporter 1 (DMT1) (Gómez et al., 2005). DMT1 can also transport other metal ions such as Cu and Mn through a proton coupling mechanism (Gómez et al., 2005). However, sharing a common pathway in intestinal absorption through DMT1 results in the concentration of Mn affecting Fe and Cu absorption and utilization (Arredondo et al., 2003; Garrick et al., 2003). Data from this experiment suggest

that the amount of Cu in feces, which is similar to Fe, showed a pattern of increasing with the amount of fecal Mn in the mineral-supplemented groups. Ca is absorbed in the GIT by metabolism-driven intercellular transport and paracellular pathway (Liu et al., 2022). Fe can reduce the bioavailability of Ca (Zhang and Liu, 2022), and in this study, the fecal calcium and iron in the LGM and MnSO<sub>4</sub> groups showed a consistent pattern, with the highest concentration on day -1 and the lowest concentration on day 14. Overall, fecal calcium concentrations were not affected by the interaction. The P contents in the feces of 4-month-old heifers were lower (0.54%) than that in the present study (Bjelland et al., 2011), probably due to different basal diets for calves. The net absorption of Mg in the small intestine and large intestine is relatively low (Care and Vantklooster, 1965), which may be the fact that Mg excretion in the feces is higher than the other trace elements.

#### 4.4. Correlation analysis of fecal minerals and fecal major bacteria

Carrothers et al. (2015) analyzed the relationship between the fecal microbiota of lactating women and their diet and found that the intake of manganese was positively correlated with the relative abundance of *Firmicutes* ( $r = 0.44$ ), and the relative abundance of *Bacteroides* was negatively correlated ( $r = -0.48$ ). *Clostridia\_UCG-014* and *Sharpea* belonged to *Firmicutes*, and their relative abundance was positively correlated with the concentration of Mn in this study. *Sharpea* is a lactic acid-producing bacterium, and it has been reported that high concentrations of Mn<sup>2+</sup> are required for the growth of lactic acid bacteria (Archibald and Fridovich, 1981; Kamke et al., 2016). In addition, this study differs from that of Carrothers et al. (2015). First, UCG-005 in *Firmicutes* was negatively correlated with the concentration of Mn, which may be because the relative abundance of this genus was higher in the group without an Mn source. Second, the relative abundance of *Bacteroidales\_RF16\_group* and *Rikenellaceae\_RC9\_gut\_group* in the *Bacteroides* phylum was positively correlated with the concentration of Mn. This may be due to the fact that the experimental animals in this study are different from the study by Carrothers et al. (2015). The experimental animals in this study were 2-month-old calves, and the dominant bacterial genus of calves during this period was *Bacteroidetes* (Jami et al., 2013).

## 5. Conclusion

The addition of LGM pre-weaning and post-weaning increased the DMI, ADG, and chest circumference compared with the control group and the inorganic Mn group as the sulfate salt. The digestibility of pre-weaning and post-weaning calves in the LGM group was not greatly affected. In addition, LGM altered the fecal microbiota, and the relative abundance of the fiber-degrading bacteria *Treponema* and *Akkermansia* increased and a more stable fecal microbiota of pre-weaning and post-weaning calves in the LGM group. LGM increased the deposition of Mn in

the body, which was beneficial to environmental protection in terms of fecal mineral element excretion. Based on the factors of fecal bacterial community and environmental protection, adding 20 mg/kg LGM to the diet containing 158.82 mg/kg Mn is the best.

## Data availability statement

The datasets presented in this study can be found in online repositories. The names of the repository/repositories and accession number(s) can be found below: <https://ngdc.cncb.ac.cn/gsa/browse/CRA009807>.

## Ethics statement

The animal study was reviewed and approved by Yangzhou University, the Institutional Animal Care and Use Committee.

## Author contributions

HJ and ML performed the experiment and included chemical analysis, statistical analysis, and manuscript writing. ML and JZ worked on the manuscript revision and gave valuable advice. DT, ZC, and YC conducted the study. All authors have read and approved the final version of this manuscript.

## Funding

This study was supported by the Jiangsu Province Special Project for Carbon Peak & Carbon Neutral Science and Technology Innovation (BE2022309), the earmarked fund for CARS (CARS-36), and the Jiangsu Province graduate practical innovation program project (SJCX21\_1618).

## Acknowledgments

The authors would like to thank Novogene Corporation (Beijing, China) for the fecal microorganism assays.

## Conflict of interest

The authors declare that the research was conducted in the absence of any commercial or financial relationships that could be construed as a potential conflict of interest.

## Publisher's note

All claims expressed in this article are solely those of the authors and do not necessarily represent those of

their affiliated organizations, or those of the publisher, the editors and the reviewers. Any product that may be evaluated in this article, or claim that may be made by its manufacturer, is not guaranteed or endorsed by the publisher.

## References

- Álvarez-Rodríguez, J., Mir, L., Seradj, A. R., Morarán, H., Balcells, J., Babot, D., et al. (2017). Nutritional strategies to cope with reduced litter weight gain and total tract digestibility in lactating sows. *J. Anim. Physiol. Anim. Nutr.* 101, 914–924. doi: 10.1111/jpn.12523
- Archibald, F. S., and Fridovich, I. (1981). Manganese and defenses against oxygen toxicity in *Lactobacillus plantarum*. *J. Bacteriol.* 145, 442–451. doi: 10.1128/jb.145.1.442-451.1981
- Arredondo, M., Muñoz, P., Mura, C. V., and Núñez, M. (2003). DMT1, a physiologically relevant apical  $\text{Cu}^{1+}$  transporter of intestinal cells. *Am. J. Physiol.* 284, C1525–C1530. doi: 10.1152/ajpcell.00480.2002
- Baldwin, R. L., McLeod, K. R., Klotz, J. L., and Heitmann, R. N. (2004). Rumen development, intestinal growth and hepatic metabolism in the pre- and postweaning ruminant. *J. Dairy Sci.* 87, e55–e65. doi: 10.3168/jds.S0022-0302(04)70061-2
- Bampidis, V., Azimonti, G., Bastos, M. D. L., Christensen, H., Dusemund, B., Durjava, M. F., et al. (2021). Safety of the feed additive consisting of manganese chelates of lysine and glutamic acid for all animal species (Zinpro Animal Nutrition). *EFSA J.* 19, e06454. doi: 10.2903/j.efsa.2021.6454
- Bibiloni, R., Fedorak, R. N., Tannock, G. W., Madsen, K. L., Gionchetti, P., Campieri, M. C., et al. (2005). VSL#3 probiotic-mixture induces remission in patients with active ulcerative colitis. *Am. J. Gastroenterol.* 100, 1539–1546. doi: 10.1111/j.1572-0241.2005.41794.x
- Bjelland, D. W., Weigel, K. A., Hoffman, P. C., Esser, N. M., and Coblenz, W. K. (2011). The effect of feeding dairy heifers diets with and without supplemental phosphorus on growth, reproductive efficiency, health, and lactation performance. *J. Dairy Sci.* 94, 6233–6242. doi: 10.3168/jds.2011-4596
- Caramalac, L. S., Netto, A. S., Martins, P. G. M. A., Moriel, P., Ranches, J., Fernandes, H. J., et al. (2017). Effects of hydroxychloride sources of copper, zinc, and manganese on measures of supplement intake, mineral status, and pre- and postweaning performance of beef calves. *J. Anim. Sci.* 95, 1739–1750. doi: 10.2527/jas.2016.0934
- Care, A. D., and Vantklooster, A. T. (1965). *In vivo* transport of magnesium and other cations across the wall of the gastrointestinal tract of sheep. *J. Physiol.* 177, 174–191. doi: 10.1113/jphysiol.1965.sp007584
- Carrothers, J. M., York, M. A., Brooker, S. L., Lackey, K. A., Williams, J. E., Shafii, B., et al. (2015). Fecal microbial community structure is stable over time and related to variation in macronutrient and micronutrient intakes in lactating women. *J. Nutr.* 145, 2379–88. doi: 10.3945/jn.115.211110
- Deng, Q., Liu, J., Li, Q., Chen, K., Liu, Z., Shen, Y., et al. (2013). Interaction of occupational manganese exposure and alcohol drinking aggravates the increase of liver enzyme concentrations from a cross-sectional study in China. *Environ. Health Prevent. Med.* 12, 30. doi: 10.1186/1476-069X-12-30
- Esaka, F. (2017). Inductively coupled plasma-mass spectrometry. *Anal. Sci.* 33, 1097–1098. doi: 10.2116/analsci.33.1097
- Faulkner, M. J., and Weiss, W. P. (2017). Effect of source of trace minerals in either forage- or by-product-based diets fed to dairy cows: 1. Production and macronutrient digestibility. *J. Dairy Sci.* 100, 5358–5367. doi: 10.3168/jds.2016-12095
- Faulkner, M. J., Wenner, B. A., Solden, L. M., and Weiss, W. P. (2017). Source of supplemental dietary copper, zinc, and manganese affects fecal microbial relative abundance in lactating dairy cows. *J. Dairy Sci.* 100, 1037–1044. doi: 10.3168/jds.2016-11680
- Flint, H. J., Bayer, E. A., Rincon, M. T., Lamed, R., and White, B. A. (2008). Polysaccharide utilization by gut bacteria: potential for new insights from genomic analysis. *Nat. Rev. Microbiol.* 6, 121–131. doi: 10.1038/nrmicro1817
- Garrick, M. D., Dolan, K. G., Horbinski, C., Ghio, A. J., Higgins, D., Porubcin, M., et al. (2003). DMT1: a mammalian transporter for multiple metals. *Biomaterials* 16, 41–54. doi: 10.1023/A:1020702213099
- Gharechahi, J., and Salekdeh, G. H. (2018). A metagenomic analysis of the camel rumen's microbiome identifies the major microbes responsible for lignocellulose degradation and fermentation. *Biotechnol. Biofuels* 11, 216. doi: 10.1186/s13068-018-1214-9
- Gómez, M. M., Garrigues, A. C., Erce, J. A. G., and Ramírez, G. R. (2005). [Fisiopathology of iron metabolism: diagnostic and therapeutic implications]. *Nefrología* 25, 9–19. Available online at: <https://europepmc.org/article/MED/15789532>
- Guilloteau, P., Zabielski, R., and Blum, J. W. (2009). Gastrointestinal tract and digestion in the young ruminant: ontogenesis, adaptations, consequences and manipulations. *J. Physiol. Pharmacol.* 60(Suppl 3), 37–46. Available online at: <https://www.semanticscholar.org/paper/Gastrointestinal-tract-and-digestion-in-the-young-Guilloteau-Zabielski/f8cf82475bdf131c84d42c5624e755bc1b198d74>
- Haase, H. (2018). Innate immune cells speak manganese. *Immunity* 48, 616–618. doi: 10.1016/j.immuni.2018.03.031
- Hill, T. M., and Bateman, H. G. 2nd., Aldrich, J. M., Schlotterbeck, R. L. (2010). Effect of milk replacer program on digestion of nutrients in dairy calves. *J. Dairy Sci.* 93, 1105–1115. doi: 10.3168/jds.2009-2458
- Ho, S. Y., Miller, W. J., Gentry, R. P., Neathery, M. W., and Blackmon, D. M. (1984). Effects of high but nontoxic dietary manganese and iron on their metabolism by calves. *J. Dairy Sci.* 67, 1489–1495. doi: 10.3168/jds.S0022-0302(84)81466-6
- Hurley, L. S., and Keen, C. L. (1987). “Manganese,” in *Trace Elements in Human and Animal Nutrition*, ed W. Mertz (Cambridge, MA: Academic Press Inc), 185–223. doi: 10.1016/B978-0-08-092468-7.50010-7
- Jami, E., Israel, A., Kotser, A., and Mizrahi, I. (2013). Exploring the bovine rumen bacterial community from birth to adulthood. *ISME J.* 7, 1069–1079. doi: 10.1038/ismej.2013.2
- Kabel, M. A., Yeoman, C. J., Han, Y., Dodd, D., Abbas, C. A., Bont, J. A., et al. (2011). Biochemical characterization and relative expression levels of multiple carbohydrate esterases of the xylanolytic rumen bacterium *Prevotella ruminicola* 23 grown on an ester-enriched substrate. *Appl. Environ. Microbiol.* 77, 5671–5681. doi: 10.1128/AEM.05321-11
- Kamke, J., Kittelmann, S., Soni, P., Li, Y., Tavendale, M., Ganesh, S., et al. (2016). Rumen metagenome and metatranscriptome analyses of low methane yield sheep reveals a Sharpea-enriched microbiome characterised by lactic acid formation and utilisation. *Microbiome* 4, 56. doi: 10.1186/s40168-016-0201-2
- Kratzer, F. H., and Vohra, P. (eds) (1996). “Chelates and chelation,” in *Chelates in Nutrition* (Boca Raton, FL: Crc. Press), 5–33. doi: 10.1201/9781351070508-2
- La Reau, A. J., and Suen, G. (2018). The ruminococci: key symbionts of the gut ecosystem. *J. Microbiol.* 56, 199–208. doi: 10.1007/s12275-018-8024-4
- Lauber, C. L., Hamady, M., Knight, R., and Fierer, N. (2009). Pyrosequencing-based assessment of soil pH as a predictor of soil bacterial community structure at the continental scale. *Appl. Environ. Microbiol.* 75, 5111–5120. doi: 10.1128/AEM.00335-09
- Li, R. W., Connor, E. E., Li, C., Baldwin Vi, R. L., and Sparks, M. E. (2012). Characterization of the rumen microbiota of pre-ruminant calves using metagenomic tools. *Environ. Microbiol.* 14, 129–139. doi: 10.1111/j.1462-2920.2011.02543.x
- Liu, J., Pu, Y. Y., Xie, Q., Wang, J. K., and Liu, J. X. (2015). Pectin induces an *in vitro* rumen microbial population shift attributed to the pectinolytic *Treponema* group. *Curr. Microbiol.* 70, 67–74. doi: 10.1007/s00284-014-0672-y
- Liu, N., Lu, W., Dai, X., Qu, X., and Zhu, C. (2022). The role of TRPV channels in osteoporosis. *Mol. Biol. Rep.* 49, 577–585. doi: 10.1007/s11033-021-06794-z
- Lozupone, C. A., Stombaugh, J. I., Gordon, J. I., Jansson, J. K., and Knight, R. (2012). Diversity, stability and resilience of the human gut microbiota. *Nature* 489, 220–230. doi: 10.1038/nature11550
- Malmuthuge, N., Griebel, P., and Guan, L. L. (2014). Taxonomic identification of commensal bacteria associated with the mucosa and digesta throughout the gastrointestinal tracts of preweaned calves. *Appl. Environ. Microbiol.* 80, 2021–2028. doi: 10.1128/AEM.03864-13
- Malmuthuge, N., Griebel, P. J., and Guan, L. L. (2015). The gut microbiome and its potential role in the development and function of newborn calf gastrointestinal tract. *Front. Vet. Sci.* 2, 36. doi: 10.3389/fvets.2015.00036
- Malmuthuge, N., and Guan, L. L. (2017). Understanding the gut microbiome of dairy calves: opportunities to improve early-life gut health. *J. Dairy Sci.* 100, 5996–6005. doi: 10.3168/jds.2016-12239
- Martinez-Garcia, M., Brazel, D., Swan, B., Arnosti, C., Chain, P., Reitenga, K. G., et al. (2012). Capturing single cell genomes of active polysaccharide

## Supplementary material

The Supplementary Material for this article can be found online at: <https://www.frontiersin.org/articles/10.3389/fmicb.2023.1163468/full#supplementary-material>



- degraders: an unexpected contribution of *Verrucomicrobia*. *PLoS ONE*. 7, e35314. doi: 10.1371/journal.pone.0035314
- Meale, S. J., Li, S., Azevedo, P., Derakhshani, H., Plaizier, J. C., Khafipour, E., et al. (2016). Development of ruminal and fecal microbiomes are affected by weaning but not weaning strategy in dairy calves. *Front. Microbiol.* 7, 582. doi: 10.3389/fmicb.2016.00582
- Meng, T., Gao, L., Xie, C., Xiang, Y. K., Huang, Y. Q., Zhang, Y. W., et al. (2021). Manganese methionine hydroxy analog chelated affects growth performance, trace element deposition and expression of related transporters of broilers. *Anim. Nutr.* 7, 481–487. doi: 10.1016/j.aninu.2020.09.005
- Mudgal, V., Saxena, N., Kumar, K., Dahiya, S. S., Punia, B. S., Sharma, M. L., et al. (2019). Sources and levels of trace elements influence some blood parameters in *Murrah Buffalo (Bubalus bubalis)* calves. *Biol. Trace Elem. Res.* 188, 393–403. doi: 10.1007/s12011-018-1439-2
- Myer, P. R., Smith, T. P., Wells, J. E., Kuehn, L. A., and Freely, H. C. (2015). Rumen microbiome from steers differing in feed efficiency. *PLoS ONE* 10, e0129174. doi: 10.1371/journal.pone.0129174
- Palmer, C., Bik, E. M., Giulio, D. B., Relman, D. A., and Brown, P. O. (2007). Development of the human infant intestinal microbiota. *PLoS Biol.* 5, e177. doi: 10.1371/journal.pbio.0050177
- Redford, A. J., and Fierer, N. (2009). Bacterial succession on the leaf surface: a novel system for studying successional dynamics. *Microb. Ecol.* 58, 189–198. doi: 10.1007/s00248-009-9495-y
- Roshanzamir, H., Rezaei, J., and Fazaeli, H. (2020). Colostrum and milk performance, and blood immunity indices and minerals of Holstein cows receiving organic Mn, Zn and Cu sources. *Anim. Nutr.* 6, 61–68. doi: 10.1016/j.aninu.2019.08.003
- Santamaria, A. B. (2008). Manganese exposure, essentiality and toxicity. *Indian J. Med. Res.* 128, 484–500.
- Shabat, S. K. B. S., Sasson, G., Doron-Faigenboim, A., Durman, T., Yaacoby, S., Miller, M. E. B., et al. (2016). Specific microbiome-dependent mechanisms underlie the energy harvest efficiency of ruminants. *ISME J.* 10, 2958–2972. doi: 10.1038/ismej.2016.62
- Sheppard, S. C., Long, J. M., and Sanipelli, B. (2010). Verification of radionuclide transfer factors to domestic-animal food products, using indigenous elements and with emphasis on iodine. *J. Environ. Radioact.* 101, 895–901. doi: 10.1016/j.jenvrad.2010.06.002
- Sheppard, S. C., and Sanipelli, B. (2012). Trace elements in feed, manure, and manured soils. *J. Environ. Qual.* 41, 1846–1856. doi: 10.2134/jeq2012.0133
- Silva, D. J., and Queiroz, A. C. (2006). *Análise de Alimentos: Métodos Químicos e Biológicos*. 3rd ed. Viçosa: UFV Viçosa, 235.
- Soest, P. J. V. (1994). *Nutritional Ecology of the Ruminant*, Vol. 2. Ithaca, NY: Cornell University Press.
- Spears, J. W. (1996). Organic trace minerals in ruminant nutrition. *Anim. Feed Sci. Technol.* 58, 151–163. doi: 10.1016/0377-8401(95)00881-0
- Tuomisto, H. (2010). A consistent terminology for quantifying species diversity? Yes, it does exist. *Oecologia* 164, 853–860. doi: 10.1007/s00442-010-1812-0
- Weller, M., Overton, T., Rourke, J., and Armstrong, F. (2014). *Inorganic Chemistry*, Vol. 6. Oxford: Oxford University Press.
- Windisch, W. (2002). Interaction of chemical species with biological regulation of the metabolism of essential trace elements. *Anal. Bioanal. Chem.* 372, 421–425. doi: 10.1007/s00216-001-1117-6
- Wong-Valle, J., Henry, P. R., Ammerman, C. B., and Rao, P. V. (1989). Estimation of the relative bioavailability of manganese sources for sheep. *J. Anim. Sci.* 67, 2409–2414. doi: 10.2527/jas1989.6792409x
- Yáñez-Ruiz, D. R., Abecia, L., and Newbold, C. J. (2015). Manipulating rumen microbiome and fermentation through interventions during early life: a review. *Front. Microbiol.* 6, 01133. doi: 10.3389/fmicb.2015.01133
- Yatsunenko, T., Rey, F. E., Manary, M. J., Trehan, I., Dominguez-Bello, M. G., Contreras, M., et al. (2012). Human gut microbiome viewed across age and geography. *Nature* 486, 222–227. doi: 10.1038/nature11053
- Zhang, M., and Liu, K. (2022). Calcium supplements and structure-activity relationship of peptide-calcium chelates: a review. *Food Sci. Biotechnol.* 31, 1111–1122. doi: 10.1007/s10068-022-01128-6



## OPEN ACCESS

## EDITED BY

Wei Qi He,  
Soochow University, China

## REVIEWED BY

Jiajia Song,  
Southwest University, China  
Juan José Valdez Alarcón,  
Universidad Michoacana de San Nicolás de  
Hidalgo, Mexico

## \*CORRESPONDENCE

Ping Li  
✉ lipingchxyy@163.com  
Rongjie Zhao  
✉ zhao\_rongjie@yahoo.com

<sup>†</sup>These authors have contributed equally to this work and share first authorship

RECEIVED 24 February 2023

ACCEPTED 22 May 2023

PUBLISHED 09 June 2023

## CITATION

Jiao Y, Zhao Z, Li X, Li L, Xiao D, Wan S, Wu T, Li T, Li P and Zhao R (2023) Salidroside ameliorates memory impairment following long-term ethanol intake in rats by modulating the altered intestinal microbiota content and hippocampal gene expression.  
*Front. Microbiol.* 14:1172936.  
doi: 10.3389/fmicb.2023.1172936

## COPYRIGHT

© 2023 Jiao, Zhao, Li, Li, Xiao, Wan, Wu, Li, Li and Zhao. This is an open-access article distributed under the terms of the [Creative Commons Attribution License \(CC BY\)](https://creativecommons.org/licenses/by/4.0/). The use, distribution or reproduction in other forums is permitted, provided the original author(s) and the copyright owner(s) are credited and that the original publication in this journal is cited, in accordance with accepted academic practice. No use, distribution or reproduction is permitted which does not comply with these terms.

# Salidroside ameliorates memory impairment following long-term ethanol intake in rats by modulating the altered intestinal microbiota content and hippocampal gene expression

Yu Jiao<sup>1†</sup>, Zhenglin Zhao<sup>2†</sup>, Xin Li<sup>3</sup>, Lulu Li<sup>2</sup>, Dan Xiao<sup>4,5</sup>,  
Siyan Wan<sup>6</sup>, Tong Wu<sup>1</sup>, Tong Li<sup>1</sup>, Ping Li<sup>1\*</sup> and Rongjie Zhao<sup>1\*</sup>

<sup>1</sup>Department of Psychiatry, Qiqihar Medical University, Qiqihar, Heilongjiang, China, <sup>2</sup>Department of Biochemistry, Qiqihar Medical University, Qiqihar, Heilongjiang, China, <sup>3</sup>Department of Psychiatry, The Fourth Affiliated Hospital of Qiqihar Medical University, Qiqihar, Heilongjiang, China, <sup>4</sup>School of Medicine and Health, Harbin Institute of Technology, Harbin, Heilongjiang, China, <sup>5</sup>Department of Medicine and Health, Zhengzhou Research Institute of Harbin Institute of Technology, Zhengzhou, Henan, China, <sup>6</sup>Department of Preventive Medicine, Qiqihar Medical University, Qiqihar, Heilongjiang, China

**Background:** Salidroside (*Sal*), the main component of a famous herb *Rhodiola rosea* L, enhances memory performance and reduces fatigue. Therefore, this study assessed the effect of *Sal* on memory impairment induced by a long-term intake of ethanol (EtOH) in rats and investigated its relevant mechanisms using gut microbiota metagenomic analysis and hippocampal transcriptomic analysis.

**Methods:** Eighteen male SD rats were divided into the normal control group (CON group), EtOH model group (Model group), and *Sal* treatment group (*Sal* group). The rats in the Model and *Sal* groups intragastrically (i.g.) received 2g/kg EtOH for 30 consecutive days, whereas the CON group was given an equal volume of distilled water. Meanwhile, the rats in the *Sal* group were administered i.g. 30mg/kg *Sal* 60min after EtOH intake. All rats were tested in the eight-arm maze for their memory function every 3days. On the 30th day, metagenomic analyses of gut microbiota and transcriptomic analyses of the hippocampus were performed.

**Results:** Compared with the Model group, *Sal* treatment reduced the total time to complete the eight-arm maze task, decreased the number of arm entries, and abated the working memory error that was significant from the 9th day. Additionally, *Sal* intervention improved the gut microbiota composition, such as the increased abundance of *Actinobacteria* and *Bifidobacterium*, which was related to the metabolism of amino acids and terpenoid carbohydrate, endocrine function, and signal transduction by neurotransmitters. In the hippocampus, the EtOH intake differentially expressed 68 genes (54 genes increased, whereas 14 genes decreased), compared with the CON group, whereas *Sal* intervention affected these changes: 15 genes increased whereas 11 genes decreased. And, enrichment analyses revealed these genes were related to the structural components of the ribosome, mRNA splicing process, protein translation, mitochondria function, and immunological reaction. Finally, a correlation analysis found the memory impairment was positively correlated with the abnormal

upregulation of *Tomm7* but negatively correlated with decreased abundance of gut *Alistipes\_indistinctus*, *Lactobacillus\_taiwanensis*, *Lactobacillus\_paragasseri*, and *Lactobacillus\_johnsonii*.

**Conclusion:** *Sal* improved memory impairment caused by long-term EtOH intake in rats, which may be related to its regulation of gut dysbiosis and hippocampal dysfunction.

#### KEYWORDS

Salidroside, ethanol, memory impairment, gut microbiota, hippocampus, metagenomics

## Introduction

In recent times, long-term alcohol use has imposed a tremendous disease burden on human health worldwide. Long-term alcohol use is associated with more than 200 diseases (Dumont et al., 2020; Ke et al., 2022). The long-term alcohol syndrome has a broad spectrum of symptoms, including severe memory dysfunction that seriously affects the quality of life of alcohol abusers. Being a small organic molecule, ethanol (EtOH) readily passes through different biomembranes, including the blood–brain barrier. More than 99% of the about 100 billion resident neurons in the brain are either glutamatergic (excitatory) or GABAergic (inhibitory) neurons, and they are linked together to construct complex networks and structures to implement appropriate functions of the brain, including learning and memory. EtOH is both an allosteric agonist of GABA<sub>A</sub> receptors and allosteric antagonist of the ionotropic glutamatergic receptors, indicating that most alcohol abusers suffer from certain kinds of memory impairment (Parsons, 1986). However, the mechanisms by which alcohol consumption causes impaired memory function have not been fully elucidated.

Long-term alcohol use leads to neurological dysfunction in different brain regions, such as prefrontal cortex, hippocampus, and amygdala, which are involved in memory processes (Topiwala et al., 2017; Caleb et al., 2022; Collin and Eric, 2022). The hippocampus is the most significant structure among the aforementioned brain regions, because it is the primary structure for encoding information and memory formation. Additionally, it is involved in almost every aspect and process of memory, such as the consolidation of information from short-term memory to long-term memory, formation of spatial and working memory, and memory extinction and reconsolidation. Moreover, a growing number of studies have shown that the hippocampus is susceptible to damage by long-term EtOH use. Memory impairment in alcohol abusers seems to greatly depend on the hippocampus (Contreras et al., 2019).

Long-term alcohol intake leads to disturbed gastrointestinal function, which can cause diverse symptoms in the body, including high cognitive dysfunction (Choi, 2021; Zhao et al., 2021). The gut microbiota and the central nervous system (CNS) have bidirectional connections with respect to the anatomy, physiology, and biochemical interactions. The gut–brain axis is involved in almost every facet of the physiologic processes of the body, such as neural, endocrine, and immune responses (Xia et al., 2021). For instance, the microbiota induce and produce neurotransmitters, hormones, and other physiological factors either by themselves or by stimulating

gastrointestinal cells, which together with their neuroactive metabolites enter the circulatory system, regulating CNS functions, including learning and memory (Marcondes Ávila et al., 2020; Pradhananga et al., 2020). In turn, the CNS controls the gut microbiota through various biological signaling molecules, such as hormones, cytokines, and neurotransmitters, affecting the composition and diversity of gut microbiota, which complete the cyclic regulation of the CNS–gut–CNS circle (Cox and Weiner, 2018). Therefore, the effect of long-term consumption of EtOH on gut microbiota and its critical role in regulating learning and memory have been the focus of research (Qamar et al., 2019).

Currently, the main drugs that are widely prescribed in clinical practice for treating cognitive impairment—including memory dysfunction—are pyranacetam (Uniyal et al., 2019), anisacetam, and other brain function improvement agents. These drugs not only improve cognitive dysfunction but also possess therapeutic effects on cerebrovascular disease, brain trauma, vascular dementia, and Alzheimer's disease. However, their effects on alcoholic memory impairment are limited. They have severe side effects, such as dry mouth, nausea, vomiting, abdominal discomfort, and insomnia, which greatly compromise their clinical use. Therefore, the development of safe herbal or alternative drugs with fewer side effects has become increasingly urgent. *Rhodiola rosea* L is a perennial herb, which has therapeutic effects on mental disorders, such as anxiety and depression (van Diermen et al., 2009). Salidroside (*Sal*) is the main component of *Rhodiola rosea* L, and like its parent herb, it can enhance mental strength and reduce fatigue (Shevtsov et al., 2003). For example, *Sal* increases the CNS levels of some neurotransmitters, such as norepinephrine (NE), dopamine (DA), serotonin (5-HT), and acetylcholine (ACh), to stimulate CNS activity, especially enhance learning and memory (Panossian et al., 2008; Li et al., 2017). However, no study on the effect of *Sal* on memory impairment induced by long-term alcohol use has yet been reported.

Taken together, the above evidence points to a possible therapeutic role of *Sal* on memory impairment caused by a long-term EtOH consumption. Therefore, in the present study, we established a long-term EtOH intake rat model and evaluated *Sal* effects on memory impairment using the eight-arm maze (EAM) test. After the confirmation of *Sal* therapeutic effects, the relevant mechanisms were explored by metagenomic analyses of gut microbiota and the hippocampus. Additionally, a triple correlation analysis was performed between behavior and gut microbiota changes and hippocampal gene expression changes. This work not only provides a basic research evidence for the development of *Sal* as a promising

candidate and potential strategy to treat memory deficit in alcoholic conditions, but also address the correlation between the gut microbiota and the hippocampus functionally interact to mediate memory impairment caused by a long-term ethanol consumption.

## Materials and methods

### Establishment of alcohol-induced memory impairment model in rats and intervention with *Sal*

Eighteen SD rats (male, 180–220 g) were purchased from the Animal Laboratory Center of Qiqihar Medical University. All rats were individually housed with controlled diet and free access to water on a 12-h dark/light cycle at a constant humidity of  $55 \pm 5\%$  and temperature of  $22 \pm 2^\circ\text{C}$ . All experimental protocols were approved by the Animal Ethics Committee of Qiqihar Medical University (QMU-AECC-2023-87). The alcoholism modeling method was slightly modified based on the experiment of Jiao Yu et al. (2021). All experimental protocols were approved by the Animal Ethics Committee of Qiqihar Medical University. The alcoholism modeling method was slightly modified based on the experiment of Sase et al. (2016). Rats (six rats in each group) were randomly divided into the control group (CON group), chronic alcoholism model group (Model group), and *Sal* group. Briefly, in the subsequent 30 days, the Model and *Sal* groups were continuously administered with EtOH (2 g/kg/day, dissolved in distilled water) by the intragastric (i.g.) route. The *Sal* group was administered with *Sal* (30 mg/kg/day, i.g., dissolved in distilled water) 60 min after alcohol intake, whereas the CON and Model groups were given the same volume of distilled water. Memory was assessed by the EAM behavior experiment on days 3, 6, 9, 12, 15, 18, 21, 24, 27, and 30 of the experiment. *Sal* (purity  $\geq 98\%$ ) was purchased from Shaanxi Wanyuan Biotechnology Co (Xi'an, Shan Xi, China).

### Cognitive status measurement

Cognitive Status Measurement was slightly modified based on the experiment of Sase et al. (2016). The EAM test consisted of eight radiation arms and a central platform. Eight arms radiate from an octagonal platform in the middle, each 50 cm long. The angle between the arms was  $45^\circ$ . A 30-cm-high baffle was placed at the beginning of each arm, and eight baffles blocked the central platform. A thermal imager was placed 180 cm above the platform and was responsible for recording data, such as the movement trajectory of the rat and number of entries into each radiation arm throughout the experiment. The entire maze was made of black organic plastic. Throughout the experiment, the maze was placed in the center of the lab at a fixed position, and the position of other objects in the lab remained unchanged.

Rats were trained once a day for 7 days prior to testing, while maintaining 80% of their normal feeding throughout the experiment. At the beginning of training, rats were placed on the central platform of the maze for 15 s, followed by removal of the eight radiating arm baffles. Rats freely chose to enter the end of the radiated arm for foraging for 10 min or completed foraging for all arms prematurely, indicating the end of training. Following each training session, the maze was wiped with acetic acid to eliminate the influence of odors

on subsequent testing. Food was placed only at the end of arms 1, 2, 5, and 7 (working arm), and no food was placed in arms 3, 4, 6, and 8 (reference arm) throughout the test. The order of placement of the entire food arm remained unchanged in this experiment. Repeated entries into the working arm were recorded as working memory errors (WMEs).

Test indicators were as follows:

(1) Total time for rats to complete all working arms of the eight-arm maze: time to pass arms 1, 2, 5, and 7. If not completed within 10 min, time was recorded as 10 min. (2) Total number of working memory errors: the total number of errors within 10 min; error was defined as repeated entry into the same working arm. (3) Total number of arm entries: total number of arm entries of rats in a test.

Changes were detected and analyzed on experimental days 3, 6, 9, 12, 15, 18, 21, 24, 27, and 30. The specific experimental flow is shown in Figure 1.

### Hippocampal and intestinal content collection

At the end of the behavioral testing on day 30, the rats were decapitated immediately to collect blood samples. Rat skull was dissected, and the hippocampus was rapidly collected. Additionally, 2 g of intestinal contents were collected from all rats and rapidly frozen in liquid nitrogen and transferred to a  $-80^\circ\text{C}$  freezer. All operations were performed on a sterile ice bath.

### Metagenomic detection of intestinal contents

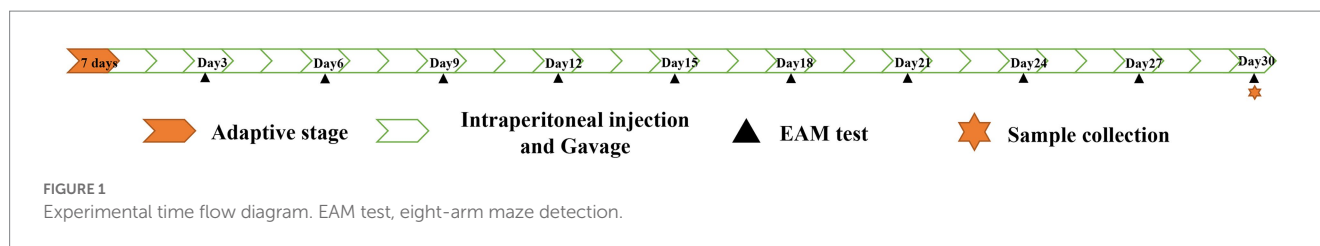
The metagenomic sequencing of intestinal contents was performed according to this order: sample DNA extraction, library sequencing, data quality control, species annotation and analysis, gene set construction and analysis, functional annotation analysis, and other processes. In this project, metagenomic analysis was performed using the Wekemo Bioincloud (Shenzhen, China).<sup>1</sup> Specific steps were as follows:

#### ① Sample extraction testing and sequencing of intestinal flora

Genomic DNA was extracted from intestinal content samples using the CTAB method. Libraries were constructed using the NEB Next® Ultra™ DNA Library Prep Kit for Illumina (NEB, Ipswich, United States). Qualified DNA samples were randomly interrupted into fragments of approximately 350 bp in length using a Covaris ultrasonic disruptor (Covaris S2 System, Massachusetts, United States), and the entire library preparation was completed by end repair, deployment A tail, sequencing adaptor, purification, and PCR amplification of the DNA fragments. Finally, the AMPure XP system purified the PCR products, detected insert size of the library using Agilent2100 (Agilent Technologies Co., Ltd., United States), and

<sup>1</sup> <https://www.bioincloud.tech>





quantified library concentration using real-time PCR (Bio-Rad, United States). Indexed coding samples were clustered on the cBot Cluster Generation System using the Illumina PE Cluster Kit (Illumina, United States). Following cluster generation, DNA libraries were sequenced on the Illumina Novaseq 6000 (Illumina, San Diego, CA, United States) platform, and 150 bp double-ended reads were generated.

## ② Data analysis

Data quality control and de-host sequence: Metagenomic sequencing was performed using the Illumina NovaSeq high-throughput sequencing platform to obtain metagenomic raw data for bacteria, fungi, and archaea in intestinal content samples. Raw sequencing data were pre-processed using the Knead data software.

## ③ Species and functional annotations

Kraken2 and self-built microbial nucleic acid databases (screened NCBI NT nucleic acid database and RefSeq whole genome database for sequences belonging to bacteria, fungi, ancient fine bacteria, and viruses) were aligned to calculate the number of sequences containing species in each group of samples, and then Bracken was used to predict the actual relative abundance of species in the samples. Sequences after quality control and de-hosting were aligned (DIAMOND based) to the Protein Data Bank (UniRef90) using the HUMAnN2 software. PCoA analysis was based on specie abundance tables and functional abundance tables. Lefse analysis and mining were performed to detect differences in species composition and functional composition between samples (Villar et al., 2015).

## ④ Resistance gene annotation

The DIAMOND software (Buchfink et al., 2015) was used to align quality control and de-hosted sequences of each sample to the CARD database, and the sequences that failed the alignment were filtered out [parameters: -e 0.001 (e-value <1e-3) -i80 (identity percent >80%)]. The relative abundance of antibiotic resistance genes in each group of samples was obtained from the alignment (Detailed results are shown in the Supplementary Figure S1).

## Hippocampal transcriptome sequencing analysis

Using the Illumina sequencing platform, all RNAs of the samples were sequenced, and the high-quality data were compared with the reference genome for further analysis of expression quantification, differential genes, and functional annotation. In this study,

transcriptome biochemistry analysis was performed using the Wekemo Bioincloud (see text footnote 1) (Shenzhen, China).

## ① Sample collection and preparation

RNA was extracted using standard extraction methods, and RNA samples were tested for RNA integrity using the Agilent 2100 bioanalyzer (Agilent Technologies Co. Ltd., United States) for quality control. The mRNA with polyA tails was enriched by Oligo(dT) magnetic beads using the NEBNext® Ultra™ RNA Library Prep Kit (Illumina), and the resulting mRNA was subsequently randomly interrupted with divalent cations in the NEB Fragmentation Buffer. The fragmented mRNA was used as a template and random oligonucleotides as primers to synthesize the first strand of cDNA in the M-MuLV reverse transcriptase system, followed by degradation of the RNA strand with RNaseH and synthesis of the second strand of cDNA with dNTPs under the DNA polymerase I system. The purified double-stranded cDNA was end-repaired, A-tailed, and connected to the sequencing junction. The cDNA of 250–300 bp was screened by AMPure XP beads and amplified by PCR, and the PCR products were purified by AMPure XP beads again to obtain the library. After library construction, initial quantification was performed using a Qubit 2.0 Fluorometer (Thermo Scientific, United States), and the insert size of the library was subsequently checked using an Agilent 2100 bioanalyzer. After the libraries passed the test, Illumina sequencing was performed to generate 150 bp paired-end reads.

## ② Data quality control and differential expression analysis

To ensure the quality and reliability of data analysis, filtration of raw data is necessary. It mainly includes removal of reads with adapter, removal of reads containing N (N indicates that base information cannot be determined), and removal of low-quality reads (reads with Qphred ≤20 bases accounting for more than 50% of the entire read length). Additionally, clean data were subjected to Q20, Q30, and GC content calculation. All subsequent analyses were based on clean data for high quality analysis. Indexing of the reference genome was constructed using HISAT2v2.0.5, and paired-end clean reads were aligned to the reference genome using HISAT2 v2.0.5. StringTie (1.3.3b) for novel gene prediction. Differential expression analysis between the two compared combinations was performed using the DESeq2 software (1.16.1).

## ③ Enrichment and pathway analysis

GO enrichment analysis of differentially expressed genes (Gene Ontology, GO) was performed using the clusterProfiler (3.4.4) software. Statistical enrichment of differentially expressed genes in

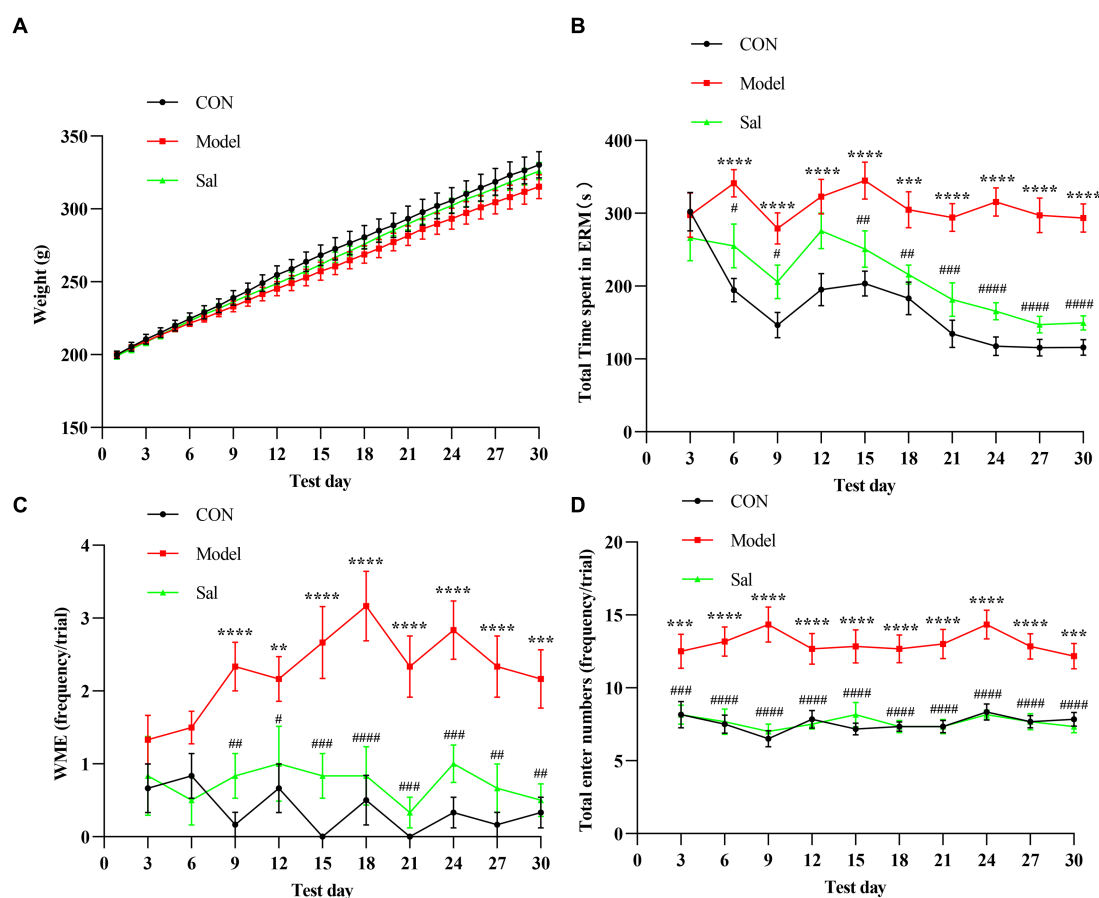


FIGURE 2

*Sal* improves the memory function during alcoholism in rats. (A) There was no significant difference in body weight among CON, Model, and *Sal* groups. (B–D) The total maze time, the number of working memory errors, and the total number of arm entries were significantly increased in the Model group compared with the other two groups. Two-way ANOVA and Tukey analyses were used for multiple group comparison. Data are shown as mean  $\pm$  SEM,  $n=6$  in each group.  $^{*}p<0.01$ ,  $^{***}p<0.001$ ,  $^{****}p<0.0001$  (CON vs. Model);  $^{*}p<0.05$ ,  $^{*}p<0.01$ ,  $^{***}p<0.001$ ,  $^{****}p<0.0001$  (Model vs. *Sal*).

KEGG pathways was analyzed using the clusterProfiler (3.4.4) software.

## Data processing and statistical analysis

All experiments were repeated three times. Data are presented as the mean  $\pm$  standard error of the mean (SEM). One- or two-way ANOVA followed by Tukey's post-hoc test was used for multiple comparisons. Data were analyzed using GraphPad Prism 8.0 software (GraphPad Software, Inc.). Correlation analyses were performed using R software (V4.2.2).

## Results

### Improving the effect of *Sal* on memory dysfunction in chronic EtOH intake rats

In successive experiments over 30 days, no apparent difference in body weight was observed among the groups (Figure 2A). Cognitive function was measured using the EAM test, and the total time to complete the EAM was generally higher in the Model group than in

the other two groups. Rats in the *Sal* group were more effective during the EAM task ( $p<0.001$ , Figure 2B). Compared with the CON group, the Model group had WMEs that began to rise on day 9 ( $p<0.01$ ), whereas the *Sal* group had a decreased number of WMEs ( $p<0.01$ , Figure 2C). Additionally, the total number of arm entries in the Model group was significantly more than that of the CON group ( $p<0.001$ ), whereas *Sal* intervention reduced the number of arm entries ( $p<0.001$ , Figure 2D). Taking these results together, we concluded that chronic administration of alcohol caused working memory impairment, whereas administration of *Sal* improved memory function against alcoholic consumption.

### *Sal* treatment affects intestinal diversity of microbes by metagenomic analysis of gut contents

#### Sequence control and de-host sequences

Double-end sequencing was performed using the Illumina sequencing platform. Raw data were obtained by sequencing. The pre-processed protocol was as follows: ① the linker sequence was removed (parameter ILLUMINACLIP: adapters\_path: 2:30:10); ② the scanned sequence (4-bp sliding window size). The removal condition

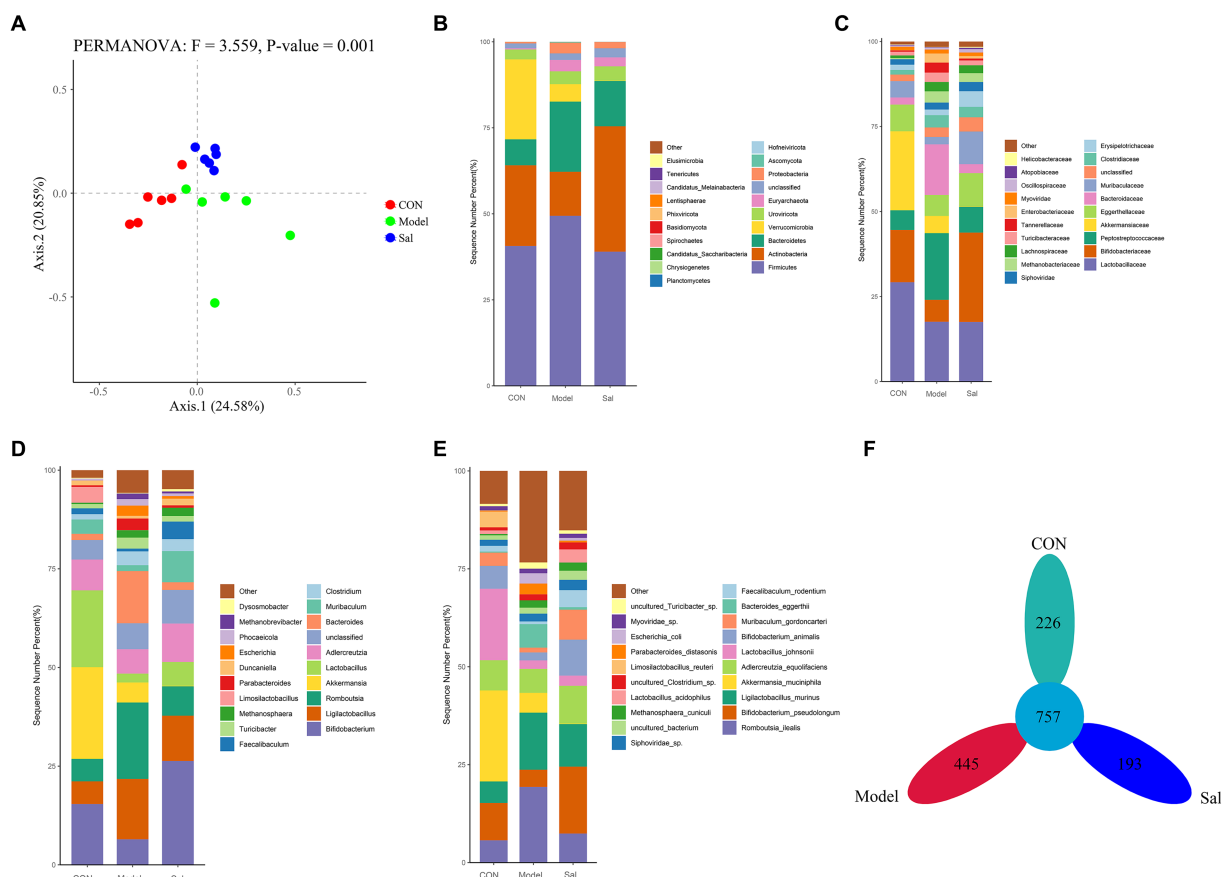


FIGURE 3

Composition of the gut microbiota in the CON, Model and Sal groups. (A) Bray-Curtis-based PCoA plots that can relatively effectively separate the Model group from the remaining two groups, indicating that the gut flora composition of the Model group is significantly different from the remaining two groups. Distribution characteristics of the gut microbiota in the CON, Model and Sal groups ( $n=6$  for each group). Histograms of relative abundance of the top 20 species at the (B) phylum level, (C) family level, (D) genus level, and (E) species level among the three groups with Wilcoxon rank-sum test. (F) Petal plots of the three groups.

of subsequent sequence was set as average mass score < 20 (99% accuracy, parameter SLIDINGWINDOW: 4:20); and ③ the sequence with a final length of < 50 bp was removed (parameter MINLEN: 50) (see [Supplementary Table S1](#) for detailed results).

## Analysis of sample composition

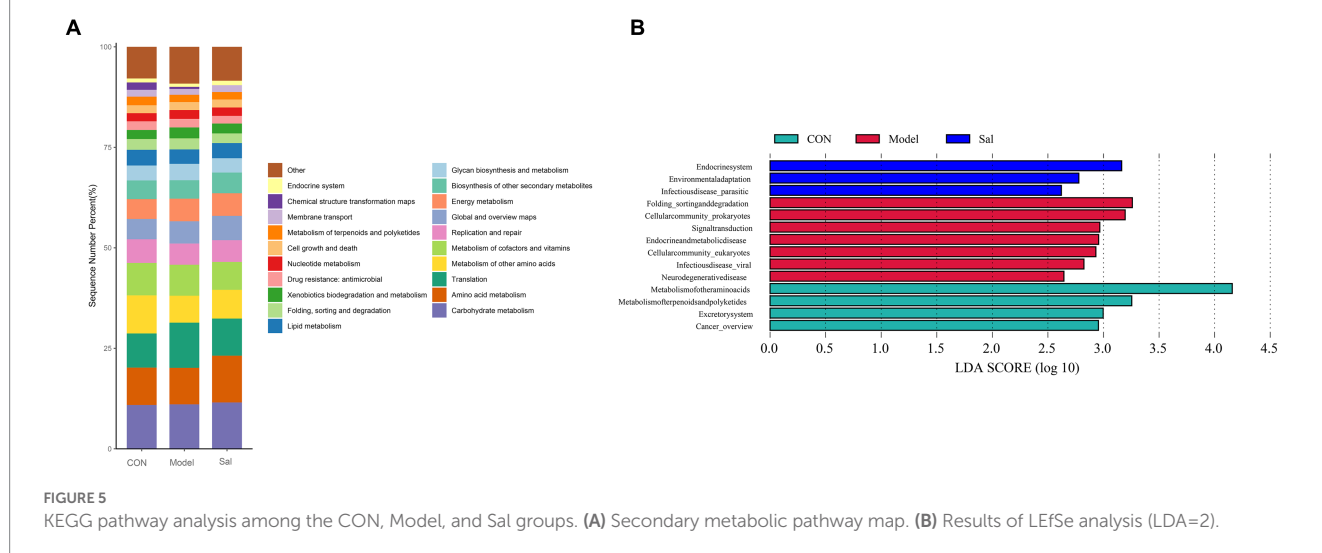
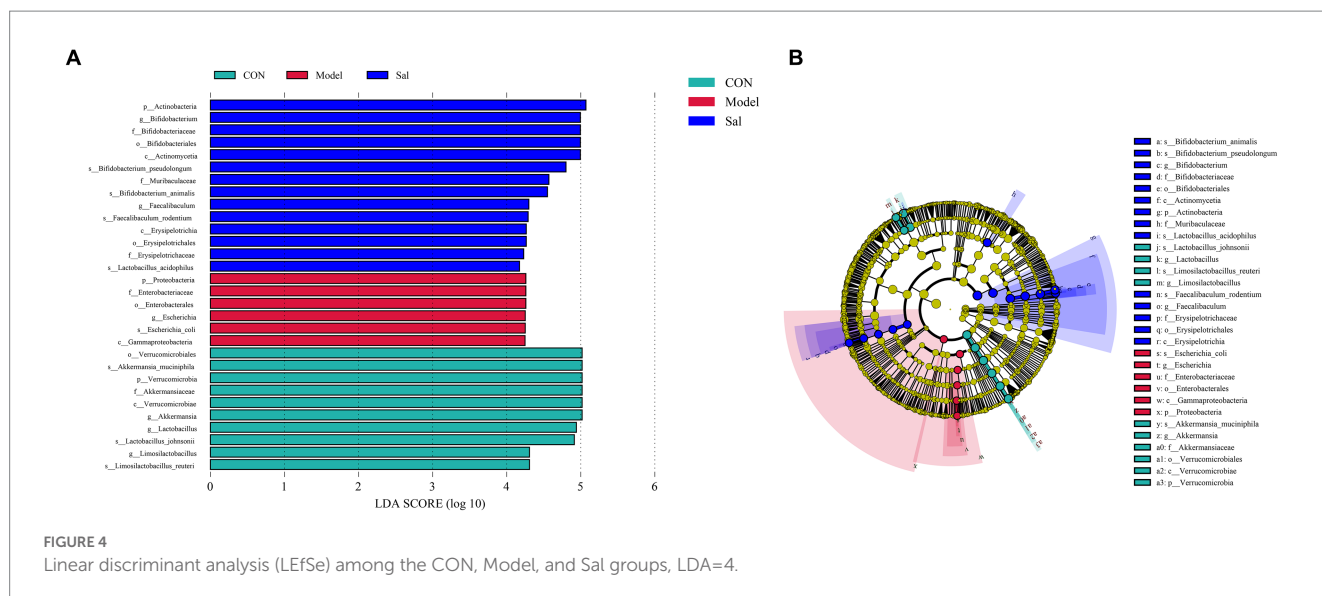
The diversity among samples was analyzed by principal component analysis (PCoA). If the samples were similar in species composition, the closer they were in the PCoA plot. The results showed ([Figure 3A](#)) that Axis 0.1 indicated 24.57% differentiation and Axis 0.2 indicated 20.88% differentiation ( $F = 3.557$ ,  $p = 0.001$ ). Compared to the relatively scattered distribution in the Model group, the distributions in the CON and Sal groups were more concentrated, indicating that Sal intervention had an effect on the composition of the intestinal flora of rats in the model of alcohol-induced memory damage and brought the composition of the intestinal flora close to that of the control group. All valid sequences of the samples were annotated and classified by Kraken2 ([Wood and Salzberg, 2014](#)) (parameter –confidence 0.2), and the proportion of the number of sequences in the samples at the Kingdom level to the total number of sequences were performed. The species detected

were Archaea (1.56%, 1,276,538), Bacteria (95.21%, 77,692,265), Fungi (0.13%, 105,304), Heunggongvirae (2.86%, 2,333,896), and Viruses (0.23%, 187,864).

Bacteria accounted for the largest number of sequences. At the phylum level, the Sal group was richer in the Actinobacteria phylum than the other two groups, and the Model group had a higher relative abundance of the thick-walled phylum and a lower relative abundance of the Actinobacteria phylum. At the family level, the Lactobacillus family was more abundant in the CON group than the other two groups. At the genus level, the genus Bifidobacterium was significantly more abundant in the Sal group than in the Model group. At the species level, *Romboutsia ilealis* was more abundant in the Model group than the CON and Sal groups. A total of 757 OTUs were detected in the three groups; 226, 445, and 193 OTUs were specific to the control, Model, and Sal groups, respectively ([Figures 3B–F](#)). The taxonomic levels of archaeobacteria and fungi are shown in [Supplementary Figure S2](#).

## Differential microbial screening

The characteristic microorganisms of each group were determined using the LefSe analysis (linear discriminant analysis



effect size method), and the relationships between different microbial groups, from phylum to species level (LDA=4), are shown in the branching diagram (Figures 4A,B). The results showed that the 30 OTUs at the phylum (3 OTUs), order (4 OTUs), order (4 OTUs), family (5 OTUs), genus (6 OTUs), and species levels (8 OTUs) differed significantly among the three groups. The relative abundance of Proteobacteria, Enterobacteriaceae, Enterobacterales, Escherichia, Escherichia\_coli, and Gammaproteobacteria was higher in the Model group. In the control group, Verrucomicrobiales, Akkermansia\_muciniphila, Verrucomicrobia, Akkermansiaceae, Verrucomicrobiae, Akkermansia, Lactobacillus Lactobacillus\_johnsonii, Limosilactobacillus, and Limosilactobacillus\_reuteri were more abundant. In the Sal group, Actinobacteria, Bifidobacterium Bifidobacteriaceae, Bifidobacteriales, Actinomycetia, Bifidobacterium\_pseudolongum, Muribaculaceae, Bifidobacterium\_animalis Faecalibaculum, Faecalibaculum\_rodentium, Erysipelotrichia, Erysipelotrichales, Erysipelotrichaceae, and Lactobacillus\_acidophilus had higher relative abundance.

## Functional analysis prediction

Based on the search of the KEGG (Kyoto Encyclopedia of Genes and Genomes) database for comparative annotations, a KEGG secondary pathway map was obtained (Figure 5A). No significant difference in the secondary pathway was observed among the three groups of samples. The LDA bar graph was obtained by LEfSe analysis of the basic metabolic pathways of KEGG (set LDA=2), and the results are shown in Figure 5B. In the CON group, the metabolic pathways involved were the metabolism of other amino acids and metabolism of terpenoids and polyketides. Additionally, Excretorysystem and Cancer\_overview were relatively high. The Model group mainly involved seven highly expressed metabolic pathways, including Folding\_sorting and degradation, Cellular community\_prokaryotes, Signal transduction Endocrine and metabolic disease, Cellular community\_eukaryotes, Infectious disease\_viral, and Neuro degenerative disease. In the Sal group, three highly expressed metabolic pathways were involved: Endocrine system, Environmental adaptation, and Infectious disease\_parasitic.



## Sal treatment affects hippocampal transcriptomics in alcohol consumption rats and data quality control and variance expression analysis

Quality control processing was performed on the raw data of each sample using the fastp software (Chen et al., 2018) to obtain clean data. A total of 273,318,968, 274,582,288, and 284,832,284 clean reads were generated from the control, Model, and Sal groups, respectively. Where the Q20 values were all higher than 97%, the Q30 values were all higher than 92%, the error rate was 0.03, and the GC content distribution was about 48% (Supplementary Table S2 for detailed results). The clean data reads after QC were compared to the reference genome using HISAT2 (Kim et al., 2015), and the comparison was evaluated using Qualimap RNA-seq (Konstantin et al., 2016). A total of 210,235,503, 211,159,294, and 220,176,485 reads were generated from the control, Model, and Sal groups mapped to the rat genome, respectively. Differentially expressed genes were screened by screening out detection rates (proportion of count not 0)  $<0.25$ ,  $|\log_2(\text{Fold Change})| > 1$  &  $\text{padj} < 0.05$ . The results revealed 68 differentially expressed genes in the Model group, compared with the CON group. Among them, 54 genes had elevated relative expression and 14 genes had decreased relative expression.

The top five relatively highly expressed genes were *Cnmd* ( $\log_2\text{Fold Change}=4.00$ ,  $\text{padj}=2.33\text{E-}03$ ), *S100a9* ( $\log_2\text{Fold Change}=3.03$ ,  $\text{padj}=2.55\text{E-}08$ ), *Tomm7* ( $\log_2\text{Fold Change}=1.63$ ,  $\text{padj}=4.40\text{E-}11$ ), *Klhl40* ( $\log_2\text{Fold Change}=1.57$ ,  $\text{padj}=1.08\text{E-}03$ ), and *Lilrb3a* ( $\log_2\text{Fold Change}=1.45$ ,  $\text{padj}=4.77\text{E-}02$ ). The first five relatively low-expressing genes were *AY172581.16* ( $\log_2\text{Fold Change}=-2.37$ ,  $\text{padj}=2.35\text{E-}06$ ), *AY172581.17* ( $\log_2\text{Fold Change}=-2.04$ ,  $\text{padj}=3.51\text{E-}05$ ), *Npsr1* ( $\log_2\text{Fold Change}=-1.98$ ,  $\text{padj}=2.74\text{E-}02$ ), *AY172581.5* ( $\log_2\text{Fold Change}=-1.43$ ,  $\text{padj}=2.88\text{E-}02$ ), and *Rxfp1* ( $\log_2\text{Fold Change}=-1.21$ ,  $\text{padj}=1.22\text{E-}03$ ). Twenty-six differentially expressed genes were identified in the Sal group, compared to the Model group. Among these genes, 15 genes were elevated and 11 genes were decreased. The top five relatively highly expressed genes were *Olr1694* ( $\log_2\text{Fold Change}=2.84$ ,  $\text{padj}=4.67\text{E-}03$ ), *Ca3* ( $\log_2\text{Fold Change}=2.17$ ,  $\text{padj}=1.26\text{E-}02$ ), *Synpo2* ( $\log_2\text{Fold Change}=1.54$ ,  $\text{padj}=1.47\text{E-}03$ ), *AY172581.17* ( $\log_2\text{Fold Change}=1.53$ ,  $\text{padj}=7.37\text{E-}03$ ), and *Spp1* ( $\log_2\text{Fold Change}=1.49$ ,  $\text{padj}=3.29\text{E-}02$ ). The top five relatively lowly expressed genes were *Ch25h* ( $\log_2\text{Fold Change}=-1.56$ ,  $\text{padj}=2.80\text{E-}02$ ), *Tubb2b* ( $\log_2\text{Fold Change}=-1.29$ ,  $\text{padj}=2.63\text{E-}07$ ), *Tomm7* ( $\log_2\text{Fold Change}=-1.13$ ,  $\text{padj}=9.61\text{E-}04$ ), *Naa38* ( $\log_2\text{Fold Change}=-1.09$ ,  $\text{padj}=3.15\text{E-}04$ ), and *Mei1* ( $\log_2\text{Fold Change}=-1.08$ ,  $\text{padj}=9.21\text{E-}03$ ). The results are shown in Figures 6A–D.

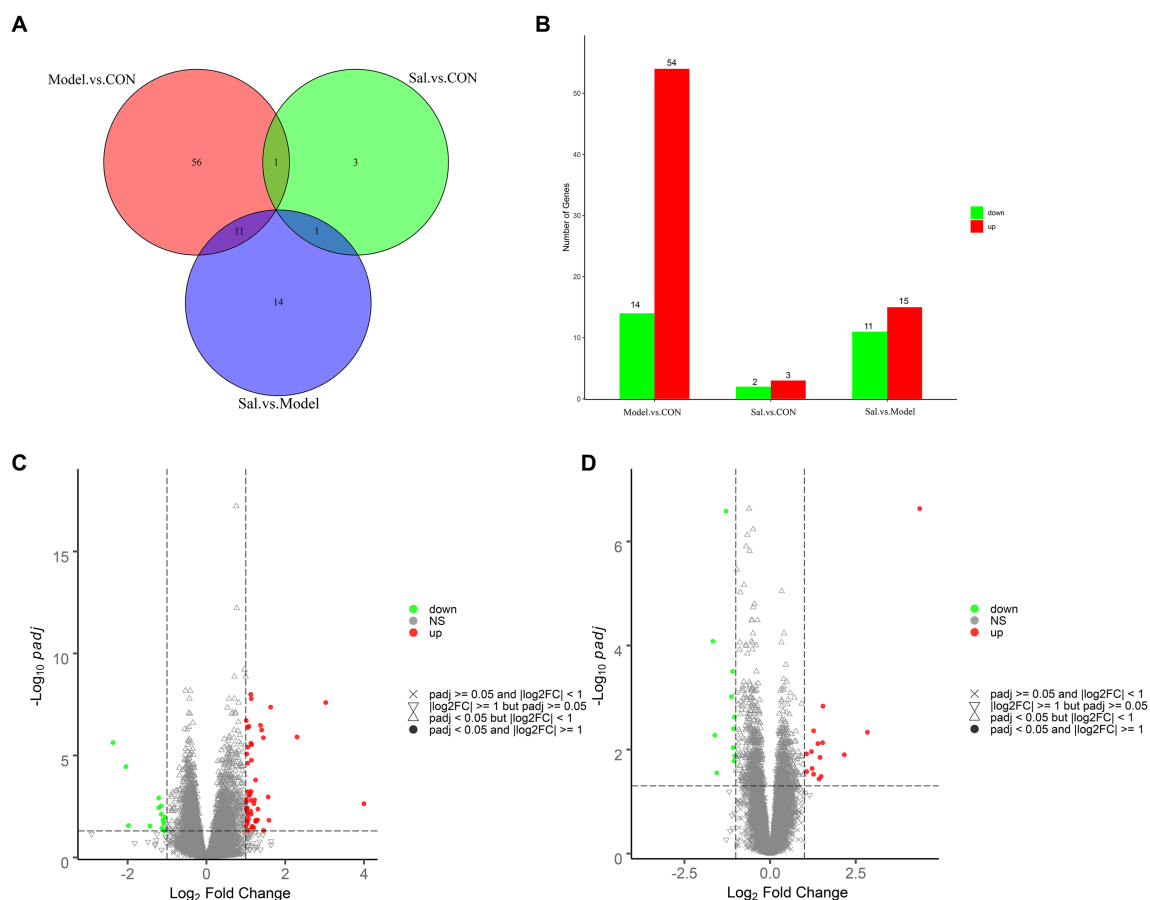


FIGURE 6

Analysis of differentially expressed genes among the CON, Model, and Sal groups. (A) Venn diagram of groups. (B) Histogram of differentially expressed genes among groups. (C) Volcano diagram of differentially expressed genes between the Model and CON groups. (D) Volcano diagram of differentially expressed genes between the Sal and Model groups. Red and green dots indicate up- and down-regulation, and gray dots indicate no differential gene expression.

## GO pathway analysis

Based on the GO database, the gene set enrichment analysis (GSEA) of the function of genes among the three groups revealed 314 GO terms with significant differences between the Model and CON groups. They included biological processes (197 subclasses), cell components (57 subclasses), and molecular functions (60 subclasses). Among them, the top five terms included mitochondrial inner membrane, translation, structural constituent of ribosome, immune response and cellular response

to tumor necrosis factor (Figure 7A). The core genes related to each term are shown in Figure 7B. A total of 652 significant GO terms were found between the *Sal* and Model groups; they included biological processes (416 subclasses), cell components (122 subclasses), and molecular functions (114 subclasses). Among them, the top five terms were mitochondrial inner member, translation, immediate response, structural constitution of ribosomes, and mRNA splicing, *via* spliceosome (Figure 7C). The core genes related to each term are shown in Figure 7D.

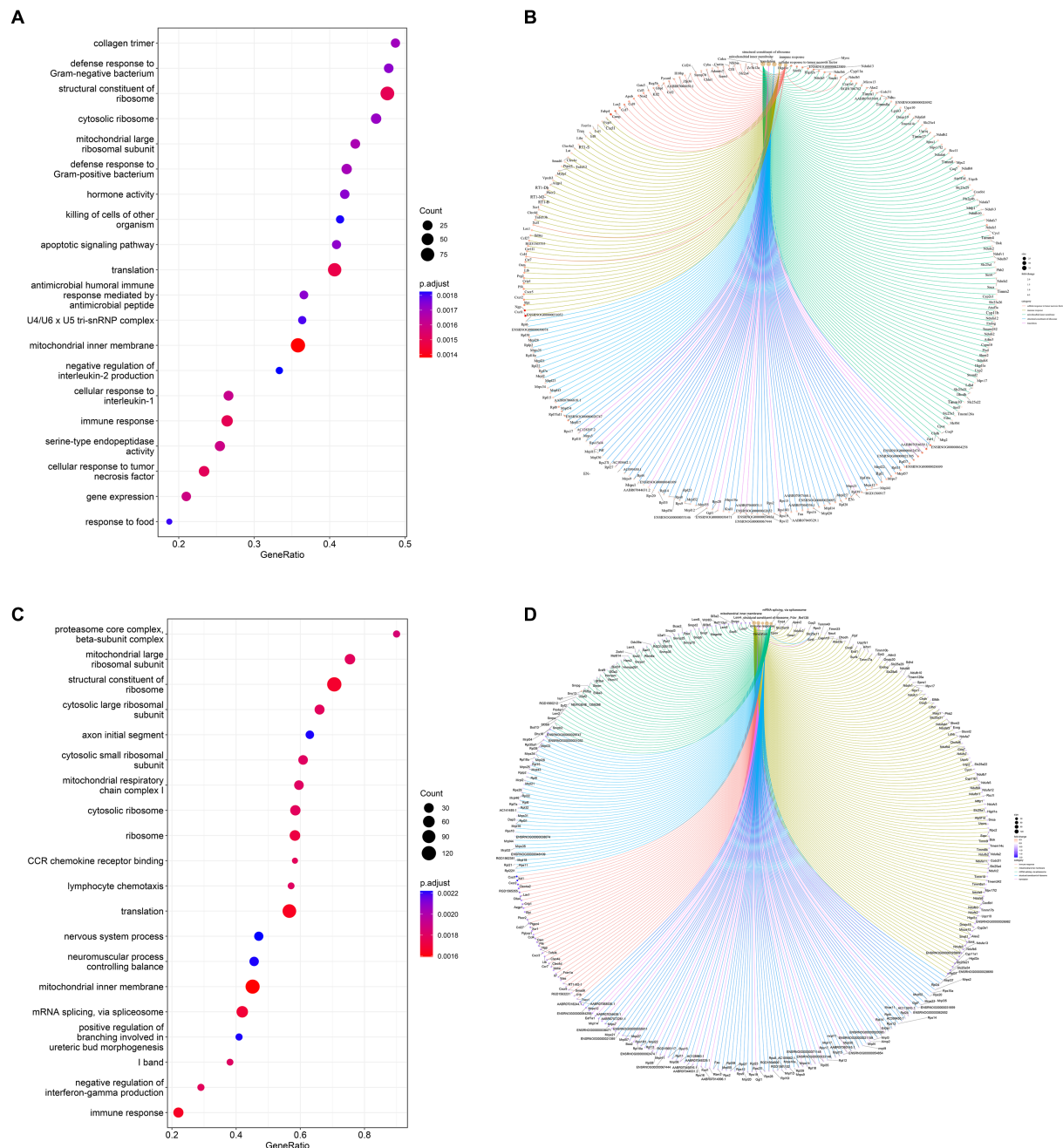
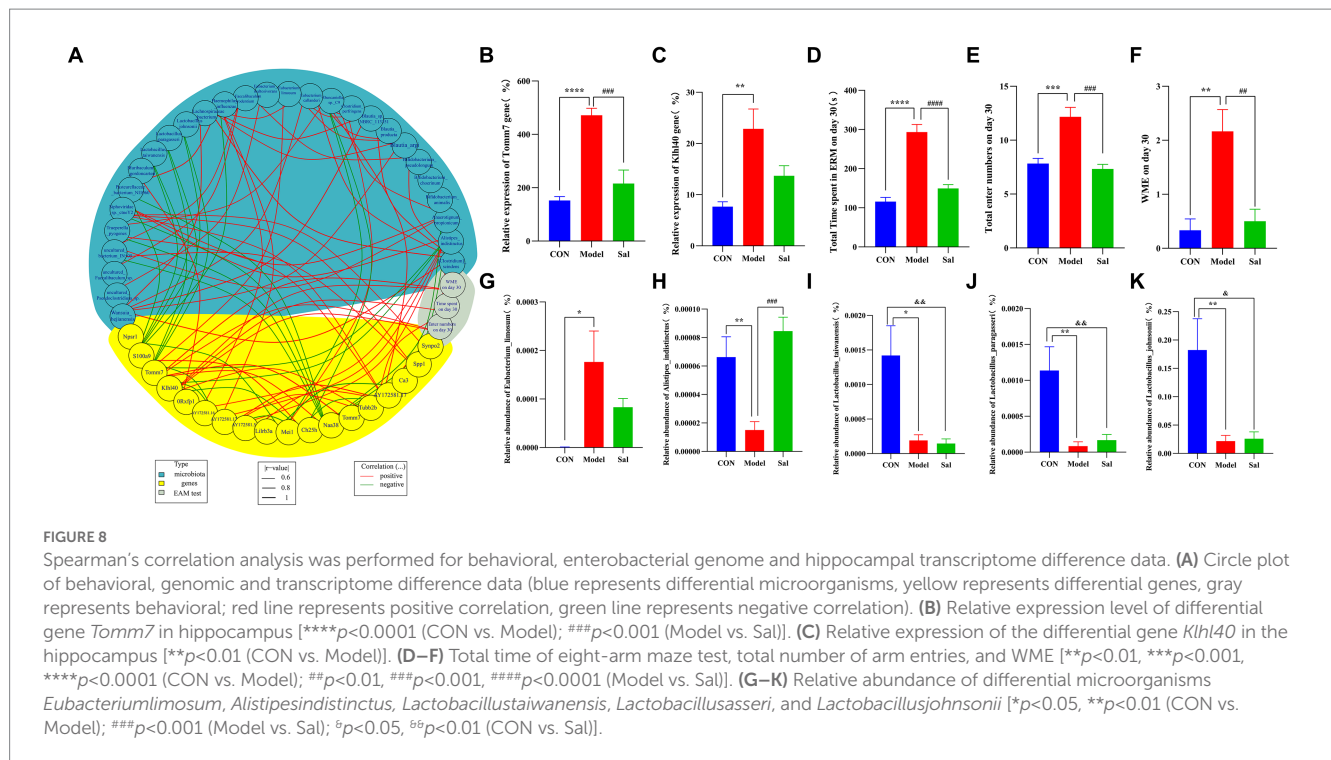


FIGURE 7

Dot plots of the main GO term enrichment analysis and core\_enrichment gene plots ( $n=6$  per group). Comparison of the 20 most important terms between (A) the Model and CON groups and (C) the *Sal* and Model groups. (B) Plots of core genes enriched to key terms between the Model and CON groups and (D) *Sal* and Model groups, with each dot representing a core gene.



## Combined multi-omics correlation analysis

Correlation analyses among data of behavioral, microbial genome, and hippocampal transcriptome were performed using the R package (R 4.2.2) (Figure 8). Compared with CON group, the Model group had a total time to complete the EAM, total number of arm entries, and WMEs on the 30th day to be positively correlated with the upregulation of *Tomm7* and *Klhl40* mRNA in rat hippocampus. The upregulation of *Tomm7* and *Klhl40* mRNA was positively correlated with the abundance of *Eubacteriumlimosum* and negatively correlated with the abundance of *Alistipesindistinctus*, *Lactobacustaiwanensis*, *Lactobacustaiwanensis*, *Lactobacustaiwanensis*, *Lactobacustaiwanensis*, and *Lactobacustaiwanensis* in the intestine of the Model group. Compared with the Model group, the Sal group had a significantly decreased mRNA expression of *Tomm7* in the hippocampus upon administration of Sal. This decreased expression was positively correlated with the abundance of *Alistipesindistinctus*, *Lactobacustaiwanensis*, *Lactobacustaiwanensis*, *Lactobacustaiwanensis*, and *Lactobacustaiwanensis* in the intestine of the Sal group.

## Discussion

In this study, we observed the ameliorative effect of Sal on memory impairment caused by long-term administration of EtOH in rats, which was manifested as the reduction in total time to complete the EAM task, decreased number of arm entries, and abated working memory errors in the EAM tests. Additionally, the metagenomic analysis revealed that the composition and diversity of intestinal flora were significantly altered in rats with memory improvement after Sal intervention, which are mainly associated with metabolism of amino acids, terpenoids, and polyketides. For instance, EtOH caused a decrease in the relative abundance of

*Actinobacteria*, *Bifidobacteriaceae*, *Akkermansiaceae*, and *Lactobacillus* and an increase in the relative abundance of *Romboutsia ilealis* in the intestinal tract of rats. The relative abundance of microorganisms in their intestinal contents improved with Sal intervention, especially the relative abundance of *Bifidobacterium*, *Ligilactobacillus*, *Adlercreutzia*, and *Lactobacillus* was increased. These findings confirmed the effect of Sal on intestinal microbes.

To verify whether Sal acts on the gut-brain axis, a transcriptomic analysis of hippocampal tissue was then performed. The overall results showed that 26 genes were differentially expressed after Sal intervention, compared with the Model group. Furthermore, enrichment analyses revealed that these differential genes were mainly involved in the mitochondrial inner membrane, translation, immune response, structural constituent of ribosome, and mRNA splicing. Finally, the multiple correlation analyses uncovered the correlation among the behaviors, gut microbiota, and changed expression of hippocampal genes. Altogether, these findings provide evidence that Sal can attenuate alcoholic memory impairment, which may be associated with an improvement in gut-brain axis function.

Memory is the physiological process of the CNS by which information or data about intra- or extra-environments are encoded, stored, and retrieved when needed. Memory is usually evaluated using the EAM test. In this study, either spatial memory or working memory performance was greatly improved by Sal treatment in rats administered with long-term EtOH. Additionally, according to the most popular theory in recent times, memory improvement by Sal treatment is likely linked to alteration in gut-brain function.

Gut microbiota are an integral part of the human body and affect human health and disease (Cockburn and Koropatkin, 2016). Studies have shown that alcohol consumption can lead to changes in the composition of gut microbes and affect immune factors,



immune system tolerance (Wang et al., 2022; Ye et al., 2022), and immune system function, which can lead to learning and memory impairment (Bishnoi et al., 2022). *Sal* plays a beneficial immunomodulatory role by regulating immune cell differentiation, inflammatory signaling pathway activation, and inflammatory factor secretion to reduce inflammatory damage in various diseases (Drayton et al., 2006; Wang et al., 2013). For example, Saldiogenin, a major component of *Rhodiola rosea* L, can reduce excessive inflammatory responses caused by asthma or cerebral ischemia by regulating the balance of helper T cells (Th1/Th2) [8] or macrophage polarization (Liu et al., 2018; Wang et al., 2018). These studies reflect the modulatory effects of Saldiogenin on various immune cells.

At this stage, the use of rats to model diseases of alcohol has been increasingly refined, and the various diseases caused by alcohol have been increasingly clearly studied (García-García et al., 2021; Crofton et al., 2022; Maccioni et al., 2022). However, changes in alcohol-induced intestinal flora and studies on brain-related brain regions are relatively rare. In the present study, the intestinal contents of rats were collected by continuous administration of *Sal* intervention. The flora of rat intestinal contents could be analyzed more accurately. By macrogenome sequencing analysis, we found significant differences in the abundance and diversity of the flora among the Model, *Sal*, and CON groups. This finding is consistent with the findings of Wang et al. (2023). The PCoA results showed that the composition of the flora was similar between the *Sal* and Model groups, but the relative abundance was differed. At the phylum level, the Model group had a higher relative abundance of the thick-walled phylum and a lower relative abundance of the *Actinobacteria* phylum, whereas the relative abundance of *Bifidobacterium* was lower. *Sal* intervention significantly increased the relative abundance of *Bifidobacterium*.

*Bifidobacterium* can pre-prevent alcoholic liver disease by modulating the intestinal microbiota in mice with chronic alcohol intake (Aldridge et al., 2022). To find the differential microorganisms between the *Sal* and Model groups using linear discriminant analysis, this study found that the significantly different families in the Model and *Sal* groups were *E. coli* and *Bifidobacterium* families, respectively. Numerous studies have found that *E. coli* can cause diarrhea and other symptoms in various organisms, including humans and mice (Shahbazi et al., 2021; Yu et al., 2023). Similarly, in this study, diarrheal symptoms were observed in the Model group. Additionally, *Bifidobacterium*, as one of the important probiotics, can regulate the balance of intestinal flora, inhibit tumor growth, and regulate immune function in the intestines (Li et al., 2022; Ren et al., 2022). In this study, we found that *Sal* significantly increased the relative abundance of *Bifidobacteria* and decreased the relative abundance of *E. coli* in rat intestine, thus acting as a regulator of the intestinal flora. This finding is consistent with the results of a previous study (Miyazaki et al., 2010). Therefore, *Sal* may play an important role in regulating intestinal flora imbalance. This finding is consistent with previous findings on the effects of other herbal medicines on intestinal flora (Mei et al., 2022; Xu et al., 2022; Chen et al., 2023). Functional enrichment analysis of the macrogenome showed that *Sal* affects the endocrine system and environmental adaptations by regulating intestinal flora.

A growing number of studies have shown that alterations in gut microbiota are closely associated with the development of neurological diseases (Hang et al., 2022), and alcohol consumption can lead to pathophysiological changes in several brain regions (Hansen et al., 2020; Varodayan et al., 2022). To further investigate whether *Sal* regulates the gut–brain axis through gut microbiota, we performed transcriptional sequencing analysis of hippocampal tissues. Transcriptional sequencing revealed 26 differentially expressed genes in the *Sal* group compared to the model group. They included 15 genes with elevated expression (*Olr1694*, *Ca3*, *Synpo2*, etc.) and 11 genes with decreased expression (*Ch25h*, *Tubb2b*, *Tomm7*, etc.). One study found that by rapidly increasing carbonic anhydrase (CA) concentrations in the cortex and hippocampus (two brain regions involved in memory processing), the extracellular signal-regulated kinase (ERK) pathway in the cortex and hippocampus—a key step in memory formation—could be rapidly increased (Canto de Souza et al., 2017).

Growing evidence indicate that brain carbonic anhydrase (CA) is a key regulator of cognition, especially in recognition and aversive memory. A study has found that injecting inhibitors of carbonic anhydrase in the hippocampal CA1 region or mPFC impairs short-term social recognition memory (Schmidt et al., 2022). The aforementioned study is consistent with the present study, in which the *Ca3* gene expression in the hippocampus was increased by *Sal* intervention, which in turn had the effect of improving memory. Abnormalities in  $\beta$ -microtubulin (*Tubb2b*) have been suggested to be probably associated with the pathophysiology of schizophrenia and have a unique role in neuronal differentiation and cell viability. In patients with schizophrenia, *Tubb2b* protein expression is reduced in the anterior cingulate cortex and increased in the dorsolateral prefrontal cortex; however, it remains unchanged in the superior temporal gyrus or hippocampus. In contrast, alcohol consumption can lead to cytoskeletal changes (Moehle et al., 2012). In the present study, we found that *Sal* intervention reduced hippocampal *Tubb2b* gene expression, which provides an idea to study memory impairment from a genetic perspective.

A GSEA of gene function based on the GO database for the *Sal* and Model groups revealed 652 significant GO terms between the two groups. The top five terms included mitochondrial inner membrane, translation, immune response, structural constituents of ribosome, and mRNA splicing, *via* spliceosome. The immune system is an important system that performs immune response and immune function, and alcohol abuse can lead to impairment of the immune system, which can be inherited by offspring through the maternal generation, resulting in severe immune deficiency (Bake et al., 2021). In the present study, we found that *Sal* is likely to improve alcohol-induced memory impairment by regulating hippocampal immune response, which provides a scientific basis for investigating the association between immune response and alcohol exquisite memory impairment.

Notably, we observed that the upregulation of *Tomm7* and *Klhl40* mRNA in rat hippocampus exhibited a positive regulatory role on behavioristics. *Tomm7* is a gene that encodes a subunit of mitochondrial outer membrane translocase and is involved in the transport and stability of mitochondrial proteins, and *klhl40* is a gene that encodes a protein containing Kelch repeat domains and



is involved in muscle development and function. Although none direct evidence, there still several hints that changes in the expression of *tomm7* and *klhl40* genes in the hippocampus of the alcohol-dependent rat model are associated with gut microbiota. One study found that acute ethanol treatment can induce neurodegeneration in cultured hippocampal neurons, leading to mitochondrial dysfunction, calcium processing defects, and synaptic damage in hippocampal neurons. This means that mitochondrial-related genes (such as *tomm7*) also play a role in this process (Pérez et al., 2020). Another study found that during the withdrawal period after alcohol exposure, the expression of miRNAs (microRNAs) and mRNAs (messenger RNAs) in the rat hippocampus area changed significantly, including some genes related to muscle development. This may mean that muscle-related genes (such as *klhl40*) also play a role in this process (Engen et al., 2015). Of course, these are only speculations and are not enough to prove a direct or indirect association between *tomm7*, *klhl40* genes and gut microbiota. More experimental data and analysis are needed to determine. Therefore, we further verified the variation of *tomm7* and *klhl40* in hippocampus by real-time PCR to ensure the viability of these hints.

Further, the administration of *Sal* leading to a downregulation of *tomm7*, as well as the positive correlation with the abundance of *Alistipesindistinctus*, *Lactobacustaiwanensis*, *Lactobacuspargi*, and *Lactobacuspargillusjohnsonii* in the intestine of the *Sal* group. Some studies suggest that *Alistipes indistinctus* can interact with other gut microbiota to influence gut barrier, immune system, and metabolism (Wang et al., 2021). None clear research on the physiological functions of *Lactobacustaiwanensis*. However, *Lactobacillus crispatus* is a common probiotic that mainly inhabits the vagina and intestine. It can produce hydrogen peroxide and has antibacterial, anti-inflammatory, and immune-regulatory effects (Lopez-Vicchi et al., 2020). *Lactobacuspargi* and *Lactobacuspargillusjohnsonii* are the type of lactic acid bacteria, belonging to the *Lactobacillus* genus. Their physiological functions have not been clearly studied. However, lactic acid bacteria generally have functions such as fermentation, lowering pH, inhibiting harmful bacteria, producing vitamins, and promoting digestion (Zhu et al., 2019). In our study, we first initiated the physiological functions of *Lactobacustaiwanensis*, *Lactobacuspargillusjohnsonii* and *Lactobacuspargi*, the type of *Lactobacillus* during *tomm7*-related *Sal* treatment in alcoholic memory impairment. There is a certain association between gut *Lactobacillus* and alcohol-induced memory impairment. Some studies suggest that supplementing with *Lactobacillus* can improve the composition and function of gut microbiota, thereby alleviating alcohol-induced damage to hippocampal neurons and cognitive function (Bloemendaal et al., 2021; Sun et al., 2022). Although none direct evidence reporting the association between *tomm7* and *Lactobacillus*. However, some studies identified that *Lactobacillus* could regulate the functions of the immune and nervous systems by producing outer membrane vesicles and soluble factors. These factors may affect the transport and stability of mitochondrial proteins, indirectly affecting the function of *tomm7* (Sun et al., 2015; Di Cerbo et al., 2016; Mata Forsberg et al., 2019). Our research suggests that *Sal* can affect the expression of *tomm7* in the hippocampus, and therefore *tomm7* can be used as a therapeutic target to improve alcohol-induced memory impairment, with *Sal* being a potential drug under

this pathological condition. Additionally, the *Alistipesindistinctus*, and three *Lactobacillus* of *Lactobacustaiwanensis*, *Lactobacuspargi*, and *Lactobacuspargillusjohnsonii* *Lactobacillus* represented can be used as dominant probiotics to affect hippocampal function and may serve as potential target microbiota for disease regulation and functional improvement, providing a compelling evidence for the translation of future drugs and the application of microbiota.

## Conclusion

Sustained intervention with *Sal* improves alcoholic memory dysfunction. Furthermore, this study revealed that *Sal* can alter the diversity and composition of gut microbiota and affect the expression of a large number of genes in the hippocampus of rats with alcohol-induced memory impairment. To our knowledge, this study is the first to report the effects of *Sal* intervention on gut microbiota and hippocampal transcriptome in rats with alcohol memory impairment. This study provides an important scientific basis for the role of the gut-brain axis in inducing alcohol memory impairment and elucidates the therapeutic role of *Sal* in the treatment of alcoholic memory impairment.

## Data availability statement

The datasets presented in this study can be found in online repositories. The name of the repository and accession number can be found at: China National Microbiology Data Center (NMDC); NMDC0000192.

## Ethics statement

The animal study was reviewed and approved by the Ethics Committee of Qiqihar Medical University.

## Author contributions

YJ, RZ, PL, and XL designed the experiments. YJ, ZZ, TW, LL, TL, XL, and DX performed the experiments. YJ, SW, PL, and XL performed the statistical analysis. RZ, PL, DX, ZZ, and YJ wrote the manuscript. All authors contributed to this article and approved the submitted version.

## Funding

This study was funded by the National Natural Science Foundation of China (82104173), and Qiqihar Academy of Medical Sciences, Grant No. QMSI2019M-09; Heilongjiang Provincial College Students Innovation and Entrepreneurship Project, Grant No. 201911230056; The Science Research Foundation of Qiqihar Medical Institute No. 2021-ZDPY-014; The Science Research Foundation of Qiqihar city, China No. LHYD-2021015; The Science Research Foundation of Qiqihar city, Qiqihar city, China No. LHYD-202011.

## Conflict of interest

The authors declare that the research was conducted in the absence of any commercial or financial relationships that could be construed as a potential conflict of interest.

## Publisher's note

All claims expressed in this article are solely those of the authors and do not necessarily represent those of their affiliated

organizations, or those of the publisher, the editors and the reviewers. Any product that may be evaluated in this article, or claim that may be made by its manufacturer, is not guaranteed or endorsed by the publisher.

## Supplementary material

The Supplementary material for this article can be found online at: <https://www.frontiersin.org/articles/10.3389/fmicb.2023.1172936/full#supplementary-material>

## References

- Aldridge, G. M., Zarin, T. A., Brandner, A. J., George, O., Gilpin, N. W., Repunte-Canonigo, V., et al. (2022). Effects of single and dual hypocretin-receptor blockade or knockdown of hypocretin projections to the central amygdala on alcohol drinking in dependent male rats. *Addict. Neurosci.* 3:100028. doi: 10.1016/j.addicn.2022.100028
- Bake, S., Pinson, M. R., Pandey, S., Chambers, J. P., Mota, R., Fairchild, A. E., et al. (2021). Prenatal alcohol-induced behavioral differences in immune, metabolic and neurobehavioral outcomes in adult rats. *Brain Ages Immun.* 98, 86–100. doi: 10.1016/j.bbi.2021.08.207
- Bishnoi, I. R., Cloutier, C. J., Tyson, C. D., Matic, V. M., Kavaliers, M., and Ossenkopp, K. P. (2022). Infection, learning, and memory: focus on immune activation and aversive conditioning. *Neurosci. Biobehav. Rev.* 142:104898. doi: 10.1016/j.neubiorev.2022.104898
- Bloemendaal, M., Szopinska-Tokov, J., Belzer, C., Boverhoff, D., Papalini, S., Michels, F., et al. (2021). Probiotics-induced changes in gut microbial composition and its effects on cognitive performance after stress: exploratory analyses. *Transl. Psychiatry* 11:300. doi: 10.1038/s41398-021-01404-9
- Buchfink, B., Xie, C., and Huson, D. H. (2015). Fast and sensitive protein alignment using DIAMOND. *Nat. Methods* 12, 59–60. doi: 10.1038/nmeth.3176
- Caleb, S. B., Julia, E. J. M., Peggy, S. K., Ethan, P. G., Abigail, L. W., and Mark, A. P. (2022). Ethanol sustains phosphorylated tau protein in the cultured rat hippocampus: implications for fetal alcohol spectrum disorders. *Alcohol* 103, 45–54. doi: 10.1016/j.alcohol.2022.07.007
- Canto de Souza, L., Provensi, G., Vullo, D., Carta, F., Scozzafava, A., Costa, A., et al. (2017). Carbonic anhydrase activation enhances object recognition in mice through phosphorylation of the extracellular signal-regulated kinase in the cortex and the hippocampus. *Neuropharmacology* 118, 148–156. doi: 10.1016/j.neuropharm.2017.03.009
- Chen, H. D., Jiang, M. Z., Zhao, Y. Y., Li, X., Lan, H., Yang, W. Q., et al. (2023). Effects of breviscapine on cerebral ischemia-reperfusion injury and intestinal flora imbalance by regulating the TLR4/MyD88/NF- $\kappa$ B pathway in rats. *J. Ethnopharmacol.* 300:115691. doi: 10.1016/j.jep.2022.115691
- Chen, S. F., Zhou, Y. Q., Chen, Y. R., and Gu, J. (2018). Fastp: an ultra-fast all-in-one FASTQ preprocessor. *Bioinformatics* 34, i884–i890. doi: 10.1093/bioinformatics/bty560
- Choi, N. G. (2021). Alcohol use disorder and treatment receipt among individuals aged 50 years and older: other substance use and psychiatric correlates. *J. Subst. Abuse Treat.* 131:108445. doi: 10.1016/j.jsat.2021.108445
- Cockburn, D. W., and Koropatkin, N. M. (2016). Polysaccharide degradation by the intestinal microbiota and its influence on human health and disease. *J. Mol. Biol.* 428, 3230–3252. doi: 10.1016/j.jmb.2016.06.021
- Collin, D. T., and Eric, J. N. (2022). Teenage drinking and adult neuropsychiatric disorders: an epigenetic connection. *Sci. Adv.* 8:eabq5934. doi: 10.1126/sciadv.abq5934
- Contreras, A., Polin, E., Miguéns, M., Pérez-García, C., Pérez, V., Ruiz-Gayo, M., et al. (2019). Intermittent-excessive and chronic-moderate ethanol intake during adolescence impair spatial learning, memory and cognitive flexibility in the adulthood. *Neuroscience* 418, 205–217. doi: 10.1016/j.neuroscience.2019.08.051
- Cox, L. M., and Weiner, H. L. (2018). Microbiota signaling pathways that influence neurological disease. *Neurotherapeutics* 15, 135–145. doi: 10.1007/s13311-017-0598-8
- Crofton, E. J., Zhu, M. H., Curtis, K. N., Nolan, G. W., O'Buckley, T. K., Morrow, A. L., et al. (2022). Medial prefrontal cortex-basolateral amygdala circuit dysfunction in chronic alcohol-exposed male rats. *Neuropharmacology* 205:108912. doi: 10.1016/j.neuropharm.2021.108912
- di Cerbo, A., Palmieri, B., Aponte, M., Morales-Medina, J. C., and Iannitti, T. (2016). Mechanisms and therapeutic effectiveness of lactobacilli. *J. Clin. Pathol.* 69, 187–203. doi: 10.1136/clinpath-2015-202976
- Drayton, D., Liao, S., Mounzer, R., and Ruddle, N. H. (2006). Lymphoid organ development: from ontogeny to neogenesis. *Nat. Immunol.* 7, 344–353. doi: 10.1038/nri1330
- Dumont, U., Sanchez, S., Olivier, B., Chateil, J. F., Deffieux, D., Quideau, S., et al. (2020). Maternal alcoholism and neonatal hypoxia-ischemia: neuroprotection by stilbenoid polyphenols. *Brain Res.* 1738:146798. doi: 10.1016/j.brainres.2020.146798
- Engen, P. A., Green, S. J., Voigt, R. M., Forsyth, C. B., and Keshavarzian, A. (2015). The gastrointestinal microbiome: alcohol effects on the composition of intestinal microbiota. *Alcohol. Res.* 37, 223–236. doi: 10.13140/RG.2.1.4342.9285
- García-García, F., Priego-Fernández, S., López-Mucio, L. A., Acosta-Hernández, M. E., and Peña-Escudero, C. (2021). Increased alcohol consumption in sleep-restricted rats is mediated by delta FosB induction. *Alcohol* 93, 63–70. doi: 10.1016/j.alcohol.2021.02.004
- Hang, Z. C., Lei, T., Zeng, Z. H., Cai, S., Bi, W., and du, H. (2022). Composition of intestinal flora affects the risk relationship between Alzheimer's disease/Parkinson's disease and cancer. *Biomed. Pharmacother.* 145:112343. doi: 10.1016/j.biopha.2021.112343
- Hansen, A. W., Almeida, F. B., Bandiera, S., Pulcinelli, R. R., Caletti, G., Agnes, G., et al. (2020). Correlations between withdrawal of GABAA and NMDA receptors after chronic alcohol treatment or subunits and the effect of taurine in the hippocampus of rats. *Alcohol* 82, 63–70. doi: 10.1016/j.alcohol.2019.08.005
- Jiao, Y., Kim, S. C., and Wang, Y. (2021). Sauchinone Blocks Ethanol Withdrawal-Induced Anxiety but Spares Locomotor Sensitization: Involvement of Nitric Oxide in the Bed Nucleus of the Stria Terminalis. *Evid Based Complement Alternat Med.* 2021:6670212. doi: 10.1155/2021/6670212
- Ke, X., Zhang, R., Li, P., Zuo, L., Wang, M., Yang, J., et al. (2022). Hydrochloride Berberine ameliorates alcohol-induced liver injury by regulating inflammation and lipid metabolism. *Biochem. Biophys. Res. Commun.* 610, 49–55. doi: 10.1016/j.bbrc.2022.04.009
- Kim, D., Langmead, B., and Salzberg, S. L. (2015). HISAT: a fast spliced aligner with low memory requirements. *Nat. Methods* 12, 357–360. doi: 10.1038/nmeth.3317
- Konstantin, O., Ana, C., and Fernando, G. (2016). Qualimap 2: advanced multi-sample quality control for high-throughput sequencing data. *Bioinformatics* 32, 292–294. doi: 10.1093/bioinformatics/btv566
- Li, N., Wang, J., Liu, P., Li, J., and Xu, C. (2022). Multi-omics reveals that *Bifidobacterium breve* M-16V may alleviate the immune dysregulation caused by nanoplastyrene. *Environ. Int.* 163:107191. doi: 10.1016/j.envint.2022.107191
- Li, Y., Zhao, Y., Li, X., Liu, T., Jiang, X., and Han, F. (2017). Characterization of global metabolic profile of *Saldiola crenulata* after oral administration in rat plasma, urine, bile and feces based on UHPLC-FT-ICR MS. *J. Pharm. Biomed. Anal.* 149, 318–328. doi: 10.1016/j.jpba.2017.10.032
- Liu, X., Wen, S., Yan, F., Liu, K., Liu, L., Wang, L., et al. (2018). Sallidroside provides neuroprotection by modulating al polarization after cerebral ischemia. *J. Neuroinflammation* 15:39. doi: 10.1186/s12974-018-1081-0
- Lopez-Vicchi, F., de Winne, C., Brie, B., Soriano, E., Ladyman, S. R., and Becu-Villalobos, D. (2020). Metabolic functions of prolactin: physiological and pathological aspects. *J. Neuroendocrinol.* 32:e12888. doi: 10.1111/jne.12888
- Maccioni, P., Bratzu, J., Lobina, C., Acciaro, C., Corrias, G., Capra, A., et al. (2022). Exposure to an enriched environment reduces alcohol self-administration in Sardinian alcohol-preferring rats. *Physiol. Behav.* 249:113771. doi: 10.1016/j.physbeh.2022.113771
- Marcondes Ávila, P. R., Fiorot, M., Michels, M., Domingui, D., Abatti, M., Vieira, A., et al. (2020). Effects of microbiota transplantation and the role of the vagus nerve in gut-brain axis in animals subjected to mild chronic stress. *J. Affect. Disord.* 277, 410–416. doi: 10.1016/j.jad.2020.08.013
- Mata Forsberg, M., Björkander, S., Pang, Y., Lundqvist, L., Ndi, M., Ott, M., et al. (2019). Extracellular membrane vesicles from lactobacilli dampen IFN- $\gamma$  responses in a monocyte-dependent manner. *Sci. Rep.* 9:17109. doi: 10.1038/s41598-019-53576-6

- Mei, B. W., Rong, S. Y., Li, Z., Gu, E., Zhou, Z., and Qi, Y. (2022). Evaluation of traditional Chinese medicine 'effect on improving the health of adults' intestinal fitness: an optical tool based on ultrasensitive bioluminescent flora and applications. *Med. Eng. Phys.* 111:103943. doi: 10.1016/j.medengphy.2022.103943
- Miyazaki, Y., Yokota, H., Takahashi, H., Fukuda, M., Kawakami, H., Kamiya, S., et al. (2010). Effect of probiotic bacterial strains of *Lactobacillus*, *Bifidobacterium*, and *Enterococcus* on enteroregulatory *Escherichia coli*. *J. Infect. Chemother.* 16, 10–18. doi: 10.1007/s10156-009-0007-2
- Moehle, M. S., Luduena, R. F., Haroutunian, V., Meador-Woodruff, J. H., and McCullumsmith, R. E. (2012). Regional differences in expression of  $\beta$ -tubulin isoforms in schizophrenia. *Schizophr. Res.* 135, 181–186. doi: 10.1016/j.schres.2011.12.010
- Panosian, A., Nikoyan, N., Ohanyan, N., Hovhannisyanyan, A., Abrahamyan, H., Gabrielyan, E., et al. (2008). Comparative behavioral study of *Sal diola* on behavioral despair of rats. *Phytomedicine* 15, 84–91. doi: 10.1016/j.phymed.2007.10.003
- Parsons, O. A. (1986). Cognitive functioning in sober social drinkers: a review and critique. *J. Stud. Alcohol* 47, 101–114. doi: 10.15288/jsa.1986.47.101
- Pérez, M. J., Loyola, R., Canelo, F., Aranguiz, A., Tapia-Monsalves, C., Osorio-Fuentealba, C., et al. (2020). NADPH oxidase contributes to oxidative damage and mitochondrial impairment induced by acute ethanol treatment in rat hippocampal neurons. *Neuropharmacology* 171:108100. doi: 10.1016/j.neuropharm.2020.108100
- Pradhananga, S., Tashtush, A. A., Allen-Vercos, E., Petrof, E. O., and Lomax, A. E. (2020). Protease-dependent excitation of nodose ganglion neurons by commensal gut bacteria. *J. Physiol* 598, 2137–2151. doi: 10.1113/JP279075
- Qamar, N., Castano, D., Patt, C., Chu, T., Cottrell, J., and Chang, S. L. (2019). Meta-analysis of alcohol-induced dysbiosis and the resulting behavioral impact. *Behav. Brain Res.* 376:112196. doi: 10.1016/j.bbr.2019.112196
- Ren, Z. Y., Chen, S. F., Lv, H., Peng, L., Yang, W., Chen, J., et al. (2022). Effect of *Bifidobacterium animalis* subsp. *lactis* SF on enhancing the tumor suppression of irinotecan by regulating the intestinal flora. *Pharmacol. Res.* 184:106406. doi: 10.1016/j.phrs.2022.106406
- Sase, A., Nawaratna, G., Hu, S., Wu, G., and Lubec, G. (2016). Decreased homoarginine and increased nitric oxide and nitric oxide synthase levels in parallel training in rats in a radial arm maze. *Amino Acids* 48, 2197–2204. doi: 10.1007/s00726-016-2251-y
- Schmidt, S. D., Nachtigall, E. G., Marcondes, L. A., Zanluchi, A., Furini, C. R. G., Passani, M. B., et al. (2022). Modulation of carbonic anhydrases activity in the hippocampus or prefrontal cortex differentially affects social recognition memory in rats. *Neuroscience* 497, 184–195. doi: 10.1016/j.neuroscience.2022.03.025
- Shahbazi, G., Rezaee, M. A., Nikkahi, F., Ebrahimzadeh, S., Hemmati, F., Namavar, B. B., et al. (2021). Characteristics of diarrheagenic *Escherichia coli* pathotypes among children under the age of 10 years with acute diarrhea. *Gene Rep.* 25:101318. doi: 10.1016/j.genrep.2021.101318
- Shevtsov, V. A., Zholus, B. I., and Shervarly, V. I., Vol'skij, V. B., Korovin, Y. P., Khristich, M. P., Roslyakova, N. A., and Wikman, G. (2003). A randomized trial of two different doses of a SHR-5 *Sallidroside diola rosea* extract versus placebo and control of capacity for mental work. *Phytomedicine* 10:95–105. doi: 10.1078/094471103321659780
- Sun, Z., Harris, H., McCann, A., Guo, C., Argimón, S., Zhang, W., et al. (2015). Expanding the biotechnology potential of lactobacilli through comparative genomics of 213 strains and associated genera. *Nat. Commun.* 6:8322. doi: 10.1038/ncomms9322
- Sun, N., Zhu, B., Xin, J., Li, L., Gan, B., Cao, X., et al. (2022). Psychoactive effects of *Lactobacillus johnsonii* BS15 on preventing memory dysfunction induced by acute ethanol exposure through modulating intestinal microenvironment and improving alcohol metabolic level. *Front. Microbiol.* 13:847468. doi: 10.3389/fmicb.2022.847468
- Topiwala, A., Allan, C. L., Valkanova, V., Zsoldos, E., Filippini, N., Sexton, C., et al. (2017). Moderate alcohol consumption as risk factor for adverse brain outcomes and cognitive decline: longitudinal cohort study. *BMJ* 357:j2353. doi: 10.1136/bmj.j2353
- Uniyal, A., Singh, R., Akhtar, A., Bansal, Y., Kuhad, A., and Sah, S. P. (2019). Co-treatment of piracetam with risperidone rescued physiological deficits in experimental paradigms of post-traumatic stress disorder by restoring the physiological alterations in cortex and hippocampus. *Pharmacol. Biochem. Behav.* 185:172763. doi: 10.1016/j.pbb.2019.172763
- van Diermen, D., Marston, A., Bravo, J., Reist, M., Carrupt, P. A., and Hostettmann, K. (2009). Monoamine oxidase inhibition by *Rhodiola rosea* L. roots. *J. Ethnopharmacol.* 122:397–401. doi: 10.1016/j.jep.2009.01.007
- Varodayan, F. P., Patel, R. R., Matzeu, A., Wolfe, S. A., Curley, D. E., Khom, S., et al. (2022). The amygdala noradrenergic system is compromised with alcohol use disorder. *Biol. Psychiatry* 91, 1008–1018. doi: 10.1016/j.biopsych.2022.02.006
- Villar, E., Farrant, G. K., Follows, M., Garczarek, L., Speich, S., Audic, S., et al. (2015). Environmental characteristics of *Agulhas* rings affect interocean plankton transport. *Science* 348:1261447. doi: 10.1126/science.1261447
- Wang, Q., Kuang, H., Su, Y., Sun, Y., Feng, J., Guo, R., et al. (2013). Naturally derived anti-inflammatory compounds from Chinese medicinal plants. *J. Ethnopharmacol.* 146, 9–39. doi: 10.1016/j.jep.2012.12.013
- Wang, X. L., Li, L., Bian, C., Bai, M., Yu, H., Gao, H., et al. (2023). Alterations and correlations of gut microbiota, fecal, and serum metabolome characteristics in a rat model of alcohol use disorder. *Front. Microbiol.* 13:1068825. doi: 10.3389/fmicb.2022.1068825
- Wang, K., Shi, J., Gao, S., Hong, H., Tan, Y., and Luo, Y. (2022). Oyster protein hydrolysates alleviated chronic alcohol-induced liver injury in mice by regulating hepatic lipid metabolism and inflammation response. *Food Res. Int.* 160:111647. doi: 10.1016/j.foodres.2022.111647
- Wang, C., Wang, Q., Lou, Y., Xu, J., Feng, Z., Chen, Y., et al. (2018). Sallidroside attenuates neuroinflammation and improves functional recovery after spinal cord injury through microglia polarization regulation. *J. Cell. Mol. Med.* 22, 1148–1166. doi: 10.1111/jcmm.13368
- Wang, B., Zhang, L., Dai, T., Qin, Z., Lu, H., Zhang, L., et al. (2021). Liquid-liquid phase separation in human health and diseases. *Sig. Transduct. Target Ther.* 6:290. doi: 10.1038/s41392-021-00678-1
- Wood, D., and Salzberg, S. (2014). Kraken: ultrafast metagenomic sequence classification using exact alignments. *Genome Biol.* 15:R46. doi: 10.1186/gb-2014-15-3-r46
- Xia, T., Duan, W., Zhang, Z., Li, S., Zhao, Y., Geng, B., et al. (2021). Polyphenol-rich vinegar extract regulates intestinal microbiota and immunity and prevents alcohol-induced inflammation in mice. *Food Res. Int.* 140:110064. doi: 10.1016/j.foodres.2020.110064
- Xu, B. G., Zheng, J. W., Tian, X. X., Yuan, F., Liu, Z., Zhou, Y., et al. (2022). Protective mechanism of traditional Chinese medicine guizhi fuling pills against carbon tetrachloride-induced kidney damage is through inhibiting oxidative stress, inflammation and regulating the intestinal flora. *Phytomedicine* 101:154129. doi: 10.1016/j.phymed.2022.154129
- Ye, M. X., Xiang, H. T., Liu, H. J., Hu, Z., Wang, Y., Gu, Y., et al. (2022). Innate immune tolerance against adolescent intermittent alcohol exposure-induced behavioral abnormalities in adult mice. *J. Int. Immunopharmacol.* 113:109250. doi: 10.1016/j.intimp.2022.109250
- Yu, F. Z., Guo, J., Ren, H. L., Lu, S., He, Z., Chang, J., et al. (2023). Tyrosol inhibits NF- $\kappa$ B pathway in the treatment of enterotoxigenic *Escherichia coli*-induced diarrhea in mice. *Microb. Pathog.* 176:105944. doi: 10.1016/j.micpath.2022.105944
- Zhao, Z., Kim, S. C., Jiao, Y., Wang, Y., Lee, B. H., Kim, H. Y., et al. (2021). Solitary nitric oxide signaling mediates mild stress-induced anxiety and norepinephrine release in the bed nucleus of the stria terminalis during protracted ethanol withdrawal. *Behav. Neurol.* 2021:2149371. doi: 10.1155/2021/2149371
- Zhu, W., Zhang, M., Chang, L., Zhu, W., Li, C., Xie, F., et al. (2019). Characterizing the composition, metabolism and physiological functions of the fatty liver in *Rana omeimontis* tadpoles. *Front. Zool.* 16:42. doi: 10.1186/s12983-019-0341-x



## OPEN ACCESS

## EDITED BY

WeiQi He,  
Soochow University, China

## REVIEWED BY

Maria Manuela Rosado,  
Sapienza University of Rome, Italy  
Silvia Pires,  
Weill Cornell Medicine, United States

## \*CORRESPONDENCE

Teruyuki Sano  
✉ tsano1@uic.edu

RECEIVED 31 January 2023

ACCEPTED 07 September 2023

PUBLISHED 13 October 2023

## CITATION

White Z, Cabrera I, Kapustka I and  
Sano T (2023) Microbiota as key factors in  
inflammatory bowel disease.  
*Front. Microbiol.* 14:1155388.  
doi: 10.3389/fmicb.2023.1155388

## COPYRIGHT

© 2023 White, Cabrera, Kapustka and Sano.  
This is an open-access article distributed under  
the terms of the [Creative Commons Attribution  
License \(CC BY\)](#). The use, distribution or  
reproduction in other forums is permitted,  
provided the original author(s) and the  
copyright owner(s) are credited and that the  
original publication in this journal is cited, in  
accordance with accepted academic practice.  
No use, distribution or reproduction is  
permitted which does not comply with these  
terms.

# Microbiota as key factors in inflammatory bowel disease

Zachary White, Ivan Cabrera, Isabel Kapustka and Teruyuki Sano\*

Department of Microbiology and Immunology, College of Medicine, University of Illinois at Chicago,  
Chicago, IL, United States

Inflammatory Bowel Disease (IBD) is characterized by prolonged inflammation of the gastrointestinal tract, which is thought to occur due to dysregulation of the immune system allowing the host's cells to attack the GI tract and cause chronic inflammation. IBD can be caused by numerous factors such as genetics, gut microbiota, and environmental influences. In recent years, emphasis on commensal bacteria as a critical player in IBD has been at the forefront of new research. Each individual harbors a unique bacterial community that is influenced by diet, environment, and sanitary conditions. Importantly, it has been shown that there is a complex relationship among the microbiome, activation of the immune system, and autoimmune disorders. Studies have shown that not only does the microbiome possess pathogenic roles in the progression of IBD, but it can also play a protective role in mediating tissue damage. Therefore, to improve current IBD treatments, understanding not only the role of harmful bacteria but also the beneficial bacteria could lead to attractive new drug targets. Due to the considerable diversity of the microbiome, it has been challenging to characterize how particular microorganisms interact with the host and other microbiota. Fortunately, with the emergence of next-generation sequencing and the increased prevalence of germ-free animal models there has been significant advancement in microbiome studies. By utilizing human IBD studies and IBD mouse models focused on intraepithelial lymphocytes and innate lymphoid cells, this review will explore the multifaceted roles the microbiota plays in influencing the immune system in IBD.

## KEYWORDS

host-pathogen interaction, gut innate immunity, IELs, ILCs, protective bacteria for IBD

## Introduction

Inflammatory bowel disease (IBD) is characterized as a chronic immune-mediated inflammatory disease affecting the gastrointestinal tract. IBD can be divided into two subgroups: Crohn's Disease (CD), and Ulcerative Colitis (UC) ([Crohn's and Colitis Foundation, 2014](#)). CD can occur anywhere along the gastrointestinal tract and involve patches of healthy tissue mixed between inflamed areas, on the other hand, UC is limited to the colon and has continuous inflammation of large areas of the colon ([Fakhoury et al., 2014](#)). The National Institute of Allergy and Infectious Diseases (NIAID) is focusing on IBD as one of the specific autoimmune diseases for intense study.<sup>1</sup> The prevalence of IBD is increasing worldwide, recent reports have recorded that an estimated 2 million people in North America,

<sup>1</sup> <https://www.niaid.nih.gov/diseases-conditions/autoimmune-disease-research>



3.2 million people in Europe, and millions more in east and southern Asia, have been diagnosed with IBD as of 2020 (Ananthakrishnan et al., 2020; Olatifafar et al., 2021; Zhao et al., 2021). With rates of IBD rising all over the world, development of new strategies to combat IBD are critically needed. Although the underlying causes of IBD are ill-defined, IBD is thought to develop due to microbial, environmental, genetic, and immune-mediated factors (Khan et al., 2019; Glassner et al., 2020; Mentella et al., 2020). Recently, the importance of the microbiome in the development of IBD has been at the forefront of study (Khan et al., 2019; Somineni and Kugathasan, 2019).

Our microbiomes contain more than 100 trillion different microorganisms, including bacteria, viruses, fungi, and protozoa. The gastrointestinal (GI) tract is one niche that harbors significant populations of these microorganisms (Figure 1). The predominant bacterial populations in a healthy microbiome are *Firmicutes*, *Actinobacteria*, *Bacteroidetes*, and *Verrucomicrobia* (Pickard et al., 2017; Kho and Lal, 2018). Importantly, the distribution of bacterial species throughout the GI tract varies (Table 1). The colon harbors the greatest number and diversity of bacteria with the highest proportion of colon colonizing bacteria being *Bacteroides*, *Bifidobacterium*, and *Clostridiales* (Vuik et al., 2019). These bacteria can survive in this location because they might be adept at using enzymes to break down and digest complex polysaccharides which are indigestible by the host (Flint et al., 2012). The stomach on the other hand contains comparatively few microorganisms due to its high-stress conditions, with its main populations being *Streptococcus*, *Prevotella*, *Rothia*, and *Veillonella* (Nardone and Compare, 2015). Moreover, the small intestine also contains lower bacterial populations compared to colon,

most likely due to its proximity to the stomach, and is rich in mono- and di-saccharides which promote *Proteobacteria* and *Firmicutes* (Vuik et al., 2019; Leite et al., 2020). This description of the “healthy” microbiome is not complete however, as it is noted that during dysbiosis there is the possibility that these normally commensal bacteria can emerge as pathobionts due to the altered environment of the gut. Therefore, a comprehensive analysis of potential pathobionts and opportunistic microbes is required before we can define a truly “healthy” microbiome (Chervy et al., 2020; Mancini et al., 2021). The gut microbiome can play a critical role in gut homeostasis, metabolism, immune activation, and defending against intestinal pathogens. Thus, the study of how the gut microbiome influences the immune system to either combat or promote IBD will provide valuable insights for new drug targets or therapeutics.

## The microbiome and inflammatory bowel disease

The gut microbiome contains high concentrations of commensals, such that immunomodulatory bacteria will constantly be providing stimuli to the host’s immune cells, especially dendritic cells and macrophages which extend their dendrites to capture such bacteria. During non-perturbed circumstances, this stimulation will lead to immunologic tolerance which prevents unwanted intestinal inflammation. It is believed that genetic susceptibility, environmental factors, and certain microbes can cause this controlled tolerance to become dysregulated and lead to the development of colitis. Although the mechanisms underlying how and why this occurs are not

TABLE 1 Distinct microbiota associations.

Tissue	Phyla: Genus	Environment	Reference
• Stomach	<ul style="list-style-type: none"> <li>Firmicutes: <i>Lactobacillus</i>, <i>Streptococcus</i>, <i>Enterococcus</i>, <i>Veillonella</i></li> <li>Proteobacteria: <i>Helicobacter</i>, <i>Haemophilus</i>, <i>Neisseria</i></li> <li>Actinobacteria: <i>Rothia</i>, <i>Propionibacterium</i></li> <li>Bacteroidetes: <i>Bacteroides</i> <i>Prevotella</i></li> </ul>	<ul style="list-style-type: none"> <li>Partially Aerobic</li> <li>Highly acidic</li> </ul>	<ul style="list-style-type: none"> <li>Nardone and Compare (2015)</li> <li>Yang et al. (2013)</li> <li>Wu et al. (2014)</li> <li>Martinez-Guryn et al. (2019)</li> </ul>
• Duodenum	<ul style="list-style-type: none"> <li>Firmicutes: <i>Lactobacillus</i>, <i>Clostridium</i>, <i>Staphylococcus</i>, <i>Streptococcus</i></li> <li>Bacteroidetes: <i>Bacteroides</i></li> <li>Actinobacteria: <i>Bifidobacterium</i></li> <li>Proteobacteria: <i>Neisseria</i></li> </ul>	<ul style="list-style-type: none"> <li>Partially Aerobic</li> <li>Neutral</li> </ul>	<ul style="list-style-type: none"> <li>Wang et al. (2005)</li> <li>Cheng et al. (2013)</li> <li>Kastl et al. (2020)</li> <li>Martinez-Guryn et al. (2019)</li> </ul>
• Jejunum	<ul style="list-style-type: none"> <li>Firmicutes: <i>Streptococcus</i>, <i>Veillonella</i>, <i>Clostridium</i>, <i>Enterococcus</i>, <i>Lactobacillus</i></li> <li>Proteobacteria: <i>Escherichia</i>, <i>Haemophilus</i>, <i>Neisseria</i>, <i>Klebsiella</i>, <i>Citrobacter</i></li> <li>Bacteroidetes: <i>Prevotella</i>, <i>Bacteroides</i></li> <li>Actinobacteria: <i>Bifidobacterium</i>, <i>Rothia</i>, <i>Actinomyces</i></li> <li>Fusobacteria: <i>Fusobacterium</i>, <i>Leptotrichia</i></li> </ul>	<ul style="list-style-type: none"> <li>Partially Aerobic</li> <li>Neutral</li> </ul>	<ul style="list-style-type: none"> <li>Sundin et al. (2017)</li> <li>Martinez-Guryn et al. (2019)</li> </ul>
• Ileum	<ul style="list-style-type: none"> <li>Firmicutes: <i>Clostridium</i>, <i>Peptostreptococcus</i>, <i>Lactobacilli</i>, <i>Enterococcus</i></li> <li>Actinobacteria: <i>Bifidobacterium</i></li> <li>Proteobacteria: <i>Helicobacter</i>, <i>Escherichia</i></li> <li>Bacteroidetes: <i>Bacteroides</i>, <i>Prevotella</i></li> </ul>	<ul style="list-style-type: none"> <li>Partially Aerobic</li> <li>Acidic</li> </ul>	<ul style="list-style-type: none"> <li>Villmones et al. (2018)</li> <li>Martinez-Guryn et al. (2019)</li> </ul>
• Colon	<ul style="list-style-type: none"> <li>Firmicutes: <i>Clostridium</i>, <i>Ruminococcus</i>, <i>Lactobacilli</i></li> <li>Proteobacteria: <i>Escherichia</i>, <i>Enterobacter</i>, <i>Helicobacter</i>, <i>Klebsiella</i></li> <li>Bacteroidetes: <i>Bacteroides</i>, <i>Prevotella</i>, <i>Alistipes</i></li> <li>Actinobacteria: <i>Bifidobacterium</i></li> <li>Verrucomicrobia: <i>Akkermansia</i></li> </ul>	<ul style="list-style-type: none"> <li>Highly Anaerobic</li> <li>Neutral</li> </ul>	<ul style="list-style-type: none"> <li>Mailhe et al. (2018)</li> <li>Thursby and Juge (2017)</li> <li>Martinez-Guryn et al. (2019)</li> </ul>

Associations of microbiota and regions of GI tract. There are specific bacteria that tend to colonize in distinct locations in the stomach and intestines. This is most likely due to the local micro-environment that promotes certain bacteria over others.

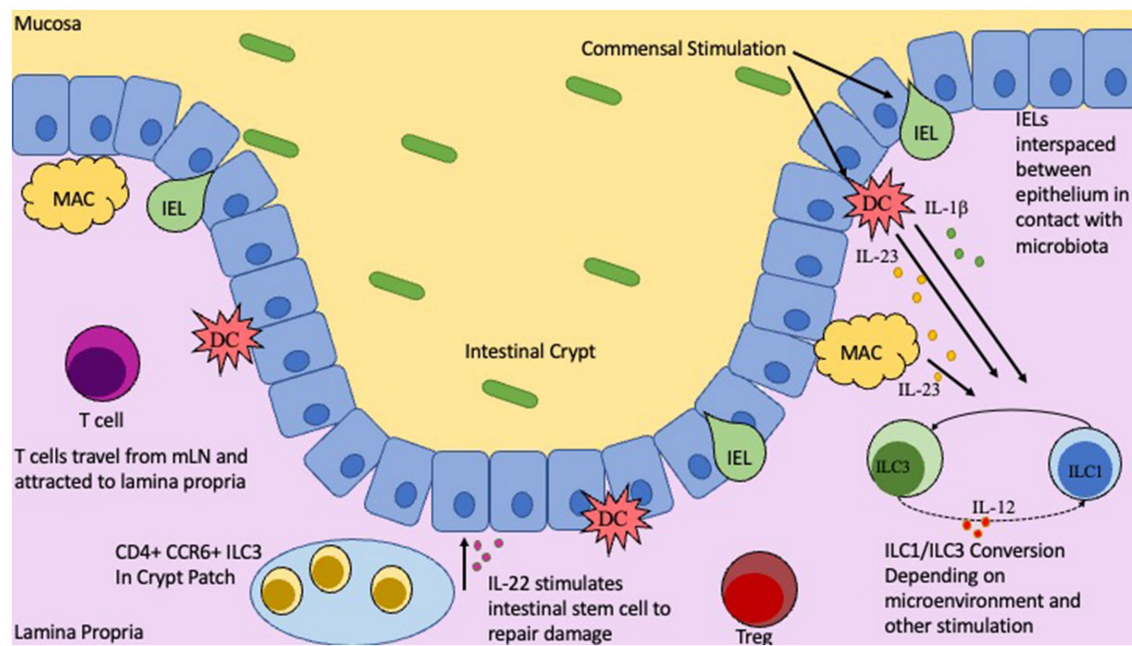


FIGURE 1

Location and functions of T cells, IELs, and ILCs in the Gut. Intestinal epithelial barrier with gut mucosa and Lamina Propria on either side. Commensal microbiota in the gut lumen will stimulate innate immune cells, DCs and Macrophages, as well as IELs. Depending on nature of stimulation and by which commensal will influence IEL cytokine production, along with IL-23 and IL-1b from DCs/Macs to trigger ILC1/ILC3 conversion. CD4+ CCR6+ ILC3s located in the crypt patch will produce IL-22 to stimulate repair and regeneration mechanisms.

completely understood, many studies have indicated that the mere presence of bacteria significantly influences these processes. Studies have shown that genetically susceptible rodents that have been housed under germ-free (GF) conditions, show little to no intestinal inflammation. Whereas mice breed under specific pathogen free (SPF) conditions show symptoms of colitis (Sartor, 1997; Sellon et al., 1998; Keubler et al., 2015). Accordingly, mice that have been genetically targeted to delete the gene responsible for IL-10, a potent anti-inflammatory cytokine, will develop inflammation in the cecum and colon spontaneously, and had increased highly activated CD4+ T cells when housed in SPF conditions (Sellon et al., 1998; Keubler et al., 2015). Interestingly, IL-10 KO GF mice on the other hand had a lack of colitis and immune activation (Sellon et al., 1998). This induction of colitis in genetically susceptible mice has long been attributed to the human enterohepatic *Helicobacter hepaticus* (*H. hepaticus*) (Danne et al., 2017; Zhu et al., 2021). However, there is conflicting evidence to suggest that *H. hepatoicus* itself is not sufficient to induce colitis unless it is co-colonized with *Lactobacillus reuteri* (Dieleman et al., 2000; Whary et al., 2011). Additionally, fecal transplants from IBD human donors are sufficient to induce IBD symptoms in GF mice and that fecal transplantation from healthy donors does not induce these symptoms (Erben et al., 2014; Weingarden and Vaughn, 2017; Jang et al., 2021). This is thought to occur by the IBD donor microbiota preferentially stimulating Th17 and Th2 T cells over Tregs, while healthy microbiota induce more Tregs (Longman et al., 2013; Britton et al., 2019). Fittingly, it has been observed that when naïve CD4+ T cells were transferred from healthy mice into immunocompromised mice, colitis was induced (Powrie et al., 1994; Kullberg et al., 2006; Ostanin et al., 2009). The degree to which these mice were susceptible to colitis was directly associated

with the composition of the mouse's unique gut microbiome (Reinoso Webb et al., 2018), and this naïve T cell transfer colitis model is widely used to study the effects of the microbiome on IBD pathogenesis (Ostanin et al., 2009).

Interestingly, it has been found that there are distinct actions that the hosts immune system with partake in response to colonization of the gut microbiota. For example, in 2014, it was observed that specific intestinal microbiota are preferentially coated with high levels of immunoglobulin A (IgA) and that the specific microbes that have this high IgA coating are found to dramatically increase susceptibility to colitis (Gaboriau-Routhiau et al., 2009; Palm et al., 2014). Utilizing this differential coating of IgA could be a powerful tool in distinguishing between potentially pathogenic bacteria and healthy commensals (Pabst and Slack, 2020). In humans, it has been demonstrated that IBD severity is closely associated with disruptions in the normal microbiota, known as dysbiosis (Schaubeck et al., 2016). Not only is the diversity of bacteria in healthy intestinal tissue much greater than that of inflamed intestinal tissue, but there is a marked change in the predominant bacteria colonized. It has been observed that patients with IBD are observed to have a reduction in Firmicutes and an increase in Proteobacteria, and a few members of Bacteroidetes (Sepehri et al., 2007; Alam et al., 2020; Lee and Chang, 2021). This change in composition and diversity is thought to lead to an impairment of several key immunomodulatory functions and reduction in intestinal barrier integrity thus allowing inflammation to occur and stimulate unnecessary immune responses (Lee and Chang, 2021). Importantly, in addition to diversity and composition of the microbiome being reduced an/or altered it has also been observed that the metagenomic, metatranscriptomic, and metabolomic profiles of the microbiomes in IBD patients are altered (Lloyd-Price et al., 2019). For

example, the measured metabolites produced by the microbiota in IBD patients are significantly less diverse than those without IBD. Additionally, they observe that Short Chain Fatty Acids (SCFAs) produced by the microbiota are reduced in patients with dysbiosis; specifically, the SCFA butyrate is consistently noted as being less abundant in dysbiosis. [Lloyd-Price et al., 2019](#), hypothesize that this loss of butyrate is due to the depletion of important metabolite producers like *F. prausnitzii* and *R. hominis* ([Lloyd-Price et al., 2019](#)). Along these lines, this same group also observed that the primary bile acid cholate and its conjugates are consistently measured higher in dysbiosis from patients with CD, and conversely that the secondary bile acids deoxycholate and lithocholate are reduced in this condition ([Duboc et al., 2013](#); [Lloyd-Price et al., 2019](#)). They conclude that the microbiota change in IBD-associated dysbiosis causes alterations in intestinal bile acid production which may lead to the inhibition of anti-inflammatory effects seen in some of the secreted bile acids resulting in chronic inflammation that is a hallmark of IBD ([Duboc et al., 2013](#)). Lastly, it was noted that IBD specific signals are significantly detectable at the RNA level in dysbiosis, this includes pathways known to be upregulated in IBD and known bacterial species that are observed to have different expression profiles in IBD patients ([Schirmer et al., 2018](#)). Adding to this complexity, recent studies showed that dysbiosis of oral microbiome in patients with periodontitis can also directly influence the development of gut inflammation by promoting harmful pathobiont colonization and supplying pathogenic T cells to the gut ([Atarashi et al., 2017](#); [Kitamoto et al., 2020](#); [Kitamoto and Kamada, 2022](#)). Microbiomes from other niches can influence microbiome-mediated gut tissue inflammation. However, treatment of IBD with antibiotics has shown conflicting outcomes; with some studies showing mild benefits and others with little to no effect ([Nitzan et al., 2016](#); [Abraham and Quigley, 2020](#)). This may be explained by the variable locations of disease occurrence and the different mechanisms of action for the varying antibiotics tested. For example, if the treated antibiotics depleted more beneficial bacteria than pathogenic bacteria, the output of the treatment for IBD will be detrimental. So far, our knowledge cannot predict such outcomes because of the diversity of bacteria and their unknown immunomodulatory functions. Finally, the genetic indicators that are known to be associated with IBD are generally related to how the immune system interacts with the gut microbiota ([Imhann et al., 2017](#); [Aschard et al., 2019](#); [Cohen et al., 2019](#)). Thus, characterizing how commensal bacteria interact with the host's tissues and immune system will be critical for combatting IBD. Taken together microbiome-dependent T cell activation and dysregulation can cause gut inflammation, while innate lymphoid cells (ILCs) and intra-epithelial lymphocytes (IELs), which are also abundant in the intestine and function similarly as T cells, likewise contribute to IBD. In this review, we will examine the contribution of T cells, ILCs and IELs in IBD pathogenesis.

## Microbiota influence on intra-epithelial lymphocytes

The microbiome has a significant impact on maturation and education of the immune system. To keep immune responses in check, commensal microbes induce immune tolerance to prevent unwanted immune activation and inflammation while still allowing for robust immune responses toward pathogens. This is a delicate process and any

perturbations, such as dysbiosis or genetic susceptibility, may lead to improper immune responses and potentially IBD. One critical player are the intraepithelial lymphocytes (IELs). IELs are interspaced between epithelial cells in the intestinal barrier located underneath the mucosal layer. IELs are considered the first line of defense in the gastrointestinal tract as they are the first immune cell to encounter microbes colonizing the mucosa ([Figure 1](#)). Once IELs arrive at the intestinal barrier and position themselves between the epithelial cells, they do not return to circulation ([Masopust et al., 2010](#); [Van Kaer and Olivares-Villagómez, 2018](#)). The distribution of IELs is not consistent along the entire gastrointestinal tract and differs between mice and humans ([Camerini et al., 1993](#); [Beagley et al., 1995](#); [Tamura et al., 2003](#)). The microbiome is seen as a potent modulator of IEL phenotypic composition and clonal expansion ([Helgeland et al., 2004](#)). It was observed that in GF rats there was a significant reduction in CD4<sup>+</sup> IELs compared to conventionalized rats that showed notable populations of both CD4<sup>+</sup> IELs as well as CD4<sup>+</sup>CD8 $\alpha$ <sup>+</sup> double positive IELs ([Helgeland et al., 2004](#); [Harada et al., 2022](#)). Interestingly, the GF rats displayed similar numbers of CD8<sup>+</sup> IELs compared to conventionalized rats, indicating that while CD4 single and double positive IELs are highly influenced by the microbiota, CD8<sup>+</sup> IELs seem to be relatively independent of microbiota ([Bousso et al., 2000](#); [Helgeland et al., 2004](#)). Although it has been difficult to identify the different bacterial species in the microbiome that influence IEL composition, it has been noted that segmented filamentous bacteria (SFB) has the ability to significantly modulate IELs ([Umesaki et al., 1999](#); [Helgeland et al., 2004](#)).

The majority of IELs express a CD8 $\alpha$  $\alpha$  homodimer with around 90% of these expressing T cell receptors (TCRs) ([Van Kaer and Olivares-Villagómez, 2018](#)). These IELs can be divided into two groups, natural or induced IELs. Induced IELs form from naïve T cells that encounter antigens in the gut-associated lymphoid tissue (GALT) and then migrate to the intestine. Induced IELs can be further classified into CD4 or CD8 $\alpha$  $\beta$  expressing. Induced IELs are typically thought to possess an effector-memory phenotype that aids in the defense against pathogens. Contrary to traditional thought there is some evidence to suggest that induced TCR $\alpha$  $\beta$ <sup>+</sup>CD4<sup>+</sup> IELs do not lose their CD8 chains such that they express both CD4 and CD8 $\alpha$  $\alpha$  ([Morrissey et al., 1995](#); [Yap and Mariño, 2018](#)). Studies have revealed that some commensals can modulate the generation and function of TCR $\alpha$  $\beta$ <sup>+</sup>CD4<sup>+</sup>CD8 $\alpha$  $\alpha$ <sup>+</sup> IELs ([Zhou C. et al., 2019](#)). They show that TCR $\alpha$  $\beta$ <sup>+</sup>CD4<sup>+</sup> IELs are absent in GF mice and that the addition of the commensal *Lactobacillus reuteri* can induce expansion of TCR $\alpha$  $\beta$ <sup>+</sup>CD4<sup>+</sup> IELs by downregulating ThPOK, a key transcriptional regulator of T cells ([Cervantes-Barragan et al., 2017](#)). Importantly, this specialized IEL subset has been associated with IBD and has been found to, upon stimulation by microbiota, induce alteration of Foxp3<sup>+</sup>Treg into TCR $\alpha$  $\beta$ <sup>+</sup>CD4<sup>+</sup>CD8 $\alpha$  $\alpha$ <sup>+</sup> IELs during intestinal inflammation ([Das et al., 2003](#); [Cervantes-Barragan et al., 2017](#); [Zhou C. et al., 2019](#)). Moreover, a very recent report from the Kasper lab showed that dietary Fatty Acids (FAs) can be bio-transformed into Conjugated Linoleic Acids (CLAs) predominantly by the microbiota in the small intestine. They demonstrate that the CLAs then act as important modulators to maintain a healthy CD4<sup>+</sup>CD8 $\alpha$  $\alpha$ <sup>+</sup> IEL pool, highlighting gut commensal's role in preserving mucosal defenses ([Song et al., 2023](#)). The other subclass of induced IELs is TCR $\alpha$  $\beta$ <sup>+</sup>CD8 $\alpha$  $\beta$ <sup>+</sup> IELs. These cells are derived from activated CD8<sup>+</sup> T cells from the periphery and account for up to 15% of total IELs in mice and 80% in humans ([Sujino et al., 2016](#)). While physiological roles of these cells in intestine during homeostasis and pathogenesis are not fully understood yet,



several studies have uncovered links between  $\text{TCR}\alpha\beta^+$   $\text{CD8}\alpha\beta^+$  IELs and the microbiome. One study demonstrated a significant increase in  $\text{TCR}\alpha\beta^+$   $\text{CD8}\alpha\beta^+$  IELs when GF mice were microbially colonized in SPF conditions (Jarry et al., 1990). Others have shown that reducing specific bacterial species with antibiotics can increase the number of  $\text{TCR}\alpha\beta^+$   $\text{CD8}\alpha\beta^+$  IELs (Imaoka et al., 1996). Natural IELs on the other hand, will home directly to the intestinal epithelium after thymic development. Natural IELs include  $\text{TCR}\gamma\delta^+$ , which are known to have high mobility throughout the intestinal epithelium (Chen B. et al., 2018). Interestingly, there is conflicting evidence for the role of  $\text{TCR}\gamma\delta^+$  IELs in colitis models. Some suggest that these cells act protectively against inflammatory damage to the epithelium; while others indicate that  $\text{TCR}\gamma\delta^+$  IELs act in a pathogenic fashion (Simpson et al., 1997; Canesso et al., 2017; Mariño et al., 2017; Nielsen et al., 2017). Some studies suggest that  $\text{TCR}\gamma\delta^+$  IELs help protect the intestinal epithelium from inflammatory damage by secreting TGF- $\beta$  and KGF (Yang et al., 2004; Hu et al., 2018; Michaudel and Sokol, 2020). Although various papers indicated the relationships between microbiota and IELs up-regulation and activation, the repertoire of TCR on the IELs had been not investigated. Recently Bousbaine et al., reported that  $\beta$ -hexosaminidase, a conserved enzyme across commensals of the Bacteroidetes phylum, as a driver of  $\text{CD4}^+$  IEL differentiation. In addition, the paper nicely showed that the  $\beta$ -hexosaminidase-specific  $\text{CD4}^+$  IELs can play a protective role in a mouse model of colitis (Bousbaine et al., 2022). Utilizing and enhancing the protective mechanisms of our immune cells is a promising path for IBD therapeutics.

## Microbiota influence on innate lymphoid cells

Innate lymphoid cells (ILCs) are a class of immune cells that form from a common lymphoid progenitor (CLP) (Liu et al., 2011; Artis

and Spits, 2015). ILCs are also associated with IBD pathogenesis by interacting directly and indirectly with the microbiota, regulating intestinal barrier integrity, and secreting cytokines. Dysfunction of ILCs will perturb gut homeostasis and can lead to gut inflammation and IBD. There are several subclasses of ILCs based on their phenotype: ILC1, ILC2, ILC3, NK/ LTi cells are usually included in descriptions of ILCs as they share many similarities in development and function (Liu et al., 2011; Panda and Colonna, 2019; Figure 2). ILCs are known to be primarily located at the mucosal surfaces. With the most well-known reservoir being the intestinal epithelial barrier, which allows extensive communication with the gut microbiota (Liu et al., 2011; Panda and Colonna, 2019). Although ILCs have been shown to modulate both innate and adaptive immunity through secretion of cytokines, they are considered a part of the innate immune system (Liu et al., 2011; Abt et al., 2015; Mortha and Burrows, 2018; Vivier et al., 2018). ILCs are seen as the innate immune systems counterpart to T cells because they produce similar effector cytokines but require no education by antigen presenting cells via TCR is required (Vivier et al., 2018; Panda and Colonna, 2019). ILCs are tissue-resident cells that are found in high numbers within the mucosa and have been associated with maintaining homeostasis, intestinal repair, and regeneration (Liu et al., 2011; Vivier et al., 2018). Importantly ILCs will constantly produce their effector cytokines at steady-state conditions and are not rapidly replenished by the circulation (Giuffrida et al., 2018; Luo et al., 2021). ILC1 cells are known to produce the key cytokines IFN- $\gamma$  and TNF- $\alpha$ , as well as provide resistance to intracellular pathogens; with their adaptive counterpart being Th1 cells which is also regulated by the same master transcription factor T-bet (Fuchs, 2016; Vivier et al., 2018). ILC2 cells, whose T cell counterpart is Th2 and master transcription factor being GATA3, secrete several interleukins: IL-4, IL-5, IL-9, and IL-13. ILC2s are involved in fighting parasitic infections and in type two mediated inflammation (Vivier et al., 2018). Next, the ILC3s are regulated by the transcription factor ROR $\gamma$ t and produce the effector

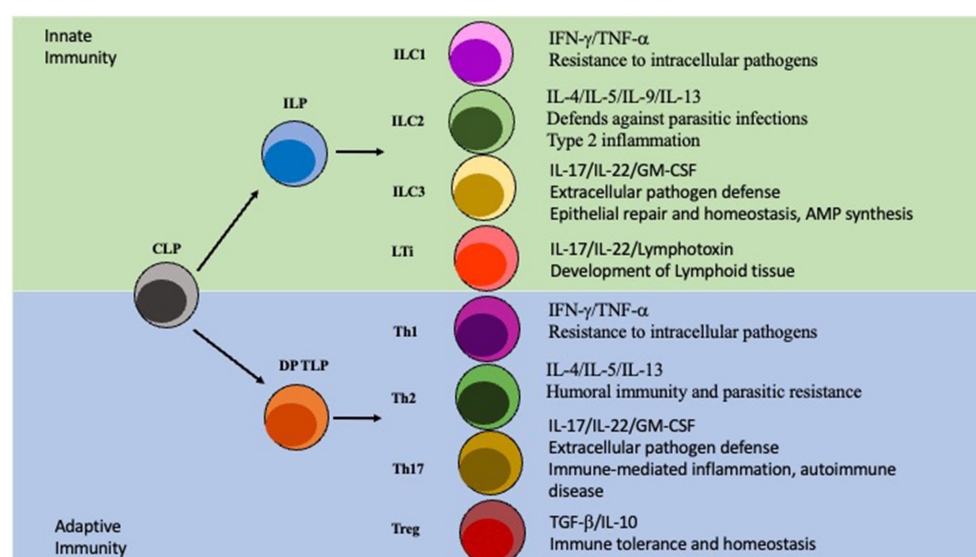


FIGURE 2

ILC vs T cell Differentiation. ILC and T cell differentiation. The Innate lymphoid progenitor (ILP) and the double positive T cell progenitor (DP TLP) arise from a common lymphoid progenitor (CLP). The ILP can then, depending on other signals, differentiate into ILC1/ILC2/ILC3/LTi cells which are part of the innate immunity. Similarly, the DP TLP can differentiate into a Th1/Th2/Th17/Treg identity and is part of the adaptive immunity.



cytokines IL-17, IL-22, and GM-CSF similarly to Th17 cells (Qiu et al., 2012; Vivier et al., 2018). They are involved in extracellular pathogen defense, epithelial repair, and homeostasis, along with stimulating AMP synthesis. LT $\alpha$  cells are important to the development of the secondary lymphoid organs, for example Peyer's Patches on the small intestine (Sonnenberg et al., 2011; Van De Pavert, 2021). Although NK cells are also regulated by the transcription factor T-bet and produce IFN $\gamma$  they are not directly differentiated into NK cells, instead arising from a separate, but related, NK progenitor that is reportedly governed by the expression of TOX, NFIL3, ID2, and ETS1 (Zhang and Huang, 2017; Vivier et al., 2018). Importantly, although the other ILCs are closely related to CD4 T cells NK cells on the other hand resemble CD8 cytotoxic T cells (Zhang and Huang, 2017).

In an IBD context, the balance between ILCs, particularly ILC1 and ILC3 is currently a major area of study, as this balance has been linked to intestinal inflammation (Chen L. et al., 2018; Castleman et al., 2020; Saez et al., 2021). However, ILC2s have recently been implicated in gut microbiome dependent inflammatory responses in the lung, indicating that ILC2s may also play a role in the development of inflammatory diseases but this is still unclear (Pu et al., 2021). ILC3s have been reported to perform several functions related to maintaining homeostasis in the gut. They can sense and communicate with the microbiota to influence intestinal epithelial cells to produce anti-microbial peptides, promote epithelial tissue repair and regeneration, and modulate the adaptive immune system (Buela et al., 2015; Diefenbach et al., 2020; Romera-Hernández et al., 2020; Zhou and Sonnenberg, 2020; Sepahi et al., 2021). The hallmark of ILC3 is the production of IL-17 and IL-22 and, in certain conditions, GM-CSF. One way the microbiome communicates with ILCs is through Short Chain Fatty Acids (SCFAs). For example, dietary fiber can be metabolized by the gut microbiome to produce SCFAs that in turn act as regulators for immune cells including ILC3s (Gasaly et al., 2021; Sepahi et al., 2021). Accordingly, the metabolites produced by commensals from dietary fibers regulate G-protein coupled receptors to promote optimal expansion of ILCs in the gut (Chun et al., 2019; Sonnenberg and Hepworth, 2019). It has been shown that metabolites produced by commensals will stimulate the AKT-STAT3 and ERK-STAT3 pathways to increase IL-22 production and ILC3 generation (Sarrabayrouse et al., 2014).

IL-22 is known to promote epithelial barrier integrity and encourage epithelial regeneration (Chun et al., 2019; Poholek et al., 2019). Its clinical relevance in IBD has been extensively documented. In short, IL-22 can induce mucosal repair and regeneration which is critical for treatment of IBD, and IL-23R, which is known to stimulate production of IL-22, is associated with the development of IBD (Geremia et al., 2011). Additionally, IL-22 is also demonstrated to stimulate the production of anti-microbial peptides (AMPs); specifically, the REGIII family (Chun et al., 2019; Willinger, 2019). ILC3s also communicate with the commensals by utilizing the ILC's TLRs. TLR stimulation by commensal PAMPs can induce secretion of IL-22, IL-13, and IL-5 (Takatsu, 2011; Reece et al., 2014; Xuan et al., 2021). In conjunction with directly regulating ILCs, commensals can also indirectly influence ILCs by modulating myeloid and epithelial cells in the intestine. In mice, commensal microbes will stimulate intestinal resident myeloid cells to secrete IL-1 $\beta$  and IL-23. These two key cytokines in turn will stimulate ILC3s to produce the GM-CSF; GM-CSF can induce Treg generation and expansion via dendritic cells, enhancing tolerance (Pickert et al., 2009; Mortha et al., 2014;

Mizoguchi et al., 2018; Miljković et al., 2021). Concurrently, IL-1 $\beta$  will also influence ILC3s to secrete IL-2 which also drives Treg generation and tolerance (Mizoguchi et al., 2018; Zhou L. et al., 2019). This occurs as Tregs will inhibit ILC3-associated colitis by preventing the secretion of IL-23 and IL-1 $\beta$  from tissue-resident macrophages that block the production of IL-22 (Saez et al., 2021).

Additionally, ILC3s are associated with the IBD susceptibility gene TNFSF15 as well as the adaptive immune response. The TNFSF15 gene encodes the protein TL1A which is the ligand for Death Receptor 3 (DR3) (Jostins et al., 2012; Castellanos et al., 2018). This ligand TL1A will act in concert with IL-23 and IL-1 $\beta$  to enhance IL-22 secretion and promote ILC3 expansion *ex vivo* (Longman et al., 2014; Ahn et al., 2015). Moreover, in mice colonized with Segmented Filamentous Bacteria (SFB) or IBD-associated microbiota such as Adherent-Invasive *E. coli* (AIEC), there is an increase in ILC3-produced IL-22 (Sano et al., 2015; Castellanos et al., 2018). It was revealed that this occurs by inducing TL1A expression on mononuclear phagocytes such that the increased expression of TL1A will lead to IL-22 secretion from ILC3s in a DR3 dependent manner. To confirm this association, ILC3 specific DR3 deletion in mice showed decreased IL-22 secretion from ILC3s and a higher susceptibility to chemical-induced colitis (Castellanos et al., 2018). Not only has it been observed that the microbiota can influence ILCs, but they also impact T cells in response to certain bacterial stimuli. For example, *E. coli* has been shown to induce Th17 mucosal immunity exacerbating colitis or arthritis severity (Viladomiu et al., 2017). In addition to commensals influencing ILCs, it has been demonstrated that cytokines produced by ILCs can regulate commensal bacteria; this is seen by T-bet $^{+}$  type 1 ILCs (ILC1) that produce IFN $\gamma$  and TNF $\alpha$  that can increase the permeability of the colonic epithelial cell line and thus influence the movement of commensals across the intestinal epithelium (Clark et al., 2005). This crosstalk between ILCs and commensals via myeloid cells is critical in maintaining homeostasis in colitis models. Expression of IFN $\gamma$  in ILC1 was dependent on proper T-bet expression and that mice deficient in T-bet developed ILC-associated colitis due to an increase in IL-17 production (Powell et al., 2012). Furthermore, ILCs are directly associated with IBD. It has been noted that in IBD tissue samples there is a reduced number of NKp44 $^{+}$  ILC3s compared to healthy control. This loss of ILC3s in IBD is accompanied by an increase of ILC1s and ILC2s in inflamed samples (Geremia and Arancibia-Cárcamo, 2017; Forkel et al., 2019). They also display a notable increase in secreted IFN $\gamma$ , which is associated with inflammation. Additionally, in inflamed intestinal tissue, there is an inverse relationship between the numbers of NKp44 $^{+}$  ILC3s and the accumulation of IL-17A and IFN $\gamma^{+}$  T cells in human (Forkel et al., 2019). Metabolites secreted by the microbiota can influence immune responses via ILCs, the modulation of ILCs by commensals can produce helpful cytokines, and the imbalance between ILC subtypes may alter the pathogenesis of IBD (Mazmanian et al., 2005; Bernink et al., 2015).

Recently, another important role of ILC3s, its ability to perform MHC dependent functions, has been reported by various laboratories but originally from the Sonnenberg lab (Hepworth et al., 2015; Akagbosu et al., 2022; Eshleman et al., 2023). They clearly showed that ILC3s express major histocompatibility complex class II (MHCII) and such MHCII $^{+}$  ILC3 play important roles to control dysregulated CD4 T cells during colitis. Recently, two groups showed that mice with specific deletions of MHCII on ROR $\gamma$ t-expressing/expressed cells

failed to develop microbiota-specific Tregs (considered as inducible Tregs or peripheral Tregs), thus, mice develop severe colitis (Hepworth et al., 2015; Lyu et al., 2022). Therefore, they concluded that MHCII-expressing ROR $\gamma$ <sup>+</sup> ILC3 generate microbiota-specific regulatory T cells to establish tolerance in the gut. Although Akagbosu et al., 2022, saw similar gut inflammation phenotype using a related model (Cre-ERT2 mediated inducible deletion), they claimed that non-ILC3 ROR $\gamma$ <sup>+</sup> antigen presenting cells as “Thetis” cells which carry combined features of mTECs and Dendritic cells. They also concluded that ILC3s were dispensable for the regulation of early-life peripheral tolerance using ROR $\alpha$ -specific MHCII conditional deletion mice (Akagbosu et al., 2022). Two mini reviews and spotlight papers explain more detailed points (Olyha and Stephanie, 2022; Stephen-Victor and Chatila, 2022), while most ILC3s express MHCII, understanding the role of MHCII-expressing ILC3 will uncover novel features of ILC3s in terms of IBD in both mice and humans.

## What are the differences among IELs, ILCs, and T cells?

Although these three cell types share similar features, they each have their own unique markers and characteristics that we are only now starting to uncover. Firstly, IELs are closely locating in-between intestinal epithelial cells to act as a first line of defense against pathogens. IELs, unlike T cells in the lamina propria, do not need to be primed, upon encountering a pathogen. IELs will immediately begin to secrete cytokines (Zhou C. et al., 2019; Ma et al., 2021). Although until recently IELs had been underappreciated as key players in intestinal homeostasis and IBD pathogenesis, recent studies have highlighted their contributions in those contexts (Hu and Edelblum, 2017). For example, during dysbiosis, IELs have increased cytolytic potential which leads to damage to the intestinal epithelium which can exacerbate inflammatory responses (Setty et al., 2015). Similarly, it was observed that the cytokine IL-23 along with endoplasmic reticulum stress can lead to enhanced IEL lytic activity (Liu et al., 2011). Lastly, gut dysbiosis can also lead to a loss of critical regulatory IELs, which in turn then allows unwanted immune activation and inflammation (Hu and Edelblum, 2017). ILCs on the other hand, are normally located directly underneath the intestinal epithelium, a perfect position to receive signals from the epithelium, but some specialized subsets of ILCs, namely the CCR6<sup>+</sup> ILC3 has been shown to home to the crypt patches to aid in crypt integrity and regeneration (Ohradanova-Repic et al., 2020). ILCs as the innate counterpart of T cells share many of the same features but importantly ILCs lack the rearranged antigen receptors that are the hallmark of conventional T cells. Since it is known that ILCs can act directly on the intestinal epithelial barrier, and can influence innate and adaptative immune responses, a comprehensive understanding on how microbiota influence ILCs is critical for future therapeutics (Ganal-Vonarburg and Duerr, 2020). It has been demonstrated that ILC3s play a critical role in IL-22 production, which leads to stimulation of repair and regenerative effects in the gut, and resistance against *Citrobacter Rodentium* infection (Guo et al., 2015). However robust study on ILC deficient mice and how specific microbiota affect them has been lacking. Finally, T cells are lymphocytes that originate as hematopoietic cells in the bone marrow and travel to the thymus to mature. For the intestines, once T cells leave the gut draining mesenteric lymph nodes

(mLNs) following the antigen presentation by antigen presenting cells, they generally will reside in the underlying Lamina Propria where they partake in many different functions (Zhou C. et al., 2019; Ma et al., 2021). Many studies have focused on the role that CD4<sup>+</sup> T helper cells (Th) play in the development of autoimmune diseases. Specifically, it was discovered that Th17 cells are strongly associated with IBD pathogenesis (Yasuda et al., 2019). During healthy intestinal conditions Th17 cells work to ensure the integrity of the intestinal epithelial barrier and communicate with other cells to produce important antimicrobial peptides (Blaschitz and Raffatellu, 2010). However, during disturbed conditions Th17 can secrete potent proinflammatory cytokines which will further enhance inflammation and IBD progression (Blaschitz and Raffatellu, 2010; Yasuda et al., 2019). Another important T cell subset is the regulatory T cell (Treg) which normally secretes immunosuppressive cytokines like IL-10 which is a key cytokine in maintaining homeostasis in the gut (Atarashi et al., 2011). It is noted that IBD patients have a distinct reduction in Tregs which might explain the increase in unwanted inflammatory responses normally seen in IBD (Mayne and Williams, 2013; Clough et al., 2020). Additionally, there is evidence that altering the precarious balance between Tregs, and T helper subsets can contribute to the pathogenesis of IBD (Mayne and Williams, 2013). A very recent paper in 2022 details how specific microbiota can influence the generation of Tregs and Th17, cells highlighting the immense influence that the microbiome has over T cell differentiation and thus what immune responses will occur (Kedmi et al., 2022). Revealing how these different cells are stimulated and the specific roles they play in IBD will enable deep analysis of the interactions between the microbiota, the intestinal epithelium, and immune cells to allow us to more precisely modulate the microbiome to enhance health of the host.

## Controlling gut inflammation with microbiota

To attenuate the inflammation in the gut during tissue damage and/or IBD, we must not only inhibit microbiome-dependent T cell dysregulation but also promote commensal-derived protective function of ILC3 and IELs. To this end, identification and characterization of specific commensal bacteria is critical to enable us to manipulate these functions. Current efforts are interested in identifying protective commensals, whether this be through their interactions with the immune cells, production of beneficial SCFAs, or inducing intestinal cell regeneration. Along these lines, it was recently revealed that there are several strains of *Clostridium* and a strain of *Faecalibacterium* that can suppress the pro inflammatory activity of NF- $\kappa$ B (Bajer et al., 2017; Giri et al., 2022). Moreover, *Butyrivibrio* can induce Treg derived IL-10 to maintain gut homeostasis via butyrate secretion. There are many other ways that the microbiome can modulate gut inflammation, including the stimulation of several different SCFAs such as butyrate, acetate, and propionate (Silva et al., 2020). Moreover, the gut microbiota's ability to stimulate IL-10, TGF- $\beta$ , IL-4, IL-27, and IL-35 is also associated with anti-inflammatory effects (Al Bander et al., 2020; Silva et al., 2020). Taking advantage of these beneficial commensals could be used as a treatment for IBD or other inflammatory gut diseases. Conversely identification of pathogenic commensals could be used to predict if

someone may develop gut inflammation or could be used to selectively eliminated with antibiotic treatment.

Importantly, IL-23 plays a key role in the pathogenesis of autoimmune and chronic inflammatory diseases, due to IL-23R susceptibility alleles being associated with IBD. Blockade of IL-23R in human IBD animal models can often decrease gut inflammation (Buonocore et al., 2010; Parigi et al., 2022), while protective IL-22 production from ILC3s requires the stimulation of IL-23R on ILC3 (Geremia et al., 2011). On the other hand, it was reported that ILC drive innate intestinal pathology via IL-23 (Eken et al., 2014). This complexity might be due to the diverse causes of IBD development. However, to control and treat IBD, we must overcome this gap in knowledge to leverage the protective commensal-driven immune responses to improve patient outcomes. There are still many questions to fully understand the relationships among gut bacteria, gut inflammation, and immune cells in the gut (Sefik et al., 2015), but current emphasis is focusing on: (1) Will TCR specificities against gut commensals on the CD4 T cell be important factors to developing gut inflammation under disease conditions such as IL-10 KO and transfer colitis model? (2) Can commensal-inducing protective responses overcome autoimmune inflammatory signals to maintain homeostasis in the gut?

## Discussion

The microbiome in IBD patients is distinctly different than that in a healthy individual. There is overwhelming evidence that suggests that the microbiome plays a critical role in maintaining homeostatic balance to prevent dysbiosis. Studies have revealed that commensal bacteria in coordination with the innate and adaptive immune systems, IELs, and ILCs all play critical roles in these processes. Current strategies, such as the use the Fecal Microbiota Transplantation (FMT) suggests that utilizing commensals to influence the microbiome interactions with the host's immune system to promote homeostasis and prevent dysbiosis and inflammation is a promising area of research (Lopez and Grinspan, 2016). This may include colonizing known helpful or protective bacteria to IBD patients to try and resolve dysbiosis or even supplementing known beneficial commensal-produced metabolites to a certain part of the intestine to promote intestinal barrier integrity in IBD patients. Although much of the specifics concerning which bacterial populations are helpful or harmful in these processes are still unknown. Elucidating the extensive communication between commensal bacteria with IELs and ILCs will be key in uncovering the precise mechanisms that govern intestinal homeostasis and development of IBD. Taken together the microbiome is a uniquely evolving target for diagnosis and treatment of IBD and that future

studies will need to focus deeply on how particular microbes interact with the host's tissue to promote intestinal epithelium barrier integrity, prevent inflammation, and maintain intestinal homeostasis.

## Future studies: distinguishing distinct features of IELs, ILCs, and T cells

Despite the similarity among these three cell types, many different functions have been reported. Since transcriptomic analysis became more reasonable to perform, researchers are re-considering not only these similarities but also their distinct and unique features in their expressing receptors and transcription factors. Moreover, their unique location has been considered more and more in these days. Zindl et al. nicely showed that a nonredundant function in IL-22 producing CD4 T cells and ILC3s against *Citrobacter rodentium* infection in the crypt and villi in the intestine (Zindl et al., 2022). In the near future, we will be able to analyze the host-pathogen interaction at the single cell/bacterium resolution.

## Author contributions

ZW wrote the review with supervision of TS following feedback from IC and IK. All authors contributed to the article and approved the submitted version.

## Funding

This work was supported by Schweppe Award in Translational Research (TS) and UIC start-up funds (TS).

## Conflict of interest

The authors declare that the research was conducted in the absence of any commercial or financial relationships that could be construed as a potential conflict of interest.

## Publisher's note

All claims expressed in this article are solely those of the authors and do not necessarily represent those of their affiliated organizations, or those of the publisher, the editors and the reviewers. Any product that may be evaluated in this article, or claim that may be made by its manufacturer, is not guaranteed or endorsed by the publisher.

## References

- Abraham, B., and Quigley, E. (2020). Antibiotics and probiotics in inflammatory bowel disease: when to use them? *Frontline Gastroenterol.* 11, 62–69. doi: 10.1136/flgastro-2018-101057
- Abt, M. C., Lewis, B. B., Caballero, S., Xiong, H., Carter, R. A., Sušac, B., et al. (2015). Innate immune defenses mediated by two ILC subsets are critical for protection against acute *Clostridium difficile* infection. *Cell Host Microbe* 18, 27–37. doi: 10.1016/j.chom.2015.06.011
- Ahn, Y. O., Weeres, M. A., Neulen, M. L., Choi, J., Kang, S. H., Heo, D. S., et al. (2015). Human group3 innate lymphoid cells express DR3 and respond to TL1A with enhanced IL-22 production and IL-2-dependent proliferation. *Eur J Immunol* 45, 2335–2342.
- Akagbosu, B., Tayyebi, Z., Shibu, G., Paucar Iza, Y. A., Deep, D., Parisotto, Y. F., et al. (2022). Novel antigen-presenting cell imparts Treg-dependent tolerance to gut microbiota. *Nature* 610, 752–760. doi: 10.1038/s41586-022-05309-5



- Alam, M. T., Amos, G. C. A., Murphy, A. R. J., Murch, S., Wellington, E. M. H., and Arasaratnam, R. P. (2020). Microbial imbalance in inflammatory bowel disease patients at different taxonomic levels. *Gut Pathog.* 12:1. doi: 10.1186/s13099-019-0341-6
- Al Bander, Z., Nitert, M. D., Mousa, A., and Naderpoor, N. (2020). The gut microbiota and inflammation: an overview. *Int. J. Environ. Res. Public Health* 17:7618. doi: 10.3390/ijerph17207618
- Ananthakrishnan, A. N., Kaplan, G. G., and Ng, S. C. (2020). Changing global epidemiology of inflammatory bowel diseases: sustaining health care delivery into the 21st century. *Clin. Gastroenterol. Hepatol.* 18, 1252–1260. doi: 10.1016/j.cgh.2020.01.028
- Artis, D., and Spits, H. (2015). The biology of innate lymphoid cells. *Nature* 517, 293–301. doi: 10.1038/nature14189
- Aschard, H., Laville, V., Tchetgen, E. T., Knights, D., Imhann, F., Seksik, P., et al. (2019). Genetic effects on the commensal microbiota in inflammatory bowel disease patients. *PLoS Genet.* 15:e1008018. doi: 10.1371/journal.pgen.1008018
- Atarashi, K., Suda, W., Luo, C., Kawaguchi, T., Motoo, I., Narushima, S., et al. (2017). Ectopic colonization of oral bacteria in the intestine drives TH1 cell induction and inflammation. *Science* 358, 359–365. doi: 10.1126/science.aan4526
- Atarashi, K., Tanoue, T., Shima, T., Imaoka, A., Kuwahara, T., Momose, Y., et al. (2011). Induction of colonic regulatory T cells by indigenous clostridium species. *Science* 331, 337–341. doi: 10.1126/science.1198469
- Bajer, L., Kverka, M., Kostovcik, M., Macinga, P., Dvorak, J., Stehlikova, Z., et al. (2017). Distinct gut microbiota profiles in patients with primary sclerosing cholangitis and ulcerative colitis. *World J. Gastroenterol.* 23, 4548–4558. doi: 10.3748/wjg.v23.i25.4548
- Beagley, K. W., Fujihashi, K., Lagoo, A. S., Lagoo-Deenadaylan, S., Black, C. A., Murray, A. M., et al. (1995). Differences in intraepithelial lymphocyte T cell subsets isolated from murine small versus large intestine. *J. Immunol.* 154, 5611–5619. doi: 10.4049/jimmunol.154.11.5611
- Bernink, J. H., Krabbendam, L., Germar, K., De Jong, E., Gronke, K., Kofoed-Nielsen, M., et al. (2015). Interleukin-12 and -23 control plasticity of CD127(+) group 1 and group 3 innate lymphoid cells in the intestinal lamina Propria. *Immunity* 43, 146–160. doi: 10.1016/j.immuni.2015.06.019
- Blaschitz, C., and Raffatellu, M. (2010). Th17 cytokines and the gut mucosal barrier. *J. Clin. Immunol.* 30, 196–203. doi: 10.1007/s10875-010-9368-7
- Bousbaine, D., Fisch, L. I., London, M., Bhagchandani, P., Rezende de Castro, T. B., Mimeo, M., et al. (2022). A conserved Bacteroidetes antigen induces anti-inflammatory intestinal T lymphocytes. *Science* 377, 660–666. doi: 10.1126/science.abg5645
- Bousso, P., Lemaître, F., Laouini, D., Kanellopoulos, J., and Kourilsky, P. (2000). The peripheral CD8 T cell repertoire is largely independent of the presence of intestinal flora. *Int. Immunol.* 12, 425–430. doi: 10.1093/intimm/12.4.425
- Britton, G. J., Contijoch, E. J., Mogno, I., Vennaro, O. H., Llewellyn, S. R., Ng, R., et al. (2019). Microbiotas from humans with inflammatory bowel disease Alter the balance of gut Th17 and RORγt+ regulatory T cells and exacerbate colitis in mice. *Immunity* 50, 212–224.e14. doi: 10.1016/j.immuni.2018.12.015
- Buela, K.-A. G., Omenetti, S., and Pizarro, T. T. (2015). Crosstalk between type 3 innate lymphoid cells and the gut microbiota in inflammatory bowel disease. *Curr. Opin. Gastroenterol.* 31, 449–455. doi: 10.1097/MOG.0000000000000217
- Buonocore, S., Ahern, P. P., Uhlig, H. H., Ivanov, I. I., Littman, D. R., Maloy, K. J., et al. (2010). Innate lymphoid cells drive IL-23 dependent innate intestinal pathology. *Nature* 464, 1371–1375. doi: 10.1038/nature08949
- Camerini, V., Sydora, B. C., Aranda, R., Nguyen, C., MacLean, C., McBride, W., et al. (1993). Regional specialization of the mucosal immune system. Intraepithelial lymphocytes of the large intestine have a different phenotype and function than those of the small intestine. *J. Immunol.* 160, 2608–2618. doi: 10.4049/jimmunol.160.6.2608
- Canesso, M., Lemos, L., Neves, T. C., Marim, F. M., Castro, T. B., Veloso, E. S., et al. (2017). The cytosolic sensor STING is required for intestinal homeostasis and control of inflammation. *Mucosal Immunol.* 11, 820–834. doi: 10.1038/mi.2017.88
- Castellanos, J. G., Woo, V., Viladomiu, M., Putzel, G., Lima, S., Diehl, G. E., et al. (2018). Microbiota-induced TNF-like ligand 1A drives group 3 innate lymphoid cell-mediated barrier protection and intestinal T cell activation during colitis. *Immunity* 49, 1077–1089.e5. doi: 10.1016/j.immuni.2018.10.014
- Castleman, M. J., Dillon, S. M., Purba, C., Cogswell, A. C., McCarter, M., Barker, E., et al. (2020). Enteric bacteria induce IFNγ and Granzyme B from human colonic group 1 innate lymphoid cells. *Gut Microbes* 12:1667723. doi: 10.1080/19490976.2019.1667723
- Cervantes-Barragan, L., Chai, J. N., Tianero, M. D., Di Luccia, B., Ahern, P. P., Merriman, J., et al. (2017). *Lactobacillus reuteri* induces gut intraepithelial CD4+CD8αα+ T cells. *Science* 357, 806–810. doi: 10.1126/science.aah5825
- Chen, B., Ni, X., Sun, R., Zeng, B., Wei, H., Tian, Z., et al. (2018). Commensal bacteria-dependent CD8αβ+ T cells in the intestinal epithelium produce antimicrobial peptides. *Front. Immunol.* 9:1065. doi: 10.3389/fimmu.2018.101065
- Cheng, J., Kalliomäki, M., Heilig, H. G. H., Palva, A., Lähteenoja, H., De Vos, W. M., et al. (2013). Duodenal microbiota composition and mucosal homeostasis in pediatric celiac disease. *BMC Gastroenterol.* 13:113. doi: 10.1186/1471-230X-13-113
- Chen, L., He, Z., Iuga, A. C., Martins Filho, S. N., Faith, J. J., et al. (2018). Diet modifies colonic microbiota and CD4+ T-cell repertoire to induce flares of colitis in mice with myeloid-cell expression of interleukin 23. *Gastroenterology* 155, 1177–1191.e16. doi: 10.1053/j.gastro.2018.06.034
- Chervy, M., Barnich, N., and Denizot, J. (2020). Adherent-Invasive E. coli: Update on the Lifestyle of a Troublemaker in Crohn's Disease. *Int J Mol Sci* 21:3734. doi: 10.3390/ijms21103734
- Chun, E., Lavoie, S., Fonseca-Pereira, D., Bae, S., Michaud, M., Hoveyda, H. R., et al. (2019). Metabolite-sensing receptor Ffar2 regulates colonic group 3 innate lymphoid cells and gut immunity. *Immunity* 51, 871–884.e6. doi: 10.1016/j.immuni.2019.09.014
- Clark, E., Hoare, C., Tanianis-Hughes, J., Carlson, G. L., and Warhurst, G. (2005). Interferon γ induces translocation of commensal *Escherichia coli* across gut epithelial cells via a lipid raft-mediated process. *Gastroenterology* 128, 1258–1267. doi: 10.1053/j.gastro.2005.01.046
- Clough, J. N., Omer, O. S., Tasker, S., and Lord, G. M. and Irving, P. M. (2020). Regulatory T-cell therapy in Crohn's disease: challenges and advances. *Gut* 69, 942–952.
- Cohen, L. J., Cho, J. H., Gevers, D., and Chu, H. (2019). Genetic factors and the intestinal microbiome guide development of microbe-based therapies for inflammatory bowel diseases. *Gastroenterology* 156, 2174–2189. doi: 10.1053/j.gastro.2019.03.017
- Crohn's and Colitis Foundation. (2014). *The facts about inflammatory bowel diseases*. New York: Crohn's and Colitis Foundation of America.
- Danne, C., Ryzhakov, G., Martínez-López, M., Ilott, N. E., Franchini, F., Cuskin, F., et al. (2017). A large polysaccharide produced by *Helicobacter hepaticus* induces an anti-inflammatory gene signature in macrophages. *Cell Host Microbe* 22, 733–745.e5. doi: 10.1016/j.chom.2017.11.002
- Das, G., Augustine, M. M., das, J., Bottomly, K., Ray, P., and Ray, A. (2003). An important regulatory role for CD4+CD8αα T cells in the intestinal epithelial layer in the prevention of inflammatory bowel disease. *Proc Natl Acad Sci U S A* 100, 5324–5329. doi: 10.1073/pnas.0831037100
- Diefenbach, A., Gnafakis, S., and Shomrat, O. (2020). Innate lymphoid cell-epithelial cell modules sustain intestinal homeostasis. *Immunity* 52, 452–463. doi: 10.1016/j.immuni.2020.02.016
- Dieleman, L. A., Arends, A., Tonkonogy, S. L., Goerres, M. S., Craft, D. W., Grenther, W., et al. (2000). *Helicobacter hepaticus* does not induce or potentiate colitis in interleukin-10-deficient mice. *Infect. Immun.* 68, 5107–5113. doi: 10.1128/IAI.68.9.5107-5113.2000
- Duboc, H., Rajca, S., Rainteau, D., Benarous, D., Maubert, M. A., Quervain, E., et al. (2013). Connecting dysbiosis, bile-acid dysmetabolism and gut inflammation in inflammatory bowel diseases. *Gut* 62, 531–539. doi: 10.1136/gutjnl-2012-302578
- Eken, A., Singh, A. K., Treuting, P. M., and Oukka, M. (2014). IL-23R+ innate lymphoid cells induce colitis via interleukin-22-dependent mechanism. *Mucosal Immunol.* 7, 143–154. doi: 10.1038/mi.2013.33
- Erben, U., Loddenkemper, C., Doerfel, K., Spieckermann, S., Haller, D., Heimesaat, M. M., et al. (2014). A guide to histomorphological evaluation of intestinal inflammation in mouse models. *Int. J. Clin. Exp. Pathol.* 7, 4557–4576.
- Eshleman, E. M., Shao, T. Y., Woo, V., Rice, T., Engleman, L., Didriksen, B. J., et al. (2023). Intestinal epithelial HDAC3 and MHC class II coordinate microbiota-specific immunity. *J. Clin. Invest.* 133:e162190. doi: 10.1172/JCI162190
- Fakhoury, M., Negrulj, R., Moorianian, A., and Al-Salami, H. (2014). Inflammatory bowel disease: clinical aspects and treatments. *J. Inflamm. Res.* 7, 113–120. doi: 10.2147/JIR.S65979
- Flint, H. J., Scott, K. P., Duncan, S. H., Louis, P., and Forano, E. (2012). Microbial degradation of complex carbohydrates in the gut. *Gut Microbes* 3, 289–306. doi: 10.4161/gmic.19897
- Forkel, M., van Tol, S., Höög, C., Michaëlsson, J., Almer, S., and Mjösberg, J. (2019). Distinct alterations in the composition of mucosal innate lymphoid cells in newly diagnosed and established Crohn's disease and ulcerative colitis. *J. Crohn's Colitis* 13, 67–78. doi: 10.1093/ecco-jcc/jyy119
- Fuchs, A. (2016). ILC1s in tissue inflammation and infection. *Front. Immunol.* 7:104. doi: 10.3389/fimmu.2016.00104
- Gaboriau-Routhiau, V., Rakotobe, S., Lécuyer, E., Mulder, I., Lan, A., Bridonneau, C., et al. (2009). The key role of segmented filamentous bacteria in the coordinated maturation of gut helper T cell responses. *Immunity* 31, 677–689. doi: 10.1016/j.immuni.2009.08.020
- Ganal-Vonarburg, S. C., and Duerr, C. U. (2020). The interaction of intestinal microbiota and innate lymphoid cells in health and disease throughout life. *Immunology* 159, 39–51.
- Gasaly, N., De Vos, P., and Hermoso, M. A. (2021). Impact of bacterial metabolites on gut barrier function and host immunity: a focus on bacterial metabolism and its relevance for intestinal inflammation. *Front. Immunol.* 12:658354. doi: 10.3389/fimmu.2021.658354
- Geremia, A., and Arancibia-Cárcamo, C. V. (2017). Innate lymphoid cells in intestinal inflammation. *Front. Immunol.* 8:1296. doi: 10.3389/fimmu.2017.01296
- Geremia, A., Arancibia-Cárcamo, C. V., Fleming, M. P. P., Rust, N., Singh, B., Mortensen, N. J., et al. (2011). IL-23-responsive innate lymphoid cells are increased in inflammatory bowel disease. *J. Exp. Med.* 208, 1127–1133. doi: 10.1084/jem.20101712



- Giri, R., Hoedt, E. C., Khushi, S., Salim, A. A., Bergot, A. S., Schreiber, V., et al. (2022). Secreted NF- $\kappa$ B suppressive microbial metabolites modulate gut inflammation. *Cell Rep.* 39:110646. doi: 10.1016/j.celrep.2022.110646
- Giuffrida, P., Corazza, G. R., and Di Sabatino, A. (2018). Old and new lymphocyte players in inflammatory bowel disease. *Dig. Dis. Sci.* 63, 277–288. doi: 10.1007/s10620-017-4892-4
- Glassner, K. L., Abraham, B. P., and Quigley, E. M. M. (2020). The microbiome and inflammatory bowel disease. *J. Allergy Clin. Immunol.* 145, 16–27. doi: 10.1016/j.jaci.2019.11.003
- Guo, X., Liang, Y., Zhang, Y., Lasorella, A., Kee, B. L., and Fu, Y. X. (2015). Innate lymphoid cells control early colonization resistance against intestinal pathogens through ID2-dependent regulation of the microbiota. *Immunity* 42, 731–743. doi: 10.1016/j.immuni.2015.03.012
- Harada, Y., Sujino, T., Miyamoto, K., Nomura, E., Yoshimatsu, Y., Tanemoto, S., et al. (2022). Intracellular metabolic adaptation of intraepithelial CD4+CD8 $\alpha\alpha$ + T lymphocytes. *iScience* 25:104021. doi: 10.1016/j.isci.2022.104021
- Helgeland, L., Dissen, E., Dai, K. Z., Midtvedt, T., Brandtzaeg, P., and Vaage, J. T. (2004). Microbial colonization induces oligoclonal expansions of intraepithelial CD8 T cells in the gut. *Eur. J. Immunol.* 34, 3389–3400. doi: 10.1002/eji.200425122
- Hepworth, M. R., Fung, T. C., Masur, S. H., Kelsen, J. R., McConnell, F. M., Dubrot, J., et al. (2015). Group 3 innate lymphoid cells mediate intestinal selection of commensal bacteria-specific CD4+ T cells. *Science* 348, 1031–1035. doi: 10.1126/science.aaa4812
- Hu, M. D., and Edelblum, K. L. (2017). Sentinels at the frontline: the role of intraepithelial lymphocytes in inflammatory bowel disease. *Curr. Pharmacol. Rep.* 3, 321–334. doi: 10.1007/s40495-017-0105-2
- Hu, M. D., Ethridge, A. D., Lipstein, R., Kumar, S., Wang, Y., Jabri, B., et al. (2018). Epithelial IL-15 Is a Critical Regulator of  $\gamma\delta$  Intraepithelial Lymphocyte Motility within the Intestinal Mucosa. *J. Immunol.* 201, 747–756. doi: 10.4049/jimmunol.1701603
- Imaoka, A., Matsumoto, S., Setoyama, H., Okada, Y., and Umesaki, Y. (1996). Proliferative recruitment of intestinal intraepithelial lymphocytes after microbial colonization of germ-free mice. *Eur. J. Immunol.* 26, 945–948. doi: 10.1002/eji.1830260434
- Imhann, F., Vich Vila, A., Bonder, M. J., Fu, J., Gevers, D., Visschedijk, M. C., et al. (2017). Interplay of host genetics and gut microbiota underlying the onset and clinical presentation of inflammatory bowel disease. *Gut* 67, 108–119. doi: 10.1136/gutjnl-2016-312135
- Jang, H.-M., Kim, J. K., Joo, M. K., Shin, Y. J., Lee, C. K., Kim, H. J., et al. (2021). Transplantation of fecal microbiota from patients with inflammatory bowel disease and depression alters immune response and behavior in recipient mice. *Sci. Rep.* 11:20406. doi: 10.1038/s41598-021-00088-x
- Jarry, A., Cerf-bensussan, N., Brousse, N., Selz, F., and Guy-grand, D. (1990). Subsets of CD3+ (T cell receptor  $\alpha/\beta$  or  $\gamma/\delta$ ) and CD3– lymphocytes isolated from normal human gut epithelium display phenotypic features different from their counterparts in peripheral blood. *Eur. J. Immunol.* 20, 1097–1103. doi: 10.1002/eji.1830200523
- Jostins, L., Ripke, S., Weersma, R. K., Duerr, R. H., McGovern, D. P., Hui, K. Y., et al. (2012). Host-microbe interactions have shaped the genetic architecture of inflammatory bowel disease. *Nature* 491, 119–124. doi: 10.1038/nature11582
- Kastl, A. J., Terry, N. A., Wu, G. D., and Albenberg, L. G. (2020). The structure and function of the human small intestinal microbiota: current understanding and future directions. *Cell. Mol. Gastroenterol. Hepatol.* 9, 33–45. doi: 10.1016/j.jcmgh.2019.07.006
- Kedmi, R., Najar, T. A., Mesa, K. R., Grayson, A., Kroehling, L., Hao, Y., et al. (2022). A ROR $\gamma$ t+ cell instructs gut microbiota-specific Treg cell differentiation. *Nature* 610, 737–743. doi: 10.1038/s41586-022-05089-y
- Keubler, L. M., Buettner, M., Häger, C., and Bleich, A. (2015). A multihit model: colitis lessons from the Interleukin-10–deficient mouse. *Inflamm. Bowel Dis.* 21, 1967–1975. doi: 10.1097/MIB.0000000000000468
- Khan, I., Ullah, N., Zha, L., Bai, Y., Khan, A., Zhao, T., et al. (2019). Alteration of gut microbiota in inflammatory bowel disease (IBD): cause or consequence? IBD treatment targeting the gut microbiome. *Pathogens* 8:126. doi: 10.3390/pathogens8030126
- Kho, Z. Y., and Lal, S. K. (2018). The human gut microbiome – a potential controller of wellness and disease. *Front. Microbiol.* 9:1835. doi: 10.3389/fmicb.2018.01835
- Kitamoto, S., and Kamada, N. (2022). Untangling the oral–gut axis in the pathogenesis of intestinal inflammation. *Int. Immunol.* 34, 485–490. doi: 10.1093/intimm/dxac027
- Kitamoto, S., Nagao-Kitamoto, H., Jiao, Y., Gilliland, M. G., Hayashi, A., Imai, J., et al. (2020). The Intermucosal connection between the mouth and gut in CommensalPathobiont-driven colitis. *Cells* 182, 447–462.e14. doi: 10.1016/j.cell.2020.05.048
- Kullberg, M. C., Jankovic, D., Feng, C. G., Hue, S., Gorelick, P. L., McKenzie, B. S., et al. (2006). IL-23 plays a key role in *Helicobacter hepaticus*-induced T cell-dependent colitis. *J. Exp. Med.* 203, 2485–2494. doi: 10.1084/jem.20061082
- Lee, M., and Chang, E. B. (2021). Inflammatory bowel diseases and the microbiome: searching the crime scene for clues. *Gastroenterology* 160, 524–537. doi: 10.1053/j.gastro.2020.09.056
- Leite, G., Morales, W., Weitsman, S., Celly, S., Parodi, G., Mathur, R., et al. (2020). The duodenal microbiome is altered in small intestinal bacterial overgrowth. *PLoS One* 15:e0234906. doi: 10.1371/journal.pone.0234906
- Liu, Z., Yadav, P. K., Xu, X., Su, J., Chen, C., Tang, M., et al. (2011). The increased expression of IL-23 in inflammatory bowel disease promotes intraepithelial and lamina propria lymphocyte inflammatory responses and cytotoxicity. *J. Leukoc. Biol.* 89, 597–606. doi: 10.1189/jlb.0810456
- Lloyd-Price, J., Arze, C., Ananthakrishnan, A. N., Schirmer, M., Avila-Pacheco, J., Poon, T. W., et al. (2019). Multi-omics of the gut microbial ecosystem in inflammatory bowel diseases. *Nature* 569, 655–662. doi: 10.1038/s41586-019-1237-9
- Longman, R. S., Diehl, G. E., Victorio, D. A., Huh, J. R., Galan, C., Miraldi, E. R., et al. (2014). CX3CR1+ mononuclear phagocytes support colitis-associated innate lymphoid cell production of IL-22. *J. Exp. Med.* 211, 1571–1583. doi: 10.1084/jem.20140678
- Longman, R. S., Yang, Y., Diehl, G. E., Kim, S. V., and Littman, D. R. (2013). Microbiota: host interactions in mucosal homeostasis and systemic autoimmunity. *Cold Spring Harb. Symp. Quant. Biol.* 78, 193–201. doi: 10.1101/sqb.2013.78.020081
- Lopez, J., and Grinspan, A. (2016). Fecal microbiota transplantation for inflammatory bowel disease. *Gastroenterol. Hepatol. (N Y)* 12, 374–379.
- Luo, W., Tian, L., Tan, B., Shen, Z., Xiao, M., Wu, S., et al. (2021). Update: innate lymphoid cells in inflammatory bowel disease. *Dig. Dis. Sci.* 67, 56–66. doi: 10.1007/s10620-021-06831-8
- Lyu, M., Suzuki, H., Kang, L., Gaspal, F., Zhou, W., Goc, J., et al. (2022). ILC3s select microbiota-specific regulatory T cells to establish tolerance in the gut. *Nature* 610, 744–751. doi: 10.1038/s41586-022-05141-x
- Ma, H., Qiu, Y., and Yang, H. (2021). Intestinal intraepithelial lymphocytes: maintainers of intestinal immune tolerance and regulators of intestinal immunity. *J. Leukoc. Biol.* 109, 339–347. doi: 10.1002/JLB.3RU0220-111
- Mailhe, M., Ricaboni, D., Vitton, V., Gonzalez, J. M., Bachar, D., Dubourg, G., et al. (2018). Repertoire of the gut microbiota from stomach to colon using culturomics and next-generation sequencing. *BMC Microbiol.* 18:157. doi: 10.1186/s12866-018-1304-7
- Mancini, N. L., Rajeev, S., Jayme, T. S., Wang, A., Keita, A. V., Workentine, M. L., et al. (2021). Crohn's disease Pathobiont adherent-invasive E coli disrupts epithelial mitochondrial networks with implications for gut permeability. *Cell. Mol. Gastroenterol. Hepatol.* 11, 551–571. doi: 10.1016/j.jcmgh.2020.09.013
- Mariño, E., Richards, J. L., McLeod, K. H., Stanley, D., Yap, Y. A., Knight, J., et al. (2017). Gut microbial metabolites limit the frequency of autoimmune T cells and protect against type 1 diabetes. *Nat. Immunol.* 18, 552–562. doi: 10.1038/ni.3713
- Martinez-Guryn, K., Leone, V., and Chang, E. B. (2019). Regional diversity of the gastrointestinal microbiome. *Cell Host Microbe* 26, 314–324. doi: 10.1016/j.chom.2019.08.011
- Masopust, D., Choo, D., Vezys, V., Wherry, E. J., Duraiswamy, J., Akondy, R., et al. (2010). Dynamic T cell migration program provides resident memory within intestinal epithelium. *J. Exp. Med.* 207, 553–564. doi: 10.1084/jem.20090858
- Mayne, C. G., and Williams, C. B. (2013). Induced and natural regulatory T cells in the development of inflammatory bowel disease. *Inflamm. Bowel Dis* 19, 1772–1788.
- Mazmanian, S. K., Liu, C. H., Tzianabos, A. O., and Kasper, D. L. (2005). An immunomodulatory molecule of symbiotic bacteria directs maturation of the host immune system. *Cells* 122, 107–118. doi: 10.1016/j.cell.2005.05.007
- Mentella, M. C., Scaldaferrri, F., Pizzoferrato, M., Gasbarrini, A., and Miggiano, G. A. D. (2020). Nutrition, IBD and gut microbiota: a review. *Nutrients* 12:944. doi: 10.3390/nu12040944
- Michaudel, C., and Sokol, H. (2020). The gut microbiota at the Service of Immunometabolism. *Cell Metab.* 32, 514–523. doi: 10.1016/j.cmet.2020.09.004
- Miljković, Đ., Jevtić, B., Stojanović, I., and Dimitrijević, M. (2021). ILC3, a central innate immune component of the gut-brain Axis in multiple sclerosis. *Front. Immunol.* 12:1025. doi: 10.3389/fimmu.2021.657622
- Mizoguchi, A., Yano, A., Himuro, H., Ezaki, Y., Sadanaga, T., and Mizoguchi, E. (2018). Clinical importance of IL-22 cascade in IBD. *J. Gastroenterol.* 53, 465–474. doi: 10.1007/s00535-017-1401-7
- Morrissey, P. J., Charrier, K., Horovitz, D. A., Fletcher, F. A., and Watson, J. D. (1995). Analysis of the intra-epithelial lymphocyte compartment in SCID mice that received co-isogenic CD4+ T cells. Evidence that mature post-thymic CD4+ T cells can be induced to express CD8 alpha in vivo. *J. Immunol.* 154, 2678–2686. doi: 10.4049/jimmunol.154.6.2678
- Mortha, A., and Burrows, K. (2018). Cytokine networks between innate lymphoid cells and myeloid cells. *Front. Immunol.* 9:191. doi: 10.3389/fimmu.2018.00191
- Mortha, A., Chudnovskiy, A., Hashimoto, D., Bogunovic, M., Spencer, S. P., Belkaid, Y., et al. (2014). Microbiota-dependent crosstalk between macrophages and ILC3 promotes intestinal homeostasis. *Science* 343:1249288. doi: 10.1126/science.1249288
- Nardone, G., and Compare, D. (2015). The human gastric microbiota: is it time to rethink the pathogenesis of stomach diseases? *United European Gastroenterol J* 3, 255–260. doi: 10.1177/2050640614566846
- Nielsen, M. M., Witherden, D. A., and Havran, W. L. (2017).  $\gamma\delta$  T cells in homeostasis and host defence of epithelial barrier tissues. *Nat. Rev. Immunol.* 17, 733–745. doi: 10.1038/nri.2017.101

- Nitzan, O., Elias, M., Peretz, A., and Saliba, W. (2016). Role of antibiotics for treatment of inflammatory bowel disease. *World J. Gastroenterol.* 22, 1078–1087. doi: 10.3748/wjg.v22.i3.1078
- Ohradanova-Repic, A., Boes, M., and Stockinger, H. (2020). *Role of metabolism in regulating immune cell fate decisions*. Lausanne, Switzerland: Frontiers Media SA.
- Olfatifar, M., Zali, M. R., Pourhoseingholi, M. A., Balaii, H., Ghavami, S. B., Ivanchuk, M., et al. (2021). The emerging epidemic of inflammatory bowel disease in Asia and Iran by 2035: a modeling study. *BMC Gastroenterol.* 21:204. doi: 10.1186/s12876-021-01745-1
- Olyha, S. J., and Stephanie, C. (2022). Eisenbarth. A new tolerogenic cell RORs onto the scene. *Science Immunology* 7:eadf0767. doi: 10.1126/sciimmunol.adf0767
- Ostanin, D. V., Bao, J., Koboziev, I., Gray, L., Robinson-Jackson, S. A., Kosloski-Davidson, M., et al. (2009). T cell transfer model of chronic colitis: concepts, considerations, and tricks of the trade. *Am. J. Physiol. Gastrointest. Liver Physiol.* 296, G135–G146. doi: 10.1152/ajpgi.90462.2008
- Pabst, O., and Slack, E. (2020). IgA and the intestinal microbiota: the importance of being specific. *Mucosal Immunol.* 13, 12–21. doi: 10.1038/s41385-019-0227-4
- Palm, N. W., de Zoete, M. R., Cullen, T. W., Barry, N. A., Stefanowski, J., Hao, L., et al. (2014). Immunoglobulin a coating identifies Colitogenic bacteria in inflammatory bowel disease. *Cells* 158, 1000–1010. doi: 10.1016/j.cell.2014.08.006
- Panda, S. K., and Colonna, M. (2019). Innate lymphoid cells in mucosal immunity. *Front. Immunol.* 10:861. doi: 10.3389/fimmu.2019.00861
- Parigi, T. L., Iacucci, M., and Ghosh, S. (2022). Blockade of IL-23: what is in the pipeline? *J. Crohns Colitis* 16, ii64–ii72. doi: 10.1093/ecco-jcc/jjab185
- Pickard, J. M., Zeng, M. Y., Caruso, R., and Núñez, G. (2017). Gut microbiota: role in pathogen colonization, immune responses, and inflammatory disease. *Immunol. Rev.* 279, 70–89. doi: 10.1111/imr.12567
- Pickert, G., Neufert, C., Leppkes, M., Zheng, Y., Wittkopf, N., Warntjen, M., et al. (2009). STAT3 links IL-22 signaling in intestinal epithelial cells to mucosal wound healing. *J. Exp. Med.*, 1472. doi: 10.1084/jem.20082683
- Poholek, C. H., Dulson, S. J., Zajac, A. J., and Harrington, L. E. (2019). Interleukin-21 controls ILC3 cytokine production and promotes a protective phenotype in a mouse model of colitis. *Immunohorizons* 3, 194–202. doi: 10.4049/immunohorizons.1900005
- Powell, N., Walker, A. W., Stolarczyk, E., Canavan, J. B., Gökmen, M. R., Marks, E., et al. (2012). The transcription factor T-bet regulates intestinal inflammation mediated by interleukin-7 receptor+ innate lymphoid cells. *Immunity* 37, 674–684. doi: 10.1016/j.immuni.2012.09.008
- Powrie, F., Coffman, R. L., and Correa-Oliveira, R. (1994). Transfer of CD4+ T cells to C.B-17 SCID mice: a model to study Th1 and Th2 cell differentiation and regulation in vivo. *Res. Immunol.* 145, 347–353. doi: 10.1016/S0923-2494(94)80198-3
- Pu, Q., Lin, P., Gao, P., Wang, Z., Guo, K., Qin, S., et al. (2021). Gut microbiota regulate gut-lung Axis inflammatory responses by mediating ILC2 compartmental migration. *J. Immunol.* 207, 257–267. doi: 10.4049/jimmunol.2001304
- Qiu, J., Heller, J. J., Guo, X., Chen, Z. M. E., Fish, K., Fu, Y. X., et al. (2012). The aryl hydrocarbon receptor regulates gut immunity through modulation of innate lymphoid cells. *Immunity* 36, 92–104. doi: 10.1016/j.immuni.2011.11.011
- Reece, P., Gauvreau, G. M., Sehmi, R., and Denburg, J. A. (2014). IL-4 and IL-13 differentially regulate TLR-induced eosinophil-basophil differentiation of cord blood CD34+ progenitor cells. *PLoS One* 9:e100734. doi: 10.1371/journal.pone.0100734
- Reinosa Webb, C., den Bakker, H., Koboziev, I., Jones-Hall, Y., Rao Kottapalli, K., Ostanin, D., et al. (2018). Differential susceptibility to T cell-induced colitis in mice: role of the intestinal microbiota. *Inflamm. Bowel Dis.* 24, 361–379. doi: 10.1093/ibd/izx014
- Romera-Hernández, M., Aparicio-Domingo, P., Papazian, N., Karrich, J. J., Cornelissen, F., Hoogenboezem, R. M., et al. (2020). Yap1-driven intestinal repair is controlled by group 3 innate lymphoid cells. *Cell Rep.* 30, 37–45.e3. doi: 10.1016/j.celrep.2019.11.115
- Saez, A., Gomez-Bris, R., Herrero-Fernandez, B., Mingorance, C., Rius, C., and Gonzalez-Granado, J. M. (2021). Innate lymphoid cells in intestinal homeostasis and inflammatory bowel disease. *Int. J. Mol. Sci.* 22:7618. doi: 10.3390/ijms22147618
- Sano, T., Huang, W., Hall, J. A., Yang, Y., Chen, A., Gavzy, S. J., et al. (2015). An IL-23R/IL-22 circuit regulates epithelial serum amyloid A to promote local effector Th17 responses. *Cells* 163, 381–393. doi: 10.1016/j.cell.2015.08.061
- Sarrabayrouse, G., Bossard, C., Chauvin, J. M., Jarry, A., Meurette, G., Quévrain, E., et al. (2014). CD4CD8 $\alpha$  lymphocytes, a novel human regulatory T cell subset induced by colonic bacteria and deficient in patients with inflammatory bowel disease. *PLoS Biol.* 12:e1001833. doi: 10.1371/journal.pbio.1001833
- Sartor, R. B. (1997). The influence of normal microbial flora on the development of chronic mucosal inflammation. *Res. Immunol.* 148, 567–576. doi: 10.1016/S0923-2494(98)80151-X
- Schaubeck, M., Clavel, T., Calasan, J., Lagkouvardos, I., Haange, S. B., Jehmlich, N., et al. (2016). Dysbiotic gut microbiota causes transmissible Crohn's disease-like ileitis independent of failure in antimicrobial defence. *Gut* 65, 225–237. doi: 10.1136/gutjnl-2015-309333
- Schirmer, M., Franzosa, E. A., Lloyd-Price, J., McIver, L. J., Schwager, R., Poon, T. W., et al. (2018). Dynamics of metatranscription in the inflammatory bowel disease gut microbiome. *Nat. Microbiol.* 3, 337–346. doi: 10.1038/s41564-017-0089-z
- Sefik, E., Geva-Zatorsky, N., Oh, S., Konnikova, L., Zemmour, D., McGuire, A. M., et al. (2015). Individual intestinal symbionts induce a distinct population of ROR $\gamma$ + regulatory T cells. *Science* 349, 993–997. doi: 10.1126/science.aaa9420
- Sellon, R. K., Tonkonogy, S., Schultz, M., Dieleman, L. A., Grenther, W., Balish, E., et al. (1998). Resident enteric bacteria are necessary for development of spontaneous colitis and immune system activation in Interleukin-10-deficient mice. *Infect. Immun.* 66, 5224–5231. doi: 10.1128/IAI.66.11.5224-5231.1998
- Sepahi, A., Liu, Q., Friesen, L., and Kim, C. H. (2021). Dietary fiber metabolites regulate innate lymphoid cell responses. *Mucosal Immunol.* 14, 317–330. doi: 10.1038/s41385-020-0312-8
- Sepehri, S., Kotlowski, R., Bernstein, C. N., and Krause, D. O. (2007). Microbial diversity of inflamed and noninflamed gut biopsy tissues in inflammatory bowel disease. *Inflamm. Bowel Dis.* 13, 675–683. doi: 10.1002/ibd.20101
- Setty, M., Discepolo, V., Abadie, V., Kamhawi, S., Mayassi, T., Kent, A., et al. (2015). Distinct and synergistic contributions of epithelial stress and adaptive immunity to functions of intraepithelial killer cells and active celiac disease. *Gastroenterology* 149, 681–691.e10. doi: 10.1053/j.gastro.2015.05.013
- Silva, Y. P., Bernardi, A., and Frozza, R. L. (2020). The role of short-chain fatty acids from gut microbiota in gut-brain communication. *Front. Endocrinol.* 11:25. doi: 10.3389/fendo.2020.00025
- Simpson, S. J., Holländer, G. A., Mizoguchi, E., Allen, D., Bhan, A. K., Wang, B., et al. (1997). Expression of pro-inflammatory cytokines by TCR $\alpha$  $\beta$ + T and TCR $\gamma$  $\delta$ + T cells in an experimental model of colitis. *Eur. J. Immunol.* 27, 17–25. doi: 10.1002/eji.1830270104
- Somineni, H. K., and Kugathasan, S. (2019). The microbiome in patients with inflammatory diseases. *Clin. Gastroenterol. Hepatol.* 17, 243–255. doi: 10.1016/j.cgh.2018.08.078
- Song, X., Zhang, H., Zhang, Y., Goh, B., Bao, B., Mello, S. S., et al. (2023). Gut microbial fatty acid isomerization modulates intraepithelial T cells. *Nature* 619, 837–843. doi: 10.1038/s41586-023-06265-4
- Sonnenberg, G. F., and Hepworth, M. R. (2019). Functional interactions between innate lymphoid cells and adaptive immunity. *Nat. Rev. Immunol.* 19, 599–613. doi: 10.1038/s41577-019-0194-8
- Sonnenberg, G. F., Monticelli, L. A., Elloso, M. M., Fouser, L. A., and Artis, D. (2011). CD4(+) lymphoid tissue-inducer cells promote innate immunity in the gut. *Immunity* 34, 122–134. doi: 10.1016/j.immuni.2010.12.009
- Stephen-Victor, E., and Chatila, T. A. (2022). An embarrassment of riches: ROR $\gamma$ t+ antigen-presenting cells in peripheral tolerance. *Immunity* 55, 1978–1980. doi: 10.1016/j.immuni.2022.10.009
- Sujino, T., London, M., Hoytema van Konijnenburg, D., Rendon, T., Buch, T., Silva, H. M., et al. (2016). Tissue adaptation of regulatory and intraepithelial CD4+ T cells controls gut inflammation. *Science* 352, 1581–1586. doi: 10.1126/science.aaf3892
- Sundin, O. H., Mendoza-Ladd, A., Zeng, M., Diaz-Arévalo, D., Morales, E., Fagan, B. M., et al. (2017). The human jejunum has an endogenous microbiota that differs from those in the oral cavity and colon. *BMC Microbiol.* 17:160. doi: 10.1186/s12866-017-1059-6
- Takatsu, K. (2011). Interleukin-5 and IL-5 receptor in health and diseases. *Proc. Jpn. Acad. Ser. B Phys. Biol. Sci.* 87, 463–485. doi: 10.2183/pjab.87.463
- Tamura, A., Soga, H., Yaguchi, K., Yamagishi, M., Toyota, T., Sato, J., et al. (2003). Distribution of two types of lymphocytes (intraepithelial and lamina-propria-associated) in the murine small intestine. *Cell Tissue Res.* 313, 47–53. doi: 10.1007/s00441-003-0706-4
- Thursby, E., and Juge, N. (2017). Introduction to the human gut microbiota. *Biochem. J.* 474, 1823–1836. doi: 10.1042/BCJ20160510
- Umesaki, Y., Setoyama, H., Matsumoto, S., Imaoka, A., and Itoh, K. (1999). Differential roles of segmented filamentous bacteria and clostridia in development of the intestinal immune system. *Infect. Immun.* 67, 3504–3511. doi: 10.1128/IAI.67.7.3504-3511.1999
- Van De Pavert, S. A. (2021). Lymphoid tissue inducer (LTi) cell ontogeny and functioning in embryo and adult. *Biom. J.* 44, 123–132. doi: 10.1016/j.bj.2020.12.003
- Van Kaer, L., and Olivares-Villagómez, D. (2018). Development, homeostasis, and functions of intestinal intraepithelial lymphocytes. *J. I.* 200, 2235–2244. doi: 10.4049/jimmunol.1701704
- Viladomiu, M., Kivoolowitz, C., Abdulhamid, A., Dogan, B., Victorio, D., Castellanos, J. G., et al. (2017). IgA-coated *E. coli* enriched in Crohn's disease spondyloarthritis promote TH17-dependent inflammation. *Sci. Transl. Med.* 9:eaf9655. doi: 10.1126/scitranslmed.aaf9655
- Villmones, H. C., Haug, E. S., Ulvestad, E., Grude, N., Stenstad, T., Halland, A., et al. (2018). Species level description of the human Ileal bacterial microbiota. *Sci. Rep.* 8:4736. doi: 10.1038/s41598-018-23198-5
- Vivier, E., Artis, D., Colonna, M., Diefenbach, A., Di Santo, J. P., Eberl, G., et al. (2018). Innate lymphoid cells: 10 years on. *Cells* 174, 1054–1066. doi: 10.1016/j.cell.2018.07.017

- Vuik, F., Dicksved, J., Lam, S. Y., Fuhler, G. M., van der Laan, L., van de Winkel, A., et al. (2019). Composition of the mucosa-associated microbiota along the entire gastrointestinal tract of human individuals. *United European Gastroenterol J* 7, 897–907. doi: 10.1177/2050640619852255
- Wang, M., Ahrné, S., Jeppsson, B., and Molin, G. (2005). Comparison of bacterial diversity along the human intestinal tract by direct cloning and sequencing of 16S rRNA genes. *FEMS Microbiol. Ecol.* 54, 219–231. doi: 10.1016/j.femsec.2005.03.012
- Weingarden, A. R., and Vaughn, B. P. (2017). Intestinal microbiota, fecal microbiota transplantation, and inflammatory bowel disease. *Gut Microbes* 8, 238–252. doi: 10.1080/19490976.2017.1290757
- Whary, M. T., Taylor, N. S., Feng, Y., Ge, Z., Muthupalani, S., Versalovic, J., et al. (2011). *Lactobacillus reuteri* promotes *Helicobacter hepaticus*-associated typhlocolitis in gnotobiotic B6.129P2-IL-10 (tm1Cgn) (IL-10 (–/–)) mice. *Immunology* 133, 165–178. doi: 10.1111/j.1365-2567.2011.03423.x
- Willinger, T. (2019). Metabolic control of innate lymphoid cell migration. *Front. Immunol.* 10:2010. doi: 10.3389/fimmu.2019.02010
- Wu, W. M., Yang, Y. S., and Peng, L. H. (2014). Microbiota in the stomach: new insights. *J. Dig. Dis.* 15, 54–61. doi: 10.1111/1751-2980.12116
- Xuan, X., Zhang, L., Tian, C., Wu, T., Ye, H., Cao, J., et al. (2021). Interleukin-22 and connective tissue diseases: emerging role in pathogenesis and therapy. *Cell Biosci.* 11:2. doi: 10.1186/s13578-020-00504-1
- Yang, H., Antony, P. A., Wildhaber, B. E., and Teitelbaum, D. H. (2004). Intestinal intraepithelial lymphocyte  $\gamma\delta$ -T cell-derived keratinocyte growth factor modulates epithelial growth in the mouse. *J. Immunol.* 172, 4151–4158. doi: 10.4049/jimmunol.172.7.4151
- Yang, I., Nell, S., and Suerbaum, S. (2013). Survival in hostile territory: the microbiota of the stomach. *FEMS Microbiol. Rev.* 37, 736–761. doi: 10.1111/1574-6976.12027
- Yap, Y. A., and Mariño, E. (2018). An insight into the intestinal web of mucosal immunity, microbiota, and diet in inflammation. *Front. Immunol.* 9:2617. doi: 10.3389/fimmu.2018.02617
- Yasuda, K., Takeuchi, Y., and Hirota, K. (2019). The pathogenicity of Th17 cells in autoimmune diseases. *Semin. Immunopathol.* 41, 283–297. doi: 10.1007/s00281-019-00733-8
- Zhang, Y., and Huang, B. (2017). The development and diversity of ILCs, NK cells and their relevance in health and diseases. *Adv. Exp. Med. Biol.* 1024, 225–244. doi: 10.1007/978-981-10-5987-2\_11
- Zhao, M., Gönczi, L., Lakatos, P. L., and Burisch, J. (2021). The burden of inflammatory bowel disease in Europe in 2020. *J. Crohn's Colitis* 15, 1573–1587. doi: 10.1093/ecco-jcc/jjab029
- Zhou, C., Qiu, Y., and Yang, H. (2019). CD4CD8 $\alpha\alpha$  IELs: they have something to say. *Front. Immunol.* 10:2269. doi: 10.3389/fimmu.2019.02269
- Zhou, L., Chu, C., Teng, F., Bessman, N. J., Goc, J., Santosa, E. K., et al. (2019). Innate lymphoid cells support regulatory T cells in the intestine through interleukin-2. *Nature* 568, 405–409. doi: 10.1038/s41586-019-1082-x
- Zhou, W., and Sonnenberg, G. F. (2020). Activation and suppression of group 3 innate lymphoid cells in the gut. *Trends Immunol.* 41, 721–733. doi: 10.1016/j.it.2020.06.009
- Zhu, L., Zhu, C., Cao, S., and Zhang, Q. (2021). *Helicobacter hepaticus* induce colitis in male IL-10–/– mice dependent by Cytolethal distending toxin B and via the activation of Jak/stat signaling pathway. *Front. Cell. Infect. Microbiol.* 11:616218. doi: 10.3389/fcimb.2021.616218
- Zindl, C. L., Witte, S. J., Laufer, V. A., Gao, M., Yue, Z., Janowski, K. M., et al. (2022). A nonredundant role for T cell-derived interleukin 22 in antibacterial defense of colonic crypts. *Immunity* 55, 494–511.e11. doi: 10.1016/j.immuni.2022.02.003

# Frontiers in Microbiology

Explores the habitable world and the potential of microbial life

The largest and most cited microbiology journal which advances our understanding of the role microbes play in addressing global challenges such as healthcare, food security, and climate change.

## Discover the latest Research Topics

[See more →](#)

### Frontiers

Avenue du Tribunal-Fédéral 34  
1005 Lausanne, Switzerland  
[frontiersin.org](https://frontiersin.org)

### Contact us

+41 (0)21 510 17 00  
[frontiersin.org/about/contact](https://frontiersin.org/about/contact)

